HUMAN AND ONCOVIRAL NONCODING RNAS AS MODULATORS OF CANCER AGGRESSIVENESS AND DISEASE PROGRESSION

EDITED BY: Deilson Elgui De Oliveira, Patricia P. Reis and Wan L. Lam

PUBLISHED IN: Frontiers in Oncology and Frontiers in Cell and Deveopmental Biology

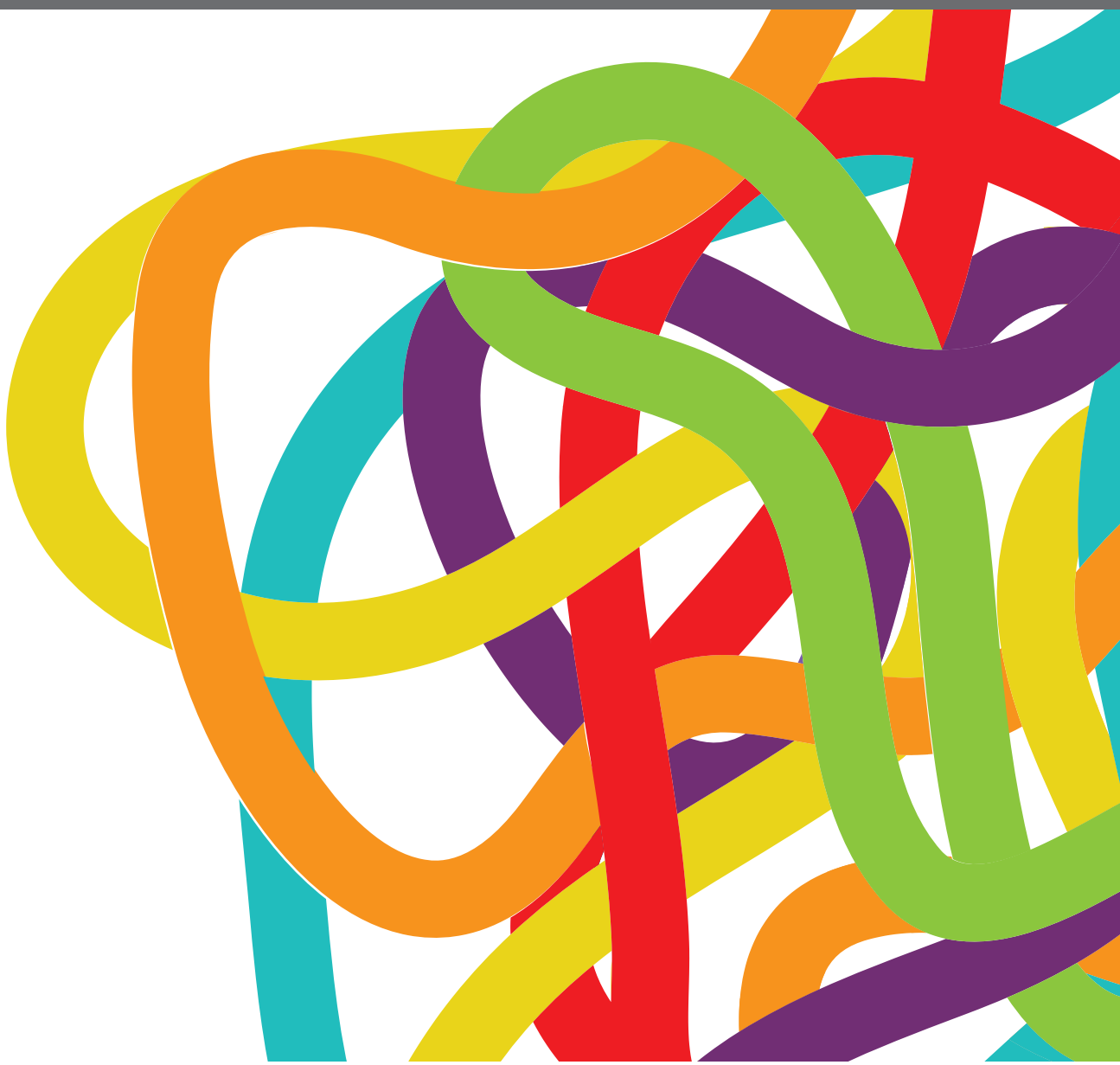

frontiers Research Topics

ISSN 1664-8714
ISBN 978-2-88966-565-5
DOI 10.3389/978-2-88966-565-5

About Frontiers

Frontiers is more than just an open-access publisher of scholarly articles: it is a pioneering approach to the world of academia, radically improving the way scholarly research is managed. The grand vision of Frontiers is a world where all people have an equal opportunity to seek, share and generate knowledge. Frontiers provides immediate and permanent online open access to all its publications, but this alone is not enough to realize our grand goals.

Frontiers Journal Series

The Frontiers Journal Series is a multi-tier and interdisciplinary set of open-access, online journals, promising a paradigm shift from the current review, selection and dissemination processes in academic publishing. All Frontiers journals are driven by researchers for researchers; therefore, they constitute a service to the scholarly community. At the same time, the Frontiers Journal Series operates on a revolutionary invention, the tiered publishing system, initially addressing specific communities of scholars, and gradually climbing up to broader public understanding, thus serving the interests of the lay society, too.

Dedication to Quality

Each Frontiers article is a landmark of the highest quality, thanks to genuinely collaborative interactions between authors and review editors, who include some of the world's best academicians. Research must be certified by peers before entering a stream of knowledge that may eventually reach the public - and shape society; therefore, Frontiers only applies the most rigorous and unbiased reviews.
Frontiers revolutionizes research publishing by freely delivering the most outstanding research, evaluated with no bias from both the academic and social point of view. By applying the most advanced information technologies, Frontiers is catapulting scholarly publishing into a new generation.

What are Frontiers Research Topics?

Frontiers Research Topics are very popular trademarks of the Frontiers Journals Series: they are collections of at least ten articles, all centered on a particular subject. With their unique mix of varied contributions from Original Research to Review Articles, Frontiers Research Topics unify the most influential researchers, the latest key findings and historical advances in a hot research area! Find out more on how to host your own Frontiers Research Topic or contribute to one as an author by contacting the Frontiers Editorial Office: frontiersin.org/about/contact

HUMAN AND ONCOVIRAL NONCODING RNAS AS MODULATORS OF CANCER AGGRESSIVENESS AND DISEASE PROGRESSION

Topic Editors:
Deilson Elgui De Oliveira, São Paulo State University, Brazil
Patricia P. Reis, São Paulo State University, Brazil
Wan L. Lam, British Columbia Cancer Research Centre, Canada

Citation: De Oliveira, D. E., Reis, P. P., Lam, W. L., eds. (2021). Human and Oncoviral Noncoding RNAs as Modulators of Cancer Aggressiveness and Disease Progression. Lausanne: Frontiers Media SA. doi: 10.3389/978-2-88966-565-5

Table of Contents

frontiers in Oncology

EDITORIAL
published: 25 January 2021
doi: 10.3389/fonc.2020.641725

Editorial: Human and Oncoviral Non-Coding RNAs as Modulators of Cancer Aggressiveness and Disease Progression

Patricia P. Reis[1]*, *Wan L. Lam*[2]* and *Deilson Elgui de Oliveira*[1]*

[1] Medical School, São Paulo State University (UNESP), Botucatu, Brazil, [2] University of British Columbia, Vancouver, BC, Canada

Keywords: non-coding RNAs, cancer biology, tumor progression, oncoviruses, cancer management, human

Editorial on the Research Topic

Human and Oncoviral Non-Coding RNAs as Modulators of Cancer Aggressiveness and Disease Progression

OPEN ACCESS

Edited and reviewed by:
Paolo Pinton,
University of Ferrara, Italy

***Correspondence:**
Patricia P. Reis
patricia.reis@unesp.br
Wan L. Lam
WanLam@bccrc.ca
Deilson Elgui de Oliveira
deilson.elgui@unesp.br

Specialty section:
This article was submitted to Molecular and Cellular Oncology, a section of the journal Frontiers in Oncology

Received: *14 December 2020*
Accepted: *17 December 2020*
Published: *25 January 2021*

Citation:
Reis PP, Lam WL and Elgui de Oliveira D (2021) Editorial: Human and Oncoviral Non-Coding RNAs as Modulators of Cancer Aggressiveness and Disease Progression. Front. Oncol. 10:641725. doi: 10.3389/fonc.2020.641725

Non-coding RNAs (ncRNAs) include a variety of molecules that modulate complex cellular networks with roles in normal physiology and cancer pathogenesis (1). Several types of ncRNAs, such as microRNAs (miRNAs) and long non-coding RNAs (lncRNAs)—either endogenous or from viral origin—have been widely investigated in human cancers. They are diagnostic, prognostic, and predictive biomarkers, detectable in biofluids (2). Human and viral ncRNAs contribute to the hallmarks of cancer, modulating target genes participating in disease development and tumor progression (3–6).

This Research Topic compiles original research and review papers that shed light on the role of human or viral ncRNAs in the molecular and cellular processes leading to cancer progression. The ncRNAs orchestrate malignant invasion and the dissemination of neoplastic cells, notably by metastasis, by targeting genes within several signaling pathways, such as those in the Epithelial-Mesenchymal Transition program. The 13 papers on this Research Topic highlight ncRNAs as key players in cancer pathogenesis, some proposed as biomarkers applicable to clinical management of patients.

Mou et al. showed that the lncRNA *Lymph Node Metastasis Associated Transcript 1* (*LNMAT1*) is upregulated in malignant melanoma. Mechanistically, *LNMAT1* enhances cancer cell migration and invasion by suppressing the *Cell Adhesion Molecule 1* (*CADM1*) tumor suppressor gene. In colorectal carcinoma (CRC), Lin et al. demonstrated that the *miR-506* targets the epigenetic modifier UHRF1 *via* the KISS1/PI3K/NF-κB signaling axis, inhibiting the proliferation, migration, and invasion of CRC cells *in vitro* and *in vivo*, suggesting new therapeutic targets for CRC. In gastric cancer (GC), Sun et al. showed that the lncRNA *AK025387* was upregulated in metastatic GC cells, putatively by regulation of the Raf-1/MAPK/MEK/ERK signaling. Zhao et al. reviewed the role of lncRNAs and miRNAs in regulating the *Programmed Cell Death 4* (*PDCD4*) tumor suppressor gene, which is involved in a variety of cellular regulatory mechanisms, to disclose relevant information for the development of novel therapies for targeting cancers disrupted in PDCD4 suppression.

Drugs and natural compounds have been widely explored regarding their activity and cytotoxicity against various cancers for decades. In this regard, Liu et al. reported that the natural glycoalkaloid

Solasonine (SS) inhibited the growth of HepG2 and QGY-7703 hepatocellular carcinoma (HCC) cells, and this effect was attributed to regulatory interaction between miR-375-3p and the lncRNA CCAT1, leading to reduction of IRF5 mediated by the SP1 transcription factor. Yan et al. showed a novel mechanism of Temozolomide resistance in glioblastoma cells based on activity of lnRNA *ADAMTS9* and the AS2/FUS/MDM2 signaling axis. LncRNA alterations may lead to the acquisition of resistance to chemotherapy. Abildgaard et al. present the landscape of lncRNA alterations associated with the hallmarks of ovarian carcer (OC), concluding that OC pathogenesis and acquisition of treatment resistance may occur through highly complex mechanisms in which ncRNAs have prominent roles.

In chronic myeloid leukemia (CML), allogeneic-hematopoietic stem cell transplantation (allo-HSCT) may be the treatment of choice for patients with resistant forms of the disease. Martins et al. evaluated the miRNA expression profiles in CML in 28 patients equally divided into groups with untreated cases of chronic phase-CML and cases with cytogenetic remission after allo-HSCT. Among the differentially expressed miRNAs, the miR-1260a and miR-409-3p were identified as the top downregulated and upregulated miRNAs, respectively. Interestingly, the signaling pathways involving MAPKs, RAS, and ROCK were enriched with components encoded by genes targeted by these miRNAs, suggesting that they may have regulatory functions in the clinical evolution of CML.

A significant fraction of human cancers is linked to infection by oncogenic viruses, such as the Human Papilloma Virus (HPV) and the Epstein-Barr virus (EBV). Tornesello et al. describe complex interactions between miRNAs, lncRNAs, and circular RNAs (circRNAs) in the pathogenesis of cervical carcer strongly linked to HPV infection. The lncRNAs *HOTAIR*, *MALAT1*, *GAS5*, and *MEG3* were reported to regulate tumor invasion and therapeutic resistance in cervical cancer. Additionally, the circRNA, circ-0018289 contributes *via* a miRNA-sponging mechanism. This network of interacting ncRNAs may also include HPV microRNAs (e.g., HPV-16-miR-H1-1 and HPV-16-miR-H2-1), but further investigation of this matter is required to clarify their role in HPV-associated cancers. Nonetheless, viral ncRNAs encoded by EBV are already recognized as key players of EBV-induced carcinogenesis. Verhoeven et al. reported that the BART region of the EBV genome encodes lncRNAs that not only contribute to EBV latency in nasopharyngeal carcinomas (NPC) cells, but also regulate genes that ultimately may cause immune evasion and contribute to NPC progression.

The discovery of previously unannotated miRNAs in several tissue types (7) has prompted the identification of new ncRNAs with biological and clinical relevance in cancers. Rock et al. reported that 146 novel miRNAs specific to head and neck squamous cell carcinomas (HNSCC) were identified from small RNA sequence data *in silico*. Interestingly, 135/146 miRNAs were found increased in HNSCC samples compared to non-neoplastic head and neck tissues. The novel miRNAs identified were validated with HNSCC samples; furthermore, a prognostic-model combining novel and known miRNAs and using multivariate Cox regression analysis was proposed, allowing improved stratification of survival and recurrence risk of patients. In pancreatic cancer, Ros et al. reported new antisense lncRNAs associated with *High Mobility Group A* (*HMGA1* and *HMGA2*) genes, and *HMGA2-AS1* lncRNA regulates the expression of its own sense gene, with implications for tumorigenesis. Finally, Wu and Chen reviewed the role of super-enhancers (SE) molecules and se-ncRNAs, which may have potent activities as effectors in the determination of cell identity and their crosstalk with immune checkpoints. SEs associated with ncRNAs have shown to play a role in several regulatory mechanisms, including immune checkpoint expression in cancer cells, and the authors highlight a number of studies that explored the use of SE blockers for improved cancer therapies.

Altogether, these papers included in this Research Topic by Frontiers shed more light on the characterization of known and novel ncRNAs with relevant roles in cancer biology and that may be valuable as biomarkers to assess prognosis, response to treatment, and monitoring of patients with aggressive cancers.

AUTHOR CONTRIBUTIONS

All authors contributed equally to this Editorial. All authors contributed to the article and approved the submitted version.

REFERENCES

1. Anastasiadou E, Jacob L, Slack F. Non-coding RNA networks in cancer. *Nat Rev Cancer* (2018) 18:5–18. doi: 10.1038/nrc.2017.99
2. Anfossi S, Babayan A, Pantel K, Calin GA. Clinical utility of circulating non-coding RNAs - an update. *Nat Rev Clin Oncol* (2018) 15:541–63. doi: 10.1038/s41571-018-0035-x
3. Michael IP, Saghafinia S, Hanahan D. A set of microRNAs coordinately controls tumorigenesis, invasion, and metastasis. *Proc Natl Acad Sci USA* (2019) 116(48):24184–95. doi: 10.1073/pnas.1913307116
4. Mirzaei H, Hamblin MR. Regulation of Glycolysis by Non-coding RNAs in Cancer: Switching on the Warburg Effect. *Mol Ther Oncolytics* (2020) 19:218–39. doi: 10.1016/j.omto.2020.10.003
5. Safarzadeh E, Asadzadeh Z, Safaei S, Hatefi A, Derakhshani A, Giovannelli F, et al. MicroRNAs and lncRNAs-A new layer of myeloid-derived suppressor cells regulation. *Front Immunol* (2020) 11:572323. doi: 10.3389/fimmu.2020.572323
6. Caetano BFR, Jorge BAS, Müller-Coan BG, Elgui de Oliveira D. Epstein-Barr virus microRNAs in the pathogenesis of human cancers. *Cancer Lett* (2021) 499:14–23. doi: 10.1016/j.canlet.2020.11.019
7. Londin E, Loher P, Telonis AG, Quann K, Clark P, Jing Y, et al. Analysis of 13 cell types reveals evidence for the expression of numerous novel primate- and tissue-specific microRNAs. *Proc Natl Acad Sci USA* (2015) 112(10):E1106–15. doi: 10.1073/pnas.1420955112

Conflict of Interest: The authors declare that the research was conducted in the absence of any commercial or financial relationships that could be construed as a potential conflict of interest.

frontiers in Oncology

ORIGINAL RESEARCH
published: 03 July 2019
doi: 10.3389/fonc.2019.00569

LNMAT1 Promotes Invasion-Metastasis Cascade in Malignant Melanoma by Epigenetically Suppressing CADM1 Expression

*Kuanhou Mou[1], Xiang Zhang[2], Xin Mu[1], Rui Ge[1], Dan Han[1], Yan Zhou[1] and Lijuan Wang[1]**

[1] Department of Dermatology, the First Affiliated Hospital of Xi'an Jiaotong University, Xi'an, China, [2] Department of Clinical Laboratory Medicine, Xijing Hospital, Fourth Military Medical University, Xi'an, China

The invasion-metastasis cascade is one of the most important factors relating to poor survival and prognosis of malignant melanoma (MM) patients. Long non-coding RNA lymph node metastasis associated transcript 1 (LNMAT1) is a key regulator in lymph node metastasis of multiple cancer types, but the roles and underlying mechanisms of LNMAT1 in the invasion-metastasis cascade of MM remain unclear. In the present study, we aimed to investigate the expression and function of LNMAT1 in MM. Here, we found that LNMAT1 was upregulated in MM tissues and cells, and its expression levels were further enhanced in MM patients with lymph node metastasis and metastatic MM cells. Using loss-of-function assays, we found that LNMAT1 promoted cell migration and invasion and lung metastasis in MM *in vitro* and *in vivo*. Moreover, we found that cell adhesion molecule 1 (CADM1), the established tumor suppressor in MM, was the downstream target of LNMAT1. Mechanistically, LNMAT1 epigenetically suppressed CADM1 expression by recruiting EZH2, the key regulator of trimethylation of histone H3 at lysine 27 (H3K27me3), to the CADM1 promoter, resulting in transcriptional inhibition of CADM1. Lastly, rescue assays demonstrated that LNMAT1 promoted cell migration and invasion of MM by suppressing CADM1 expression. Our findings elucidate a new mechanism for LNMAT1-mediated invasion-metastasis cascade in MM and suggest that LNMAT1 may be a new therapeutic target and prognostic predictor for MM.

Keywords: LNMAT1, EZH2, CADM1, invasion-metastasis cascade, malignant melanoma

OPEN ACCESS

Edited by:
Patricia P. Reis,
São Paulo State University, Brazil

Reviewed by:
Jessamy Tiffen,
Centenary Institute Australia, Australia
Pei Yan Liu,
University of New South Wales, Australia

****Correspondence:***
Lijuan Wang
6945216juan@163.com

Specialty section:
This article was submitted to Molecular and Cellular Oncology, a section of the journal Frontiers in Oncology

Received: *13 April 2019*
Accepted: *12 June 2019*
Published: *03 July 2019*

Citation:
Mou K, Zhang X, Mu X, Ge R, Han D, Zhou Y and Wang L (2019) LNMAT1 Promotes Invasion-Metastasis Cascade in Malignant Melanoma by Epigenetically Suppressing CADM1 Expression. Front. Oncol. 9:569. doi: 10.3389/fonc.2019.00569

INTRODUCTION

It is estimated that there will be 96,480 newly diagnosed malignant melanoma (MM) cases in 2019 in the United States following a drastically increased incidence throughout the last decade (1). Despite continuous improvement in diagnosis and treatment, the current recommended maintenance schedules, from radical resection to molecular-targeted drugs, are only effective in a subset of patients (2, 3). Tumors spread to distant sites or visceral organs in some early diagnosed patients, and the 5-year overall survival rate remains extremely disappointing for this subset of patients (4). Hence, it is highly important to explore new detailed mechanisms that account for the invasion-metastasis cascade in MM.

Long non-coding RNAs (lncRNAs) are reported to play pivotal roles in a wide range of vital biological processes (5, 6). More importantly, lncRNAs have also been identified as crucial regulators in the metastasis of multiple cancer types and function as oncogenes or tumor suppressors depending on the cancer type or circumstance (7). Regarding MM, it was reported that lncRNAs could function as molecular scaffolds to regulate the expression levels and functions of established oncogenes or tumor suppressors by interacting with RNA-binding proteins (8–10). Nevertheless, only a few lncRNAs have been functionally characterized in MM, and the mechanisms underlying their biological functions are yet to be fully elucidated. Long intergenic non-coding RNA 01296 (Linc01296), also known as lymph node metastasis associated transcript 1 (LNMAT1), is located in chromosome 14q11.2 and was identified as a metastasis-promoting gene in multiple cancer types (11, 12). It was reported that LNMAT1 could promote invasion and metastasis by either functioning as a ceRNA (13) or by interacting with RNA-binding proteins (14). However, the expression pattern and functions of LNMAT1 in MM remain unclear.

CADM1, a member of the cell adhesion molecule family, has been proven to be a tumor suppressor in many cancers, including breast cancer (15), esophageal squamous cell carcinoma (16), and hepatocellular carcinoma (17). In MM, it was reported that the expression of CADM1 was also significantly downregulated and functions as a tumor suppressor by suppressing matrix metalloproteinases (MMPs) in MM (18, 19). However, the regulating mechanism of CADM1 in MM is not fully elucidated.

In the current study, we determined that LNMAT1 was upregulated in MM tissues and cells, with enhanced expression in patients with lymph node metastasis and metastatic MM cell lines. More importantly, we found that LNMAT1 inhibited invasion and lung metastasis by suppressing CADM1 expression by recruiting EZH2 to its promoter. Our study indicates that LNMAT1 promotes the invasion-metastasis cascade and may be a potential therapeutic target in MM.

MATERIALS AND METHODS

Clinical Specimens

This study was carried out in accordance with the recommendations of Ethical Committee of the First Affiliated Hospital of Xi'an Jiaotong University. The protocol was approved by the Ethical Committee of the First Affiliated Hospital of Xi'an Jiaotong University. All subjects gave written informed consent in accordance with the Declaration of Helsinki. A total of 13 human MM tissues of diagnosed MM patients and 13 benign nevi (BN) tissues of healthy controls were resected and collected at the First Affiliated Hospital of Xi'an Jiaotong University from 2010 to 2017. Written informed consent was obtained from the participants enrolled in this study. Detailed information about the MM patients is provided in **Supplementary Table 1**.

Cell Culture

Human malignant melanoma cell lines WM35, A375, A2058, and mouse malignant melanoma cell line B16/F10 were purchased from GeneChem (Shanghai, China), and human epidermal melanocytes HEMa-LP were purchased from ThermoFisher (ThermoFisher, MA, USA). HEMa-LP cells were cultured in Medium 254 (ThermoFisher, MA, USA) supplemented with human melanocyte growth supplement, and WM35, A375, A2058, and B16/F10 cells were cultured in Dulbecco's modified eagle medium (DMEM, Gibco, NY, USA) supplemented with 10% fetal bovine serum (Cellmax, Beijing, China) at 37°C in a humidified atmosphere of 5% CO_2.

shRNA Infection and siRNA Transfection

Lentiviral small hairpin RNA (shRNA) directed against LNMAT1 in human and mouse-derived cells and scrambled negative control (NC) shRNA were designed and provided by GeneChem (Shanghai, China). Briefly, the LNMAT1 shRNAs targeting human LNMAT1 and NC shRNAs were cloned into the Bam I and Age I sites of the CV146 core vector (Ubi-MCS-SV40-firefly-Luciferase-IRES-Puromycin). The LNMAT1 shRNAs targeting mouse LNMAT1 and NC shRNAs were cloned into the Bam I and Age I sites of the GV260 core vector (hU6-MCS-Ubi-firefly-Luciferase-IRES-Puromycin). Then, 20 μg CV146-LNMAT1 shRNAs/NC shRNAs for human LNMAT1 knockdown or GV246-LNMAT1 shRNA/NC shRNAs for mouse LNMAT1 knockdown along with lentiviral packaging helper plasmid Helper 1.0 (15 μg) and Helper 2.0 (10 μg) were co-transfected into 293T cells by Lipofectamine 2000. The cell supernatant was collected 48 h later and then centrifuged to concentrate and purify human and mouse LNMAT1 shRNAs and NC shRNAs. LNMAT1 siRNA, CADM1 siRNA, and scrambled NC siRNA were synthesized and provided by Ribobio (Guangzhou, China). The sequences for shRNAs and siRNAs used in our study are provided in **Supplementary Table 2**.

For shRNA infection, MM cells were seeded in six-well plates and infected by HiTransG A (Genechem) according to the manufacturer's protocol. Then, MM cells were selected with puromycin for 2 weeks to remove uninfected MM cells and obtain stable LNMAT1 knockdown cells. The stable LNMAT1 knockdown MM cells were collected for qRT-PCR, western blot (WB), transwell assays, wound healing assays, and animal experiments.

For siRNA transfection, MM cells were seeded in six-well plates and transfected by Lipofectamine 2000 (ThermoFisher) according to the manufacturer's protocol. After 48 h, cells were collected for qRT-PCR, WB, transwell, and wound healing assays.

Migration and Invasion Assays, Wound Healing Assays, and WB

The number of migratory and invasive cells with LNMAT1 NC and LNMAT1 shRNA were measured by transwell assay (Corning, NY, USA) with or without Matrigel (BD, CA, USA), and the migratory distance of cells with LNMAT1 NC and LNMAT1 shRNA was measured by wound healing assays. CADM1 protein levels in MM cells infected with LNMAT1 NC and LNMAT1 shRNA were measured by WB. All procedures for transwell assays, wound healing assays, and WB were performed as described in our previous study (20).

Chromatin Immunoprecipitation (ChIP)-qPCR Assay

ChIP-qPCR assays were performed using the EZ-Magna ChIP A/G kit (Millipore, MA, USA) following the manufacturer's instructions. First, 1×10^6 MM cells were fixed in formaldehyde for 10 min, cell lysates were sonicated and sheared to generate chromatin DNA between 100 and 200 bp in length, and then the lysates were immunoprecipitated with anti-EZH2 (Cell Signaling Technology, USA) or anti-H3K27me3 (Abcam, UK). IgG served as the control. Then, the precipitated chromatin DNA was analyzed by qRT-PCR.

RNA Immunoprecipitation (RIP)

RIP assays were performed using the EZ-Magna RIP kit (Merck Millipore, USA) following the manufacturer's protocol. MM cells were lysed in RIP lysis buffer, and cell extracts were incubated with anti-EZH2 (Cell Signaling Technology, USA) or IgG for 6 h. Then, purified RNA was analyzed by qRT-PCR to identify the presence of LNMAT1.

Quantitative Real-Time Polymerase Chain Reaction (qRT-PCR)

RNA extraction and qRT-PCR were performed as described in our previous study. The primers used in this study were purchased from Sangon Biotech (Shanghai, China) and are displayed in **Supplementary Table 3**.

Animal Experiment

This study was carried out in accordance with the recommendations of Animal Care and Use Committee of Xi'an Jiaotong University. For lung metastasis assays, B16/F10 cells were seeded in six-well plates, and LNMAT1 shRNA targeting mouse LNMAT1 was infected by HiTransG A (Genechem) according to the manufacturer's protocol. Then, B16/F10 cells were selected with puromycin for 2 weeks to remove uninfected B16/F10 cells and obtain stable LNMAT1 knockdown B16/F10 cells. LNMAT1 stably silencing B16/F10 cells (1×10^6) or control cells were injected into the tail vein of 6-week-old C57/B6 mice (Animal Center of Xi'an Jiaotong University, Xi'an, China; $n = 5$ for each group). All mice were housed and maintained under specific pathogen-free conditions, and all experiments were approved by the Animal Care and Use Committee of Xi'an Jiaotong University and performed in accordance with institutional guidelines. Lung metastases were monitored and quantified by the Xenogen IVIS Kinetic Imaging System (PerkinElmer, MA, USA).

Statistical Analysis

IBM SPSS statistical software (version 22.0) was used to perform statistical analyses. Student's *t*-test was used for data analysis, and *P*-values were determined using 2-sided tests. $P < 0.05$ was considered to have statistical significance.

RESULTS

LNMAT1 Is Upregulated in MM Cells and Tissues With High Metastasis Potential

qRT-PCR analysis indicated that LNMAT1 is upregulated in MM tissues (cutaneous and acral melanoma) compared to BN tissues (**Figure 1A**, $P < 0.05$). Furthermore, LNMAT1 was found in higher levels in MM patients with lymph node (LN) metastasis than those without LN metastasis (**Figure 1B**, $P < 0.05$). Accordingly, the TCGA database from GEPIA (http://gepia.cancer-pku.cn) also showed enhanced LNMAT1 expression in MM ($P < 0.05$, **Figure 1C**), and enhanced LNMAT1 levels were observed in metastatic MM ($P < 0.05$, **Figure 1D**). Furthermore, LNMAT1 was also higher in MM cells than in HEMa-LP cells, and enhanced LNMAT1 levels were observed in MM cell lines with high metastatic potential (A375 and A2058) compared to primary MM cells (**Figure 1E**, $P < 0.05$). More importantly, after silencing LNMAT1 expression in MM cells with shRNAs (**Figure 1F**, $P < 0.05$), the mRNA expression levels of MMP-2, MMP-9, and N-cadherin, which are markers of tumor invasion-metastasis cascade, were found to be downregulated by qRT-PCR. Meanwhile, the expression of E-cadherin, one of the most important tumor metastasis suppressors and epithelial–mesenchymal transition (EMT) markers, was upregulated (**Figures 1G,H**). These results indicated that LNMAT1 may play an oncogenic role in the invasion-metastasis cascade in MM.

LNMAT1 Promotes the Invasion-Metastasis Cascade in MM *in vitro* and *in vivo*

To further elucidate the functions of LNMAT1 in the invasion-metastasis cascade of MM, wound healing, transwell, and B16/F10 pulmonary metastasis models were employed. Wound healing assays demonstrated that the migratory distance was decreased in MM cells infected with LNMAT1 shRNA lentivirus compared to that in control cells (**Figure 2A**, $P < 0.05$). Furthermore, silencing LNMAT1 expression in MM cells could attenuate cell migratory and invasive abilities (Migration assays: **Figures 2B,C**, invasion: **Figures 2D,E**; all $P < 0.05$), Then, we infected B16/F10 cells with LNMAT1 shRNA to stably silence LNMAT1 expression in B16/F10 and investigate the effects of LNMAT1 on lung metastasis in B16/F10 *in vivo* (**Figure 2F**). As shown by the Bioluminescence imaging (BLI) data (**Figures 2G,H**) and *ex vivo* photography of lung tissues (**Figures 2I,J**), LNMAT1 depletion significantly decreased lung colonization of B16/F10; this was consistent with the *in vitro* results. These results indicated that LNMAT1 promotes the migration and invasion of MM *in vitro* and *in vivo*.

CADM1 Is the Downstream Target of LNMAT1 in MM

Previously, it was found that CADM1, an established metastasis suppressor gene, could inhibit cell migration and invasion in MM by suppressing the expression of MMP-2 and MMP-9 (18). Thus, we investigated whether a regulatory mechanism existed between LNMAT1 and CADM1 in MM. As shown by qRT-PCR and WB, mRNA (**Figure 3A**, $P < 0.05$) and protein (**Figure 3B**)

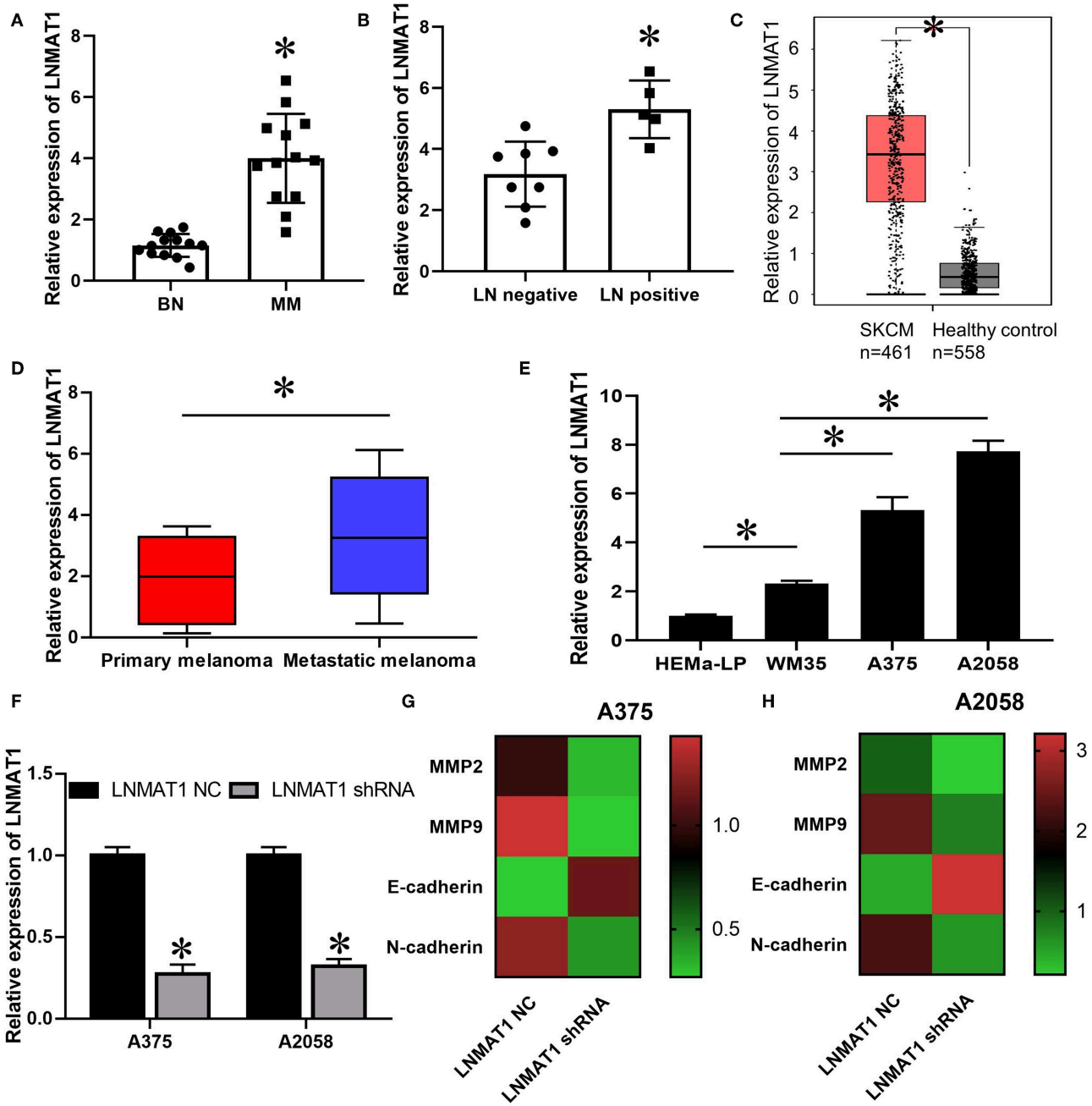

FIGURE 1 | LNMAT1 is upregulated in MM cell and tissues with high metastasis potential. **(A)** The expression of LNMAT1 in BN and MM (8 cutaneous melanoma and 5 acral melanoma); **(B)** The expression of LNMAT1 in MM patients with or without lymph node metastasis; **(C)** The expression of LNMAT1 in 461 patients with skin cutaneous malignant melanoma (SCKM, red box) and 558 healthy controls (Benign nevi ($n = 346$) and normal skin ($n = 212$), black box). TCGA data was analyzed by GEPIA (http://gepia.cancer-pku.cn/). **(D)** The expression of LNMAT1 in 101 patients with primary cutaneous MM (Red box) and 360 patients with metastatic cutaneous MM (Blue box). TCGA data was analyzed by GEPIA (http://gepia.cancer-pku.cn/). **(E)** The expression of LNMAT1 in human epidermal melanocytes and primary and metastatic MM cells; **(F)** The silencing effects of LNMAT1 shRNA in MM cells; **(G,H)** The expression of MMP-2, MMP-9, E-cadherin, and N-cadherin in A375 **(G)** and A2058 **(H)** cells infected with LNMAT1 shRNA or NC. Data are shown as the mean ± S.E. *$P < 0.05$, ns: not significant. The representative results of three independent experiments are shown.

levels of CADM1 were enhanced after silencing LNMAT1 expression in MM cells. Additionally, CADM1 expression was downregulated in MM tissues compared to BN tissues (**Figure 3C**, $P < 0.05$). More importantly, CADM1 expression was inversely correlated with LNMAT1 expression in MM tissues (**Figure 3D**, $P < 0.05$).

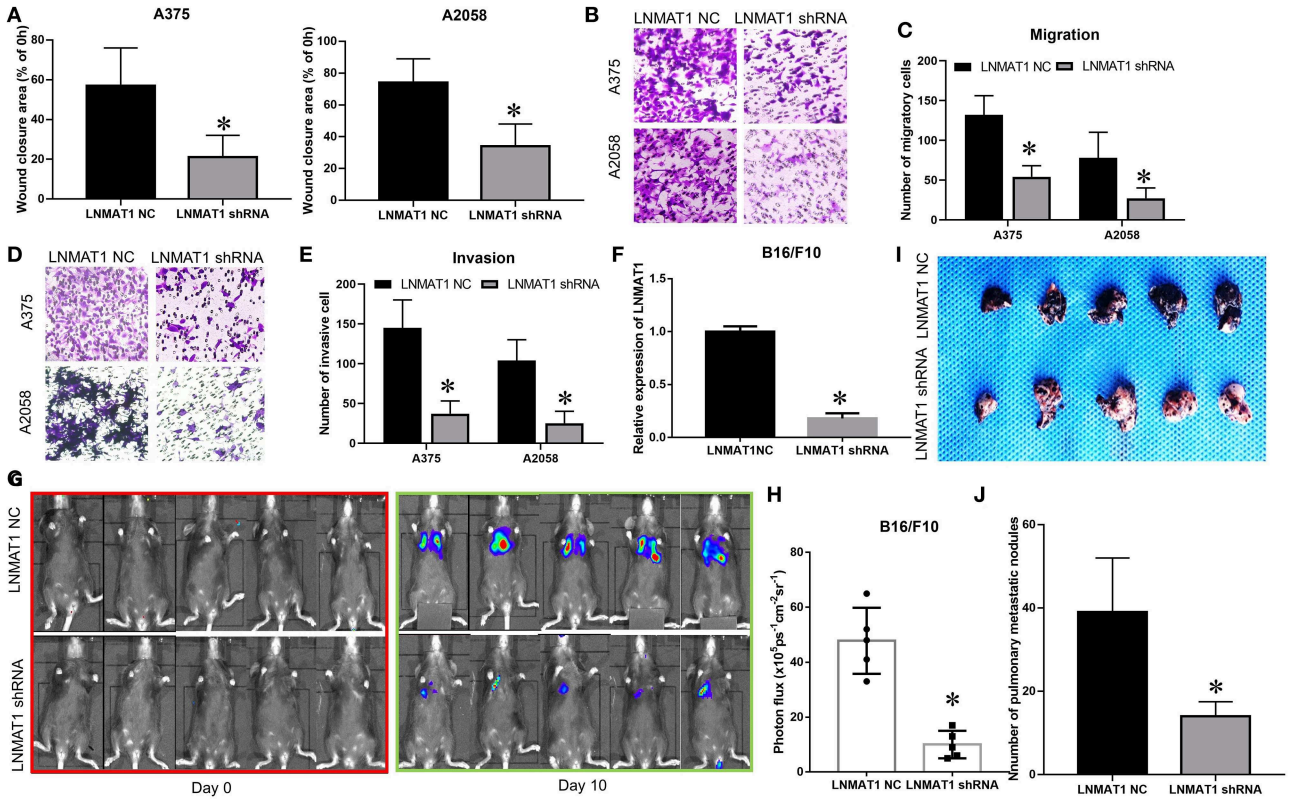

FIGURE 2 | LNMAT1 promotes the invasion-metastasis cascade in MM *in vitro* and *in vivo*. **(A)** MM cells were infected with LNMAT1 NC or shRNA. Wound healing assays were performed to detect the migratory distance in the indicated groups. The representative results of three independent experiments are shown; **(B,C)** Transwell assays were performed to detect the number of migratory cells in the indicated groups. The representative results of three independent experiments are shown; **(D,E)** Transwell assays were performed to detect the number of invasive cells in the indicated groups. The representative results of three independent experiments are shown; **(F)** The silencing effects of LNMAT1 shRNA in B16/F10 cells; **(G,H)** Bioluminescence images at day 0 and day 10 **(G)** and statistical analysis **(H)** of bioluminescence at day 10 (lung colonization) in C57/B6 mice ($n = 5$) that were intravenously injected with LNMAT1 stably silencing B16/F10 cells or NC cells; **(I,J)** Bright field imaging **(I)** and number of metastatic nodules **(J)** at day 10 in the lungs of C57/B6 mice ($n = 5$) that were intravenously injected with LNMAT1 stably silencing B16/F10 cells or NC cells. Data are shown as the mean ± S.E. *$P < 0.05$, ns: not significant.

LNMAT1 Epigenetically Suppresses CADM1 Expression by Recruiting EZH2 to Its Promoter

It has been reported that LNMAT1 could epigenetically suppress KLF2 expression by interacting with EZH2, an RNA-binding protein and crucial regulator for the trimethylation of histone H3 at lysine 27 (H3K27me3) (14). Thus, we hypothesized that LNMAT1 might suppress CADM1 expression by recruiting EZH2 to its promoter. RIP assays determined that LNMAT1 could directly bind with EZH2 in MM cells (**Figure 3E**, $P < 0.05$). Chip-qPCR assays further revealed that LNMAT1 depletion decreased EZH2 binding and H3K27me3 modification in the CADM1 promoter (**Figures 3F,G**; $P < 0.05$). These results indicated that LNMAT1 suppressed CADM1 expression by recruiting EZH2 to its promoter and inducing the modification of histone methylation to mediate epigenetic silencing.

CADM1 Mediates the Function of LNMAT1 in MM Cells

Lastly, we performed rescue experiments to further identify whether LNMAT1 promoted the invasion-metastasis cascade by inhibiting CADM1 expression. Overall, qRT-PCR (**Figures 4A,B**; all $P<0.05$), wound healing (**Figures 4C,D**; all $P < 0.05$), and transwell assays (Migration: **Figures 4E,F**, invasion: **Figures 4G,H**; all $P < 0.05$) demonstrated that silencing CADM1 expression could partly rescue the inhibitory effects on cell migration and invasion induced by LNMAT1 depletion in MM cells. These results indicated that CADM1 mediates the function of LNMAT1 in MM.

DISCUSSION

LncRNAs have been identified as crucial regulators and biomarkers in multiple cancers, including MM, and LNMAT1 has been confirmed as an oncogenic lncRNA in various cancers. In non-small-cell lung cancer and cholangiocarcinoma, LNMAT1 could function as a competitive endogenous RNA (ceRNA) and promote cell proliferation and migration by sponging miR-5095 (21, 22). In colorectal cancer, LNMAT1 promoted liver metastasis and tumorigenesis and activated the PI3K/AKT cascade by competitively binding with miR-26a (23). In esophageal squamous cell carcinoma, LNMAT1

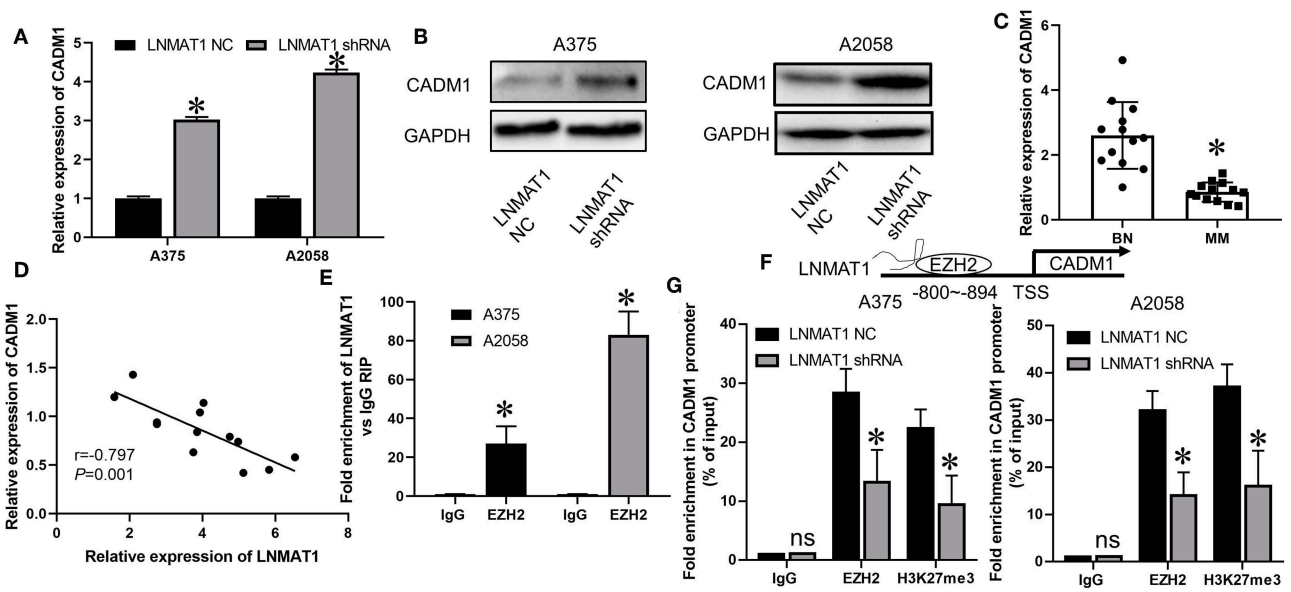

FIGURE 3 | LNMAT1 epigenetically suppresses CADM1 expression by recruiting EZH2 to its promoter. **(A,B)** The mRNA **(A)** and protein **(B)** levels of CADM1 in response to LNMAT1 silencing were detected in MM cells by qRT-PCR and WB; **(C)** The relative expression of CADM1 was detected in BN and MM tissues of by qRT-PCR; **(D)** Correlations between CADM1 and LNMAT1 expression in MM tissues; **(E)** RIP with anti-EZH2 and IgG from extracts of MM cells infected with LNMAT1 NC or shRNA and qRT-PCR were performed to confirm the interactions between LNMAT1 and EZH2/IgG; **(F)** Schematic diagram showing mechanism of LNMAT1 at the EZH2 binding site on LNMAT1 gene promoters. **(G)** ChiP-qPCR assays of MM cells infected with LNMAT1 NC or shRNA were performed to reveal the effects of LNMAT1 on EZH2 and H3K27me3 occupancy in the CADM1 promoter. Data are shown as the mean ± S.E. $^*P < 0.05$, ns: not significant. The representative results of three independent experiments are shown.

promoted cell proliferation and invasion by epigenetically suppressing KLF2 (14). In bladder cancer, LNMAT1 was found to be upregulated in patients with lymph node metastasis and was a potential lymphatic metastasis promoter. Mechanistic experiments confirmed that LNMAT1 upregulated CCL2 expression by interacting with hnRNPL and enhancing H3K4me3 modification (11). Consistent with these previous studies, we also identified that LNMAT1 plays a role in promoting metastasis in MM. We found that LNMAT1 was upregulated in MM tissues and cells compared to those of BN and melanocytes. Moreover, we also found that LNMAT1 expression was further upregulated in patients with lymph node metastasis and cells with highly metastatic potential. Lastly, we determined that silencing LNMAT1 inhibited cell migration and invasion in MM *in vitro* and *in vivo*. Combined with previous studies concerning the functions of LNMAT1, our study further confirmed that LNMAT1 plays an oncogenic role in carcinogenesis and cancer progression.

CADM1 expression is relatively lower in metastatic breast cancer (24) and lung adenocarcinoma (25) patients than in patients with non-invasive cancer. In MM, it was reported that CADM1 expression was significantly downregulated in melanoma tissues (19). Furthermore, CADM1 upregulation inhibited MM cell motility and invasiveness (18). It was also found that the expression levels of matrix metalloproteinase-2 (MMP-2) and matrix metalloproteinase-9 (MMP-9) were downregulated by CADM1 over-expression (18). As MMP-2 and MMP-9 are key regulators of extracellular matrix (ECM) degradation and tumor invasion (26), CADM1 is therefore a metastasis susceptibility gene and is involved in the invasion-metastasis cascade in MM. In the current study, we found that silencing LNMAT1 resulted in the inhibition of MMP-2 and MMP-9 expression. An increase in E-cadherin and decrease in N-cadherin were also found after silencing LNMAT1 in MM, indicating that LNMAT1 potentially plays an important role in EMT and the invasion-metastasis cascade in MM. As both LNMAT1 and CADM1 are key regulators of MMP expression and EMT and induced the invasion-metastasis cascade, we further investigated the relationships between CADM1 and LNMAT1 in MM. We found that LNMAT1 expression was inversely correlated with CADM1 in MM tissues and cells. In addition, LNMAT1 could suppress CADM1 expression by recruiting EZH2 to its promoter and induce modifications of histone methylation. Thus, we conclude that the metastasis-promoting role of LNMAT1 in MM is mediated by CADM1 suppression.

In conclusion, we revealed that LNAMT1 is a potential oncogene in MM. LNAMT1 was upregulated in MM tissues and cells with highly metastatic potential. Furthermore, LNAMT1 could promote the invasion-metastasis cascade of MM *in vivo* and *in vitro*. Studies on the underlying mechanism showed that LNAMT1 epigenetically suppressed CADM1 expression by recruiting EZH2 to its promoter, and silencing CADM1 expression rescued the inhibitory

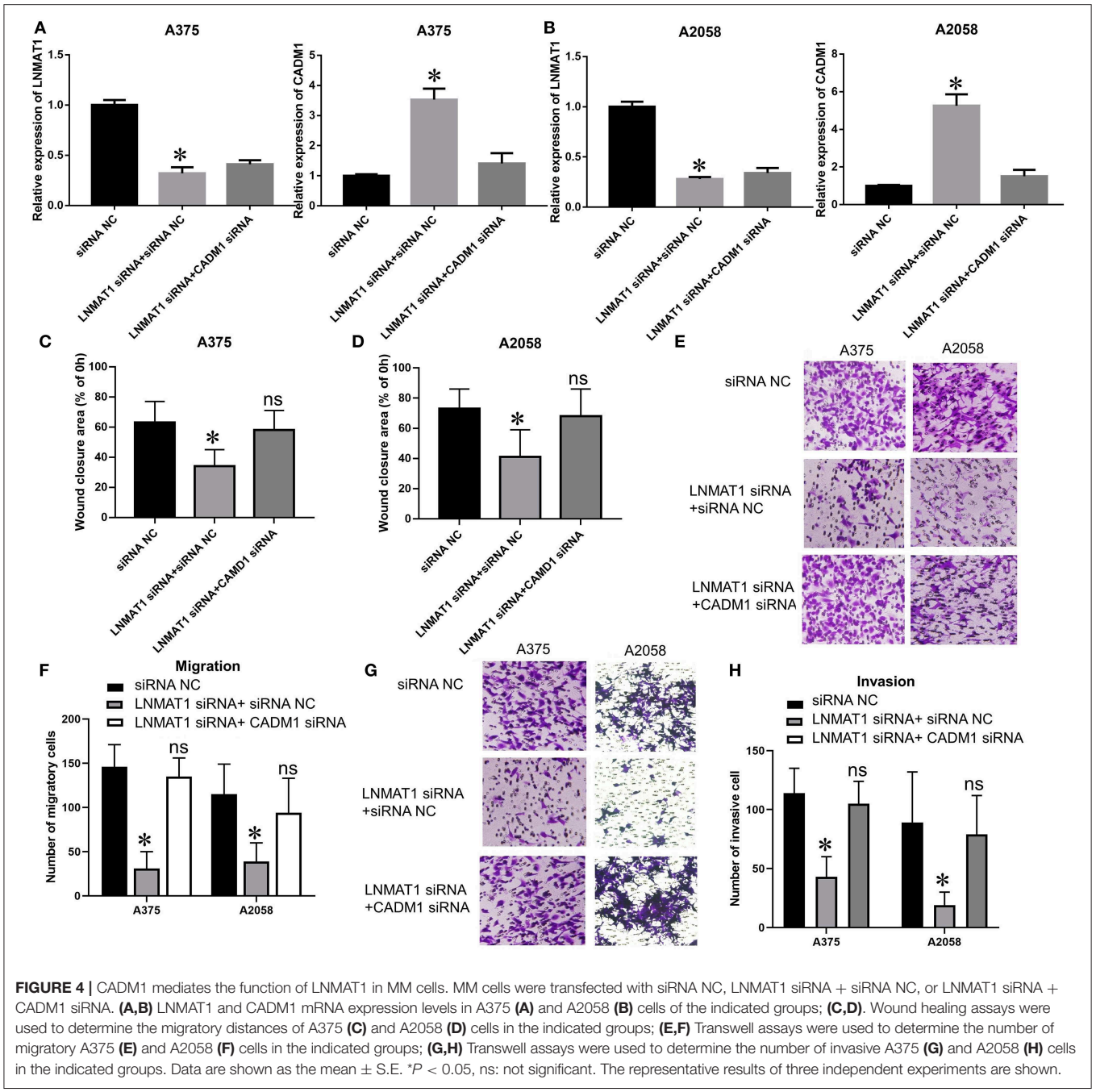

FIGURE 4 | CADM1 mediates the function of LNMAT1 in MM cells. MM cells were transfected with siRNA NC, LNMAT1 siRNA + siRNA NC, or LNMAT1 siRNA + CADM1 siRNA. **(A,B)** LNMAT1 and CADM1 mRNA expression levels in A375 **(A)** and A2058 **(B)** cells of the indicated groups; **(C,D)**. Wound healing assays were used to determine the migratory distances of A375 **(C)** and A2058 **(D)** cells in the indicated groups; **(E,F)** Transwell assays were used to determine the number of migratory A375 **(E)** and A2058 **(F)** cells in the indicated groups; **(G,H)** Transwell assays were used to determine the number of invasive A375 **(G)** and A2058 **(H)** cells in the indicated groups. Data are shown as the mean ± S.E. $^*P < 0.05$, ns: not significant. The representative results of three independent experiments are shown.

effects on MM cell migration and invasion induced by LNAMT1 depletion. Our study helps to reveal the regulatory mechanism of LNMAT1 and CADM1 in MM and may provide a novel target for MM treatment in the future.

DATA AVAILABILITY

All datasets generated for this study are included in the manuscript and/or the **Supplementary Files**.

ETHICS STATEMENT

This study was carried out in accordance with the recommendations of institutional guideline, Ethnical committee of the First Affiliated Hospital of Xi'an Jiaotong University. The protocol was approved by the Ethnical committee of the First Affiliated Hospital of Xi'an Jiaotong University. All subjects gave written informed consent in accordance with the Declaration of Helsinki. The animal experiments were carried out in accordance with the recommendations of institutional guideline, Animal Care and Use Committee of Xi'an Jiaotong University. The

protocol was approved by the Animal Care and Use Committee of Xi'an Jiaotong University.

AUTHOR CONTRIBUTIONS

KM, XZ, RG, and XM performed the research. LW designed the research study. YZ contributed essential reagents or tools. DH analyzed the data. LW wrote the paper. All authors have read and approved the final manuscript.

FUNDING

This work was supported by the National Natural Science Foundation of China (No. 81802935) and Foundation of the First Affiliated Hospital of Xi'an Jiaotong University (grant number: 2018MS-04).

ACKNOWLEDGMENTS

We would like to express our gratitude to Dr. Shengjia Shi (Department of Urology, Xijing Hospital, Airforce Military Medical University, China) for the generous help in ChIP assays, RIP assays and animal experiments.

SUPPLEMENTARY MATERIAL

The Supplementary Material for this article can be found online at: https://www.frontiersin.org/articles/10.3389/fonc.2019.00569/full#supplementary-material

REFERENCES

1. Siegel RL, Miller KD, Jemal A. Cancer statistics, 2019. *CA Cancer J Clin.* (2019) 69:7–34. doi: 10.3322/caac.21551
2. Zhou J, Jin B, Jin Y, Liu Y, Pan J. The antihelminthic drug niclosamide effectively inhibits the malignant phenotypes of uveal melanoma *in vitro* and *in vivo*. *Theranostics.* (2017) 7:1447–62. doi: 10.7150/thno.17451
3. Rozeman EA, Dekker TJA, Haanen J, Blank CU. Advanced melanoma: current treatment options, biomarkers, and future perspectives. *Am J Clin Dermatol.* (2018) 19:303–17. doi: 10.1007/s40257-017-0325-6
4. Maio M, Grob JJ, Aamdal S, Bondarenko I, Robert C, Thomas L, et al. Five-year survival rates for treatment-naive patients with advanced melanoma who received ipilimumab plus dacarbazine in a phase III trial. *J Clin Oncol.* (2015) 33:1191–6. doi: 10.1200/JCO.2014.56.6018
5. Richtig G, Ehall B, Richtig E, Aigelsreiter A, Gutschner T, Pichler M. Function and clinical implications of long non-coding RNAs in melanoma. *Int J Mol Sci.* (2017) 18:e715. doi: 10.3390/ijms18040715
6. Yu X, Zheng H, Tse G, Chan MT, Wu WK. Long non-coding RNAs in melanoma. *Cell Prolif.* (2018) 51:e12457. doi: 10.1111/cpr.12457
7. Weidle UH, Birzele F, Kollmorgen G, Ruger R. Long non-coding RNAs and their role in metastasis. *Cancer Genomics Proteomics.* (2017) 14:143–60. doi: 10.21873/cgp.20027
8. Lu Q, Zhao N, Zha G, Wang H, Tong Q, Xin S. LncRNA HOXA11-AS exerts oncogenic functions by repressing p21 and miR-124 in uveal melanoma. *DNA Cell Biol.* (2017) 36:837–44. doi: 10.1089/dna.2017.3808
9. Zhang H, Bai M, Zeng A, Si L, Yu N, Wang X. LncRNA HOXD-AS1 promotes melanoma cell proliferation and invasion by suppressing RUNX3 expression. *Am J Cancer Res.* (2017) 7:2526–35.
10. Yin Y, Zhao B, Li D, Yin G. Long non-coding RNA CASC15 promotes melanoma progression by epigenetically regulating PDCD4. *Cell Biosci.* (2018) 8:42. doi: 10.1186/s13578-018-0240-4
11. Chen C, He W, Huang J, Wang B, Li H, Cai Q, et al. LNMAT1 promotes lymphatic metastasis of bladder cancer via CCL2 dependent macrophage recruitment. *Nat Commun.* (2018) 9:3826. doi: 10.1038/s41467-018-06152-x
12. Wang X, Wang L, Gong Y, Liu Z, Qin Y, Chen J, et al. Long noncoding RNA LINC01296 promotes cancer-cell proliferation and metastasis in urothelial carcinoma of the bladder. *Onco Targets Ther.* (2019) 12:75–85. doi: 10.2147/OTT.S192809
13. Qin QH, Yin ZQ, Li Y, Wang BG, Zhang MF. Long intergenic noncoding RNA 01296 aggravates gastric cancer cells progress through miR-122/MMP-9. *Biomed Pharmacother.* (2018) 97:450–7. doi: 10.1016/j.biopha.2017.10.066
14. Wang L, Meng D, Wang Y, Hu J. Long non-coding RNA LINC01296 promotes esophageal squamous cell carcinoma cell proliferation and invasion by epigenetic suppression of KLF2. *Am J Cancer Res.* (2018) 8:2020–9.
15. Saito M, Goto A, Abe N, Saito K, Maeda D, Ohtake T, et al. Decreased expression of CADM1 and CADM4 are associated with advanced stage breast cancer. *Oncol Lett.* (2018) 15:2401–6. doi: 10.3892/ol.2017.7536
16. Qian JB, Liu HB, Zhu Y, Lu F, Yang QC, Shen Y. CADM1 mRNA expression and clinicopathological significance in esophageal squamous cell carcinoma tissue. *Genet Mol Res.* (2017) 16:gmr16029178. doi: 10.4238/gmr16029178
17. Zhang W, Xie HY, Ding SM, Xing CY, Chen A, Lai MC, et al. CADM1 regulates the G1/S transition and represses tumorigenicity through the Rb-E2F pathway in hepatocellular carcinoma. *HBPD INT.* (2016) 15:289–96. doi: 10.1016/S1499-3872(16)60099-1
18. You Y, Zhang J, Li Y, Li Y, Shi G, Ma L, et al. CADM1/TSLC1 inhibits melanoma cell line A375 invasion through the suppression of matrix metalloproteinases. *Mol Med Rep.* (2014) 10:2621–6. doi: 10.3892/mmr.2014.2556
19. Munhoz de Paula Alves Coelho K, Stall J, Fronza Junior H, Blasius R, de Franca PHC. Evaluation of expression of genes CADM1, TWIST1 and CDH1 by immunohistochemestry in melanocytic lesions. *Pathol Res Pract.* (2017) 213:1067–71. doi: 10.1016/j.prp.2017.07.028
20. Mou K, Liu B, Ding M, Mu X, Han D, Zhou Y, et al. lncRNA-ATB functions as a competing endogenous RNA to promote YAP1 by sponging miR-590-5p in malignant melanoma. *Int J Oncol.* (2018) 53:1094–104. doi: 10.3892/ijo.2018.4454
21. Zhang D, Li H, Xie J, Jiang D, Cao L, Yang X, et al. Long noncoding RNA LINC01296 promotes tumor growth and progression by sponging miR-5095 in human cholangiocarcinoma. *Int J Oncol.* (2018) 52:1777–86. doi: 10.3892/ijo.2018.4362
22. Hu X, Duan L, Liu H, Zhang L. Long noncoding RNA LINC01296 induces non-small cell lung cancer growth and progression through sponging miR-5095. *Am J Transl Res.* (2019) 11:895–903.
23. Liu B, Pan S, Xiao Y, Liu Q, Xu J, Jia L. LINC01296/miR-26a/GALNT3 axis contributes to colorectal cancer progression by regulating O-glycosylated MUC1 via PI3K/AKT pathway. *J Exp Clin Cancer Res.* (2018) 37:316. doi: 10.1186/s13046-018-0994-x

24. Wikman H, Westphal L, Schmid F, Pollari S, Kropidlowski J, Sielaff-Frimpong B, et al. Loss of CADM1 expression is associated with poor prognosis and brain metastasis in breast cancer patients. *Oncotarget.* (2014) 5:3076–87. doi: 10.18632/oncotarget.1832
25. Goto A, Niki T, Chi-Pin L, Matsubara D, Murakami Y, Funata N, et al. Loss of TSLC1 expression in lung adenocarcinoma: relationships with histological subtypes, sex and prognostic significance. *Cancer Sci.* (2005) 96:480–6. doi: 10.1111/j.1349-7006.2005.00075.x
26. Shay G, Lynch CC, Fingleton B. Moving targets: emerging roles for MMPs in cancer progression and metastasis. *Matrix Biol.* (2015) 44–6:200–6. doi: 10.1016/j.matbio.2015.01.019

Conflict of Interest Statement: The authors declare that the research was conducted in the absence of any commercial or financial relationships that could be construed as a potential conflict of interest.

frontiers in Oncology

REVIEW
published: 18 September 2019
doi: 10.3389/fonc.2019.00919

The Regulatory Role of Non-coding RNAs on Programmed Cell Death Four in Inflammation and Cancer

Mengxiang Zhao[1†], Nisha Zhu[1†], Fengyao Hao[1], Yuxian Song[1], Zhiyong Wang[2], Yanhong Ni[1*] and Liang Ding[1*]*

[1] *Central Laboratory Nanjing Stomatological Hospital, Medical School of Nanjing University, Nanjing, China,* [2] *Department of Oral and Maxillofacial Surgery, Nanjing Stomatological Hospital, Nanjing, China*

Programmed cell death 4 (PDCD4) is a tumor suppressor gene implicated in many cellular functions, including transcription, translation, apoptosis, and the modulation of different signal transduction pathways. The downstream mechanisms of PDCD4 have been well-discussed, but its upstream regulators have not been systematically summarized. Noncoding RNAs (ncRNAs) are gene transcripts with no protein-coding potential but play a pivotal role in the regulation of the pathogenesis of solid tumors, cardiac injury, and inflamed tissue. In recent studies, many ncRNAs, especially microRNAs (miRNAs) and long noncoding RNAs (lncRNAs), were found to interact with PDCD4 to manipulate its expression through transcriptional regulation and function as oncogenes or tumor suppressors. For example, miR-21, as a classic oncogene, was identified as the key regulator of PDCD4 by targeting its 3′-untranslated region (UTR) to promote tumor proliferation, migration, and invasion in colon, breast, and bladder carcinoma. Therefore, we reviewed the recently emerging pleiotropic regulation of PDCD4 by ncRNAs in cancer and inflammatory disorders and aimed to shed light on the mechanisms of associated diseases, which could be conducive to the development of novel treatment strategies for PDCD4-induced diseases.

Keywords: PDCD4, miRNA, lncRNA, cancer, inflammation

OPEN ACCESS

Edited by:
Deilson Elgui De Oliveira, São Paulo State University, Brazil

Reviewed by:
Hua Zhang, Guangdong Medical University, China
Giuseppe Palma, National Cancer Institute G. Pascale Foundation (IRCCS), Italy

****Correspondence:***
Liang Ding
879269339@qq.com
Yanhong Ni
niyanhong12@163.com
Zhiyong Wang
wangzhiyong67@163.com

† These authors have contributed equally to this work

Specialty section:
This article was submitted to Molecular and Cellular Oncology, a section of the journal Frontiers in Oncology

Received: *06 May 2019*
Accepted: *03 September 2019*
Published: *18 September 2019*

Citation:
Zhao M, Zhu N, Hao F, Song Y, Wang Z, Ni Y and Ding L (2019) The Regulatory Role of Non-coding RNAs on Programmed Cell Death Four in Inflammation and Cancer. Front. Oncol. 9:919. doi: 10.3389/fonc.2019.00919

INTRODUCTION

The Function and Structure of PDCD4

The main functions of Programmed cell death 4 (PDCD4)(NCBI GeneID: 27250) are reflected in the following two aspects. First, it acts as a suppressor in tumor progression; second, it is an inflammatory factor that participates in inflammation (1–3). An alteration in PDCD4 expression is pivotal to the pathogenesis of cancer and inflammation diseases. The expression of PDCD4 is downregulated in many kinds of human cancers, such as breast carcinoma, hepatocellular carcinoma, oral carcinoma, and ovarian cancer (4–7). The overexpression of PDCD4 induces apoptosis or cell cycle arrest, inhibits the invasion, proliferation and migration of cancer cells, and increases the sensitivity of cancer cells to antineoplastic drugs (8–11). In addition, knockdown of PDCD4 expression by an siRNA or shRNA stimulates invasion and migration in nasopharyngeal and lung cancer cells (12, 13). In brief, aberrant PDCD4 expression levels are associated with the progression of multiple diseases. Understanding the regulatory mechanisms of PDCD4 expression and targeting the homeostasis of PDCD4 is beneficial for related treatment. Thus, therapeutic strategies based on PDCD4 manipulation are promising treatments for cancer or inflammatory disorders.

The human gene *PDCD4* is located at human chromosome 10q24 (14). The PDCD4 protein was identified independently from different species, including humans, mice, and chickens. The deduced amino acid sequences are highly conserved among these species (15). *PDCD4* encodes a 469-amino acid peptide composed of two conserved alpha helical MA3 domains (amino acids 164–275 and 329–440). These two domains are also present in eukaryotic translation initiation factors, eIF4G I, and eIF4G II (16). A yeast two-hybrid assay (16), a mammalian two-hybrid assay and analyses of the PDCD4-eIF4A cocrystal structure revealed that PDCD4 interacts with eIF4A by its MA-3 domains, limits ribosomal recombination and protein synthesis and inhibits malignant behaviors (17). eIF4A1(NCBI GeneID: 1973) is an RNA helicase that catalyzes the unwinding of the secondary structure at the 5′-untranslated region (UTR) of mRNAs. PDCD4 binds to two molecules of eIF4A through its MA3 domains to inhibit translation initiation by preventing eIF4G from binding to eIF4A (18). The PDCD4 protein contains two nuclear export signals (NESs), suggesting that the protein might be able to shuttle between the nucleus and cytoplasm (19). The phosphorylation of PDCD4 by Akt and S6K1 at Ser67 and Ser457 causes the nuclear translocation of PDCD4, contributing to its ubiquitination via an E3 ligase β-transducin repeat-containing protein (β-TRCP) and subsequent proteasome-dependent degradation (20, 21). It has also been reported that PDCD4 binds to RNA through its two positively charged amino acid clusters, RBM1 and RBM2, at the N-terminal domain [(22); **Figure 1**].

DOWNSTREAM SIGNALS OF PDCD4

PDCD4 are reported to participate into the control of several cellular signaling pathways. PDCD4 interacts and inhibits eIF4A and activator protein 1 (AP-1)-dependent transcription in a concentration-dependent manner through many transcription factors, including JNK, MAP4K1, c-Myc, E-cadherin, β-catenin, and Snail. The overexpression of PDCD4 in mouse epidermal JB6 cells inhibits both basal and 12-O-tetradecanoylphorbol-13-acetate (TPA)-induced AP-1 transactivation through the inhibition of c-Jun activation (23). In colon tumor cells, PDCD4 regulates the expression of the JNK upstream kinase MAP4K1 by c-Myc, resulting in the activation of JNK and c-Jun, to control the activation of AP-1. A mutation in the c-Myc binding site of the MAP4K1 promoter could reduce MAP4K1 promoter activity, and the downregulation of c-Myc can restore MAP4K1 expression and the activation of AP1 in *PDCD4*-knockdown colon tumor GEO and HT29 cells (24). In addition, *PDCD4* knockdown suppresses E-cadherin expression through elevated protein levels of Snail, causing the activation of β-catenin-dependent transcription and stimulating the expression of c-Myc and urokinase-type plasminogen activator (u-PAR) (25). u-PAR is a 55–60 kDa glycosylated receptor for the degradation of extracellular matrix components by binding to its ligand and allowing human osteosarcoma cells to penetrate the basal membrane during invasion (26). Snail is a transcriptional repressor that binds to E-boxes on the E-cadherin promoter for transcription inhibition (27). The regulation of Snail by PDCD4 was demonstrated through Akt, and the knockdown of Akt abolishes *PDCD4* knockdown-induced Snail expression in colon cancer (28). Akt can also activate NF-κB to upregulate Snail (29). PDCD4 was also found to inhibit carbonic anhydrase type II (CAII) expression in HEK-293 (human embryonic kidney) cells. CAII is an important substrate for the synthesis of amino acids, lipids, and pyrimidine for tumor growth (30). In addition, PDCD4 could decrease CDK4/6 (cyclin-dependent kinase 4/6) via the upregulation of $p21^{Waf1/Cip1}$ and repress the CDK1 and cdc2 (cell division cycle 2) promoter in a neuroendocrine cell line, thus leading to reduced cell proliferation (31). By manipulating these pathways, PDCD4 ultimately inhibits cell survival, proliferation, and metastasis (**Figure 2**).

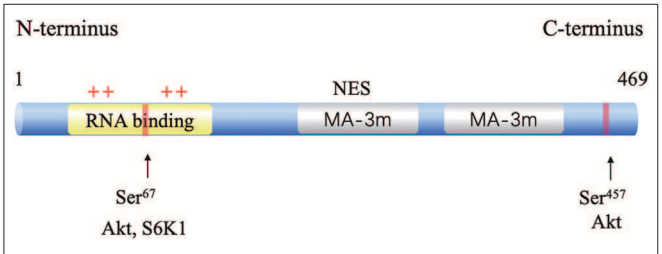

FIGURE 1 | Structure and functional sites of PDCD4. The two conserved MA-3 domains are in green, the phosphorylation sites are shown in red, and the RNA-binding site in blue.

NCRNAS AS UPSTREAM REGULATORS OF PDCD4

The downstream mechanisms of PDCD4 have been well-discussed, but its upstream regulators have not been systematically summarized. In recent years, most studies have focused on the regulation of PDCD4 expression by noncoding RNAs (ncRNAs). In the following review, we will emphasize the regulation of PDCD4 expression by ncRNAs, which should provide a reference for upcoming clinical and laboratory studies on PDCD4 regulation.

Recent reports have revealed that ncRNAs contribute to the regulation of PDCD4 expression and function. ncRNAs are RNA molecules that cannot code proteins and were found to engage in the regulation of multiple cellular activities, including proliferation, differentiation, apoptosis, stress, and immune responses (32–36). ncRNAs consist of microRNAs (miRNAs), long noncoding RNAs (lncRNAs) and circular RNAs (circRNAs), which regulate specific gene expression through regulating transcriptional, posttranscriptional, and posttranslational processes. miRNA are 20–25 nucleotides in length, and mature miRNAs usually bind to the 3′-UTR of their target mRNAs through their seed sequences to cause the degradation of target mRNAs and to block translational protein synthesis. The seed sequence is usually located 2–7 nucleotides from the 5′-end of the miRNA and is complementary to a site in the 3′-UTR of its target mRNA (37). LncRNAs have

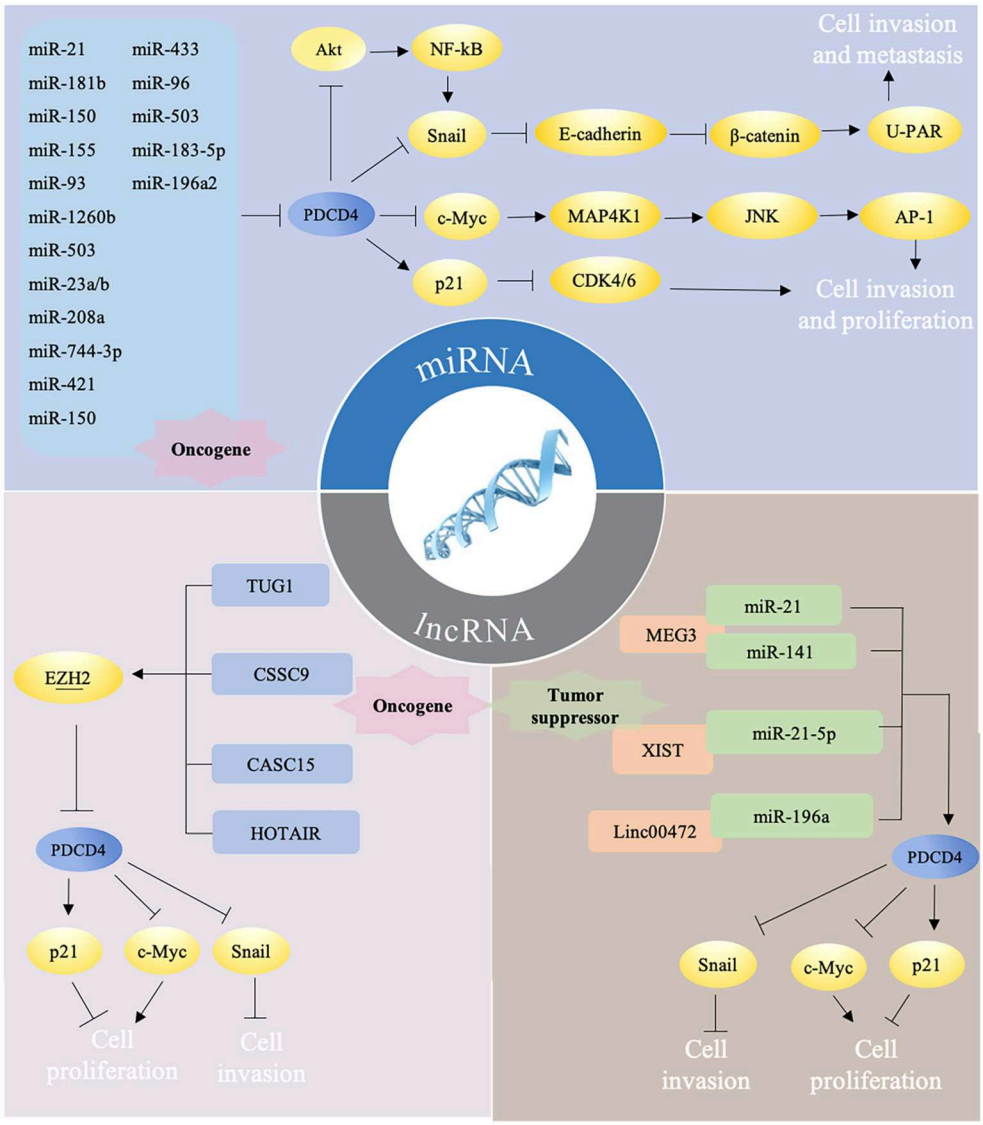

FIGURE 2 | Different ncRNAs regulate PDCD4 in mutiple ways. (i) miRNAs target PDCD4 directly to promote tumor progression via several pathways. Briefly, PDCD4 reduces the expression of Snail directly or by NF-κB/Akt pathway and leads to up-regulation of E-cadherin, inhibition of β-catenin dependent transcription, and decrease of the expression of c-Myc and uPAR. Down-regulated c-Myc subsequently inhibits MAP4K1 expression, thereby inhibiting AP-1 transcription to impede proliferation, promotion, and invasion. PDCD4 could decrease CDK4/6 via the upregulation of p21, thus leading to reduced cell proliferation. (ii) LncRNAs could function as oncogene and downregulate PDCD4 expression by recruiting EZH2. (iii) LncRNAs could also function as tumor suprefessor to sponge miRNAs, which may counteract the effects of miRNAs on PDCD4.

more than 200 nucleotides in length with little protein-coding potential, which have been defined to regulate gene expression by transcriptional regulation, genetic imprinting, chromatin remodeling, posttranscriptional regulation, and translational regulation (38). In recent years, ncRNAs have been demonstrated to manipulate the availability of PDCD4 via different ways (**Figure 2**), including directly targeting the 3′-UTR of PDCD4 by a miRNA or epigenetic modification and miRNA sponging on PDCD4 by a lncRNA. ncRNAs, including miRNAs and lncRNAs, are key regulators of PDCD4 dosage, and delicately modulate PDCD4 expression (**Table 1**).

MIRNA-REGULATED PDCD4 PROMOTES TUMOR PROGRESSION

Most recent studies of PDCD4 have focused on miRNAs, and now we will focus on regulatory mechanisms in tumors. More than 30 miRNAs were reported to be direct negative regulators of PDCD4, and many of them showed enhanced expression in tumors (40, 60). Furthermore, bioinformatics analyses predict that more than 80 miRNAs potentially target PDCD4, implying an essential role for miRNAs in regulating PDCD4 expression (61). These miRNAs downregulate PDCD4 levels and function

TABLE 1 | The summary of ncRNA that regulate PDCD4 in different cancers and inflammatory disorders.

Cancer	ncRNA	Functional responses and targets	References
Laryngeal cancer	miR-503	miR-503 inhibits apoptosis by directly targeting PDCD4	(39)
	miR-744-3p	miR-744-3p regulates PDCD4 to reduce AKT and NF-κB activation as well as MMP-9 expression	(40)
Gastric cancer	miR-23a/b	miR-23a/b promotes tumor growth and suppress apoptosis by targeting PDCD4	(41)
	miR-208a-3p	miR-208a-3p suppresses cell apoptosis by targeting PDCD4	(42)
	miR-93	miR-93 functions as an oncomiR for the downregulation of PDCD4	(43)
	miR-196a2	miR-196a2 inhibits apoptosis by directly targeting PDCD4	(44)
Colorectal cancer	miR-1260b	miR-1260b inhibitor enhances the chemosensitivity 5-FU due to downregulation of PDCD4	(45)
	miR-181b	Activation of IL-6/STAT3 suppressed PDCD4 by upregulating miR-181b	(46)
Cervical cancer	miR-150	miR-150 functions as a tumor promoter in reducing chemosensitivity and promoting invasiveness via targeting PDCD4	(47)
Breast cancer	miR-421	PDCD4 is a direct target gene of miR-421	(10)
	miR-183-5p	Inhibition of miR-183-5p could repress the progression of breast cancer through restoring PDCD4 levels	(48)
Melanoma	CASC15	CASC15 acts as an oncogene by negatively regulating PDCD4 expression via recruiting EZH2 and subsequently increasing H3K27me3 level	(49)
	miR-150	Knockdown of miR-150 enhanced cell apoptosis via direct targeting of PDCD4	(50)
Osteosarcoma	miR-433	miR-433 suppresses the expression of PDCD4	(51)
Lung cancer	miR-155	miR-155 exerts an onco- genic role in NSCLC by directly targeting PDCD4	(52)
Liver cancer	miR-93	miR-93 dramatically promoted HCC invasion and metastasis by EMT via targeting PDCD4	(53)
Glioblastoma	miR-503	microRNA-503 increases proliferation of glioblastoma cells and inhibits apoptosis by directly targeting PDCD4	(54)
Osteosarcoma	XIST/ miR-21-5p	lncRNA-XIST acts as a miRNA sponge, impedes miR-21-5p to maintain the expression of PDCD4	(55)
Colorectal cancer	Linc00472/ miR-196a	Linc00472 suppressed proliferation and induced apoptosis through up-regulating PDCD4 by decoying miR-196a	(56)
Esophageal carcinoma	TUG1	TUG1 suppressed PDCD4 expression by recruiting EZH2 to the promoter region of PDCD4 and increasing H3K27me3 level in ESCC cells	(57)
	CASC9	lncRNA CASC9 functions as an oncogene by negatively regulating PDCD4 expression through recruiting EZH2 and subsequently altering H3K27me3 level	(58)
Glioma	HOTAIR	Suppression of PDCD4 mediated by HOTAIR inhibits glioma cell proliferation and invasion in a PRC2-dependent manner	(59)

by binding to the 3′-UTR of *PDCD4* mRNA. Among these miRNAs, studies conducted on miR-21(NCBI GeneID: 406991) are the most extensive. The human gene miR-21 was one of the first identified mammalian miRNAs and is located at chromosome 17q23.2 within the highly conserved gene encoding TMEM49 (62). Through early lineage tracing studies, miR-21 was found to be upregulated in various diseases, such as oropharyngeal cancer (63) and salivary adenoid cystic carcinoma (64). Asangani et al. performed a bioinformatic search and uncovered a potentially conserved site for miR-21 within the 3′-UTR of *PDCD4* mRNA and demonstrated that miR-21 inhibited PDCD4 levels to reduce the ability of invasion, intravasation and metastasis (65). miR-21 is associated with therapeutic outcome and poor survival in malignant cancer (66). For instance, miR-21 is overexpressed in salivary adenoid cystic carcinoma (SACC) cells, and the suppression of miR-21 with a miR-21 inhibitor in SACC cells could increase the activity of the PDCD4 promoter and the expression of PDCD4 protein, suppress p-STAT3 protein expression, through further feedback, reduce miR-21 expression, and finally lead to the inhibition of cell invasion and migration (64). Moreover, further recent studies confirmed the regulation of PDCD4 by miR-21 in colon, breast, and bladder carcinoma (67).

In colorectal cancer (CRC) cells, activated IL-6/STAT3 signals increased the expression of miR-181, which leaded to downregulating the expression of PDCD4 and promoting cell proliferation and metastasis and inhibit the apoptosis of CRC cells (46). In cervical cancer, overexpressed miR-150 can also promote the proliferation, migration and invasion of cervical cancer cells *in vitro* by directly targeting the expression of PDCD4 (47). miR-155(NCBI GeneID: 406947) decreases PDCD4 levels by binding to the 3′-UTR of PDCD4. PDCD4 is a functional target of miR-155 and regulates proliferation or invasion by targeting PDCD4 in non-small-cell lung cancer (52). In human hepatocellular carcinoma (HCC), the downregulation of PDCD4 by miR-93 (NCBI GeneID: 407050) promotes HCC cell migration and invasion via the epithelial-mesenchymal transition (EMT) pathway (68). In laryngeal squamous cell carcinoma, miR-744-3p (NCBI GeneID: 100126313) could activate the MMP-9 regulatory axis by provoking the signaling pathway controlled by NF-κB p65 by suppressing PDCD4 (40). The inhibition of

miR-1260b induces a decrease in PDCD4 expression, as well as phosphorylated Akt (p-Akt) and phosphorylated extracellular signal-regulated kinase (p-ERK) (45). In glioblastoma, miRNA-503 (NCBI GeneID: 574506), induced by TGF-α1, inhibits apoptosis and increases the proliferation of glioblastoma cells by directly targeting PDCD4 (54). miR-421 (NCBI GeneID: 693122) regulates the proliferation, migration, invasion and apoptosis of breast cancer cells, including MCF-7 and MDA-MB-231 cells, by targeting PDCD4 (10). miR-433 (NCBI GeneID: 574034) is significantly overexpressed in osteosarcoma tissues and cell lines. The transfection of miR-433 mimics into osteosarcoma cell lines could decrease apoptosis by PDCD4. In contrast, the inhibition of miR-433 enhanced the apoptosis of tumor cells (51). Similarly, miR-23a/b (NCBI GeneID: 407010) (41), miR-208a-3p (NCBI GeneID: 406990) (42), miR-150 (NCBI GeneID: 406942)(47), miR-96 (NCBI GeneID: 407053) (69), miR-503 (NCBI GeneID: 574506) (39), miRNA-183-5p (NCBI GeneID: 406959) (48), and miR-196 (NCBI GeneID: 406972) also decrease protein levels by binding to the 3′-UTR of PDCD4 (44).

MIRNA-MEDIATED PDCD4 DOWNREGULATION PROTECTS AGAINST INFLAMMATION

In addition to carcinogenesis, the regulation of PDCD4 by miRNAs also plays an important role in various inflammatory responses. Das et al. demonstrated that the miR-21/PDCD4 axis plays a key role in the process of turning on an anti-inflammatory phenotype in efferocytosis-the digestion and elimination of dead or dying cells by phagocytes. Elevated miR-21 in LPS-activated macrophages promotes efferocytosis and silences the target gene PDCD4, which in turn results in the elevated production of anti-inflammatory IL-10 and accounts for a net anti-inflammatory phenotype (70). The miR-21/PDCD4 axis also regulates mesenchymal stem cells (MSCs) to secrete stanniocalcin 1 (STC1) and other neuroprotective factors to inhibit retinal ganglion cell (RGC) apoptosis and microglial activation and promote RGC survival in a mouse model of acute glaucoma (71). The increased miR-21 expression level following spinal cord injury (SCI) may enhance neurite outgrowth to promote the repair of injured spinal cords by inhibiting the expression of PDCD4 (72). miR-16 targets and inhibits PDCD4 expression in atherosclerosis to suppress the activation of inflammatory macrophages through mitogen-activated protein kinase (MAPK) and NF-κB signaling, and suppresse the expression of proinflammatory factors, including interleukin (IL)-6 and tumor necrosis factor-α (TNF-α), whereas it enhanced the expression of the anti-inflammatory factor IL-10. Thus, the miR-16-PDCD4 axis suppresses the activation of inflammatory macrophages in atherosclerosis (73). In another study, the overexpression of miR-499 (NCBI GeneID: 574501) protected cardiomyocytes against LPS-induced apoptosis by inhibiting PDCD4. However, the experiment was performed in rats, and the experimental results may not be directly extrapolated to humans (74). Increased miRNA expression has also been reported in diseases caused by inflammation, including colitis and atherosclerosis. In these cases, triggering a regulatory response through miRNA would be beneficial. These findings suggest that the regulation of PDCD4 by miRNAs, in addition to its negative effects on tumors, can also play a positive role in other diseases.

LNCRNAS ACT AS ONCOGENES TO REGULATE PDCD4 BY EPIGENETIC MODIFICATION

LncRNAs have also been identified as critical regulators in a variety of cancer types [4], including epigenetic modification, transcriptional regulation, RNA decay, and miRNA sponging. Bioinformatic analysis revealed that the promoter region of PDCD4 was enriched in the repressive marker histone H3 lysine 27 trimethylation (H3 K27me3) and enhancer of zeste homolog 2 (EZH2) binding sites, demonstrating that PDCD4 expression is under the regulation of epigenetic modification (58). EZH2, an important catalytic subunit of polycomb repressive complex 2 (PRC2), is a histone methyltransferase that epigenetically represses target gene expression by promoting H3 K27me3 (57). Cancer susceptibility candidate 15 (CASC15) (NCBI GeneID: 401237), also named linc00340, is located on chromosome 6p22.3 and was initially identified as a highly active lncRNA (75). The expression of CASC15 is upregulated in melanoma, hepatocellular carcinoma and gastric cancer. It acts as an oncogene in cancer progression and phenotype switching. In melanoma, CASC15 may recruit EZH2, and EZH2 could subsequently directly bind to the promoter of PDCD4 in melanoma cells and inhibit PDCD4 expression (49). Wu et al. found that CASC9 (NCBI GeneID: 101805492) knockdown decreased the enrichment of EZH2 and H3K27me3 in the PDCD4 promoter region, which resulted in the upregulation of PDCD4 (58). Downregulation of the lncRNA HOTAIR (NCBI GeneID: 100124700) was demonstrated to activate the expression of PDCD4 at the transcriptional level in glioma stem cells by reducing the recruitment of downstream molecules, including EZH2 and LSD1 (76). The lncRNA taurine upregulated gene 1 (TUG1) (NCBI GeneID: 55000) was also demonstrated to suppress PDCD4 by recruiting EZH2 in esophageal squamous cell carcinoma (ESCC) through epigenetic modification (57, 59).

LNCRNAS ACT AS TUMOR SUPPRESSORS TO REGULATE PDCD4 THROUGH MIRNA SPONGING

The regulation of PDCD4 by lncRNAs is also promoted by another mechanism by which the dysregulated lncRNAs could sponge special miRNAs to suppress their target genes, such as PDCD4, through a competing endogenous RNA (ceRNA) mechanism. The ceRNA hypothesis accounts for the fact that specific RNAs are able to attenuate miRNA activity through sequestration and elevate miRNA target gene expression. The hypothesis potentially accounts for the function of a substantial proportion of the thousands of yet uncharacterized lncRNAs (77). LncRNAs block the effects of miRNAs via the competition

for the seed sites of miRNAs with their target mRNAs. For instance, the lncRNA maternally expressed gene 3 (MEG3) (NCBI GeneID: 55384) is located at chromosome 14q32 and could enhance the sensitivity of colorectal cancer (CRC) cells to oxaliplatin via the upregulation of PDCD4 by sponging miR-141 and overcoming oxaliplatin resistance in CRC (78). In addition to its role in cancer, MEG3 also functions as a ceRNA for miR-21 to regulate PDCD4 expression in ischemic neuronal death followed by reperfusion (79). The lncRNA growth arrest-specific transcript 5 (GAS5) (NCBI GeneID: 60674) is downregulated in several kinds of cancers, including cervical cancer and breast cancer, and HCC tissues. The knockdown of GAS5 leads to the repression of cell viability. GAS5 as a ceRNA competes with PDCD4 to bind to miR-21, and the depletion or overexpression of GAS5 could lead to the downregulation or upregulation of PDCD4 levels in tumor cells. In HCCs, GAS5 acts as a tumor suppressor through the negative regulation of miR-21 and its target PDCD4 to suppress the migration and invasion of cancer cells (80). Similarly, GAS5 deficiency by siGAS5 also reduced miR-21 target protein PDCD4 expression in cervical cancer cells. The malignant behaviors of cervical cancer cells, manifested by cell migration and invasion, were enhanced by siGAS5 (81). Linc00472 (NCBI GeneID: 79940) is downregulated in CRC tissues and cells, and it acts as a tumor suppressor by upregulating PDCD4 by sponging miR-196a (56). miR-93-5p, a direct target of linc00472, directly targets PDCD4. The miR-93-5p/PDCD4 pathway mediated the suppressive role of linc00472 in HCC cells (82). The lncRNA DGCR5 and miR-320a regulate each other in a reciprocal manner, and DGCR5 could reverse the inhibition of PDCD4 by miR-320a, which is involved in the regulation of the pancreatic ductal adenocarcinoma cell phenotype (83). The expression of the lncRNA NBAT1 is downregulated in osteosarcoma tissues and cell lines. NBAT1 (NCBI GeneID: 729177) functions as a ceRNA against miR-21 to increase the expression of the miR-21 target gene PDCD4 and then suppresses osteosarcoma growth and metastasis *in vitro* and *in vivo* (84). Similarly, the lncRNA XIST inhibits cell growth and mobility by competitively binding to miR-21-5p for PDCD4 up-regulation in osteosarcoma (55).

These findings show that PDCD4 expression and activity are controlled by the network of ncRNAs, and the dysregulation of these ncRNAs can contribute to changes in PDCD4 function in various diseases.

TARGETING THE NCRNA/PDCD4 SIGNALING PATHWAY: THERAPEUTIC APPLICATIONS

Since drug resistance commonly occurs in cancer patients, it is critical to develop alternative therapeutic strategies to resensitize resistant cancer cells and patient-derived models (PDX) (85, 86). Recently, published studies have demonstrated that the miRNA/PDCD4 axis could modulate chemosensitivity in resistant cancers. Treatment with a combination of drugs and miRNA inhibitors is a viable strategy for enhancing chemosensitivity though their synergistic effects. PDCD4 can downregulate the 5-fluorouracil (5-FU) resistance induced by miR-21 in pancreatic cancer cells and rescue the phenotypic characteristics disrupted by miR-21 (87). The role of miR-21/PDCD4 in drug resistance also concerns gemcitabine resistance in breast cancer, glioblastoma cancer, and pancreatic cancer.

In addition to affecting the resistance of cancer cells, there are also some drugs that can directly regulate the level of miRNA/PDCD4, thus serving as a potential therapeutic application. Treatment with isoalantolactone remarkably increased the expression of PDCD4 via the downregulation of miR-21, which exerts anticancer effects against esophageal squamous cell carcinoma (88). Quercetin is a kind of flavonoid that was reported to inhibit both acute and chronic Cr(VI)-induced miR-21 elevation and PDCD4 reduction in human bronchial epithelial cells. Besides, the Cr(VI)-induced binding of miR-21 to the 3′-UTR of PDCD4 was reduced by treatment with quercetin (89). It has been demonstrated that curcumin can inhibit tumor proliferation, invasion and metastasis by inhibiting the miR-21 transcription to stabilize the PDCD4 expression in CRC (90). In addition, the long intergenic noncoding RNA 152 (linc00152) was upregulated and promoted tumor progression and conferred oxaliplatin resistance in colon cancer by functioning as a ceRNA to release erb-b2 receptor tyrosine kinase 4 (ERBB4) by sponging miR-193a-3p (91).

The abovementioned evidence illustrates that targeting these transcription factors through small molecule drugs that regulate miRNA/PDCD4 expression may be effective in treating cancers.

CONCLUSIONS

We here summarize the roles of miRNAs and lncRNAs in PDCD4 regulation. Recent studies have demonstrated that ncRNAs interact with PDCD4 at the transcriptional and posttranscriptional levels. Several miRNAs directly target PDCD4 to repress the PDCD4 protein level and function, which promotes tumorigenesis. Then, the miRNA/PDCD4 axis could exert a protective effect in inflammation by downregulating miRNA levels. lncRNAs have been reported to regulate PDCD4 in multiple ways. By epigenetic modification, a lncRNA could down-regulate PDCD4 expression by recruiting EZH2 to its promoter region and increasing the H3K27me3 enrichment of its promoter. In addition, as a miRNA sponge, lncRNAs also counteract the effects of miRNAs on their target mRNAs. The regulation of miRNAs by ceRNAs has added a new layer of complexity to PDCD4 regulation by miRNAs. However, there is also controversy about the ceRNA hypothesis. The essence of the doubt against the ceRNA hypothesis is that any change in the expression of an individual miRNA target would constitute only a small fraction of the target site abundance (77), implicating that physiological changes of one individual lncRNA might be insufficient to suppress miRNA activity.

DISCUSSION

The abovementioned studies deepen our understanding of the diverse roles of the ncRNA/PDCD4 pathway in inflammation and cancer. An urgent issue for clinicians is whether the ncRNA/PDCD4 pathway can be used as a potential target for therapeutic intervention; however, related clinical studies are lacking. Interestingly, miRNAs targeting PDCD4, including miR-21 and miR-23, have been tested in clinical trials via liposomes or other strategies for the treatment of inflammatory diseases and cancer (92). For example, treatment with anti-miR-21 oligonucleotides reduced breast cancer MCF-7 xenograft growth (93); therefore, PDCD4 might also be a new therapeutic target for cancer. However, based on the dual role of the ncRNA/PDCD4 pathway in tumor and inflammatory diseases, research on anticancer interventions must ensure that targeting ncRNA/PDCD4 would not render the side effects that induce an inflammatory response, such as endothelial inflammatory damage through the NF-κB/TNF-α signaling pathway (1). Since certain elevated levels of miRNAs and lncRNAs may also contribute to cancer promotion, more consideration should be taken in targeting of the ncRNA/PDCD4 pathway during the treatment of inflammatory diseases. Further dissection of ncRNAs in the PDCD4 pathway at the molecular and cellular levels will provide insights into the underlying mechanisms of PDCD4 in tumor suppression and devise novel avenues in drug development against cancer and other PDCD4-associated diseases.

AUTHOR CONTRIBUTIONS

MZ, NZ, FH, YS, ZW, YN, and LD collected the related paper and drafted the manuscript. MZ, NZ, ZW, YN, and LD participated in the design of the review and draft the manuscript. All authors read and approved the final manuscript.

FUNDING

This study was supported by National Natural Science Foundation of China (Nos. 81902754 to LD, 81702680 to YS, and 81772880 to YN). China Postdoctoral Science Foundation (No. 2019M651789 to LD). Nanjing Medical Science and Technology Development Foundation, Nanjing Department of Health (Nos. YKK17138 to YS and ZKX17032 to ZW). Jiangsu Key Research & Development Program (No. BE2018618 to ZW). Fundamental Research Funds for the Central Universities (No. 021014380117 to LD).

REFERENCES

1. Zhang YH, He K, Shi G. Effects of MicroRNA-499 on the inflammatory damage of endothelial cells during coronary artery disease via the targeting of PDCD4 through the NF-Kappabeta/TNF-alpha signaling pathway. *Cell Physiol Biochem*. (2017) 44:110–24. doi: 10.1159/000484588
2. Yang Z, Tang Y, Zhao Q, Lu H, Xu G. Down-regulation of microRNA-23b aggravates LPS-induced inflammatory injury in chondrogenic ATDC5 cells by targeting PDCD4. *Iranian J Basic Med Sci*. (2018) 21:529–35. doi: 10.22038/IJBMS.2018.25856.6364
3. Wang L, Jiang Y, Song X, Guo C, Zhu F, Wang X, et al. Pdcd4 deficiency enhances macrophage lipoautophagy and attenuates foam cell formation and atherosclerosis in mice. *Cell Death Dis*. (2016) 7:e2055. doi: 10.1038/cddis.2015.416
4. Chen Z, Yuan YC, Wang Y, Liu Z, Chan HJ, Chen S. Down-regulation of programmed cell death 4 (PDCD4) is associated with aromatase inhibitor resistance and a poor prognosis in estrogen receptor-positive breast cancer. *Breast Cancer Res Treat*. (2015) 152:29–39. doi: 10.1007/s10549-015-3446-8
5. Wei ZT, Zhang X, Wang XY, Gao F, Zhou CJ, Zhu FL, et al. PDCD4 inhibits the malignant phenotype of ovarian cancer cells. *Cancer Sci*. (2009) 100:1408–13. doi: 10.1111/j.1349-7006.2009.01210.x
6. Zhang H, Ozaki I, Mizuta T, Hamajima H, Yasutake T, Eguchi Y, et al. Involvement of programmed cell death 4 in transforming growth factor-beta1-induced apoptosis in human hepatocellular carcinoma. *Oncogene*. (2006) 25:6101–12. doi: 10.1038/sj.onc.1209634
7. Reis PP, Tomenson M, Cervigne NK, Machado J, Jurisica I, Pintilie M, et al. Programmed cell death 4 loss increases tumor cell invasion and is regulated by miR-21 in oral squamous cell carcinoma. *Mol Cancer*. (2010) 9:238. doi: 10.1186/1476-4598-9-238
8. Jansen AP, Camalier CE, Stark C, Colburn NH. Characterization of programmed cell death 4 in multiple human cancers reveals a novel enhancer of drug sensitivity. *Mol Cancer Ther*. (2004) 3:103–10.
9. Jia LF, Wei SB, Gan YH, Guo Y, Gong K, Mitchelson K, et al. Expression, regulation and roles of miR-26a and MEG3 in tongue squamous cell carcinoma. *Int J Cancer*. (2014) 135:2282–93. doi: 10.1002/ijc.28667
10. Wang Y, Liu Z, Shen J. MicroRNA-421-targeted PDCD4 regulates breast cancer cell proliferation. *Int J Mol Med*. (2018) 43:267–75. doi: 10.3892/ijmm.2018.3932
11. Li Y, Wang X, Wang X, Wan L, Liu Y, Shi Y, et al. PDCD4 suppresses proliferation, migration, and invasion of endometrial cells by inhibiting autophagy and NF-kappaB/MMP2/MMP9 signal pathway. *Biol Reprod*. (2018) 99:360–72. doi: 10.1093/biolre/ioy052
12. Zhen Y, Fang W, Zhao M, Luo R, Liu Y, Fu Q, et al. miR-374a-CCND1-pPI3K/AKT-c-JUN feedback loop modulated by PDCD4 suppresses cell growth, metastasis, and sensitizes nasopharyngeal carcinoma to cisplatin. *Oncogene*. (2017) 36:275–85. doi: 10.1038/onc.2016.201
13. Jiang LP, He CY, Zhu ZT. Role of microRNA-21 in radiosensitivity in non-small cell lung cancer cells by targeting PDCD4 gene. *Oncotarget*. (2017) 8:23675–89. doi: 10.18632/oncotarget.15644
14. Soejima H, Miyoshi O, Yoshinaga H, Masaki Z, Ozaki I, Kajiwara S, et al. Assignment of the programmed cell death 4 gene (PDCD4) to human chromosome band 10q24 by *in situ* hybridization. *Cytogenet Cell Genet*. (1999) 87:113–4. doi: 10.1159/000015408
15. Lankat-Buttgereit B, Goke R. Programmed cell death protein 4 (pdcd4): a novel target for antineoplastic therapy? *Biol Cell*. (2003) 95:515–9. doi: 10.1016/j.biolcel.2003.09.003
16. Goke A, Goke R, Knolle A, Trusheim H, Schmidt H, Wilmen A, et al. DUG is a novel homologue of translation initiation factor 4G that binds eIF4A. *Biochem Biophys Res Commun*. (2002) 297:78–82. doi: 10.1016/S0006-291X(02)02129-0
17. Zakowicz H, Yang HS, Stark C, Wlodawer A, Laronde-Leblanc N, Colburn NH. Mutational analysis of the DEAD-box RNA helicase eIF4AII characterizes its interaction with transformation suppressor Pdcd4 and eIF4GI. *RNA*. (2005) 11:261–74. doi: 10.1261/rna.7191905
18. Lu WT, Wilczynska A, Smith E, Bushell M. The diverse roles of the eIF4A family: you are the company you keep. *Biochem Soc Trans*. (2014) 42:166–72. doi: 10.1042/BST20130161
19. Bohm M, Sawicka K, Siebrasse JP, Brehmer-Fastnacht A, Peters R, Klempnauer KH. The transformation suppressor protein Pdcd4 shuttles between nucleus and cytoplasm and binds RNA. *Oncogene*. (2003) 22:4905–10. doi: 10.1038/sj.onc.1206710

20. Palamarchuk A, Efanov A, Maximov V, Aqeilan RI, Croce CM, Pekarsky Y. Akt phosphorylates and regulates Pdcd4 tumor suppressor protein. *Cancer Res*. (2005) 65:11282–6. doi: 10.1158/0008-5472.CAN-05-3469
21. Dorrello NV, Peschiaroli A, Guardavaccaro D, Colburn NH, Sherman NE, Pagano M. S6K1- and betaTRCP-mediated degradation of PDCD4 promotes protein translation and cell growth. *Science*. (2006) 314:467–71. doi: 10.1126/science.1130276
22. Wedeken L, Ohnheiser J, Hirschi B, Wethkamp N, Klempnauer KH. Association of tumor suppressor protein Pdcd4 with ribosomes is mediated by protein-protein and protein-RNA interactions. *Genes Cancer*. (2010) 1:293–301. doi: 10.1177/1947601910364227
23. Yang HS, Knies JL, Stark C, Colburn NH. Pdcd4 suppresses tumor phenotype in JB6 cells by inhibiting AP-1 transactivation. *Oncogene*. (2003) 22:3712–20. doi: 10.1038/sj.onc.1206433
24. Wang Q, Zhang Y, Yang HS. Pdcd4 knockdown up-regulates MAP4K1 expression and activation of AP-1 dependent transcription through c-Myc. *Biochim Biophys Acta*. (2012) 1823:1807–14. doi: 10.1016/j.bbamcr.2012.07.004
25. Wang Q, Sun ZX, Allgayer H, Yang HS. Downregulation of E-cadherin is an essential event in activating beta-catenin/Tcf-dependent transcription and expression of its target genes in Pdcd4 knockdown cells. *Oncogene*. (2010) 29:128–38. doi: 10.1038/onc.2009.302
26. Kariko K, Kuo A, Boyd D, Okada SS, Cines DB, Barnathan ES. Overexpression of urokinase receptor increases matrix invasion without altering cell migration in a human osteosarcoma cell line. *Cancer Res*. (1993) 53:3109–17.
27. Cano A, Perez-Moreno MA, Rodrigo I, Locascio A, Blanco MJ, del Barrio MG, et al. The transcription factor snail controls epithelial-mesenchymal transitions by repressing E-cadherin expression. *Nat Cell Biol*. (2000) 2:76–83. doi: 10.1038/35000025
28. Wang Q, Zhu J, Wang YW, Dai Y, Wang YL, Wang C, et al. Tumor suppressor Pdcd4 attenuates Sin1 translation to inhibit invasion in colon carcinoma. *Oncogene*. (2017) 36:6225–34. doi: 10.1038/onc.2017.228
29. Gaubitz C, Prouteau M, Kusmider B, Loewith R. TORC2 structure and function. *Trends Biochem Sci*. (2016) 41:532–45. doi: 10.1016/j.tibs.2016.04.001
30. Lankat-Buttgereit B, Gregel C, Knolle A, Hasilik A, Arnold R, Goke R. Pdcd4 inhibits growth of tumor cells by suppression of carbonic anhydrase type II. *Mol Cell Endocrinol*. (2004) 214:149–53. doi: 10.1016/j.mce.2003.10.058
31. Goke R, Barth P, Schmidt A, Samans B, Lankat-Buttgereit B. Programmed cell death protein 4 suppresses CDK1/cdc2 via induction of p21(Waf1/Cip1). *Am J Physiol Cell Physiol*. (2004) 287:C1541–6. doi: 10.1152/ajpcell.00025.2004
32. Panda AC, Abdelmohsen K, Gorospe M. SASP regulation by noncoding RNA. *Mech Ageing Dev*. (2017) 168:37–43. doi: 10.1016/j.mad.2017.05.004
33. Qu S, Zeng C, Wang WE. Noncoding RNA and cardiomyocyte proliferation. *Stem Cells Int*. (2017) 2017:6825427. doi: 10.1155/2017/6825427
34. Ding L, Ren J, Zhang D, Li Y, Huang X, Hu Q, et al. A novel stromal lncRNA signature reprograms fibroblasts to promote the growth of oral squamous cell carcinoma via LncRNA-CAF/interleukin-33. *Carcinogenesis*. (2018) 39:397–406. doi: 10.1093/carcin/bgy006
35. Ding L, Ren J, Zhang D, Li Y, Huang X, Ji J, et al. The TLR3 agonist inhibit drug efflux and sequentially consolidates low-dose cisplatin-based chemoimmunotherapy while reducing side effects. *Mol Cancer Ther*. (2017) 16:1068–79. doi: 10.1158/1535-7163.MCT-16-0454
36. Liang D, Xiao-Feng H, Guan-Jun D, Er-Ling H, Sheng C, Ting-Ting W, et al. Activated STING enhances Tregs infiltration in the HPV-related carcinogenesis of tongue squamous cells via the c-jun/CCL22 signal. *Biochim Biophys Acta*. (2015) 1852:2494–503. doi: 10.1016/j.bbadis.2015.08.011
37. Bartel DP. MicroRNAs: target recognition and regulatory functions. *Cell*. (2009) 136:215–33. doi: 10.1016/j.cell.2009.01.002
38. Sun W, Yang Y, Xu C, Guo J. Regulatory mechanisms of long noncoding RNAs on gene expression in cancers. *Cancer Genet*. (2017) 216–217:105–10. doi: 10.1016/j.cancergen.2017.06.003
39. Shuang Y, Zhou X, Li C, Huang Y, Zhang L. MicroRNA503 serves an oncogenic role in laryngeal squamous cell carcinoma via targeting programmed cell death protein 4. *Mol Med Rep*. (2017) 16:5249–56. doi: 10.3892/mmr.2017.7278
40. Li JZ, Gao W, Lei WB, Zhao J, Chan JY, Wei WI, et al. MicroRNA 744–3p promotes MMP-9-mediated metastasis by simultaneously suppressing PDCD4 and PTEN in laryngeal squamous cell carcinoma. *Oncotarget*. (2016) 7:58218–33. doi: 10.18632/oncotarget.11280
41. Hu X, Wang Y, Liang H, Fan Q, Zhu R, Cui J, et al. miR-23a/b promote tumor growth and suppress apoptosis by targeting PDCD4 in gastric cancer. *Cell Death Dis*. (2017) 8:e3059. doi: 10.1038/cddis.2017.447
42. Yin K, Liu M, Zhang M, Wang F, Fen M, Liu Z, et al. miR-208a-3p suppresses cell apoptosis by targeting PDCD4 in gastric cancer. *Oncotarget*. (2016) 7:67321–32. doi: 10.18632/oncotarget.12006
43. Liang H, Wang F, Chu D, Zhang W, Liao Z, Fu Z, et al. miR-93 functions as an oncomiR for the downregulation of PDCD4 in gastric carcinoma. *Sci Rep*. (2016) 6:23772. doi: 10.1038/srep23772
44. Fawzy MS, Toraih EA, Ibrahiem A, Abdeldayem H, Mohamed AO, Abdel-Daim MM. Evaluation of miRNA-196a2 and apoptosis-related target genes: ANXA1, DFFA and PDCD4 expression in gastrointestinal cancer patients: a pilot study. *PLoS ONE*. (2017) 12:e0187310. doi: 10.1371/journal.pone.0187310
45. Zhao J, Cao J, Zhou L, Du Y, Zhang X, Yang B, et al. MiR-1260b inhibitor enhances the chemosensitivity of colorectal cancer cells to fluorouracil by targeting PDCD4/IGF1. *Oncol Lett*. (2018) 16:5131–9. doi: 10.3892/ol.2018.9307
46. Liu Y, Uzair Ur R, Guo Y, Liang H, Cheng R, Yang F, et al. miR-181b functions as an oncomiR in colorectal cancer by targeting PDCD4. *Protein Cell*. (2016) 7:722–34. doi: 10.1007/s13238-016-0313-2
47. Zhang Z, Wang J, Li J, Wang X, Song W. MicroRNA-150 promotes cell proliferation, migration, and invasion of cervical cancer through targeting PDCD4. *Biomed Pharmacother*. (2018) 97:511–7. doi: 10.1016/j.biopha.2017.09.143
48. Cheng Y, Xiang G, Meng Y, Dong R. MiRNA-183–5p promotes cell proliferation and inhibits apoptosis in human breast cancer by targeting the PDCD4. *Reprod Biol*. (2016) 16:225–33. doi: 10.1016/j.repbio.2016.07.002
49. Yin Y, Zhao B, Li D, Yin G. Long non-coding RNA CASC15 promotes melanoma progression by epigenetically regulating PDCD4. *Cell Biosci*. (2018) 8:42. doi: 10.1186/s13578-018-0240-4
50. Wan J, Yang J, Huang Y, Deng L. MicroRNA-150 inhibitors enhance cell apoptosis of melanoma by targeting PDCD4. *Oncol Lett*. (2018) 15:1475–82. doi: 10.3892/ol.2017.7445
51. Sun Y, Wang F, Wang L, Jiao Z, Fang J, Li J. MicroRNA-433 regulates apoptosis by targeting PDCD4 in human osteosarcoma cells. *Oncol Lett*. (2017) 14:2353–8. doi: 10.3892/ol.2017.6441
52. Liu F, Song D, Wu Y, Liu X, Zhu J, Tang Y. MiR-155 inhibits proliferation and invasion by directly targeting PDCD4 in non-small cell lung cancer. *Thoracic Cancer*. (2017) 8:613–9. doi: 10.1111/1759-7714.12492
53. Huang H, Wang X, Wang C, Zhuo L, Luo S, Han S. The miR-93 promotes proliferation by directly targeting PDCD4 in hepatocellular carcinoma. *Neoplasma*. (2017) 64:770–7. doi: 10.4149/neo_2017_516
54. Guo P, Yu Y, Li H, Zhang D, Gong A, Li S, et al. TGF-a1-induced miR-503 controls cell growth and apoptosis by targeting PDCD4 in glioblastoma cells. *Sci Rep*. (2017) 7:11569. doi: 10.1038/s41598-017-11885-8
55. Zhang R, Xia T. Long non-coding RNA XIST regulates PDCD4 expression by interacting with miR-21–5p and inhibits osteosarcoma cell growth and metastasis. *Int J Oncol*. (2017) 51:1460–70. doi: 10.3892/ijo.2017.4127
56. Ye Y, Yang S, Han Y, Sun J, Xv L, Wu L, et al. Linc00472 suppresses proliferation and promotes apoptosis through elevating PDCD4 expression by sponging miR-196a in colorectal cancer. *Aging*. (2018) 10:1523–33. doi: 10.18632/aging.101488
57. Xu C, Guo Y, Liu H, Chen G, Yan Y, Liu T. TUG1 confers cisplatin resistance in esophageal squamous cell carcinoma by epigenetically suppressing PDCD4 expression via EZH2. *Cell Biosci*. (2018) 8:61. doi: 10.1186/s13578-018-0260-0
58. Wu Y, Hu L, Liang Y, Li J, Wang K, Chen X, et al. Up-regulation of lncRNA CASC9 promotes esophageal squamous cell carcinoma growth by negatively regulating PDCD4 expression through EZH2. *Mol Cancer*. (2017) 16:150. doi: 10.1186/s12943-017-0715-7
59. Chen Y, Bian Y, Zhao S, Kong F, Li X. Suppression of PDCD4 mediated by the long non-coding RNA HOTAIR inhibits the proliferation and invasion of glioma cells. *Oncol Lett*. (2016) 12:5170–6. doi: 10.3892/ol.2016.5323
60. Zhao MY, Wang LM, Liu J, Huang X, Liu J, Zhang YF. MiR-21 suppresses anoikis through targeting PDCD4 and PTEN in

human esophageal adenocarcinoma. *Curr Med Sci*. (2018) 38:245–51. doi: 10.1007/s11596-018-1872-7
61. Dweep H, Sticht C, Pandey P, Gretz N. miRWalk–database: prediction of possible miRNA binding sites by "walking" the genes of three genomes. *J Biomed Informatics*. (2011) 44:839–47. doi: 10.1016/j.jbi.2011.05.002
62. Ge Y, Zhang L, Nikolova M, Reva B, Fuchs E. Strand-specific *in vivo* screen of cancer-associated miRNAs unveils a role for miR-21(*) in SCC progression. *Nat Cell Biol*. (2016) 18:111–21. doi: 10.1038/ncb3275
63. Zhang X, Gee H, Rose B, Lee CS, Clark J, Elliott M, et al. Regulation of the tumour suppressor PDCD4 by miR-499 and miR-21 in oropharyngeal cancers. *BMC Cancer*. (2016) 16:86. doi: 10.1186/s12885-016-2109-4
64. Jiang LH, Ge MH, Hou XX, Cao J, Hu SS, Lu XX, et al. miR-21 regulates tumor progression through the miR-21-PDCD4-Stat3 pathway in human salivary adenoid cystic carcinoma. *Lab Invest*. (2015) 95:1398–408. doi: 10.1038/labinvest.2015.105
65. Asangani IA, Rasheed SA, Nikolova DA, Leupold JH, Colburn NH, Post S, et al. MicroRNA-21 (miR-21) post-transcriptionally downregulates tumor suppressor Pdcd4 and stimulates invasion, intravasation and metastasis in colorectal cancer. *Oncogene*. (2008) 27:2128–36. doi: 10.1038/sj.onc.1210856
66. Guo YB, Ji TF, Zhou HW, Yu JL. Effects of microRNA-21 on nerve cell regeneration and neural function recovery in diabetes mellitus combined with cerebral infarction rats by targeting PDCD4. *Mol Neurobiol*. (2018) 55:2494–505. doi: 10.1007/s12035-017-0484-8
67. Allgayer H. Pdcd4, a colon cancer prognostic that is regulated by a microRNA. *Crit Rev Oncol Hematol*. (2010) 73:185–91. doi: 10.1016/j.critrevonc.2009.09.001
68. Ji C, Liu H, Yin Q, Li H, Gao H. miR-93 enhances hepatocellular carcinoma invasion and metastasis by EMT via targeting PDCD4. *Biotechnol Lett*. (2017) 39:1621–9. doi: 10.1007/s10529-017-2403-5
69. Ma QQ, Huang JT, Xiong YG, Yang XY, Han R, Zhu WW. MicroRNA-96 regulates apoptosis by targeting PDCD4 in human glioma cells. *Technol Cancer Res Treat*. (2017) 16:92–8. doi: 10.1177/1533034616629260
70. Das A, Ganesh K, Khanna S, Sen CK, Roy S. Engulfment of apoptotic cells by macrophages: a role of microRNA-21 in the resolution of wound inflammation. *J Immunol*. (2014) 192:1120–9. doi: 10.4049/jimmunol.1300613
71. Su W, Li Z, Jia Y, Zhu Y, Cai W, Wan P, et al. microRNA-21a-5p/PDCD4 axis regulates mesenchymal stem cell-induced neuroprotection in acute glaucoma. *J Mol Cell Biol*. (2017) 9:289–301. doi: 10.1093/jmcb/mjx022
72. Jiang Y, Zhao S, Ding Y, Nong L, Li H, Gao G, et al. MicroRNA21 promotes neurite outgrowth by regulating PDCD4 in a rat model of spinal cord injury. *Mol Med Rep*. (2017) 16:2522–8. doi: 10.3892/mmr.2017.6862
73. Liang X, Xu Z, Yuan M, Zhang Y, Zhao B, Wang J, et al. MicroRNA-16 suppresses the activation of inflammatory macrophages in atherosclerosis by targeting PDCD4. *Int J Mol Med*. (2016) 37:967–75. doi: 10.3892/ijmm.2016.2497
74. Zhu J, Yao K, Wang Q, Guo J, Shi H, Ma L, et al. Ischemic postconditioning-regulated miR-499 protects the rat heart against ischemia/reperfusion injury by inhibiting apoptosis through PDCD4. *Cell Physiol Biochem*. (2016) 39:2364–80. doi: 10.1159/000452506
75. Glusman G, Qin S, El-Gewely MR, Siegel AF, Roach JC, Hood L, et al. A third approach to gene prediction suggests thousands of additional human transcribed regions. *PLoS Comput Biol*. (2006) 2:e18. doi: 10.1371/journal.pcbi.0020018
76. Fang K, Liu P, Dong S, Guo Y, Cui X, Zhu X, et al. Magnetofection based on superparamagnetic iron oxide nanoparticle-mediated low lncRNA HOTAIR expression decreases the proliferation and invasion of glioma stem cells. *Int J Oncol*. (2016) 49:509–18. doi: 10.3892/ijo.2016.3571
77. Thomson DW, Dinger ME. Endogenous microRNA sponges: evidence and controversy. *Nat Rev Genet*. (2016) 17:272–83. doi: 10.1038/nrg.2016.20
78. Wang H, Li H, Zhang L, Yang D. Overexpression of MEG3 sensitizes colorectal cancer cells to oxaliplatin through regulation of miR-141/PDCD4 axis. *Biomed Pharmacother*. (2018) 106:1607–15. doi: 10.1016/j.biopha.2018.07.131
79. Yan H, Rao J, Yuan J, Gao L, Huang W, Zhao L, et al. Long non-coding RNA MEG3 functions as a competing endogenous RNA to regulate ischemic neuronal death by targeting miR-21/PDCD4 signaling pathway. *Cell Death Dis*. (2017) 8:3211. doi: 10.1038/s41419-017-0047-y
80. Hu L, Ye H, Huang G, Luo F, Liu Y, Liu Y, et al. Long noncoding RNA GAS5 suppresses the migration and invasion of hepatocellular carcinoma cells via miR-21. *Tumour Biol*. (2016) 37:2691–702. doi: 10.1007/s13277-015-4111-x
81. Yao T, Lu R, Zhang J, Fang X, Fan L, Huang C, et al. Growth arrest-specific 5 attenuates cisplatin-induced apoptosis in cervical cancer by regulating STAT3 signaling via miR-21. *J Cell Physiol*. (2019) 234:9605–15. doi: 10.1002/jcp.27647
82. Chen C, Zheng Q, Kang W, Yu C. Long non-coding RNA LINC00472 suppresses hepatocellular carcinoma cell proliferation, migration and invasion through miR-93–5p/PDCD4 pathway. *Clin Res Hepatol Gastroenterol*. (2018) 43:436–45. doi: 10.1016/j.clinre.2018.11.008
83. Yong S, Yabin Y, Bing Z, Chuanrong Z, Dianhua G, Jianhuai Z, et al. Reciprocal regulation of DGCR5 and miR-320a affects the cellular malignant phenotype and 5-FU response in pancreatic ductal adenocarcinoma. *Oncotarget*. (2017) 8:90868–78. doi: 10.18632/oncotarget.18377
84. Yang C, Wang G, Yang J, Wang L. Long noncoding RNA NBAT1 negatively modulates growth and metastasis of osteosarcoma cells through suppression of miR-21. *Am J Cancer Res*. (2017) 7:2009–19.
85. Rea D, Del Vecchio V, Palma G, Barbieri A, Falco M, Luciano A, et al. Mouse models in prostate cancer translational research: from xenograft to PDX. *Biomed Res Int*. (2016) 2016:9750795. doi: 10.1155/2016/9750795
86. Rea D, Coppola G, Palma G, Barbieri A, Luciano A, Del Prete P, et al. Microbiota effects on cancer: from risks to therapies. *Oncotarget*. (2018) 9:17915–27. doi: 10.18632/oncotarget.24681
87. Wei X, Wang W, Wang L, Zhang Y, Zhang X, Chen M, et al. MicroRNA-21 induces 5-fluorouracil resistance in human pancreatic cancer cells by regulating PTEN and PDCD4. *Cancer Med*. (2016) 5:693–702. doi: 10.1002/cam4.626
88. Wen SW, Zhang YF, Li Y, Xu YZ, Li ZH, Lu H, et al. Isoalantolactone inhibits esophageal squamous cell carcinoma growth through downregulation of microRNA-21 and derepression of PDCD4. *Digest Dis Sci*. (2018) 63:2285–93. doi: 10.1007/s10620-018-5119-z
89. Pratheeshkumar P, Son YO, Divya SP, Wang L, Turcios L, Roy RV, et al. Quercetin inhibits Cr(VI)-induced malignant cell transformation by targeting miR-21-PDCD4 signaling pathway. *Oncotarget*. (2017) 8:52118–31. doi: 10.18632/oncotarget.10130
90. Mudduluru G, George-William JN, Muppala S, Asangani IA, Kumarswamy R, Nelson LD, et al. Curcumin regulates miR-21 expression and inhibits invasion and metastasis in colorectal cancer. *Biosci. Rep*. (2011) 31:185–97. doi: 10.1042/BSR20100065
91. Yue B, Cai D, Liu C, Fang C, Yan D. Linc00152 functions as a competing endogenous RNA to confer oxaliplatin resistance and holds prognostic values in colon cancer. *Mol Ther*. (2016) 24:2064–77. doi: 10.1038/mt.2016.180
92. Krichevsky AM, Gabriely G. miR-21: a small multi-faceted RNA. *J Cell Mol Med*. (2009) 13:39–53. doi: 10.1111/j.1582-4934.2008.00556.x
93. Si ML, Zhu S, Wu H, Lu Z, Wu F, Mo YY. miR-21-mediated tumor growth. *Oncogene*. (2006) 26:2799–803. doi: 10.1038/sj.onc.1210083

Conflict of Interest Statement: The authors declare that the research was conducted in the absence of any commercial or financial relationships that could be construed as a potential conflict of interest.

frontiers in Cell and Developmental Biology

ORIGINAL RESEARCH
published: 02 October 2019
doi: 10.3389/fcell.2019.00217

Novel Function of lncRNA ADAMTS9-AS2 in Promoting Temozolomide Resistance in Glioblastoma via Upregulating the FUS/MDM2 Ubiquitination Axis

Yuanliang Yan[1,2†], Zhijie Xu[3†], Xi Chen[1,2], Xiang Wang[1,2], Shuangshuang Zeng[1,2], Zijin Zhao[4], Long Qian[1,2], Zhi Li[5], Jie Wei[1,2], Lei Huo[4], Xuejun Li[4], Zhicheng Gong[1,2] and Lunquan Sun[5*]*

[1] Department of Pharmacy, Xiangya Hospital, Central South University, Changsha, China, [2] National Clinical Research Center for Geriatric Disorders, Xiangya Hospital, Central South University, Changsha, China, [3] Department of Pathology, Xiangya Hospital, Central South University, Changsha, China, [4] Department of Neurosurgery, Xiangya Hospital, Central South University, Changsha, China, [5] Key Laboratory for Molecular Radiation Oncology of Hunan Province, Center for Molecular Medicine, Xiangya Hospital, Central South University, Changsha, China

OPEN ACCESS

Edited by:
Deilson Elgui De Oliveira, São Paulo State University, Brazil

Reviewed by:
Vishwa Jeet Amatya, Hiroshima University, Japan
Sathish Kumar Mungamuri, National Institute of Nutrition, India

***Correspondence:**
Zhicheng Gong
gongzhicheng@csu.edu.cn
Lunquan Sun
lunquansun@csu.edu.cn

† These authors have contributed equally to this work

Specialty section:
This article was submitted to Molecular and Cellular Oncology, a section of the journal Frontiers in Cell and Developmental Biology

Received: *26 June 2019*
Accepted: *18 September 2019*
Published: *02 October 2019*

Citation:
Yan Y, Xu Z, Chen X, Wang X, Zeng S, Zhao Z, Qian L, Li Z, Wei J, Huo L, Li X, Gong Z and Sun L (2019) Novel Function of lncRNA ADAMTS9-AS2 in Promoting Temozolomide Resistance in Glioblastoma via Upregulating the FUS/MDM2 Ubiquitination Axis. Front. Cell Dev. Biol. 7:217. doi: 10.3389/fcell.2019.00217

Background: LncRNAs have been shown to play essential roles in cancer therapeutic response. However, the detailed mechanism of lncRNAs in temozolomide (TMZ) resistance in glioblastoma (GBM) remain to be elucidated.

Methods: To elucidate the mechanism maintaining TMZ resistance, we constructed two TMZ-resistant GBM cell lines (T98G-R/U118-R). LncRNAs from four public datasets were reanalyzed, and the candidate lncRNA ADAMTS9-AS2 was evaluated in TMZ-treated GBM patients and *in vitro* cell lines.

Results: Reanalysis of lncRNA expression profiles identified ADAMTS9-AS2 as significantly overexpressed in TMZ-resistant GBM cells and as positively associated with the IC_{50} of TMZ in GBM cells. Overexpression of ADAMTS9-AS2 was also significantly associated with poor TMZ response and shorter progression-free survival (PFS) in TMZ-treated GBM patients. Knockdown of ADAMTS9-AS2 inhibited proliferation and attenuated the IC_{50} of TMZ, as well as mitigating invasion and migration in TMZ-resistant GBM cells. Subsequent investigations indicated that reduced expression of ADAMTS9-AS2 significantly suppressed expression of the FUS protein, which was predicted as a direct substrate of ADAMTS9-AS2. Expression trends of FUS were directly correlated with those of ADAMTS9-AS2, as shown by increasing concentrations and prolonged treatment with TMZ. RNA pull-down and RIP assays indicated that both endogenous and exogenous ADAMTS9-AS2 directly binds to the RRM and Znf_RanBP2 domains of FUS, consequently increasing FUS protein expression. Knockdown of ADAMTS9-AS2 reduced the half-life of FUS and decreased FUS protein stability via K48 ubiquitin degradation. Moreover, the E3 ubiquitin-protein ligase MDM2 interacts with and down

regulates FUS, while the RRM and Znf_RanBP2 domains of FUS facilitate its binding with MDM2. ADAMTS9-AS2 decreased the interaction between MDM2 and FUS, which mediates FUS K48 ubiquitination. Additionally, knockdown of the ADAMTS9-AS2/FUS signaling axis significantly alleviated progression and metastasis in TMZ-resistant cells.

Conclusion: ADAMTS9-AS2 possessed a novel function that promotes TMZ resistance via upregulating the FUS/MDM2 axis in GBM cells. The RRM or Znf_RanBP2 domains of FUS facilitate the combination of ADAMTS9-AS2 and FUS, competitively inhibiting MDM2-dependent FUS K48 ubiquitination and resulting in enhanced FUS stability and TMZ resistance. Our results suggest that the ADAMTS9-AS2/FUS/MDM2 axis may represent a suitable prognostic biomarker and a potential target in TMZ-resistant GBM therapy.

Keywords: glioblastoma, TMZ resistance, ADAMTS9-AS2, FUS, MDM2, ubiquitination

INTRODUCTION

Glioblastoma (GBM), the most lethal form of primary intrinsic brain tumor in both pediatric and adult populations, has the highest mortality rate among all malignant nervous system neoplasms, with a median survival of only 12–15 months. In 2005, the US Food and Drug Administration (FDA) approved combination temozolomide (TMZ) and radiotherapy treatment in adults with newly diagnosed glioblastoma, as well as the use of TMZ alone as a maintenance treatment (Hombach-Klonisch et al., 2018). TMZ remains the most widely used and effective first-line chemotherapeutic for GBM patients, with high bioavailability and tolerability. However, over time, the majority of patients with GBM gradually develop resistance to TMZ during treatment, leading to GBM recurrence and treatment failure (Kaur et al., 2018; Teng et al., 2018).

Several pathways have been elucidated that regulate TMZ resistance, and expression of the DNA repair protein O^6-methylguanine-DNA-methyltransferase (MGMT) is considered the predominant cause of TMZ resistance. MGMT expression can be silenced by methylation of the promoter/enhancer region, and polymorphisms in MGMT gene promote MGMT expression and TMZ resistance (Wang et al., 2017; Chen X. et al., 2018). Other plausible mechanisms are involved in TMZ resistance as well, including activation of base excision repair (BER), reduced activity of mismatch repair (MMR) genes, histone posttranslational modifications, GBM stem cells and dysregulation of other effectors (Garnier et al., 2018). Epigenetic variations have been shown to play major roles in mediating the resistance to targeted therapies and conventional cytotoxic agents. Aberrant miRNA expression, such as in mIR-93, noted in clinically relevant tumor subtypes of GBM, influences tumor response to therapy through epigenetic miRNA-based silencing or sensitizing effects (Huang et al., 2019). Recent studies suggest that long non-coding RNAs (lncRNAs) are indispensable for the regulation of cellular processes in glioma tumorigenesis and in therapeutic responses (Yan et al., 2017). Specifically, several clinically relevant lncRNAs have been correlated with patient outcome in GBM and mediate biological functions, including stemness, immunity, development, regulation of gene expression, and regulation of protein synthesis (Schmitt and Chang, 2016). Thus, understanding the most relevant mechanisms of TMZ resistance may help identify novel drug targets and more effective therapies.

The discovery of lncRNAs has provided insight into the underlying biological mechanisms of glioma phenotypes, which is mediated through their interactions with other cellular macromolecules, including proteins, RNA and DNA (Peng et al., 2018). LncRNA nuclear-enriched abundant transcript 1 (NEAT1) contributes to glioma cell growth and invasion through the WNT/β-catenin pathway by scaffolding the EZH2 protein (Chen Q. et al., 2018). Findings from Sa's group have shown that lncRNA homeobox transcript antisense intergenic RNA (HOTAIR) promotes drug delivery across the blood tumor barrier (BTB) in glioma treatment by sponging miR-148b-3p (Sa et al., 2017). Chen reported that lncRNA AC003092.1 may act as an endogenous "sponge" of miR-195, promoting expression of TFPI-2 and overcoming TMZ resistance in glioma cells (Xu et al., 2018). Through chromatin modification, LncPRESS1 disrupts deacetylation of H3K56 by sequestering SIRT6 from chromatin to safeguard pluripotency-specific stem cells (Jain et al., 2016). Using RNA expression profiling, Mazor G et al. found that lncRNA TP73-AS1 comprises a clinically relevant lncRNA that influences metabolism-related genes and ALDH1A1, conferring TMZ resistance to GBM stem cells (Mazor et al., 2019). In addition, studies have shown that lncRNA metastasis-associated lung adenocarcinoma transcript 1 (MALAT1) plays a promising role in TMZ therapeutic response to GBM (Amodio et al., 2018). Nanocomplex-mediated silencing of MALAT1 effectively sensitizes glioma cells to temozolomide therapy (Kim et al., 2018). Furthermore, ML Zhang et al. showed that circRNAs generated from lncRNA LINC-PINT, containing short open reading

Abbreviations: ADAMTS9-AS2, ADAM metallopeptidase with thrombospondin type 1 motif 9 antisense RNA 2; BER, Base excision repair; DNMT1, DNA methyltransferase-1; FUS, Fused in sarcoma; GBM, Glioblastoma; IC_{50}, Half maximal inhibitory concentration; lncRNAs, Long non-coding RNAs; IP, Immunoprecipitation; MALAT1, Metastasis-associated lung adenocarcinoma transcript 1; MGMT, O^6-methylguanine-DNA-methyltransferase; MMR, Mismatch repair; PFS, Progression-free survival; RIP, RNA immunoprecipitation; smsiRNAs, Smart silencer; TMZ, Temozolomide.

frames, encode functional peptides that suppress oncogenic transcriptional elongation in glioblastoma (Zhang et al., 2018). However, it remains largely unknown how specific lncRNAs influence in the mechanical properties of glioma cells in response to TMZ exposure.

To address these challenges, we reanalyzed lncRNA profiles in TMZ-resistant glioma cells using four public glioma-associated lncRNAs datasets. Our data identified 12 differentially expressed lncRNAs in TMZ-resistant glioma cells. Among these, lncRNA ADAMTS9-AS2 (ADAM metallopeptidase with thrombospondin type 1 motif 9 antisense RNA 2) was significantly overexpressed. Moreover, alterations in ADAMTS9-AS2 were correlated with TMZ response in glioma patients. Using subsequent functional assays, ADAMTS9-AS2 was found to be involved in fused in sarcoma (FUS)/MDM2 mediated progression in TMZ-resistant GBM.

MATERIALS AND METHODS

Cell Culture

T98G and U118 human glioma cell lines, identified by the short tandem repeat (STR) analysis (**Supplementary Data Sheet S1**), were obtained from the Cancer Research Institute, Central South University, China, and have been authenticated by short tandem repeat genotyping (Genesky Biotechnologies Inc., Shanghai). As described in our previous study (Dai et al., 2017), we established T98G-R and U118-R TMZ-resistant cell lines with continuous stepwise selection using increasing concentrations of TMZ for greater than 6 months. Next, the half maximal inhibitory concentration (IC_{50}) was determined to confirm stable resistance to TMZ. Glioma cells and HEK 293T cells were maintained in DMEM supplemented (C11995500, HyClone) with 10% fetal bovine serum (10099141C, Gibco) and 1% penicillin/streptomycin (10378016, Gibco) at 37°C with 5% CO_2.

Reagents

TMZ was purchased from Sigma-Aldrich Corporation Chemicals (PHR1437). Cycloheximide (CHX) was purchased from MedChemExpress (HY-12320). The proteasome inhibitor MG132 was purchased from Selleck Chemicals (S2619). All reagents were dissolved in dimethylsulfoxide (Amresco). Specific siRNAs and smart silencer (smsiRNAs) RNAs were purchased from Ribo (China) with sequences shown in **Supplementary Table S1**. Full-length ADAMTS9-AS2 and MDM2 were PCR-amplified from human cDNA and subcloned into pcDNA3.1(+) to create ADAMTS9-AS2 expression plasmids. A FUS expression plasmid, along with truncation constructs used in this study, were purchased from Addgene (29609, 29610, 29611, 29612) and Vigene Biosciences. The constructs His-Ubiquitin (WT) and His-Ubiquitin (K48R) were kind gifts from Prof. Gang Huang (Cincinnati Children's Hospital, Cincinnati, OH, United States). Overexpressing plasmids (1 μg) or smsiRNAs/siRNAs (100 nM) of indicated genes were transfected into cells using Lipofectamine 3000 (L3000015, Invitrogen) for overexpression and knockdown of indicated genes, respectively, followed by analysis 48–72 h later.

Human Tissues

One hundred forty-four glioma tissues were collected between 2015 and 2018 from the Department of Neurosurgery, Xiangya Hospital of Central South University. This project was approved by the Chinese Clinical Trial Register (ChiCTR-RPC-16008569) and the ethics committee of Xiangya Hospital (Changsha, China). Data do not contain any information that could identify patients. Detailed clinical information was collected from patient records and is listed in **Supplementary Table S2**. Samples were obtained from patients during surgery and were immediately snap-frozen in liquid nitrogen until use. Chemotherapy response status was assigned to patients based on progression-free survival (PFS) in GBM patients with TMZ treatment (Stupp et al., 2015, 2017) denoted as TMZ response (no recurrence within 4 months after surgical resection) and TMZ non-response (recurrence within 4 months after surgical resection).

MTS Assays and IC_{50}

T98G, U118, and their TMZ-resistant cell lines were seeded in 96-well plates (2×10^3 cells/well) and cultured overnight. Various concentrations of TMZ (0, 0.2, 2, 20, 200, 2,000 μM) or/and indicated transfection reagents were added into the medium for 72 h. Then, MTS assays were performed to determine cell viability following the manufacturer's protocols. Briefly, 20 μl MTS solution (G358C, Promega) was added into each well and incubated for 6 h. Absorbance was detected at 490 nm using a VICTOR X2 microplate reader (PerkinElmer, United States). IC_{50} was determined using sigmoidal concentration-response curve-fitting mode using SPSS software. Variable slope was employed to calculate IC_{50} values [non-linear regression; dose-response-inhibition; log(inhibitor) vs. response- variable slope (4 parameters)]. Cell proliferation was determined by treating TMZ-sensitive or TMZ-resistant glioma cells (1×10^3 cells/well) with 100 μM TMZ for 5 days in 96-well plates. Cell proliferation of TMZ-sensitive or TMZ-resistant glioma cells (1×10^3 cells/well) after indicated transfection was determined for 5 days in 96-well plates.

Cell Cycle Analysis

After serum starvation and cell cycle synchronization for 12 h, cells were seeded into T25 flasks at 1×10^6 cells each. As cells adhered to the plate, drug treatments were added to the flask, and cells were incubated for 48 h. For each condition, detached and adherent cells were harvested, fixed in 70% ethanol at −20°C for at least 12 h, and incubated with propidium iodide (20 μg/ml), phosphate-buffered saline (PBS) and RNase A (50 μg/ml) in the dark. Stained cells were detected using flow cytometry (Guava easyCyte 8HT, Millipore, United States).

Scratch Assay

The scratch assay was used to measure cell migration *in vitro*. In brief, cells were seeded into 60 mm dishes (2.5×10^5 cells/well) and cultured until they formed a fused monolayer for 24 h. The smsiRNAs or/and siRNAs treatments were administered for each group according to the experimental design. A P200 pipette tip was used to create a scratch. After 48 h,

wound closure was imaged using a microscope with mounted camera. Relative migration distance was measured, using ImageJ software, by determining the fraction of cell coverage across the scratch. Relative migration distance was calculated as follows: (%) = migration area/total area × 100%.

Transwell Assay

The transwell assay was used to measure cell invasion *in vitro*. Matrigel (BD Biosciences, NJ, United States) was mixed with medium in a ratio of 1:8 and placed on the upper surface of each insert in 24-well transwell plates (BD Biosciences, NJ, United States). The chambers were held 6 h in the incubator. In brief, 1×10^4 cells were added to the upper chamber, and 10% FBS was added to the lower chamber. The smsiRNAs or/and siRNAs treatments were administered for each group according to the experimental design. After 48 h, chambers were fixed and stained with 0.05% crystal violet for 2 h. Cells on the upper surface were gently scraped, and stained cells were imaged and quantified under the microscope. The ImageJ software was used to assist cell counting in cell invasion assays.

RNA Extraction and qPCR

Total RNA was extracted using TRIzol reagent (Invitrogen) according to the manufacturer's instructions. The RNA quality was checked after 1% agarose gel electrophoresis with ChemiDoc XRS system (Bio-Rad, United States) and using Protein nucleic acid spectrophotometer (Beckman Coulter, United States). The A260/A280 ratios of RNA are allowed between 1.8 and 2.2. Total RNA was then reverse-transcribed to cDNA using the PrimeScript^{TM} strand cDNA synthesis kit (6210, Takara). The PARIS Kit (AM1921, Invitrogen) was used to separate nuclear and cytoplasmic RNAs in GBM cells. The qPCR reaction was then performed by CFX96 Touch Real-Time PCR Detection System (Bio-Rad, United States) to determine the expression levels of targets, and performed in triplicate in three independent experiments. The primer sequences of qPCR are shown in **Supplementary Table S1**. Changes in target mRNA levels relative to a reference gene (β-actin) were determined using the $2^{-\Delta\Delta ct}$ method with iTaq Universal SYBR green Supermix as previous reported (1725121, Bio-Rad) (Song et al., 2019).

RNA Pull-Down Assay

LncRNA ADAMTS9-AS2 was transcribed *in vitro* from the pcDNA3.1(+) vector using the T7 RiboMAX large-scale RNA production system (P1300) and was biotin labeled using the Pierce RNA 3′ end biotinylation kit (20160). Two milligrams of protein extract from T98G-R cells were then mixed with 100 pmol biotinylated RNA, incubated with nucleic-acid-compatible streptavidin magnetic beads and washed (Pierce magnetic RNA-Protein pull-down kit, 20164). Proteins that bound to the streptavidin-coupled dynabeads were resolved using reducing sample buffer and then subjected to western blot.

RNA Immunoprecipitation (RIP)

RIP analysis was performed using the Magna RIP RNA-Binding Protein Immunoprecipitation Kit (Millipore, Bedford, MA, United States) according to the manufacturer's instructions. Antibodies to FUS and the V5-tag used for RIP were the same as those used for western blot. C-immunoprecipitated RNAs were detected by strand specific qPCR.

Western Blot Analysis

Whole cell protein was isolated using Pierce IP Lysis Buffer (Thermo Fisher Scientific, United States). The PARIS Kit (AM1921, Invitrogen) was used to separate nuclear and cytoplasmic protein fractions in GBM cells. Protein concentrations were quantified using the Micro BCA Protein Assay Kit (23229, Thermo Scientific). Purified proteins were boiled with 4 × loading buffer, and denatured protein samples were separated by SDS-PAGE on 10% polyacrylamide gels. Then, samples were transferred to NC membranes (HATF00010, Millipore). After blocking with 5% non-fat milk for 1 h, membranes were probed with appropriate primary antibodies overnight at 4°C. The next day, membranes were washed with PBS/Tween (PBST) and incubated with appropriate secondary antibodies for approximately 1 h at room temperature. Protein bands were visualized by Immobilon Western chemiluminescent reagents (WBKLS0500, Millipore). Information for utilized primary antibodies is shown in **Supplementary Table S3**.

Immunoprecipitation (IP)

For ubiquitination assays, cells were transfected according to the experimental requirements followed by treatment with 1 μM MG132 for 6 h. Then, 500 μg protein lysates were incubated with 1 mg/ml specific primary antibody with gentle rocking for 3 h at 4°C. Protein A/G beads (10002D, Invitrogen) were subsequently added to precipitate protein complexes and further incubated with gentle rocking overnight at 4°C. Precipitates were collected, and supernatants were discarded. Pellets were fixed and resuspended in SDS sample loading buffer before boiling. Samples were then subjected to SDS-PAGE for western blot analysis.

Data Acquisition and Reanalysis Using Different Bioinformatics Methods

The bioinformatics analysis of lncRNA profiling in GBM tissues was conducted through several independent bioinformatics databases. LncRNA Modulator Atlas in Pan-cancer (LncMAP) is a user-friendly web platform, providing lncRNA-mediated transcriptional signatures in human cancer tissues (Li et al., 2018). Using the Cancer RNA-Seq Nexus (CRN), we selected two studies (CRN Glioma and CRN Glioblastoma) to explore the lncRNA profiles between the normal and GBM tissues (Li J. R. et al., 2016). The Atlas of Non-coding RNAs in Cancer (TANRIC) was used for the further confirmation of the changes of lncRNAs in GBM (Li et al., 2015). Then, the consistently dysregulated genes were identified using a Venn analysis and Heatmap diagram.

In addition, to evaluate the roles of lncRNAs in protein complexes, we used the RAID database to version 2.0 (RAID v2.0) (Yi et al., 2017), which integrated diverse RNA-associated interactions. Using this tool, we explore the proteins that

bind to disregulated lncRNAs. Furthermore, another integrated bioinformatics platform, UbiBrowser (Li et al., 2017), was used to investigate the human E3 ubiquitin-protein ligase-substrate interaction network.

Statistical Analysis

Statistics were calculated using SPSS 20.0 (SPSS Inc., United States). One-way ANOVA (Kruskal–Wallis test) and Chi-square tests were employed to analyze differences in demographic characteristics and clinical data among different groups. Receiver operating characteristic (ROC) curves were established to discriminate GBM response patients from non-response patients. Area under the ROC curve was used as an accuracy index for evaluating the predictive performance of the hypothesized lncRNA. $^{*}p < 0.05$ and $^{**}p < 0.01$ were regarded as statistically significant.

RESULTS

Establishment of T98G-R and U118-R TMZ-Resistant GBM Cell Lines

To confirm resistant phenotypes, T98G-R and U118-R cancer cells were exposed to various doses of TMZ. After approximately 72 h, we measured cell viability and IC_{50} using MTS assay. Compared to the parental cells, T98G and U118, cell viability rates in T98G-R and U118-R cells were much higher in response to TMZ treatment (**Figure 1A** and **Supplementary Figure S1A**). IC_{50} values of TMZ-resistant cells were increased more than fourfold compared to parental cells (T98G vs. T98G-R: 163.4 μM vs. 1850.7 μM; U118 vs. U118-R: 87.6 μM vs. 383.6 μM) (**Figure 1A** and **Supplementary Figure S1A**). To further compare the proliferation capacity of parental and TMZ-resistant GBM cells, the cells were treated with 100 μM TMZ for 3 or 5 days. Significantly different cell cycle distribution was observed between TMZ-resistant cells and their parental cell lines. Upon TMZ treatment, T98G and U118 cells caused marked cell cycle arrest in G2/M phase in a time-dependent manner, while there were no significant changes in T98G-R and U118-R cells (**Figure 1B** and **Supplementary Figure S1B**). These findings are consistent with the TMZ-resistant phenotype of T98G-R and U118-R cell lines.

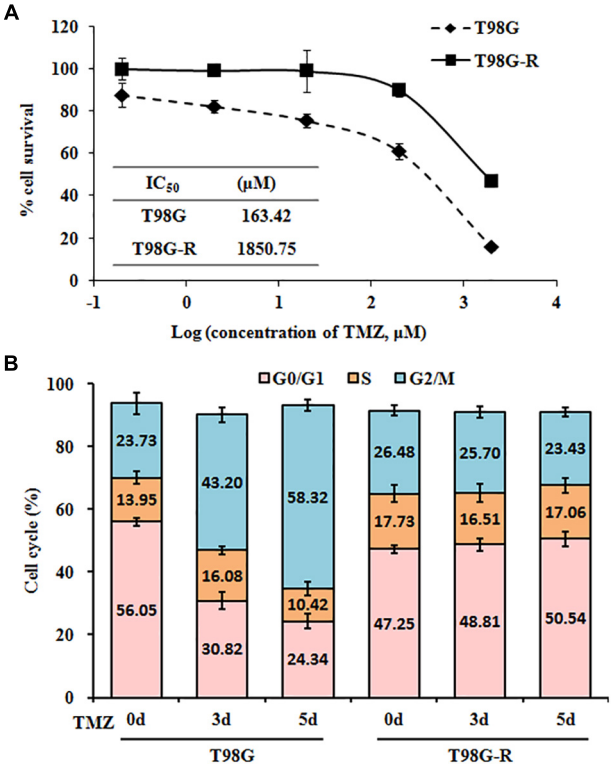

FIGURE 1 | Establishment and characterization of TMZ-resistant GBM cell lines. **(A)** Cell viability and IC_{50} analysis was performed to evaluate cytotoxicity of TMZ to T98G and T98G-R cells in response to the indicated concentrations of TMZ for 72 h. **(B)** T98G and T98G-R cells were treated with 100 μM TMZ for 3 and 5 days, and cell cycle was examined by flow cytometry. The above experiments were repeated independently three times with similar results. Each data point represents mean ± SD.

LncRNA ADAMTS9-AS2 Is Overexpressed in TMZ-Resistant GBM Cell Lines

LncRNAs are essential epigenetic regulators with critical roles in tumor initiation and malignant progression. To examine whether changes in lncRNA are involved in therapeutic response to TMZ in GBM cells, we first performed data mining using CRN Glioma (Li J. R. et al., 2016), CRN Glioblastoma (Li J. R. et al., 2016), TANRIC-GBM-CHINA (Li et al., 2015), and LncMAP GBM (Li et al., 2018) datasets and evaluated overlapping lncRNAs in GBM samples. The Venn diagram revealed that approximately 68 lncRNAs are common among these four published datasets (**Figure 2A**). After a preliminary screen through strand-specific qPCR, we identified 12 co-differentially expressed lncRNAs in TMZ-resistant T98G-R and U118-R cells. Among these, nine lncRNAs were frequently upregulated, and three were frequently downregulated (**Figures 2B,C**). Furthermore, the ADAMTS9-AS2 was the most consistently and markedly overexpressed RNA transcript in TMZ-resistant T98G-R and U118-R cells ($p < 0.01$, $p < 0.05$, respectively) (**Figures 2D,E**). Thus, in subsequent experiments, we primarily evaluated the functional roles of ADAMTS9-AS2 in TMZ response in GBM samples.

Overexpressed ADAMTS9-AS2 Predicts Poor TMZ Response in GBM Patients

To investigate whether ADAMTS9-AS2 expression is associated with TMZ response in GBM patients, we assessed ADAMTS9-AS2 transcriptional levels in TMZ response and TMZ non-response GBM tissues. The results revealed that ADAMTS9-AS2 was significantly upregulated in non-responding tissues compared to responding tissues (7.13 ± 1.07 vs. 1.21 ± 0.12, $p < 0.001$) (**Figure 3A**). A ROC curve was drawn to investigate the potential diagnostic value of ADAMTS9-AS2 expression in differentiating response status in GBM patients. The AUC was 0.84, with the diagnostic sensitivity and specificity reaching

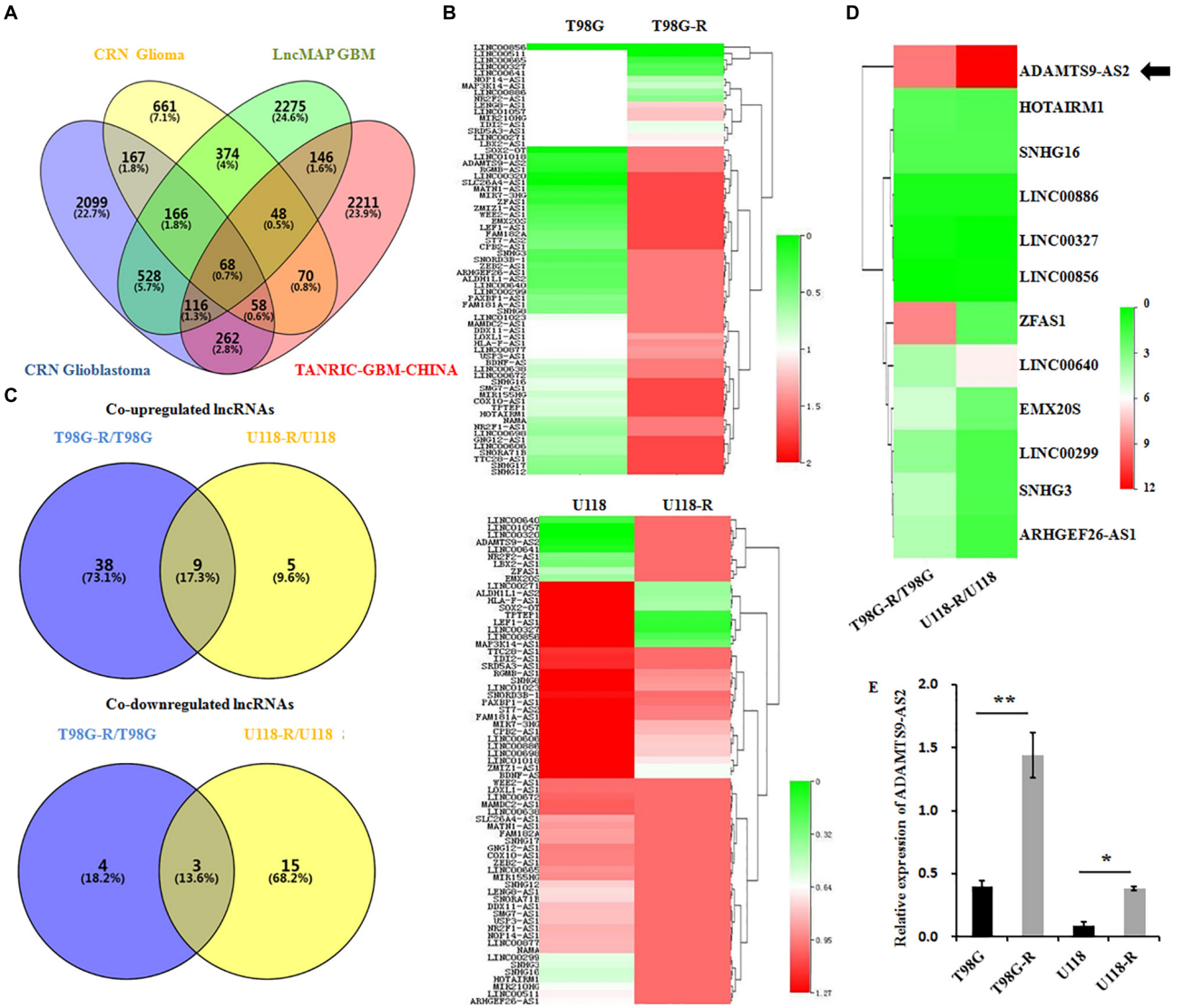

FIGURE 2 | ADAMTS9-AS2 is significantly overexpressed in TMZ-resistant GBM cells. **(A)** Venn diagram of four datasets from different databases. **(B)** Changes in 68 glioma-related lncRNAs were examined between T98G/T98G-R and U118/U118-R. **(C)** The Venn diagram indicates the co-upregulated and co-downregulated lncRNAs in TMZ-resistant cells, T98G-R and U118-R. **(D)** Heatmap showing the 12 co-differentially expressed lncRNAs in TMZ-resistant cells, T98G-R and U118-R. **(E)** qPCR assay of ADAMTS9-AS2 transcript expression in TMZ-resistant GBM cell lines. Quantitative results are from three independent experiments and are shown as the mean ± SD. *$p < 0.05$, **$p < 0.01$.

63.87 and 69.99%, respectively (**Figure 3B**). Moreover, we observed improved PFS among patients with lower ADAMTS9-AS2 expression compared to those with higher ADAMTS9-AS2 expression (6.77 vs. 2.66 months, $p < 0.001$) (**Figure 3C**). Collectively, these clinical data on our patients support the conclusion that ADAMTS9-AS2 represents a significant prognostic marker in GBM patients after TMZ treatment.

ADAMTS9-AS2 Induces TMZ Resistance by Regulating Metastasis

To investigate the effects of ADAMTS9-AS2 on TMZ-resistant behaviors, we determined the Spearman correlation between ADAMTS9-AS2 levels and TMZ sensitivity (IC_{50}) in 6 GBM cell lines (T87G, U118, MGR2, U251, U87, C6). IC_{50} values of TMZ were positively correlated with ADAMTS9-AS2 expression levels in these glioma cells (Spearman $r = 0.98$, $p < 0.001$) (**Figure 4A**). Next, we used a smsiRNAs-mediated knockdown strategy to inhibit ADAMTS9-AS2 expression in TMZ-resistant cells, T98G-R and U118-R (**Figure 4B** and **Supplementary Figure S2A**). Upon knockdown of ADAMTS9-AS2, T98G-R cells showed enhanced sensitivity to TMZ, which manifested as reduced cell proliferation rates (**Figure 4C**) and about an 40-fold decrease in IC_{50} (**Figure 4D**). Similar results were observed in U87-R cells (**Supplementary Figures S2B,C**). In addition, given one of the well-documented mechanisms in

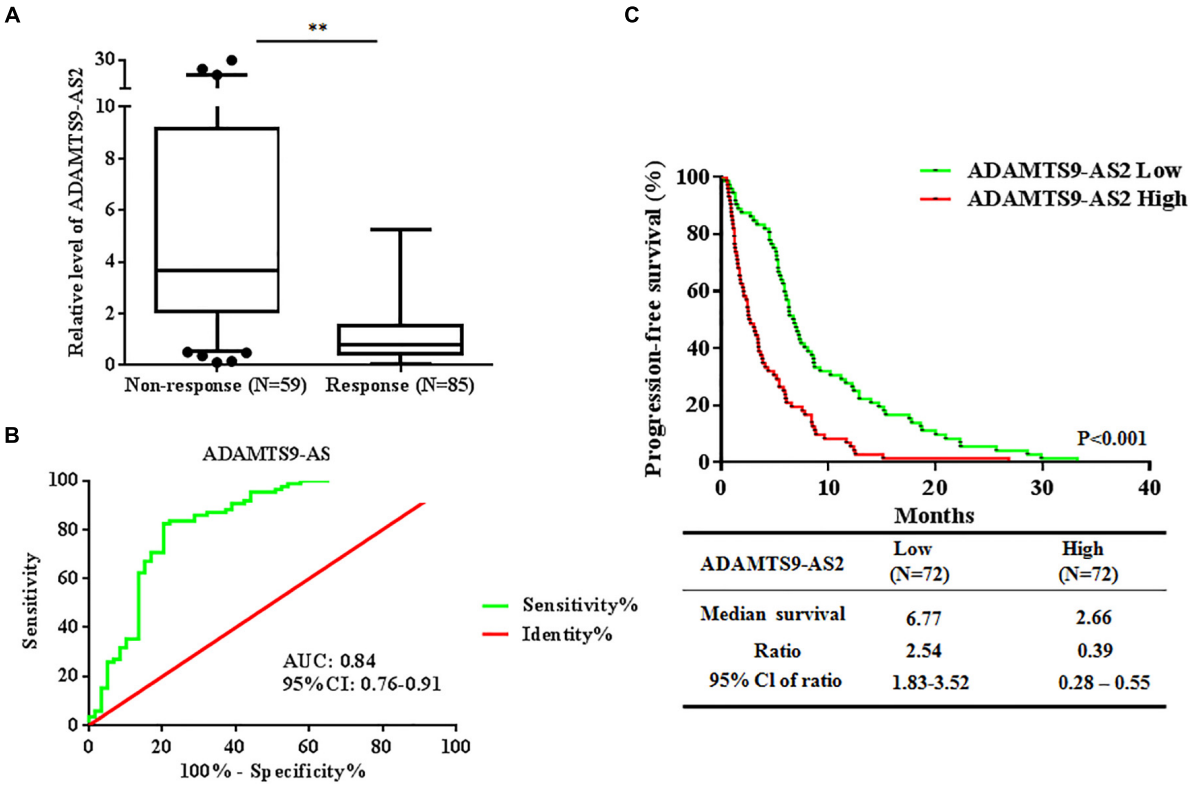

ADAMTS9-AS2	Low (N=72)	High (N=72)
Median survival	6.77	2.66
Ratio	2.54	0.39
95% CI of ratio	1.83-3.52	0.28 – 0.55

FIGURE 3 | Altered expression of ADAMTS9-AS2 is associated with TMZ response in 144 GBM patients. **(A)** qPCR assay of ADAMTS9-AS2 transcript expression in patients with differential TMZ response status. **(B)** ROC curves were established to discriminate TMZ responding patients from non-responding patients. **(C)** PFS among patients with ADAMTS9-AS2 low (green, median PFS: 6.77 mouths) and ADAMTS9-AS2 high (red, median PFS: 2.66 mouths) groups. $^{**}p < 0.01$ were regarded as statistically significant.

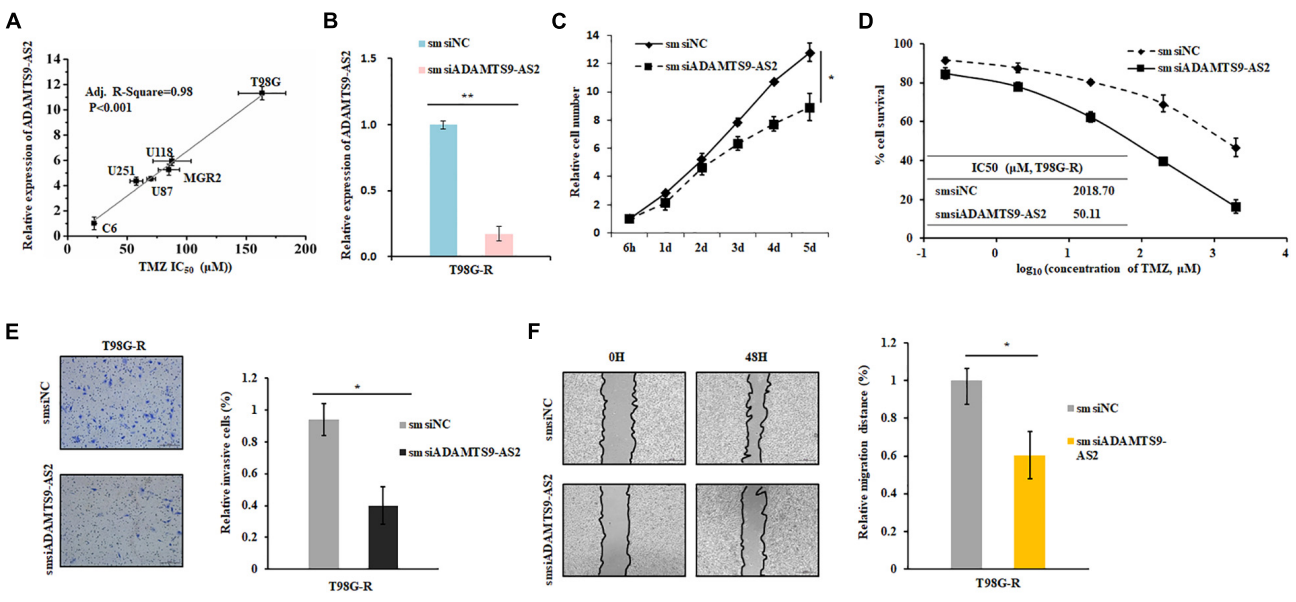

FIGURE 4 | ADAMTS9-AS2 supports TMZ resistance in T98G-R GBM cells. **(A)** The correlation between ADAMTS9-AS2 mRNA expression and IC_{50} values in six GBM cells was quantified by Spearman's rank correlation. **(B)** qPCR confirmed that smsiRNAs mediate knockdown of ADAMTS9-AS2. Relative cell number **(C)**, TMZ IC50 value **(D)**, invasion ability **(E)** and migration ability **(F)** were examined in T98G-R cells after knockdown of ADAMTS9-AS2. Quantitative results of three independent experiments are shown as the mean ± SD. $^{*}p < 0.05$, $^{**}p < 0.01$.

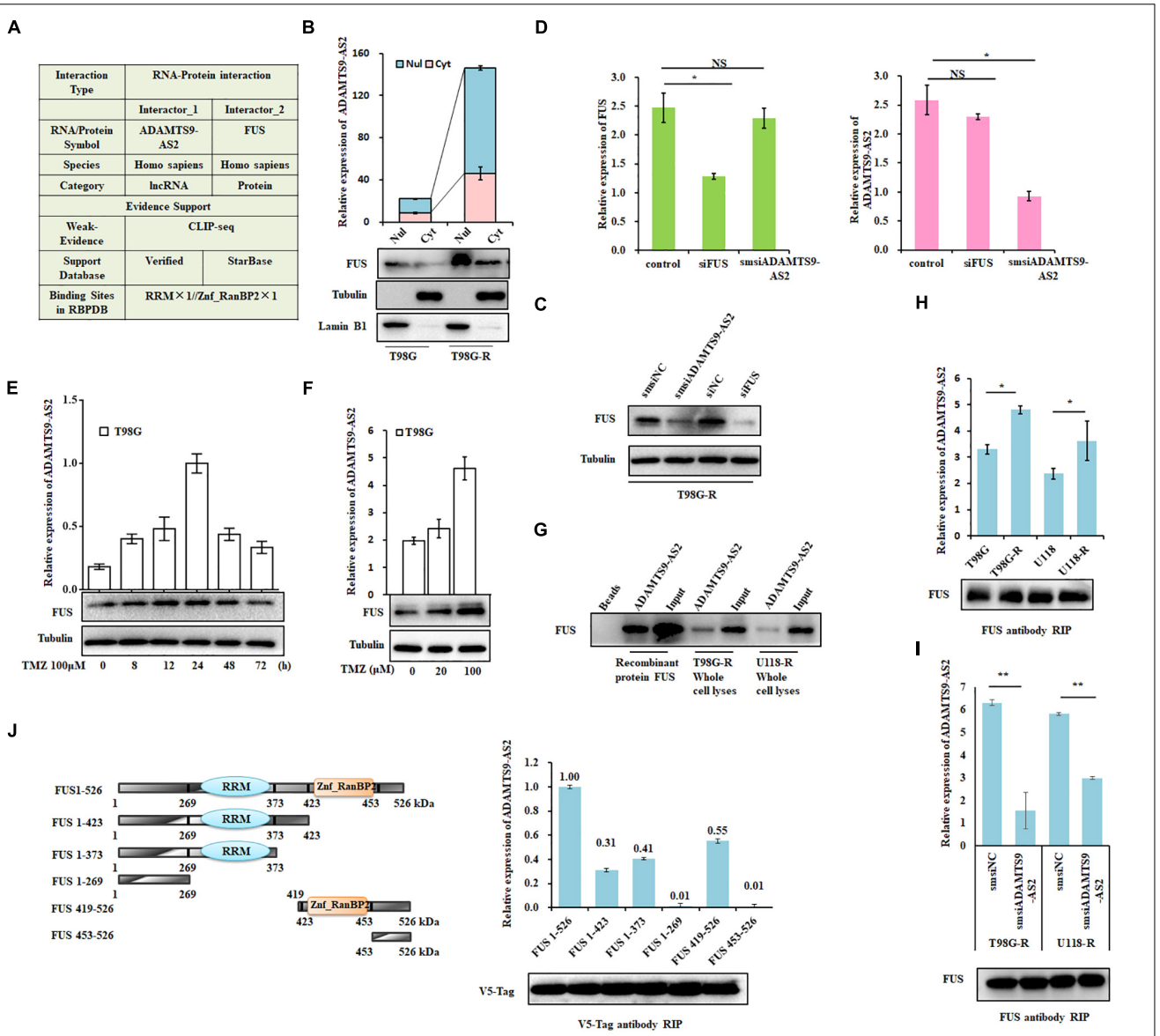

FIGURE 5 | ADAMTS9-AS2 interacts with the co-localized FUS protein. **(A)** The RAID algorithm was used to predict the binding affinity of ADAMTS9-AS2 to FUS. **(B)** Subcellular localization of ADAMTS9-AS2 and FUS analyzed from nuclear and cytoplasmic extracts. **(C)** Protein levels of FUS determined by western blot analyses of lysates from ADAMTS9-AS2 knockdown cells T98G-R. **(D)** qPCR assay of ADAMTS9-AS2 and FUS transcript expression in ADAMTS9-AS2 or FUS knock down T98G-R cells. Upon different durations **(E)** or doses **(F)** of TMZ treatment, the variation tendency of ADAMTS9-AS2 and FUS was analyzed in T98G cells. **(G)** Proteins isolated from the RNA pull-down assays with biotinylated ADAMTS9-AS2 RNA were identified by western blot analyses using specific anti-FUS antibodies. mRNA isolated from the RIP assays with anti-FUS antibody was identified by qPCR using specific ADAMTS9-AS2 primers in T98G-R and U118-R cells without **(H)** or with **(I)** ADAMTS9-AS2 knockdown. **(J)** Truncated versions of V5-FUS were produced according to the predicted ADAMTS9-AS2/FUS binding domain. mRNA isolated from the RIP assays with anti-V5 tag antibody was identified by qPCR analysis using specific ADAMTS9-AS2 primers in HEK293T cells. All images displayed are representatives of three independent experiments. $*p < 0.05$, $**p < 0.01$.

TMZ response involves elevated methylation of O6MeG DNA methyltransferase (MGMT) (Yan et al., 2016), we further want to evaluate whether the ADAMTS9-AS2 modulated TMZ-resistant behaviors was dependent on the MGMT methylation status in different GBM cells. Interestingly, ectopic expression of ADAMTS9-AS2 significantly upregulated the IC50 values of TMZ in both MGMT-positive cell lines T98G and U118 (**Supplementary Figures S2D,E**) and MGMT-negative cell lines U251 and U87 (**Supplementary Figures S2F,G**). These data collectively support that ADAMTS9-AS2 might represent a predictive marker of TMZ chemosensitivity in GBM cells in MGMT-independent mechanisms.

In addition, it has been previously demonstrated that the cancer cells with chemoresistance phenotype exhibit a mesenchymal phenotype with increased migration and invasion capacity compared with the parental cells. Given that metastasis

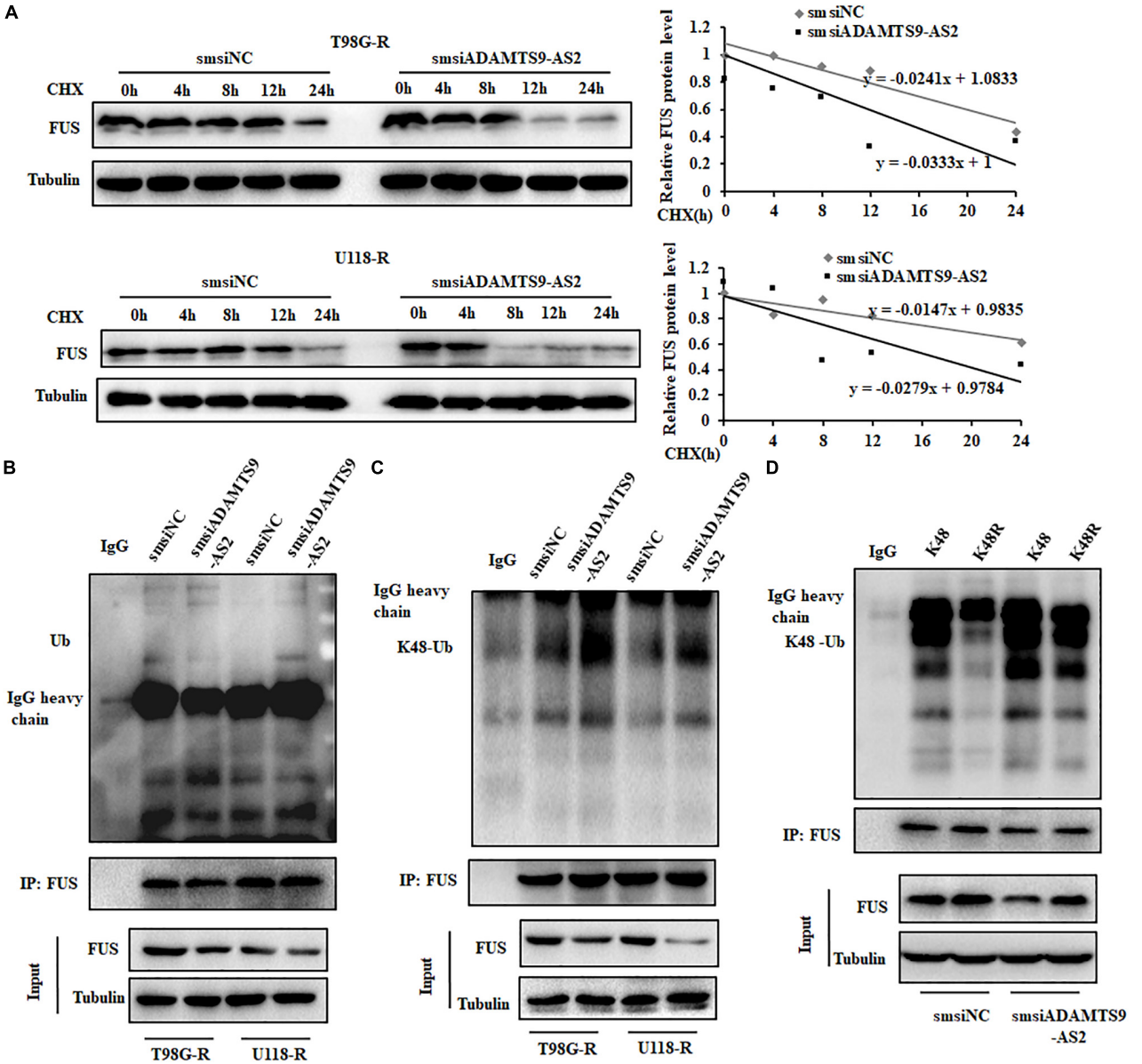

FIGURE 6 | ADAMTS9-AS2 enhances FUS stability by weakening its K48-linked ubiquitination. **(A)** After treatment with CHX (20 μg/ml) for indicated times, protein levels of FUS were determined by western blot analyses of lysates from ADAMTS9-AS2 knockdown cells T98G-R and U118-R. Western blot analysis of ubiquitin **(B)** and K48-ubiquitin **(C)** immunoprecipitated with anti-FUS antibodies in T98G-R and U118-R cells. **(D)** Western blot analysis of K48-ubiquitin immunoprecipitated with anti-FUS antibodies in ADAMTS9-AS2 downregulated HEK293T cells. Experiments were repeated three times with similar results.

might have promising roles in chemotherapeutic responses (Park et al., 2016; Ingham and Schwartz, 2017), we further assessed whether ADAMTS9-AS2 might influence invasion and migration. As expected, compared to the untreated group, ADAMTS9-AS2 knockdown significantly inhibited invasion in chemoresistant T98G-R and U118-R cells (**Figure 4E** and **Supplementary Figure S2H**). Scratch analysis showed reduced migratory ability in ADAMTS9-AS2 knock down T98G-R and U87-R cells (**Figure 4F** and **Supplementary Figure S2I**). Taken together, these finding illustrate that ADAMTS9-AS2 expression induces TMZ resistance via modulation of metastasis, and inhibition of ADAMTS9-AS2 resensitizes TMZ-resistant GBM cells to TMZ.

ADAMTS9-AS2 Binds to FUS and Reduces Its K48-Linked Ubiquitination

To screen for interactions between ADAMTS9-AS2 and protein complexes that potentially act as protein scaffolds, we used the RAID algorithm (Yi et al., 2017) to identify proteins that bind to ADAMTS9-AS2. FUS, an RNA-binding protein, was identified as the main protein associated with ADAMTS9-AS2

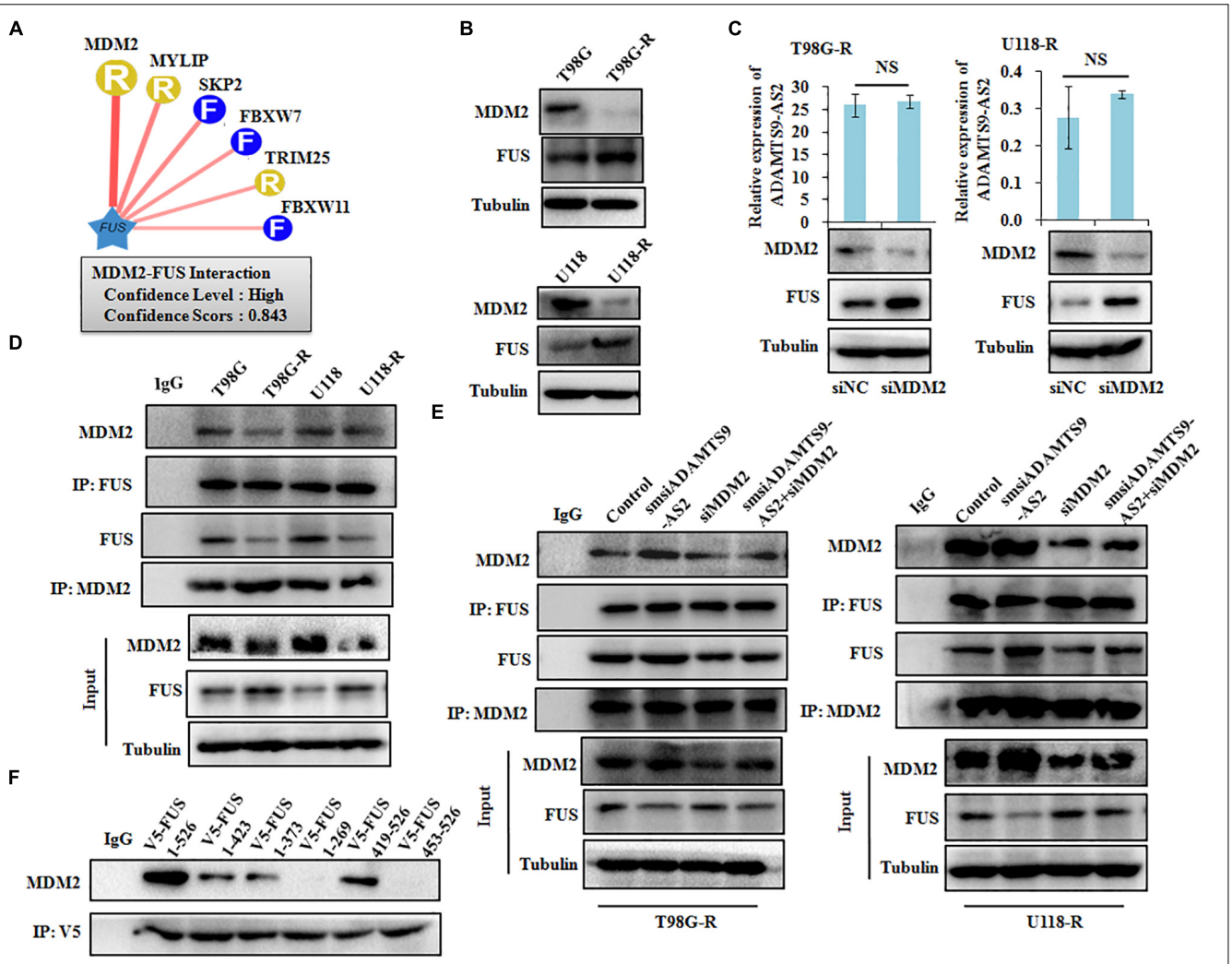

FIGURE 7 | ADAMTS9-AS2 attenuates MDM2-mediated FUS ubiquitination and degradation. **(A)** The UbiBrowser tool identified the E3 ligase that interacts with FUS. **(B)** Protein levels of FUS and MDM2 were determined by western blot analyses of lysates from T98G-R and U118-R TMZ-resistant cells. **(C)** Expression levels of ADAMTS9-AS2 and FUS were analyzed in MDM2 knockdown cells T98G-R and U118-R. **(D)** IP analysis revealed the FUS/MDM2 interaction in T98G-R and U118-R cells. **(E)** IP analysis revealed the FUS/MDM2 interaction in ADAMTS9-AS2 and MDM2 downregulated cells T98G-R and U118-R. **(F)** After transfection with the truncated versions of V5-FUS in HEK293T cells, proteins isolated from IP assays using anti-V5 tag antibody were identified by western blot analyses using a specific MDM2 antibody. All data are representative of three independent experiments, and representative images are shown.

(**Figure 5A**). First, we applied nuclear and cytoplasmic extraction to visualize the cellular localization and relative abundance of ADAMTS9-AS2 and FUS in TMZ-resistant cells, T98G-R and U118-R. We found that ADAMTS9-AS2 and FUS are primarily distributed in the nuclear region (**Figure 5B** and **Supplementary Figure S3A**). Furthermore, knockdown of ADAMTS9-AS2 by smsiRNAs downregulated FUS protein levels in T98G-R and U118-R cells (**Figure 5C** and **Supplementary Figure S3B**). However, no significant changes in ADAMTS9-AS2 were seen in FUS siRNA-treated cells (**Figure 5D** and **Supplementary Figure S3C**). These data indicate that FUS is a downstream effector of ADAMTS9-AS2. Resistance to TMZ is partly implicated to the low MGMT promoter methylation status and enhanced DNA repair function. To illustrated the mechanism, ADAMTS9-AS2 and FUS expression were analyzed in both MGMT-negative cell lines U251 and U87 and MGMT-positive cell lines U118 and T98G (**Supplementary Figure S3D**). The results showed higher expression of ADAMTS9-AS2 and FUS in relative TMZ-resistant cells than the sensitive GBM cell lines. In addition, we evaluated the effects of ADAMTS9-AS2/FUS on TMZ response in GBM cells. In response to different doses or durations of TMZ treatment, the variation of ADAMTS9-AS2 was very similar to that of FUS in the parent cells, T98G and U118 (**Figures 5E,F** and **Supplementary Figures S3E,F**), supporting the idea that the ADAMTS9-AS2/FUS axis is involved in TMZ chemotherapy.

Next, to confirm the association between ADAMTS9-AS2 and FUS, we used proteins isolated from the RNA pull-down assays and found that ADAMTS9-AS2 directly interacts with both endogenous and exogenous FUS (**Figure 5G**). Moreover, RIP was performed using a specific FUS antibody to ensure that

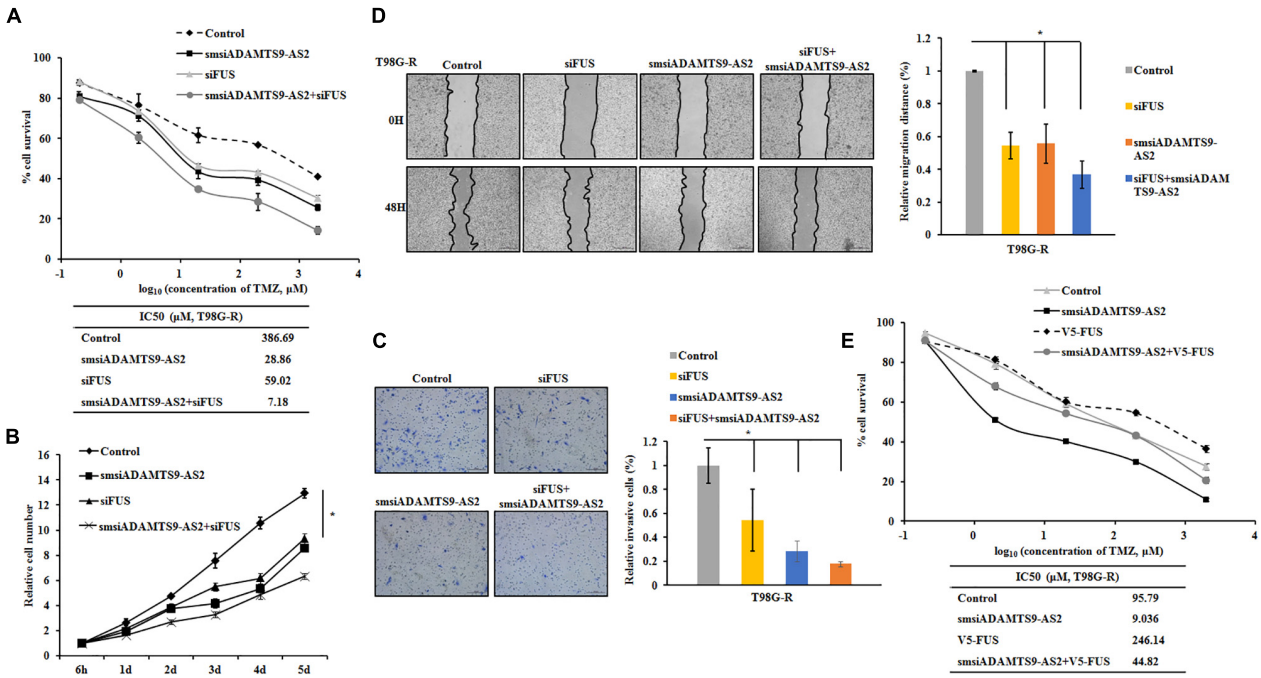

FIGURE 8 | Knockdown of ADAMTS9-AS2/FUS promotes TMZ chemosensitivity in T98G-R cells. TMZ IC_{50} value **(A)**, relative cell number **(B)**, invasion **(C)**, and migration **(D)** were examined in T98G-R cells after knockdown of ADAMTS9-AS2 and FUS. **(E)** FUS overexpression could rescue the inhibitory effects of ADAMTS9-AS2 knockdown in T98G-R cells. The above experiments were repeated independently three times with similar results. *$p < 0.05$ were regarded as statistically significant.

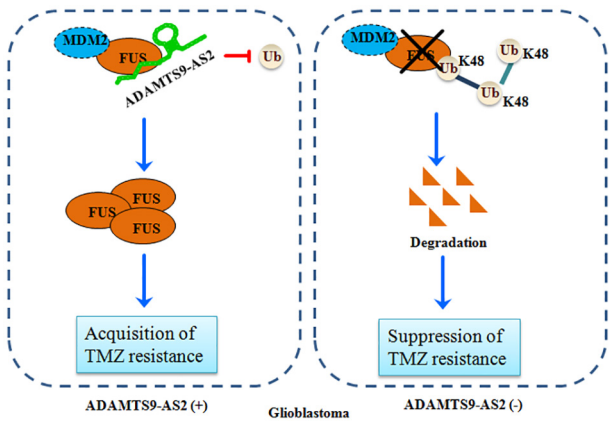

FIGURE 9 | A schematic for FUS stabilization by ADAMTS9-AS2, which promotes TMZ resistance in GBM cells. ADAMTS9-AS2 binds to FUS and interferes with its MDM2-mediated K48 polyubiquitination and degradation. The FUS protein is stabilized by ADAMTS9-AS2 overexpression and promotes cell metastasis, which is required for development of TMZ resistance in GBM cells.

ADAMTS9-AS2 was specifically immunoprecipitated from cell lysates. The binding capacity in TMZ-resistant cells was much stronger than in parent cells (**Figure 5H**), and knockdown of ADAMTS9-AS2 significantly weakened the association between ADAMTS9-AS2 and FUS (**Figure 5I**). In addition, based on the predicted binding sites of ADAMTS9-AS2 in the FUS protein sequence (**Figure 5A**), we obtained a series of vectors encoding V5-tagged FUS deletion mutants. RIP was performed using a specific V5 antibody to determine that ADAMTS9-AS2 specifically immunoprecipitates FUS through both the RRM and Znf_RanBP2 domains (**Figure 5J**). Thus, these data confirm that ADAMTS9-AS2 directly binds to FUS *in vitro*.

As FUS transcriptional levels did not change in ADAMTS9-AS2-downregulated T98G-R or U118-R cells (**Figure 5D** and **Supplementary Figure S3C**), we performed CHX chase assays to determine the protein stability of FUS. While knockdown of ADAMTS9-AS2 surprisingly attenuated the half-life of the FUS protein in TMZ-resistant cells, T98G-R and U118-R (**Figure 6A**), its overexpression promoted it (**Supplementary Figure S4**). Moreover, global and K48-linked ubiquitination of FUS in ADAMTS9-AS2-downregulated T98G-R and U118-R cells was more augmented than in controls (**Figures 6B,C**). In HEK293T cells transfected with ADAMTS9-AS2, V5-FUS, and K48-Ubiquitin, ADAMTS9-AS2 knockdown robustly enhanced FUS K48-linked ubiquitination, but this effect was compromised in the presence of the K48R mutant (**Figure 6D**). These data indicate that ADAMTS9-AS2 inhibits proteasome-dependent degradation of FUS.

To identify characteristics of the E3 ligase that interact with FUS, we used a computational predictive system, UbiBrowser (Li et al., 2017). As shown in **Figure 7A**, FUS interacts most strongly with the murine double minute 2 (MDM2) E3 ligase, with a confidence score of 0.843. Western blot

analysis revealed that low MDM2 levels and high FUS levels are clearly seen in T98G-R and U118-R cells (**Figure 7B**). Furthermore, FUS expression was upregulated in MDM2-downregulated cells, whereas there was no significant change in ADAMTS9-AS2 transcription (**Figure 7C**). Moreover, the FUS-MDM2 interaction was decreased in T98G-R and U118-R cells (**Figure 7D**). Knockdown of MDM2 weakened its FUS binding ability, leading to upregulated FUS expression (**Figure 7E**). We further scanned the interaction between MDM2 and FUS when ADAMTS9-AS2 was knocked down. The FUS/MDM2 interaction was enhanced in ADAMTS9-AS2 knock down T98G-R and U118-R cells (**Figure 7E**). Then, after full-length and truncated FUS proteins were expressed in HEK293T cells, IP analysis determined that all of FUS fragments containing the RRM or Znf_RanBP2 domains specifically immunoprecipitated MDM2 (**Figure 7F**). Together, these results demonstrate that ADAMTS9-AS2 might attenuate the interaction between FUS and MDM2, inhibiting MDM2-mediated FUS K48-ubiquitination and degradation.

The Effect of Modulating ADAMTS9-AS2/FUS on TMZ Chemosensitivity

To further determine the role of ADAMTS9-AS2/FUS in regulating therapeutic response to TMZ, we used T98G-R and U118-R cell lines stimulated with RNA interference silencing technology to downregulate the ADAMTS9-AS2/FUS signaling pathway. Under these conditions, IC_{50} values and cell proliferation rates were both significantly inhibited in ADAMTS9-AS2 or FUS downregulated cells (**Figures 8A,B** and **Supplementary Figures S5A,B**), indicating enhanced TMZ chemosensitivity. In addition, transwell and scratch assay showed similar effects for ADAMTS9-AS2 and FUS knockdown with significant inhibition of migration and invasion in both T98G-R and U118-R cells (**Figures 8C,D** and **Supplementary Figures S5C,D**). Moreover, combined knockdown of ADAMTS9-AS2 and FUS further promoted the sensitivity of TMZ-resistant cells to TMZ (**Figures 8A–D** and **Supplementary Figures S5A–D**). However, overexpression of FUS could rescue the inhibitory effects of ADAMTS9-AS2 knockdown in both T98G-R and U118-R cells (**Figure 8E** and **Supplementary Figure S5E**). These data indeed support the conclusion that ADAMTS9-AS2 inhibition enhances the antitumor effect of TMZ in GBM cells by down-regulating FUS expression.

DISCUSSION AND CONCLUSION

Over the last decade, it has been increasingly demonstrated that the majority of the mammalian genome is pervasively transcribed, resulting in the production of numerous lncRNAs (Kopp and Mendell, 2018). Accumulating evidence indicates that abnormal lncRNAs play multiple roles in maintaining tumor initiation and progression, demonstrating their crucial clinical potential as biomarkers and therapeutic targets (Slaby et al., 2017; Xu et al., 2017). However, the detailed functions of lncRNAs in GBM resistance to TMZ remains to be elucidated in detail. In this present study, we demonstrated that ADAMTS9-AS2 could directly bind to FUS and interfere with its MDM2-mediated K48 polyubiquitination. FUS stabilization by ADAMTS9-AS2 overexpression promotes the cell metastatic behavior, which is required for the TMZ resistance of GBM cells (**Figure 9**).

Growing evidence indicates that lncRNAs regulate the expression of target genes in glioma cells. While dependent upon the cellular and environmental context, interesting conflicting outcomes have been shown regarding lncRNAs in cancer diagnose and prognosis. For example, the lncRNA MALAT1 was categorized as a tumor-suppressive gene in glioma via ERK/MAPK-mediated growth and MMP2-mediated invasiveness, while Xiong et al. found that MALAT1 enhances glioma stem cell viability and promotes gliomagenesis through suppressing miR-129 and facilitating *SOX2* expression (Han et al., 2016; Xiong Z. et al., 2018). ADAMTS9-AS2 was first identified as a novel tumor suppressor that is regulated by DNA methyltransferase-1 (DNMT1). Knockdown of ADAMTS9-AS2 by siRNA inhibited the migration of glioma cells (Yao et al., 2014). Recent studies have revealed ADAMTS9-AS2 is a double-edged sword in the initiation and malignant progression of human cancers. Compared to adjacent normal tissue, ADAMTS9-AS2 is downregulated in colorectal cancer and predicts improved prognosis in colorectal cancer patients (Li Q. et al., 2016). In contrast, ADAMTS9-AS2 levels have been found at significantly higher levels in epithelial ovarian cancer than in normal ovaries and benign ovarian cysts shown by lncRNA microarray profiling (Wang H. et al., 2016). Upregulation of ADAMTS9-AS2 facilitates cell migration and invasion via targeting miR-143-3p/integrin α6 signaling in salivary adenoid cystic carcinoma (Xie et al., 2018). However, the roles of ADAMTS9-AS2 in TMZ-resistant GBM remain unclear. We performed the first ADAMTS9-AS2/FUS combination analysis in GBM and identified ADAMTS9-AS2 as a proto-oncogene that promotes TMZ resistance through stabilizing the FUS protein. Further clarifying the functions of ADAMTS9-AS2 might uncover the nature of GBM and provide novel targets for treatment.

The RNA-binding-protein FUS, also known as translocated in liposarcoma (TLS), is a critical regulator during the characteristic pathological features of amyotrophic lateral sclerosis (Sun et al., 2015). Recently, studies have found that FUS mRNA or protein expression is upregulated in liposarcoma (Spitzer et al., 2011), breast cancer (Ke et al., 2016), cervical cancer (Zhu et al., 2018), and FUS promotes malignant progression in non-small cell lung cancer (Xiong D. et al., 2018). Functioning as an oncoprotein, FUS has been proven to be essential for the growth of prostate cancer cells by activating androgen receptor signaling (Haile et al., 2011). Reducing FUS expression significantly abrogated lncRNA NEAT1 mediated cell survival in breast cancer cells (Ke et al., 2016). FUS also regulates the expression of 19 circRNAs by binding to introns in the splice regions, such as for circ_3279 and circ_5306. In glioma, silencing of the FUS gene inhibits the proliferation and migration of neuroblastoma cells and increases their chemical sensitivity to cisplatin by promoting

expression of miRNA-141 (Wang Z. et al., 2016). In glioma-exposed endothelial cells (GECs), the FUS protein combines with circ_002136, which acts as a miR-138-5p molecular sponge, upregulating SOX13 and SPON2 and increasing angiogenesis of GECs (He et al., 2019). However, the biological significance of the FUS-mediated therapeutic response is not fully understood. Our study is the first to demonstrate that ADAMTS9-AS2 interacts with FUS in the nucleus to inhibit MDM2-medicated FUS K48-ubiquitination and degradation, which inhibits migration and proliferation in GBM TMZ-resistant cells. Identifying cellular mechanism that drive GBM to be recur and TMZ resistant is critical to improving outcomes in patients. Additional studies are needed to focus on how this resistance developed during the course of GBM progression, especially the development of TMZ resistance at different time interval. Also, the addition of primary GBM cells obtained from patients are needed to determine ADAMTS9-AS2 mediated FUS/MDM2 ubiquitination axis in future studies.

This is the first study to provide a detailed characterization of the ADAMTS9-AS2/FUS/MDM2 axis in GBM TMZ resistance. A better understanding of the potential roles of lncRNAs in GBM biology, especially the characteristics of glioma patients, is of great significance for the progression of gene-targeted therapy.

DATA AVAILABILITY STATEMENT

The raw data supporting the conclusions of this manuscript will be made available by the authors, without undue reservation, to any qualified researcher.

ETHICS STATEMENT

The studies involving human participants were reviewed and approved by the Chinese Clinical Trial Register (ChiCTR-RPC-16008569) and the ethics committee of Xiangya Hospital (Changsha, China). The patients/participants provided their written informed consent to participate in this study.

AUTHOR CONTRIBUTIONS

YY, ZX, and ZG performed most of the experiments, analyzed the data, and wrote the manuscript. LQ, SZ, XC, and JW helped to perform some of the experiments. ZL, ZZ, XL, and LH provided the study material and supported administrative management. LS conceived and supervised the study, and reviewed and approved the manuscript. All authors read and approved the final manuscript.

FUNDING

This study was supported by grants from the National Natural Science Foundation of China (81572946, 81803035, and 81703036), Natural Science Foundation of Hunan Province, China (2019JJ50932), and Youth Fund of Xiangya Hospital (2017Q17).

ACKNOWLEDGMENTS

We thank Elsevier's Language Editing for assistance with English language polishing.

SUPPLEMENTARY MATERIAL

The Supplementary Material for this article can be found online at: https://www.frontiersin.org/articles/10.3389/fcell.2019.00217/full#supplementary-material

FIGURE S1 | Establishment and characterization of the U118-R TMZ-resistant GBM cell line. **(A)** Cell viability and IC_{50} analysis was performed to evaluate cytotoxicity of TMZ to U118 and U118-R cells in response to treatment with indicated concentrations of TMZ for 72 h. **(B)** U118 and U118-R cells were treated with 100 μM TMZ for 3 and 5 days, and cell cycle was examined by flow cytometry. The above experiments were repeated independently three times with similar results. Each data point represents mean ± SD.

FIGURE S2 | ADAMTS9-AS2 supports TMZ resistance in GBM cells U118-R. **(A)** qPCR confirmed smart silencer-mediated knockdown of ADAMTS9-AS2. Relative cell number **(B)** and IC_{50} values **(C)** were examined in U118-R cells after knockdown of ADAMTS9-AS2. **(D,E)** Ectopic expression of ADAMTS9-AS2 significantly upregulated IC50 values of TMZ in MGMT-positive cell lines T98G and U118. **(F,G)** Ectopic expression of ADAMTS9-AS2 significantly upregulated IC50 values of TMZ in MGMT-negative cell lines U251 and U87. Invasion ability **(H)** and migration ability **(I)** were examined in U118-R cells after knockdown of ADAMTS9-AS2. Quantitative results shown are of three independent experiments and represent the mean ± SD. $^{*}p < 0.05$, $^{**}p < 0.01$.

FIGURE S3 | ADAMTS9-AS2 upregulates the FUS protein, which is involved in TMZ response in U118-R cells. **(A)** Subcellular localization of ADAMTS9-AS2 and FUS analyzed from nuclear and cytoplasmic extracts in U118-R cells. **(B)** Protein levels of FUS were determined by western blot analyses of lysates from U118-R ADAMTS9-AS2 downregulated cells. **(C)** qPCR assay of ADAMTS9-AS2 and FUS transcript expression in U118-R ADAMTS9-AS2 or FUS knock down cells. **(D)** ADAMTS9-AS2 and FUS Protein levels were evaluated in both MGMT-negative cell lines U251 and U87 and MGMT-positive cell lines U118 and T98G. Upon different durations **(E)** or doses **(F)** of TMZ treatment, the variation tendency of ADAMTS9-AS2 and FUS was analyzed in U118 cells.

FIGURE S4 | ADAMTS-AS2 regulate the FUS protein stability in parental cells. After treatment with CHX (20 μg/ml) for indicated times, protein levels of FUS were determined by western blot analyses of lysates from ADAMTS9-AS2 over-expressed cells T98G and U118.

FIGURE S5 | ADAMTS9-AS2/FUS knockdown promotes TMZ chemosensitivity in U118-R cells. TMZ IC_{50} value **(A)**, relative cell number **(B)**, invasion **(C)**, and migration **(D)** were examined in U118-R cells after knockdown of ADAMTS9-AS2 and FUS. **(E)** FUS overexpression could rescue the inhibitory effects of ADAMTS9-AS2 knockdown in U118-R cells. The above experiments were repeated independently three times with similar results. $^{*}p < 0.05$, $^{**}p < 0.01$.

TABLE S1 | The sequences for the primers, siRNAs and smsiRNAs.

TABLE S2 | Baseline demographic and clinical characteristics according to ADAMTS9-AS2 expression.

TABLE S3 | The information of indicated primary antibodies.

DATA SHEET S1 | The certificates of cell authenticity by STR analysis. The data sheet contains original STR analysis results, as well as final certification report of glioma cells.

REFERENCES

Amodio, N., Raimondi, L., Juli, G., Stamato, M. A., Caracciolo, D., Tagliaferri, P., et al. (2018). MALAT1: a druggable long non-coding RNA for targeted anti-cancer approaches. *J. Hematol. Oncol.* 11:63. doi: 10.1186/s13045-018-0606-4

Chen, Q., Cai, J., Wang, Q., Wang, Y., Liu, M., Yang, J., et al. (2018). Long noncoding RNA NEAT1, regulated by the EGFR pathway, contributes to glioblastoma progression through the WNT/beta-Catenin pathway by scaffolding EZH2. *Clin. Cancer Res.* 24, 684–695. doi: 10.1158/1078-0432.CCR-17-0605

Chen, X., Zhang, M., Gan, H., Wang, H., Lee, J. H., Fang, D., et al. (2018). A novel enhancer regulates MGMT expression and promotes temozolomide resistance in glioblastoma. *Nat. Commun.* 9:2949. doi: 10.1038/s41467-018-05373-4

Dai, S., Yan, Y., Xu, Z., Zeng, S., Qian, L., Huo, L., et al. (2017). SCD1 confers temozolomide resistance to human glioma cells via the Akt/GSK3beta/beta-catenin signaling axis. *Front. Pharmacol.* 8:960. doi: 10.3389/fphar.2017.00960

Garnier, D., Meehan, B., Kislinger, T., Daniel, P., Sinha, A., Abdulkarim, B., et al. (2018). Divergent evolution of temozolomide resistance in glioblastoma stem cells is reflected in extracellular vesicles and coupled with radiosensitization. *Neuro Oncol.* 20, 236–248. doi: 10.1093/neuonc/nox142

Haile, S., Lal, A., Myung, J. K., and Sadar, M. D. (2011). FUS/TLS is a co-activator of androgen receptor in prostate cancer cells. *PLoS One* 6:e24197. doi: 10.1371/journal.pone.0024197

Han, Y., Wu, Z., Wu, T., Huang, Y., Cheng, Z., Li, X., et al. (2016). Tumor-suppressive function of long noncoding RNA MALAT1 in glioma cells by downregulation of MMP2 and inactivation of ERK/MAPK signaling. *Cell Death Dis.* 7:e2123. doi: 10.1038/cddis.2015.407

He, Z., Ruan, X., Liu, X., Zheng, J., Liu, Y., Liu, L., et al. (2019). FUS/circ_002136/miR-138-5p/SOX13 feedback loop regulates angiogenesis in Glioma. *J. Exp. Clin. Cancer Res.* 38:65. doi: 10.1186/s13046-019-1065-7

Hombach-Klonisch, S., Mehrpour, M., Shojaei, S., Harlos, C., Pitz, M., Hamai, A., et al. (2018). Glioblastoma and chemoresistance to alkylating agents: involvement of apoptosis, autophagy, and unfolded protein response. *Pharmacol. Ther.* 184, 13–41. doi: 10.1016/j.pharmthera.2017.10.017

Huang, T., Wan, X., Alvarez, A. A., James, C. D., Song, X., Yang, Y., et al. (2019). MIR93 (microRNA -93) regulates tumorigenicity and therapy response of glioblastoma by targeting autophagy. *Autophagy* 15, 1100–1111. doi: 10.1080/15548627.2019.1569947

Ingham, M., and Schwartz, G. K. (2017). Cell-cycle therapeutics come of age. *J. Clin. Oncol.* 35, 2949–2959. doi: 10.1200/JCO.2016.69.0032

Jain, A. K., Xi, Y., McCarthy, R., Allton, K., Akdemir, K. C., Patel, L. R., et al. (2016). LncPRESS1 Is a p53-regulated LncRNA that safeguards pluripotency by disrupting SIRT6-mediated de-acetylation of histone H3K56. *Mol. Cell* 64, 967–981. doi: 10.1016/j.molcel.2016.10.039

Kaur, S., Ramdzan, Z. M., Guiot, M. C., Li, L., Leduy, L., Ramotar, D., et al. (2018). CUX1 stimulates APE1 enzymatic activity and increases the resistance of glioblastoma cells to the mono-alkylating agent temozolomide. *Neuro Oncol.* 20, 484–493. doi: 10.1093/neuonc/nox178

Ke, H., Zhao, L., Feng, X., Xu, H., Zou, L., Yang, Q., et al. (2016). NEAT1 is required for survival of breast cancer cells through FUS and miR-548. *Gene Regul. Syst. Biol.* 10(Suppl. 1), 11–17. doi: 10.4137/GRSB.S29414

Kim, S. S., Harford, J. B., Moghe, M., Rait, A., Pirollo, K. F., and Chang, E. H. (2018). Targeted nanocomplex carrying siRNA against MALAT1 sensitizes glioblastoma to temozolomide. *Nucleic Acids Res.* 46, 1424–1440. doi: 10.1093/nar/gkx1221

Kopp, F., and Mendell, J. T. (2018). Functional classification and experimental dissection of long noncoding RNAs. *Cell* 172, 393–407. doi: 10.1016/j.cell.2018.01.011

Li, J., Han, L., Roebuck, P., Diao, L., Liu, L., Yuan, Y., et al. (2015). TANRIC: an interactive open platform to explore the function of lncRNAs in cancer. *Cancer Res.* 75, 3728–3737. doi: 10.1158/0008-5472.CAN-15-0273

Li, J. R., Sun, C. H., Li, W., Chao, R. F., Huang, C. C., Zhou, X. J., et al. (2016). Cancer RNA-Seq nexus: a database of phenotype-specific transcriptome profiling in cancer cells. *Nucleic Acids Res.* 44, D944–D951. doi: 10.1093/nar/gkv1282

Li, Q., Dai, Y., Wang, F., and Hou, S. (2016). Differentially expressed long non-coding RNAs and the prognostic potential in colorectal cancer. *Neoplasma* 63, 977–983. doi: 10.4149/neo_2016_617

Li, Y., Li, L., Wang, Z., Pan, T., Sahni, N., Jin, X., et al. (2018). LncMAP: pan-cancer atlas of long noncoding RNA-mediated transcriptional network perturbations. *Nucleic Acids Res.* 46, 1113–1123. doi: 10.1093/nar/gkx1311

Li, Y., Xie, P., Lu, L., Wang, J., Diao, L., Liu, Z., et al. (2017). An integrated bioinformatics platform for investigating the human E3 ubiquitin ligase-substrate interaction network. *Nat. Commun.* 8:347. doi: 10.1038/s41467-017-00299-9

Mazor, G., Levin, L., Picard, D., Ahmadov, U., Caren, H., Borkhardt, A., et al. (2019). The lncRNA TP73-AS1 is linked to aggressiveness in glioblastoma and promotes temozolomide resistance in glioblastoma cancer stem cells. *Cell Death Dis.* 10:246. doi: 10.1038/s41419-019-1477-5

Park, J. S., Kim, I. K., Han, S., Park, I., Kim, C., Bae, J., et al. (2016). Normalization of tumor vessels by Tie2 activation and Ang2 inhibition enhances drug delivery and produces a favorable tumor microenvironment. *Cancer Cell* 30, 953–967. doi: 10.1016/j.ccell.2016.10.018

Peng, Z., Liu, C., and Wu, M. (2018). New insights into long noncoding RNAs and their roles in glioma. *Mol. Cancer* 17:61. doi: 10.1186/s12943-018-0812-2

Sa, L., Li, Y., Zhao, L., Liu, Y., Wang, P., Liu, L., et al. (2017). The role of HOTAIR/miR-148b-3p/USF1 on regulating the permeability of BTB. *Front. Mol. Neurosci.* 10:194. doi: 10.3389/fnmol.2017.00194

Schmitt, A. M., and Chang, H. Y. (2016). Long noncoding RNAs in cancer pathways. *Cancer Cell* 29, 452–463. doi: 10.1016/j.ccell.2016.03.010

Slaby, O., Laga, R., and Sedlacek, O. (2017). Therapeutic targeting of non-coding RNAs in cancer. *Biochem. J.* 474, 4219–4251. doi: 10.1042/BCJ20170079

Song, E. L., Xing, L., Wang, L., Song, W. T., Li, D. B., Wang, Y., et al. (2019). LncRNA ADAMTS9-AS2 inhibits cell proliferation and decreases chemoresistance in clear cell renal cell carcinoma via the miR-27a-3p/FOXO1 axis. *Aging* 11, 5705–5725. doi: 10.18632/aging.102154

Spitzer, J. I., Ugras, S., Runge, S., Decarolis, P., Antonescu, C., Tuschl, T., et al. (2011). mRNA and protein levels of FUS, EWSR1, and TAF15 are upregulated in liposarcoma. *Genes Chromosomes Cancer* 50, 338–347. doi: 10.1002/gcc.20858

Stupp, R., Taillibert, S., Kanner, A., Read, W., Steinberg, D., Lhermitte, B., et al. (2017). Effect of tumor-treating fields plus maintenance temozolomide vs maintenance temozolomide alone on survival in patients with glioblastoma: a randomized clinical trial. *JAMA* 318, 2306–2316. doi: 10.1001/jama.2017.18718

Stupp, R., Taillibert, S., Kanner, A. A., Kesari, S., Steinberg, D. M., Toms, S. A., et al. (2015). maintenance therapy with tumor-treating fields plus temozolomide vs temozolomide alone for glioblastoma: a randomized clinical trial. *JAMA* 314, 2535–2543. doi: 10.1001/jama.2015.16669

Sun, S., Ling, S. C., Qiu, J., Albuquerque, C. P., Zhou, Y., Tokunaga, S., et al. (2015). ALS-causative mutations in FUS/TLS confer gain and loss of function by altered association with SMN and U1-snRNP. *Nat. Commun.* 6:6171. doi: 10.1038/ncomms7171

Teng, J., Hejazi, S., Hiddingh, L., Carvalho, L., de Gooijer, M. C., Wakimoto, H., et al. (2018). Recycling drug screen repurposes hydroxyurea as a sensitizer of glioblastomas to temozolomide targeting de novo DNA synthesis, irrespective of molecular subtype. *Neuro Oncol.* 20, 642–654. doi: 10.1093/neuonc/nox198

Wang, H., Fu, Z., Dai, C., Cao, J., Liu, X., Xu, J., et al. (2016). LncRNAs expression profiling in normal ovary, benign ovarian cyst and malignant epithelial ovarian cancer. *Sci. Rep.* 6:38983. doi: 10.1038/srep38983

Wang, H. W., Xu, Z. K., Song, Y., and Liu, Y. G. (2017). Correlations of MGMT genetic polymorphisms with temozolomide resistance and prognosis of patients with malignant gliomas: a population-based study in China. *Cancer Gene Ther.* 24, 215–220. doi: 10.1038/cgt.2017.7

Wang, Z., Lei, H., and Sun, Q. (2016). MicroRNA-141 and its associated gene FUS modulate proliferation, migration and cisplatin chemosensitivity in neuroblastoma cell lines. *Oncol. Rep.* 35, 2943–2951. doi: 10.3892/or.2016.4640

Xie, S., Yu, X., Li, Y., Ma, H., Fan, S., Chen, W., et al. (2018). Upregulation of lncRNA ADAMTS9-AS2 promotes salivary adenoid cystic carcinoma metastasis via PI3K/Akt and MEK/Erk signaling. *Mol. Ther.* 26, 2766–2778. doi: 10.1016/j.ymthe.2018.08.018

Xiong, D., Wu, Y. B., Jin, C., Li, J. J., Gu, J., Liao, Y. F., et al. (2018). Elevated FUS/TLS expression is negatively associated with E-cadherin expression and prognosis of patients with non-small cell lung cancer. *Oncol. Lett.* 16, 1791–1800. doi: 10.3892/ol.2018.8816

Xiong, Z., Wang, L., Wang, Q., and Yuan, Y. (2018). LncRNA MALAT1/miR-129 axis promotes glioma tumorigenesis by targeting SOX2. *J. Cell Mol. Med.* 22, 3929–3940. doi: 10.1111/jcmm.13667

Xu, N., Liu, B., Lian, C., Doycheva, D. M., Fu, Z., Liu, Y., et al. (2018). Long noncoding RNA AC003092.1 promotes temozolomide chemosensitivity through miR-195/TFPI-2 signaling modulation in glioblastoma. *Cell Death Dis.* 9:1139. doi: 10.1038/s41419-018-1183-8

Xu, Z., Yan, Y., Qian, L., and Gong, Z. (2017). Long non-coding RNAs act as regulators of cell autophagy in diseases (Review). *Oncol. Rep.* 37, 1359–1366. doi: 10.3892/or.2017.5416

Yan, Y., Xu, Z., Dai, S., Qian, L., Sun, L., and Gong, Z. (2016). Targeting autophagy to sensitive glioma to temozolomide treatment. *J. Exp. Clin. Cancer Res.* 35:23. doi: 10.1186/s13046-016-0303-5

Yan, Y., Xu, Z., Li, Z., Sun, L., and Gong, Z. (2017). An insight into the increasing role of LncRNAs in the pathogenesis of gliomas. *Front. Mol. Neurosci.* 10:53. doi: 10.3389/fnmol.2017.00053

Yao, J., Zhou, B., Zhang, J., Geng, P., Liu, K., Zhu, Y., et al. (2014). A new tumor suppressor LncRNA ADAMTS9-AS2 is regulated by DNMT1 and inhibits migration of glioma cells. *Tumour Biol.* 35, 7935–7944. doi: 10.1007/s13277-014-1949-2

Yi, Y., Zhao, Y., Li, C., Zhang, L., Huang, H., Li, Y., et al. (2017). RAID v2.0: an updated resource of RNA-associated interactions across organisms. *Nucleic Acids Res.* 45, D115–D118. doi: 10.1093/nar/gkw1052

Zhang, M., Zhao, K., Xu, X., Yang, Y., Yan, S., Wei, P., et al. (2018). A peptide encoded by circular form of LINC-PINT suppresses oncogenic transcriptional elongation in glioblastoma. *Nat. Commun.* 9:4475. doi: 10.1038/s41467-018-06862-2

Zhu, H., Zheng, T., Yu, J., Zhou, L., and Wang, L. (2018). LncRNA XIST accelerates cervical cancer progression via upregulating Fus through competitively binding with miR-200a. *Biomed. Pharmacother.* 105, 789–797. doi: 10.1016/j.biopha.2018.05.053

Conflict of Interest: The authors declare that the research was conducted in the absence of any commercial or financial relationships that could be construed as a potential conflict of interest.

frontiers in Oncology

ORIGINAL RESEARCH
published: 18 October 2019
doi: 10.3389/fonc.2019.01081

The Reciprocal Interaction Between LncRNA CCAT1 and miR-375-3p Contribute to the Downregulation of IRF5 Gene Expression by Solasonine in HepG2 Human Hepatocellular Carcinoma Cells

Zheng Liu[1], ChangJu Ma[1], XiaoJuan Tang[1], Qing Tang[1], LiJie Lou[2], Yaya Yu[1], Fang Zheng[1], JingJing Wu[1], Xiao-bo Yang[3], Wei Wang[2,3]* and Swei Sunny Hann[1,3]**

[1] *Laboratory of Tumor Biology, The Second Clinical College of Guangzhou University of Chinese Medicine, Guangzhou University of Chinese Medicine, Guangzhou, China,* [2] *Department of Gastrointestinal Surgery, The Second Clinical College of Guangzhou University of Chinese Medicine, Guangzhou University of Chinese Medicine, Guangzhou, China,* [3] *Guangdong Provincial Key Laboratory of Clinical Research on Traditional Chinese Medicine Syndrome, The Second Clinical College of Guangzhou University of Chinese Medicine, Guangzhou University of Chinese Medicine, Guangzhou, China*

OPEN ACCESS

Edited by:
Deilson Elgui De Oliveira, São Paulo State University, Brazil

Reviewed by:
Hua Zhang, Guangdong Medical University, China
Zexian Liu, Sun Yat-sen University Cancer Center (SYSUCC), China

***Correspondence:**
Xiao-bo Yang
yangxiaobomd@163.com
Wei Wang
ww1640@yeah.net
Swei Sunny Hann
hann20102@outlook.com

Specialty section:
This article was submitted to Molecular and Cellular Oncology, a section of the journal Frontiers in Oncology

Received: *18 June 2019*
Accepted: *30 September 2019*
Published: *18 October 2019*

Citation:
Liu Z, Ma C, Tang X, Tang Q, Lou L, Yu Y, Zheng F, Wu J, Yang X, Wang W and Hann SS (2019) The Reciprocal Interaction Between LncRNA CCAT1 and miR-375-3p Contribute to the Downregulation of IRF5 Gene Expression by Solasonine in HepG2 Human Hepatocellular Carcinoma Cells. Front. Oncol. 9:1081. doi: 10.3389/fonc.2019.01081

Solasonine (SS), a natural glycoalkaloid component, has been shown to have potent inhibitory activity and cytotoxicity against many cancer types. However, the precise mechanisms underlying this, particularly in hepatocellular carcinoma (HCC) are poorly understood. In this study, we showed that SS inhibited growth of HCC cells. Mechanistically, we observed that SS increased the expression of miR-375-3p, whereas reducing levels of long non-coding RNAs (lncRNAs) CCAT1 was noticed in HepG2 HCC and other cells. In addition, we found that SS repressed transcription factors, SP1 and interferon regulatory factor 5 (IRF5), protein expressions. There was a reciprocal interaction among miR-375-3p, CCAT1, and SP1. Moreover, SS inhibited IRF5 promoter activity, which was not observed in cells transfected with excessive expressed SP1 vectors. Interestingly, exogenously expressed IRF5 was shown to reverse expressions of SS-inhibited CCAT1 and induced-miR-375-3p; and neutralized SS-inhibited growth of HCC cells. Similar results were also found *in vivo* mouse model. Collectively, our results show that SS inhibits HepG2 HCC growth through the reciprocal regulation between the miR-375-3p and lncRNA CCAT1, and this results in transcription factor SP1-mediated reduction of IRF5 expression. The regulations and interactions among miR-375-3p, CCAT1, SP1, and IRF5 axis unveil a novel molecular mechanism underlying the anti-HCC growth by SS. IRF5 may be a potential target for treatment of HCC.

Keywords: solasonine, HCC, IRF5, lncRNA CCAT1, miR-375-3p, SP1

INTRODUCTION

Hepatocellular carcinoma (HCC) is one of the most common malignancies with high frequencies of recurrence and metastasis. The treatment of HCC requires multidisciplinary treatment modalities (1). Although substantial treatment improvements have been made, HCC still remains to have a poor prognosis (1). Currently, there are limited treatment options for advanced HCC. The novel

therapeutic advances with several small molecules kinase inhibitors and immunotherapy, such as programmed death-ligand 1 (PD-L1)/programmed cell death 1 (PD-1) pathway, may likely change the treatment scenario of HCC (2, 3). Thus, searching and exploring novel strategies for the treatment of HCC is of great importance.

Numerous anti-cancer agents have been isolated from natural products, such as plants including their semi-synthetic and synthetic derivates. Among these, solasonine (SS), one major glycoalkaloid extracted from *S. lycocarpum* and found *Solanum* species, has been demonstrated anti-proliferative activity against many cancer types (4–7). SS could inhibit cell proliferation, migration and colony formation of glioma cells through targeting the anti-inflammatory molecules, NF-κB and mitogen-activated protein kinase (MAPK) signaling axis cascade (8). Another report investigated the anti-proliferative activity of SS against several cancer types and demonstrated that SS may be a potential anticancer drug candidate (5). Nevertheless, the precise molecular mechanism underlying the anti-cancer effects of SS still remains to be determined.

Long non-coding RNAs (lncRNAs), which lack a complete open reading frame and play an important role in biological processes, have been illustrated to function as important regulators in several biological functions, such as cell proliferation, differentiation and apoptosis, in cancer (9). Many lncRNAs are dysregulated and involved in tumorigenesis, progression, metastasis, prognosis, or diagnosis and even treatment in HCC (10). Among these, the expression of lncRNA, CCAT1, was markedly increased in the HCC tissues compared to that in the pair-matched non-cancerous tissues. CCAT1 promoted the proliferation and migration of HCC cells by functioning as a molecular sponge for miRNA let-7, and led to the control of endogenous targets, such as high-mobility group protein A2 (HMGA2) and c-Myc, suggesting that CCAT1 played a critical role in the growth and progression of HCC via competitively sponging to let-7 (11). In addition, Kaplan–Meier analysis found that the patients with reduced CCAT1 levels showed better overall survival compared to those with increased CCAT1 expression. Moreover, Cox proportional hazards analyses demonstrated that CCAT1 could be used as an independent prognostic indicator in patients with HCC (12). This finding, together with other reports, indicated that the aberrant expression of CCAT1 promoted proliferation, migration and invasion in HCC both *in vivo* and *in vitro* (13). However, the role of CCAT1 and the detailed molecular mechanism underlying the involvement of HCC development and progression still remain unknown.

MicroRNAs (miRNAs) have been involved in many types of diseases, including human cancer. A large body of evidence has demonstrated that miRNAs regulate multiple biological functions, such as cancer cell differentiation, growth, apoptosis and metastasis (14). MiR-375, which acted as a candidate tumor suppressor miRNA, has been showed to suppress growth and induce apoptosis in several cancer types (15–17). Studying the expression of miR-375 and its target gene SMAD family member 7 (SMAD7) polymorphisms (rs4939827) in colorectal cancer (CRC) patients found that there was a significant association between miR-375 and the susceptibility to CRC, and that miR-375 and rs4939827 SNP in SMAD7 could be considered as a potential biomarker for early diagnosis of CRC (18). MiR-375 was among the most downregulated miRNAs in resistant breast cancer cells. Forced expression of miR-375 could sensitize tamoxifen-resistant cells to tamoxifen and reversed epithelial-to-mesenchymal transition (EMT) in breast cancer cells, suggesting that miR-375 might be used for potential therapeutic approaches for the treatment of tamoxifen-resistant breast cancer (19). The lncRNA-miRNA regulatory networks, such as CCAT1 interacted with miRNAs, have been implicated to regulate tumorigenesis and progression in cancers including HCC (11, 14, 20). CCAT1 functions as a molecular regulator for miRNA by competitively sponging, and leading to regulate endogenous target gene expression and subsequent biological function (11, 21, 22).

Transcription factor interferon regulatory factor 5 (IRF5) has been shown to regulate the expression of genes involved in the inflammatory responses and the stimulation of the immune system (23). Moreover, studies have demonstrated that IRF5 negatively regulated cell growth and oncogene activation, favoring cell differentiation, apoptosis, and sensitivity to oncolytic therapy (24–26). IRF5 proved to be an adverse independent prognostic factor for overall survival (OS) and recurrence free survival (RFS) in clear cell renal cell carcinoma (ccRCC) cells (27). On the contrary, IRF5 also acts as a tumor suppressor in several human cancers (28, 29). Thus, the true role of this transcription factor in tumor biology remains to be undetermined. Given the role of IRF5 in pathogenesis, its clinical and prognostic value in cancer, IRF5 may represent a potential therapeutic target for cancer. The connection and interaction of miRNA and IRF5 have also been studied. MiR-146b was shown to target IRF5, resulting in the regulation of macrophage activation (30). miR-let7a also directly targeted pro-inflammatory gene high-mobility group protein A2 (HMGA2), thereby suppressing anti-citrullinated protein antibodies (ACPAs)-induced IRF5 expression through phosphoinositide 3-kinase (PI3-K) signaling in macrophages (31). However, until now, there has been less information demonstrating the links between IRF5 and lncRNA expression and function.

In the current study, we explored the potential mechanism underlying the anti-HCC cell growth by SS. We observed that SS inhibited HCC cell growth through the reciprocal regulation of miR-375-3p and CCAT1; this resulted in transcription factor SP1-mediated inhibition of IRF5 gene expression.

MATERIALS AND METHODS

Reagents and Cell Culture

Liver cancer cell line, HepG2, was obtained from the Cell Line Bank at the Laboratory Animal Center of Sun Yat-sen University (Guangzhou, China), Cell line, QGY-7703, and human normal hepatocyte (LO2) cells were obtained from Cell Bank of Chinese Academy of Science (Shanghai, China). All cell lines had no HCV infection. Monoclonal antibodies against SP1 and IRF5 were purchased from Cell Signaling Technology Inc. (Beverly, MA, USA) and AB

TABLE 1 | The information of critical reagents used in this study.

		Dilutions	Catalog numbers	Resources	Final concentration
Antibody	SP1	1:1,000	#9389	Cell Signaling Technology	
	IRF5	1:750	A1149	ABclonal Technology	
	GAPDH	1:20,000	ab128915	Abcam	
	Anti-rabbit IgG HRP-linked	1:2,000	#7074	Cell Signaling Technology	
Plasmids	pcDNA3.1			Dr. Thomas E. Eling	0.2 μg/mL
	EX-NEG-M02		EX-NEG-MO2	GeneCopoeia	0.2 μg/mL
	pcDNA3.1-SP1			Dr. Thomas E. Eling	2.0 μg/mL
	EX-NEG-M02-IRF5		EX-Z4372-MO2	GeneCopoeia	1.5 μg/mL
	EX-NEG-M02-CCAT1		CS-GS3356-MO2	GeneCopoeia	0.5 μg/mL
	pEZX-PL01-IRF5 promoter		HPRM33965-PL01	GeneCopoeia	1.0 μg/mL
NC/mimics	NC		miR 01101	Ribo Biological Co., Ltd.	100 nM
	miR-375-3p mimics		miR 10005307	Ribo Biological Co., Ltd.	100 nM

Colonel Technology Inc. (Wuhan, China), separately. 3-(4, 5-Dimethylthiazol-2-yl)-2, 5-diphenyltetra-zolium bromide (MTT) powder was provided by Sigma-Aldrich (St. Louis, MO, USA). 5-Ethynyl-2′-deoxyuridine (EdU) detection kit and miR-375-3p mimics were purchased from Ribo Biological Co., Ltd. (Guangzhou, China). Lipofectamine 3000 reagent was obtained from Life Technologies (Carlsbad, CA, USA). The pcDNA3.1 (control vector) and the SP1 overexpression plasmid were kindly provided by Dr. Thomas E. Eling (NIEHS, Research Triangle Park, NC, USA). The detailed information for the critical reagents used was summarized in **Table 1** (**Supplementary Material**). SS was purchased from Chengdu Must Biotechnology Company (Chengdu, Sichuan, China). Cells were cultured at 37°C in 5% CO2 in RPMI-1640 medium (GIBCO, Life Technologies, Grand Island, NY, USA) supplemented with 10% FBS (HyClone, Invitrogen, Camarillo, CA, USA), 100 U/mL penicillin and 100 μg/mL streptomycin (Invitrogen, Carlsbad, CA, USA). In addition, the medium grown HepG2-Luc was added with Geneticin G-418 Sulfate (Life Technologies, Carlsbad, CA, USA) (200 μg/mL).

Cell Viability Assay

HepG2 and QGY-7703 cells (3–5 x 10^3 cells/well) and normal hepatocyte (LO2) cells (3–5 x 10^3 cells/well) were seeded into a 96-well microtiter plate and treated with increasing concentrations of SS for up to 72 h. Cell viability was detected by MTT assay. The operational approach has been reported in a previous study (32). Lastly, an ELISA reader (Perkin Elmer, Victor X5, Waltham, MA, USA) was used to measure the absorbance at 570 nm. The calculation formula of cell viability (%) was as follows: (absorbance of test sample/absorbance of control) × 100. The cells treated with vehicle only (DMSO, 0.1% in media) was served as a zero control and the control values were set to 1 by default.

EdU Incorporation Assay

HepG2 and QGY-7703 cells (5 x 10^3 cells/well) were seeded into 96-well plates followed by treating with SS (45 μM) for 24 h. After 24 h, the medium was removed and the cells was cultured in a resuspended RPMI-1640 medium with 50 μM EdU for 2 h at 37°C, stained with Apollo reaction reagent. All DNA contents of the cells were stained with Hoechst 33342. At last, an inverted fluorescence microscope (Nikon, Ts2RFL, Tokyo, Japan) was used to take pictures at × 400 magnifications. Three captured fields were selected randomly and the EdU-positive cells were calculated. The calculation formula was as follows: percentage of EdU-positive cells = (EdU-positive cells/Hoechst stain cells) × 100.

TABLE 2 | The primer sequences of gene amplification by qRT-PCR.

Symbol	Primer	Primer sequence(5′-3′)
CCAT1	F-primer	5′-GCCGTGTTAAGCATTGCGAA-3′
	R-primer	5′-TCATGTCTCGGCACCTTTCC-3′
GAPDH	F-primer	5′-AAGCCTGCCGGTGACTAAC-3′
	R-primer	5′-GCGCCCAATACGACCAAATC-3′
miR-375-3p	F-primer	5′-TGCTTTGTTCGTTCGGCTC-3′
	R-primer	5′-TATGGTTGTTCACGACTCCTTCAC-3′
U6	F-primer	5′-ATTGGAACGATACAGAGAAGATT-3′
	R-primer	5′-GGAACGCTTCACGAATTTG-3′

Quantitative Real-time PCR

Total RNA of HepG2 and QGY-7703 cells from different treatment were extracted by using Trizol reagent (Invitrogen). RNA was reversed transcribed into cDNAs using the RT-PCR kit (TaKaRa, Dalian, China). The reverse-transcription step was carried out in triplicate and the total RNA concentration was the same in every sample. A quantitative real-time RT-PCR (qRT-PCR) assay was performed on an ABI 7500 Real-Time PCR System (Applied Biosystems, Grand Island, NY, USA) for the quantification of miR-375-3p and CCAT1 transcript using the SYBR Premix Dimmer Eraser kit (TaKaRa) and fluorescent RNA-binding dyes. All conductions were in accordance with the instructions provided by the manufacturer. Each sample was tested in triplicate, and reference genes were applied to normalize the results. The PCR conditions were as follows: 10 min at 95°C, followed by 40 cycles of 15 s at 95°C, and 1 min at 60°C. Threshold quantification cycle (C_q) was determined

for each sample/primer pair and the 2−ΔΔCt method was used to calculate the relative levels of specific molecules. The copy numbers were consistent with the anticipated result. The amplification efficiency for miR-375-3p and CCAT1 was 100.95 and 100.35%, respectively. The forward and reverse primer sequences used in qRT-PCR are shown in **Table 2** (**Supplementary Material**). The procedure was based on the guidelines of the minimum information for publication of qRT-PCR experiments (MIQE) (33).

Western Blot Analysis

HepG2 and QGY-7703 cells were seeded into 6-well plates at a density of 4×10^5 cells/well or 2×10^5 cells/well and treated with different conditions of SS for up to 48 h. The cells were lysed with 1 × RIPA buffer, which contained proteinase inhibitor cocktail, and the protein concentrations were measured. Equal amounts of protein were mixed in volumetric 3 × SDS sample buffer and separated on 10% SDS polyacrylamide gels. Primary antibody was incubated at 4°C overnight. Afterwards, secondary antibody raised against rabbit IgG conjugated to horse-radish peroxidase (Cell Signaling, Beverly, MA, USA) was incubated for 1 h at room temperature. Finally, signals were detected using a freshly prepared enhanced chemiluminescence solution (Millipore, Burlington, MA, USA) with a ChemiDoc XRS +System (Bio-Rad, Hercules, CA, USA). ImageJ software (National Institutes of Health, Bethesda, MD, USA) was used to quantify and compare the intensity of single band between the control and proteins of interest.

Transient Transfection Assays

HepG2 and QGY-7703 cells (2×10^5 cells/well) were seeded into 6-well plates and reached to 50–60% confluence before treatment. The mimics, inhibitors and the negative control of miR-375-3p were mixed with the ribo FECT™ CP transfection reagent (RiboBio Co., Guangzhou, China) in accordance with the instructions provided by the manufacturer; compounds were added to the cells and maintained for 48 h at 37°C. In separate experiments, HepG2 and QGY-7703 cells were seeded into 6-well plates at a density of 3×10^5 cells/well and transfected with the pcDNA3.1 (control plasmid), pcDNA3.1-SP1, overexpression plasmids of CCAT1 and IRF5 (EX-NEG-M02-CCAT1, EX-NEG-M02-IRF5), and the respective controls obtained from GeneCopoeia, Inc. (Rockville, MD, USA) with Lipofectamine 3000 reagent at a final concentration of 2 μg/mL for 6 h at 37°C followed by treatment with SS for the indicated time for all other experiments.

Luciferase Reporter Assay

HepG2 and QGY-7703 cells were seeded into 24-well plates at a density of 6.5×10^4 cells/well and reached to 50–60% confluence before treatment. The control plasmid pEZX-PL01 and pEZX-PL01-IRF5 promoter plasmids purchased from GeneCopoeia (Rockville, MD, USA) were transfected into the cells with Lipofectamine 3000 for 6 h, followed by treating with SS for an additional 24 h. The wild and mutation types of CCAT1 3′-UTR luciferase vectors were designed and synthesized by GeneCopoeia, Inc. (Rockville, MD, USA). These vectors were co-transfected into the cells with either miR-375-3p mimic or a negative control using Lipofectamine 3000 Reagent, followed by exposure of the cells to SS for an additional 24 h. The preparation of cell lysis and the measurement of luciferase activities were determined using the Luc-Pair™ Dual-Luminescence Assay Kit (GeneCopoeia), in accordance with the instructions provided by the manufacturer. In a separate experiment, the control and IRF5 promoter were transfected into the cells for 6 h before transfecting with the pcDNA3.1 and SP1 overexpression plasmids, and treated with SS for 24 h, followed by measuring luciferase activity using the Luc-Pair™ Dual-Luminescence Assay Kit (GeneCopoeia).

RNA Immunoprecipitation (RIP) Assay

The RNA immunoprecipitation (RIP) assay was performed using the Magna RIP™ RNA-Binding Protein Immunoprecipitation Kit (Millipore, Billerica, MA, USA), according to the manufacturer's instructions. Briefly, HepG2 and QGY-7703 cells (2.0×10^7) were rinsed and scraped with cold PBS, then lysed in complete RIP lysis buffer containing protease and RNase inhibitors. The cell lysis was incubated with RIP immunoprecipitation buffer containing magnetic beads conjugated with human anti-Ago2 antibody (Millipore, Billerica, MA, USA) (5 μg of total antibody used per immunoprecipitation) at room temperature for 30 min, and negative control IgG (Millipore, Billerica, MA, USA). The beads were then thoroughly washed and digested with proteinase K (30 min at 55°C) to disengage Ago2, containing ribonucleoprotein (RNP) complexes. Purified RNA was obtained and then applied to quantitative PCR with reverse transcription analysis. The expression of Ago2 was measured by Western blot.

Xenograft Tumor Study

Female nude mice (weight of 18–20 g), which were purchased from Beijing Vital River Laboratory Animal Technology Co., Ltd. (Beijing, China), were kept in a SPF environment at the Animal Center of Guangdong Provincial Hospital of Chinese Medicine. All animal experimental procedures were performed in accordance with the protocol approved by the Animal Care and Use Committee of Guangdong Provincial Hospital of Chinese Medicine and the National Institutes of Health Guide for the Care and Use of Laboratory Animals (the Ethics Approval Number 2018067). HepG2-Luc cells carrying luciferase reporter gene (HepG2-Luc, obtained from the Guangzhou Land Biological Technology Co., Guangzhou, China) were resuspended in 0.2 mL of phenol red-free RIPM 1640 with 2% FBS in a number of 2.0×10^6. The resuspended cells were then injected into the upper hind limb of the nude mice. Xenografts were expected to grow for 1 week when starting the first measurements. Mice were randomly divided into three groups: the control, low-dose group (SS, 5 mg/kg), and high-dose group (SS, 20 mg/kg), and were injected with reference substance or SS once a day via intraperitoneal injection for up to 15 days ($n = 9$ per group). Mice were then anesthetized by inhalation of 2% isoflurane and injected with the substrate D-Luciferin (Caliper Life Sciences, Hopkinton, MA, USA) at a dose of 150 mg/kg in 100 μL into the peritoneal cavity of the nude mice. The bioluminescence

imaging signal was determined using the IVIS200 Imaging System (Xenogen/Caliper, Alameda, CA, USA) at the first and end of the experiments (on day 2 and 15) and expressed as photons/sec. Tumor volume was calculated using the formula for a spheroid: volume = (width^2 × length) × 0.5 and the mice weights were measured once a week. All mice were sacrificed on the 15th day in accordance with the Guidelines for the Care and Use of Laboratory Animals. At the end of the experiments, xenograft tumors were isolated and expressions of miR-214-3p, CCAT1, SP1, and IRF5 were determined by qRT-PCR and Western blot, respectively.

Statistical Analysis

Data were generated from at least three separated experiments. Continuous variable of the date are presented as the mean ± SD. One-way ANOVA was used to detect the differences between groups, and significance of difference between particular treatment groups was analyzed by Dunnett's multiple comparison tests. GraphPad Prism software was used to create the diagram, and asterisks which indicated $P < 0.05$, showed the significant differences between experimental groups and the corresponding control condition.

RESULTS

Solasonine (SS) Inhibited Growth of HCC Cells

Previous studies from ours and others have shown that bioactive glycoalkaloids, such as SS, solasodine, and solamargine, inhibited growth of different cancer cells (8, 34, 35). In the current study, we showed that SS inhibited the growth of HCC cells in time-and dose-dependent manner as determined by MTT assay (**Figure 1A**). The IC50 values were 37.70, 33.88, 35.48 μM and 29.17, 31.83, 35.01 μM from 24 to 72 h in HepG2 and QGY7703 cells, respectively. This finding was also proven by another method for detecting cell proliferation-EdU incorporation assay. Please note that much lower toxicity profiles were observed when human hepatocytes LO2 cells were exposed to the same concentration of SS (IC50 values were 62.43, 49.84, 51.91 μM) from 24 to 72 h (**Figure 1A**). We demonstrated that the percentage of EdU positive HCC cells was significantly reduced in the SS-treated group compared to the control one (**Figure 1B**). These results suggested that SS inhibited the growth of HCC HepG2 and QGY7703 cells.

SS Increased the Expression of miR-375-3p and Inhibited the Levels of lncRNA CCAT1, and There Was Reciprocal Interaction of CCAT1 and miR-375-3p in HCC Cells

We next examined the possible targets that may be involved in the inhibitory effect of SS on cell growth. Studies have demonstrated the important roles of lncRNAs and miRNA, such as CCAT1 and miR-375, in different types of cancers, including HCC, and aberrant expressions of CCAT1 and miR-375 have been involved in several biological processes, such as cell proliferation, migration, and invasion, via regulating different target genes and signaling pathways (36–40). However, the biological role of either CCAT1 or miR-375 in HCC remains to be incompletely characterized. It was for these reasons that we explored the role of CCAT1 and miR-375 in mediating the anti-HCC effect of SS. Herein, our results unveiled that SS significantly increased miR-375-3p, while reduced lncRNA CCAT1 expression levels were observed in HepG2 and QGY7703 cells (**Figures 2A,B**). Of note, either the inhibitors of miR-375-3p or exogenously expressed CCAT1 significantly stimulated the growth of HepG2 and QGY7703 cells as determined by MTT assay (**Figures 2C,D**). Bioinformatics analyses have found that miR-375-3p could physical bind to CCAT1, we therefore want to examine whether miR-375-3p regulated expression of CCAT1. We found that the mimics of miR-375-3p reduced the luciferase activity in 3-UTR region of CCAT1 in HepG2 and QGY7703 cells (**Figure 2E**), and suppressed the expression of CCAT1 (**Figure 2F**). In addition, AGO_2 RIP assays showed that CCAT1 could bind with miR-375-3p (**Figure 2G**). Interestingly, we showed that exogenously expressed CCAT1 reduced the expression of miR-375-3p in HepG2 and QGY7703 cells (**Figure 2H**). Together, our results demonstrated that CCAT1 was a target of miR-375-3p and there was a reciprocal interaction between CCAT1 and miR-375-3p, which may be important targets of SS. Furthermore, inhibition of CCAT1 and induction of miR-375-3p were involved in the SS-mediated inhibition of HepG2 and QGY7703 cell growth.

SS and the Mimics of miR-375-3p Reduced SP1 Protein Expression Whereas Overexpressed CCAT1 Enhanced SP1 Protein Expression

To investigate the mechanism underlying the SS-regulated CCAT1 and miR-375-3p expressions, and identify relevant downstream target, we next began to test the biological significance of the interaction of CCAT1 and miR-375-3p in mediating the effect of SS. Transcription factors, such as SP1, have been shown to regulate the expression of multiple genes implicated in several biological functions, such as cell proliferation, progression, and cell death (41). More importantly, bioinformatics analysis and other experimental procedures showed that SP1 was a direct target of miR-375-3p (42–44). We found that SS reduced SP1 protein expressions (**Figure 3A**). Moreover, the mimics of miR-375-3p reduced, whereas excessive expression of CCAT1 enhanced SP1 protein expression in HepG2 and QGY7703 cells (**Figures 3B,C**). Interestingly, exogenously expressed SP1 was found to feedback resist SS-inhibited CCTA1 expression (**Figure 3D**), and SS-stimulated miR-375-3p (**Figure 3E**). These findings indicated that both CCAT1 and miR-375-3p acted as upstream factors, regulated the expression of SP1, and there were feedback regulatory loops between CCAT1, miR-375-3p and SP1, leading to the reciprocal interactive axis in this process.

SS Reduced IRF-5 Protein Expressions and Promoter Activity, Which Were Reversed by Excessive Expressed SP1

The master transcription factor IRF5 has been involved in the occurrence and progression of numerous diseases, including cancer (45). Bioinformatics analyses showed that the IRF5

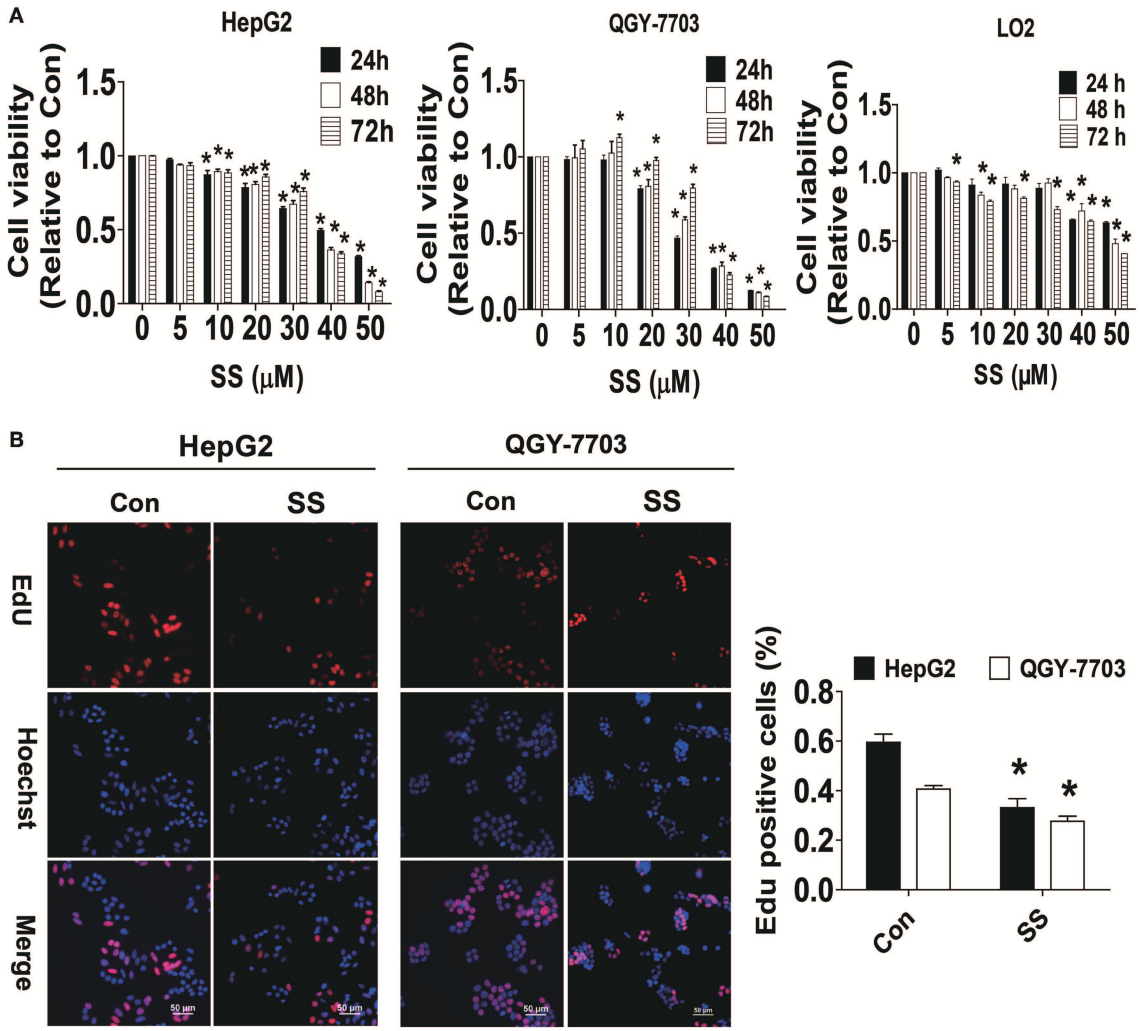

FIGURE 1 | SS inhibited growth of HCC cells. **(A)** HCC HepG2 and QGY-7703 cells (3–5 x 10^3 cells/well), normal hepatocyte (LO2) cells (3–5 x 10^3 cells/well) were treated with different concentrations of SS for up to 72 h. The cells were collected and processed for MTT assay as described in the Materials and Methods section. **(B)** HepG2 and QGY7703 cells were treated with SS (45 μM) for 24 h, followed by processing for measuring the cell growth by EdU DNA cell proliferation kit described in the Materials and Methods section. The image was magnified 10×. Hoechst was used to stain all the nuclei. At least 5 captured fields were randomly selected, and the percentage of EdU positive cells = (EdU positive cells/Hoechst stain cells) × 100. Scale bars, 50 μM. Values are given as the mean ± SD, from three independent experiments performed in triplicate. *Indicates significant difference as compared to the untreated control group ($P < 0.05$).

promoter region contained putative SP1 binding sites, and a series of gain and off-functional experiments suggested that the SP1 transcription factor was the primary determinant for activating the basal transcription of the IRF5 (46). Herein, we further delineate the association and role of IRF5 in this process. We showed that SS inhibited IRF5 protein expression in a dose-dependent fashion (**Figure 4A**) and the promoter activity in HepG2 and QGY7703 cells (**Figure 4B**), which was overcome in cells overexpressed SP1 gene in HepG2 and QGY7703 cells (**Figures 4C,D**). These findings confirmed that SP1, which acts as upstream factor of IRF5, regulated the expression of IRF5 in this process.

IRF5 Feedback Regulated CCAT1 Expression and Neutralized SS-Inhibited Cell Growth

To further delineate the role and illustrate the function of IRF5 in HCC growth, we assess the possibility of feedback regulatory loops. We showed that exogenously expressed IRF5 unexpectedly antagonized the SS-inhibited CCAT1, and SS-induced miR-375-3p expressions (**Figures 5A,B**), and more importantly, neutralized SS-inhibited HCC cell growth (**Figure 5C**). Three findings indicated that there were feedback regulatory loops and IRF5 played a critical role in mediating the SS-inhibited HCC cell proliferation.

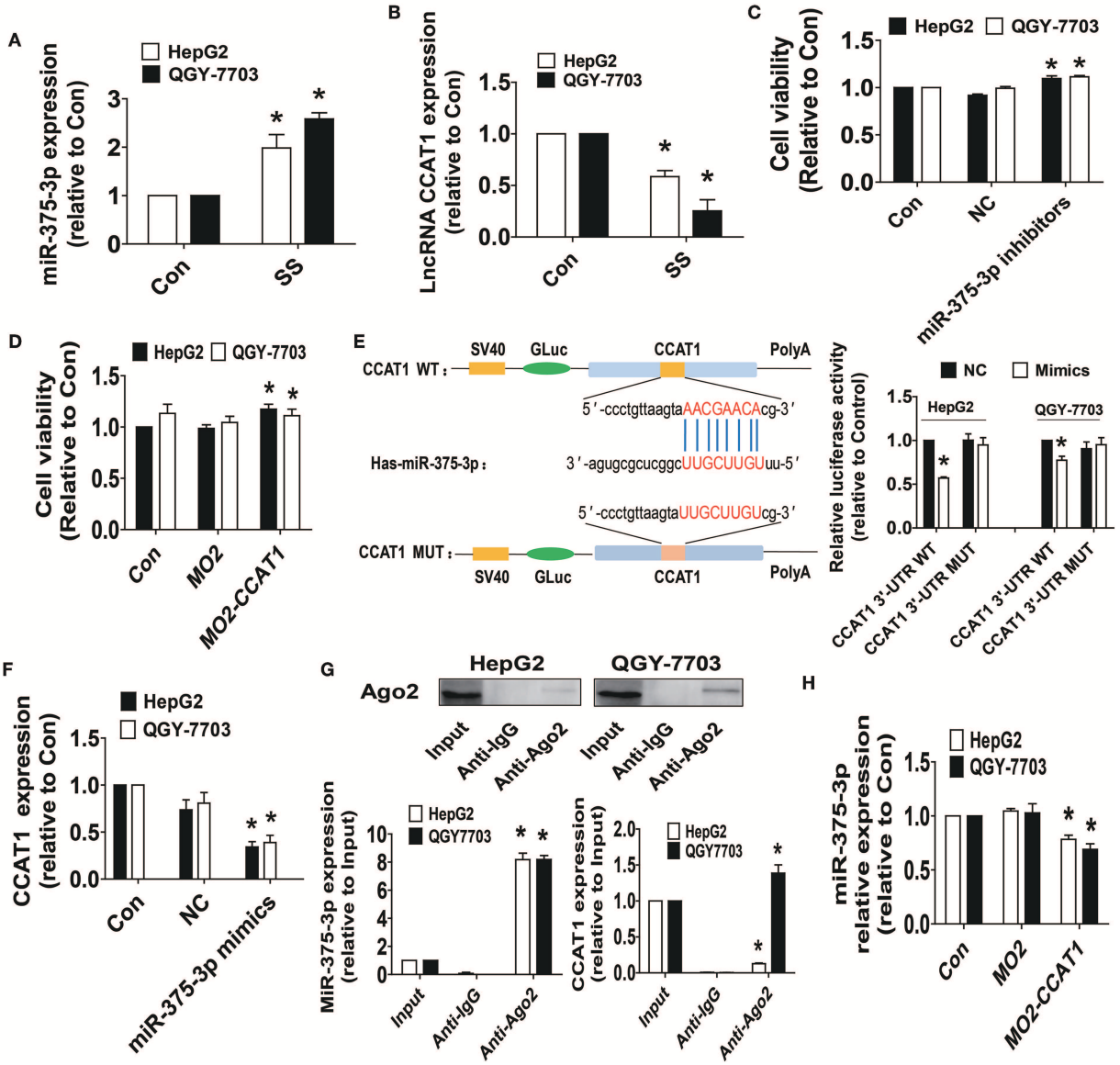

FIGURE 2 | SS increased the expression of miR-375-3p and inhibited the levels of lncRNA CCAT1, and there was reciprocal interaction of CCAT1 and miR-375-3p in HCC cells. **(A,B)** HepG2 and QGY7703 cells were treated with SS (45 μM) for 24 h, and the expression levels of miR-375-3p and CCAT1 were measured via qRT-PCR. **(C,D)** HepG2 and QGY7703 cells were transfected with the control or miR-375-3p mimics (100 nM), CCAT1 expression vectors for up to 48 h followed by determining cell growth via MTT assays. **(E)** The luciferase reporter constructs containing the wild type and mutant binding sites in 3′-UTR region of CCAT1 were shown (upper panel). HepG2 and QGY7703 cells were transfected with the CCAT1 3'UTR-WT or CCAT1 3′-UTR-Mut vectors (1.25 μg/mL each) for 24 h, then treated with the miR-375-3p mimics (100 nM) or miR-negative control (NC) for an additional 48 h. Afterwards, the luciferase activity was detected using Secrete-Pair™ Dual Luminescence Assay Kit as described in the Materials and Methods section (lower panel). **(F)** HepG2 and QGY7703 cells were treated with the control or miR-375-3p mimics (100 nM) for up to 48 h followed by determining the expression levels of CCAT1 via qRT-PCR. **(G)** Cell lysates from HepG2 and QGY7703 cells were incubated with Ago2 antibody-coated magnetic beads. Precipitates ware subjected to Western blot for Ago2 protein and qRT-PCR for detecting CCAT1 and miR-375-3p expression levels. Preimmune IgG and input from cell extracts were used as controls. **(H)** HepG2 and QGY7703 cells were transfected with the control or CCAT1 overexprssion vectors for up to 48 h followed by determining the expression levels of miR-375-3p via qRT-PCR. Values in bar graphs were given as the mean ± SD from three independent experiments. *Indicates significant difference as compared to the untreated control group ($P < 0.05$).

The Anti-HCC Effects by SS in a Mouse Xenograft Tumor Model

Finally, we further examined the role of SS on tumor growth *in vivo*. Mice bearing xenografted HCC HepG2-Luc cells were treated via intraperitoneal injection with either the control or SS for up to 15 days, followed by being given D-luciferin via intraperitoneal injection. The xenografts were assessed by *in vivo* bioluminescence imaging at the start and end of the

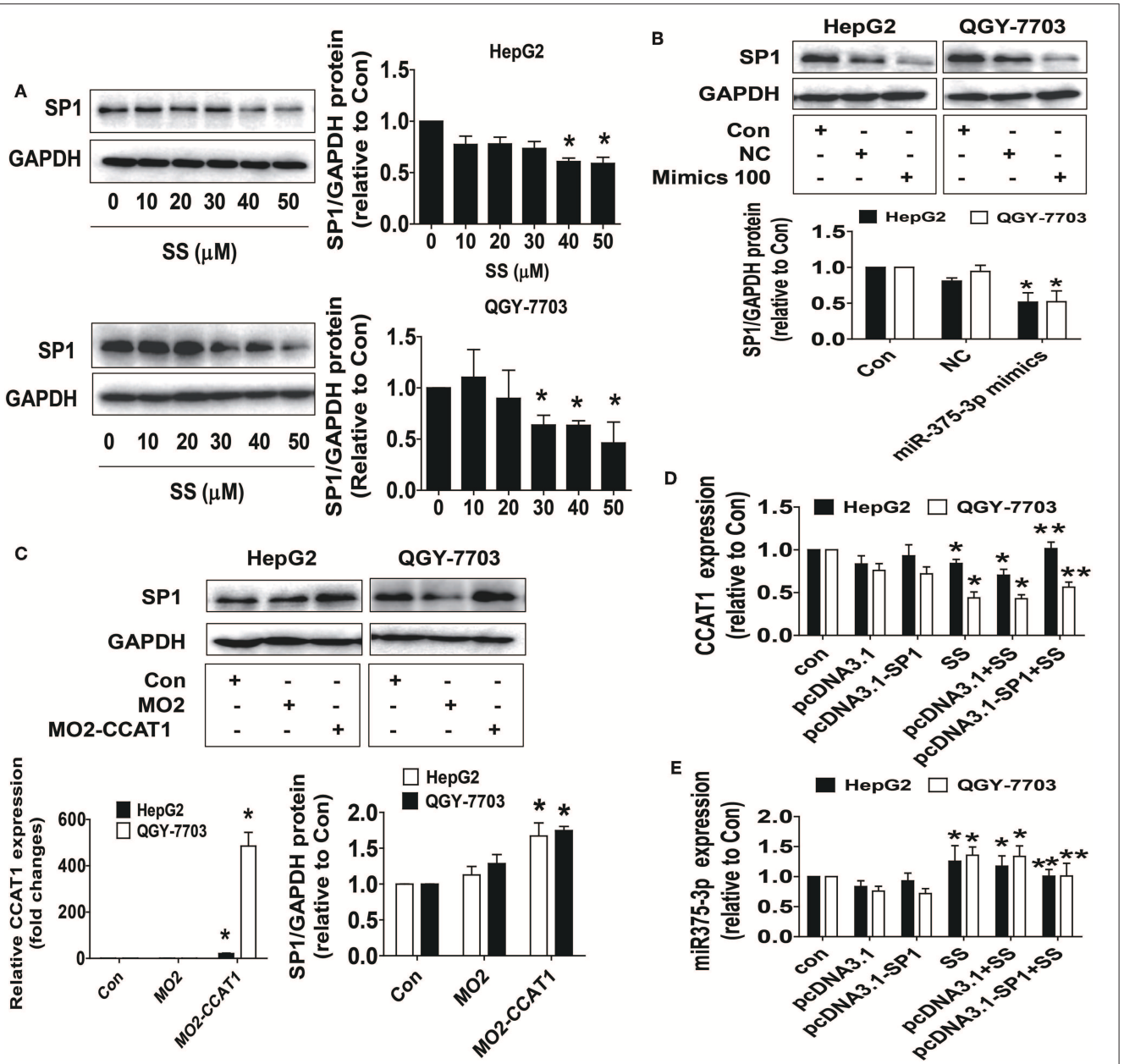

FIGURE 3 | SS and the mimics of miR-375-3p reduced SP1 protein expression whereas overexpressed CCAT1 enhanced SP1 protein expression. **(A)** HepG2 and QGY7703 cells were treated with different concentrations of SS for 24 h. The expression of SP1 protein was detected by Western blot. GAPDH was used as a loading control. **(B,C)** HepG2 and QGY7703 cells were treated with mimics of miR-375-3p or transfected with the control and excessive expressed CCAT1 vector for up to 24 h before exposing the cells to SS (45 μM) for an additional 24 h. Afterwards, the expressions of SP1 proteins were detected by Western blot. GAPDH was used as a loading control. The figures are representative cropped gels/blots that have been run under the same experimental conditions. **(D,E)** HepG2 and QGY7703 cells were transfected with the control or SP1 expression vectors for 24 h before exposing the cells to SS (45 μM) for an additional 24 h followed by measuring the expression levels of CCAT1 and miR-375-3p via qRT-PCR. Values in bar graphs were given as the mean ± SD from three independent experiments. *Indicates significant difference as compared to the untreated control group ($P < 0.05$); **Indicates significant difference from SS treated alone ($P < 0.05$).

experiments (on day 2 and 15). Through the Xenogen IVIS200 system, we found that the high doses of (20 mg/kg) SS-treated mice had a substantial inhibitory effect on tumor growth as compared to that in the control group (**Figure 6A**). In addition, compared to that in the control group, a significant reduction in the xenografted tumor weight and size (volume) was observed in the high dose of SS-treated group (**Figures 6B–D**). Moreover, consistent with the results from the *in vitro*, we observed the induction of miR-375-3p and reductions of CCAT1 expressions and SP1 and IRF5 protein levels from

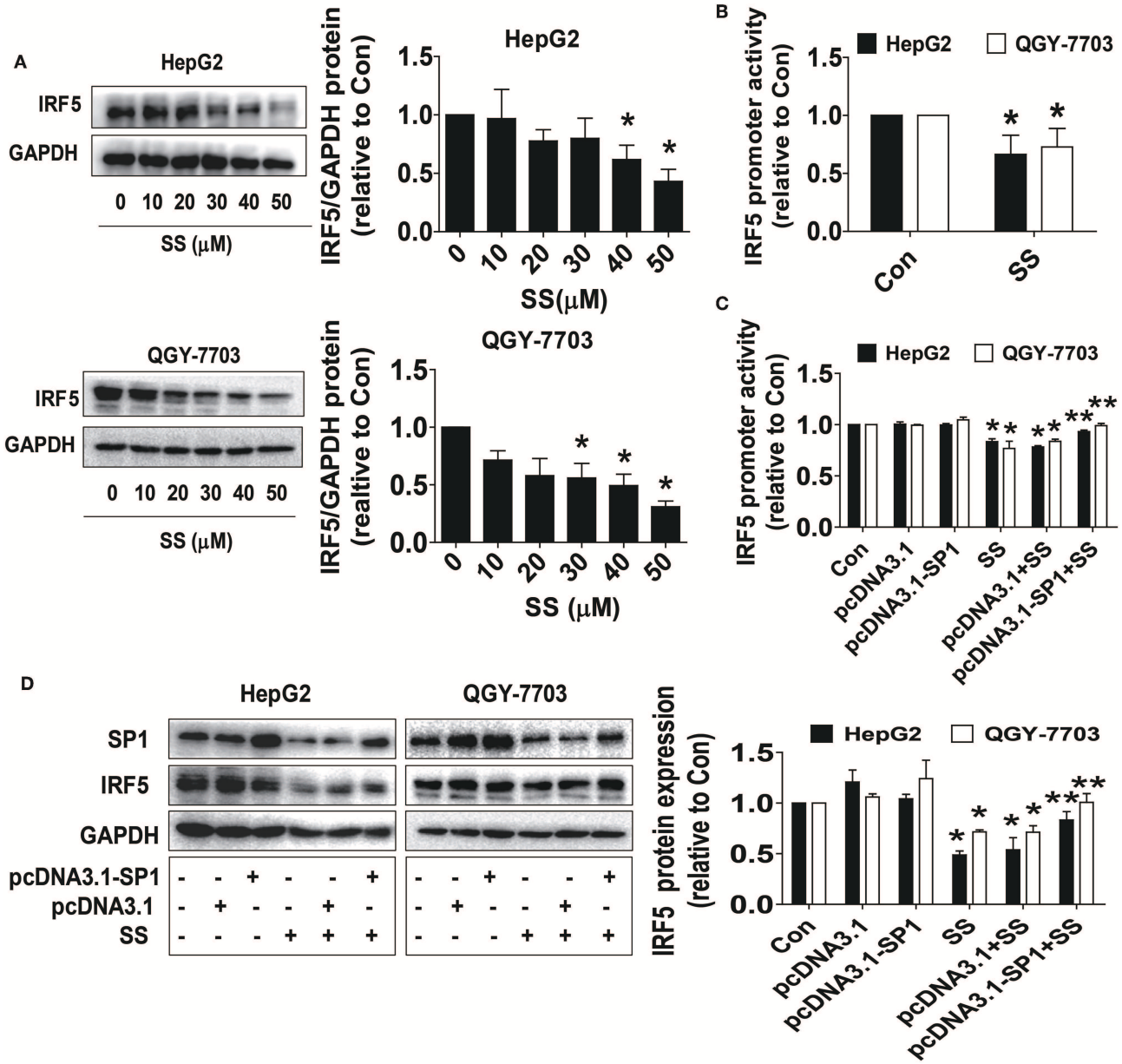

FIGURE 4 | SS reduced IRF-5 protein expressions and excessive expressed IRF5 neutralized SS-inhibited cell growth. **(A,B)** HepG2 and QGY7703 cells were treated with different concentrations of SS for 24 h or a wild type human IRF5 promoter reporter construct ligated to luciferase reporter gene and the internal control for 24 h, followed by treating with the SS (45 μM) for an additional 24 h. The expression of IRF5 protein and promoter activities were determined by Western Blot **(A)** and Dual-Luciferase Reporter Assay System **(B)** described in the Materials and Methods section. The figures are representative cropped gels/blots that have been run under the same experimental conditions. **(C,D)** HepG2 and QGY7703 cells were transfected with the control or SP1 expression vectors for 24 h, or a wild type human IRF5 promoter reporter construct ligated to luciferase reporter gene and the internal control for 24 h, followed by treating with the SS (45 μM) for an additional 24 h. Afterwards, The expression of IRF5 protein and promoter activities were determined by Dual-Luciferase Reporter Assay System **(C)** and Western Blot **(D)** and described in the Materials and Methods section. The figures are representative cropped gels/blots that have been run under the same experimental conditions. Values in bar graphs were given as the mean ± SD from three independent experiments. *Indicates significant difference as compared to the untreated control group ($P < 0.05$); **Indicates significant difference from SS treated alone ($P < 0.05$).

xenografted tumors obtained from the above experiments in the high dose SS-treated group, as compared to that in the control one, as determined by qRT-PCR and Western Blot, respectively (**Figures 6E–G**).

DISCUSSION

Several natural compounds and phytochemicals demonstrated many biological activities, such as antibacterial and anticancer

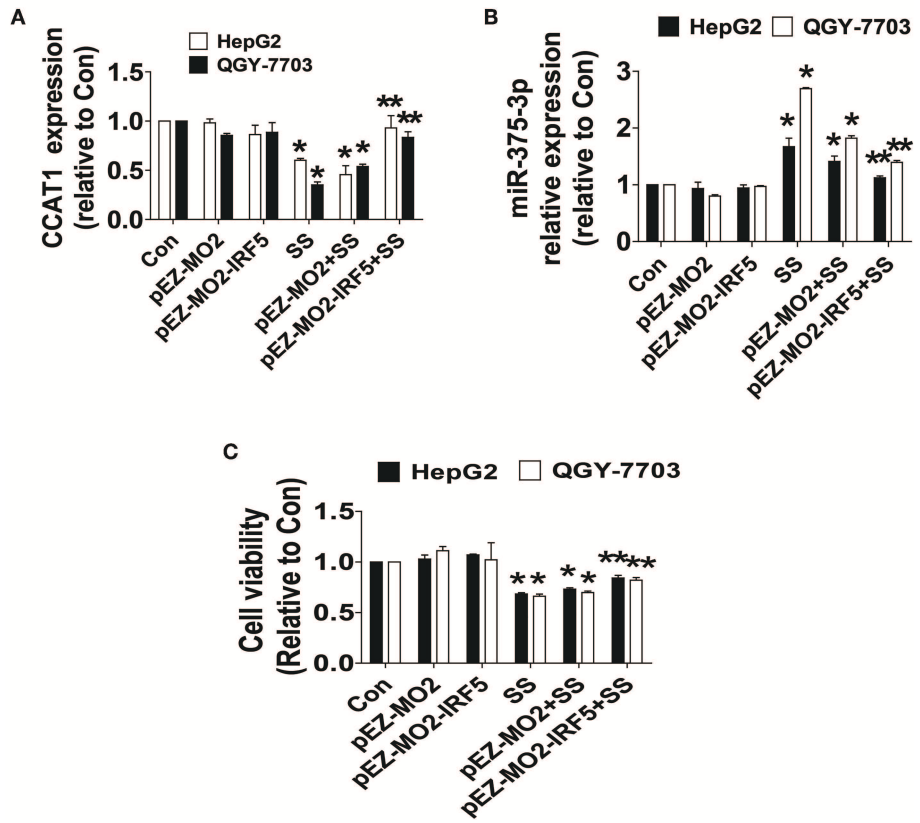

FIGURE 5 | IRF5 feedback regulated CCAT1 and miR-375-3p expression and neutralized SS-inhibited cell growth. **(A–C)** HepG2 and QGY7703 cells were transfected with the control or IRF5 expression vectors for 24 h followed by treating with the SS (45 μM) for an additional 24 h. Afterwards, The expression of CCAT1 and miR-375-3p, and cell growth were determined by qRT-PCR and MTT described in the Materials and Methods section, respectively. Values in bar graphs were given as the mean ± SD from three independent experiments. *Indicates significant difference as compared to the untreated control group ($P < 0.05$); **Indicates significant difference from SS treated alone ($P < 0.05$).

(47). Previous studies from ourselves and others have shown that bioactive glycoalkaloids, such as SS, solasodine, and solamargine, inhibited growth of several different cancer cells (8, 34, 35). These results suggested the therapeutic potential of SS in cancer treatment. However, the underlying molecular mechanisms in controlling human cancer proliferation by this agent still need to be determined. In the current study, we provided new evidence demonstrating the anti-HCC effect of SS. We observed that SS inhibited growth of HCC HepG2 cells through the reciprocal regulation between the miR-375-3p and lncRNA CCAT1, and this resulted in transcription factor SP1-mediated reduction of IRF5 gene expression. Our results showed relatively high IC50 values of SS in HepG2 and QGY7703 cells, respectively. We believe that the cell culturing and growth conditions when cells are exposed to SS, the genetic and biological variation of the HCC cell line itself and other unknown factors may have contributed to this relatively high dose response, although this may be the result of physiological ranges without noticeable toxicity. Consistent with this, one recent study showed that SS had cytotoxicity on HepG2 cells with IC50 of 91.8 ± 9.4 μM, while solamargine showed comparable potency against HepG2 cells with IC50 of 10.8 ± 0.1 μM, suggesting relatively weak cytotoxicity of SS in HCC cells (34). Of note, low IC50 value was reported in other cancer cell types using SS (5). Regardless, more experiments are strongly required to confirm potential anti-proliferative/cytotoxic effects of SS against cancer.

In this study, we demonstrated a role of miR-375-3p and lncRNA CCAT1 in mediating the anti-HCC cell growth. Our results indicated that the induction of miR-375-3p and reduction of CCAT1 involved in the SS-inhibited growth of HCC HepG2 cells and QGY7703 cells. MiR-375, acting as tumor suppressor, significantly inhibited cell proliferation and induced apoptosis in cancer cells via different mechanisms (36, 48, 49). However, the role of miR-375 in HCC has not been reported. Consistent with this, our results confirmed the tumor suppressor role and suggested the involvement of this miRNA in mediating the anti-HCC cell growth by SS. Our results also implied the oncogenic role of CCAT1 in this study. Studied have shown that CCAT1 played important roles in many cancers by stimulating cell proliferation, migration, invasion and metastasis (50). Interestingly, we demonstrated a reciprocal regulation between the miR-375-3p and CCAT1 in mediating the SS effect

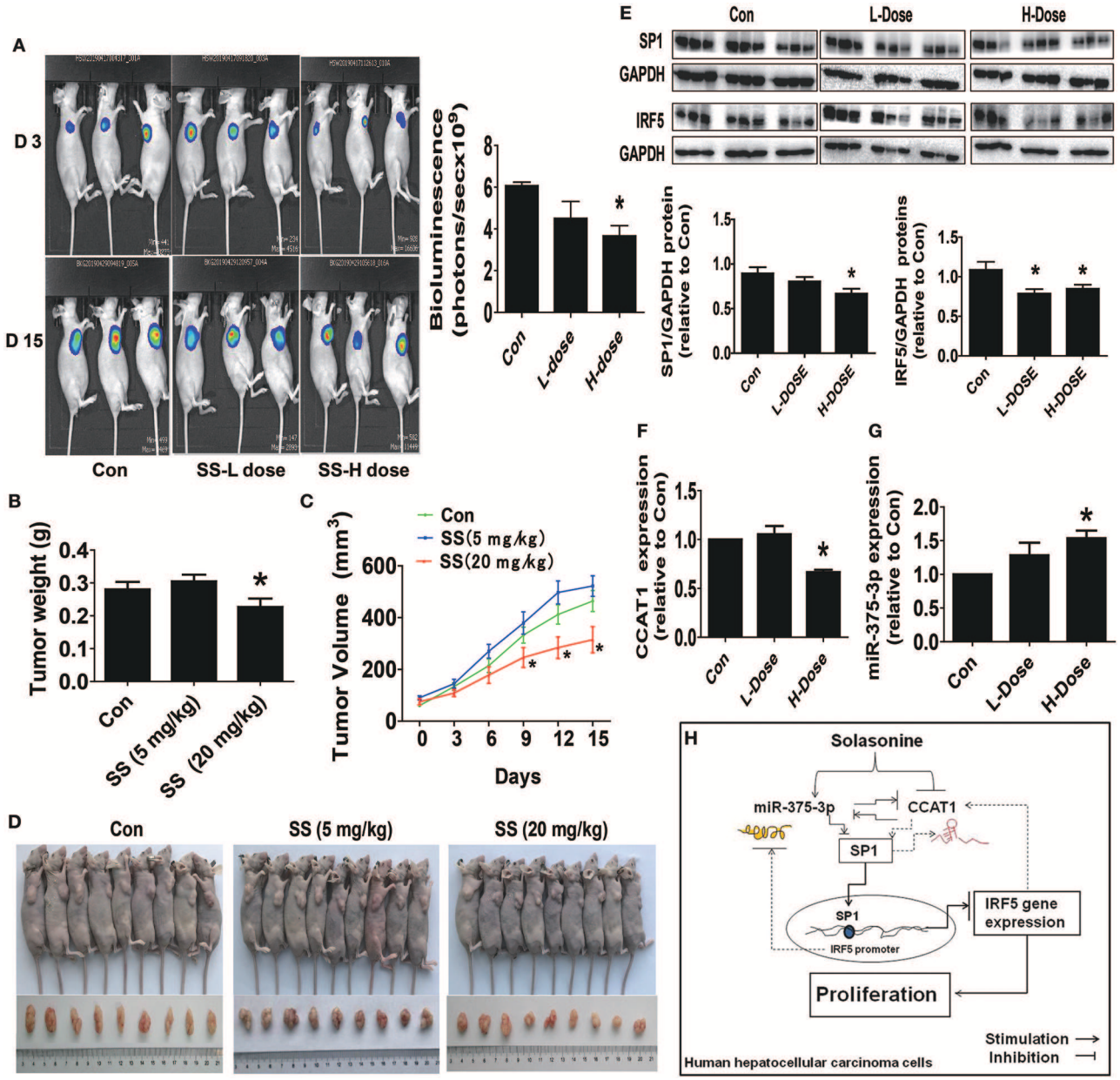

FIGURE 6 | The anti-HCC effects by SS in a mouse xenograft tumor model. **(A)** HepG2-Luc cells carrying luciferase reporter gene (HepG2-Luc, obtained from the Guangzhou Land Biological Technology Co., Guangzhou, China) were resuspended in 0.2 mL of phenol red-free RIPM 1640 with 2% FBS in a number of 2.0×10^6. Then, the resuspended cells were injected into the upper hind limb of the nude mice. Xenografts were expected to grow for 1 week when starting the first measurements. Mice were randomly divided into three groups: the control, low-dose group (SS, 5 mg/kg), and high-dose group (SS, 20 mg/kg), and were injected with reference substance or SS once a day via intraperitoneal injection for up to 15 days ($n = 9$ per group). The xenografts were assessed by *in vivo* bioluminescence imaging at the first and end of the experiments (on day 2 and 15). The tumor growth was monitored by injecting luciferin in the mice followed by measuring bioluminescence using IVIS Imaging System. Imaging and quantification of signals were controlled by the acquisition and analysis software living image as described in the Materials and Methods section. Representative images are shown. **(B,C)** The xenografts were harvested on day 15, and the weight **(B)** and volume **(C)** of tumors were measured. **(D)** The photographs of the vehicle- and drugs-treated xenografts derived from nude mice are shown. **(E–G)** At the end of the experiments, xenograft tumors were isolated from individual animals, and the corresponding lysates were processed and detected miR-375-3p and CCAT1 levels, SP1 and IRF5 protein expressions by qRT-PCR and Western blot, respectively. GAPDH was used as a loading control. The figures are representative cropped gels/blots that have been run under the same experimental conditions. The bar graphs represented the tumor weight and volume of mice results of as mean ± SD. *Indicates the significant difference from the untreated control ($p < 0.05$). **(H)** The diagram shows that SS inhibits HCC growth through the reciprocal regulation between the miR-375-3p and lncRNA CCAT1, this result in transcription factor SP1-mediated reduction of IRF5 gene expression. The interactions among miR-375-3p, CCAT1, SP1, and IRF5 axis unveil a novel molecular mechanism underlying the anti-HCC growth by SS.

in this process suggesting that there is direct binding of miR-375-3p to CCAT1, and CCAT1 was a direct target of miR-375-3p. The interaction of CCAT1 with miRNAs, other than miR-375, have been largely reported in other studies in different cancer types (38, 51, 52). CCAT1 was highly expressed in HCC tissues and cells, and involved in growth and metastasis. CCAT1 stimulated proliferation of HCC cells via regulation of CCNE1 expression by acting as a ceRNA to sponge miR-30c-2-3p (38). Our findings suggested that the CCAT1/miR-375-3p regulatory axis could be a potential target for HCC treatment. Other regulatory axes, such as CCAT1/let-7/high mobility group A2 (HMGA2) and c-Myc, have been reported to be involved in the HCC growth and invasion and metastasis (11). We believed that this would add the significant role of CCAT1, and implicate the potential application of CCAT1 for the prognosis and treatment of HCC. These also suggest that multiple targets and regulatory pathways have been involved in the anti-HCC effects. More importantly, we have observed how CCAT1 acted as ceRNA to sponge miR-375-3p, and there was a physical binding of CCAT1 to miR-375-3p affected in the presence of SM, resulting in the inhibition of CCAT1 expression. The true significance of this association and detailed mechanism underlying this process still needs to be determined in the future research.

We observed the role of transcription factor SP1. Our results suggested that both CCAT1 and miR-375-3p acted as upstream factors, regulating the expression of SP1 in this process. As a common transcription factor, SP1 has been associated with many biological processes, such as growth, apoptosis, metastasis, drug resistance, differentiation, DNA damage response and angiogenesis (41, 53, 54). Studies using bioinformatics analysis and other experimental procedures, such as 3′-UTR luciferase activity assays, have confirmed that SP1 is a target of miR-375-3p (42–44). Consistent with this, our results suggested the oncogenic role of SP1 in mediating the anti-HCC effect of SS. We also demonstrated the feedback role of SP1 on CCAT1 and miR-375-3p expressions, suggesting a potential complex regulatory loops, which needs to be determined in the future. As a critical transcription factor, IRF5 regulated immune and inflammatory responses in host defense and disease (55). Studies also showed the role of this transcription factor in cancer biology (56–58). IRF5 expression and function in hepatocytes infected with HCV virus, HCV replicon cells, and human primary tissues from patients with HCV-positive and -negative HCC were examined and identified that IRF5 was a new negative regulator of HCV-associated HCC pathogenesis. IRF5 induced apoptosis, inhibited autophagy, and suppressed migration, invasion of hepatocytes infected with HCV virus and HCV replicon cells. Thus, IRF5 acted as an important suppressor of HCV replication and HCC pathogenesis (45). On the contrary, IRF5 played an adverse role in predicting both OS and RFS in patients with non-metastatic ccRCC (27). Although limited data demonstrated the dual role of IRF5, our results suggested that repression of IRF5 contributed to the overall effect of SS in HCC inhibition. More specifically, our results indicated that the inhibition of HCC by SS was partly due to the observation that SP1 could bind to the promoter regions of IRF5, thereby directly regulating the expression of the IRF5 gene. Consistent with these findings, one study demonstrated the association between SP1 and IRF5. Bioinformatic analyses showed that the promoter region of IRF5 contained several putative SP1 binding sites. Excessive expression of SP1 enhanced the promoter activity and increased the expression of IRF5, suggesting that SP1 transcription factor is the primary positive determinant for increasing the expression of IRF5 (46). Overall, our findings demonstrated that the regulation, interplay and potential regulatory mechanisms among CCAT1 and miR-375-3p, and SP1 and IRF5, converge in the anti-HCC effect of SS. More studies are still required to further elucidate the in-depth mechanism underlying these correlations that contributed to overall effect of SS in HCC growth inhibition.

Moreover, our *in vivo* results were consistent with the findings *in vitro,* confirming the suppressive effects of SS on HCC HepG2 tumor growth and regulations of CCAT1, miR-375-3p, SP1, and IRF5 expressions. The doses of SS used were based on previous studies (8, 59), which demonstrated remarkable inhibitory effects without noticeable toxicities. Our findings suggested that SS suppressed growth of human HCC HepG2 cells, via targeting CCAT1/miR-375-3p/SP1/IRF5 signaling regulatory axis.

Of note, one major limitation in this study was that the only true HepG2 HCC cell line was used, as the previously considered HCC cell line, QGY-7703, was recently identified to be an unreliable cell line model for HCC due to the potential contamination of other human cell lines. Although similar results were also obtained from this cell lines in the current study. We believe that using other reliable HCC cell lines, such as Hep3B, HCCLM3, and MHCC-97H, is required to confirm our findings.

In summary, our results show that SS inhibited growth of HepG2 HCC and QGY-7703 cells through the reciprocal regulation between the miR-375-3p and lncRNA CCAT1, which leads to transcription factor SP1-mediated reduction of IRF5 expression (**Figure 6H**). The interactions and inter-regulations among miR-375-3p, CCAT1, SP1, and IRF5 axis unveil a novel molecular mechanism underlying the anti-HCC growth by SS. IRF5 may be a potential target for HCC therapy. Additional experiments using other reliable cell line models for HCC are strongly desirable to support the conclusion. Moreover, the available data of correlations among IRF5, CCAT1, and miR-375 and HCC patient survival were scarce and the public datasets had little such information thus far, although the differential expressions of these molecules between HCC tumor and normal tissues have been shown and associated with the prognosis, and patient survival (27), and have acted as potential biomarkers in diagnosis and prognosis of HCC (11, 12, 60). Regardless, future, well-designed, large-size, and high quality patient cohort studies are required to elucidate the clinic-pathological implications of IRF5, CCAT1, and miR-375 in patients with HCC. For example, overall survival using GEPIA (Gene Expression Profiling Interactive Analysis) web server (http://gepia2.cancer-pku.cn/) is a valuable resource for gene expression analysis based on tumor and normal samples from The Cancer Genome Atlas (TCGA) and Genotype-Tissue Expression (GTEx) datasets, and will be one of the most preferred tools for biologists and clinicians to explore cancer genomics data (61).

DATA AVAILABILITY STATEMENT

The raw data supporting the conclusions of this manuscript will be made available by the authors that uploaded in the supplementary section to any qualified researcher.

ETHICS STATEMENT

All animal experimental procedures were performed in accordance with the protocol approved by the Animal Care and Use Committee of Guangdong Provincial Hospital of Chinese Medicine and the National Institutes of Health Guide for the Care and Use of Laboratory Animals (the Ethics Approval Number 2018067).

AUTHOR CONTRIBUTIONS

SH conceived of the study, participated in its design and coordination, draft and finalized the manuscript. ZL, CM, and XT carried out the cell growth, siRNA, Western Blot assays, transfection and luciferase reporter assays, and statistical analysis. QT, FZ, and LL participated in performed the cell viability, siRNA, transfection assays, and protein expression experiments. YY and JW performed statistical analysis. XY and WW coordinated and provided important suggestions including some reagents, and critical reading the manuscript. All authors read and approved the final manuscript.

FUNDING

This work was supported in part by the grants from the National Natural Science Foundation of China (Nos. 81703551 and 81871863), the Science and Technology Program of Guangzhou (No. 201607010385), and the Major Program of National Natural Science Foundation of Guangdong (No. 2018B030311061), the Special Science and Technology Join fund from Guangdong Provincial Department of Science and Technology-Guangdong Academy of Traditional Chinese Medicine (No. 2014A020221024), the Science and Technology Planning Project of Guangdong Province (No. 2017A050506042), and the Specific Research Fund for TCM Science and Technology of Guangdong Provincial Hospital of Chinese Medicine (Nos. YN2015MS19 and YN2016ZD02).

SUPPLEMENTARY MATERIAL

The Supplementary Material for this article can be found online at: https://www.frontiersin.org/articles/10.3389/fonc.2019.01081/full#supplementary-material

REFERENCES

1. Siegel RL, Miller KD, Jemal A. Cancer statistics, 2018. *CA Cancer J Clin.* (2018) 68:7–30. doi: 10.3322/caac.21442
2. Personeni N, Pressiani T, Santoro A, Rimassa L. Regorafenib in hepatocellular carcinoma: latest evidence and clinical implications. *Drugs Context*. (2018) 7:212533. doi: 10.7573/dic.212533
3. Zou J, Zhuang M, Yu X, Li N, Mao R, Wang Z, et al. MYC inhibition increases PD-L1 expression induced by IFN-γ in hepatocellular carcinoma cells. *Mol Immunol.* (2018) 101:203–29. doi: 10.1016/j.molimm.2018.07.006
4. Lezama-Davila CM, McChesney JD, Bastos JK, Miranda MA, Tiossi RF, da Costa Jde, et al. A New antileishmanial preparation of combined solamargine and solasonine heals cutaneous leishmaniasis through different immunochemical pathways. *Antimicrob Agents Chemother.* (2016) 60:2732–8. doi: 10.1128/AAC.02804-15
5. Munari CC, de Oliveira PF, Campos JC, Martins Sde P, Da Costa JC, Bastos JK, et al. Antiproliferative activity of *Solanum lycocarpum* alkaloidic extract and their constituents, solamargine and solasonine, in tumor cell lines. *J Nat Med.* (2014) 68:236–41. doi: 10.1007/s11418-013-0757-0
6. Lee KR, Kozukue N, Han JS, Park JH, Chang EY, Baek EJ, et al. Glycoalkaloids and metabolites inhibit the growth of human colon (HT29) and liver (HepG2) cancer cells. *J Agric Food Chem.* (2004) 52:2832–9. doi: 10.1021/jf030526d
7. Burger T, Mokoka T, Fouche G, Steenkamp P, Steenkamp V, Cordier W. Solamargine, a bioactive steroidal alkaloid isolated from *Solanum aculeastrum* induces non-selective cytotoxicity and P-glycoprotein inhibition. *BMC Complement Altern Med.* (2018) 18:137. doi: 10.1186/s12906-018-2208-7
8. Wang X, Zou S, Lan YL, Xing JS, Lan XQ, Zhang B. Solasonine inhibits glioma growth through anti-inflammatory pathways. *Am J Transl Res.* (2017) 9:3977–89.
9. Wu J, Hann SS. Functions and roles of long-non-coding RNAs in human nasopharyngeal carcinoma. *Cell Physiol Biochem.* (2018) 45:1191–204. doi: 10.1159/000487451
10. He Y, Meng XM, Huang C, Wu BM, Zhang L, Lv XW, et al. Long noncoding RNAs: novel insights into hepatocelluar carcinoma. *Cancer Lett.* (2014) 344:20–7. doi: 10.1016/j.canlet.2013.10.021
11. Deng L, Yang SB, Xu FF, Zhang JH. Long noncoding RNA CCAT1 promotes hepatocellular carcinoma progression by functioning as let-7 sponge. *J Exp Clin Cancer Res.* (2015) 34:18. doi: 10.1186/s13046-015-0136-7
12. Zhu HQ, Zhou X, Chang H, Li HG, Liu FF, Ma CQ, et al. Aberrant expression of CCAT1 regulated by c-Myc predicts the prognosis of hepatocellular carcinoma. *Asian Pac J Cancer Prev.* (2015) 16:5181–5. doi: 10.7314/APJCP.2015.16.13.5181
13. Zhu H, Zhou X, Chang H, Li H, Liu F, Ma C, et al. CCAT1 promotes hepatocellular carcinoma cell proliferation and invasion. *Int J Clin Exp Pathol.* (2015) 8:5427–34.
14. Mo Y, He L, Lai Z, Wan Z, Chen Q, Pan S, et al. LINC01287/miR-298/STAT3 feedback loop regulates growth and the epithelial-to-mesenchymal transition phenotype in hepatocellular carcinoma cells. *J Exp Clin Cancer Res.* (2018) 37:149. doi: 10.1186/s13046-018-0831-2
15. Tsukamoto Y, Nakada C, Noguchi T, Tanigawa M, Nguyen LT, Uchida T, et al. MicroRNA-375 is downregulated in gastric carcinomas and regulates cell survival by targeting PDK1 and 14-3-3zeta. *Cancer Res.* (2010) 70:2339–49. doi: 10.1158/0008-5472.CAN-09-2777
16. Szczyrba J, Nolte E, Wach S, Kremmer E, Stohr R, Hartmann A, et al. Downregulation of Sec23A protein by miRNA-375 in prostate carcinoma. *Mol Cancer Res.* (2011) 9:791–800. doi: 10.1158/1541-7786.MCR-10-0573
17. Zhang LX, Jin W, Zheng J, Dai YX, Song Y, Ni HB, et al. MicroRNA-375 regulates proliferation and apoptosis of glioma cancer cells by inhibiting CTGF-EGFR signaling pathway. *Bratisl Lek Listy.* (2018) 119:17–21. doi: 10.4149/BLL_2018_004
18. Shaker OG, Mohammed SR, Mohammed AM, Mahmoud Z. Impact of microRNA-375 and its target gene SMAD-7 polymorphism on susceptibility of colorectal cancer. *J Clin Lab Anal.* (2018) 32:e22215. doi: 10.1002/jcla.22215
19. Ward A, Balwierz A, Zhang JD, Kublbeck M, Pawitan Y, Hielscher T, et al. Re-expression of microRNA-375 reverses both tamoxifen resistance and accompanying EMT-like properties in breast cancer. *Oncogene.* (2013) 32:1173–82. doi: 10.1038/onc.2012.128
20. Xie CR, Wang F, Zhang S, Wang FQ, Zheng S, Li Z, et al. Long noncoding RNA HCAL facilitates the growth and metastasis of hepatocellular carcinoma

by acting as a ceRNA of LAPTM4B. *Mol Ther Nucleic Acids.* (2017) 9:440–51. doi: 10.1016/j.omtn.2017.10.018
21. Ma MZ, Chu BF, Zhang Y, Weng MZ, Qin YY, Gong W, et al. Long non-coding RNA CCAT1 promotes gallbladder cancer development via negative modulation of miRNA-218-5p. *Cell Death Dis.* (2015) 6:e1583. doi: 10.1038/cddis.2014.541
22. Lai Y, Chen Y, Lin Y, Ye L. Down-regulation of LncRNA CCAT1 enhances radiosensitivity via regulating miR-148b in breast cancer. *Cell Biol Int.* (2018) 42:227–36. doi: 10.1002/cbin.10890
23. Kaur A, Lee LH, Chow SC, Fang CM. IRF5-mediated immune responses and its implications in immunological disorders. *Int Rev Immunol.* (2018) 37:229–48. doi: 10.1080/08830185.2018.1469629
24. Massimino M, Vigneri P, Fallica M, Fidilio A, Aloisi A, Frasca F, Manzella L. IRF5 promotes the proliferation of human thyroid cancer cells. *Mol Cancer.* (2012) 11:21. doi: 10.1186/1476-4598-11-21
25. Li Q, Tainsky MA. Epigenetic silencing of IRF7 and/or IRF5 in lung cancer cells leads to increased sensitivity to oncolytic viruses. *PLoS ONE.* (2011) 6:e28683 doi: 10.1371/journal.pone.0028683
26. Babaian A, Romanish MT, Gagnier L, Kuo LY, Karimi MM, Steidl C, et al. Onco-exaptation of an endogenous retroviral LTR drives IRF5 expression in Hodgkin lymphoma. *Oncogene.* (2016) 35:2542–6. doi: 10.1038/onc.2015.308
27. Bai Q, Liu L, Xia Y, Wang J, Xi W, Qu Y, et al. IRF5 is associated with adverse postoperative prognosis of patients with non-metastatic clear cell renal cell carcinoma. *Oncotarget.* (2017) 8:44186–94. doi: 10.18632/oncotarget.17777
28. Fresquet V, Robles EF, Parker A, Martinez-Useros J, Mena M, Malumbres R, et al. High-throughput sequencing analysis of the chromosome 7q32 deletion reveals IRF5 as a potential tumour suppressor in splenic marginal-zone lymphoma. *Br J Haematol.* (2012) 158:712–26. doi: 10.1111/j.1365-2141.2012.09226.x
29. Bi X, Feng D, Korczeniewska J, Alper N, Hu G, Barnes BJ. Deletion of Irf5 protects hematopoietic stem cells from DNA damage-induced apoptosis and suppresses γ-irradiation-induced thymic lymphomagenesis. *Oncogene.* (2014) 33:3288–97. doi: 10.1038/onc.2013.295
30. Peng L, Zhang H, Hao Y, Xu F, Yang J, Zhang R, et al. Reprogramming macrophage orientation by microRNA 146b targeting transcription factor IRF5. *EBioMedicine.* (2016) 14:83–96. doi: 10.1016/j.ebiom.2016.10.041
31. Zhu W, Yu J, Qiu S, Liu H, Wang Y, Xu X, et al. MiR-let-7a regulates anti-citrullinated protein antibody-induced macrophage activation and correlates with the development of experimental rheumatoid arthritis. *Int Immunopharmacol.* (2017) 51:40–6. doi: 10.1016/j.intimp.2017.08.001
32. Zheng F, Tang Q, Zheng XH, Wu J, Huang H, Zhang H, et al. Inactivation of Stat3 and crosstalk of miRNA155-5p and FOXO3a contribute to the induction of IGFBP1 expression by beta-elemene in human lung cancer. *Exp Mol Med.* (2018) 50:121. doi: 10.1038/s12276-018-0146-6
33. Bustin SA, Benes V, Garson JA, Hellemans J, Huggett J, Kubista M, et al. The MIQE guidelines: minimum information for publication of quantitative real-time PCR experiments. *Clin Chem.* (2009) 55:611–22. doi: 10.1373/clinchem.2008.112797
34. Fekry MI, Ezzat SM, Salama MM, Alshehri OY, Al-Abd AM. Bioactive glycoalkaloides isolated from *Solanum melongena* fruit peels with potential anticancer properties against hepatocellular carcinoma cells. *Sci Rep.* (2019) 9:1746. doi: 10.1038/s41598-018-36089-6
35. Chen Y, Tang Q, Xiao Q, Yang L, Hann SS. Targeting EP4 downstream c-Jun through ERK1/2-mediated reduction of DNMT1 reveals novel mechanism of solamargine-inhibited growth of lung cancer cells. *J Cell Mol Med.* (2017) 21:222–33. doi: 10.1111/jcmm.12958
36. Cheng L, Zhan B, Luo P, Wang B. miRNA375 regulates the cell survival and apoptosis of human nonsmall cell carcinoma by targeting HER2. *Mol Med Rep.* (2017) 15:1387–92. doi: 10.3892/mmr.2017.6112
37. Yu J, Jiang L, Gao Y, Sun Q, Liu B, Hu Y, et al. LncRNA CCAT1 negatively regulates miR-181a-5p to promote endometrial carcinoma cell proliferation and migration. *Exp Ther Med.* (2019) 17:4259–66. doi: 10.3892/etm.2019.7422
38. Zhang J, Cai M, Jiang D, Xu L. Upregulated LncRNA-CCAT1 promotes hepatocellular carcinoma progression by functioning as miR-30c-2-3p sponge. *Cell Biochem Funct.* (2019) 37:84–92. doi: 10.1002/cbf.3375
39. Li L, Jia L, Ding Y. Upregulation of miR-375 inhibits human liver cancer cell growth by modulating cell proliferation and apoptosis via targeting ErbB2. *Oncol Lett.* (2018) 16:3319–26. doi: 10.3892/ol.2018.9011
40. Fan YP, Liao JZ, Lu YQ, Tian DA, Ye F, Zhao PX, et al. MiR-375 and doxorubicin co-delivered by liposomes for combination therapy of hepatocellular carcinoma. *Mol Ther Nucleic Acids.* (2017) 7:181–9. doi: 10.1016/j.omtn.2017.03.010
41. Yang C, Li J, Yu L, Zhang Z, Xu F, Jiang L, et al. Regulation of RIP3 by the transcription factor Sp1 and the epigenetic regulator UHRF1 modulates cancer cell necroptosis. *Cell Death Dis.* (2017) 8:e3084. doi: 10.1038/cddis.2017.483
42. Wang F, Li Y, Zhou J, Xu J, Peng C, Ye F, et al. miR-375 is down-regulated in squamous cervical cancer and inhibits cell migration and invasion via targeting transcription factor SP1. *Am J Pathol.* (2011) 179:2580–8. doi: 10.1016/j.ajpath.2011.07.037
43. Xu H, Jiang J, Zhang J, Cheng L, Pan S, Li Y. MicroRNA-375 inhibits esophageal squamous cell carcinoma proliferation through direct targeting of SP1. *Exp Ther Med.* (2019) 17:1509–16. doi: 10.3892/etm.2018.7106
44. Wang Z, Gai Y, Zhou J, Liu J, Cui S. miR-375 mediates the CRF signaling pathway to regulate catecholamine biosynthesis by targeting Sp1 in porcine adrenal gland. *Stress.* (2019) 22:332–46. doi: 10.1080/10253890.2018.1561845
45. Cevik O, Li D, Baljinnyam E, Manvar D, Pimenta EM, Waris G, et al. Interferon regulatory factor 5 (IRF5) suppresses hepatitis C virus (HCV) replication and HCV-associated hepatocellular carcinoma. *J Biol Chem.* (2017) 292:21676–89. doi: 10.1074/jbc.M117.792721
46. Shu J, Wang XH, Zhou LB, Jiang CM, Yang WX, Jin R, et al. Expression of interferon regulatory factor 5 is regulated by the Sp1 transcription factor. *Mol Med Rep.* (2016) 14:2815–22. doi: 10.3892/mmr.2016.5565
47. Sparg SG, Light ME, van Staden J. Biological activities and distribution of plant saponins. *J Ethnopharmacol.* (2004) 94:219–43. doi: 10.1016/j.jep.2004.05.016
48. Wu S, Chen H. Anti-Condyloma acuminata mechanism of microRNAs-375 modulates HPV in cervical cancer cells via the UBE3A and IGF-1R pathway. *Oncol Lett.* (2018) 16:3241–7. doi: 10.3892/ol.2018.8983
49. Zhou N, Qu Y, Xu C, Tang Y. Upregulation of microRNA-375 increases the cisplatin-sensitivity of human gastric cancer cells by regulating ERBB2. *Exp Ther Med.* (2016) 11:625–30. doi: 10.3892/etm.2015.2920
50. Li J, Qi Y. Ginsenoside Rg3 inhibits cell growth, migration and invasion in Caco-2 cells by downregulation of lncRNA CCAT1. *Exp Mol Pathol.* (2019) 106:131–8. doi: 10.1016/j.yexmp.2019.01.003
51. Liu J, Ding D, Jiang Z, Du T, Liu J, Kong Z. Long non-coding RNA CCAT1/miR-148a/PKCzeta prevents cell migration of prostate cancer by altering macrophage polarization. *Prostate.* (2019) 79:105–12. doi: 10.1002/pros.23716
52. Hu B, Zhang H, Wang Z, Zhang F, Wei H, Li L. LncRNA CCAT1/miR-130a-3p axis increases cisplatin resistance in non-small-cell lung cancer cell line by targeting SOX4. *Cancer Biol Ther.* (2017) 18:974–83. doi: 10.1080/15384047.2017.1385679
53. Wu J, Tang Q, Ren X, Zheng F, He C, Chai X, et al. Reciprocal interaction of HOTAIR and SP1 together enhance the ability of Xiaoji decoction and gefitinib to inhibit EP4 expression. *J Ethnopharmacol.* (2019) 237:128–40. doi: 10.1016/j.jep.2019.03.027
54. Beishline K, Azizkhan-Clifford J. Sp1 and the 'hallmarks of cancer'. *FEBS J.* (2015) 282:224–58. doi: 10.1111/febs.13148
55. Zhao Y, Zagani R, Park SM, Yoshida N, Shah P, Reinecker HC. Microbial recognition by GEF-H1 controls IKKepsilon mediated activation of IRF5. *Nat Commun.* (2019) 10:1349. doi: 10.1038/s41467-019-09283-x
56. Okazaki S, Stintzing S, Sunakawa Y, Cao S, Zhang W, Yang D, et al. Predictive value of TLR7 polymorphism for cetuximab-based chemotherapy in patients with metastatic colorectal cancer. *Int J Cancer.* (2017) 141:1222–30. doi: 10.1002/ijc.30810
57. Wang Q, Lingel A, Geiser V, Kwapnoski Z, Zhang L. Tumor suppressor p53 stimulates the expression of epstein-barr virus latent membrane protein 1. *J Virol.* (2017) 91:e00312-17. doi: 10.1128/JVI.00312-17
58. Thompson CD, Matta B, Barnes BJ. Therapeutic targeting of IRFs: pathway-dependence or structure-based? *Front Immunol.* (2018) 9:2622. doi: 10.3389/fimmu.2018.02622

59. Zhong Y, Li S, Chen L, Liu Z, Luo X, Xu P, et al. *In vivo* toxicity of solasonine and its effects on cyp450 family gene expression in the livers of male mice from four strains. *Toxins*. (2018) 10:E487. doi: 10.3390/toxins10120487
60. An Y, Gao S, Zhao WC, Qiu BA, Xia NX, Zhang PJ, et al. Novel serum microRNAs panel on the diagnostic and prognostic implications of hepatocellular carcinoma. *World J Gastroenterol*. (2018) 24:2596–604. doi: 10.3748/wjg.v24.i24.2596
61. Stoddard BL, Fox KR. Editorial: Preprints, citations and nucleic acids research. *Nucleic Acids Res*. (2019) 47:1–2. doi: 10.1093/nar/gky1229

Conflict of Interest: The authors declare that the research was conducted in the absence of any commercial or financial relationships that could be construed as a potential conflict of interest.

frontiers in Oncology

ORIGINAL RESEARCH
published: 22 October 2019
doi: 10.3389/fonc.2019.01120

Epstein-Barr Virus BART Long Non-coding RNAs Function as Epigenetic Modulators in Nasopharyngeal Carcinoma

*Rob J. A. Verhoeven[1], Shuang Tong[1], Bobo Wing-Yee Mok[1], Jiayan Liu[1], Songtao He[1], Jingfeng Zong[2], Yixin Chen[3], Sai-Wah Tsao[4], Maria Li Lung[5] and Honglin Chen[1]**

[1] State Key Laboratory for Emerging Infectious Diseases, Department of Microbiology and the Collaborative Innovation Center for Diagnosis and Treatment of Infectious Diseases, Li Ka Shing Faculty of Medicine, The University of Hong Kong, Hong Kong, China, [2] Department of Radiation Oncology, Fujian Provincial Cancer Hospital, Fuzhou, China, [3] School of Life Sciences, National Institute of Diagnostics and Vaccine Development in Infectious Diseases, Xiamen University, Xiamen, China, [4] Li Ka Shing Faculty of Medicine, School of Biomedical Sciences, The University of Hong Kong, Hong Kong, China, [5] Department of Clinical Oncology, Li Ka Shing Faculty of Medicine, The University of Hong Kong, Hong Kong, China

OPEN ACCESS

Edited by:
Patricia P. Reis, São Paulo State University, Brazil

Reviewed by:
Duohui Jing, Children's Cancer Institute Australia, Australia
Renato Franco, University of Campania Luigi Vanvitelli, Italy

***Correspondence:**
Honglin Chen
hlchen@hku.hk

Specialty section:
This article was submitted to Molecular and Cellular Oncology, a section of the journal Frontiers in Oncology

Received: *11 July 2019*
Accepted: *08 October 2019*
Published: *22 October 2019*

Citation:
Verhoeven RJA, Tong S, Mok BW-Y, Liu J, He S, Zong J, Chen Y, Tsao S-W, Lung ML and Chen H (2019) Epstein-Barr Virus BART Long Non-coding RNAs Function as Epigenetic Modulators in Nasopharyngeal Carcinoma. Front. Oncol. 9:1120. doi: 10.3389/fonc.2019.01120

Epstein-Barr virus (EBV) establishes lifelong latent infection in humans and is associated with several lymphoid and epithelial cancers. In nasopharyngeal carcinoma (NPC), EBV expresses few viral proteins but elevated levels of *Bam*-HI A rightward transcripts (BARTs) RNA, which includes viral microRNAs and long non-coding RNAs (lncRNAs). BART lncRNAs localize within the nucleus of EBV-infected cells and knockdown of BART lncRNAs significantly affects the expression of genes associated with cell adhesion, oxidoreductase activity, inflammation, and immunity. Notably, downregulation of *IKAROS* family zinc finger 3 (*IKZF3*/Aiolos), which plays a role in lymphocyte development and cell attachment, occurred in NPC C666-1 cells following BART lncRNA-knockdown. Since Aiolos expression is normally restricted to lymphoid cells and rarely observed in epithelial cells, induction of Aiolos by BART lncRNA was confirmed by expressing the major BART lncRNA isoform, *RPMS1*, in EBV-positive and -negative cells. BART lncRNA associated with the CBP/p300 complex and RNA polymerase II (Pol II) in the nucleus, suggesting that BART lncRNAs may mediate epigenetic regulation of gene expression through interaction with the chromatin remodeling machinery. This contention is further supported by evidence that BART lncRNA appears to stall Pol II at the promoter region and may regulate *IFNB1* and *CXCL8* expression by inhibiting transcription by Pol II in NPC. We hypothesize that EBV BART lncRNA expression modulates host gene expression and maintains EBV latency by interfering with histone methylation and acetylation processes. Aberrant expression of affected host genes mediated by BART lncRNA may lead to immune evasion, progression, and metastasis of NPC.

Keywords: Epstein-Barr virus, nasopharyngeal carcinoma, lncRNA, BART, epigenetics, Aiolos

INTRODUCTION

Epstein-Barr virus (EBV) infects more than 95% of the human population. Primary infection with EBV is usually asymptomatic, however, if infection first occurs in young adulthood, mononucleosis may develop (1). EBV remains latent in memory B cells and is kept in check by a competent immune surveillance system which continuously removes EBV-infected cells in which EBV has become activated from its stringent latency program (2). When the human immune system is compromised, latently EBV-infected cells may be transformed into lymphoblasts, which are characterized by increased cell proliferation, as seen in lymphoproliferative diseases. Reactivation of EBV occurs regularly *in vivo*, as demonstrated by virus shedding in the saliva of EBV-positive individuals. While latent infection of resting B cells with EBV and virus shedding from oral pharyngeal tissues normally cause no serious risk to the health of immunocompetent individuals, the presence of EBV can give rise to certain epithelial cancers, including nasopharyngeal carcinoma (NPC), when combined with genetic abnormalities or undefined environmental factors. We postulate that infection with activated EBV in nasopharyngeal epithelial cells predisposed toward establishment of viral latency may lead to the origin or development of NPC. The questions of how EBV-infected NPC cells can evade immune surveillance in apparently immune competent individuals and what the exact contribution of EBV is to the oncogenesis of NPC remain unanswered. However, in NPC cells EBV is known to turn off the expression of most of its latency genes which are critical for B cell transformation, presumably to avoid immune surveillance. But how does EBV maintain latency in NPC cells without these viral functions? It is likely that the mechanism regulating the EBV latency program in NPC cells also drives EBV oncogenesis.

In NPC cells, EBV mainly expresses EBNA1, EBV-encoded RNAs (EBERs), and elevated levels of *Bam*HI-A rightwards transcripts (BARTs). EBNA1 is essential for EBV replication and EBERs have been reported to play a role in antagonizing host antiviral innate immunity. While EBV LMP1 is a recognized viral oncogene, expression of LMP1 protein is not consistently observed in EBV-infected NPC cells. EBV BARTs were first identified as multi-spliced transcripts in NPC tissues and were later found to be expressed in all types of EBV-infected cells and EBV-associated tumors (3–6). However, no clear role could be attributed to BARTs in EBV infection until it was revealed that BARTs encode two clusters of EBV microRNAs with versatile functions in all forms of EBV latency (7). It is now clear that EBV BARTs comprise two groups of non-coding RNAs; a group of microRNAs (miRNAs) which are produced from introns prior to splicing and a complex family of alternatively spliced polyadenylated RNAs (7, 8). BART RNAs and miRNAs are both highly expressed in NPC, and to a lesser extent in EBV-positive gastric carcinoma and EBV-infected B cells. Our previous studies have characterized the promoters driving transcription of BARTs and show that this abundant transcription is driven by C/EBP and aberrant NF-κB signaling, and that BART miRNAs in turn modulate NF-κB activation through LMP1 in an auto-regulatory loop in NPC cells (9, 10). Expression of *C/EBP* is mainly found in epithelial cells while aberrant NF-κB signaling has been reported in NPC cells (10–12), which may contribute to the elevated level of BARTs in NPC cells. Alternative splicing of BARTs results in multiple spliced forms of BART RNA, with putative open reading frames in BARF0, RK-BARF0, RPMS1, and A73 (3, 13). However, attempts to identify proteins translated from these transcripts have been unsuccessful. Previous reports indicated that BART RNAs are restricted to the nucleus, which supports the idea that these BART RNAs may function as regulatory RNAs, rather than coding for a protein (14, 15). One recent study reported that ectopic expression of one isoform of BART RNA altered transcription of cellular genes in AGS cells, suggesting that BART RNAs may function as long non-coding RNAs (lncRNAs) (14). However, the role of BART RNAs in EBV latency and NPC, including whether they act as lncRNAs, is yet to be defined in detail.

To determine if EBV BART RNAs function as lncRNAs in NPC, this study first confirmed that BART RNAs are predominantly localized within the nucleus, as many lncRNAs tend to be nuclear. RNA-seq analysis revealed that knockdown of BART RNAs in NPC cells resulted in altered expression of genes associated with host immune/inflammatory responses, and oxidoreductase and cell adhesion activities, supporting the idea that they function as lncRNAs in NPC. Our data suggest that BART lncRNAs may affect host gene expression through epigenetic regulation and chromatin remodeling. Expression of the host transcription factor, Aiolos, is normally restricted to lymphoid cells, but it is aberrantly expressed in NPC and appears to be regulated by BART lncRNAs (16, 17). This study highlights a mechanism in which EBV expresses BART lncRNAs to modulate host gene expression, generating a cellular environment that supports EBV latency, and driving the oncogenic process in NPC.

MATERIALS AND METHODS

Cell Lines and Cell Culture Conditions

Human embryonic kidney (HEK) 293T cells, CNE2, and HeLa-Bx1 cells were maintained in Dulbecco's Minimal Essential Medium (Gibco) supplemented with 10% fetal bovine serum (FBS) and 1% P/S. The EBV-positive NPC cell line C666-1 and the Burkitt's lymphoma lines Mutu III, Mutu I and DG-75 were grown in RPMI-1640 medium (Gibco) supplemented with 10% fetal bovine serum (FBS) and 1% P/S. The hTERT immortalized NP epithelial cell lines NP361-hTERT-EBV and NP460-hTERT-EBV were grown in a 1:1 mixture of Defined Keratinocyte-SFM (Gibco) and Epilife^{TM} medium (Gibco) supplemented with 1% P/S. The EBV-positive and -negative gastric cancer cell line AGS-Bx1 and AGS, respectively, were cultured in F-12K Nutrient Mixture (Gibco) supplemented with 10% fetal bovine serum (FBS) and 1% P/S. Cells were cultured at 37°C with 5% CO_2.

Plasmids

The MAVS expression plasmid pEF-BOS MAVS was a gift from Kate Fitzgerald (Addgene, plasmid 27224). The pcDNA3-BART expression plasmid contains a full-length BART clone representing the major isoform of BART RNA, *RPMS1* (13).

The BART clone, almost 4-kb in length, contains exons I, IIIa, IIIb, IV, V, VI, and VII, which was confirmed by sequencing. The oriPtL expression plasmid was created by amplifying and cloning the oriPtL sequence spanning nucleotides 7,143–9,247 of the EBV genome from cell line C666-1 (GenBank: KJ411974.1) into pcDNA3.

ChIP Assay

Briefly, C666-1 cells transfected with LNA™ BART or negative control A GapmeRs (Exiqon) and HEK 293T cells transfected with pEF-BOS MAVS and pcDNA3-BART or empty vector were harvested after 48 h. The ChIP extract was sonicated into DNA fragments sized between 100- and 1000-bp using a Sonicator S-4000 (Misonix). For immunoprecipitation, 5 μg of rabbit anti-Pol II (sc-899, Santa Cruz Biotechnology) or 5 μg of normal rabbit IgG (sc-2027, Santa Cruz Biotechnology) was used and antibody-protein-DNA complexes were pulled-down using Dynabeads Protein A (Invitrogen). The level of immunoprecipitated DNA was determined by qPCR.

Luciferase Reporter Assay

HEK 293T cells were seeded at a density of approximately 70% in 24-well plates a day before transfection, and subsequently co-transfected with 100 ng of pEF-BOS-MAVS, 500 ng of pcDNA3-BART or pcDNA3-oriPtL, and 100 ng of a Firefly luciferase reporter plasmid driven by the IFN-β promoter (Promega), using Lipofectamine® 2000 (Invitrogen). For data normalization purposes, 10 ng of the plasmid phRL-TK (Promega) expressing *Renilla* luciferase was co-transfected with the Firefly reporter plasmid in each experiment. Cells were harvested 2 days after transfection.

Immunoblotting

Membranes were incubated overnight with primary antibodies in 3% milk in PBST. The antibodies used for immunoblotting included rabbit anti-IKZF3 (ab139408, Abcam), rabbit anti-CDK8 (A302-501A, Bethyl Laboratories), and mouse anti-β-tubulin (T8328, Sigma-Aldrich) at a 1:2,000 dilution and rabbit anti-SHC (ab24787, Abcam), rabbit anti-SEPT9 (sc-899, Santa Cruz Biotechnology), and mouse anti-MAVS (sc-166583, Santa Cruz Biotechnology) at a 1:1,000 dilution. Membranes were then incubated with IRDye700-labeled donkey anti-mouse or anti-rabbit or IRDye800-labeled donkey anti-mouse (LI-COR Biosciences) at a 1:5,000 dilution. Blots were detected using an Odyssey® Infrared Imaging System (LI-COR Biosciences).

Reverse Transcription and qPCR Amplification

RNA was extracted from cells using RNAiso Plus reagent (TaKaRa) and reverse transcribed with random primers using the High-Capacity cDNA Reverse Transcription Kit (Applied Biosystems). Real-time PCR reactions were performed using SYBR Premix Ex Taq (Tli RNase H Plus) mix (Takara) in a LightCycler 480 instrument (Roche). Primers used in this study are listed in **Supplementary Table 2** and gene expression was normalized to that of glyceraldehyde-3-phosphate dehydrogenase (GAPDH).

RNA FISH and Immunofluorescence

Stellaris fluorescent *in situ* hybridization (FISH) probes were designed and purchased from Biosearch Technologies with Quasar 570 fluorophore to detect BART lncRNA and CAL Fluor Red 635 to detect GAPDH mRNA. FISH combined with indirect immunofluorescence (IF) was performed according to the Biosearch Technologies online protocol for sequential IF + FISH in adherent cells. Cells were fixed, permeabilized, and incubated overnight at 37°C with 125 nM FISH probes and a 1:100 dilution of primary antibody in hybridization buffer (100 mg/mL dextran sulfate, 10% formamide in 2X SSC). After incubation, cells were washed with wash buffer (10% formamide in 2X SSC) and then incubated with secondary antibodies conjugated with FITC at a 1:200 dilution in wash buffer for 30 min at 37°C. Finally, the cells were washed and mounted using mounting medium with DAPI (Vectashield) and the signals were visualized using a Carl Zeiss LSM 710 confocal microscope.

Histone Acetyltransferase Activity Assay

Nuclear extracts were prepared by lysing cells in phosphate buffered saline (PBS) containing 1% NP-40 and after a short centrifugation the supernatant (cytoplasmic fraction) was removed. The nuclear extracts were washed twice with 1% NP-40 in PBS and lysed using RIPA lysis buffer. HAT assay was performed using a Histone acetyltransferase activity assay kit (ab65352, Abcam) according to the manufacturer's protocol. For each assay 30 μg nuclear extract was used and the OD was measured at 450 nm at 1-h intervals.

RNA Sequencing

Two total RNA extracts from C666-1 cells were independently prepared 2 days after transfection with BART or control GapmeRs, using the NucleoSpin RNA II kit (Macherey Nagel) in accordance with the manufacturer's instructions. Four micrograms of total RNA was used as starting material for ribosomal RNA (rRNA) depletion, performed using the human Ribo-Zero Gold rRNA Removal Kit (Illumina). Library preparation and sequencing was performed by the University of Hong Kong Center of Genomic Sciences using the HiSeq SBS Kit v4 (Illumina) and the HiSeq PE Cluster Kit v4 cBot (Illumina) on an Illumina HiSeq 1500 instrument for pair-end 101 bp sequencing. Sequencing reads were first filtered for adapter and low-quality sequences, followed by retaining only reads with a read length $\geq$ 40 bp by using Cutadapt (http://code.google.com/p/cutadapt/). Low quality reads were defined as reads with more than 5% unknown bases (N) and reads having more than 50% of bases with a quality value $\leq$ 10. Sequence reads were subsequently filtered for rRNA sequences and the remaining reads were used for downstream analysis.

Computational and Statistical Analyses

Filtered RNA sequencing reads were first aligned to the human genome (GRCh38, gencode v24), downloaded from GENCODE (18), and the remaining unaligned reads then aligned to the wild type EBV genome (GenBank: NC_007605) using STAR version 2.5.2a (19). Quantification of expression and identification of differential gene expression was performed using Partek

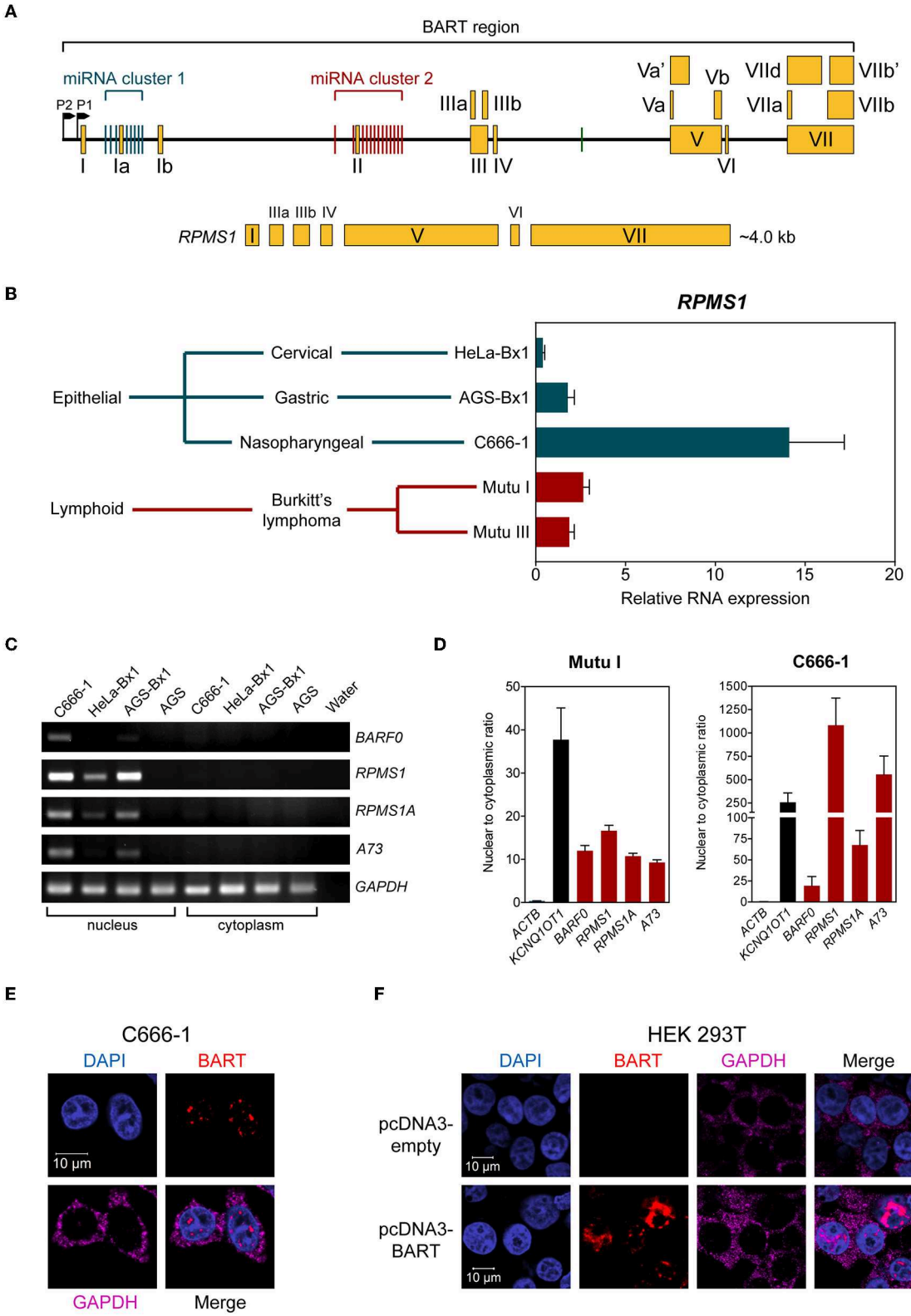

FIGURE 1 | BART RNA expression and localization. **(A)** Position and structure of the BART RNA *RPMS1* variant. Exons are indicated by yellow boxes while the black line in between represents intronic sequences, with miRNA clusters indicated by green (cluster 1) and red (cluster 2) vertical bars. **(B)** Relative expression of *RPMS1*

(Continued)

FIGURE 1 | RNA in various EBV-positive cell lines with different latency programs, analyzed by RT-qPCR. Gene expression is shown as RNA expression relative to that of *GAPDH*. The average and SEM of three independent experiments are shown. **(C)** RT-PCR and agarose gel analysis of nuclear and cytoplasmic RNA from different EBV-positive epithelial cell lines. AGS is an EBV-negative cell line, included as a control. **(D)** Nuclear to cytoplasmic ratio of BART RNA variants in Mutu I and C666-1 cell lines, analyzed by RT-qPCR. *KCNQ1OT1* was analyzed as a nuclear transcript control, and *ACTB* was analyzed as a cytoplasmic control. Data shown represent the average and SEM of three independent experiments. **(E,F)** RNA FISH showing localization of BART RNA in C666-1 and HEK 293T cell lines, respectively. RNA FISH probes against *GAPDH* mRNA were used as a cytoplasmic control.

Genomics Suite (version 6.6). Annotation for the EBV genome was manually edited into the GenBank record before importing alignment files into Partek Genomics Suite. Statistical analysis of RT-qPCR data was performed using GraphPad Prism 5 software. Significance values (*P*-values) were calculated using the two-tailed Student's *t*-test, with Welch's correction, where appropriate.

RESULTS

BART lncRNA Is Localized in the Nucleus of EBV-Infected Cells

The EBV *Bam*HI-A region encodes BART-miRNAs and BART RNA, which are derived from the introns and exons, respectively (**Figure 1A**). EBV BART RNA comprises multiple spliced forms of transcripts; *RPMS1* BART RNA has a size of about 4 kb and is the most abundant of the BART transcript species expressed in NPC cells (3). We and others have previously described EBV-derived miRNAs in EBV positive epithelial and B cell lines (9, 20). Here we compared the levels of the BART RNA, *RPMS1*, in the C666-1 NPC cell line and other EBV-infected cell lines. EBV expresses the highest levels of BART *RPMS1* in C666-1, which is naturally infected with EBV, while relatively lower levels of *RPMS1* are detected in HeLa-Bx1 and AGS-Bx1, which have been artificially infected with EBV *in vitro,* and in both latency I and III Mutu cell lines, which are derived from Burkitt's lymphoma (**Figure 1B**). It has been suggested that BART RNAs may represent a group of viral lncRNAs with as yet undefined functions (14). BART lncRNAs are predominantly detected in the nuclear fractions of EBV-harboring C666-1 and EBV-infected AGS cell lines (15). We confirmed the localization of BART lncRNAs in the nuclear fraction of all tested EBV-positive cell lines by quantitative RT-PCR (**Figures 1C,D**). The nuclear localization of BART lncRNA was further analyzed by RNA fluorescent *in-situ* hybridization (FISH) assay in C666-1 cells and pcDNA3-BART-transfected HEK 293T cells. RNA FISH clearly demonstrated distinctive dotted patterns of BART RNA exclusively in the nucleus (**Figures 1E,F**). These results further confirm that BART lncRNA is expressed at elevated levels in the nucleus of NPC cells.

GapmeR-Mediated Targeting of BART lncRNA in C666-1 Cells

To characterize the effect of BART RNA on host gene expression in NPC cells, knockdown of BART RNA was achieved by targeting it for GapmeR-mediated RNase H cleavage to disrupt its function. Three different GapmeRs targeting different locations within the BART region were tested in C666-1 cells, and all showed equal cleavage efficiency (**Figure 2A**). Pilot experiments with the *RPMS1* expression plasmid revealed that BART lncRNA overexpression and *IL6* gene expression were negatively correlated. Expression of *IL6* mRNA was used to determine the impact of targeting BART RNA with GapmeRs in C666-1. Consistently, GapmeR targeting of the splicing junction at the start of exon III, exon V, and VII all caused the significant change in host *IL6* gene expression. Gap-BART exon III was then used in subsequent experiments to knockdown endogenous expression of BART RNA in C666-1 cells (**Figure 2B**). The expression of various BART miRNAs from BART miRNA clusters 1 and 2 was also analyzed to determine how targeting BART RNA affects their expression. Of the 21 BART miRNAs tested, the 14 miRNAs with the greatest changes in expression are shown in **Figure 2C**. Only miR-BART6-5p and miR-BART9-3p showed clearly lowered expression, with only the miR-BART9-3p result being statistically significant; other tested BART miRNAs demonstrated a moderate and statistically insignificant reduction in expression following knockdown of BART lncRNA (**Figure 2C**). Since the BART GapmeR used does not target a region near the sites from which BART miRNAs are produced, it is likely that miRNA production remains largely intact.

BART lncRNA Modulates Host Gene Expression

Using the GapmeR knockdown strategy described above, we analyzed the transcriptional profile in C666-1 cells treated with either Gap-BART exon III (from here on referred to as Gap-BART) or control GapmeRs (Gap-CTL) by RNA-seq. Sequence reads generated by pair-end 101-bp sequencing on the Illumina HiSeq 1500 sequencer were first aligned to the human genome (hg38), after which the unmapped reads were manually aligned to the wild type EBV genome (GenBank: NC_007605). The vast majority of filtered reads, between 94.9 and 95.5%, were mapped to the human genome, while only 0.11–0.30% were mapped to EBV (**Supplementary Tables 1A,B**). The low frequency of EBV sequences is consistent with the fact that EBV infection in NPC C666-1 is latent. Notably, transcripts mapped to EBV were mainly derived from the *Bam*HI-A region (**Supplementary Figure 1**).

Targeting BART lncRNA with GapmeRs resulted in the downregulation of 54 genes and the upregulation of 90 genes in C666-1 cells (>2-fold change for both upregulation and downregulation), when a false discovery rate (FDR) threshold of <0.1 was applied (**Figure 3A**). The influence of BART RNA on expression of other genes, together with its nuclear location, indicates that it most likely functions as lncRNA in NPC, and will henceforth be referred to as BART lncRNA. Differentially expressed genes identified through RNA-seq analysis were further analyzed using Partek Genomics Suite (version 6.6), which revealed gene ontology groupings with high enrichment scores and low *P*-values that are relevant to cancer (e.g., cell

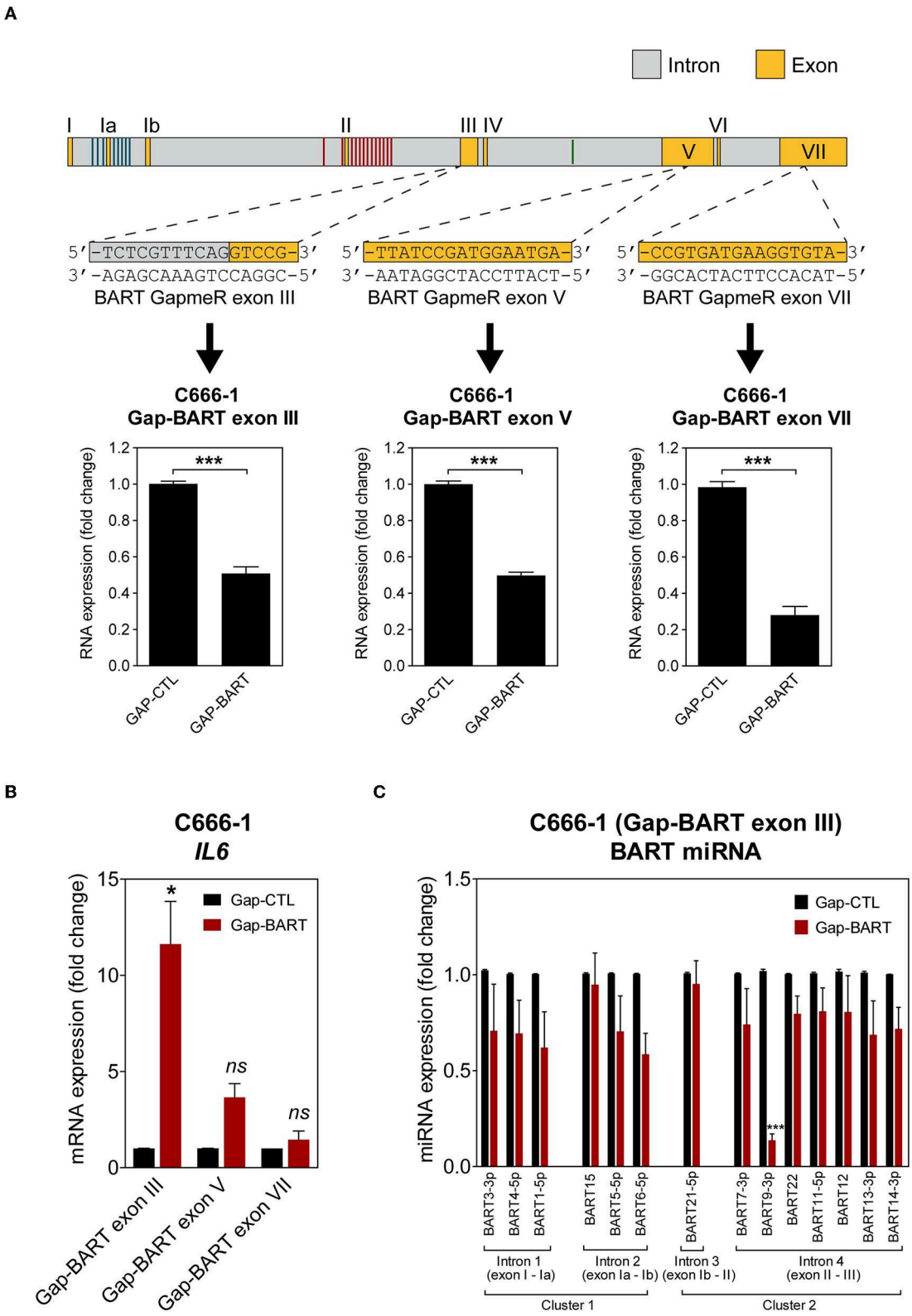

FIGURE 2 | Targeting of BART RNA with LNA™ longRNA GapmeRs. C666-1 cells were transfected with 100 nM LNA™ longRNA GapmeRs and RNA extracted 48 h later. **(A)** Three GapmeRs targeting different sequences within the BART region were analyzed to check their ability to cleave their target sequence and reduce BART

(Continued)

FIGURE 2 | RNA expression. Gene expression is shown as fold change in RNA expression relative to that of *GAPDH*. **(B)** Validation of the effect of GapmeRs targeting BART RNA on host gene expression in C666-1 cells. Expression of *IL6* was estimated by RT-qPCR following Gap-BART targeting of exons III, V, and VII. Gene expression is shown as fold change in RNA expression relative to that of *GAPDH*. **(C)** Analysis of BART miRNA expression in C666-1 cells after Gap-BART transfection. Expression is shown as fold change in miRNA expression relative to that of miR-Hsa-16. Results represent the average and SEM of three independent experiments. Statistical significance was calculated using the two-tailed Student's *t*-test. $^{*}P < 0.05$, $^{***}P < 0.001$, ns, not significant.

adhesion) and EBV infection (e.g., inflammatory and immune responses) (**Figure 3B**). The largest functional group consists of genes involved in the inflammatory response, which were all upregulated when BART lncRNAs were knocked down using GapmeRs. Similarly, most of the genes related to the immune response (6/7) and cell adhesion (6/8) were upregulated following targeting of BART lncRNA. Representative genes from the four gene ontology groups most relevant to EBV infection and cancer, namely inflammatory response, oxidoreductase activity, immune response, and cell adhesion were examined by quantitative RT-PCR (RT-qPCR) analysis to validate their response to BART lncRNA-knockdown (**Supplementary Figure 2**).

Among the differentially expressed genes, three genes from the downregulated group (*CDK8*, *SEPT9*, and *IKZF3*) were validated by both RT-qPCR and immunoblot (**Figure 3C**) to confirm the effect of BART lncRNA on the expression of these genes. These affected genes are associated with tumor progression, migration, and aberrant signaling in cancers (21–25). In particular, *IKZF3*, which encodes Aiolos and is normally not expressed in epithelial cells (26), was identified as being a potentially important target of BART lncRNA and was further examined in subsequent experiments.

Aiolos Is Expressed in NPC and Regulated by BART lncRNA

Aiolos, encoded by the *IKZF3* gene, is a lymphocyte-restricted transcription factor which is normally not expressed in epithelial cells (26). However, Aiolos expression has been detected in various malignant solid tumor cell lines and was found to downregulate adhesion-related genes in lung cancer cells (17). Since BART lncRNA expression seems to positively regulate *IKZF3* expression in C666-1 cells and negatively regulate cell adhesion-associated genes like *PCDHAC2* (**Figures 3A,C**), we first determined whether Aiolos is truly expressed in NPC cells. Indirect immunofluorescence with HEK 293T and C666-1 cells confirmed that Aiolos is expressed in the nucleus of NPC cells, but not in HEK 293T cells (**Figure 4A**). This result was further supported by immunoblotting, where moderate Aiolos expression could only be detected in C666-1 cells, with barely perceptible expression in AGS-Bx1 and none in any of the other epithelial cell lines tested, which included both EBV-positive and -negative cell lines (**Figure 4B**). As expected, both EBV-positive and -negative Burkitt's lymphoma cell lines exhibited high levels of Aiolos protein. In addition, all Aiolos-expressing cell lines exhibited no or very low $p66^{Shc}$ expression levels, which is consistent with a previous observation in lung cancer cells (17), and suggests that expression of Aiolos may also facilitate anchorage independence in NPC. This inverse relationship between *IKZF3* and $p66^{Shc}$ expression was also observed at the mRNA level (**Supplementary Figures 3A,B**). To further confirm regulation of Aiolos expression by BART lncRNA, we examined HEK 293T cells and AGS-Bx1 cells after transfection with a BART lncRNA expression vector. Compared to C666-1, AGS-Bx1 normally expresses relatively low levels of BART lncRNA and Aiolos (**Figures 1B**, **4B**). When transfected with pcDNA3-BART, expression of Aiolos is activated in HEK 293T cells, and significantly enhanced in AGS-Bx1 cells (**Figure 4C**). While GapmeR targeting of BART lncRNA not only results in downregulation of *IKZF3* expression, but also upregulates $p66^{Shc}$ mRNA expression, increased expression of $p66^{Shc}$ at the protein level is not apparent (**Figures 4A,D**). Next, we examined Aiolos expression by immunohistochemistry and observed positive staining in about 60% of NPC biopsies (17/26). Aiolos staining was apparent in tumor cells, but not in infiltrated non-cancerous cells (**Figure 4E**). It seems that EBV BART lncRNA may be involved in the regulation of host gene expression associated with anchorage independence in NPC cancers. These results suggest that modulation of Aiolos expression and associated pathways by EBV BART lncRNA may play an important role in NPC oncogenesis.

BART lncRNA Modulates Immune-Related Genes

Besides modulating expression of *IKZF3* and a variety of cell adhesion genes, we also found that BART lncRNA affects inflammatory and immune response-related genes, such as *IL6*, *IL13*, and *IL7R* (**Figure 3A**). Analysis of the RNA-seq data revealed that several immune-related genes were differentially expressed following targeted knockdown of BART lncRNA, and although the differences were not statistically significant in the RNA-seq analysis, they could be validated by RT-qPCR (**Figure 5**). Expression of two type III (*IFNL1* and *IFNL2*) and two type I (*IFNB1* and *IFNA1*) interferon genes was clearly upregulated, and various interferon-stimulated genes (ISGs) (*OAS2*, *ISG20*, *IFIT2*, and *IFIT1*), cytokine genes (*IL5*, *CXCL8*, and *IL10*), and a chemokine-related gene (*CXCR2*) were also upregulated by BART lncRNA-specific GapmeR treatment in C666-1 cells, indicating that EBV BART lncRNA may modulate the host immune response to facilitate immune evasion. The *CXCL8* gene, which encodes IL-8, and its corresponding receptor gene, *CXCR2*, are interesting targets of BART lncRNA because IL-8 is regulated by LMP1, functions as a chemotactic factor, and has been reported to promote metastasis of NPC by inducing epithelial-mesenchymal transition and downregulating E-cadherin through activation of Akt signaling (27, 28). While knockdown of BART lncRNA seems to cause upregulation of most interferons, ISGs, cytokines, and chemokine-related genes, it is interesting to note that *CXCL10* and *IFIH1*, which encodes

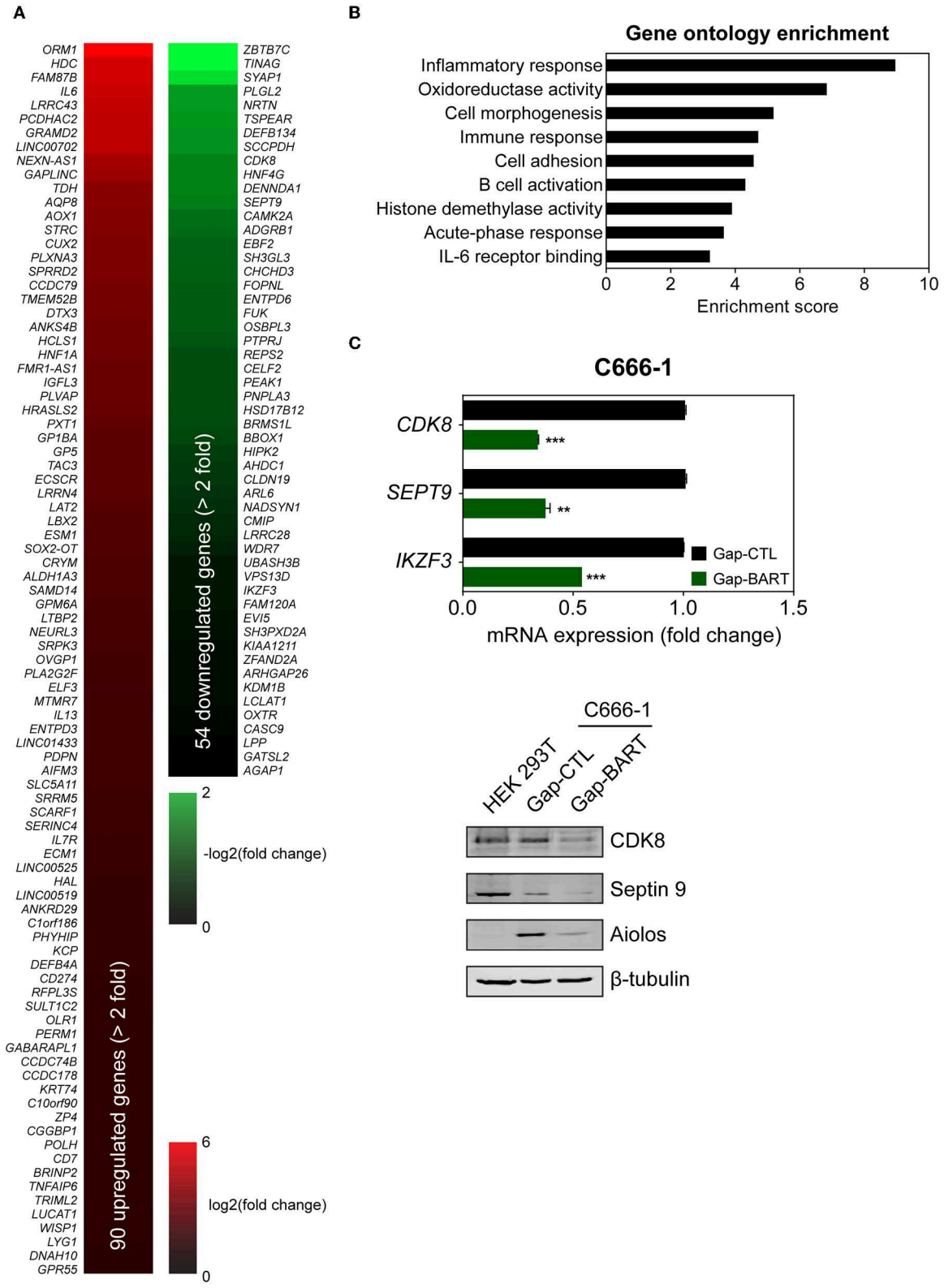

FIGURE 3 | Differential host gene expression following BART lncRNA knockdown, analyzed by RNA-seq. C666-1 cells were transfected with 100 nM LNA™ longRNA GapmeRs and RNA extracted for RNA-seq analysis 48 h later. **(A)** Upregulated (red) and downregulated (green) genes with a more than 2-fold change in expression

(Continued)

FIGURE 3 | with an FDR threshold of 0.1. **(B)** Gene ontology (GO) enrichment analysis of the up- and down-regulated genes was performed to group genes affected by BART lncRNA-targeting according to their involvement in biological processes and molecular functions. **(C)** RT-qPCR and immunoblot validation of mRNA and protein expression of *CDK8*, *SEPT9*, and *IKZF3*, which are downregulated following knockdown of BART lncRNA. Gene expression is shown as fold change in mRNA expression relative to that of *GAPDH*. C_P value > 35 were considered unreliable. The average and SEM of three independent experiments are shown. $^{**}P < 0.01$, $^{***}P < 0.001$.

MDA5, a cytoplasmic sensor of viral nucleic acids in host antiviral responses, were downregulated.

We then sought to confirm the effect of BART lncRNA on the expression of immune-related genes by overexpressing the BART lncRNA isoform *RPMS1* together with mitochondrial antiviral signaling protein (MAVS) in HEK 293T cells. A plasmid expressing the EBV-encoded nuclear lncRNA, *oriPtL*, was used as a control in these experiments (29). We found that BART lncRNA significantly inhibited MAVS-induced IFN-β promoter activity, while *oriPtL* did not show any effect (**Figure 6A**). Analysis of mRNA levels by RT-qPCR showed that expression of BART lncRNA downregulates a range of MAVS-induced interferons and ISGs in HEK 293T cells (**Figure 6B**). These results confirm an immunomodulatory role for BART lncRNA, consistent with the data from C666-1 cells treated with GapmeRs targeting EBV BART lncRNA.

BART lncRNA Inhibits Gene Expression by Affecting Transcription by RNA Polymerase II

The results described above indicate that BART lncRNA regulates expression of host genes associated with innate immunity and the oncogenesis process, so we then investigated how BART lncRNA regulates host gene expression. Using indirect immunofluorescence and RNA FISH, we found that BART lncRNA co-localizes with RNA polymerase II (Pol II) in HEK 293T cells (**Figure 7A**), indicating that BART lncRNA may play a role in transcriptional regulation by interacting with the Pol II complex. To verify that BART lncRNA may be involved with the Pol II-promoter complex, HEK 293T cells were transfected with pcDNA3-BART, followed by chromatin-immunoprecipitation (ChIP) of the promoter or coding regions of the *IFNB1* gene, which is negatively regulated by BART lncRNA. ChIP analysis with anti-Pol II showed a higher enrichment at the promoter region (−22) of the *IFNB1* gene, but this higher enrichment was not observed downstream near the end of the *IFNB1* gene (+662) (**Figure 7B**). It is tempting to hypothesize that elongation of transcription by Pol II from the promoter region (−22) may be blocked or stalled, resulting in reduced transcription of the BART lncRNA-targeted gene. To further test this hypothesis, we analyzed Pol II occupation at the promoter regions of *IFNB1* and *CXCL8* in C666-1 cells and observed that knockdown of BART lncRNA resulted in significantly less Pol II enrichment at the promoters of both genes (**Figure 7C**). The reduced enrichment of Pol II following targeting of BART lncRNA with GapmeRs is in line with the increase in *IFNB1* and *CXCL8* gene expression shown in **Figure 5**. These findings suggest a mechanism by which BART lncRNA can downregulate gene expression by interfering with Pol II-mediated transcription (**Figure 7D**).

To further examine our hypothesis that EBV BART lncRNA is involved in epigenetic regulation of gene expression, we explored a possible association between BART lncRNA and the CREB-binding protein (CBP), which interacts with various transcription factors. CBP belongs to the p300/CBP co-activator family and plays a key role in the transcriptional activation of *IFNB1* and many other cellular genes. In HEK 293T cells transfected with pcDNA3-BART, RNA-FISH, and co-staining of CBP showed that BART lncRNA and CBP co-localize in the nucleus (**Figure 7E**). Similarly, co-localization of BART lncRNA and CBP was observed in C666-1 cells which harbor EBV and express abundant levels of BART lncRNA endogenously (**Figure 7E**). These results suggest a mechanism by which BART lncRNA regulates host gene expression through interaction with CBP in EBV infected cells. To further test this contention a histone acetyltransferase (HAT) assay was performed, which showed that BART lncRNA expression can inhibit MAVS-induced HAT activity, further indicating that BART lncRNA may play a role in regulating chromatin remodeling during the gene transcription process (**Figure 7F**).

DISCUSSION

EBV is recognized as one of the etiological factors for nasopharyngeal carcinoma, in addition to genetic predisposition and putative environmental factors (30). While considerable attention has been focused on oncogenesis in EBV-associated lymphomas, the role of EBV in nasopharyngeal carcinoma is less well-understood. Studies into the role of EBV in NPC may have been hampered by the perception that NPC is a rare cancer, a lack of suitable *in vitro* and *in vivo* models and, most importantly, the fact that EBV expresses very few viral proteins in NPC cells, despite all cancer cells harboring the EBV genome. Nevertheless, it has long been known that EBV expresses elevated levels of BART non-coding RNAs, including miRNAs, and lncRNAs, in NPC cells (3, 31). The biological significance of EBV BART miRNA has been extensively analyzed and various functions associated with cell growth, immune evasion and anti-apoptotic activities have been revealed or are being actively explored (32). However, little is known regarding the role of BART lncRNAs expressed from the same transcripts. Here we present results from analysis of RNA expression profiles from NPC C666-1 cells where BART lncRNA is knocked down. Our findings show that BART lncRNA is involved in modulation of host cell expression of genes involved in cell adhesion, and those encoding interferons, ISGs, cytokines, and chemokines. Notably, BART lncRNA was found to activate expression of *IKZF3* (Aiolos), which is normally restricted to lymphocytes. We further showed that nuclear BART lncRNA associates with Pol II and the CBP/p300 complex. These results suggest that EBV BART lncRNA may play a role in epigenetic modulation of host gene expression through interaction with the host DNA methylation machinery and chromatin remodeling process during gene transcription.

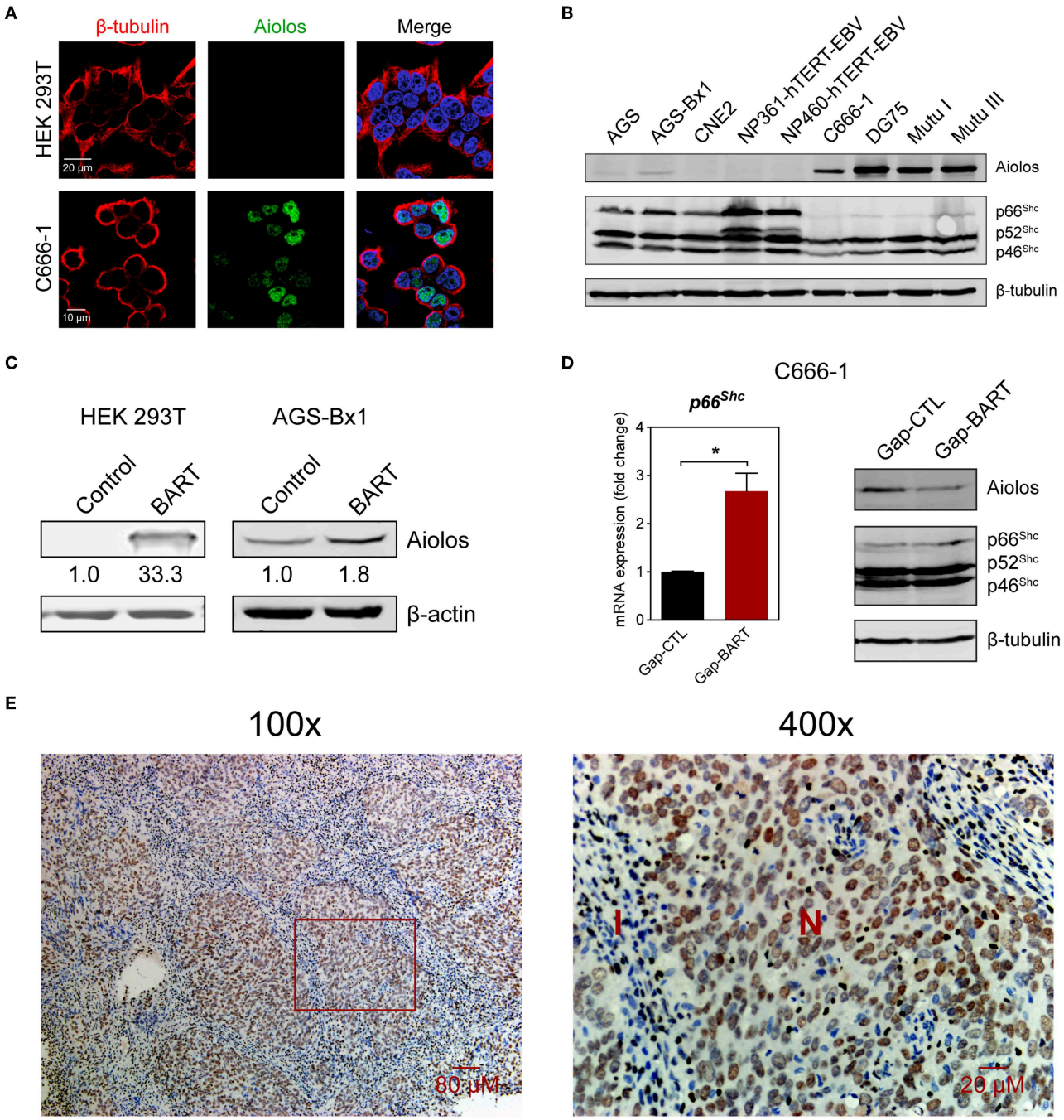

FIGURE 4 | Aiolos expression in NPC. **(A)** Aiolos protein expression was analyzed by indirect immunofluorescence in HEK 293T and C666-1 cells. **(B)** Immunoblot analysis showing Aiolos and p66^{Shc} expression in various cell lines. AGS, AGS-Bx1, CNE2, NP361-hTERT-EBV, NP460-hTERT-EBV, and C666-1 are epithelial cell lines, while DG75, Mutu I, and Mutu III are Burkitt's lymphoma cell lines. All cell lines are EBV-positive, except for AGS, CNE2, and DG75. **(C)** Effect of BART lncRNA on Aiolos expression. A plasmid containing one of the major species of BART lncRNAs (*RPMS1*) was transfected into HEK 293T and AGS-Bx1 cells. **(D)** Effect of targeting BART lncRNA with GapmeRs on levels of p66^{Shc} mRNA expression and Aiolos protein expression. The average and SEM of three independent experiments are shown. Gene expression is shown as fold change in mRNA expression relative to that of *GAPDH*. $^{*}P < 0.05$. **(E)** Immunohistochemistry for Aiolos was performed on 26 NPC biopsies. A representative image shows Aiolos staining (brown) in NPC cells at 100× and 400× magnification. I, cellular infiltrate; N, NPC cells.

EBV adopts different latency programs to evade immune surveillance *in vivo*. The hallmark of EBV latency in NPC is expression of elevated levels of EBV BARTs, including miRNAs, and lncRNAs. It is possible that EBV BARTs perform latency-associated functions in NPC cells that are performed by EBV latency proteins in B cells. Advances in recognizing the function

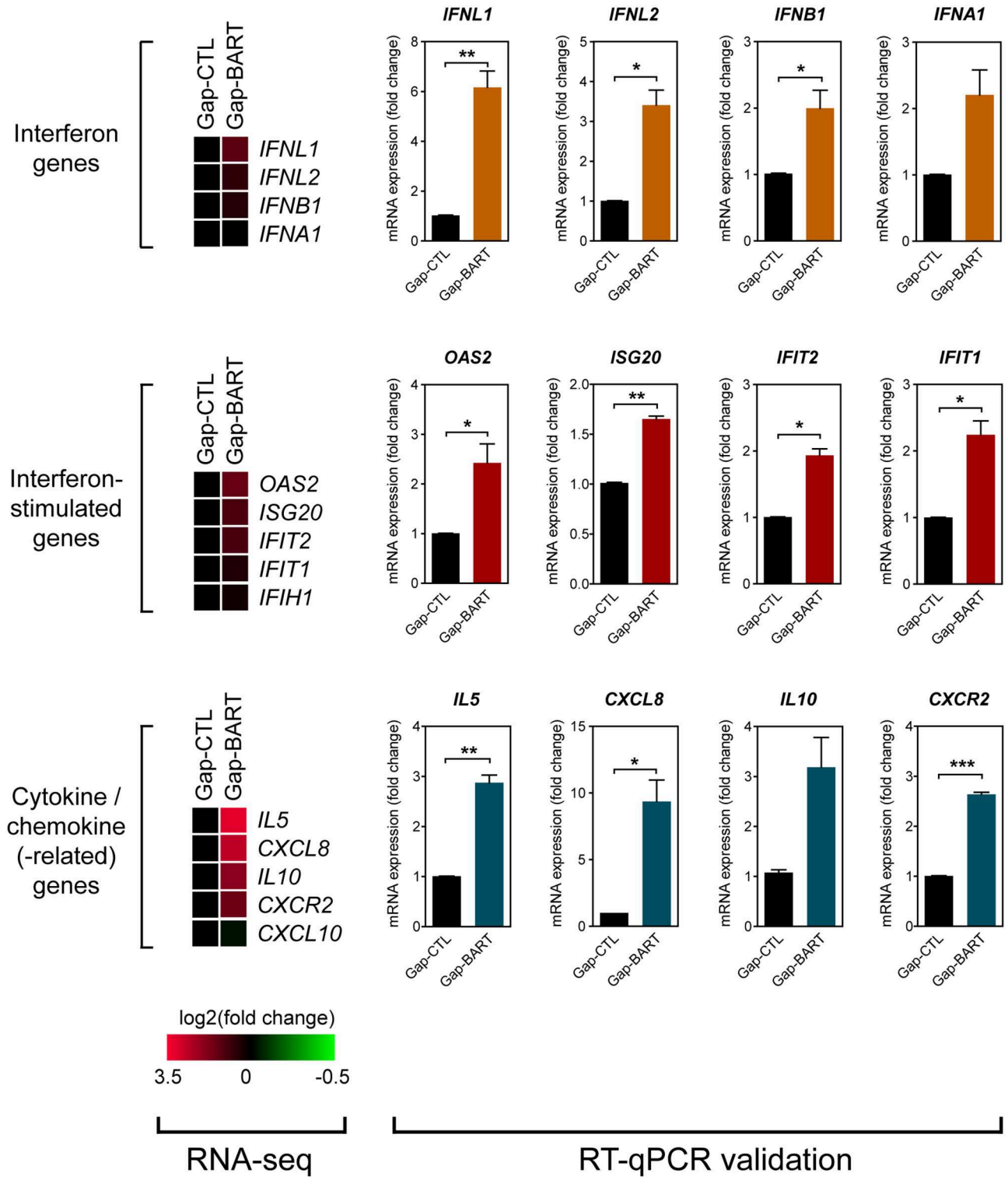

FIGURE 5 | Targeting BART lncRNA affects immune-related gene expression. Differential expression of various interferon, interferon-stimulated, cytokine and chemokine genes not fitting the RNA-seq analysis criteria (>2-fold up- or down-regulation, 0.1 FDR) was analyzed by RT-qPCR. Gene expression is shown as fold change in mRNA expression relative to that of *GAPDH*. Results represent the average and SEM of three independent experiments. $^{*}P < 0.05$, $^{**}P < 0.01$, $^{***}P < 0.001$.

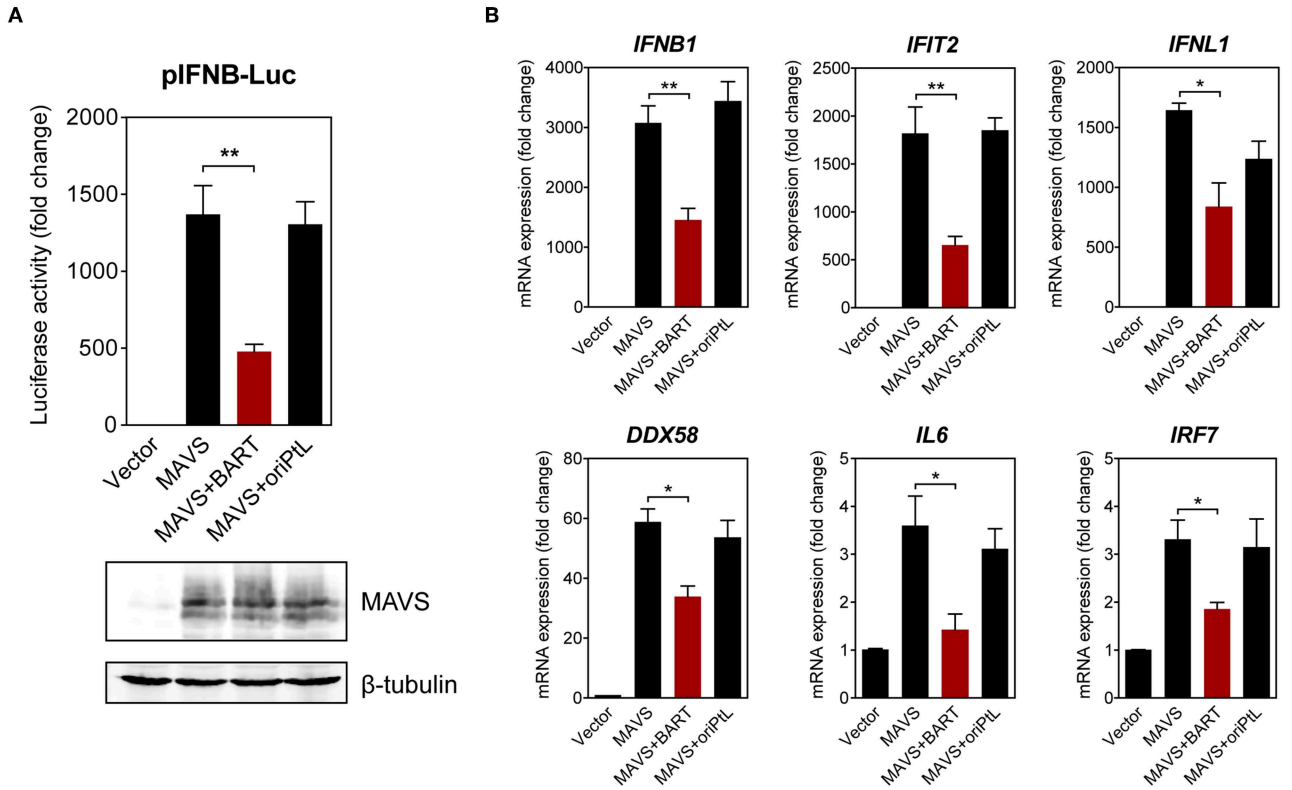

FIGURE 6 | BART lncRNA expression modulates immune-related gene expression. **(A)** HEK 293T cells were co-transfected with an empty vector or an MAVS expression vector, with or without a BART or oriPtL expression vector, plus an IFN-β promoter reporter. Luciferase activities are expressed as fold change in luciferase activity, calculated by normalizing firefly/renilla ratios to the vector control. The expression of MAVS and β-tubulin was detected by immunoblotting using specific antibodies. **(B)** RT-qPCR analysis of the expression of various immune-related genes following transfection of HEK 293T cells with an empty vector or an MAVS expression vector, with or without a BART or oriPtL expression vector. Gene expression is shown as fold change in mRNA expression relative to that of *GAPDH*. The average and SEM of three independent experiments are shown. $^{*}P < 0.05$, $^{**}P < 0.01$.

of lncRNAs in modulating gene expression has opened up new directions for exploring the biological significance of EBV BARTs in EBV infection and EBV-associated tumors. The expression of one of the isoforms of BART lncRNA can modulate cellular gene expression in a manner similar to that of EBV infection in AGS cells (33). Cellular lncRNAs have been found to interact with chromatin, protein, and RNA in both the nucleus and cytoplasm to modulate gene expression in cancer pathways (34). We have confirmed nuclear localization of BART lncRNA in both epithelial and lymphoid EBV-infected cell lines in different forms of latency by cellular fraction and RNA FISH analyses, supporting the idea that BART RNAs function as non-protein-coding transcripts in the nucleus. It seems likely that EBV has developed a strategy to shut off expression of most viral proteins to avoid immune surveillance, while utilizing BART lncRNAs to modulate host gene expression and enable establishment of latency in NPC cells. Consequently, this altered cellular gene expression may generate an environment that drives the oncogenesis process in NPC.

One of the interesting findings in this study is that *IKZF3* expression is downregulated upon knock down of BART lncRNA. Aiolos, encoded by *IKZF3*, is a member of the *Ikaros* zinc-finger protein family and its expression is usually restricted to lymphoid cells (26). Expression of Aiolos is accompanied by a sustained loss of lymphocyte adhesion to its matrix-rich microenvironment, enabling lymphocyte entry into the bloodstream and subsequent circulation to other organs (35). High levels of Aiolos expression have been reported in both liquid and solid tumors, where it promotes tumor cell survival and acts as an epigenetic driver of lymphocyte mimicry in metastatic epithelial cancers (24, 36). Aiolos promotes anchorage independence in lung cancer by downregulating several adhesion-related genes, and also by blocking anoikis through the silencing of the anchorage reporter gene $p66^{Shc}$, an isoform of the *SHC1* gene (17). Notably, we detected Aiolos expression *in vitro* in C666-1 cells and *in vivo* in NPC biopsies, but not in many other epithelial cell lines (**Figure 4B**). We suspected that expression of Aiolos may be caused by BART lncRNA, and indeed found that ectopic expression of BART lncRNA induces Aiolos expression in HEK 293T cells and upregulates expression of Aiolos in AGS-Bx1 cells. Apart from BART lncRNA expression, high NF-κB and STAT3 activity also occurs in NPC cells (11, 37, 38); these two cell signaling pathways are known to activate the *IKZF3* promoter and may also contribute to Aiolos expression (16, 39).

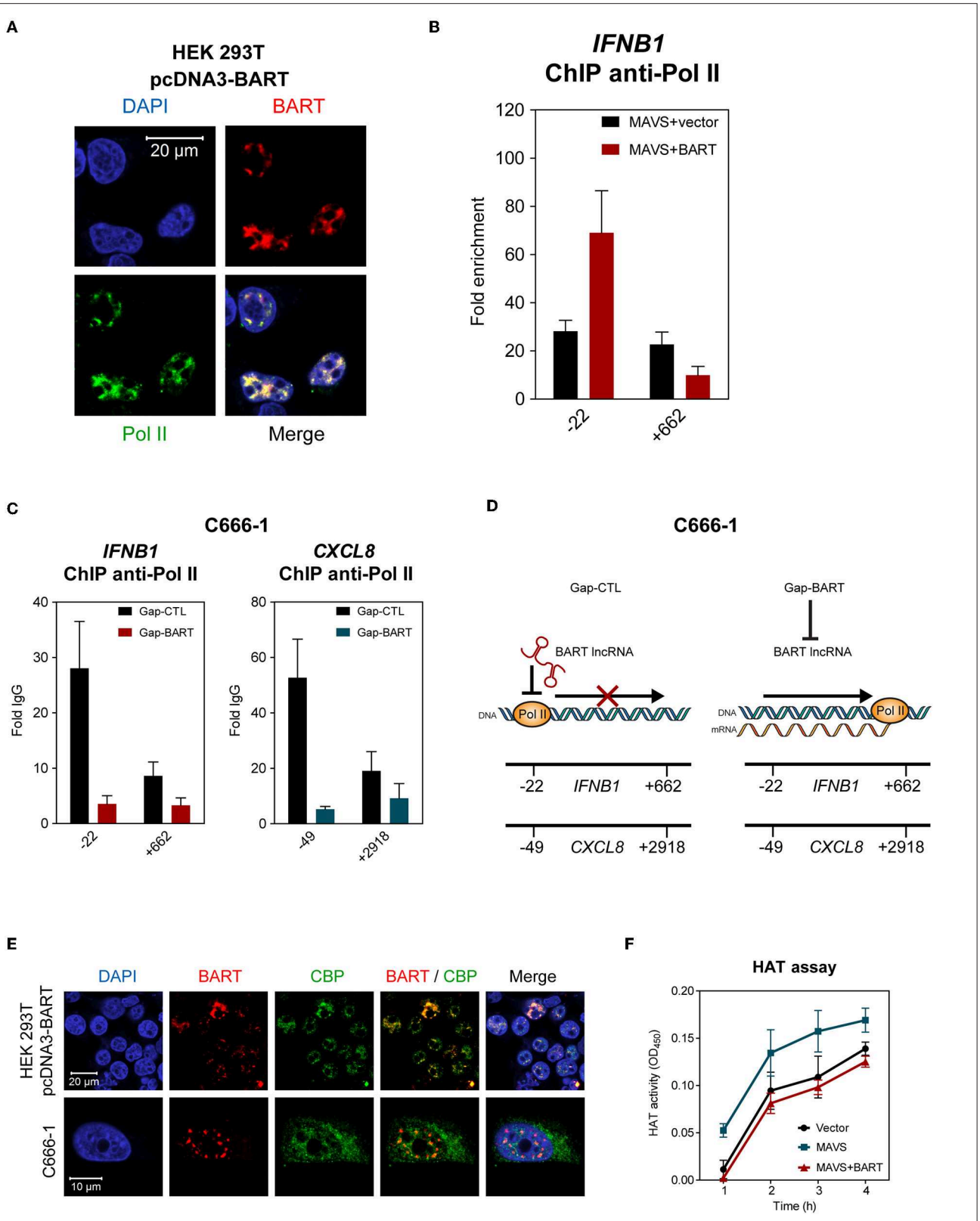

FIGURE 7 | BART lncRNA affects gene transcription through Pol II. **(A)** Combined RNA FISH and indirect immunofluorescence was performed to detect BART lncRNA and Pol II expression in HEK 293T cells transfected with the BART expression vector. **(B)** ChIP analysis of *IFNB1* promoter (−22) and downstream (+662)

(Continued)

FIGURE 7 | DNA with Pol II antibodies in HEK 293T cells where MAVS was expressed alone, or together with BART lncRNA. The average and SEM of three independent experiments are shown. **(C)** ChIP analysis of *IFNB1* and *CXCL8* promoter and downstream DNA with Pol II antibodies in BART lncRNA-knockdown C666-1 cells. The average and SEM of three independent experiments are shown. **(D)** A model suggesting how *IFNB1* and *CXCL8* expression is increased following knockdown of BART lncRNA. **(E)** Combined RNA FISH and indirect immunofluorescence analysis of HEK 293T cells transfected with the BART expression vector and C666-1 cells, showing expression of BART lncRNA and CBP. **(F)** MAVS-induced HAT activity in HEK 293T cells transfected with a MAVS expression vector, with or without a BART expression vector. For transfection experiments, extracts were obtained 48 h after transfection. The average and SEM of three independent experiments are shown.

The upregulation of adhesion genes, as well as $p66^{Shc}$, following targeting of BART lncRNA may therefore be explained in part by lower expression of Aiolos (**Figure 4D**). It seems possible that expression of BART lncRNAs inhibits cell adhesion and anoikis and may thereby facilitate anchorage independence and metastasis of cancer cells. Still unanswered is how altered cellular expression of genes, such as *IKZF3*, may contribute to the EBV latency program in NPC cells.

Most data obtained in this study seems to suggest that EBV BART lncRNA has a role in epigenetic activation. Septin 9, a well-established biomarker for colorectal cancer that is hypermethylated in several cancers (21), is upregulated by EBV BART lncRNA. However, epigenetic suppression of *GAPLINC*, *DTX3*, and *ELF3* were also observed (**Figure 3A**). The biological significance of the epigenetic modulation of these cancer-associated genes needs to be further evaluated. The role of BART lncRNA in epigenetic regulation of host genes is further supported by evidence that BART lncRNA associates with p300/CBP and Pol II in the nucleus. Both *IFNB1* and *CXCL8* genes were upregulated in C666-1 cells by knocking down BART lncRNA; this also resulted in increased Pol II occupation at the promoter region, but not near the 3' end of these genes. It seems that BART lncRNA may stall Pol II at the promoter region, preventing transcription of the targeted genes, and resulting in lower gene expression. Other mechanisms of BART lncRNA regulation may involve histone methylation and acetylation through interaction with p300/CBP. Further studies are necessary to reveal the molecular basis of epigenetic regulation of host genes by BART lncRNA, and how consequently altered cellular gene expression may facilitate EBV latency and drive oncogenesis in EBV-associated tumors.

Our findings clearly suggest that BART lncRNAs are involved in epigenetic regulation of host gene expression in NPC. While more work needs to be done to fully characterize the role of BART lncRNA in EBV-associated tumors, it seems reasonable to postulate that EBV adopts a strategy to turn off expression of most antigenic latency proteins and instead express abundant levels of BART lncRNA to suppress the immune response in NPC cells. In NPC cells, most of the latent genes are highly methylated with only EBNA1 being expressed. BART lncRNA functions as an epigenetic modulator to generate a microenvironment that is conducive to EBV latency in NPC. Consequently, aberrant expression of genes mediated by BART lncRNA may lead to evasion of the immune response, cancer progression, and metastasis in NPC.

DATA AVAILABILITY STATEMENT

RNA-seq data has been uploaded to NCBI: https://www.ncbi.nlm.nih.gov/sra/PRJNA556573. This data can be accessed using the accession number: PRJNA556573.

AUTHOR CONTRIBUTIONS

RV and HC conceived the study and designed the experiments. RV, ST, BM, JL, SH, JZ, and YC performed experiments. RV, S-WT, ML, and HC analyzed data. RV and HC wrote the paper.

FUNDING

This study was supported in part by the Research Grants Council of the Hong Kong SAR (17154516, 17119618, and C7027-16G), the Collaborative Research Fund, the Health and Medical Research Fund (14131032), the Areas of Excellence Scheme of the University Grants Committee (Grant AoE/M-06/08), and the Cross Trait Joint Funds of the National Natural Science Foundation of China (Grant No. U1405221).

ACKNOWLEDGMENTS

The authors are grateful to Dr. Jane Rayner for editing the manuscript. We would like to thank Nick Lin from the HKU Centre for Genomic Sciences for his help with the RNA-seq procedure and analysis.

SUPPLEMENTARY MATERIAL

The Supplementary Material for this article can be found online at: https://www.frontiersin.org/articles/10.3389/fonc.2019.01120/full#supplementary-material

REFERENCES

1. Rickinson AB, Kieff ED. Epstein-Barr virus. In: Knipe DM, Howley PM, editors. *Fields Virology*, 5th ed. Vol. 2. Philadelphia: Lippincott Williams & Wilkins (2007). p. 2655–700.
2. Kieff ED, Rickinson AB. Epstein-Barr virus and its replication. In: Knipe DM, Howley PM, editors. *Fields Virology*, 5th edn. Vol. 2. Philadelphia: Lippincott Williams & Wilkins (2007). p. 2655–700.
3. Chen HL, Lung MM, Sham JS, Choy DT, Griffin BE, Ng MH. Transcription of BamHI-A region of the EBV genome in NPC tissues and B cells. *Virology*. (1992) 191:193–201. doi: 10.1016/0042-6822(92)90181-N
4. Hitt MM, Allday MJ, Hara T, Karran L, Jones MD, Busson P, et al. EBV gene expression in an NPC-related tumour.

EMBO J. (1989) 8:2639–51. doi: 10.1002/j.1460-2075.1989.tb08404.x
5. Gilligan K, Sato H, Rajadurai P, Busson P, Young L, Rickinson A, et al. Novel transcription from the Epstein-Barr virus terminal EcoRI fragment, DIJhet, in a nasopharyngeal carcinoma. *J Virol.* (1990) 64:4948–56.
6. Chen H, Smith P, Ambinder RF, Hayward SD. Expression of Epstein-Barr virus BamHI-A rightward transcripts in latently infected B cells from peripheral blood. *Blood.* (1999) 93:3026–32. doi: 10.1182/blood.V93.9.3026
7. Pfeffer S, Zavolan M, Grasser FA, Chien M, Russo JJ, Ju J, et al. Identification of virus-encoded microRNAs. *Science.* (2004) 304:734–6. doi: 10.1126/science.1096781
8. Edwards RH, Marquitz AR, Raab-Traub N. Epstein-Barr virus BART microRNAs are produced from a large intron prior to splicing. *J Virol.* (2008) 82:9094–106. doi: 10.1128/JVI.00785-08
9. Verhoeven RJ, Tong S, Zhang G, Zong J, Chen Y, Jin DY, et al. NF-kappaB signaling regulates expression of Epstein-Barr virus BART MicroRNAs and long noncoding RNAs in nasopharyngeal carcinoma. *J Virol.* (2016) 90:6475–88. doi: 10.1128/JVI.00613-16
10. Chen H, Huang J, Wu FY, Liao G, Hutt-Fletcher L, Hayward SD. Regulation of expression of the Epstein-Barr virus BamHI-A rightward transcripts. *J Virol.* (2005) 79:1724–33. doi: 10.1128/JVI.79.3.1724-1733.2005
11. Lo AK, Lo KW, Tsao SW, Wong HL, Hui JW, To KF, et al. Epstein-Barr virus infection alters cellular signal cascades in human nasopharyngeal epithelial cells. *Neoplasia.* (2006) 8:173–80. doi: 10.1593/neo.05625
12. Zheng H, Dai W, Cheung AK, Ko JM, Kan R, Wong BW, et al. Whole-exome sequencing identifies multiple loss-of-function mutations of NF-kappaB pathway regulators in nasopharyngeal carcinoma. *Proc Natl Acad Sci USA.* (2016) 113:11283–8. doi: 10.1073/pnas.1607606113
13. Smith PR, de Jesus O, Turner D, Hollyoake M, Karstegl CE, Griffin BE, et al. Structure and coding content of CST (BART) family RNAs of Epstein-Barr virus. *J Virol.* (2000) 74:3082–92. doi: 10.1128/JVI.74.7.3082-3092.2000
14. Marquitz AR, Mathur A, Edwards RH, Raab-Traub N. Host gene expression is regulated by two types of noncoding RNAs transcribed from the Epstein-BamHI a rightward transcript region. *J Virol.* (2015) 89:11256–68. doi: 10.1128/JVI.01492-15
15. Al-Mozaini M, Bodelon G, Karstegl CE, Jin B, Al-Ahdal M, Farrell PJ. Epstein-Barr virus BART gene expression. *J Gen Virol.* (2009) 90:307–16. doi: 10.1099/vir.0.006551-0
16. Quintana FJ, Jin H, Burns EJ, Nadeau M, Yeste A, Kumar D, et al. Aiolos promotes TH17 differentiation by directly silencing Il2 expression. *Nat Immunol.* (2012) 13:770–7. doi: 10.1038/ni.2363
17. Li X, Xu Z, Du W, Zhang Z, Wei Y, Wang H, et al. Aiolos promotes anchorage independence by silencing $p66^{Shc}$ transcription in cancer cells. *Cancer Cell.* (2014) 25:575–89. doi: 10.1016/j.ccr.2014.03.020
18. Dobin A, Davis CA, Schlesinger F, Drenkow J, Zaleski C, Jha S, et al. STAR: ultrafast universal RNA-seq aligner. *Bioinformatics.* (2013) 29:15–21. doi: 10.1093/bioinformatics/bts635
19. Landt SG, Marinov GK, Kundaje A, Kheradpour P, Pauli F, Batzoglou S, et al. ChIP-seq guidelines and practices of the ENCODE and modENCODE consortia. *Genome Res.* (2012) 22:1813–31. doi: 10.1101/gr.136184.111
20. Zhang GH, Zong JF, Lin SJ, Verhoeven RJA, Tong S, Chen YX, et al. Circulating Epstein-Barr virus microRNAs miR-BART7 and miR-BART13 as biomarkers for nasopharyngeal carcinoma diagnosis and treatment. *Int J Cancer.* (2015) 136:E301–12. doi: 10.1002/ijc.29206
21. Force USPST, Bibbins-Domingo K, Grossman DC, Curry SJ, Davidson KW, Epling JW Jr, et al. Screening for colorectal cancer: US Preventive Services Task Force Recommendation statement. *JAMA.* (2016) 315:2564–75. doi: 10.1001/jama.2016.5989
22. Gatza ML, Silva GO, Parker JS, Fan C, Perou CM. An integrated genomics approach identifies drivers of proliferation in luminal-subtype human breast cancer. *Nat Genet.* (2014) 46:1051–9. doi: 10.1038/ng.3073
23. Hu Y, Wang J, Qian J, Kong X, Tang J, Wang Y, et al. Long noncoding RNA GAPLINC regulates CD44-dependent cell invasiveness and associates with poor prognosis of gastric cancer. *Cancer Res.* (2014) 74:6890–902. doi: 10.1158/0008-5472.CAN-14-0686
24. Antica M, Cicin-Sain L, Kapitanovic S, Matulic M, Dzebro S, Dominis M. Aberrant ikaros, aiolos, and helios expression in hodgkin and non-hodgkin lymphoma. *Blood.* (2008) 111:3296–7. doi: 10.1182/blood-2007-12-125682
25. Duhamel M, Arrouss I, Merle-Beral H, Rebollo A. The Aiolos transcription factor is up-regulated in chronic lymphocytic leukemia. *Blood.* (2008) 111:3225–8. doi: 10.1182/blood-2007-09-113191
26. Morgan B, Sun L, Avitahl N, Andrikopoulos K, Ikeda T, Gonzales E, et al. Aiolos, a lymphoid restricted transcription factor that interacts with Ikaros to regulate lymphocyte differentiation. *EMBO J.* (1997) 16:2004–13. doi: 10.1093/emboj/16.8.2004
27. Li XJ, Peng LX, Shao JY, Lu WH, Zhang JX, Chen S, et al. As an independent unfavorable prognostic factor, IL-8 promotes metastasis of nasopharyngeal carcinoma through induction of epithelial-mesenchymal transition and activation of AKT signaling. *Carcinogenesis.* (2012) 33:1302–9. doi: 10.1093/carcin/bgs181
28. Yoshizaki T, Horikawa T, Qing-Chun R, Wakisaka N, Takeshita H, Sheen TS, et al. Induction of interleukin-8 by Epstein-Barr virus latent membrane protein-1 and its correlation to angiogenesis in nasopharyngeal carcinoma. *Clin Cancer Res.* (2001) 7:1946–51.
29. Cao S, Moss W, O'Grady T, Concha M, Strong MJ, Wang X, et al. New noncoding lytic transcripts derived from the Epstein-Barr virus latency origin of replication, oriP, are hyperedited, bind the paraspeckle protein, NONO/p54nrb, and support viral lytic transcription. *J Virol.* (2015) 89:7120–32. doi: 10.1128/JVI.00608-15
30. Raab-Traub N. Epstein-Barr virus and nasopharyngeal carcinoma. *Semin Cancer Biol.* (1992) 3:297–307. doi: 10.1007/978-1-4612-0405-3_1
31. Qiu J, Cosmopoulos K, Pegtel M, Hopmans E, Murray P, Middeldorp J, et al. A novel persistence associated EBV miRNA expression profile is disrupted in neoplasia. *PLoS Pathog.* (2011) 7:e1002193. doi: 10.1371/journal.ppat.1002193
32. Klinke O, Feederle R, Delecluse HJ. Genetics of Epstein-Barr virus microRNAs. *Semin Cancer Biol.* (2014) 26:52–9. doi: 10.1016/j.semcancer.2014.02.002
33. Matsusaka K, Kaneda A, Nagae G, Ushiku T, Kikuchi Y, Hino R, et al. Classification of Epstein-Barr virus-positive gastric cancers by definition of DNA methylation epigenotypes. *Cancer Res.* (2011) 71:7187–97. doi: 10.1158/0008-5472.CAN-11-1349
34. Schmitt AM, Chang HY. Long noncoding RNAs in cancer pathways. *Cancer Cell.* (2016) 29:452–63. doi: 10.1016/j.ccell.2016.03.010
35. Wang JH, Avitahl N, Cariappa A, Friedrich C, Ikeda T, Renold A, et al. Aiolos regulates B cell activation and maturation to effector state. *Immunity.* (1998) 9:543–53. doi: 10.1016/S1074-7613(00)80637-8
36. Terada LS, Liu Z. Aiolos and lymphocyte mimicry in lung cancer. *Mol Cell Oncol.* (2014) 1:e29912. doi: 10.4161/mco.29912
37. Chen H, Lee JM, Wang Y, Huang DP, Ambinder RF, Hayward SD. The Epstein-Barr virus latency BamHI-Q promoter is positively regulated by STATs and Zta interference with JAK/STAT activation leads to loss of BamHI-Q promoter activity. *Proc Natl Acad Sci USA.* (1999) 96:9339–44. doi: 10.1073/pnas.96.16.9339
38. Thornburg NJ, Pathmanathan R, Raab-Traub N. Activation of nuclear factor-kappaB p50 homodimer/Bcl-3 complexes in nasopharyngeal carcinoma. *Cancer Res.* (2003) 63:8293–301.
39. Billot K, Soeur J, Chereau F, Arrouss I, Merle-Beral H, Huang ME, et al. Deregulation of Aiolos expression in chronic lymphocytic leukemia is associated with epigenetic modifications. *Blood.* (2011) 117:1917–27. doi: 10.1182/blood-2010-09-307140

Conflict of Interest: The authors declare that the research was conducted in the absence of any commercial or financial relationships that could be construed as a potential conflict of interest.

frontiers in Cell and Developmental Biology

ORIGINAL RESEARCH
published: 15 November 2019
doi: 10.3389/fcell.2019.00266

MiR-506 Targets *UHRF1* to Inhibit Colorectal Cancer Proliferation and Invasion via the *KISS1/PI3K/NF-κB* Signaling Axis

Yilin Lin[1†], Zhihua Chen[1†], Yan Zheng[1], Yisu Liu[1], Ji Gao[2], Suyong Lin[1] and Shaoqin Chen[1†]*

[1] Department of Gastrointestinal Surgery, The First Affiliated Hospital of Fujian Medical University, Fuzhou, China, [2] School of Nursing, Fujian Medical University, Fuzhou, China

OPEN ACCESS

Edited by:
Patricia P. Reis,
São Paulo State University, Brazil

Reviewed by:
Hua Zhang,
Guangdong Medical University, China
Marc Mousli,
Université de Strasbourg, France

***Correspondence:**
Shaoqin Chen
chenshaoqln1613@163.com

[†] These authors have contributed equally to this work

Specialty section:
This article was submitted to Molecular and Cellular Oncology, a section of the journal Frontiers in Cell and Developmental Biology

Received: 15 July 2019
Accepted: 18 October 2019
Published: 15 November 2019

Citation:
Lin Y, Chen Z, Zheng Y, Liu Y, Gao J, Lin S and Chen S (2019) MiR-506 Targets UHRF1 to Inhibit Colorectal Cancer Proliferation and Invasion via the KISS1/PI3K/NF-κB Signaling Axis. Front. Cell Dev. Biol. 7:266. doi: 10.3389/fcell.2019.00266

Background: The *UHRF1* gene is an epigenetic modification factor that mediates tumor suppressor gene silencing in a variety of cancers. Related studies have reported that *UHRF1* can inhibit the expression of the *KISS1* gene. However, the regulatory mechanism underlying *UHRF1* expression in colorectal cancer (CRC) is still unclear. The aim of this study was to gain a better understanding of the regulation of *UHRF1* expression in CRC and to determine whether it regulates the mechanism by which *KISS1* promotes CRC metastasis.

Methods: In the present study, the levels of *miR-506*, *UHRF*1 and *KISS1* expression in CRC tissues and in human CRC cell lines were studied using quantitative real-time PCR (qRT-PCR) and Western blotting. Cell proliferation, migration, and invasion assays are used to detect cell proliferation, migration, and invasion. A dual-luciferase reporter system was used to confirm the target gene of *miR-506*.

Results: This study found that *UHRF1* protein is highly expressed in CRC tissues and negatively correlated with *KISS1* protein expression. *UHRF1* overexpression activates the *PI3K/NF-κB* signaling pathway by inhibiting the mRNA expression levels of pathway mediators. Bioinformatics analysis and luciferase reporter gene assays confirmed that *miR-506* targets *UHRF1*.

Conclusion: This study identified the regulation of *UHRF1* expression in CRC and the mechanism of CRC metastasis. *UHRF1* may be a new potential target molecule for future CRC metastasis treatment.

Keywords: CRC, *miR-506*, *UHRF1*, proliferation, invasion

Abbreviations: BSP, bisulfite sequencing PCR; CRC, colorectal cancer; DAPI, 4,6-diamidino-2-phenylindole; ECL, electrochemiluminescence; EdU, 5-ethynyl-2′-deoxyuridine; PVDF, polyvinylidene fluoride; qRT-PCR, quantitative real-time PCR; RIPA, radioimmunoprecipitation assay; ROS, reactive oxygen species; UHRF1, ubiquitin-like with plant homeodomain and RING finger domains 1; 3′ UTR, 3′ untranslated region.

INTRODUCTION

Colorectal cancer (CRC) is a common malignant tumor of the digestive tract. Globally, the incidence of CRC ranks third among malignancies, below lung cancer and breast cancer (Bray et al., 2018). The lack of typical clinical symptoms is one of the reasons for the low rate of early CRC diagnosis. Comprehensive treatments such as surgery, radiation therapy, chemotherapy, biological targeting, and immunotherapy are currently the standard treatment approaches for CRC (Ni et al., 2018; Ganesh et al., 2019; Li S. et al., 2019; Siravegna et al., 2019). However, CRC metastasis remains an urgent problem, as metastasis negatively affects patient prognosis. Gene-targeted therapy has great potential, and finding effective therapeutic targets is the focus of current research (de Mel et al., 2019; Erel-Akbaba et al., 2019; Schiza et al., 2019). Studies have shown that the occurrence and development of CRC involve the activation of proto-oncogenes and the inactivation of tumor suppressor genes (Sanz-Garcia et al., 2017; Zhang and Shay, 2017), as well as microRNA changes in the tumor microenvironment (Vu and Datta, 2017; De Robertis et al., 2018; Lin X. et al., 2019; Yu et al., 2019).

The *UHRF1* (ubiquitin-like with plant homeodomain and RING finger domains 1) gene is an epigenetic modification factor (Harrison et al., 2016; Xie and Qian, 2018). Studies have shown that *UHRF1* recognizes hemi-methylated DNA, which appears at DNA replication forks, and assists *DNMT1* in DNA methylation (Lu and Wang, 2013; Ferry et al., 2017). A large number of studies have shown that *UHRF1* is highly expressed in a variety of malignant tumor tissues, including breast cancer, bladder cancer, and prostate cancer (Geng et al., 2013; Ying et al., 2015; Wan et al., 2016; Li J. et al., 2019) and that it is involved in tumorigenesis and cancer progression (Alhosin et al., 2011, 2016). In addition, *UHRF1* can inhibit cell apoptosis through the *ROS*-related signaling pathway in gastric cancer (Zhang et al., 2018), and *UHRF1* was found to enhance the invasive ability of tumor cells through the *Keap1-Nrf2* pathway in pancreatic cancer (Abu-Alainin et al., 2016). A recent study found that *UHRF1* silencing can inhibit retinoblastoma proliferation and promote apoptosis through the *PI3K/AKT* signaling pathway (Liu et al., 2019). Studies have found that the expression of *UHRF1* in CRC is related to the depth of invasion of the tumor and that knocking down the expression of *UHRF1* can inhibit the proliferation of CRC cells (Kofunato et al., 2012). Additionally, *UHRF1* silences *PPARG* expression and mediates the progression of CRC (Sabatino et al., 2012). Furthermore, *UHRF1* may promote CRC growth and metastasis by inhibiting p16 (ink4a) (Wang et al., 2012). Ashraf et al. (2017) highlighted the deregulation of *UHRF1* in various cancers, including CRC, and its prognostic value in cancers. This highlights *UHRF1* dysregulation and the importance of identifying different strategies to target *UHRF1* in cancers, as well as the prognostic value of *UHRF1* (Ashraf et al., 2017). Therefore, *UHRF1* may be an important biomarker in the diagnosis, treatment, and prognosis of CRC.

KISS1 was first discovered in melanoma; subsequently, *KISS1* was reported to affect the growth, invasion, and migration of tumor cells and confirmed to be an important tumor suppressor gene in multiple types of malignant tumors (Manley et al., 2017; Liu et al., 2018; Platonov et al., 2018). Suppression of *KISS1* expression is closely related to DNA methylation in CRC tissues (Chen et al., 2014), while *KISS1* overexpression has been reported to inhibit the invasion of CRC cells by blocking *PI3K/AKT* signaling (Chen et al., 2016; Chipman and Pasquinelli, 2019). Studies have also shown that overexpression of *UHRF1* can inhibit the expression of *KISS1* mRNA in bladder cancer (Zhang et al., 2014). However, whether *UHRF1* can inhibit *KISS1* and activate the *PI3K/NF-κB* signaling pathway in CRC remains unclear.

MicroRNAs are a class of non-coding RNAs that are abundantly found in various organisms ranging from viruses to humans. They are approximately 22 nucleotides in length. One of the functions of miRNAs is to bind to the 3′-non-coding regions of target mRNAs [3′ untranslated region (3′UTR)] to inactivate the genes (Chipman and Pasquinelli, 2019). Studies have found that at least one-third of protein-coding genes are regulated by miRNAs, including those involved in cellular differentiation, proliferation, metabolism, apoptosis, and migration (Farazi et al., 2013; Hayes et al., 2014). Studies have found that *miR-501-3p* promotes CRC progression via activation of *Wnt/*β catenin signaling (Wu et al., 2019), that *miR-4319* suppresses CRC progression by targeting *ABTB1* (Huang et al., 2019), and that *miR-144* suppresses aggressive phenotypes of tumor cells by targeting *ANO1* in CRC (Jiang et al., 2019). These studies have shown that miRNA plays an important role in CRC. Previous studies have found that *miR-202* inhibits CRC proliferation and invasion by targeting *UHRF1* (Lin Y. et al., 2019). *MiR-9* targets *UHRF1* and inhibits the proliferation and apoptosis of CRC cells (Zhu et al., 2015). Choudhry et al. (2018) reported the importance of the miRNA/*UHRF1* strategy for targeting various cancers. The study revealed the importance of miRNA therapy targeting *UHRF1*, particularly in CRC. Therefore, it is important to identify miRNAs that target *UHRF1* and to study their mechanisms of action in cancer. *MiR-506* is located on the X chromosome and is a member of the *miR-506-514* sequence family (Bentwich et al., 2005). Increased expression of *miR-506* inhibits tumor cell proliferation and promotes tumor cell senescence and apoptosis, and it has been reported to exert anticancer effects in ovarian cancer, breast cancer, and liver cancer (Wang et al., 2014; Sun et al., 2015; Yu et al., 2015). However, studies have also confirmed that *miR-506* acts as a carcinogenic factor in melanoma (Streicher et al., 2012). At present, *miR-506* has been reported to be differentially expressed in different tumors and to play oncogenic or tumor-suppressive roles in different tumors. To date, the expression and mechanism of *miR-506* in CRC remains unclear.

This study demonstrates that *UHRF1* activates the *PI3K/AKT/NF-κB* signaling pathway by inhibiting *KISS1* mRNA expression in CRC. Furthermore, *miR-506* targets *UHRF1* via the *KISS1/PI3K/NF-κB* signaling axis to inhibit CRC proliferation, migration, and invasion both *in vivo* and *in vitro*. Our findings provide new insights into the underlying mechanisms of *UHRF1* in CRC and provide potential therapeutic targets for the treatment of CRC.

MATERIALS AND METHODS

Human Tissues

A total of 121 CRC tissues and 121 adjacent normal tissues were collected from the First Affiliated Hospital of Fujian Medical University in 2017 and 2018. All tissue samples were immediately frozen in liquid nitrogen for histological examination. Tumor burden was determined using the American Joint Committee on Cancer TNM staging system. Patients provided informed consent for the use of human materials in the study, which was approved by the Ethics Committee of Fujian Medical University.

Immunohistochemical Staining and Analysis

Immunohistochemistry was performed on 4-μm-thick paraffin-embedded sections of both CRC tissues and adjacent normal tissues. Sections were stained to determine the expression levels of the *UHRF1* and *KISS1* proteins. The slides were incubated overnight at 4°C with an anti-*UHRF1* antibody (Sigma, United States) or anti-*KISS1* antibody (Sigma, United States) diluted 1:200. After incubation, the slides were washed with phosphate-buffered saline (PBS) and incubated with a fluorescein isothiocyanate-conjugated goat anti-mouse IgG secondary antibody (ZSGB-BIO, Beijing, China) for 30 min. The slides were washed with PBS and then mounted with anti-fade reagent (Invitrogen, Carlsbad, CA, United States). Finally, the stained slides were observed using an Olympus CX41 fluorescence microscope (Olympus, Tokyo, Japan). The stained tumor sections were examined for positively stained tumor cells and the intensity of immunohistochemical signals and scored independently by two observers. According to the proportion of positively stained tumor cells, the sections were scored as follows: (0) no positive tumor cells; (1) <10% positive tumor cells; (2) 10–50% positive tumor cells; and (3) >50% positive tumor cells. The staining intensity was graded according to the following criteria: (0) no staining; (1) weak staining (light yellow); (2) moderate staining (yellow brown); and (3) strong staining (brown). A total score of > 3 points was considered high expression, and ≤ 3 points was considered low expression.

Detection of *miR-506* and *UHRF1* mRNA Expression in Human Specimens

Human tissue specimens were ground into a powder using liquid nitrogen. Tissue RNA was extracted with TRIzol reagent (TransGen Biotech, Beijing, China), and then, *miR-506* and *UHRF1* mRNA expression levels were analyzed by quantitative real-time PCR (qRT-PCR). The qRT-PCR assay was performed as follows: RNA was detected using a reverse transcription kit (TaKaRa, Dalian, China) and an amplification kit (TaKaRa) following the manufacturer's instructions. *U6* was used as the internal control for *miR-506* expression levels, and *GAPDH* was used as the internal control for the *UHRF1* gene. The reaction mixture contained 10 μl of SYBR Premix Ex Taq 2, 1 μl of each primer, 2 μl of the cDNA template, and 6 μl of ddH_2O for a final volume of 20 μl. The thermal cycling parameters for amplification were as follows: a denaturation step at 95°C for 30 s, followed by 40 cycles at 95°C for 5 s and a final holding step at 60°C for 34 s. Relative gene expression was evaluated with Data Assist software version 3.0 (Applied Biosystems, Foster City, CA, United States). The relative expression levels were determined according to the $2^{-\Delta\Delta CT}$ method. The assays were performed in triplicate. Primer sequences for each gene were shown in **Table 1**.

Cell Culture

The four human CRC cell lines HCT116, LoVo, HT29, and SW480 were purchased from the Cell Bank of the Chinese Academy of Sciences (Shanghai, China). HCT116 cells and HT29 cells were grown in McCOY's 5A medium, LoVo cells were grown in F12K medium, and SW480 cells were grown in L-15 medium (Gibco, Carlsbad, CA, United States) containing 10% fetal bovine serum (FBS) (Gibco), and cells were incubated at 37°C with 5% CO_2.

Screening of Cell Lines

Cells from each cell line were plated on six-well plates (2×10^5 cells per well) and incubated for 48 h to achieve a cell density of 80%. One milliliter of TRIzol reagent was added to lyse the cells. RNA was extracted with TRIzol reagent (TransGen Biotech, Beijing, China). *MiR-506* and *UHRF1* mRNA expression levels were detected by qRT-PCR. The assays were performed in triplicate.

Vector Construction and Cell Infection

Pre-miR-506 lentivirus, *miR-506* inhibitor lentivirus, *UHRF1*-overexpressing lentivirus, *sh-UHRF1* lentivirus, *KISS1*-overexpressing lentivirus and *PI3K*-overexpressing lentivirus were purchased from GeneChem (Shanghai, China). Infection was performed using polybrene (GeneChem). A lentivirus infection efficiency of more than 80% was considered successful. According to the manufacturer's instructions, the multiplicity of infection for HCT116 cells was 10, and the multiplicity of infection for SW480 cells was 30. After 48 h of infection, the cells were digested for further cell culture. All experiments were performed according to the manufacturer's instructions.

Detection of *miR-506*, *UHRF1,* and *KISS1* mRNA Expression

Cells from each cell line were plated on six-well plates (2×10^5 cells per well) and then incubated for 48 h to achieve a cell

TABLE 1 | Primer sequences for each gene.

Gene	Primer sequence	
UHRF1	Forward	5′-CGACGGAGCGTACTCCCTAG-3′
	Reverse	5′-TCATTGATGGGAGCAAAGCA-3′
GAPDH	Forward	5′-CCCTTCATTGACCTCAACTACATG-3′
	Reverse	5′-TGGGATTTCCATTGATGACAAGC-3′
U6	Forward	5′-CGCTTCGGCAGCCACATATACTA-3′
	Reverse	5′-CGCTTCACGAATTTGCGTGTCA-3′
KISS1	Forward	5′-AGCCGCCAGATCCCCGCA-3′
	Reverse	5′-GCCGAAGGAGTTCCAGTTGT-3′
MiR-506	Forward	5′-GCGGCTTTGTGCTTGATCTAA-3′
	Reverse	5′-GTGCAGGGTCCGAGGT-3′

density of 80%. One milliliter of TRIzol reagent was added to lyse the cells. Then, *miR-506*, *UHRF1,* and *KISS1* mRNA expression levels were analyzed by qRT-PCR. All assays were performed in triplicate.

Western Blot Analysis

Radioimmunoprecipitation assay buffer was added to each group of transfected cells for protein extraction, and approximately 60 μg of total protein was loaded onto an 8% SDS-PAGE gel (Beyotime) and transferred to a PVDF membrane at 300 mA for 1.5 h. The PVDF membrane was blocked with 5% skim milk for 2 h at room temperature and then incubated with anti-*UHRF1*, anti-*KISS1* or anti-*GAPDH* (1:1000; Sigma, St. Louis, MO, United States) and anti-*p-PI3K*, anti-*AKT*, anti-*p-AKT*, anti-*NF-κB* (*p65*) or anti-*MMP9* (1:1000; Abcam, United States) antibodies overnight at 4°C. After washing, the membrane was incubated with HRP-conjugated goat anti-mouse IgG (1:5000; Beyotime) at room temperature for 90 min, washed three times in PBS and then visualized using ECL reagent. All assays were performed in triplicate.

Proliferation Assay

Each group of transfected cells (1×10^5 cells per well) was seeded in 24-well plates and then incubated for 24 h at 37°C and 5% CO_2. The reagent 5-ethynyl-2′-deoxyuridine (EdU; Beyotime, Haimen, China) was added to each well, and then, the cells were incubated for another 2 h. The cells were subsequently fixed with paraformaldehyde and stained with 4,6-diamidino-2-phenylindole (DAPI) and Alexa Fluor 555 azide (Beyotime). Proliferating cells were stained red with Alexa Fluor 555 azide, and all nuclei were stained blue with DAPI. Five fields of view were randomly photographed under a microscope for statistical analysis and measurement. The statistical method used was as follows: cell proliferation rate = number of proliferating cells/total number of cells. All assays were performed in triplicate.

Migration Assay

Transwell chambers (Corning, NY, United States) were used for the migration assay. Infected HCT116 cells (6×10^4 cells per well) or SW480 cells (9×10^4 cells per well) were suspended in serum-free culture medium and seeded into the upper chamber, and 800 μl of complete medium was added to the lower chamber. After incubation for 48 h at 37°C and 5% CO_2, the cells were fixed with paraformaldehyde and stained with crystal violet. Five random fields of view were photographed under a microscope for statistical analysis and measurements. Images were obtained using an Olympus CX41 microscope (Nikon, Tokyo, Japan), and the number of cells in different treatment groups was assessed by manual counting. All assays were performed in triplicate.

Invasion Assay

Transwell chambers (Corning, NY, United States) were used for the invasion assays. Matrigel (100 μl) (Becton Dickinson, Franklin Lake, NJ, United States) was placed into the upper chamber. Transfected HCT116 cells (9×10^4 cells per well) or SW480 cells (12×10^4 cells per well) were suspended in serum-free culture medium and seeded into the upper chamber, and 800 μl of complete medium was added to the lower chamber. After incubation for 48 h at 37°C and 5% CO_2, the cells were fixed with paraformaldehyde and stained with crystal violet. Five random fields of view were photographed under a microscope for statistical analysis and measurements. Images were obtained using an Olympus CX41 microscope (Nikon, Tokyo, Japan), and the number of cells in different treatment groups was assessed by manual counting. All assays were performed in triplicate.

Target Gene Screening Assay

TargetScan[1], MiRanda[2], and PicTar[3] online tools were applied to jointly predict miRNAs that bind to *UHRF1*. Through predictive analysis, we obtained four miRNAs, of which *miR-124-3p* and *miR-9-5p* had been previously reported, and we therefore excluded them from our analysis. We found that the function of *miR-2836* had not been reported in the literature, so it was also excluded from our analysis. As *miR-506* is known to act as a tumor suppressor in other cancer tissues, we speculated that *UHRF1* may be the target of *miR-506*.

Luciferase Assay

MiR-506 mimics and *miR-506* negative control vectors were purchased from GenePharma (Shanghai, China). The *UHRF1* wild-type vector with a potential binding sequence and the mutant vector were purchased from GeneChem (Shanghai, China). Transfection was performed using Lipofectamine 3000 (Invitrogen). HCT116 cells transfected with *miR-506* mimics (5′-UAAGGCACCCUUCUGAGUAGA-3′, 5′-UACUCAGAAGGGUGCCUUAUU-3′) or miR-506 negative control vectors (sense 5′-UUCUCCGAACGUACGUTT-3′, antisense 5′-ACGUGACACGUUCGGAGAATT-3′) were cultured for 24 h. Firefly/Renilla luciferase activity was used as an internal control. The wild-type vector and mutant vector (1 μg) were transfected into the cells, and the cells were collected after 48 h of culture. A fluorescein assay kit (Beyotime) was used to extract fluorescein from each group, and then, the fluorescence level of each group was determined by a multi-function microplate reader. All assays were performed in triplicate.

Tumor Formation in a Nude Mouse Model

Athymic male BALB/c nude mice (SLAC, Shanghai, China) were bred in the absence of specific pathogens. The trial protocol was approved by the Experimental Animal Ethics Committee of Fujian Medical University. MiR-506-overexpressing cells and vector control cells were trypsinized, and then, the cells were resuspended in medium at a concentration of 3×10^7 cells/ml. HCT116 cells (0.2 ml) were injected subcutaneously into the left flanks of 5-week-old mice (4 mice per group). *MiR-506* inhibitor cells and the vector control cells were trypsinized, and then, the

[1]http://www.targetscan.org/

[2]http://www.microrna.org/microrna/home.do

[3]http://www.pictar.org/

cells were resuspended in medium at a concentration of 3×10^7 cells/ml. SW480 cells (0.2 ml) were injected subcutaneously into the left flank of 5-week-old mice (4 mice per group). The subcutaneously growing tumors were evaluated twice weekly after transplantation. The mice were sacrificed 4 weeks (HCT116 cells) or 6 weeks (SW480 cells) later, and the weights of the subcutaneous tumors were recorded. The tissues were embedded in paraffin, sectioned, and then stained to determine the protein expression of *UHRF1*, *KISS1*, *p-PI3K*, *NF-κB,* and *MMP9* via immunohistochemistry.

Statistical Analysis

Data were statistically analyzed using SPSS 16.0 software. Quantitative data were analyzed by Student's *t*-test, and the results are expressed as the mean ± SD. The results of immunohistochemistry were tested by an independent sample χ^2 test. $p < 0.05$ was considered significant.

RESULTS

UHRF1 Is Highly Expressed in CRC Tissues Compared to Adjacent Normal Tissues

In our investigations into the expression of *UHRF1* in CRC, we found that *UHRF1* was highly expressed in CRC according to The Cancer Genome Atlas (TCGA) database ($p < 0.001$; **Figure 1A**). Next, we collected human CRC specimens (T1, $n = 28$; T2, $n = 26$; T3, $n = 31$; and T4, $n = 36$) and adjacent normal tissues ($n = 27$) and examined the expression of *UHRF1* in each sample by qRT-PCR. The results showed that the expression of *UHRF1* was significantly higher in T1 than in adjacent normal tissues ($p < 0.001$; **Figure 1B**). Additionally, no significant difference in *UHRF1* expression was found between T1 and T2 ($p = 0.356$); *UHRF1* expression in T4 and T3 was significantly higher than that in T2 ($p < 0.001$; **Figure 1B**), but *UHRF1* expression was significantly higher in T4 than in T3 ($p < 0.001$; **Figure 1B**). The immunohistochemistry results revealed that among CRC tissues, 87 cases were positive for *UHRF1* expression, and 34 cases were negative for *UHRF1* expression; among the adjacent normal tissues, 29 cases were positive for *UHRF1* expression, and 92 cases were negative for *UHRF1* expression. Altogether, these results demonstrate that *UHRF1* expression is significantly higher in CRC than in adjacent normal tissues ($p < 0.001$; **Figure 1C** and **Table 2**).

UHRF1 Inhibits *KISS1* Expression in CRC

To investigate the association between the *UHRF1* and *KISS1* proteins in CRC, immunohistochemistry was used to detect the expression of *KISS1* in 121 CRC specimens. The results showed that in 87 CRC tissues with high UHRF1 protein expression, 23 cases were positive for *KISS1* protein expression, and 64 cases were negative. Among the 34 cases of CRC with low levels of *UHRF1* protein, 21 and 13 cases were positive and negative, respectively, for *KISS1* protein expression. Thus, *UHRF1* protein and *KISS1* protein expression were found to be negatively correlated in CRC ($p < 0.0001$; **Figure 1D** and **Table 2**). Next, we investigated whether *UHRF1* inhibits *KISS1* expression. We detected the expression of *UHRF1* mRNA in four colorectal cell lines (HCT116, LoVo, HT29, and SW480) by qRT-PCR. The results showed that the expression of *UHRF1* mRNA was highest in HCT116 cells and lowest in SW480 cells (**Figure 2A**). SW480 cells were infected with UHRF1-overexpressing lentivirus, and HCT116 cells were infected with *sh-UHRF1* lentivirus. The results of the qRT-PCR analyses showed that *UHRF1* expression was significantly higher in the *UHRF1*-overexpressing group than in the negative control group and that the expression of *UHRF1* was significantly lower in the *sh-UHRF1* group than in the negative control group (**Figure 2B**), confirming that the cells were successfully infected. *KISS1* mRNA expression was decreased in the *UHRF1*-overexpression group, while it was increased in the *sh-UHRF1* group (**Figure 2C**).

UHRF1 Promotes the Proliferation, Migration, and Invasion of CRC Cells by Inhibiting *KISS1*-Induced Activation of the *PI3K/NF-κB* Signaling Pathway

Next, we explored the mechanism of *UHRF1* in CRC metastasis. Western blotting results revealed that the overexpression of *UHRF1* inhibits *KISS1* protein expression and promotes the expression of *PI3K/NF-κB* signaling pathway-related proteins; when we activated KISS1 protein expression in cells infected with the *UHRF1* overexpression vector, the expression of PI3K/NF-κB signaling pathway-associated proteins was subsequently inhibited (**Figure 3A**). Infection of CRC cells with *sh-UHRF1* promoted the expression of the *KISS1* protein and inhibited the expression of *PI3K/NF-κB* signaling pathway-related proteins. When we activated the expression of *PI3K* protein in cells infected with the *sh-UHRF1* vector, the expression of the *PI3K/NF-κB* signaling pathway-associated proteins was then activated (**Figure 3B**). This result revealed that *UHRF1* activates the *PI3K/NF-κB* signaling pathway by inhibiting *KISS1* in CRC. To further explore whether this mechanism is involved in the malignant behavior of CRC, we performed proliferation, migration, and invasion assays and further verified that *UHRF1* promotes the proliferation, migration, and invasion of CRC; however, the activation of *KISS1* reversed this trend. Additionally, *sh-UHRF1* inhibited the proliferation, migration and invasion of CRC, but the activation of *PI3K* reversed this trend (**Figures 4A–C**). Therefore, the results of this study revealed that *UHRF1* inhibits the proliferation, migration, and invasion of CRC by inhibiting *KISS1*-induced activation of the *PI3K/NF-κB* signaling pathway.

MiR-506 Is Expressed at Low Levels in CRC and Targets *UHRF1*

To further explore the mechanism of *UHRF1* expression in CRC, this study used data from three databases to predict miRNAs that might bind to *UHRF1*. The results revealed that four miRNAs (*miR-1283*, *miR-506*, *miR-9-5p,* and *miR-124-3p*) may bind to *UHRF1* (**Figure 5A**). A review of the literature revealed

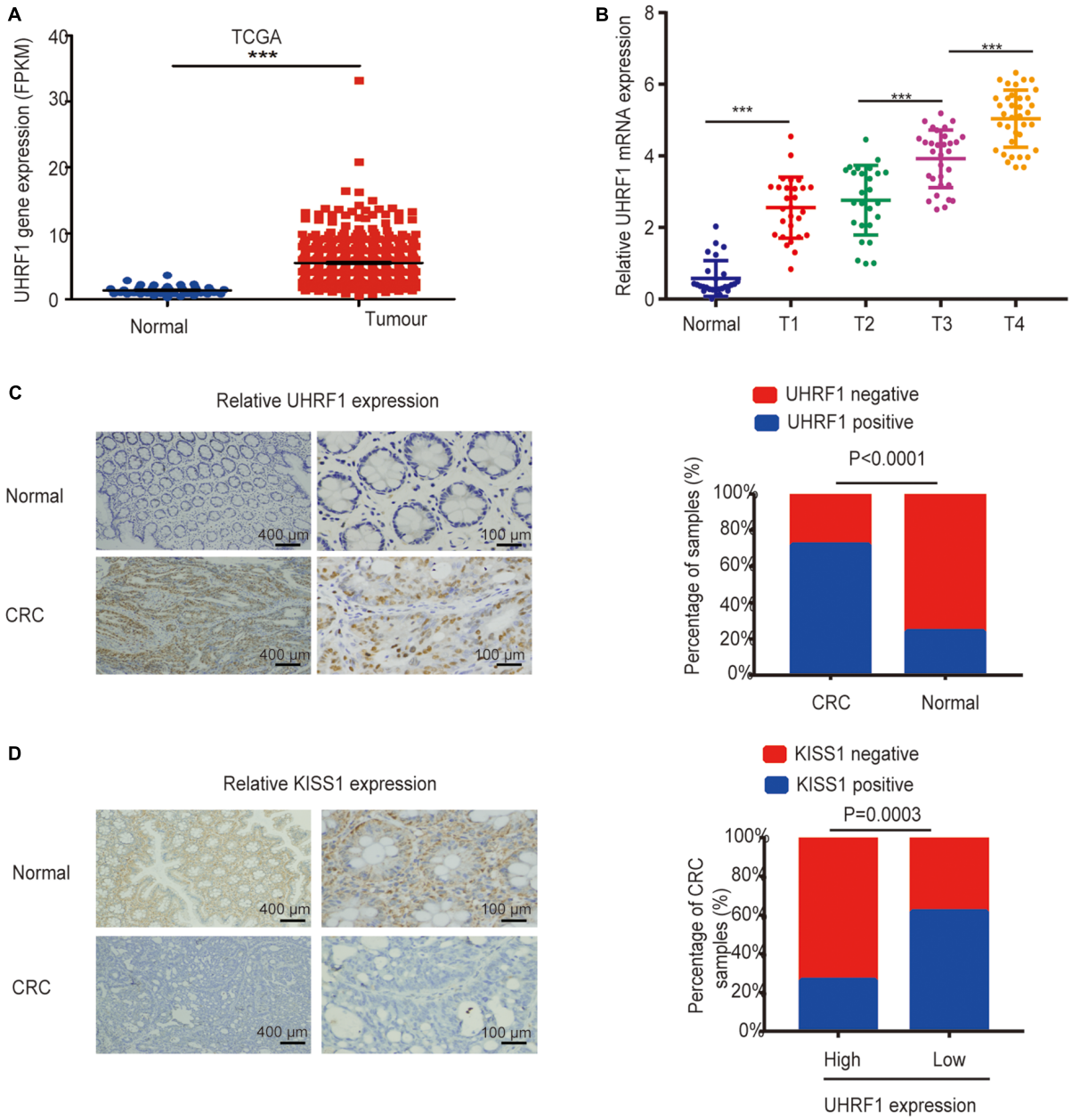

FIGURE 1 | Expression of *UHRF1* and *KISS1* in CRC. **(A)** Expression of *UHRF1* mRNA in CRC and adjacent normal tissues from the TCGA database. **(B)** The expression level of *UHRF1* mRNA in tissues was detected by qRT-PCR. **(C)** Immunohistochemistry results showed that *UHRF1* protein expression was significantly different between cancer tissues and adjacent normal tissues. **(D)** Immunohistochemistry showed that *UHRF1* protein and *KISS1* protein expression were negatively correlated in colorectal cancer. ***$p < 0.001$.

that low *miR-506* expression has been reported in a variety of tumors. Moreover, by qRT-PCR, we found that *miR-506* was downregulated in CRC and negatively correlated with *UHRF1* mRNA expression (**Figures 5B,C**). Potential binding sites were predicted by the TargetScan database (**Figure 5D**). Finally, the results of a luciferase reporter assay revealed that h-*UHRF1*-WT significantly inhibited luciferase expression in HCT116 cells and SW480 cells, whereas h-*UHRF1*-MU failed to inhibit luciferase expression (**Figure 5E**).

MiR-506 Inhibits CRC Proliferation, Migration, and Invasion via the *UHRF1/KISS1* Signaling Axis

Next, we investigated whether *miR-506* targets *UHRF1* in CRC and found that the proliferation, migration, and invasion of CRC are affected by the *KISS1/PI3K/NF-κB* signaling axis. We detected the expression of *miR-506* in four colorectal cell lines (HCT116, LoVo, HT29, and SW480) by qRT-PCR. The results showed that

TABLE 2 | Relationship between the *UHRF1* levels and clinicopathological features of 121 patients with CRC.

Variable		*n*	*UHRF1* level		*p*
			Low	High	
Age	<60	58	13	45	0.1819
	≥60	63	21	42	
Sex	Male	69	23	46	0.1401
	Female	52	11	41	
Histological grade	Well	37	14	23	0.1137
	Moderate, poor	84	20	64	
Depth of invasion	T1 + T2	54	22	32	0.0055
	T3 + T4	67	12	55	
KISS1 level	Low	77	13	64	0.0003
	High	44	21	23	

the expression of *miR-506* was highest in SW480 cells and lowest in HCT116 cells (**Figure 6A**). Therefore, this study used *miR-506* knockdown lentivirus to infect SW480 cells and infected HCT116 cells with *pre-miR-506* lentivirus. The qRT-PCR results showed that *miR-506* expression was significantly higher in the *pre-miR-506* group than in the negative control group and significantly lower in the *miR-506* inhibitor group than in the negative control group (**Figure 6B**). These results confirmed that the cells were successfully infected with lentivirus. The Western blotting results further showed that *pre-miR-506* inhibited the expression of the *UHRF1* protein and activated *KISS1* expression to suppress the expression of *PI3K/NF-κB* signaling pathway-related proteins. When the expression of *UHRF1* was activated, the expression of the *KISS1/PI3K/NF-κB* signaling axis was reversed. The *miR-506* inhibitor led to the opposite effect (**Figures 6C,D**). Finally, the results of the proliferation, migration, and invasion experiments further confirmed that *miR-506* inhibited the proliferation, migration, and invasion of CRC and that the activation of *UHRF1* reversed this trend (**Figures 7A–C**).

MiR-506 Inhibits Cell Proliferation and Invades CRC Cells in Xenograft Nude Mice

Finally, we further verified the previous results through *in vivo* experiments. Compared with the negative control group, CRC proliferation was significantly inhibited in the *miR-506* group (**Figure 8A**), and CRC proliferation was significantly enhanced in the *miR-506* inhibitor group (**Figure 8B**). Immunohistochemistry revealed that *miR-506* inhibits *UHRF1*, *p-PI3K*, *NF-κB*, and *MMP9* protein expression and promotes *KISS1* protein expression in xenograft nude mice. In contrast,

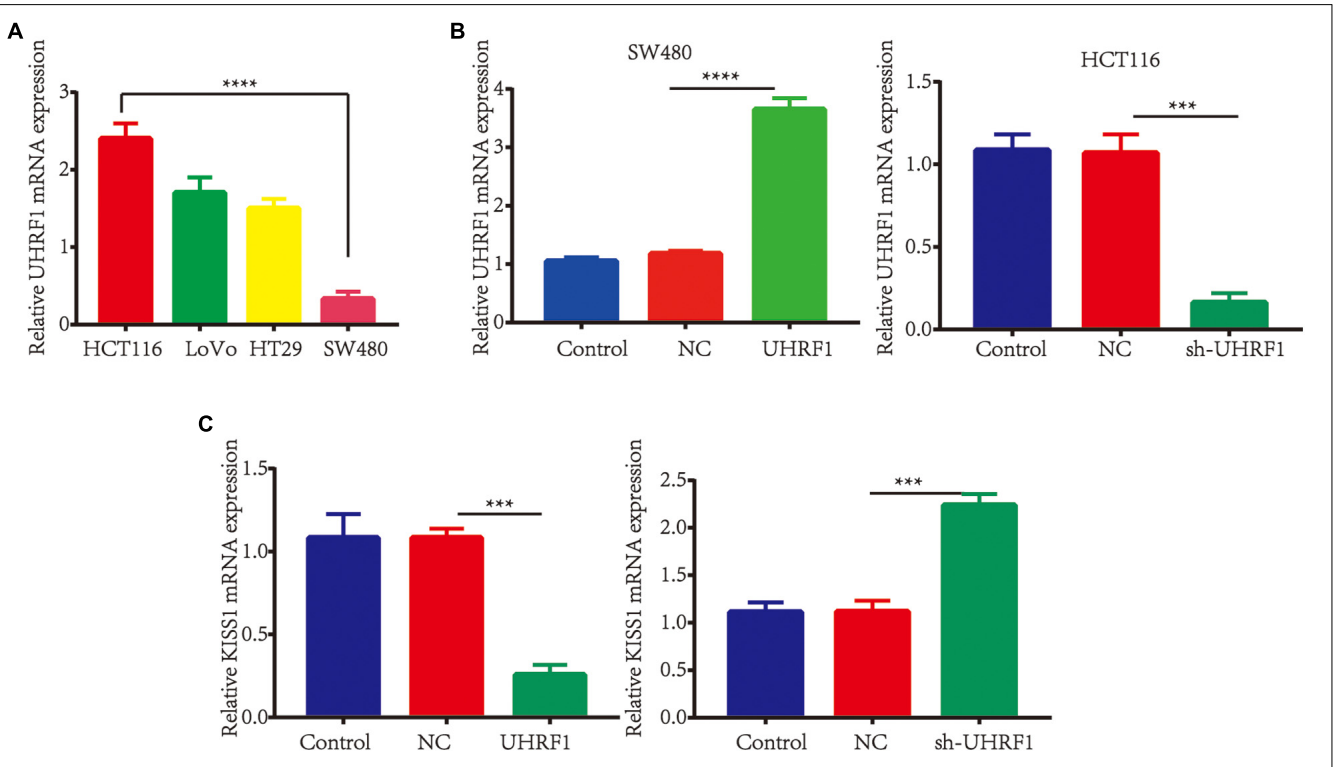

FIGURE 2 | *UHRF1* inhibits *KISS1* mRNA expression. **(A)** qRT-PCR was used to detect the expression of *UHRF1* mRNA in four colorectal cancer cell lines. The expression of *UHRF1* mRNA in HCT116 cells was significantly higher than that in SW480 cells (****$p < 0.0001$). **(B)** SW480 and HCT116 cells were infected with *UHRF1*-overexpressing and knockdown lentivirus. The expression of *UHRF1* mRNA and protein in each group was detected by qRT-PCR. **(C)** The overexpression of *UHRF1* significantly inhibited the expression of *KISS1* mRNA, and the knockdown of *UHRF1* expression significantly promoted *KISS1* mRNA expression. ***$p < 0.001$, ****$p < 0.0001$.

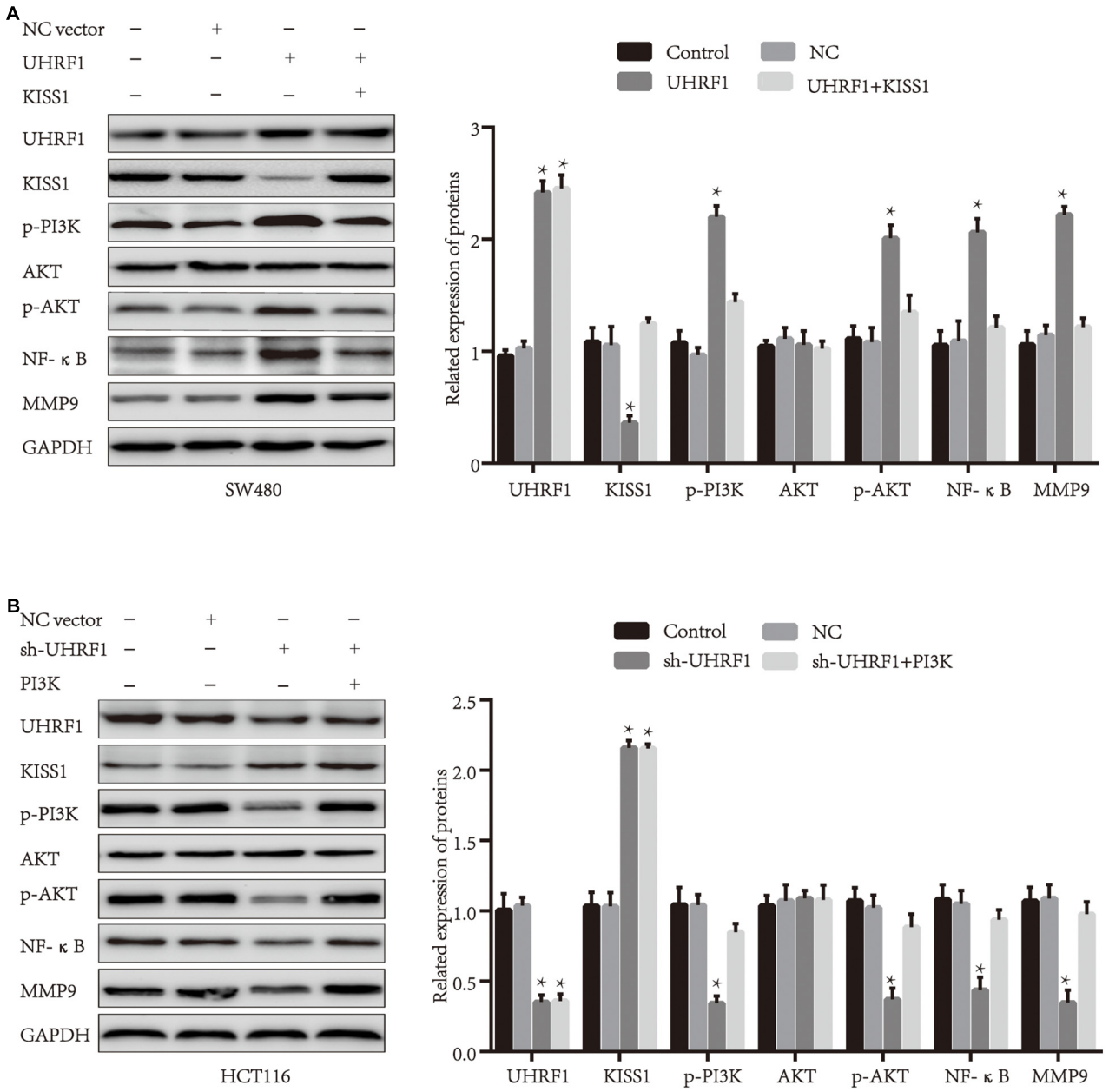

FIGURE 3 | *UHRF1* activates the *PI3K/NF-κB* signaling pathway by inhibiting *KISS1* protein expression. **(A)** *UHRF1* overexpression inhibits *KISS1* protein expression and activates *PI3K/NF-κB* signaling pathway-related proteins. When *KISS1* protein is activated, *PI3K/NF-κB* signaling axis-related protein expression levels are reversed. **(B)** Similarly, the knockdown of *UHRF1* promotes *KISS1* protein expression and inhibits *PI3K/NF-κB* signaling pathway-related proteins. When *PI3K* protein is activated, *PI3K/NF-κB* signaling axis-related protein expression levels are reversed. $^*p < 0.05$.

the *miR-506* inhibitor promotes *UHRF1*, *p-PI3K*, *NF-κB,* and *MMP9* protein expression and inhibits *KISS1* protein expression (**Figure 8C**).

DISCUSSION

Colorectal cancer is a type of malignant tumor with high invasive and metastatic abilities. CRC is currently ranked third among all cancer deaths, and CRC metastasis is an important factor in increasing mortality (Bray et al., 2018). Although multimodal treatments improve the prognosis of CRC (Ganesh et al., 2019; Li S. et al., 2019; Siravegna et al., 2019), the distant metastasis of cancer cells remains the chief culprit of treatment failure. Therefore, a better understanding of the mechanisms of CRC metastasis is essential for the development of new therapeutic strategies.

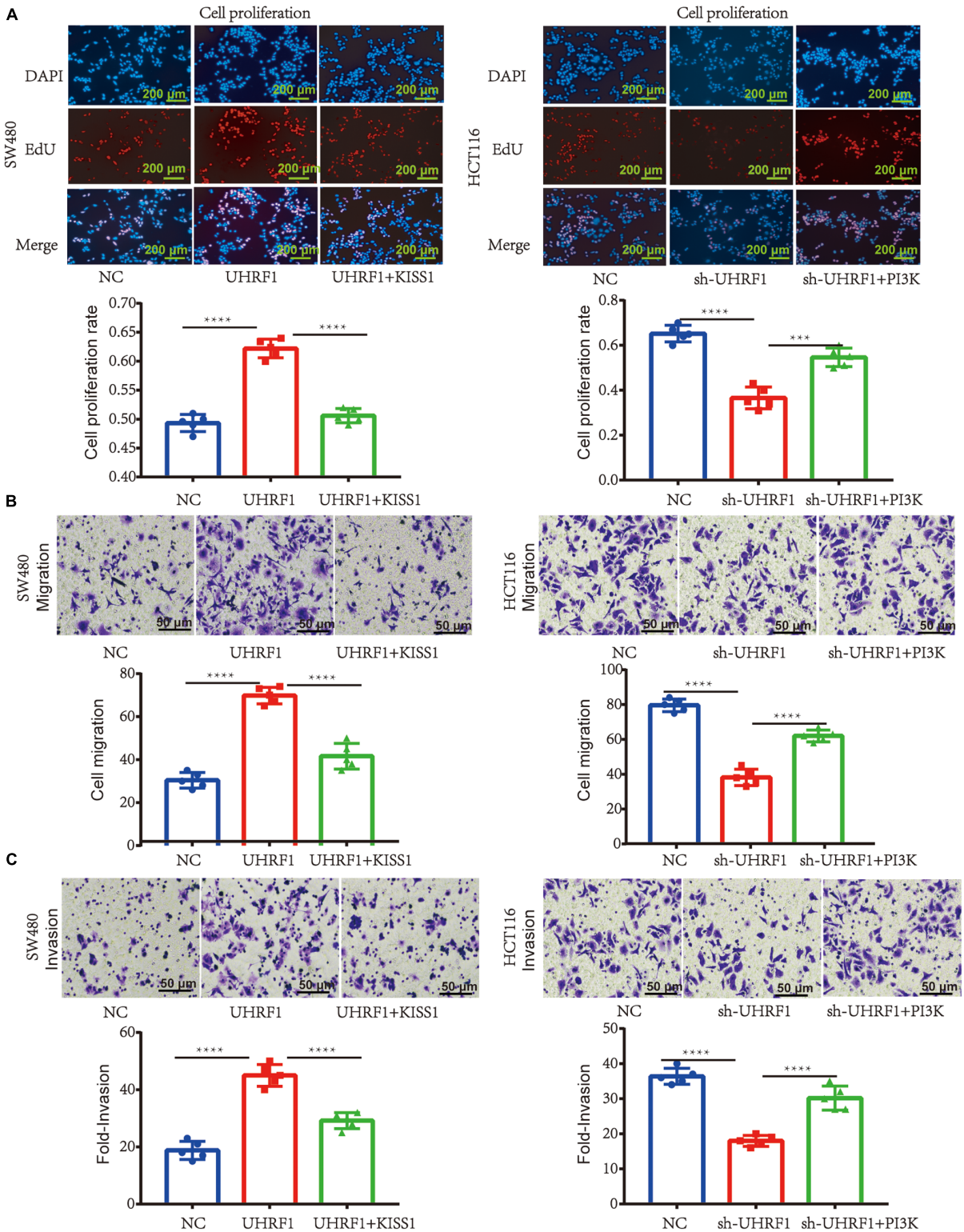

FIGURE 4 | *UHRF1* promotes the proliferation, migration, and invasion of CRC through the *KISS1/PI3K/NF-κB* signaling axis. **(A)** The proliferation of cells in each group is shown. **(B)** The migration of cells in each group is shown. **(C)** The invasion of each group of cells is shown. This result demonstrates that *KISS1* overexpression reverses the proliferation, migration, and invasion of CRC cells transfected with *UHRF1*-overexpressing lentivirus. *sh-UHRF1* inhibits the proliferation, migration, and invasion of colorectal cancer cells in HCT116 cells; the overexpression of *PI3K* reverses the proliferation, migration, and invasion of CRC cells transfected with *sh-UHRF1*. ***$p < 0.001$, ****$p < 0.0001$.

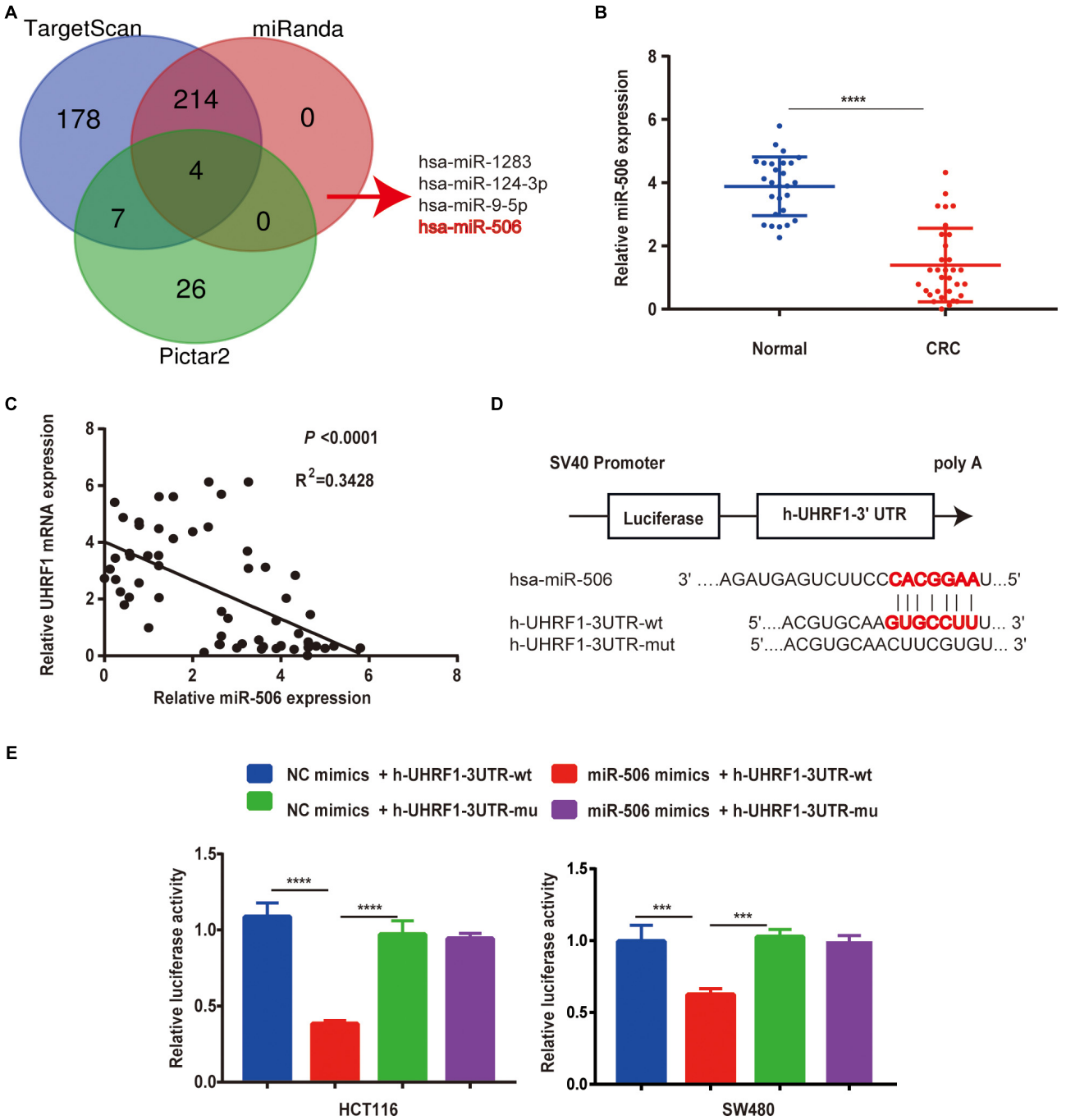

FIGURE 5 | *MiR-506* targets *UHRF1* and is negatively correlated with *UHRF1* expression in CRC. **(A)** Three databases were used to jointly predict miRNAs that may bind to *UHRF1*. **(B)** The expression level of *miR-506* in adjacent normal tissues ($n = 27$) was significantly higher than that in CRC tissues ($n = 32$). **(C)** A negative correlation was found between *miR-506* and *UHRF1* expression in CRC. **(D)** The prediction of potential binding sites for *miR-506* and *UHRF1* by bioinformatics and the design of mutant vector sequences. **(E)** WT or MU *UHRF1* luciferase constructs were transfected into HCT116 cells and SW480 cells with the *miR-506* mimics or *miR-NC*, and luciferase activity was detected 48 h later. *MiR-506* reduced the intensity of the luciferase-*UHRF1* reporter vector in HCT116 cells (****$p < 0.0001$) and SW480 cells (***$p < 0.001$).

The occurrence and development of CRC is accompanied by the activation of proto-oncogenes and the loss of tumor suppressor genes (Sanz-Garcia et al., 2017; Zhang and Shay, 2017). DNA methylation has been found to play an important role in the inactivation of tumor suppressor genes (Schubeler, 2015; Li Z. et al., 2019), and studies have

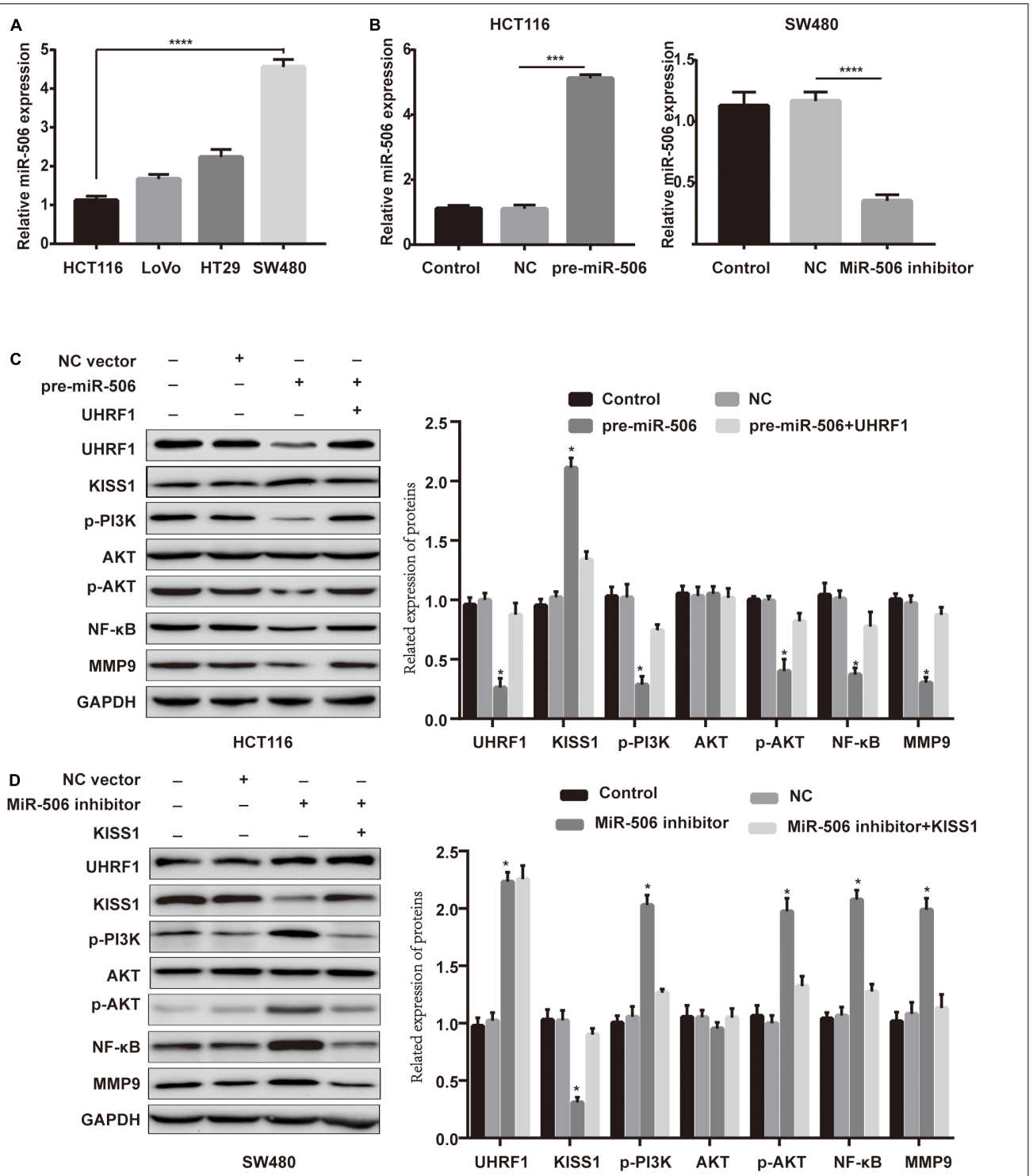

FIGURE 6 | *MiR-506* activates *KISS1* expression and inhibits the *PI3K/NF-κB* signaling axis by targeting *UHRF1*. **(A)** qRT-PCR was used to detect the expression level of *miR-506* in four CRC cells. **(B,C)** HCT116 cells and SW480 cells were infected with *pre-miR-506* lentivirus and *miR-506* knockdown lentivirus. The expression level of *miR-506* in each group was examined by qRT-PCR. **(C)** *Pre-miR-506* activated KISS1 to repress *PI3K/NF-κB* signaling pathway-associated proteins by inhibiting *UHRF1* protein; when *UHRF1* protein was activated, *KISS1/PI3K/NF-κB* signaling axis-related protein expression levels were reversed. **(D)** The *miR-506* inhibitor inhibited *KISS1* activation of *PI3K/NF-κB* signaling pathway-related proteins by promoting *UHRF1* protein expression; when *KISS1* protein was activated, *PI3K/NF-κB* signal transduction axis-related protein expression levels were reversed. $^{*}p < 0.05$, $^{***}p < 0.001$, $^{****}p < 0.0001$.

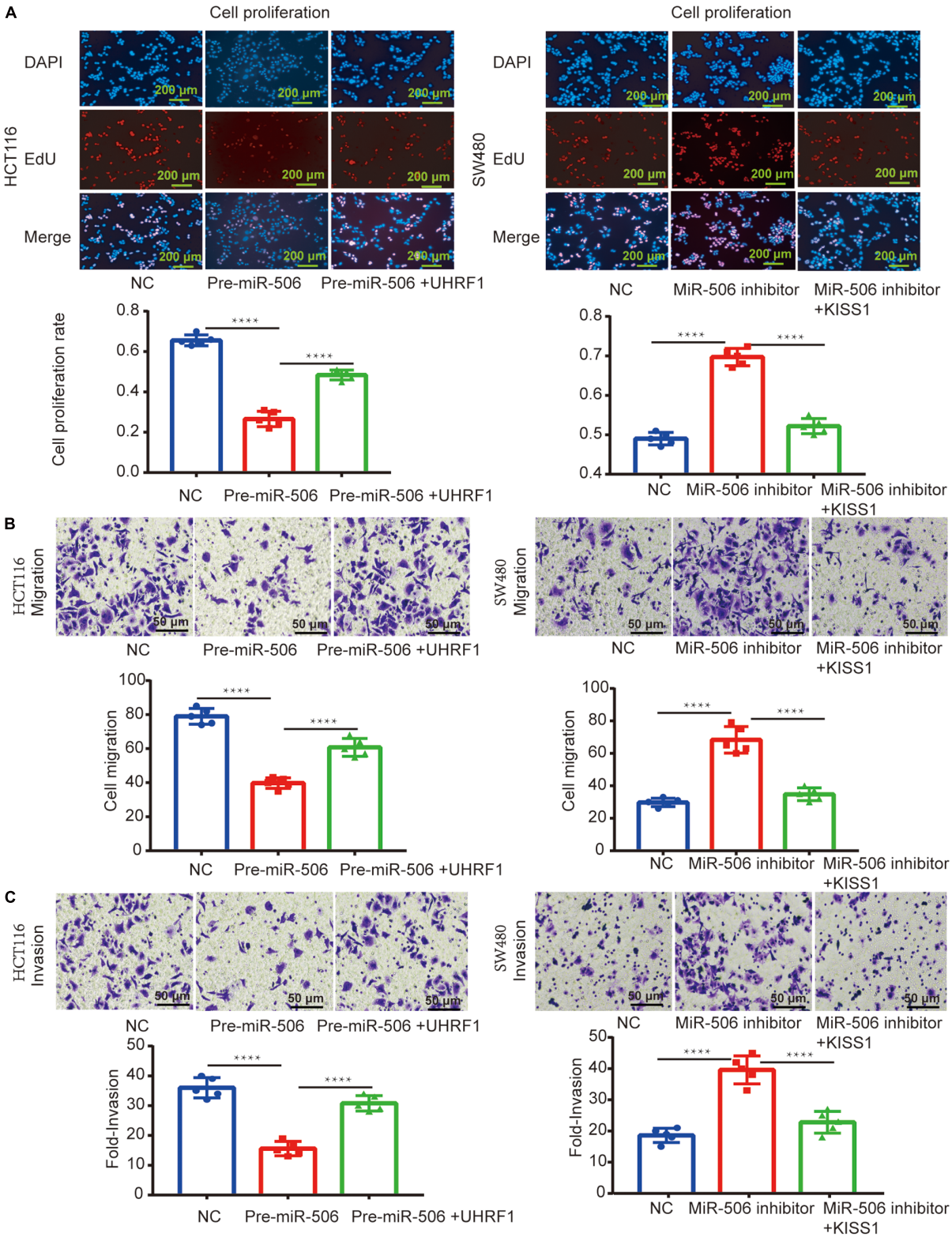

FIGURE 7 | *MiR-506* inhibits the proliferation, migration, and invasion of CRC through the *UHRF1/KISS* signaling axis. **(A–C)** *Pre-miR-506* inhibits the proliferation, migration, and invasion of HCT116 cells. *UHRF1* overexpression reversed the proliferation, migration, and invasion of CRC cells infected with the *pre-miR-506* lentivirus. The *miR-506* inhibitor promoted the proliferation of SW480 cells. Regarding migration and invasion, the overexpression of *KISS1* reversed the proliferation, migration, and invasion of CRC cells transfected with the *miR-506* inhibitor. ****$p < 0.0001$.

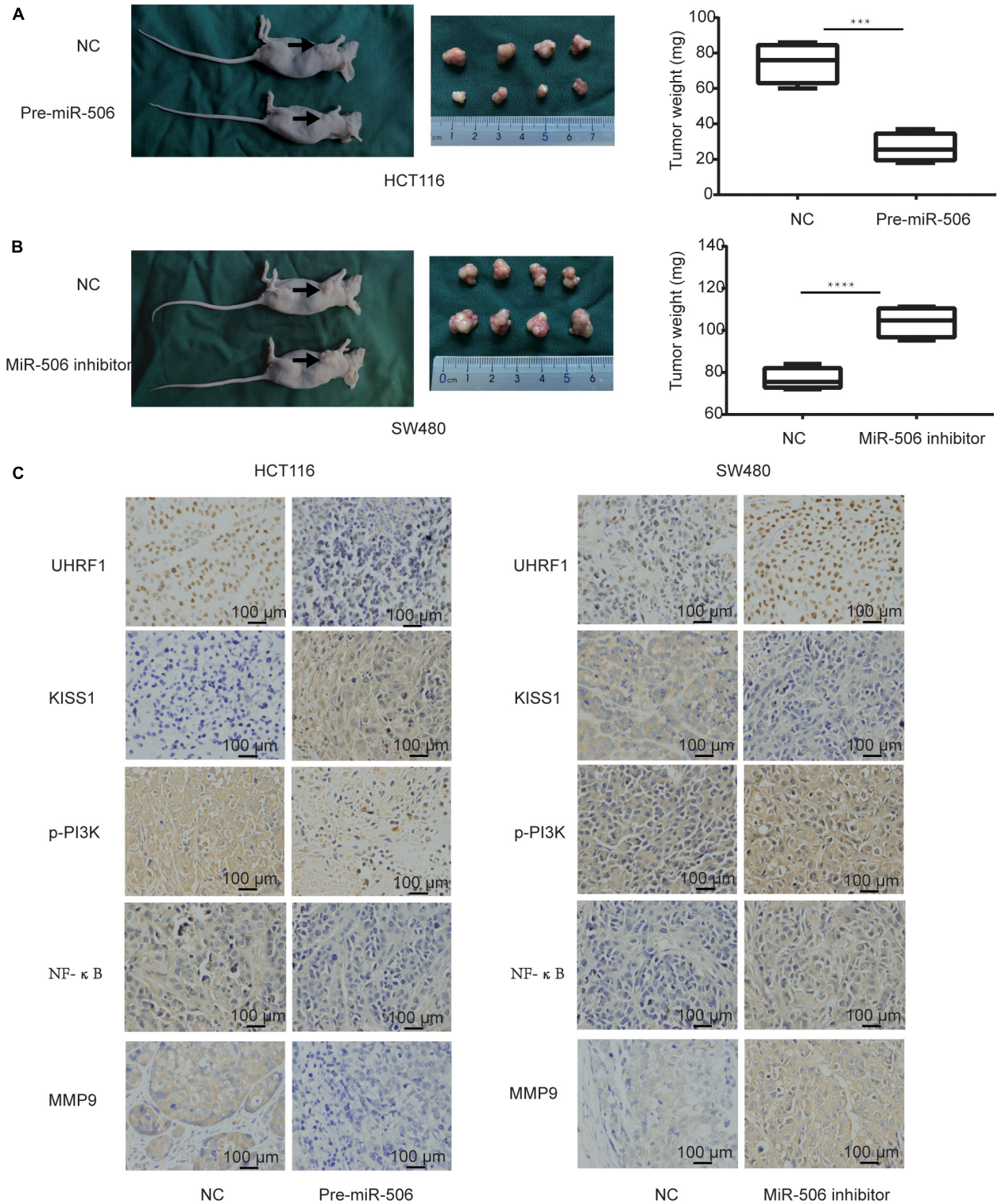

FIGURE 8 | *MiR-506* inhibits the proliferation and invasion of CRC *in vivo*. **(A)** *Pre-miR-506* significantly inhibited CRC proliferation compared with the negative control group. **(B)** The *miR-506* inhibitor significantly promoted CRC proliferation compared with the negative control group. **(C)** Immunohistochemistry was used to detect the expression of *UHRF1*, *KISS1*, *p-PI3K*, *NF-κB,* and *MMP9* proteins in each group of tumors. Compared with the negative control group, *pre-miR-506* significantly promoted *KISS1* protein expression and inhibited *UHRF1*, *p-PI3K*, *NF-κB,* and *MMP9* protein expression. Compared with the negative control group, the *miR-506* inhibitor significantly promoted *UHRF1*, *p-PI3K*, *NF-κB,* and *MMP9* protein expression and inhibited *KISS1* protein expression. ***$p < 0.001$, ****$p < 0.0001$.

shown that DNA methylation requires the involvement of *UHRF1* (Nishiyama et al., 2013; Ferry et al., 2017; Li et al., 2018b). High expression of *UHRF1* in tumor tissues has been reported to promote tumor metastasis (Oh et al., 2018; Hu et al., 2019). Related studies have also found that *UHRF1* is highly expressed in breast cancer, bladder cancer, prostate cancer, and CRC (Jenkins et al., 2005; Zhu et al., 2015; Wan et al., 2016; Saidi et al., 2017). In this study, *UHRF1* was found to be highly expressed in CRC tissues through the TCGA database. The expression of *UHRF1* in T1- and T2-stage tumors was significantly higher than that in adjacent normal tissues but significantly lower than that in T3- and T4-stage tumors. In addition, *UHRF1* overexpression was found to promote the proliferation, migration and invasion of CRC, which suggests that the high expression of *UHRF1* in CRC is closely related to CRC initial and development. However, the specific mechanism by which *UHRF1* regulates CRC metastasis remains unclear.

The *KISS1* gene is an important tumor suppressor. The loss of *KISS1* expression in CRC has been reported (Chen et al., 2014); *KISS1* expression is low in various tumor tissues, which can enhance the growth, invasion, and migration of tumor cells (Chen et al., 2016). In this study, immunohistochemical analysis revealed that *KISS1* protein expression in CRC was negatively correlated with *UHRF1* expression. Moreover, *UHRF1* overexpression promotes CRC proliferation, migration, and invasion by inhibiting *KISS1* gene expression and activating the *PI3K/NF-κB* signaling pathway. Conversely, knockdown of *UHRF1* expression can promote *KISS1* gene expression to block the *PI3K/NF-κB* signaling pathway, inhibiting the proliferation, migration, and invasion of CRC.

The aim of gene-targeted therapy is the design of a therapeutic drug that is appropriate at the cellular and molecular level and that exhibits specificity to a well-defined carcinogenic site. After entering the body, the drug should target a carcinogenic site and cause tumor cell-specific death. Previous studies have found that the drug targeting- and drug encapsulation-related challenges in designing targeted drugs are the high molecular weight and the difficulty in encapsulating these drugs to keep them stable in body fluids prior to reaching the target cancer cells.

MiRNAs are a class of non-coding RNAs that are approximately 22 nucleotides in length. These molecules play an important role in tumor metastasis because they are involved in tumor cell proliferation, apoptosis, invasion, and autophagy (Chipman and Pasquinelli, 2019). Previous studies have shown that in a variety of tumor tissues, targeted binding of miRNAs to mRNAs leads to gene silencing and can thus affect the biological behavior of tumor cells (Farazi et al., 2013). Related studies have found that miRNAs can be encapsulated into nanoparticles by exosomes, which can remain stable in the blood and that miRNAs encapsulated by exosomes can affect the metastatic ability of cancer cells in nude mice. MiRNAs have the advantages of their small molecular weights and ease of packaging and are currently being researched for targeted therapy. Therefore, miRNAs are highly promising for targeted therapy. Studies have shown that *miR-92a-3p* is upregulated in CRC and promotes the migration of CRC by targeting *NF2* (Alcantara and Garcia, 2019). *MiR-452* activates *Wnt*/β-catenin to promote CRC metastasis (Li et al., 2018a). In addition to upregulated miRNAs, downregulated miRNAs such as *miR-144*, *miR-548c-5p,* and *miR-198* also play important roles in tumorigenesis. *MiR-144* has been reported to target *GSPT1* to inhibit the metastasis of CRC (Xiao et al., 2015), and *miR-548c-5p* has been found to act as a tumor suppressor in CRC by targeting *PGK1* (Ge et al., 2019). The above results indicate that dysregulated miRNA expression has been observed in CRC and that the abnormal expression of specific miRNAs is associated with metastasis and prognosis in CRC.

The results of our study revealed that the expression of *UHRF1* in CRC is closely related to pathological stage (**Figure 1B**) and that *UHRF1* can promote the metastasis of CRC (**Figure 4**), but a miRNA targeting *UHRF1* expression in CRC has not yet been reported. Through bioinformatics analysis, we found that *miR-506* has a potential binding site on *UHRF1*. Related studies have reported that *miR-506* targets *ZEB2* to inhibit gastric cancer invasion and is associated with the poor prognosis of gastric cancer (Wang et al., 2019). In pancreatic cancer, the overexpression of *miR-506* blocks the *SPHK1/AKT/NF-κB* signaling pathway and inhibits pancreatic cancer metastasis (Li et al., 2016). However, the expression of *miR-506* in CRC and its mechanism of action are still unclear. We detected *miR-506* in CRC and adjacent normal tissues by PCR and found that *miR-506* was downregulated in normal tissues adjacent to cancer tissues. In addition, the expression of *miR-506* was negatively correlated with the expression of *UHRF1*, suggesting that *UHRF1* is the target molecule of *miR-506*. Luciferase reporter assays confirmed that *miR-506* targets *UHRF1*. Then, we performed Western blotting and cell proliferation assays. Migration and invasion assays further confirmed that *miR-506* targets *UHRF1* to inhibit the proliferation, migration, and invasion of CRC cells via the *KISS1/PI3K/NF-κB* signaling axis. The opposite results were found with the knockdown of *miR-506*. Finally, through *in vivo* ectopic tumor formation experiments, we further confirmed that *miR-506* targets *UHRF*1 to inhibit the proliferation and invasion of CRC by the *KISS1/PI3K/NF-κB* signaling pathway.

Current studies in the literature have indicated that *UHRF1*, as an oncogene in CRC, activates the *PI3K/NF-κB* signaling pathway by inhibiting the expression of *KISS1* to promote tumorigenesis and progression. In this work, the expression of *UHRF1* was found to be regulated by *miR-506*, which affects the biological behavior of CRC. As precision medicine continues to advance, gene-targeted therapy is an important next step. MiRNA-based targets are promising and may be important potential molecules in future targeted therapies for CRC.

DATA AVAILABILITY STATEMENT

We declare that the materials described in the manuscript, including all relevant raw data, will be freely available to any

scientist wishing to use them for non-commercial purposes, without breaching participant confidentiality.

ETHICS STATEMENT

The studies involving human participants were reviewed and approved by the Ethics Committee of the First Affiliated Hospital of Fujian Medical University. The patients/participants provided their written informed consent to participate in this study. The animal study was reviewed and approved by the Ethics Committee of the First Affiliated Hospital of Fujian Medical University.

AUTHOR CONTRIBUTIONS

SC designed the study and provided funding for the study. YLn participated in the entire experiment, and writing and modifying the manuscript. ZC helped to solve problems throughout the experiment, and participated in the editing and revision of the manuscript. YZ, YLu, JG, and SL participated in the Western blotting experiments and statistical analysis of the data.

FUNDING

This work was supported by the Fujian Provincial Key Specialist Construction Projects (No. 2016-SLCZD), the Training Project of Young Talents in the Health System of Fujian Province (No. 2016-ZQN-45), and the Start-up Fund for Scientific Research, Fujian Medical University (No. 2017-XQ1061).

ACKNOWLEDGMENTS

We thank the reviewers and editors for their constructive comments.

REFERENCES

Abu-Alainin, W., Gana, T., Liloglou, T., Olayanju, A., Barrera, L. N., Ferguson, R., et al. (2016). UHRF1 regulation of the Keap1-Nrf2 pathway in pancreatic cancer contributes to oncogenesis. *J. Pathol.* 238, 423–433. doi: 10.1002/path.4665

Alcantara, K. M. M., and Garcia, R. L. (2019). MicroRNA92a promotes cell proliferation, migration and survival by directly targeting the tumor suppressor gene NF2 in colorectal and lung cancer cells. *Oncol. Rep.* 41, 2103–2116. doi: 10.3892/or.2019.7020

Alhosin, M., Omran, Z., Zamzami, M. A., Al-Malki, A. L., Choudhry, H., Mousli, M., et al. (2016). Signalling pathways in UHRF1-dependent regulation of tumor suppressor genes in cancer. *J. Exp. Clin. Cancer Res.* 35:174.

Alhosin, M., Sharif, T., Mousli, M., Etienne-Selloum, N., Fuhrmann, G., Schini-Kerth, V. B., et al. (2011). Down-regulation of UHRF1, associated with re-expression of tumor suppressor genes, is a common feature of natural compounds exhibiting anti-cancer properties. *J. Exp. Clin. Cancer Res.* 30:41. doi: 10.1186/1756-9966-30-41

Ashraf, W., Ibrahim, A., Alhosin, M., Zaayter, L., Ouararhni, K., Papin, C., et al. (2017). The epigenetic integrator UHRF1: on the road to become a universal biomarker for cancer. *Oncotarget* 8, 51946–51962. doi: 10.18632/oncotarget.17393

Bentwich, I., Avniel, A., Karov, Y., Aharonov, R., Gilad, S., Barad, O., et al. (2005). Identification of hundreds of conserved and nonconserved human microRNAs. *Nat. Genet.* 37, 766–770. doi: 10.1038/ng1590

Bray, F., Ferlay, J., Soerjomataram, I., Siegel, R. L., Torre, L. A., and Jemal, A. (2018). Global cancer statistics: GLOBOCAN estimates of incidence and mortality worldwide for 36 cancers in 185 countries. *CA Cancer J. Clin.* 68, 394–424. doi: 10.3322/caac.21492

Chen, S., Chen, W., Zhang, X., Lin, S., and Chen, Z. (2016). Overexpression of KiSS-1 reduces colorectal cancer cell invasion by downregulating MMP-9 via blocking PI3K/Akt/NF-kappaB signal pathway. *Int. J. Oncol.* 48, 1391–1398. doi: 10.3892/ijo.2016.3368

Chen, S. Q., Chen, Z. H., Lin, S. Y., Dai, Q. B., Fu, L. X., and Chen, R. Q. (2014). KISS1 methylation and expression as predictors of disease progression in colorectal cancer patients. *World J. Gastroenterol.* 20, 10071–10081. doi: 10.3748/wjg.v20.i29.10071

Chipman, L. B., and Pasquinelli, A. E. (2019). miRNA Targeting: growing beyond the Seed. *Trends Genet.* 35, 215–222. doi: 10.1016/j.tig.2018.12.005

Choudhry, H., Zamzami, M. A., Omran, Z., Wu, W., Mousli, M., Bronner, C., et al. (2018). Targeting microRNA/UHRF1 pathways as a novel strategy for cancer therapy. *Oncol. Lett.* 15, 3–10. doi: 10.3892/ol.2017.7290

de Mel, S., Hue, S. S., Jeyasekharan, A. D., Chng, W. J., and Ng, S. B. (2019). Molecular pathogenic pathways in extranodal NK/T cell lymphoma. *J. Hematol. Oncol.* 12:33. doi: 10.1186/s13045-019-0716-7

De Robertis, M., Poeta, M. L., Signori, E., and Fazio, V. M. (2018). Current understanding and clinical utility of miRNAs regulation of colon cancer stem cells. *Semin. Cancer Biol.* 53, 232–247. doi: 10.1016/j.semcancer.2018.08.008

Erel-Akbaba, G., Carvalho, L. A., Tian, T., Zinter, M., Akbaba, H., Obeid, P. J., et al. (2019). Radiation-induced targeted nanoparticle-based gene delivery for brain tumor therapy. *ACS Nano.* 13, 4028–4040. doi: 10.1021/acsnano.8b08177

Farazi, T. A., Hoell, J. I., Morozov, P., and Tuschl, T. (2013). MicroRNAs in human cancer. *Adv. Exp. Med. Biol.* 774, 1–20. doi: 10.1007/978-94-007-5590-1_1

Ferry, L., Fournier, A., Tsusaka, T., Adelmant, G., Shimazu, T., Matano, S., et al. (2017). Methylation of DNA Ligase 1 by G9a/GLP Recruits UHRF1 to replicating DNA and regulates DNA Methylation. *Mol. Cell.* 67, 550–565.e. doi: 10.1016/j.molcel.2017.07.012

Ganesh, K., Stadler, Z. K., Cercek, A., Mendelsohn, R. B., Shia, J., Segal, N. H., et al. (2019). Immunotherapy in colorectal cancer: rationale, challenges and potential. *Nat. Rev. Gastroenterol. Hepatol.* 16, 361–375. doi: 10.1038/s41575-019-0126-x

Ge, J., Li, J., Na, S., Wang, P., Zhao, G., and Zhang, X. (2019). miR-548c-5p inhibits colorectal cancer cell proliferation by targeting PGK1. *J. Cell Physiol.* 234, 18872–18878. doi: 10.1002/jcp.28525

Geng, Y., Gao, Y., Ju, H., and Yan, F. (2013). Diagnostic and prognostic value of plasma and tissue ubiquitin-like, containing PHD and RING finger domains 1 in breast cancer patients. *Cancer Sci.* 104, 194–199. doi: 10.1111/cas.12052

Harrison, J. S., Cornett, E. M., Goldfarb, D., DaRosa, P. A., Li, Z. M., Yan, F., et al. (2016). Hemi-methylated DNA regulates DNA methylation inheritance through allosteric activation of H3 ubiquitylation by UHRF1. *eLife* 5:e17101. doi: 10.7554/eLife.17101

Hayes, J., Peruzzi, P. P., and Lawler, S. (2014). MicroRNAs in cancer: biomarkers, functions and therapy. *Trends Mol. Med.* 20, 460–469. doi: 10.1016/j.molmed.2014.06.005

Hu, Q., Qin, Y., Ji, S., Xu, W., Liu, W., Sun, Q., et al. (2019). UHRF1 promotes aerobic glycolysis and proliferation via suppression of SIRT4 in pancreatic cancer. *Cancer Lett.* 452, 226–236. doi: 10.1016/j.canlet.2019.03.024

Huang, L., Zhang, Y., Li, Z., Zhao, X., Xi, Z., Chen, H., et al. (2019). MiR-4319 suppresses colorectal cancer progression by targeting ABTB1.

United European Gastroenterol. J. 7, 517–528. doi: 10.1177/2050640619837440

Jenkins, Y., Markovtsov, V., Lang, W., Sharma, P., Pearsall, D., Warner, J., et al. (2005). Critical role of the ubiquitin ligase activity of UHRF1, a nuclear RING finger protein, in tumor cell growth. *Mol. Biol. Cell.* 16, 5621–5629. doi: 10.1091/mbc.e05-03-0194

Jiang, Y., Cai, Y., Shao, W., Li, F., Guan, Z., Zhou, Y., et al. (2019). MicroRNA144 suppresses aggressive phenotypes of tumor cells by targeting ANO1 in colorectal cancer. *Oncol. Rep.* 41, 2361–2370. doi: 10.3892/or.2019.7025

Kofunato, Y., Kumamoto, K., Saitou, K., Hayase, S., Okayama, H., Miyamoto, K., et al. (2012). UHRF1 expression is upregulated and associated with cellular proliferation in colorectal cancer. *Oncol. Rep.* 28, 1997–2002. doi: 10.3892/or.2012.2064

Li, J., Wang, R., Hu, X., Gao, Y., Wang, Z., Li, J., et al. (2019). Activated MEK/ERK pathway drives widespread and coordinated overexpression of UHRF1 and DNMT1 in cancer cells. *Sci. Rep.* 9:907. doi: 10.1038/s41598-018-37258-3

Li, J., Wu, H., Li, W., Yin, L., Guo, S., Xu, X., et al. (2016). Downregulated miR-506 expression facilitates pancreatic cancer progression and chemoresistance via SPHK1/Akt/NF-kappaB signaling. *Oncogene* 35, 5501–5514. doi: 10.1038/onc.2016.90

Li, T., Jian, X., He, H., Lai, Q., Li, X., Deng, D., et al. (2018a). MiR-452 promotes an aggressive colorectal cancer phenotype by regulating a Wnt/beta-catenin positive feedback loop. *J. Exp. Clin. Cancer Res.* 37:238. doi: 10.1186/s13046-018-0879-z

Li, T., Wang, L., Du, Y., Xie, S., Yang, X., Lian, F., et al. (2018b). Structural and mechanistic insights into UHRF1-mediated DNMT1 activation in the maintenance DNA methylation. *Nucleic Acids Res.* 46, 3218–3231. doi: 10.1093/nar/gky104

Lin, X., Wang, S., Sun, M., Zhang, C., Wei, C., Yang, C., et al. (2019). miR-195-5p/NOTCH2-mediated EMT modulates IL-4 secretion in colorectal cancer to affect M2-like TAM polarization. *J. Hematol. Oncol.* 12:20. doi: 10.1186/s13045-019-0708-7

Lin, Y., Chen, Z., Lin, S., Zheng, Y., Liu, Y., Gao, J., et al. (2019). MiR-202 inhibits the proliferation and invasion of colorectal cancer by targeting UHRF1. *Acta Biochim. Biophys. Sin.* 51, 598–606. doi: 10.1093/abbs/gmz042

Li, S., Xu, K., Gu, D., He, L., Xie, L., Chen, Z., et al. (2019). Genetic variants in RPA1 associated with the response to oxaliplatin-based chemotherapy in colorectal cancer. *J. Gastroenterol.* doi: 10.1007/s00535-019-01571-z [Epub ahead of print].

Li, Z., Li, Z., Wang, L., Long, C., Zheng, Z., and Zhuang, X. (2019). ZCCHC13-mediated induction of human liver cancer is associated with the modulation of DNA methylation and the AKT/ERK signaling pathway. *J. Transl. Med.* 17:108. doi: 10.1186/s12967-019-1852-0

Liu, G., Zhao, X., Zhou, J., Cheng, X., Ye, Z., and Ji, Z. (2018). LncRNA TP73-AS1 promotes cell proliferation and inhibits cell apoptosis in clear cell renal cell carcinoma through repressing KISS1 expression and inactivation of PI3K/Akt/mTOR signaling pathway. *Cell Physiol. Biochem.* 48, 371–384. doi: 10.1159/000491767

Liu, Y., Liang, G., Zhou, T., and Liu, Z. (2019). Silencing UHRF1 inhibits cell proliferation and promotes cell apoptosis in retinoblastoma Via the PI3K/Akt signalling pathway. *Pathol. Oncol. Res.* doi: 10.1007/s12253-019-00656-7 [Epub ahead of print].

Lu, R., and Wang, G. G. (2013). Tudor: a versatile family of histone methylation 'readers'. *Trends Biochem. Sci.* 38, 546–555. doi: 10.1016/j.tibs.2013.08.002

Manley, S. J., Liu, W., and Welch, D. R. (2017). The KISS1 metastasis suppressor appears to reverse the warburg effect by shifting from glycolysis to mitochondrial beta-oxidation. *J. Mol. Med.* 95, 951–963. doi: 10.1007/s00109-017-1552-2

Ni, K., Lan, G., Veroneau, S. S., Duan, X., Song, Y., and Lin, W. (2018). Nanoscale metal-organic frameworks for mitochondria-targeted radiotherapy-radiodynamic therapy. *Nat. Commun.* 9:4321. doi: 10.1038/s41467-018-06655-7

Nishiyama, A., Yamaguchi, L., Sharif, J., Johmura, Y., Kawamura, T., Nakanishi, K., et al. (2013). Uhrf1-dependent H3K23 ubiquitylation couples maintenance DNA methylation and replication. *Nature* 502, 249–253. doi: 10.1038/nature12488

Oh, Y. M., Mahar, M., Ewan, E. E., Leahy, K. M., Zhao, G., and Cavalli, V. (2018). Epigenetic regulator UHRF1 inactivates REST and growth suppressor gene expression via DNA methylation to promote axon regeneration. *Proc. Natl. Acad. Sci. U.S.A.* 115, E12417–E12426. doi: 10.1073/pnas.1812518115

Platonov, M. E., Borovjagin, A. V., Kaverina, N., Xiao, T., Kadagidze, Z., Lesniak, M., et al. (2018). KISS1 tumor suppressor restricts angiogenesis of breast cancer brain metastases and sensitizes them to oncolytic virotherapy in vitro. *Cancer Lett.* 417, 75–88. doi: 10.1016/j.canlet.2017.12.024

Sabatino, L., Fucci, A., Pancione, M., Carafa, V., Nebbioso, A., Pistore, C., et al. (2012). UHRF1 coordinates peroxisome proliferator activated receptor gamma (PPARG) epigenetic silencing and mediates colorectal cancer progression. *Oncogene* 31, 5061–5072. doi: 10.1038/onc.2012.3

Saidi, S., Popov, Z., Janevska, V., and Panov, S. (2017). Overexpression of UHRF1 gene correlates with the major clinicopathological parameters in urinary bladder cancer. *Int. Braz J. Urol.* 4, 224–229. doi: 10.1590/S1677-5538.IBJU.2016.0126

Sanz-Garcia, E., Argiles, G., Elez, E., and Tabernero, J. (2017). BRAF mutant colorectal cancer: prognosis, treatment, and new perspectives. *Ann. Oncol.* 28, 2648–2657. doi: 10.1093/annonc/mdx401

Schiza, N., Georgiou, E., Kagiava, A., Medard, J. J., Richter, J., Tryfonos, C., et al. (2019). Gene replacement therapy in a model of charcot-marie-tooth 4C neuropathy. *Brain* 142, 1227–1241. doi: 10.1093/brain/awz064

Schubeler, D. (2015). Function and information content of DNA methylation. *Nature* 517, 321–326. doi: 10.1038/nature14192

Siravegna, G., Sartore-Bianchi, A., Nagy, R. J., Raghav, K., Odegaard, J. I., Lanman, R. B., et al. (2019). Plasma HER2 (ERBB2) copy number predicts response to HER2-targeted therapy in metastatic colorectal cancer. *Clin. Cancer Res.* 25, 3046–3053. doi: 10.1158/1078-0432.CCR-18-3389

Streicher, K. L., Zhu, W., Lehmann, K. P., Georgantas, R. W., Morehouse, C. A., Brohawn, P., et al. (2012). A novel oncogenic role for the miRNA-506-514 cluster in initiating melanocyte transformation and promoting melanoma growth. *Oncogene* 31, 1558–1570. doi: 10.1038/onc.2011.345

Sun, Y., Hu, L., Zheng, H., Bagnoli, M., Guo, Y., Rupaimoole, R., et al. (2015). MiR-506 inhibits multiple targets in the epithelial-to-mesenchymal transition network and is associated with good prognosis in epithelial ovarian cancer. *J. Pathol.* 235, 25–36. doi: 10.1002/path.4443

Vu, T., and Datta, P. K. (2017). Regulation of EMT in colorectal cancer: a culprit in metastasis. *Cancers* 9:E171. doi: 10.3390/cancers9120171

Wan, X., Yang, S., Huang, W., Wu, D., Chen, H., Wu, M., et al. (2016). UHRF1 overexpression is involved in cell proliferation and biochemical recurrence in prostate cancer after radical prostatectomy. *J. Exp. Clin. Cancer Res.* 35:34. doi: 10.1186/s13046-016-0308-0

Wang, F., Yang, Y. Z., Shi, C. Z., Zhang, P., Moyer, M. P., Zhang, H. Z., et al. (2012). UHRF1 promotes cell growth and metastasis through repression of p16(ink(4)a) in colorectal cancer. *Ann. Surg. Oncol.* 19, 2753–2762. doi: 10.1245/s10434-011-2194-1

Wang, G. J., Jiao, B. P., Liu, Y. J., Li, Y. R., and Deng, B. B. (2019). Reactivation of microRNA-506 inhibits gastric carcinoma cell metastasis through ZEB2. *Aging* 11, 1821–1831. doi: 10.18632/aging.101877

Wang, Y., Cui, M., Sun, B. D., Liu, F. B., Zhang, X. D., and Ye, L. H. (2014). MiR-506 suppresses proliferation of hepatoma cells through targeting YAP mRNA 3'UTR. *Acta Pharmacol. Sin.* 35, 1207–1214. doi: 10.1038/aps.2014.59

Wu, F., Xing, T., Gao, X., and Liu, F. (2019). miR5013p promotes colorectal cancer progression via activation of Wnt/betacatenin signaling. *Int. J. Oncol.* 55, 671–683. doi: 10.3892/ijo.2019.4852

Xiao, R., Li, C., and Chai, B. (2015). miRNA-144 suppresses proliferation and migration of colorectal cancer cells through GSPT1. *Biomed. Pharmacother.* 74, 138–144. doi: 10.1016/j.biopha.2015.08.006

Xie, S., and Qian, C. (2018). The growing complexity of UHRF1-mediated maintenance DNA methylation. *Genes* 9:E600. doi: 10.3390/genes9120600

Ying, L., Lin, J., Qiu, F., Cao, M., Chen, H., Liu, Z., et al. (2015). Epigenetic repression of regulator of G-protein signaling 2 by ubiquitin-like with PHD and ring-finger domain 1 promotes bladder cancer progression. *FEBS J.* 282, 174–182. doi: 10.1111/febs.13116

Yu, F., Lv, M., Li, D., Cai, H., Ma, L., Luo, Q., et al. (2015). MiR-506 over-expression inhibits proliferation and metastasis of breast cancer cells. *Med. Sci. Monit.* 21, 1687–1692. doi: 10.12659/MSM.893522

Yu, X., Wang, D., Wang, X., Sun, S., Zhang, Y., Wang, S., et al. (2019). CXCL12/CXCR4 promotes inflammation-driven colorectal cancer progression through activation of RhoA signaling by sponging miR-133a-3p. *J. Exp. Clin. Cancer Res.* 38:32. doi: 10.1186/s13046-018-1014-x

Zhang, H., Song, Y., Yang, C., and Wu, X. (2018). UHRF1 mediates cell migration and invasion of gastric cancer. *Biosci. Rep.* 38:BSR20181065. doi: 10.1042/BSR20181065

Zhang, L., and Shay, J. W. (2017). Multiple roles of APC and its therapeutic implications in colorectal cancer. *J. Natl. Cancer Inst.* 109. doi: 10.1093/jnci/djw332

Zhang, Y., Huang, Z., Zhu, Z., Zheng, X., Liu, J., Han, Z., et al. (2014). Upregulated UHRF1 promotes bladder cancer cell invasion by epigenetic silencing of KiSS1. *PLoS One* 9:e104252. doi: 10.1371/journal.pone.0104252

Zhu, M., Xu, Y., Ge, M., Gui, Z., and Yan, F. (2015). Regulation of UHRF1 by microRNA-9 modulates colorectal cancer cell proliferation and apoptosis. *Cancer Sci.* 106, 833–839. doi: 10.1111/cas.12689

Conflict of Interest: The authors declare that the research was conducted in the absence of any commercial or financial relationships that could be construed as a potential conflict of interest.

frontiers in Oncology

REVIEW
published: 22 November 2019
doi: 10.3389/fonc.2019.01307

From Super-Enhancer Non-coding RNA to Immune Checkpoint: Frameworks to Functions

*Manqing Wu and Jun Shen**

State Key Laboratory for Oncogenes and Related Genes, Key Laboratory of Gastroenterology & Hepatology, Division of Gastroenterology and Hepatology, Ministry of Health, School of Medicine, Shanghai Cancer Institute, Shanghai Institute of Digestive Disease, Ren Ji Hospital, Shanghai Jiao Tong University, Shanghai, China

Super-enhancers (SEs) are clusters of enhancers that play a key role in regulating genes that determine cell identity. Enhancer RNAs (eRNAs) are non-coding RNAs transcribed from enhancers that function to promote the enhancer's functions via multiple mechanisms, such as recruiting transcription factors to specific enhancers, promoting enhancer-promoter looping, directing chromatin accessibility, interacting with RNA polymerase II and facilitating histone acetylation. Understanding how super-enhancer RNAs (seRNAs) contribute to specific gene regulation has thus become an area of active interest. Immune checkpoint deregulation is one of the key characteristics of tumors and autoimmune diseases, and is also closely related to cell identity. Recent studies revealed a potential pathway for seRNA's involvement in regulating the expression of immune checkpoints. The present study reviews the current knowledge of eRNA function, immune checkpoint blockage mechanism, and its effect. In addition, for the first time, we explore the direct and indirect roles of seRNAs in regulating immune checkpoint expression in cancer and autoimmune diseases.

Keywords: super-enhancer, non-coding RNA, cell identity, immune checkpoint, cancer, autoimmune disease

OPEN ACCESS

Edited by:
Patricia P. Reis, São Paulo State University, Brazil

Reviewed by:
Giuseppe Palma, National Cancer Institute G. Pascale Foundation (IRCCS), Italy
Leonardo Marques da Fonseca, Federal University of Rio de Janeiro, Brazil

***Correspondence:**
Jun Shen
shenjunrj@126.com

Specialty section:
This article was submitted to Molecular and Cellular Oncology, a section of the journal Frontiers in Oncology

Received: *12 August 2019*
Accepted: *11 November 2019*
Published: *22 November 2019*

Citation:
Wu M and Shen J (2019) From Super-Enhancer Non-coding RNA to Immune Checkpoint: Frameworks to Functions. Front. Oncol. 9:1307. doi: 10.3389/fonc.2019.01307

INTRODUCTION

The identification of substantial amounts of non-protein coding transcripts and their versatile functions is one of the most striking findings of contemporary genomic research. Only ∼2% of the transcribed human genome is accounted for by protein coding exons, thus non-coding RNAs constitute the majority of transcripts (1). Long non-coding RNAs (lncRNAs) are non-coding RNAs that are longer than 200 nucleotides, which play a significant role in the regulation of gene expression, splicing, translation, and epigenetic regulation.

Enhancers are DNA elements of a few hundred base pairs in length that are characterized by acetylation. Enhancers interact with transcription factors (TFs) and promoters. A mammalian cell contains thousands of active enhancers and ∼1 million active enhancers have been found in all human cells (2). Super-enhancers (SEs), also known as stretch enhancers, are regions where multiple enhancers are clustered together. They exert more potent effects than typical enhancers and are associated with genes that are involved in determining cell identity in both the physiological and pathological state. Cell identity genes are a cluster of functionally interconnected genes that jointly establish the unique phenotype of a given cell type on epigenomic, transcriptomic, proteomic, and metabolomic level. For instance, *NPC1L1*, *APOC3*, and *LCT* in enterocytes, *FOXP3, CTLA1,* and *IL2RA* in T regulatory cells (3, 4). *OCT4*, *NANOG,* and *PRDM14* are cell identity

genes of ESC, they encode core transcription factors of embryonic stem cell (ESC) (5). These genes function together to enable expression of genes necessary to maintain its ESC pluripotency. The suppression of their expression leads to loss of pluripotency and self-renewal ability in ESC. Super-enhancers are required for cell type-specific processes and are linked with disease-associated genomic variations. Enhancer RNAs (eRNAs), another marker of active enhancers, are a novel species of non-coding RNA molecules that are transcribed from enhancer regions. Two types of eRNAs have been identified, comprising short, bi-directional and non-polyadenylated eRNAs and long, unidirectional, and polyadenylated eRNAs. The exact function of eRNAs is not clearly understood, and it has been hypothesized that eRNAs are transcription noise that do not contribute to gene expression (6). However, recent findings suggested that at least some eRNAs have a role in enhancer function by recruiting TFs to specific enhancers, promoting enhancer-promoter looping, directing chromatin accessibility, interacting with RNA polymerase II (RNAP II), and stimulating histone acetylation (7–12). Research into enhancers has expanded over the last decade and the biological function of enhancers has become increasingly clear. However, the exact function and mechanism of eRNAs are currently under investigation.

The immune system comprises innate and adaptive immunity. Immune checkpoints, consisting of co-stimulatory checkpoints and co-inhibitory checkpoints, are vital for the maintenance of self-response and prevention of autoimmunity. They are paired molecules that act as a double check before the stimulation or inhibition of an immune response. Immune checkpoints are expressed in a tissue or cell subset-specific manner. The application of immunotherapy in a wide variety of cancers has led to significant tumor shrinkage and improved clinical outcomes in patients by revitalizing the anti-tumor immune response (13, 14). The mostly widely studied inhibitory checkpoints are programmed cell death receptor-1 (PD-1), programmed cell death ligand (PD-L1), and cytotoxic T lymphocyte-associated molecule-4 (CTLA-4).

Recent studies have shown that SEs play key roles in determining cell identity in both healthy and pathological states. Over 25,000 enhancers were identified as deferentially activated in renal, breast, and prostate tumor cells, as compared with normal cells (15). This suggested a potential network between malignancy and enhancer activity. In addition, SEs are located at oncogenes and other genes that are essential for tumor pathogenesis in cancer cells, indicating their possible utility as biomarkers for tumor-specific pathologies (2). Considering the notion that evading immune destruction as a hallmark of malignancy, it is suspected that SEs in immune cells may be involved in the regulation of inhibitory checkpoint expression (16). In this review, we summarize the current understanding of eRNA function, their mechanism of action, and immune checkpoints. Then, we focus on the crosstalk between eRNA and immune checkpoints in pathological stages. A better understanding of the link between SEs, eRNAs, and immune checkpoints, may lead to eRNAs being developed as potential markers or therapeutic targets in the future.

SUPER ENHANCER NON-CODING RNA

Enhancers are often occupied by multiple signature TFs. The typical chromatin signature of enhancers includes a high H3K4me1 to H3K4me3 ratio, histone H3 lysine 27 acetylation, P300 acetyltransferase binding, CREB binding protein (CBP) binding, mediator complex subunit 12 binding, and a high sensitivity to nucleases (17–22). A typical enhancer activates its target gene transcription via its *cis*-acting function along with interactions with the promoter and multiple TFs, including Yin-Yang 1 (YY1) and myogenic differentiation 1 (MYOD) (9, 23). Enhancers can exert their function in an orientation and distance-independent manner, being capable of targeting both upstream and downstream genes (24). RNAP II occupation at some enhancers leads to the transcription of eRNAs, which is considered as another hallmark of an active enhancer (12). SEs are tissue specific regulatory regions of DNA consisting of clusters of enhancers. In various murine cell types (macrophages, Th cells, pro-B cells, embryonic stem cells, and myotubes), SEs and their target genes, which encode cell-type specific TFs, have been identified (20). By investigating the distribution of disease-associated DNA sequence variation in enhancers and SEs in human cells and tissues, Hnisz et al. found that trait-associated single-nucleotide polymorphisms (SNPs) were highly enriched in SEs, indicating their potential disease-associated role (2). In addition, SEs are characterized by specific histone modifications and they bind with a higher level of mediators, nipped-B-like protein, P300, chromodomain-helicase-DNA-binding protein 7 (CHD7), Bromodomain-containing protein 4 (BRD4), kruppel-like factor 4, estrogen-related receptor beta, and cohesin compared with typical enhancers (2, 20). The level of histone modifications H3K27ac and H3K4me1 at SEs exceeded those at typical enhancers significantly (20). Moreover, RNAP II is clustered at SEs at a greater density than at typical enhancers, resulting in a higher level of super-enhancer RNA (seRNA) production (25) (**Figure 1**).

RNAs transcribed from enhancers can be classified as short, bi-directional, and non-polyadenylated eRNAs, and long, unidirectional, and polyadenylated eRNAs. The majority of seRNAs are capped and polyadenylated RNAs (25). This feature makes seRNAs more stable and capable of having a wider effect in physiological and pathological conditions. eRNAs are transcribed by the binding of RNAP II to enhancer DNA in various types of cells, such as macrophages, neurons, keratinocytes, and breast cancer cells (26, 27). It was proposed that TFs that are bound at enhancers interact directly or indirectly with the promoter via a cofactor to exert a stimulatory effect on RNAP II. Upon this dynamic interaction, RNAP II and its accessory effectors come close to enhancer DNA, resulting in initiation of eRNA transcription (28).

The exact function of eRNAs is incompletely understood; nevertheless, evidence suggests that at least some eRNAs play an active part in the regulation of enhancer activity and gene expression. Nicholas et al. found that the synthesis of eRNAs precedes the transcription of target gene transcription in lipopolysaccharide-activated macrophages (29). This indicated

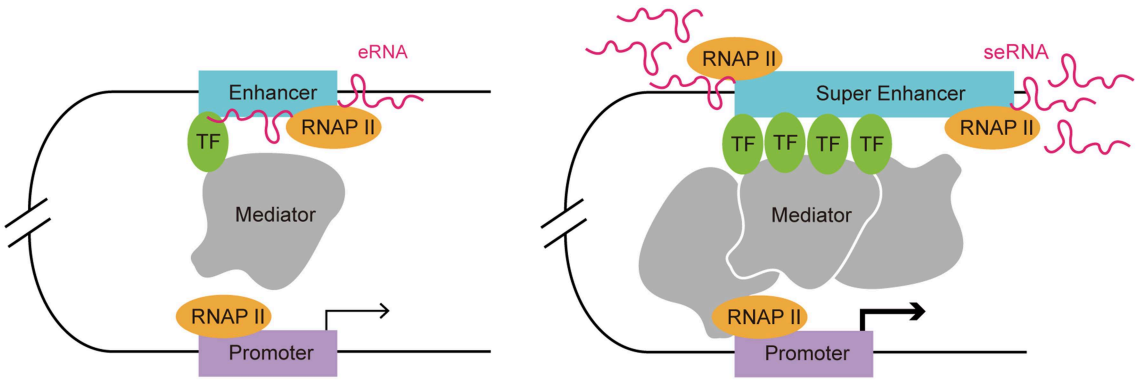

FIGURE 1 | Comparison of a typical enhancer and super enhancer. Compared with typical enhancers, super enhancers are enriched with more transcription factors, mediators, and RNAP II. Hence, the transcription activity at a super enhancer is usually higher than at a typical enhancer. Functionally, super enhancers have a higher potential to promote target cell-identity-related gene transcription.

that eRNAs might be associated with transcription activation of target gene. The transcript level of the majority eRNAs correlates highly correlated with the mRNA expression level of the nearby target gene, suggesting an activating function in promoting mRNA synthesis (27, 30). Consistently, knockdown of eRNAs leads to decreased expression of nearby target genes (31, 32).

THE ROLE OF eRNAs IN ENHANCER FUNCTION

The actions of eRNAs have been widely studied in recent decades and several functional mechanisms have been proposed. The biological functions of eRNA are associated with TF recruitment, enhancer-promoter looping, chromatin conformation, and histone acetylation (**Figure 2**) (7–12, 33, 34). In addition to their functional contributions, eRNAs are also markers of enhancer activity. As an independent indicator of enhancer activity, the presence of eRNAs can distinguish whether the enhancer is active or silent. In macrophages, nearly all SEs express seRNAs (93.3%) within intergenic regions, which indicated that the presence of seRNAs could be used to mark SEs (35).

First, recent studies showed that eRNAs can promote the recruitment of TFs. YY1 is a TF that not only binds to active enhancers and promoters, but also binds to eRNA and RNA transcribed from promoters in murine embryonic stem cells. Further investigations revealed that YY1 binding to DNA is stabilized by an eRNA that is tethered by RNAP II (23). It is possible that the eRNA captures free YY1, which allows this TF to bind to a nearby DNA locus. This creates a positive feedback loop in the stimulation of local transcription and allows more TFs to bind the genomic locus. Recently, Weintraub et al. found that YY1 could form dimers and bind to enhancers and promoters to facilitate enhancer-promoter looping (36), which suggested an indirect facilitation effect of the eRNA on enhancer-promoter looping. Similarly, Charles et al. found a novel group of interferon gamma (*IFNG*) eRNAs that bind nuclear factor kappa B (NF-κB) to enhance its function. Treatment of chromatin with ribonuclease led to decreased NF-κB binding to the *IFNG* genomic sites. Using cell transfection techniques, the authors illustrated that knockout of *IFNG-R-49*, an *IFNG* eRNA, resulted in the reduction of NF-κB binding to the *IFNG-D-49* genomic site, which demonstrated that *IFNG* eRNAs contribute to maintaining the binding between NF-κB and the *IFNG* locus (7).

Second, Amartya et al. identified a significant correlation between promoter-enhancer looping, the presence of eRNAs, and gene expression, which suggested that eRNAs are involved in the interaction between enhancers and promoters (37). As part of the gene regulatory mechanism, enhancer-promoter looping is necessary for gene activation (38). A previous study showed that enhancer-promoter looping was modulated in part by the mediator complex and cohesin (21). Following the binding of the mediator complex and cohesin to the enhancer and promoter, looping of the enhancer and promoter brings the eRNA close to the target gene promoter to allow coordination and activation. Knockdown of specific eRNAs reduced enhancer-promoter looping and limited the interplay between transcription effectors that are located within the loop, such as mediator 1, P300 and early growth response 1 (8, 31, 39, 40). Knockdown of the growth regulating estrogen receptor binding (GREB) eRNA led to suppression of enhancer-promoter looping and inhibition of *GREB1* gene induction. Further investigations showed a reduction in cohesin recruitment after eRNA knockdown. This finding suggested that eRNAs promote enhancer-promoter looping via collaborating with cohesin (33).

Third, eRNAs also contribute to directing chromatin accessibility and thus promote specific gene expression. Mousavi et al. identified two seRNAs transcribed from CE and DRR enhancers in MYOD1, a recently labeled SE, in skeletal muscle satellite cells. Depletion of these eRNAs caused reduced chromatin accessibility and RNAP II occupancy at the *MYOD1* and *MYOG* (Myogenin) loci, respectively. Normally, the *MYOG* locus remains inaccessible to nucleases, and chromatin remodeling is needed for the transcription activation of this locus. Using deoxyribonulcease I (DNase I) accessibility as an indicator for remodeling, the authors detected a reduction of

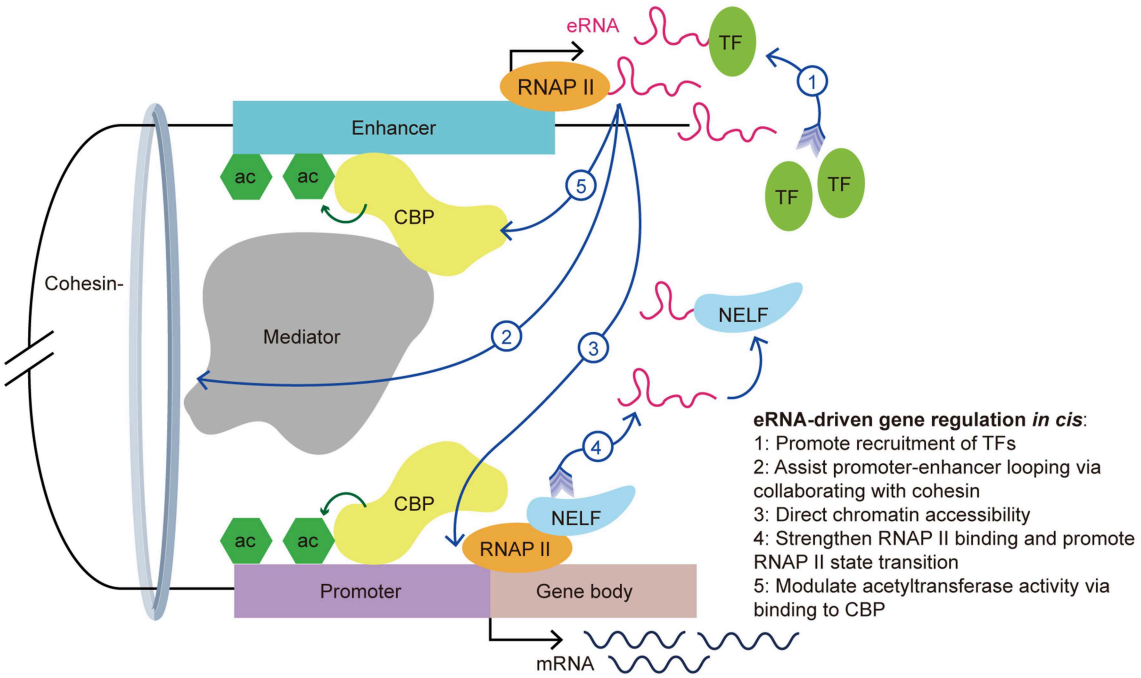

FIGURE 2 | eRNA-driven gene regulation *in cis*. *Cis*-regulatory elements, distal enhancers, and proximal promoters interact with transcription-associated proteins by forming an enhancer-promoter loop. The looping conformation brings the eRNA near to the promoter of the target gene, allowing it exert its function *in cis*. eRNAs exert their gene regulation function via interaction with a variety of transcription-associated proteins, including transcription factors, cohesin, mediators, RNAP II, and CBP.

DNase I accessibility at specific loci in eRNA-depleted cells. Additionally, they hypothesized that eRNAs are involved in regulating the assembly of transcriptional systems by observing that eRNAs affects RNAP II residency at target genes (9).

Fourth, studies have suggested that eRNAs exert various roles in the interaction with RNAP II. For example, eRNAs strengthen the binding of RNAP II to enhancer regions and promoters (9). Maruyama et al. disclosed the attenuation of diethyl maleate-induced RNAP II binding to promoters in eRNA knockdown cells (41). Moreover, eRNA promotes the paused RNAP II transition into the gene body by acting as a decoy. *Arc* eRNA depletion resulted in a decrease in the elongating form of RNAP II, which indicated that eRNAs promote the state transition of RNAP II. This hypothesis was further supported by the finding that knockdown of *Arc* eRNA led to maintenance of the negative elongation factor complex (NELF) on the promoter. NELF induces RNAP II pausing by binding to RNAP II, the promoter, and the newly generated RNA. Katie et al. suggested that eRNAs bind to NELF via competing with the nascent RNA, leading to the detachment of NELF from RNAP II, thereby enabling RNAP II elongation and mRNA synthesis (11). The state transition of RNAP II from paused to productive elongation is extremely important for target transcript production.

Last but not the least, eRNAs can bind to CBP and modulate the acetyltransferase activity at the enhancer, thus increasing the transcription of target genes. CBP binding to P300 and the resulting high levels of H3K27ac, are hallmarks of enhancers. Having noticed that there was more active transcription from loci with CBP bound to eRNAs than from the no-RNA binding control CBP binding sites, Daniel et al. found that this effect is stimulated by eRNAs binding to the histone acetyltransferase (HAT) domain of CBP. This domain determines the HAT enzymatic activity and this process promotes CBP acetyltransferase activity. The authors demonstrated that eRNA binding exposes the activation loop in CBP/P300. Thus, there is an increase of H3K27ac and H3K18ac at the enhancer and promoter, which increases transcription of the target genes (12). Taken together, eRNAs stimulate target gene transcription in part by stimulating histone acetylation.

HOW SUPER-ENHANCER RNAs REGULATE GENE EXPRESSION: *CIS* REGULATION AND *TRANS* REGULATION

The functions of seRNAs can be classified as *cis*-regulation and *trans*-regulation. The *cis* regulation by eRNAs has been widely accepted, in which the enhancer-promoter looping structure brings the eRNA close to the target gene. Using chromosome conformation capture (3C) technology, this looping model has been supported by a wide range of studies. As previously discussed, the *cis*-acting function of eRNAs is accomplished via their dynamic interactions with TFs, modifiers, and cohesin subunits within or near the enhancer-promoter loop. Depletion of seRNAs from distal super enhancers at the *NANOG* locus led to significantly decreased expression of *DPPA3* (encoding

developmental pluripotency associated 3). *DPPA3* is the nearest gene to the *NANOG* super enhancer apart from *NANOG* itself. Using 3C, the authors demonstrated that the looping of the distal super-enhancer at the *DPPA3* promoter decreased by ∼50%, suggesting that the distal seRNA stabilizes the looping and chromatin interactions *in cis*, thereby regulating the expression of *DPPA3* (31). Similarly, the transcription of another seRNA, named *CARMEN* (Cardiac mesoderm enhancer-associated non-coding RNA), was found to cause activation the expression of direct downstream genes (42). Taken together, these results demonstrated that seRNA functions as a scaffold that guides TFs and looping-associated protein complexes *in cis*.

Intriguingly, some recent studies suggested seRNAs might also function interchromosomally (*trans* activity) to direct target gene expression (**Figure 3**) (8, 25, 32, 43). For instance, the MYOD Upstream Non-coding RNA (*MUNC*), an eRNA originating from the distal regulatory region enhancer of *MYOD*, was observed to induce the transcription of specific myogenic genes [e.g., *MYOD*, *MYOG*, and *MYH3* (myosin heavy chain 3)] *in trans*. Overexpression of *MUNC* in $MYOD^{-/-}$ cells caused *MYOG* and *MYH3* transcription and expression. Notably, these two genes are located on different chromosomes, validating MUNC's *trans* activity (32). Alcarez-Dominguez et al. reported that a polyadenylated-eRNA-producing Band 3 SE transcribes an seRNA called *Bloodlinc* that can facilitate gene expression and stimulate red cell production *in trans* (25). Strikingly, they found that *Bloodlinc* diffused beyond its domain of transcription and 81 direct gene targets located across multiple chromosomes were identified as regulated reciprocally upon *Bloodlinc* depletion or overexpression. This is quite different from typical eRNAs, which usually remain in proximity to their parent enhancers. Many of the regulated genes were located outside the super-enhancer domain. Further investigations showed that *Bloodlinc* binds to *trans*-chromosomal loci that encode key erythroid modulators and TFs. Using mass spectrometry [comprehensive identification of RNA-binding proteins by mass spectrometry (ChiIRP-MS)] techniques, the authors found that *Bloodlinc* interacted with multiple protein complexes that function as RNA helicases (e.g., DExD-box helicase 21), RNA transporters (e.g., heterogeneous nuclear ribonucleoprotein A1), RNA splicers (e.g., KH-type splicing regulatory protein), chromatin organization regulators (e.g., marker of proliferation Ki-67 (MKI67), and Lamin A/C), and transcription coactivators or co-repressors [e.g., MYB binding protein 1a (MYBBP1A) and heat shock protein family A member 8 (HSPA8)]. Moreover, immunoprecipitates of endogenous heterogeneous nuclear ribonucleoprotein U (HNRNPU), a nuclear matrix protein that stabilizes RNA-chromatin associations, were specifically enriched for *Bloodlinc*, which confirmed the interaction between *Bloodlinc* and HNRNPU (25). Thus, these findings suggested a model for how *Bloodlinc* acts *in trans*. Specifically, *Bloodlinc* accesses its *trans* target genes via chromatin interactions stabilized by HNRNPU. *Bloodlinc* stimulates or represses target genes expression via interacting with transcription coactivators (e.g., MYBBP1A) or transcriptional repressors (e.g., HSPA8). This process is stabilized by chromatin organization regulators that also interact with *Bloodlinc*.

CANCER ASSOCIATED SUPER ENHANCER RNA

To determine whether enhancers or eRNAs correlate with disease-associated DNA sequence variations, Hnisz et al. investigated the distribution of SNPs within enhancers and super-enhancers. They found that SNPs were enriched in enhancers and SEs, with trait-associated SNPs occurring in SEs at a strikingly higher rate than in enhancers. Analysis in a colorectal cancer cell line demonstrated that more than one-third of SE genes have functions that are closely related with cancer hallmarks,

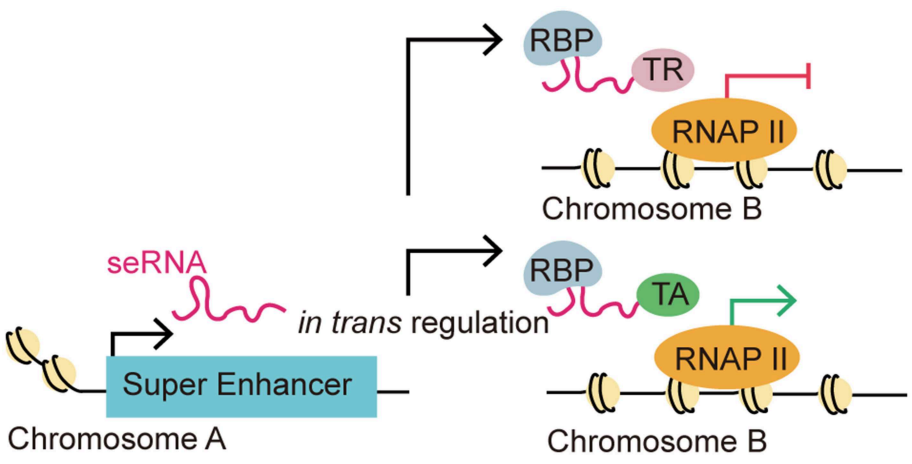

FIGURE 3 | eRNA-driven gene regulation *in trans*. Recent studies identified that eRNAs could regulate gene transcription *in trans*, which means that an eRNA could affect gene regulation in a distal target gene in a different chromosome. This distal regulation function is accomplished via interactions with RNA-binding proteins (RBPs) and other transcription-associated proteins. The *trans* regulation by eRNAs can be classified as repressive or activating depending on their interaction with transcription repressors (TRs) or transcription activators (TAs).

such as evading growth suppressors (e.g., Cyclin D1, Epiregulin), avoiding immune destruction (e.g., F2R like trypsin receptor 1) and sustaining proliferative signaling (e.g., insulin receptor substrate 1, KIT ligand) (2, 16). Consistently, other studies found that SEs are associated with critical tumor oncogenes in various types of cancers. Lovén et al. found that in multiple myeloma, disruption of *BRD4* (bromodomain-containing Protein-4) and mediator occupancy in an SE led to inhibition of tumor oncogenes, including MYC (44). Recently, eRNAs were found to participate in regulating gene transcription and cell-cycle progression with *TP53* (p53 tumor suppressor). Melo et al. found some of the *TP53* binding regions encompass enhancer activity and produce eRNAs in a p53-dependent manner. Knockdown of these eRNAs significantly inhibited downstream target gene transcription upon *TP53* activation, suggesting the eRNAs produced from *TP53* bound enhancer regions that are required for efficient *TP53* transcription enhancement and p53-dependent cell-cycle arrest (45). Moreover, Jiao et al. found a heparanase eRNA that is elevated in cancer cell lines, and enhances tumorgenesis and aggressiveness of cancer cells by facilitating chromatin looping between a super enhancer and the *HPSE* (heparanase) promoter (39). The results from these studies indicated that seRNAs might have significant roles in tumorgenesis and could serve as potential targets for cancer clinical therapy.

IMMUNE CHECKPOINT

Immune checkpoints, including stimulatory and inhibitory pathways, are regulatory signals that play vital roles in the maintenance of the delicate balance between activation of adaptive immunity and retaining self-tolerance from autoimmunopathy. Stimulatory checkpoint molecules encompass CD28 and the inducible T cell costimulator (both from the B7-CD28 superfamily) as well as CD27, CD40, OX40 (TNF receptor superfamily member 4), and CD137 (TNF receptor superfamily member 9), which are all from the tumor necrosis factor (TNF) receptor superfamily. Inhibitory checkpoint molecules include members of the B7-family [such as CTLA-4 (CD 152), PD-1 (CD 279)], Lymphocyte Activation gene-3, and nicotinamide adenine dinucleotide phosphate. Through unique and non-redundant pathways, these molecules work as secondary signals to determine the activation or inhibition of immune cells upon antigen recognition, which modulates the duration and amplitude of physiological immune responses.

Cancer cells are capable of evading immune recognition and immune-mediated destruction by downregulating the expression of tumor antigens, seizing inhibitory immune checkpoints, and inducing immune exhaustion, which leads to the increased expression of inhibitory receptors on T cells, such as CTLA-4 and PD-1 (16). Exhausted T cells often feature CTLA-4 expression. CTLA-4, as a B7/CD28 family member, is involved in tumor immune evasion via down-regulation of $CD4^+$ effector cells (T_{eff}) and promotion of T_{reg} cell activity (13). PD-1, another marker of T cell exhaustion, is expressed at a characteristically high level in tumor infiltrating T cells, which is in consistent with a reduction in interleukin (IL)-2 and IFNγ production and cell cycle arrest in T cells (46). In addition, tumor cells and tumor associated antigen presenting cells (APCs) often express higher levels of co-inhibitory molecules than co-stimulatory molecules, which enhances the activation threshold of T cell and leads to T cell anergy (47).

Rheumatic diseases are characterized by abnormal activation of the immune system, which leads to chronic inflammation and tissue damage. Immune checkpoints are actively involved in the manifestation of rheumatic disease. Genetic polymorphisms in the PD-1 gene (*PDCD1*) in humans correlate with a variety of autoimmune diseases, including type 1 diabetes (T1D), rheumatoid arthritis (RA), multiple sclerosis, and systemic lupus erythematosus (SLE) (48). Mice deficient for a single inhibitory receptor (such as CTLA-4 or PD1) often display enhanced susceptibility to experimentally-induced autoimmune diseases or may spontaneously develop a lupus-like disease (49). CTLA-4 has a fundamental role in establishing immune tolerance. *Ctla4* knockout mice showed premature death caused by the development of lymphoproliferative disease with multiple organ involvement (50), while human patients with mutations that caused loss of function of CTLA-4 also manifested widespread immune dysregulation (51). Jury et al. identified CTLA-4 dysfunction as a possible cause of abnormal T-cell activation in patients with SLE (52). In addition, autoimmunity activation and inflammatory toxicities, such as colitis, hepatitis, pneumonitis, dermatitis, and myasthenia gravis, are major adverse events caused by the use of immune-checkpoint blockers in tumor immunotherapy (53–56). The use of Ipilimumab, a CTLA-4-blocking antibody, was reported to cause inflammatory exacerbation in 25% of patients who had preexisting autoimmune diseases (57). This led to the hypothesis that enhancing inhibitory pathways would be beneficial to treat autoimmune disease. Abatacept, a CTLA4–Fc fusion protein, is the first checkpoint-targeting drug to be approved to treat rheumatic diseases. CTLA-4 Fc prevents costimulatory signaling, thus reducing T cell activation in RA, SLE, and psoriatic arthritis (58–60).

PD-1 and CTLA-4 are the most widely studied inhibitory checkpoint molecules because of their superior performance in the treatment of tumors (**Table 1**). PD-1 is expressed on T cells, B cells, dendritic cells (DCs), monocytes, natural killer (NK) T cells, exhausted cells, and T_{reg} cells. When engaged to its receptor PD-L1, which is widely expressed on antigen-presenting cells, $CD4^+$ T cells, and non-lymphoid tissues, PD-1 delivery an inhibitory signal via direct and indirect pathways. In the direct pathway, PD-L1-engaged PD1 potently counteracts CD28-co-stimulation and T cell receptor (TCR) signal transduction via terminating zeta chain of T cell receptor associated protein kinase 70 and phosphoinositide-3-kinase (PI3K) phosphorylation, leading to recruitment of protein tyrosine phosphatase non-receptor type 11 (PTPN11), which in turn inhibits IL2 production and reduces the transcription of pro-survival factor BCL-2-like protein 1 (73). In the indirect inhibitory mechanism, engaged PD1 decreases casein kinase 2 alpha 1 expression and activity, which results in the maintenance of phosphatase and tensin homolog activity, shutting off both the protein kinase B (AKT) pathway and

TABLE 1 | Overview of PD-1/PD-L1 and CTLA-4 blockage.

Molecule	Ligand (s)	Expressing cells	Blockage approved for	Blockage effects	References
PD-1	PD-L1, PD-L2	T cells, NK cells, B cells, macrophages, DC subsets, mast cells	Metastatic melanoma, non-small-cell lung cancer, head and neck squamous cell cancer, Hodgkin's lymphoma, renal cell carcinoma	Restore TCR signaling. Enhance IFN-γ and associated chemokines. Promote $CD8^+$ T cell influx in tumor microenvironment. T cell metabolic reprogramming	(61–66)
PD-L1	PD-1, B7-1 (CD80)	Tumor cells, tumor-associated APCs (e.g., DC, monocytes, macrophages, mast cells, T cells, B cells, NK cells)	Non-small-cell lung cancer, bladder cancer, urothelial carcinoma, Merkel cell carcinoma	Target: Cancer cell: Block PD-1/PD-L1 signaling pathway. Block interaction with CD80. Inhibit immune-independent cancer cell intrinsic growth. Macrophage: Suppress T cell extrusion from tumor microenvironment	(66–69)
CTLA-4	CD80, CD86	T cells (resting and activating)	Metastatic melanoma, renal cell carcinoma	Block competitive inhibition of CD28 co-stimulation. T cell metabolic reprogramming Broaden the peripheral TCR repertoire	(70–72)

subsequent T cell growth (73). In addition, the inhibitory function of PD-1 is exemplified by the promotion of TCR endocytosis and shifting the metabolic status of T cells toward fatty acid beta-oxidation, which leads to metabolic restriction (73). While CTLA-4 plays a pivotal role in attenuating the activation of naïve and memory T cells via competing with CD28-mediated signaling (74). Downstream of both CTLA-4 and PD-1 abrogates AKT activity, which is related to limiting cellular metabolism (70).

CLINICAL IMPLICATIONS OF IMMUNE CHECKPOINTS

Immunotherapy, especially PD-1/PD-L1 blockage and CTLA-4 blockage, has revolutionized the landscape of cancer treatment in recent years. The FDA has approved immune checkpoint inhibitors for the treatment of a range of tumor types, such as melanoma, non-small cell lung cancer, renal cell carcinoma, Hodgkin lymphoma, and head and neck squamous cell carcinoma.

PD-1/PD-L1 Blockage: Mechanism and Effect

By counteracting the pathological function of PD-1, antibodies that block PD-1 (e.g., Pembrolizumab and Nivolumab) and its ligand PD-L1 (e.g., Atezolizumab, Avelumab, and Duralumab) inhibit adaptive immune resistance and reinvigorate the immune response against cancer cells. PD-1 mediates immune suppression via a variety of mechanisms in cancer. In T cells, PD-L1-bound PD-1 inhibits TCR signaling by recruiting PTPN11 to the immunoreceptor tyrosine-based switch motif domain, which results in dephosphorylation of downstream signaling molecules, decreased IL-2 production, reduction in cell cycle progression, and reduced expression of TFs involved in effector function (T-bet and eomesodermin) (74). An elevated level of circulating IFNγ and its associated chemokines [C-X-C motif chemokine ligand (CXCL)-9 and CXCL-10] and T cell activation markers (MKI67 and major histocompatibility complex, class II, DR) were detected in the serum of patients undergoing anti-PD-1 and anti-PD-L1 treatment (61). PD-1 blockage restores T cell activation and an influx of $CD8^+$ T cells was detected in the tumor microenvironment (62). In addition, PD-1 signaling interferes with CD28-mediated activation of PI3K and AKT, which in turn limits glucose metabolism (70). The resulting bioenergetic insufficiencies inhibit mammalian target of rapamycin (mTOR) activity and IFNγ production, impair EZH2 (enhancer of zeste 2 polycomb repressive complex 2 subunit) expression in T cells, and reduce the level of phosphoenolpyruvate, which is linked with a lack of activation of $CD4^+$ tumor-infiltrating lymphocytes (61). The process of metabolic restriction is a driver of T cell exhaustion. Antagonists of PD-1 cause T cell metabolic reprogramming and restore their glycolytic capacity, as well as the subsequent effector function (63). PD-1 and PD-L1 blockage also decrease E3 ubiquitin ligase CBL-B expression thus inhibiting the downregulation of TCR (64).

PD-L1 expression is especially high in tumor cells and tumor-associated APCs (e.g., tumor environment DCs, macrophages, and fibroblasts) (75). As a result of adaptive immune resistance, PD-L1 overexpression on tumor cells is induced by IFNγ that is produced by activated T cells. High levels of PD-L1 expression have been associated with poor prognosis in many types of cancer. PD-L1 antibodies exert their antitumor effect partly by blocking the PD-1–PD-L1 interaction. Manish et al. found that PD-L1 also interacts with B7-1

(CD80) to inhibit T cell activation and proliferation (67). Therefore, PD-L1 blockage also may restore T cell activation by inhibiting the CD80–PD-L1 interaction. A recent study showed that tumor-expressed PD-L1 has tumor-intrinsic effects in addition to delivering an inhibitory signal to PD-1 on T cells. PD-L1 promotes cell-intrinsic growth in an immune-independent manner in both melanoma and ovarian cancer. PD-L1 represses tumor autophagy and enhances the mTOR pathway in both ovarian cancer and melanoma (68). Thus, PD-L1 blockage may exert its effect by mediating PD-L1-related intrinsic tumor signaling. PD-L1 expression on macrophages may result in active extrusion of T cells from the tumor microenvironment, indicating another possible pathway for PD-L1 blockage (69).

CROSSTALK BETWEEN seRNAs AND IMMUNE CHECKPOINTS

Super-enhancers play a critical role in the regulation of genes that define cell identity, and increasing evidence suggests that SEs and eRNAs have functions in tumorgenesis. However, the exact function and mechanism of seRNAs in the regulation of tumorgenesis and tumor immunotolerance is not fully understood. Lovén et al. found that cancer cells acquire SEs at oncogenes and at genes that are important for tumor pathogenesis. They found that SEs assist the high level transcription of genes [e.g., *MYC*, *IRF4* (interferon regulatory factor 4), *XBP1* (X-box binding protein 1), *CCND2* (Cyclin D2)] that are deregulated in multiple myeloma cells (44). Ding et al. revealed the oncogenic role of eGREB1, an eRNA of an estrogen-responsive gene enhancer, growth regulating estrogen receptor binding 1 (GREB1), in bladder cancer. Upregulated eGREB1 is associated with higher level TNM stages of bladder cancer. Consistently, proliferation, migration, and invasion were inhibited upon eGREB1 knockdown, while apoptosis was promoted (76). In addition, for a variety of cancer cells (e.g., pancreatic cancer and T cell leukemia), SEs were identified around the *MYC* gene in cancer cells. However, these SEs were not identified in their healthy counterparts (2). Besides, Hnisz et al. provided a list of tumor-specific SEs that fall into different categories of hallmark cancer genes in colorectal cancer. For instance, the identified SEs of *PCDH7* (protocadherin 7), *CCND1* (Cyclin D1), and *F2RL1* are associated with activating invasion and metastasis, evading growth suppressors, and avoiding immune destruction, respectively (2). Taken together, these findings indicated that SEs might act as keys for amplified oncogene expression. This hypothesis was supported by the results of Wong et al., who found that multiple oncogenic TFs are regulated by SEs in acute T cell lymphoblastic leukemia. Disruption of SE-related gene expression and cancer cell death were identified after treating cancer cells with RNAP II activation blocker (77). SeRNAs play an active role in promoting SE function; therefore, we suspected seRNAs could also function in this inhibitory process.

Super-Enhancer RNA Induces PD-L1 Expression via Enhancing MYC Expression

MYC is an oncogene that has been studied in depth. The activation and overexpression of *MYC* is a characteristic feature of tumorgenesis and cancer maintenance. As a TF, MYC activates the expression of many pro-proliferative genes by binding at enhancers and recruiting HATs (78). One of the mechanisms by which the *MYC* gene is believed to maintain cancer cell survival is to exempt itself from immune surveillance and the anti-tumor immune response (79). This hypothesis was supported by the finding that *MYC* expression correlated highly with *PDCD1L1* (PD-L1) gene expression in non-small cell lung cancer cell (79). Kim et al. also identified poorer clinical outcome for patients with both MYC and PD-L1 dysregulation and overexpression (79). Consistently, Casey et al. demonstrated that MYC upregulates the expression of immune checkpoints, *CD47* and *PDCD1L1*, on cancer cells by direct interaction with the promoters of these two genes. In multiple types of cancer, silencing of *MYC* leads to a significant reduction in the transcription and expression of *CD47* and *PDCD1L1*, both *in vitro* and *in vivo* (80). Therefore, MYC may be a key regulator for immune checkpoint expression in cancer. For a variety of cancer cells, SEs are found specifically clustered at genes surrounding the *MYC* gene (2). SEs tend to express seRNAs at higher levels than typical enhancers; therefore, we wondered whether seRNAs participate in the regulation of immune checkpoint expression. Human colorectal cancer-specific nucleus retained Colorectal Cancer Associated Transcript 1-long isoform (CCAT1-L) is a 2,600 nucleotide long lncRNA that is transcribed from an SE and therefore is considered as an seRNA. A recent study suggested that the seRNA CCAT1-L contributes to the regulation of *MYC* expression *in cis* in colorectal cancer. CCAT1-L is transcribed from a locus 515 kb upstream of the *MYC* gene (MYC-515) in the human 8q24 region. This SE forms an enhancer-promoter loop with the *MYC* promoter, thus bringing CCAT1-L in to close proximity with the promoter. Such chromatin interactions are present specifically in colorectal, breast, and prostate cancer (81). Xiang et al. reported that CCAT1-L assists in the maintenance of chromatin looping between the SE and the *MYC* promoter (82). Previous studies revealed that eRNAs participate in gene regulation by stabilizing enhancer-promoter looping and by dynamic interactions with TFs and mediators in the surrounding area. The accumulation of CCAT1-L surrounding its SE indicates its possible function in the regulation of its target gene. By examining the expression of mRNA after CCAT1-L knockdown, reduced *MYC* transcription and expression were detected. However, overexpression of CCAT1-L from a plasmid showed no apparent activation of *MYC* expression. This could be explained by the possibility that extrinsic CCAT1-L localized to many nuclear sites but not its *in cis* site. To confirm this hypothesis, Xiang et al. (82) used transcription activator-like engineered nucleases to achieve *in cis* overexpression of CCAT1-L in a low CCAT1-L expression cell line. CCAT1-L overexpression resulted in higher *MYC* expression and faster cell growth than that in the control cancer cell group. Thus, CCAT1-L enhances *MYC* expression *in cis*. The most common form of seRNA

function is *in cis* regulation; however, how is CCAT1-L brought close to its target gene from 515 kb away? To answer this question, Xiang et al. applied the 3C technique to investigate the interaction frequencies between possible enhancers and *MYC* promoter segments. Intriguingly, they found an interaction between a locus 335 kb upstream of the *MYC* promoter (MYC-335), and the *MYC* promoter showed the highest interaction frequency with this site, while the interaction between MYC-515 and MYC-355 ranked as second. Earlier Pomerantz et al. found an enhancer located at MYC-355, which forms a loop between the MYC promoters to promote its transcription (83). The result of 3C analysis suggested that CCAT1-L locates to MYC-335, bringing it closer to *MYC*. Knockdown of CCAT1-L resulted in a prominent decrease in the chromatin interactions between MYC-335 and the *MYC* promoter and between MYC-515 and MYC-335. Taken together, the results suggested that a looping conformation is formed between *MYC* and MYC-335 and between MYC-335 and MYC-515. In addition, CCAT1-L is required to maintain the specific loops between the *MYC* enhancers and the *MYC* promoter. Further investigation into the exact mechanism by which CCAT1-L functions to promote enhancer-promoter looping revealed that TFs transcription factor 4 and CCCTC-binding factor (CTCF) are enriched at the loops of the *MYC* promoter, and the MYC-335 and MYC-515 segments. Moreover, knockdown of *CTCF* is associated with decreased transcription of *MYC* and CCAT1-L, suggesting that the enhancer-promoter looping at *MYC* is CTCF-mediated. In addition, RNA immunoprecipitation showed a specific interaction between CTCF and CCAT1-L. Reduced CTCF occupation of the loop region at *MYC* was detected after depletion of CCAT1-L, indicating that CCAT1-L assists the binding of CTCF to chromatin and contributes to the looping formation at the *MYC* locus (82). In summary, Xiang et al. demonstrated the involvement of seRNA CCAT1-L in the regulation of key oncogene *MYC* in colon rectal cancer. CCAT1-L regulates the expression of *MYC* by interacting with CTCF and assisting its binding with chromatin to sustain the enhancer-promoter looping conformation between the *MYC* promoter and MYC-335 and between MYC-335 and MYC-515. *MYC* expression has been linked to the regulation of a variety of cancer hallmark-related genes in tumors. As mentioned above, MYC upregulates the expression of immune checkpoints *CD47* and *PDCD1L1* on cancer cells by direct interaction with promoters of these two genes. Therefore, it is possible that seRNA CCAT1-L participates in the regulation of *CD47* and *PDCD1L1* expression indirectly by promoting *MYC* gene expression *in cis*.

Additionally, Jiang et al. recently demonstrated that CCAT1 interacts with the TFs tumor protein p63 (TP63) and SRY-box 2 (SOX2) to regulate the expression of the epidermal growth factor receptor (EGFR) in esophageal squamous cell carcinoma (ESCC) (84). With identification of TP63 and SOX2 co-occupied at an SE, the authors wondered whether there is interplay between the seRNA and TP63 and SOX2. Further investigation showed that transcription of seRNA CCAT1 is activated or inhibited by TP63 and SOX2 co-binding or depletion at the promoter and SE of CCAT1. Thus, seRNA CCAT1 was validated as the downstream interaction target for TP63 and SOX2. Moreover, seRNA CCAT1 forms a complex with TP63 and SOX2 and then binds to SEs of *EGFR* to enhance its transcription and expression. The transcription of *EGFR* activates the downstream PD-L1 expression related pathways, including RAS/mitogen activated protein kinase (MAPK) and PI3K/AKT signaling pathways (84). Consistently, the expression of PD-L1 is elevated significantly in response to EGFR signaling activation in esophageal squamous cancer cells. By contrast, inhibition of the EGFR pathway led to a sharp decline in PD-L1 expression (85, 86). Further investigation showed that EGFR-dependent expression of PD-L1 in ESCC is affected by EGFR/PI3K/AKT, EGFR/RAS/MAPK and EGR-phospholipase C gamma 1 (PLC-γ) signaling pathways (84). Many studies have revealed the close connection between PD-L1 expression and *EGFR* mutation (87–89). Higher PD-L1 expression usually indicates poor prognosis (88, 89). For instance, in non-small-cell lung cancer, mutation in *EGFR* lead to upregulation of PD-L1 by activating PI3K/AKT and RAS/extracellular signal-regulated kinase (ERK) signaling (90). Notably, the *EGFR* gene is located in the 7p11 region in the human genome, indicating that CCAT1 promotes *EGFR* transcription *in trans*. Taken together, we propose that seRNA CCAT1 could be involved in the regulation of *PDCD1L1* transcription *in trans* by forming a seRNA-TF complex to promote *EGFR* expression and activate the downstream signaling pathways (**Figure 4**).

CDK7 affects transcription initiation and elongation by blocking SE normal function. As for its potential clinical application, Chipumuro et al. found cyclin-dependent kinase 7 (CDK7) inhibitor, THZ1, selectively downregulates SE-regulated *MYCN* overexpression and MYCN-driven transcription amplification in neuroblastoma (91). Similarly, other researchers revealed THZ1 suppressed SE-driven oncogenic transcriptional amplification in other cancers (92, 93).

Relationship Between BRDs, seRNAs, and PD-L1

BRD4 is a member of BET family, which includes BRD2, BRD3, and bromodomain testis-specific proteins (BRDT). As a transcription co-activator, BRD4 is often required for the expression of oncogenes, including *MYC* (94–96). The functions of BET proteins include initiation and elongation of transcription, and cell cycle control. BRD4 recruits a variety of transcription complexes, including mediator and positive transcriptional elongation factor b (P-TEFb), to acetylated chromatin, leading to the activation of gene expression via phosphorylation of RNAP II (97, 98). Studies showed accumulation of BRD4 at SEs, which facilitated eRNA transcription via interacting with acetylated histones to assist RNAP II progression (99). Recently, BET inhibitors (i.e., JQ1) have been developed for anticancer treatment. JQ1 displaces BRD4 from chromatin, breaks the cell cycle, and induces apoptosis in tumor cells. JQ1 also inhibits BRD4-associated seRNA synthesis by targeting SEs preferentially (44, 99). When treated with JQ1, SEs displayed a higher level of loss of BRD4 accumulation than typical enhancers (44). eRNAs have a role in enhancer function; therefore, it is possible that BRD4 might

regulate target gene expression indirectly via its effect on eRNA synthesis. A recent study demonstrated co-occupancy of BRD4 and mediator at *MYC* SEs, and the use of BET inhibitor JQ1 resulted in transcription elongation defects in *MYC* (44). JQ1 displacement of BRD4 from the *MYC* promoter/enhancer also led to suppression of MYC-driven malignancies, such as

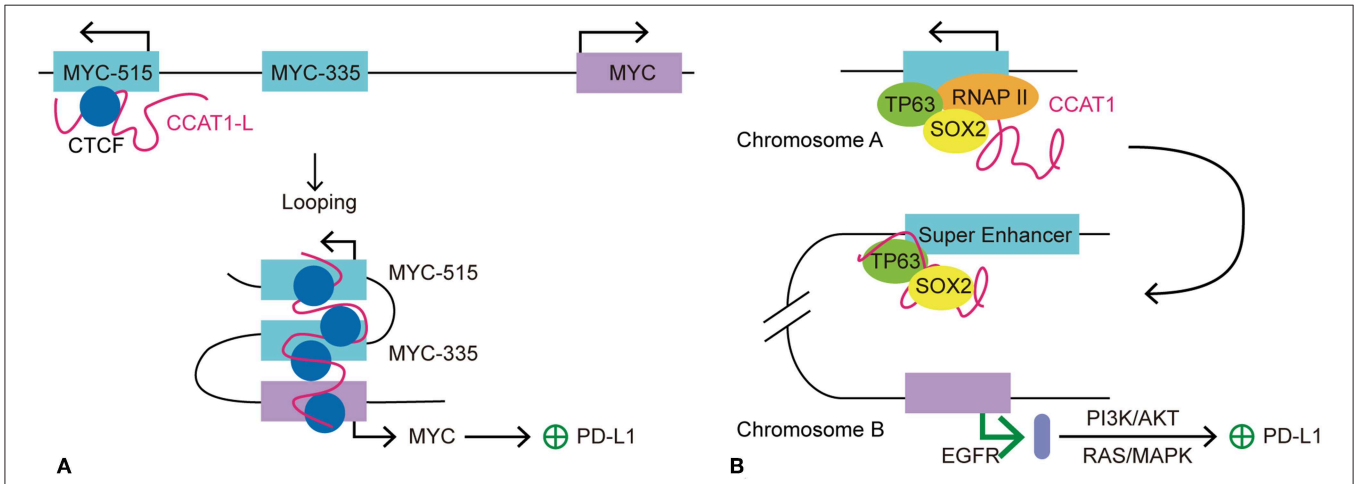

FIGURE 4 | Models of seRNA CCAT1 in the regulation of PD-L1 expression. CCAT1 is an oncogenic seRNA that can regulate the expression of PD-L1 via *cis* and *trans* actions. **(A)** SeRNA CCAT1-L induces the expression of PD-L1 via enhancing the expression of *MYC in cis*. With the help of CTCF, CCAT1-L is brought close to the *MYC* promoter via MYC-515-MYC-335-*MYC* looping. This looping conformation promotes *MYC* transcription, which allows its further promotion of PD-L1 expression. **(B)** TP63 and SOX2 are two transcription factors that promote seRNA CCAT1 transcription. CCAT1 interacts with TP63 and SOX2 to further act *in trans* on another chromosome to promote the transcription of *EGFR*. EGFR promotes PD-L1 expression via its downstream pathways, PI3K/AKT and RAS/MAPK.

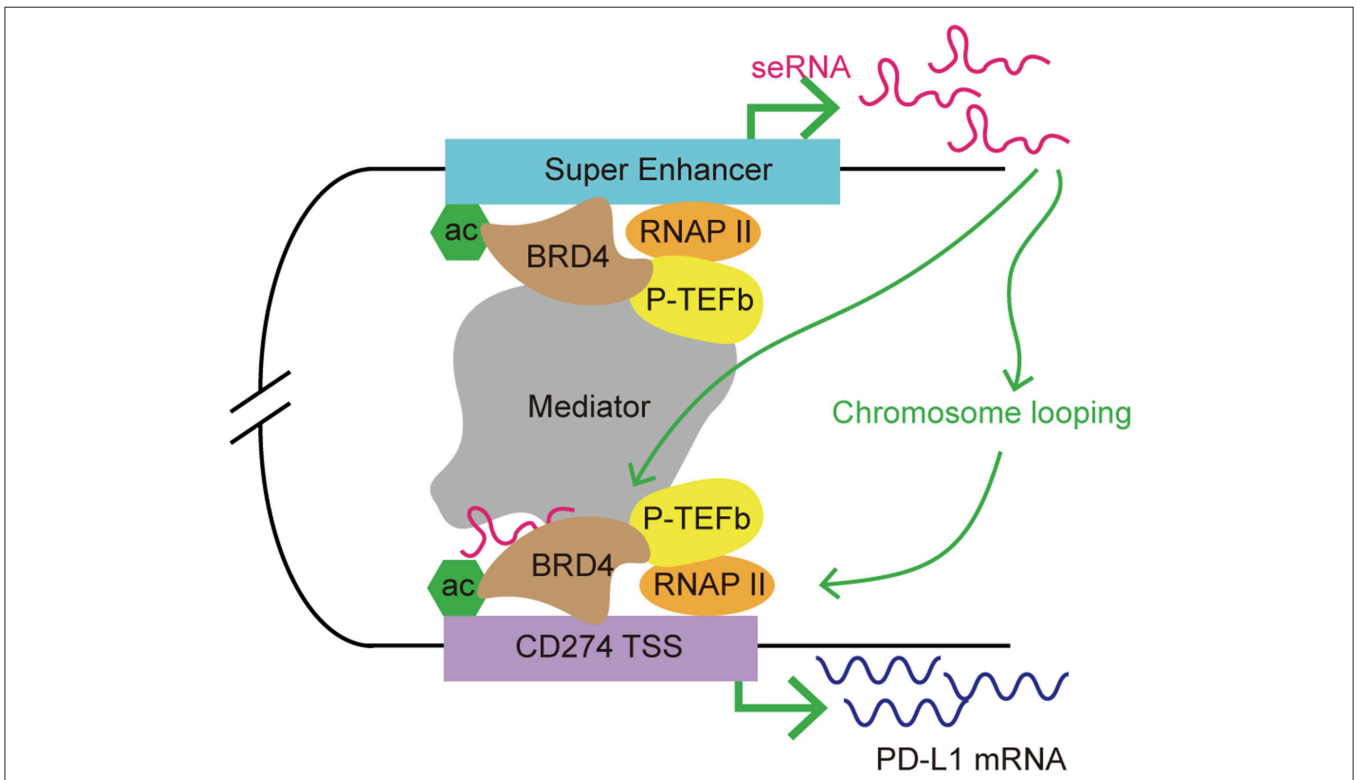

FIGURE 5 | A model of seRNA in the regulation of PD-L1 expression via BRD4. BRD4 is enriched at super enhancers and contributes to seRNA transcription. *PDCD1L1* (also known as *CD274*; encoding PD-L1) is a direct target of BRD4. BRD4 recruits mediator and P-TEFb to acetylated chromatin, leading to the activation of gene expression via phosphorylating RNAP II. An seRNA transcribed from a distal super enhancer proximal to *CD274* is found to loop with the *CD274* transcription start site (TSS). This seRNA enhances the chromosome looping stability and interacts with BRD4 to promote CD274 expression.

multiple myeloma and acute myeloid leukemia (95, 96). Zhu et al. found that treatment with a BET inhibitor suppressed PD-L1 expression in ovarian cancer (100). In a mouse model, the authors observed a dose- and time-dependent reduction in the level of *PDCD1L1* transcription and expression during treatment with JQ1 in tumor cells, macrophages and tumor-associated DCs. Knockdown of *BRD4* decreased PD-L1 expression, indicating that PD-L1 expression is at least partly regulated by BRD4. Further investigation demonstrated that the PD-L1 encoding gene, *PDCD1L1* (also known as *CD274*), is a direct target of BRD4. In addition, the application of JQ1 increased $CD8^+$ cytotoxic T cell activity; thus promoting anti-tumor immunity, limiting ovarian cancer progression, and improving mouse survival (101). The mechanism by which BRD4 regulates *PDCD1L1* expression in cancer cell has been determined. Hogg et al. demonstrated that the inhibition of *PDCD1L1* transcription by the BET inhibitor is independent of *MYC* expression, which is usually involved in PD-L1 expression regulation and is also as a target for BET inhibitors in hematologic malignancies (102, 103). The authors found that downregulation of *PDCD1L1* under JQ1 treatment was not associated with changes in *MYC* regulation. Ectopic overexpression of *MYC* did not affect JQ1's suppression of PD-L1 expression. In addition, depletion of BRD4 led to *PDCD1L1* transcription inhibition in the absence of putative changes in *MYC* expression. Using chromatin immunoprecipitation sequencing and analysis of RNAP II occupancy, the authors further identified a distal SE proximal to the *PDCD1L1* gene. Moreover, this distal SE bridged to the *PDCD1L1* transcription start site (TSS), forming a chromatin loop. The accumulation of BRD4 at the *PDCD1L1* TSS decreased substantially upon JQ1 treatment, indicating that disruption of the TSS and SE loop might contribute to JQ1-mediated PD-L1 expression inhibition (103). As mentioned previously, BRD4 promotes eRNA transcription by interacting with acetylated histones. A recent study demonstrated that the BRD4–eRNA interaction promotes the binding of BRD4 to acetylated histone. This interaction further potentiates BRD4 recruitment to enhancers and promotes subsequent transcription events (104). Therefore, we hypothesized that seRNAs might be involved in BRD4-mediated PD-L1 regulation by contributing to stability of the chromatin loop formed by the distal SE and the *PDCD1L1* TSS, which promotes RNAP II progression. BRD4 regulates the expression of *PDCD1L1* indirectly by promoting the transcription of an SE, and the resulting seRNA contributes to promoting enhancer activity, thus affecting the transcription of *PDCD1L1* (**Figure 5**).

Super-Enhancer RNA and PD-L1 Expression in Autoimmune Disease

The application of immune checkpoints in oncology sometimes triggers auto-inflammatory adverse effects, which has prompted further investigations of the contribution of immune checkpoints to autoimmunity. The expression and functions of inhibitory immune checkpoints are often dysregulated in autoimmune diseases. Promoting the inhibitory function of immune checkpoints should be beneficial to restore the immune balance in rheumatic disease. However, Farh et al. found that distinct enhancers and eRNAs are involved in autoimmune disease (**Table 2**). Genome-wide association studies revealed that risk loci for autoimmunity are enriched in immune cell-specific SEs and enhancers (111). Peeters et al. revealed a disease-specific super-enhancer signature in $CD4^+$ memory/effector cells in the synovial fluid of patients with juvenile idiopathic arthritis (105). These SEs are associated with inflammatory arthritis SNPs, indicating the contribution of SEs and, possibly, seRNAs in the control of disease pathogenesis. Moreover, the application of BET inhibitors suppressed SE-associated gene expression subsequent to a reduction in proinflammatory markers (105). A previous study found that in T cells, one-third of the non-coding RNAs are transcribed from SEs, indicating their potential role in regulating the T cell immune response (112). In T cells, cytokine receptors and cytokines are the predominant type of genes that have an SE architecture (112). ADAM like decysin 1 (ADAMDEC1) is a member of the ADAMs (A Disintegration And Metalloproteinase) protein family. *ADAMDEC1* and *ADAM28*, which is located upstream of *ADAMDEC1*, are overexpressed in SLE and are upregulated in inflammatory states. Further investigation showed that the interaction between eRNAs and P300 is involved in *ADAMDEC1* expression regulation (106). One of the functions of eRNAs is to bind CBP and modulate the acetyltransferase activity at enhancers. NF-κB is recruited to the enhancer upon activation of the inflammatory signal cascade. The accumulation of NF-κB leads to assembly of P300 on the enhancer, which can be activated by eRNAs. Activation of P300 leads to increased histone acetylation and transcription elongation (106). That study revealed the participation of eRNAs in the regulation of autoimmune-associated gene expression. Therefore, it was suggested that there is crosstalk between immune checkpoints and seRNAs in the context of autoimmunity. BTB domain and CNC homolog 2 (BACH2), a TF that functions to suppress effector programs to maintain the T_{reg}-mediated immune homeostasis, has the most prominent super-enhancer in its gene locus in T cells (113). BACH2 regulates the expression of a variety of cytokines in T cells. Genetic variation in the *BACH2* locus is associated with autoimmune-related diseases, such as Crohn's disease, RA, and T1D (114–116). Vahedi et al. found that the *BACH2* locus is SE-regulated, with high P300 occupancy. Knockdown of *BACH2* led to a significant increase in the expression of genes with an SE architecture in T cells, including those encoding cytokines and cytokine receptors (112). In addition, seRNA-related transcription is inhibited by BACH2 (112). Therefore, the authors identified a network in which the expression levels of genes and eRNAs are negatively regulated by BACH2, which itself is also SE-regulated (112). Recent research found that BACH2 promotes tumor immunosuppression via IFNγ and T_{reg}-mediated intratumoral $CD8^+$ T cell inhibition. Elevated levels of IFNγ were observed in tumors of mice with BACH2 deficiency. Further analysis revealed that suppression of IFNγ is caused by BACH2-mediated T_{reg}-dependent tumor immunosuppression (117). Thus, the results demonstrated a pathway for BACH2 to regulate the expression of IFNγ immunosuppression. There are two interferon regulatory

factor-1 (IRF-1) binding sites on the promoter of *PDCD1L1*. Diaz et al. revealed that IFNγ signaling is the primarily regulating signal for *PDCD1L1* expression in melanoma cells. Diaz et al. identified the IFNγ-Janus kinase (JAK)-signal transducer and activator of transcription (STAT)-IRF1 axis that regulates PD-L1 expression (118). Such findings link BACH2 with PD-L1 expression, indicating its potential influence on immune checkpoint expression. Similarly, in the context of autoimmune disease, Osum et al. demonstrated that IFNγ drives PD-L1 expression on islet beta cells in T1D (119). T cell-directed beta cell destruction is the main cause of T1D. *In vivo* and *in vitro* experiments showed that T cell infiltration-dependent islet beta cell PD-L1 upregulation is mediated by IFNγ (119). In addition, the increased PD-L1 expression correlated with the level of T cell infiltration and insulitis, indicating that elevated PD-L1 expression is a salvage response to islet destruction (119). These findings led us to hypothesize that SE-regulated TF BACH2 might play a role in regulating the expression of PD-L1 indirectly by mediating the expression of IFNγ in autoimmune disease. Moreover, seRNAs might also contribute to this regulation by promoting SE function. However, little research has been performed on the contribution of seRNAs to the regulation of immune checkpoint expression in autoimmune diseases, and the exact contribution of seRNAs to autoimmune diseases remains poorly understood. Further investigation and more direct evidence are required to reveal the details of the crosstalk between seRNAs and immune checkpoints in autoimmune diseases.

TABLE 2 | Involvement of SE in autoimmune diseases.

Disease	Cell type	Disease associated SE/seRNA	SE or eRNA regulated gene(s)	Gene function	References
Juvenile idiopathic arthritis	$CD4^+$ memory /effector cells	CTLA4 SE CXCR4 SE	*CTLA4* *CXCR4*	Preserve self-tolerance Control chemokine binding receptor expression	(105)
SLE	Monocytes Peripheral blood mononuclear cells	Enhancer1, Enhancer2, eRNA157 PDCD1 enhancer	*ADADMEC1* *PDCD1*	Escape inhibition by tissue inhibitor of metalloprotease-3 (TIMP-3). Preserve self-tolerance	(106) (107)
Inflammatory bowel disease	CD14+ cells	IFNG-R-49	Not specified	Control of IL22 and IL26 expression levels	(108)
Multiple sclerosis	THP-1 cells	Vitamin D receptor super enhancers (VSE) 1-3	*ZMIZ1 DENND6B USP2 ASAP2 SEMA6B LRG1*	Leukocyte aggregation, actin filament organization, axon guidance, pro-inflammatory cytokine production regulation	(109)
Autoimmune uveitis	Th1	T-bet SE and T-bet seRNA	*IFNγ, TNF, FASL, ILL8RL*, and *CTLA4*	Inflammatory cell infiltration	(110)

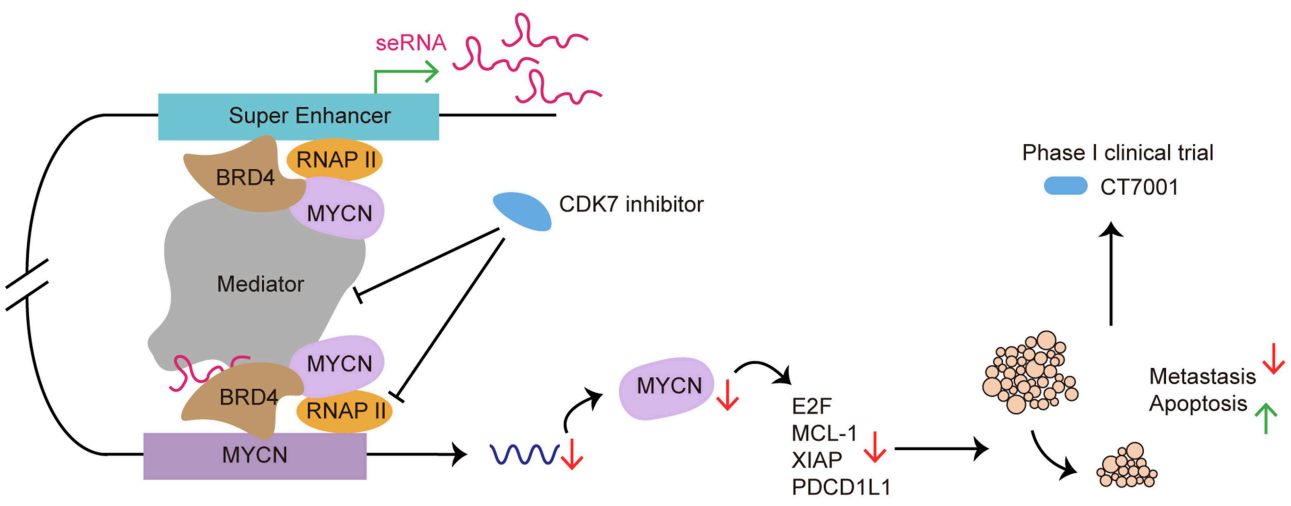

FIGURE 6 | SE as a therapeutic target in cancer treatment: from preclinical to clinical. CDK7 inhibitor targets SE to suppress SE-regulated MYCN driven oncogenic transcription amplification, including *E2F, MCL-1, XIAP* (93). CDK7 inhibitor blocks SE functioning by affecting RNAP II and Mediator complex. Use of CDK7 inhibitor induces tumor regression, cancer cell apoptosis and reduces metastasis both *in vivo* and *in vitro* (120). CT7001, a CDK7 inhibitor, has been approved for phase I clinical trial in patients with advanced malignancies.

CONCLUSIONS

Current knowledge of immune checkpoints and SEs has increased our understanding of immune checkpoint expression in oncology and autoimmunity. Evading immune destruction is a major hallmark of cancer, suggesting that the expression of inhibitory immune checkpoints could be a critical identity character of tumor cells (16). Super enhancers are clusters of enhancers that facilitate gene expression that is important for cell identity. eRNAs contribute to enhancer function via multiple approaches, including enhancing promoter-enhancer looping, facilitating TF assembly, and promoting RNAP II activation. In the present review, we proposed several ways by which seRNAs contribute to immune checkpoint regulation indirectly by mediating the expression of key genes that regulate immune checkpoint expression, and play critical roles in determining cell identity.

As a potential therapeutic target, many researchers had focus on exploring the application of SE blockers in cancers and autoimmune diseases (**Figure 6**). He et al. recently summarized the role of SE as therapeutic target in cancer treatment. By using BET inhibitor, CDK7 inhibitor, AKT inhibitors, demethylases, and acetyltransferase, researchers target carcinogenic SEs to inhibit cancer growth, invasion, immune escape and progression (121).

Although remarkable process has been made in revealing the regulation of immune checkpoint expression and eRNA function, many questions and challenges remain. For instance, the exact function and mechanism of seRNAs have not been clearly demonstrated. Additional and direct evidence of seRNA function in immune checkpoint expression is required to further support the indirect gene regulation effect by seRNAs. Recent findings also revealed that the exact boundaries between eRNAs and lncRNAs are not absolute, suggesting that some eRNAs might have been mistakenly identified as lncRNAs (28). Despite having a similar frequency of transcription to protein-coding genes, eRNAs have a shorter half-life compared with that of mRNAs and lncRNAs, which represents an obstacle for their thorough study (122). Such characteristics and uncertainty of seRNA make research into the interaction between seRNAs and TFs or chromatin a challenge. Joint efforts should be made by biologists and immunologists to further identify the correlations between SEs, seRNAs, and immune checkpoints. We are only starting to comprehend the full panoply of eRNAs' functions. In the future, a thorough understanding of the mechanism by which seRNAs regulate gene expression and their contribution to disease pathogenesis might help to identify new therapeutic targets and disease biomarkers.

AUTHOR CONTRIBUTIONS

All authors listed have made a substantial, direct and intellectual contribution to the work, and approved it for publication.

FUNDING

This work was supported by grants from National Natural Science Foundation of China (No. 81770545), and by MDT Project of Clinical Research Innovation Foundation, Renji Hospital, School of Medicine, Shanghai Jiao Tong University (PYI-17-003).

ACKNOWLEDGMENTS

We acknowledge support from National Natural Science Foundation of China and Renji Hospital, School of Medicine, Shanghai Jiao Tong University.

REFERENCES

1. International Human Genome Sequencing C. Finishing the euchromatic sequence of the human genome. *Nature.* (2004) 431:931–45. doi: 10.1038/nature03001
2. Hnisz D, Abraham BJ, Lee TI, Lau A, Saint-Andre V, Sigova AA, et al. Super-enhancers in the control of cell identity and disease. *Cell.* (2013) 155:934–47. doi: 10.1016/j.cell.2013.09.053
3. Chen L, Toke NH, Luo S, Vasoya RP, Fullem RL, Parthasarathy A, et al. A reinforcing HNF4-SMAD4 feed-forward module stabilizes enterocyte identity. *Nat Genet.* (2019) 51:777–85. doi: 10.1038/s41588-019-0384-0
4. Li X, Zheng Y. Regulatory T cell identity: formation and maintenance. *Trends Immunol.* (2015) 36:344–53. doi: 10.1016/j.it.2015.04.006
5. Di Micco R, Fontanals-Cirera B, Low V, Ntziachristos P, Yuen Stephanie K, Lovell Claudia D, et al. Control of embryonic stem cell identity by BRD4-dependent transcriptional elongation of super-enhancer-associated pluripotency genes. *Cell Rep.* (2014) 9:234–47. doi: 10.1016/j.celrep.2014.08.055
6. Struhl K. Transcriptional noise and the fidelity of initiation by RNA polymerase II. *Nat Struct Mol Biol.* (2007) 14:103–5. doi: 10.1038/nsmb0207-103
7. Spurlock CF III, Shaginurova G, Tossberg JT, Hester JD, Chapman N, Guo Y, et al. Profiles of long noncoding RNAs in human naive and memory T cells. *J Immunol.* (2017) 199:547–58. doi: 10.4049/jimmunol.1700232
8. Hsieh CL, Fei T, Chen Y, Li T, Gao Y, Wang X, et al. Enhancer RNAs participate in androgen receptor-driven looping that selectively enhances gene activation. *Proc Natl Acad Sci USA.* (2014) 111:7319–24. doi: 10.1073/pnas.1324151111
9. Mousavi K, Zare H, Dell'orso S, Grontved L, Gutierrez-Cruz G, Derfoul A, et al. eRNAs promote transcription by establishing chromatin accessibility at defined genomic loci. *Mol Cell.* (2013) 51:606–17. doi: 10.1016/j.molcel.2013.07.022
10. Lai F, Orom UA, Cesaroni M, Beringer M, Taatjes DJ, Blobel GA, et al. Activating RNAs associate with Mediator to enhance chromatin architecture and transcription. *Nature.* (2013) 494:497–501. doi: 10.1038/nature11884
11. Schaukowitch K, Joo JY, Liu X, Watts JK, Martinez C, Kim TK. Enhancer RNA facilitates NELF release from immediate early genes. *Mol Cell.* (2014) 56:29–42. doi: 10.1016/j.molcel.2014.08.023
12. Bose DA, Donahue G, Reinberg D, Shiekhattar R, Bonasio R, Berger SL. RNA binding to CBP stimulates histone acetylation and transcription. *Cell* 168:135–49.e122. doi: 10.1016/j.cell.2016.12.020
13. Alsaab HO, Sau S, Alzhrani R, Tatiparti K, Bhise K, Kashaw SK, et al. PD-1 and PD-L1 checkpoint signaling inhibition for cancer immunotherapy: mechanism, combinations, and clinical outcome. *Front Pharmacol.* (2017) 8:561. doi: 10.3389/fphar.2017.00561
14. Pardoll DM. The blockade of immune checkpoints in cancer immunotherapy. *Nat Rev Cancer.* (2012) 12:252–64. doi: 10.1038/nrc3239

15. Rhie SK, Guo Y, Tak YG, Yao L, Shen H, Coetzee GA, et al. Identification of activated enhancers and linked transcription factors in breast, prostate, and kidney tumors by tracing enhancer networks using epigenetic traits. *Epigenet Chrom.* (2016) 9:50. doi: 10.1186/s13072-016-0102-4
16. Hanahan D, Weinberg RA. Hallmarks of cancer: the next generation. *Cell.* (2011) 144:646–74. doi: 10.1016/j.cell.2011.02.013
17. Rada-Iglesias A, Bajpai R, Swigut T, Brugmann SA, Flynn RA, Wysocka J. A unique chromatin signature uncovers early developmental enhancers in humans. *Nature.* (2011) 470:279–83. doi: 10.1038/nature09692
18. Creyghton MP, Cheng AW, Welstead GG, Kooistra T, Carey BW, Steine EJ, et al. Histone H3K27ac separates active from poised enhancers and predicts developmental state. *Proc Natl Acad Sci USA.* (2010) 107:21931–6. doi: 10.1073/pnas.1016071107
19. Ogryzko VV, Schiltz RL, Russanova V, Howard BH, Nakatani Y. The transcriptional coactivators p300 and CBP are histone acetyltransferases. *Cell.* (1996) 87:953–9 doi: 10.1016/S0092-8674(00)82001-2
20. Whyte WA, Orlando DA, Hnisz D, Abraham BJ, Lin CY, Kagey MH, et al. Master transcription factors and mediator establish super-enhancers at key cell identity genes. *Cell.* (2013) 153:307–19. doi: 10.1016/j.cell.2013.03.035
21. Kagey MH, Newman JJ, Bilodeau S, Zhan Y, Orlando DA, van Berkum NL, et al. Mediator and cohesin connect gene expression and chromatin architecture. *Nature.* (2010) 467:430–5. doi: 10.1038/nature09380
22. May D, Blow MJ, Kaplan T, McCulley DJ, Jensen BC, Akiyama JA, et al. Large-scale discovery of enhancers from human heart tissue. *Nat Genet.* (2011) 44:89–93. doi: 10.1038/ng.1006
23. Sigova AA, Abraham BJ, Ji X, Molinie B, Hannett NM, Guo YE, et al. Transcription factor trapping by RNA in gene regulatory elements. *Science.* (2015) 350:978–81. doi: 10.1126/science.aad3346
24. Heintzman ND, Stuart RK, Hon G, Fu Y, Ching CW, Hawkins RD, et al. Distinct and predictive chromatin signatures of transcriptional promoters and enhancers in the human genome. *Nat Genet.* (2007) 39:311–8. doi: 10.1038/ng1966
25. Alvarez-Dominguez JR, Knoll M, Gromatzky AA, Lodish HF. The super-enhancer-derived alncRNA-EC7/bloodlinc potentiates red blood cell development in trans. *Cell Rep.* (2017) 19:2503–14. doi: 10.1016/j.celrep.2017.05.082
26. Lam MT, Li W, Rosenfeld MG, Glass CK. Enhancer RNAs and regulated transcriptional programs. *Trends Biochem Sci.* (2014) 39:170–82. doi: 10.1016/j.tibs.2014.02.007
27. Kim TK, Hemberg M, Gray JM, Costa AM, Bear DM, Wu J, et al. Widespread transcription at neuronal activity-regulated enhancers. *Nature.* (2010) 465:182–7. doi: 10.1038/nature09033
28. Espinosa JM. Revisiting lncRNAs: how do you know yours is not an eRNA? *Mol Cell.* (2016) 62:1–2. doi: 10.1016/j.molcel.2016.03.022
29. Nicholas NE II, Heward JA, Roux B, Tsitsiou E, Fenwick PS, Lenzi L, et al. Long non-coding RNAs and enhancer RNAs regulate the lipopolysaccharide-induced inflammatory response in human monocytes. *Nat Comm.* (2014) 5:3979. doi: 10.1038/ncomms4979
30. Ren C, Liu F, Ouyang Z, An G, Zhao C, Shuai J, et al. Functional annotation of structural ncRNAs within enhancer RNAs in the human genome: implications for human disease. *Sci Rep.* (2017) 7:15518. doi: 10.1038/s41598-017-15822-7
31. Blinka S, Reimer MH Jr, Pulakanti K, Rao S. Super-enhancers at the nanog locus differentially regulate neighboring pluripotency-associated genes. *Cell Rep.* (2016) 17:19–28. doi: 10.1016/j.celrep.2016.09.002
32. Cichewicz MA, Kiran M, Przanowska RK, Sobierajska E, Shibata Y, Dutta A. MUNC, an eRNA upstream from the MYOD gene, induces a subgroup of myogenic transcripts in trans, independently of MyoD. *Mol Cell Biol.* (2018) 38:e00655–17. doi: 10.1128/MCB.00655-17.
33. Li W, Notani D, Ma Q, Tanasa B, Nunez E, Chen AY, et al. Functional roles of enhancer RNAs for oestrogen-dependent transcriptional activation. *Nature.* (2013) 498:516–20. doi: 10.1038/nature12210
34. Bose DA, Berger SL. eRNA binding produces tailored CBP activity profiles to regulate gene expression. *RNA Biol.* (2017) 14:1655–9. doi: 10.1080/15476286.2017.1353862
35. Hah N, Benner C, Chong LW, Yu RT, Downes M, Evans RM. Inflammation-sensitive super enhancers form domains of coordinately regulated enhancer RNAs. *Proc Natl Acad Sci USA.* (2015) 112:E297–302. doi: 10.1073/pnas.1424028112
36. Weintraub AS, Li CH, Zamudio AV, Sigova AA, Hannett NM, Day DS, et al. YY1 is a structural regulator of enhancer-promoter loops. *Cell.* (2017) 171:1573–88.e1528. doi: 10.1016/j.cell.2017.11.008
37. Sanyal A, Lajoie BR, Jain G, Dekker J. The long-range interaction landscape of gene promoters. *Nature.* (2012) 489:109–13. doi: 10.1038/nature11279
38. Deng W, Lee J, Wang H, Miller J, Reik A, Gregory PD, et al. Controlling long-range genomic interactions at a native locus by targeted tethering of a looping factor. *Cell.* (2012) 149:1233–44. doi: 10.1016/j.cell.2012.03.051
39. Jiao W, Chen Y, Song H, Li D, Mei H, Yang F, et al. HPSE enhancer RNA promotes cancer progression through driving chromatin looping and regulating hnRNPU/p300/EGR1/HPSE axis. *Oncogene.* (2018) 37:2728–45. doi: 10.1038/s41388-018-0128-0
40. Pnueli L, Rudnizky S, Yosefzon Y, Melamed P. RNA transcribed from a distal enhancer is required for activating the chromatin at the promoter of the gonadotropin alpha-subunit gene. *Proc Natl Acad Sci USA.* (2015) 112:4369–74. doi: 10.1073/pnas.1414841112
41. Maruyama A, Mimura J, Itoh K. Non-coding RNA derived from the region adjacent to the human HO-1 E2 enhancer selectively regulates HO-1 gene induction by modulating Pol II binding. *Nucleic Acids Res.* (2014) 42:13599–614. doi: 10.1093/nar/gku1169
42. Ounzain S, Micheletti R, Arnan C, Plaisance I, Cecchi D, Schroen B, et al. CARMEN, a human super enhancer-associated long noncoding RNA controlling cardiac specification, differentiation and homeostasis. *J Mol Cell Cardiol.* (2015) 89(Pt A):98–112. doi: 10.1016/j.yjmcc.2015.09.016
43. Feng J, Bi C, Clark BS, Mady R, Shah P, Kohtz JD. The Evf-2 noncoding RNA is transcribed from the Dlx-5/6 ultraconserved region and functions as a Dlx-2 transcriptional coactivator. *Genes Dev.* (2006) 20:1470–84. doi: 10.1101/gad.1416106
44. Loven J, Hoke HA, Lin CY, Lau A, Orlando DA, Vakoc CR, et al. Selective inhibition of tumor oncogenes by disruption of super-enhancers. *Cell.* (2013) 153:320–34. doi: 10.1016/j.cell.2013.03.036
45. Melo CA, Drost J, Wijchers PJ, van de Werken H, de Wit E, Oude Vrielink JA, et al. eRNAs are required for p53-dependent enhancer activity and gene transcription. *Mol Cell.* (2013) 49:524–35. doi: 10.1016/j.molcel.2012.11.021
46. Crespo J, Sun H, Welling TH, Tian Z, Zou W. T cell anergy, exhaustion, senescence, and stemness in the tumor microenvironment. *Curr Opin Immunol.* (2013) 25:214–21. doi: 10.1016/j.coi.2012.12.003
47. Zou W, Chen L. Inhibitory B7-family molecules in the tumour microenvironment. *Nat Rev Immunol.* (2008) 8:467–77. doi: 10.1038/nri2326
48. Zamani MR, Aslani S, Salmaninejad A, Javan MR, Rezaei N. PD-1/PD-L and autoimmunity: a growing relationship. *Cell Immunol.* (2016) 310:27–41. doi: 10.1016/j.cellimm.2016.09.009
49. Olde Nordkamp MJ, Koeleman BP, Meyaard L. Do inhibitory immune receptors play a role in the etiology of autoimmune disease? *Clin Immunol.* (2014) 150:31–42. doi: 10.1016/j.clim.2013.11.007
50. Waterhouse P, Penninger JM, Timms E, Wakeham A, Shahinian A, Lee KP, et al. Lymphoproliferative disorders with early lethality in mice deficient in Ctla-4. *Science.* (1995) 270:985–8. doi: 10.1126/science.270.5238.985
51. Kuehn HS, Ouyang W, Lo B, Deenick EK, Niemela JE, Avery DT, et al. Immune dysregulation in human subjects with heterozygous germline mutations in CTLA4. *Science.* (2014) 345:1623–7. doi: 10.1126/science.1255904
52. Jury EC, Flores-Borja F, Kalsi HS, Lazarus M, Isenberg DA, Mauri C, et al. Abnormal CTLA-4 function in T cells from patients with systemic lupus erythematosus. *Eur J Immunol.* (2010) 40:569–78. doi: 10.1002/eji.200939781
53. Siakavellas SI, Bamias G. Checkpoint inhibitor colitis: a new model of inflammatory bowel disease? *Curr Opin Gastroenterol.* (2018) 34:377–83. doi: 10.1097/MOG.0000000000000482
54. Dougan M. Checkpoint blockade toxicity and immune homeostasis in the gastrointestinal tract. *Front Immunol.* (2017) 8:1547. doi: 10.3389/fimmu.2017.01547
55. Makarious D, Horwood K, Coward JIG. Myasthenia gravis: an emerging toxicity of immune checkpoint inhibitors. *Eur J Cancer.* (2017) 82:128–36. doi: 10.1016/j.ejca.2017.05.041
56. Abdel-Wahab N, Shah M, Suarez-Almazor ME. Adverse events associated with immune checkpoint blockade in patients with

cancer: a systematic review of case reports. *PLoS ONE.* (2016) 11:e0160221. doi: 10.1371/journal.pone.0160221
57. Johnson DB, Sullivan RJ, Ott PA, Carlino MS, Khushalani NI, Ye F, et al. Ipilimumab therapy in patients with advanced melanoma and preexisting autoimmune disorders. *JAMA Oncol.* (2016) 2:234–40. doi: 10.1001/jamaoncol.2015.4368
58. Blair HA, Deeks ED. Abatacept: a review in rheumatoid arthritis. *Drugs.* (2017) 77:1221–33. doi: 10.1007/s40265-017-0775-4
59. Pimentel-Quiroz VR, Ugarte-Gil MF, Alarcon GS. Abatacept for the treatment of systemic lupus erythematosus. *Expert Opin Invest Drugs.* (2016) 25:493–9. doi: 10.1517/13543784.2016.1154943
60. Mease PJ, Gottlieb AB, van der Heijde D, FitzGerald O, Johnsen A, Nys M, et al. Efficacy and safety of abatacept, a T-cell modulator, in a randomised, double-blind, placebo-controlled, phase III study in psoriatic arthritis. *Ann Rheum Dis.* (2017) 76:1550–8. doi: 10.1136/annrheumdis-2016-210724
61. Granier C, De Guillebon E, Blanc C, Roussel H, Badoual C, Colin E, et al. Mechanisms of action and rationale for the use of checkpoint inhibitors in cancer. *ESMO Open.* (2017) 2:e000213. doi: 10.1136/esmoopen-2017-000213
62. Choueiri TK, Fishman MN, Escudier B, McDermott DF, Drake CG, Kluger H, et al. Immunomodulatory activity of nivolumab in metastatic renal cell carcinoma. *Clin Cancer Res.* (2016) 22:5461–71. doi: 10.1158/1078-0432.CCR-15-2839
63. Chang CH, Qiu J, O'Sullivan D, Buck MD, Noguchi T, Curtis JD, et al. Metabolic competition in the tumor microenvironment is a driver of cancer progression. *Cell.* (2015) 162:1229–41. doi: 10.1016/j.cell.2015.08.016
64. Ostrand-Rosenberg S, Horn LA, Haile ST. The programmed death-1 immune-suppressive pathway: barrier to antitumor immunity. *J Immunol.* (2014) 193:3835–41. doi: 10.4049/jimmunol.1401572
65. Wei SC, Duffy CR, Allison JP. Fundamental mechanisms of immune checkpoint blockade therapy. *Cancer Disc.* (2018) 8:1069–86. doi: 10.1158/2159-8290.CD-18-0367
66. Abril-Rodriguez G, Ribas A. SnapShot: immune checkpoint inhibitors. *Cancer Cell.* (2017) 31:848–e841. doi: 10.1016/j.ccell.2017.05.010
67. Butte MJ, Keir ME, Phamduy TB, Sharpe AH, Freeman GJ. Programmed death-1 ligand 1 interacts specifically with the B7-1 costimulatory molecule to inhibit T cell responses. *Immunity.* (2007) 27:111–22. doi: 10.1016/j.immuni.2007.05.016
68. Clark CA, Gupta HB, Sareddy G, Pandeswara S, Lao S, Yuan B, et al. Tumor-Intrinsic PD-L1 signals regulate cell growth, pathogenesis, and autophagy in ovarian cancer and melanoma. *Cancer Res.* (2016) 76:6964–74. doi: 10.1158/0008-5472.CAN-16-0258
69. Kortlever RM, Sodir NM, Wilson CH, Burkhart DL, Pellegrinet L, Brown Swigart L, et al. Myc cooperates with ras by programming inflammation and immune suppression. *Cell.* (2017) 171:1301–15.e1314. doi: 10.1016/j.cell.2017.11.013
70. Parry RV, Chemnitz JM, Frauwirth KA, Lanfranco AR, Braunstein I, Kobayashi SV, et al. CTLA-4 and PD-1 receptors inhibit T-cell activation by distinct mechanisms. *Mol Cell Biol.* (2005) 25:9543–53. doi: 10.1128/MCB.25.21.9543-9553.2005
71. Kim ES, Kim JE, Patel MA, Mangraviti A, Ruzevick J, Lim M. Immune checkpoint modulators: an emerging antiglioma armamentarium. *J Immunol Res.* (2016) 2016:4683607. doi: 10.1155/2016/4683607
72. Robert L, Tsoi J, Wang X, Emerson R, Homet B, Chodon T, et al. CTLA4 blockade broadens the peripheral T-cell receptor repertoire. *Clin Cancer Res.* (2014) 20:2424–32. doi: 10.1158/1078-0432.CCR-13-2648
73. Arasanz H, Gato-Canas M, Zuazo M, Ibanez-Vea M, Breckpot K, Kochan G, et al. PD1 signal transduction pathways in T cells. *Oncotarget.* (2017) 8:51936–45. doi: 10.18632/oncotarget.17232
74. Seidel JA, Otsuka A, Kabashima K. Anti-PD-1 and Anti-CTLA-4 therapies in cancer: mechanisms of action, efficacy, and limitations. *Front Oncol.* (2018) 8:86. doi: 10.3389/fonc.2018.00086
75. Zou W, Wolchok JD, Chen L. PD-L1. (B7-H1). and PD-1 pathway blockade for cancer therapy: mechanisms, response biomarkers, and combinations. *Sci Transl Med.* (2016) 8:328rv324. doi: 10.1126/scitranslmed.aad7118
76. Ding M, Liu Y, Li J, Yao L, Liao X, Xie H, et al. Oestrogen promotes tumorigenesis of bladder cancer by inducing the enhancer RNA-eGREB1. *J Cell Mol Med.* (2018) 22:5919–27. doi: 10.1111/jcmm.13861
77. Wong RWJ, Ngoc PCT, Leong WZ, Yam AWY, Zhang T, Asamitsu K, et al. Enhancer profiling identifies critical cancer genes and characterizes cell identity in adult T-cell leukemia. *Blood.* (2017) 130:2326–38. doi: 10.1182/blood-2017-06-792184
78. Cotterman R, Jin VX, Krig SR, Lemen JM, Wey A, Farnham PJ, et al. N-Myc regulates a widespread euchromatic program in the human genome partially independent of its role as a classical transcription factor. *Cancer Res.* (2008) 68:9654–62. doi: 10.1158/0008-5472.CAN-08-1961
79. Kim EY, Kim A, Kim SK, Chang YS. MYC expression correlates with PD-L1 expression in non-small cell lung cancer. *Lung Cancer.* (2017) 110:63–7. doi: 10.1016/j.lungcan.2017.06.006
80. Casey SC, Tong L, Li Y, Do R, Walz S, Fitzgerald KN, et al. MYC regulates the antitumor immune response through CD47 and PD-L1. *Science.* (2016) 352:227–31. doi: 10.1126/science.aac9935
81. Ahmadiyeh N, Pomerantz MM, Grisanzio C, Herman P, Jia L, Almendro V, et al. 8q24 prostate, breast, and colon cancer risk loci show tissue-specific long-range interaction with MYC. *Proc Natl Acad Sci USA.* (2010) 107:9742–6. doi: 10.1073/pnas.0910668107
82. Xiang JF, Yin QF, Chen T, Zhang Y, Zhang XO, Wu Z, et al. Human colorectal cancer-specific CCAT1-L lncRNA regulates long-range chromatin interactions at the MYC locus. *Cell Res.* (2014) 24:513–31. doi: 10.1038/cr.2014.35
83. Pomerantz MM, Ahmadiyeh N, Jia L, Herman P, Verzi MP, Doddapaneni H, et al. The 8q24 cancer risk variant rs6983267 shows long-range interaction with MYC in colorectal cancer. *Nat Genet.* (2009) 41:882–4. doi: 10.1038/ng.403
84. Jiang Y, Jiang YY, Xie JJ, Mayakonda A, Hazawa M, Chen L, et al. Co-activation of super-enhancer-driven CCAT1 by TP63 and SOX2 promotes squamous cancer progression. *Nat Commun.* (2018) 9:3619. doi: 10.1038/s41467-018-06081-9
85. Zhang W, Pang Q, Yan C, Wang Q, Yang J, Yu S, et al. Induction of PD-L1 expression by epidermal growth factor receptor-mediated signaling in esophageal squamous cell carcinoma. *OncoTargets Ther.* (2017) 10:763–71. doi: 10.2147/OTT.S118982
86. Akbay EA, Koyama S, Carretero J, Altabef A, Tchaicha JH, Christensen CL, et al. Activation of the PD-1 pathway contributes to immune escape in EGFR-driven lung tumors. *Cancer Disc.* (2013) 3:1355–63. doi: 10.1158/2159-8290.CD-13-0310
87. Tang Y, Fang W, Zhang Y, Hong S, Kang S, Yan Y, et al. The association between PD-L1 and EGFR status and the prognostic value of PD-L1 in advanced non-small cell lung cancer patients treated with EGFR-TKIs. *Oncotarget.* (2015) 6:14209–19. doi: 10.18632/oncotarget.3694
88. Azuma K, Ota K, Kawahara A, Hattori S, Iwama E, Harada T, et al. Association of PD-L1 overexpression with activating EGFR mutations in surgically resected nonsmall-cell lung cancer. *Ann Oncol.* (2014) 25:1935–40. doi: 10.1093/annonc/mdu242
89. Okita R, Maeda A, Shimizu K, Nojima Y, Saisho S, Nakata M. PD-L1 overexpression is partially regulated by EGFR/HER2 signaling and associated with poor prognosis in patients with non-small-cell lung cancer. *Cancer Immunol Immunother.* (2017) 66:865–76. doi: 10.1007/s00262-017-1986-y
90. Ota K, Azuma K, Kawahara A, Hattori S, Iwama E, Tanizaki J, et al. Induction of PD-L1 expression by the EML4-ALK oncoprotein and downstream signaling pathways in non-small cell lung cancer. *Clin Cancer Res.* (2015) 21:4014–21. doi: 10.1158/1078-0432.CCR-15-0016
91. Chipumuro E, Marco E, Christensen CL, Kwiatkowski N, Zhang T, Hatheway CM, et al. CDK7 inhibition suppresses super-enhancer-linked oncogenic transcription in MYCN-driven cancer. *Cell.* (2014) 159:1126–39. doi: 10.1016/j.cell.2014.10.024
92. Chen CH, Yang N, Zhang Y, Ding J, Zhang W, Liu R, et al. Inhibition of super enhancer downregulates the expression of KLF5 in basal-like breast cancers. *Int J Biol Sci.* (2019) 15:1733–42. doi: 10.7150/ijbs.35138
93. Rasool RU, Natesan R, Deng Q, Aras S, Lal P, Sander Effron S, et al. CDK7 inhibition suppresses castration-resistant prostate cancer through MED1 inactivation. *Cancer Disc.* (2019) 9:1538–55. doi: 10.1158/2159-8290.CD-19-0189
94. Dawson MA, Prinjha RK, Dittmann A, Giotopoulos G, Bantscheff M, Chan WI, Inhibition of BET recruitment to chromatin as an

effective treatment for MLL-fusion leukaemia. *Nature.* (2011) 478:529–33. doi: 10.1038/nature10509
95. Delmore JE, Issa GC, Lemieux ME, Rahl PB, Shi J, Jacobs HM, et al. BET bromodomain inhibition as a therapeutic strategy to target c-Myc. *Cell.* (2011) 146:904–17. doi: 10.1016/j.cell.2011.08.017
96. Da Costa D, Agathanggelou A, Perry T, Weston V, Petermann E, Zlatanou A, et al. BET inhibition as a single or combined therapeutic approach in primary paediatric B-precursor acute lymphoblastic leukaemia. *Blood Cancer J.* (2013) 3:e126. doi: 10.1038/bcj.2013.24
97. Chiang CM. Brd4 engagement from chromatin targeting to transcriptional regulation: selective contact with acetylated histone H3 and H4. *F1000 Biol Rep.* (2009) 1:98. doi: 10.3410/B1-98
98. Wu SY, Chiang CM. The double bromodomain-containing chromatin adaptor Brd4 and transcriptional regulation. *J Biol Chem.* (2007) 282:13141–5. doi: 10.1074/jbc.R700001200
99. Kanno T, Kanno Y, LeRoy G, Campos E, Sun HW, Brooks SR, et al. BRD4 assists elongation of both coding and enhancer RNAs by interacting with acetylated histones. *Nat Struct Mol Biol.* (2014) 21:1047–57. doi: 10.1038/nsmb.2912
100. Zhu H, Bengsch F, Svoronos N, Rutkowski MR, Bitler BG, Allegrezza MJ, et al. BET bromodomain inhibition promotes anti-tumor immunity by suppressing PD-L1 expression. *Cell Rep.* (2016) 16:2829–37. doi: 10.1016/j.celrep.2016.08.032
101. Yokoyama Y, Zhu H, Lee JH, Kossenkov AV, Wu SY, Wickramasinghe JM, et al. BET inhibitors suppress ALDH activity by targeting ALDH1A1 super-enhancer in ovarian cancer. *Cancer Res.* (2016) 76:6320–30. doi: 10.1158/0008-5472.CAN-16-0854
102. Doroshow DB, Eder JP, LoRusso PM. BET inhibitors: a novel epigenetic approach. *Ann Oncol.* (2017) 28:1776–87. doi: 10.1093/annonc/mdx157
103. Hogg SJ, Vervoort SJ, Deswal S, Ott CJ, Li J, Cluse LA, et al. BET-bromodomain inhibitors engage the host immune system and regulate expression of the immune checkpoint ligand PD-L1. *Cell Rep.* (2017) 18:2162–74. doi: 10.1016/j.celrep.2017.02.011
104. Rahnamoun H, Lee J, Sun Z, Lu H, Ramsey KM, Komives EA, et al. RNAs interact with BRD4 to promote enhanced chromatin engagement and transcription activation. *Nat Struct Mol Biol.* (2018) 25:687–97. doi: 10.1038/s41594-018-0102-0
105. Peeters JG, Vervoort SJ, Tan SC, Mijnheer G, de Roock S, Vastert SJ, et al. Inhibition of super-enhancer activity in autoinflammatory site-derived T cells reduces disease-associated gene expression. *Cell Rep.* (2015) 12:1986–96. doi: 10.1016/j.celrep.2015.08.046
106. Shi L, Li S, Maurer K, Zhang Z, Petri M, Sullivan KE. Enhancer RNA and NFkappaB-dependent P300 regulation of ADAMDEC1. *Mol Immunol.* (2018) 103:312–21. doi: 10.1016/j.molimm.2018.09.019
107. Prokunina L, Castillejo-López C, Oberg F, Gunnarsson I, Berg L, Magnusson V, et al. A regulatory polymorphism in PDCD1 is associated with susceptibility to systemic lupus erythematosus in humans. *Nat Genet.* (2002) 32:666–9. doi: 10.1038/ng1020
108. Aune TM, Crooke PS III, Patrick AE, Tossberg JT, Olsen NJ, Spurlock CF III. Expression of long non-coding RNAs in autoimmunity and linkage to enhancer function and autoimmune disease risk genetic variants. *J Autoimm.* (2017). 81:99–109. doi: 10.1016/j.jaut.2017.03.014
109. Lu M, McComish BJ, Burdon KP, Taylor BV, Korner H. The association between vitamin d and multiple sclerosis risk: 1,25. (OH)2D3 induces super-enhancers bound by VDR. *Front Immunol.* (2019) 10:488. doi: 10.3389/fimmu.2019.00488
110. Hertweck A, Evans CM, Eskandarpour M, Lau JC, Oleinika K, Jackson I, et al. T-bet activates Th1 genes through mediator and the super elongation complex. *Cell Rep.* (2016) 15:2756–70. doi: 10.1016/j.celrep.2016.05.054
111. Farh KK, Marson A, Zhu J, Kleinewietfeld M, Housley WJ, Beik S, et al. Genetic and epigenetic fine mapping of causal autoimmune disease variants. *Nature.* (2015) 518:337–43. doi: 10.1038/nature13835
112. Vahedi G, Kanno Y, Furumoto Y, Jiang K, Parker SC, Erdos MR, et al. Super-enhancers delineate disease-associated regulatory nodes in T cells. *Nature.* (2015) 520:558–62. doi: 10.1038/nature14154
113. Afzali B, Gronholm J, Vandrovcova J, O'Brien C, Sun HW, Vanderleyden I, et al. BACH2 immunodeficiency illustrates an association between super-enhancers and haploinsufficiency. *Nat Immunol.* (2017) 18:813–23. doi: 10.1038/ni.3753
114. McAllister K, Yarwood A, Bowes J, Orozco G, Viatte S, Diogo D, et al. Identification of BACH2 and RAD51B as rheumatoid arthritis susceptibility loci in a meta-analysis of genome-wide data. *Arthr Rheum.* (2013) 65:3058–62. doi: 10.1002/art.38183
115. Franke A, McGovern DP, Barrett JC, Wang K, Radford-Smith GL, Ahmad T, et al. Genome-wide meta-analysis increases to 71 the number of confirmed Crohn's disease susceptibility loci. *Nat Genet.* (2010) 42:1118–25. doi: 10.1038/ng.717
116. Cooper JD, Smyth DJ, Smiles AM, Plagnol V, Walker NM, Allen JE, et al. Meta-analysis of genome-wide association study data identifies additional type 1 diabetes risk loci. *Nat Genet.* (2008) 40:1399–401. doi: 10.1038/ng.249
117. Roychoudhuri R, Eil RL, Clever D, Klebanoff CA, Sukumar M, Grant FM, et al. The transcription factor BACH2 promotes tumor immunosuppression. *J Clin Invest.* (2016) 126:599–604. doi: 10.1172/JCI82884
118. Garcia-Diaz A, Shin DS, Moreno BH, Saco J, Escuin-Ordinas H, Rodriguez GA, et al. Interferon receptor signaling pathways regulating PD-L1 and PD-L2 expression. *Cell Rep.* (2017) 19:1189–201. doi: 10.1016/j.celrep.2017.04.031
119. Osum KC, Burrack AL, Martinov T, Sahli NL, Mitchell JS, Tucker CG, et al. Interferon-gamma drives programmed death-ligand 1 expression on islet beta cells to limit T cell function during autoimmune diabetes. *Sci Rep.* (2018) 8:8295. doi: 10.1038/s41598-018-26471-9
120. Zhang J, Liu S, Ye Q, Pan J. Transcriptional inhibition by CDK7/9 inhibitor SNS-032 abrogates oncogene addiction and reduces liver metastasis in uveal melanoma. *Mol Cancer.* (2019) 18:140. doi: 10.1186/s12943-019-1070-7
121. Zhang Z, Lee JH, Ruan H, Ye Y, Krakowiak J, Hu Q, et al. Transcriptional landscape and clinical utility of enhancer RNAs for eRNA-targeted therapy in cancer. *Nat Commun.* (2019) 10:4562. doi: 10.1038/s41467-019-12543-5
122. Lam MT, Cho H, Lesch HP, Gosselin D, Heinz S, Tanaka-Oishi Y, et al. Rev-Erbs repress macrophage gene expression by inhibiting enhancer-directed transcription. *Nature.* (2013) 498:511–5. doi: 10.1038/nature12209

Conflict of Interest: The authors declare that the research was conducted in the absence of any commercial or financial relationships that could be construed as a potential conflict of interest.

frontiers in Oncology

ORIGINAL RESEARCH
published: 27 November 2019
doi: 10.3389/fonc.2019.01305

Expanding the Transcriptome of Head and Neck Squamous Cell Carcinoma Through Novel MicroRNA Discovery

Leigha D. Rock[1,2,3,4], Brenda C. Minatel[3], Erin A. Marshall[3], Florian Guisier[3,5], Adam P. Sage[3], Mateus Camargo Barros-Filho[3,6], Greg L. Stewart[3], Cathie Garnis[3] and Wan L. Lam[3]*

[1] Department of Cancer Control Research, British Columbia Cancer Research Centre, Vancouver, BC, Canada, [2] Faculty of Dentistry, University of British Columbia, Vancouver, BC, Canada, [3] Department of Integrative Oncology, British Columbia Cancer Research Centre, Vancouver, BC, Canada, [4] Faculty of Dentistry, Dalhousie University, Halifax, NS, Canada, [5] Department of Pulmonology and CIC-CRB 1404, Rouen University Hospital, Rouen, France, [6] International Research Center—A.C.Camargo Cancer Center, São Paulo, Brazil

OPEN ACCESS

Edited by:
Luisa Lanfrancone, European Institute of Oncology (IEO), Italy

Reviewed by:
Luigi Fattore, Sapienza University of Rome, Italy
Marco Sciacovelli, University of Cambridge, United Kingdom

***Correspondence:**
Leigha D. Rock
leigha.rock@dal.ca

Specialty section:
This article was submitted to Molecular and Cellular Oncology, a section of the journal Frontiers in Oncology

Received: *12 July 2019*
Accepted: *11 November 2019*
Published: *27 November 2019*

Citation:
Rock LD, Minatel BC, Marshall EA, Guisier F, Sage AP, Barros-Filho MC, Stewart GL, Garnis C and Lam WL (2019) Expanding the Transcriptome of Head and Neck Squamous Cell Carcinoma Through Novel MicroRNA Discovery. Front. Oncol. 9:1305. doi: 10.3389/fonc.2019.01305

Head and neck squamous cell carcinoma (HNSCC) has a poor survival rate mainly due to late stage diagnosis and recurrence. Despite genomic efforts to identify driver mutations and changes in protein-coding gene expression, developing effective diagnostic and prognostic biomarkers remains a priority to guide disease management and improve patient outcome. Recent reports of previously-unannotated microRNAs (miRNAs) from multiple somatic tissues have raised the possibility of HNSCC-specific miRNAs. In this study, we applied a customized *in-silico* analysis pipeline to identify novel miRNAs from raw small-RNA sequencing datasets from public repositories. We discovered 146 previously-unannotated sequences expressed in head and neck samples that share structural properties highly characteristic of miRNAs. The combined expression of the novel miRNAs revealed tissue and context-specific patterns. Furthermore, comparison of tumor with non-malignant tissue samples ($n = 43$ pairs) revealed 135 of these miRNAs as differentially expressed, most of which were overexpressed or exclusively found in tumor samples. Additionally, a subset of novel miRNAs was significantly associated with HPV infection status and patient outcome. A prognostic-model combining novel and known miRNA was developed (multivariate Cox regression analysis) leading to an improved death and relapse risk stratification (log rank $p < 1e\text{-}7$). The presence of these miRNAs was corroborated both in an independent dataset and by RT-qPCR analysis, supporting their potential involvement in HNSCC. In this study, we report the discovery of 146 novel miRNAs in head and neck tissues and demonstrate their potential biological significance and clinical relevance to head and neck cancer, providing a new resource for the study of HNSCC.

Keywords: microRNAs, non-coding RNA, gene expression profiling, head and neck cancer, computational biology

INTRODUCTION

Head and neck squamous cell carcinoma (HNSCC) is the eighth most common cancer worldwide (1) and has a poor survival rate, mainly due to late stage diagnosis, and frequent disease recurrence (2). Despite advances in surgical techniques, chemotherapy, radiation therapy, and targeted therapy, the 5-years survival rate of patients remains at 50% (3). Hence there is a need to expand the repertoire of head and neck specific diagnostic and prognostic biomarkers. Furthermore, in order to improve patient outcome a better understanding of the genetic and epigenetic events associated with disease progression are needed.

MicroRNAs (miRNAs) are a class of single-stranded small non-coding RNAs (sncRNAs) ∼21–23 nucleotides in length, which act as regulators of gene expression by binding to complementary sequences within mRNAs (4). A single miRNA transcript can act on multiple mRNA targets, and therefore, miRNAs are involved in many biological and pathological processes. In fact, miRNA dysregulation has been shown as a frequent and important event across all stages of cancer (5–8), as well as in many different cancer types (9–15). Their stability in biofluids and tissue biopsies presents opportunities for biomarker discovery (4, 16) and subsequently drug target detection (17–19). Among the dysregulated miRNAs in HNSCC, miR-21, miR-34, miR-93, miR-155, miR-196, and miR-211 are the most studied (20). Functional assays and target prediction have demonstrated that these miRNAs play important roles in regulation of cell proliferation, immune invasion, and resistance to cell death (21–24), corroborating their role as regulators in HNSCC (20, 25). Furthermore, miRNAs have demonstrated utility as biomarkers in the diagnosis and prognostication of HNSCC. For example, under-expression of let-7d and miR-205 are associated with poor survival in HNSCC (26), and circulating miR-142, miR-186, miR-195, miR-374b, and miR-574 have been shown to be promising markers for monitoring therapy in HNSCC patients (27).

While current miRNA repositories contain ∼2,500 unique miRNA sequences, they are primarily comprised of those that are either conserved across several tissues or abundantly expressed, for the most part discounting lineage- and tissue-specific miRNAs (28). However, recent studies show that numerous miRNAs may be expressed only in specific tissues or contexts (29–33), and may have utility as clinical markers of disease (8, 34).

Mining of large-scale datasets using bioinformatic algorithms has become an important tool for expanding the current annotation of miRNA repositories and discovering these tissue/context-specific miRNAs, particularly due to the data's high coverage depth and sample size. The discovery of novel miRNAs not only provides a novel resource for the research community, but may also guide future clinical efforts on the design of new drug targets and disease biomarkers. Thus, we hypothesize the existence of previously-unannotated and tissue-specific miRNAs in head and neck samples, which may have been overlooked due to their tissue/context specificity. In this study, we use a large-scale analysis of high-throughput sequencing data to uncover these novel miRNAs and explore their relevance to HNSCC tumourigenesis.

MATERIALS AND METHODS

Clinical Data Sets

A discovery cohort consisting of publicly available high-throughput raw small-RNA sequencing data from 523 tumors along with 43 paired non-malignant samples was retrieved from The Cancer Genome Atlas (TCGA) on the cgHUB data repository (dbgap Project ID: 6208), available at: https://cancergenome.nih.gov/ (accessed October 2018). Clinical information on the cases, summarized in **Table 1**, was obtained from the University of California Santa Cruz Xena Browser, available at: https://xenabrowser.net/ (accessed August 2018). HPV status was obtained from the Cancer Genome Atlas Network (35).

Publicly available small-RNA sequencing data from an independent cohort ($n = 20$) of oral squamous cell carcinoma samples were obtained from the Gene Expression Omnibus (GEO) repository (Accession GSE52663) (36).

Validation was carried out using formalin-fixed paraffin-embedded (FFPE) tissue from 25 oral squamous cell carcinoma (OSCC) tumors and 5 non-malignant oral tissue samples.

Data Processing and Novel MicroRNA Discovery

The data were analyzed using a customized *in-silico* analysis pipeline. The study design is summarized in **Figure 1**, and

TABLE 1 | Clinicopathological information of the HNSCC patients from TCGA*.

Clinical feature		Total (%)$
Histology	Malignant	523
Anatomical Site	Oral cavity	316 (60.4)
	Pharynx	90 (17.2)
	Larynx	117(22.4)
Age†	Range	19–90
	Median	61
Gender	Male	382 (73.0)
	Female	141 (27.0)
Smoking status	Never smoker	121 (23.1)
	Former smoker	211 (40.3)
	Current smoker	176 (33.7)
	Not determined	15 (2.9)
Disease stage	I	21 (4.0)
	II	97 (18.5)
	III	105 (20.1)
	IVA, IVB, and IVC	286 (54.7)
	Not determined	14 (2.7)
HPV status#	Positive	73 (14.0)
	Negative	40 (7.6)
	Not determined	410 (78.4)

*Information retrieved August 2018 from UCSC Xena (https://xenabrowser.net).
$Column percentage.
†Age data missing for one patient.
#Determined by p16 testing.

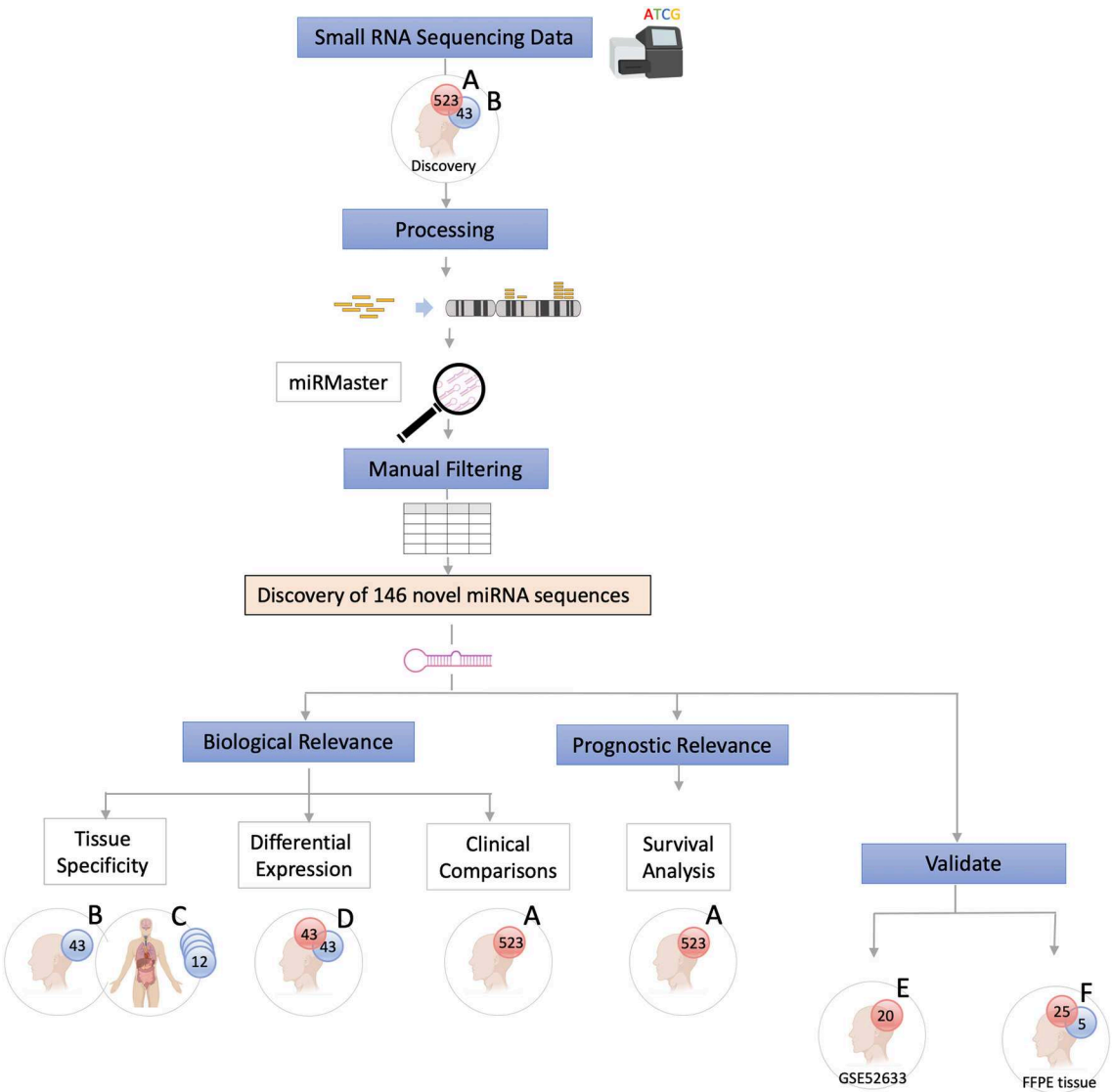

FIGURE 1 | Study Flow Chart. High throughput small RNA-sequencing data from head and neck squamous cell carcinoma (HNSCC) ($n = 523$, dataset A) and matched non-malignant tissue ($n = 43$, dataset B) were obtained from The Cancer Genome Atlas (TCGA). Raw sequence data (BAM files) were converted into unaligned reads (FASTQ) and inputted into miRMaster for miRNA detection and quantification. A threshold criteria of ≥1 read per million (RPM) in ≥10% of samples per group was employed. To determine whether these novel sequences have potential biological relevance group comparison and association analyses were performed. Tissue specificity of the novel candidate sequences was assessed by comparing non-malignant samples (dataset B) with those from 12 other non-malignant tissue types from TCGA Pan-Cancer Atlas (dataset C) using non-linear t-Distributed Stochastic Neighbor Embedding. Differentially expressed novel miRNAs were detected by comparing tumor and matched non-malignant samples (dataset D). Clinicopathological features of the novel miRNA transcripts ($n = 130$) that were found to be expressed exclusively in tumor samples (dataset A) were compared. Survival analysis was performed to further characterize the novel sequences. Cox regression analysis showed that candidate novel miRNA sequences behave similarly to known miRNAs and may have prognostic value. Validation was performed on an independent dataset (Gene Expression Omnibus GSE52633) (dataset E) and by performing RT-qPCR of the most relevant miRNA candidates in formalin-fixed paraffin-embedded (FFPE) tissues (dataset F).

the data subsets used for the step-wise comparisons that were conducted are summarized in **Table 2**.

Raw sequence data from both HNSCC tumors and non-malignant head and neck tissue samples (**Table 2**, datasets A and B) obtained from TCGA in the form of BAM files were converted into unaligned (FASTQ) files using Partek Flow® (http://www.partek.com/partek-flow/). FASTQ files were then analyzed for novel miRNA expression using the online analysis platform miRMaster (https://ccb-compute.cs.uni-saarland.de/mirmaster) (accessed October 2018). This platform predicts novel miRNAs based on the miRDeep2 algorithm, a well-established novel miRNA discovery tool which identifies miRNA-like configurations by considering relative free-energy and the probability of random folding (37). Default parameters were used

TABLE 2 | Description of clinical data sets.

Data set	Description of samples
A	HNSCC samples obtained from TCGA ($n = 523$)
B	Non-malignant head and neck samples obtained from TCGA ($n = 43$)
C	Non-malignant samples from different organs* from TCGA Pan-Cancer Atlas
D	Matched HNSCC and non-malignant samples from TCGA ($n = 43$ pairs)
E	OSCC from the GEO (GSE52633) ($n = 20$)
F	FFPE OSCC tissue ($n = 25$) and FFPE non-malignant tissue from the buccal mucosa ($n = 5$)
Analyses	
A and B	MiRNA discovery
B and C	Tissue specificity* of novel miRNAs
D	Differential expression between non-malignant samples and HNSCC
A	Association of miRNAs with clinical features
A	Survival analysis
E	Detection of novel miRNAs in an independent cohort
F	Experimental validation of most relevant miRNA by RT-qPCR in FFPE tissues

HNSCC, head and neck squamous cell carcinoma; TCGA, The Cancer Genome Atlas; OSCC, oral squamous cell carcinoma; FFPE, formalin-fixed paraffin-embedded.
**bile duct (n = 9), bladder (n = 19), brain (n = 5), cervix (n = 3), colon (n = 9), kidney (n = 71), liver (n = 47), lung (n = 91), pancreas (n = 4), prostate (n = 52), stomach (n = 45), and thyroid (n = 59).*

to perform quality filtering and read collapsing. The adapters were trimmed (Illumina TruSeq small RNA 3p), followed by the alignment of the reads to the hg38 build of the human genome (38). Sequences previously annotated in miRBase v.22 were excluded. The list of candidate novel miRNA transcripts was then further curated to include only sequences with a detectable expression of $\geq$1 read per million (RPM) in at least 10% of samples, for each group. Those miRNA candidates that remained after filtering were considered putative novel miRNAs.

To verify their designation as true miRNA sequences, we assessed whether these novel miRNA candidates shared structural properties and sequence features with known miRNA sequences. Nucleotide composition of the seed sequence and guanine-cytosine (GC) content were compared between the novel candidates and currently-annotated miRNAs, as well as their distribution across the genome.

Group Comparison and Association Studies

To determine the tissue-specificity of these novel miRNA candidates, normalized expression levels of the 146 candidate novel miRNA sequences from the non-malignant head and neck tissues (**Table 2**, datasets B and D) were queried against non-malignant samples from 12 different organ sites from TCGA Pan-Cancer Atlas using non-linear t-Distributed Stochastic Neighbor Embedding (t-SNE) dimensionality reduction. The tissues investigated included bile duct ($n = 9$), bladder ($n = 19$), brain ($n = 5$), cervix ($n = 3$), colon ($n = 9$), kidney ($n = 71$), liver ($n = 47$), lung ($n = 91$), pancreas ($n = 4$), prostate ($n = 52$), stomach ($n = 45$), thyroid ($n = 59$) and head & neck ($n = 43$).

To assess their involvement in HNSCC development, we sought to determine whether these novel transcripts are dysregulated in corresponding tumor samples.

An unsupervised hierarchal clustering analysis (Pearson correlation and complete linkage) was performed including novel miRNAs present in both tumor and non-malignant sample groups (**Table 2**, dataset D). Paired sample *t*-test (Benjamini-Hochberg [BH] adjusted $p < 0.05$ and fold change [FC] > 1.5) was applied to compare the novel miRNA expression between malignant and non-malignant samples ($n = 43$ pairs).

Clinical-pathological associations, examining anatomical site (oral cavity, pharynx, and larynx), smoking status (lifelong non-smoker versus continuing smoker) and HPV status (negative vs. positive), were observed for the novel miRNAs ($n = 130$) expressed exclusively in tumor samples (**Table 2**, dataset A) (*t*-test BH adjusted $p < 0.05$ and FC > 1.5).

To explore a potential prognostic relevance of the sequences discovered, the miRNA expression was associated with overall (OS) and recurrence-free survival (RFS) using the TCGA tumor samples (**Table 2**, dataset A). MicroRNAs associated with survival ($p < 0.01$) in a univariate log-rank test were included in a multivariate Cox proportional hazard model.

Target Prediction and Pathway Enrichment

To investigate the possible genes targeted by our recently discovered miRNAs and their biological roles, we performed target prediction and pathway enrichment analysis. Target prediction was performed using the miRanda v 3.3a algorithm, against all human genes 3′ UTR sequences acquired from Ensembl through Biomart tool (https://www.ensembl.org/) (39). The prediction algorithm was executed using strict alignment, alignment score $\geq$180 and energy threshold $\leq$-20 kcal/mol parametrizations. Next, to gain further functional insights into the pathways these targets may be involved, we submitted the gene symbols identified to a comprehensive pathway enrichment analysis using pathDIP, which includes 15 distinct pathways resources (Extended pathway associations. Experimental plus orthologs plus FpClass – High Confidence; Minimum confidence level for predicted associations: 0.99) (40).

Confirmation Using an Independent Cohort

Publicly available small-RNA sequencing data from a second cohort ($n = 20$) (**Table 2**, dataset E) of oral squamous cell carcinoma (OSCC) tissue samples were downloaded from GEO (Accession GSE52663) (36). SRA files were converted to FASTQ and mapped to human genome build 38 using the STAR aligner in Partek Flow® (41). Novel miRNA candidates were then quantified by their genomic loci. Expression values were averaged to create an average expression value per sample. A detection threshold $\geq$10 reads across the averaged samples was employed.

Confirmation by RT-qPCR

To further confirm the presence of these miRNAs in HNSCC, we selected five of the most highly-expressed HNnov-miRNAs and confirmed their expression by PCR in an independent cohort of

OSCC. Formalin-fixed paraffin-embedded (FFPE) tissue blocks ($n = 25$ OSCC and 5 normal oral tissue from the buccal mucosa) (**Table 2**, dataset F) were obtained from the British Columbia Oral Biopsy Service using written informed consent and a study protocol approved by the University of British Columbia—BC Cancer Research Ethics Board. Five 10 μm sections were cut from each block, and immediately placed into clean 1.5 mL microtubes. Deparaffinization was performed in xylene, and extraction was performed using the miRNeasy FFPE kit (QIAGEN, Hilden Germany) following manufacturer's guidelines.

Custom reverse-transcription and PCR primers were designed using the Custom TaqMan® Small RNA Assay Design Tool from Thermo Fisher. Primers were designed specific to the mature miRNA sequences for five of the highest-expressing novel HNnov-miRNAs, including HNnov-miR-59-5p (UGAGUUCUGGGCUGUAGUGUGCU), HNnov-miR-3-5p (AAUUACAGAUUGUCUCAGAGA), HNnov-miR-45-5p (GGGGGUGUAGCUCAGUGGUAGA), HNnov-miR-19-5p (CCCUGAUGAGCUUGACUCUAG), and HNnov-miR-48-3p (AAGUUUCUCUGAACGUGUAGAGC), according to **Table S1**. Reverse transcription of miRNA species was performed using the TaqMan™ MicroRNA Reverse Transcription Kit (Applied Biosystems™, Cat#4366596) and RT-qPCR in TaqMan™ Universal Master Mix II, with UNG (Applied Biosystems™, Cat#4440044) according to protocols established by the manufacturer. RT-qPCR was performed in an Applied Biosystems® 7500 Real-Time PCR System, and expression of mature miRNA transcripts in tumors was calculated in reference to normal oral epithelium using the $2^{(-\Delta\Delta Ct)}$ method and normalized to U6 (TaqMan Cat#4427975, Assay ID: 001973).

RESULTS

Discovery of Novel miRNA Sequences in Head and Neck Samples

In order to identify novel miRNAs in HNSCC non-malignant and tumor tissues, we submitted the raw HNSCC sncRNA sequence data from TCGA (**Table 2**, datasets A and B) to the online platform miRMaster and applied a miRNA-discovery algorithm as described in Materials and Methods. This initial analysis resulted in a list of miRNA candidates that were curated to exclude sequences highly homologous to those previously annotated in miRBase v.22. After curation, 146 previously unannotated miRNAs were identified (**Table S1**). These novel miRNA sequences are herein referred to as HNnov-miRs. The discovery of these 146 miRNAs represents a 5.5% increase to the total number of 2,656 currently-annotated miRNAs quantified by miRMaster, and an outstanding increase of 25% to the 583 currently-annotated miRNAs that were also found to be expressed at our threshold levels (1 RPM in 10% of the samples) in the TCGA HNSCC cohort (**Figure 2A**). Like currently-annotated miRNAs, the HNnov-miRs where shown to be widely distributed across the genome (**Figure 2C**). Additionally, they were found to have similar overall molecular features compared to annotated miRNAs, further supporting their identity as miRNA sequences (**Table S1**).

Tissue- and Context-Specific Expression Patterns of the Novel miRNAs

Next, we sought to investigate the tissue-specificity of the HNnov-miRs by comparing their combined expression patterns in head and neck against other tissue types. This analysis showed that the HNnov-miRs are indeed head and neck-specific and their combined expression patterns were able to clearly distinguish non-malignant head and neck samples from other types of non-malignant tissue (bile duct, bladder, brain, cervix, colon, kidney, liver, lung, pancreas, prostate, stomach, and thyroid), as evidenced by t-Distributed Stochastic Neighbor Embedding (t-SNE) analysis (**Figure 3**). This tissue-specific nature highlights their potential relevance to head and neck biology.

Differential Expression in HNSCC Tumor and Non-malignant Head and Neck Tissue

From our curated list of 146 HNnov-miRs, a total of 16 HNnov-miR sequences were exclusively expressed in non-malignant samples, 80 in tumors only, and 50 shared between both sample types (**Figure 2B**, **Table S2**). Of the 50 HNnov-miRs detected in both matched tumor and non-malignant tissue samples ($n = 43$ pairs), 39 were differentially expressed (BH-$p < 0.05$). Most sequences ($n = 38$) were found to be significantly over-expressed in HNSCC, while only one was under-expressed in tumors compared to non-malignant tissue (**Table S2**). Hierarchical clustering analysis of the HNnov-miRs detected in both tumor and matched non-malignant tissue samples demonstrated a clear difference in expression patterns between the two groups (**Figure 4**), which highlights that the HNnov-miRs are not only tissue-specific but also context-specific.

To further explore the role of these 39 HNnov-miRNAs found to be significantly over-expressed in HNSCC, we performed target prediction analysis. This analysis revealed a total of 10,221 possible unique protein-coding gene targets (**Table S2**), in which 3,273 were targeted by at least 10% of the 39 miRNAs. We also performed pathway enrichment analysis on the 10,221 gene targets to investigate the biological pathways they may be involved and reported the top 20 enriched pathways (**Table S6**). In this analysis, none of the pathways were found to be significantly enriched after Benjamini-Hochberg correction, however it suggests the target genes to be involved mainly with interleukin signaling.

We also investigated if HNnov-miRs expression patterns differed according to different clinical parameters. Expression patterns of the novel miRNAs did not differ significantly between oral cavity and pharynx/larynx subsites. Likewise, expression between smokers and non-smokers did not differ significantly. Interestingly, three of the predicted novel miRNAs (HNnov-miR-2, HNnov-miR-30, and HNnov-miR-125) were significantly associated with HPV status (BH-$p < 0.05$ and fold change>1.5), where their downregulation was associated with the presence of HPV infection (**Table S3**).

Potential Prognostic Relevance of the Novel miRNAs

The prognostic impact of novel and known miRNAs was assessed in the TCGA cohort ($n = 523$) (dataset A in **Table 2**).

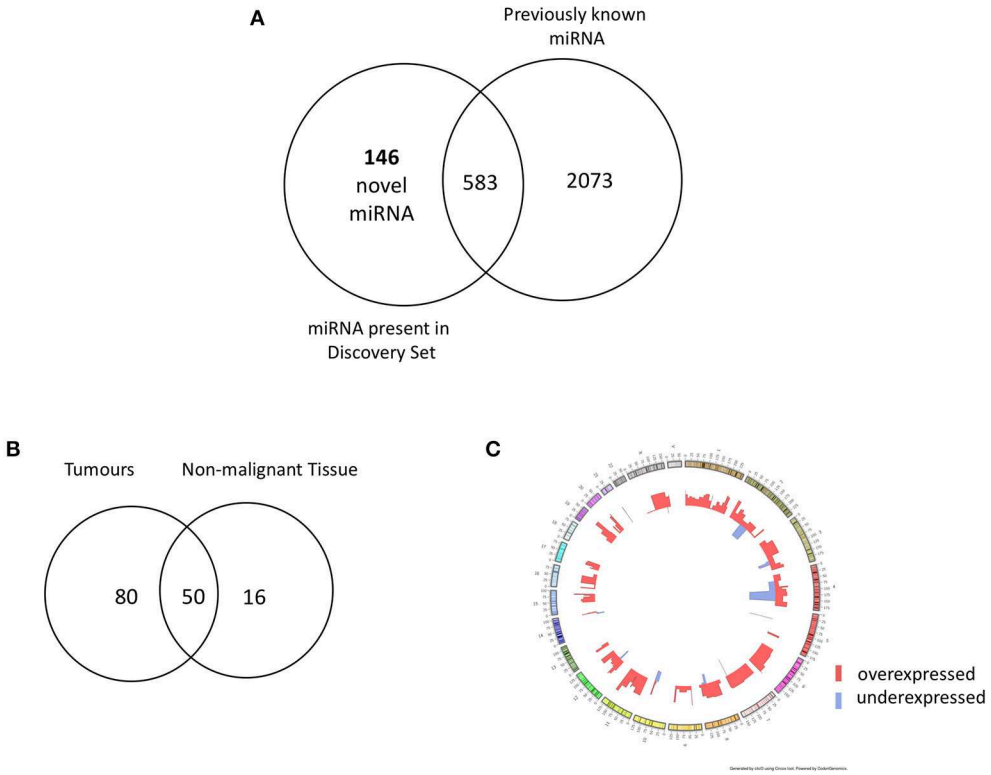

FIGURE 2 | (A) Venn diagram summarizing the relative proportion of novel vs. previously identified miRNAs expressed to the same levels in the TCGA cohort compared to the current annotation of miRNA repositories. An addition of 146 novel miRNAs to 583 previously annotated sequences expressed to the same d level in the TCGA increases the transcriptome head and neck tissues substantially. **(B)** Venn diagram of novel miRNAs identified in head and neck squamous cell carcinoma tumor tissue ($n = 523$) and non-malignant ($n = 43$) tissue. Our results revealed 146 novel miRNA candidates; 80 and 16 were observed exclusively in non- malignant and tumor tissues, respectively, with 50 miRNA candidates detected in both groups. **(C)** Circos plot displaying the genomic localization of the novel miRNAs. The outermost circle displays the human autosomal chromosomes, and the inner layers show the expression fold changes (logged) of the novel miRNAs in head and neck squamous cell carcinoma tumors in relation to matched non-malignant tissue [created by ClicO FS: An interactive web-based service of Circos (42)].

Three predicted novel miRNAs were significantly associated with overall survival (OS; HNnov-miR-104, HNnov-miR-120, and HNnov-miR-136) and three were significantly associated with recurrence free survival (RFS; HNnov-miR-3, HNnov-miR-87, and HNnov-miR-135) in univariate analyses (**Table S4**, **Figure S1**). In a multivariate Cox proportional hazard model including both novel and known miRNAs, one novel miRNA remained independently associated with OS (HNnov-miR-120), and two with RFS (HNnov-miR-3 and HNnov-miR-135). We then established scores for OS and RFS using either known miRNAs alone or both novel and known miRNAs. Scores using novel and known miRNAs were more powerful in the segregation of patients within prognostic groups (**Table S4**, **Figure S2**).

Confirmation of the Novel miRNAs in an Independent Cohort

To confirm the existence of our novel miRNAs, we also investigated their presence in an additional RNA-sequencing dataset using the same analysis and filtering criteria performed in our discovery cohort. In the validation dataset (**Table 2**, dataset E), 102 of the 146 HNnov-miRs were detected (**Table S5**, **Figure S3**), including all three of the HNnov-miRs that were found to be overexpressed in HPV negative samples and all six of the HNnov-miRs that were associated with OS or RFS.

Validation by RT-qPCR

For this verification, we found that, compared to normal tissues, the 5 miRNA selected were all more highly expressed in OSCC, confirming not only their existence within the tumor, but their importance to tumor biology (**Figure S4**).

DISCUSSION

In this study, we report a comprehensive analysis of undiscovered miRNAs that has led to the expansion of the head and neck transcriptome. By analyzing raw small-RNA sequencing data for both quantity and secondary RNA structure, we discovered 146 HNnov-miRs previously undescribed in head and neck tissues. Our characterization of these novel transcripts has revealed not only their tissue-specific nature and their context-specific expression patterns relevance to head and neck cancer biology, but also their diagnostic and prognostic potential.

The current annotation of the human miRNA transcriptome mainly contains miRNA sequences that are abundant and

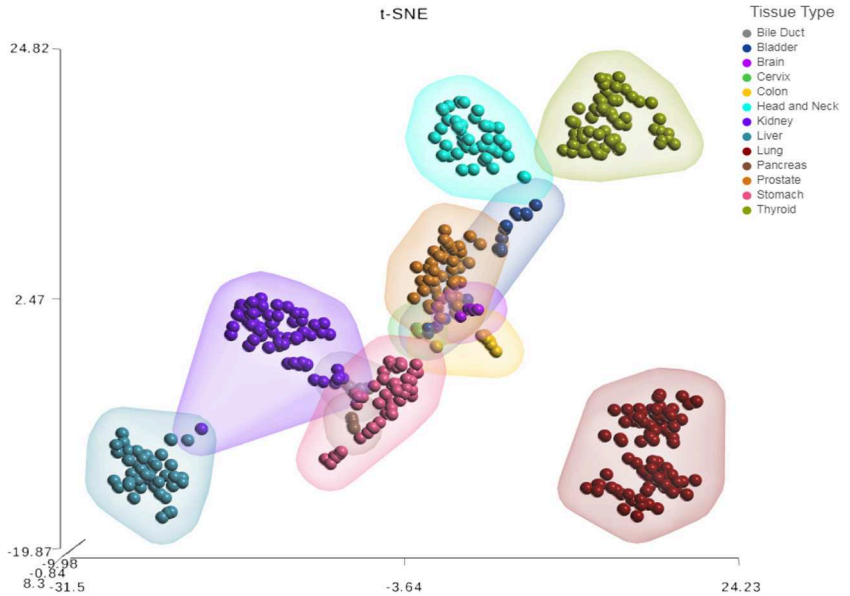

FIGURE 3 | Tissue-specific expression patterns of unannotated miRNA transcripts. t-Distributed Stochastic Neighbor Embedding (t-SNE) analysis T-SNE shows tissue specificity of head and neck non-malignant tissue compared to other non-malignant tissue from The Cancer Genome Atlas (TCGA); bile duct ($n = 9$), bladder ($n = 19$), brain ($n = 5$), cervix ($n = 3$), colon ($n = 9$), were compared to head & neck ($n = 43$), kidney ($n = 71$), liver ($n = 47$), lung ($n = 91$), pancreas ($n = 4$), prostate ($n = 52$), stomach ($n = 45$), and thyroid ($n = 59$).

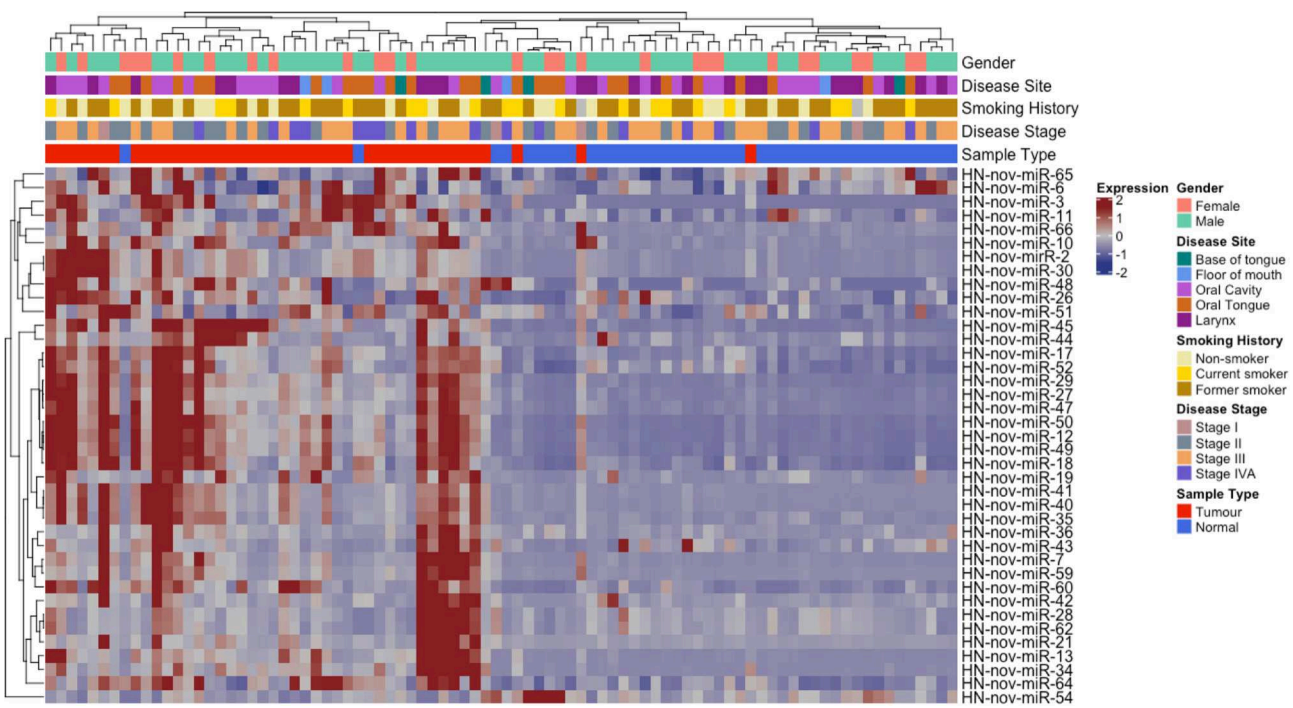

FIGURE 4 | Unsupervised hierarchal clustering analysis comprising 39 HNnov-miR expressed in both tumors and non-malignant tissue. The dendogram shows two clusters, the first enriched by non-neoplastic samples (novel miRNA expression predominantly low) and the second by tumor samples (novel miRNA expression predominantly high). Heatmap annotation bars show some of the clinical parameters associated with each tissue sample, including gender, disease site and stage, smoking history, and tissue type.

conserved. Therefore, cell lineage- and tissue-specific miRNAs, especially those that are less abundant, may not be included in current miRBase annotations (29). This study, like several recent studies of other organs, has shown that re-analyses of high-throughput sequencing data, can lead to large-scale discoveries of novel miRNAs that are expressed in a tissue-specific manner, thus expanding the human miRNA transcriptome (29–33).

In order to validate the expression of the 146 HNnov-miRs, we analyzed an independent dataset of HNSCC ($n = 20$). High throughput sequencing data of small-RNAs are scarce, and despite the limited sample size of this validation set, 102 of our HNnov-miRNAs were detected in this independent cohort. To provide an additional layer of verification, experimental validation of the miRNAs was carried out by performing RT-qPCR of the most relevant miRNA candidates in OSCC tissues, thereby strengthening the position that these novel miRNAs may serve as a new resource for the exploration of head and neck cancer specific transcripts in future investigations.

Interestingly, our study did not show a difference in expression pattern of HNnov-miRNA between HNSCC tumors from smokers and non-smokers. These observations are sustained by similar studies. Kolokythas et al. have reported similar miRNA expression in oral squamous cell carcinoma in never-smokers and ever-smokers (43). Similarly, a study that looked at genome wide analysis in 30 oral potentially malignant lesions that progressed to cancer and a study that examined loss of heterozygosity at 9p, 17p, and 4q in 455 lesions with oral epithelial dysplasia showed similar genetic alterations between smokers and nonsmokers (44, 45). However, Irimie et al. have reported that the overall variation in gene expression profiles was different for patients who smoked compared to those who have never smoked. The interaction between genetics and exposure to non-tobacco environmental carcinogens complicates the identification of a single effect, such as smoking, related to HNSCC.

Our results showed that three of the predicted novel miRNAs (HNnov-miR-2, HNnov-miR-30, and HNnov-miR-125) were significantly associated with HPV status. Interestingly, all of these novel genes map to chromosome 12, and both HNnov-miR-2 and HNnov-miR30 lie within the genes *KRT6C* and *KRT6B*, respectively. This is interesting as both KRT6C, and B, have previously described to have roles in various cancers, and are included in a gene signature separating lung adenocarcinoma, from lung squamous cell carcinoma (46, 47). Further, we also find expression of these genes to be associated with HPV status. Additional studies will be needed to determine if these novel miRNAs work in conjunction with, or have specific functions independent of these cancer associated protein coding genes (**Figure 5**).

The potential utility of the HNnov-miRNAs is highlighted by our observations that a subset of these transcripts is significantly associated with patient outcome (**Figure S1**), and that combining novel and known miRNAs improved the prognostic signature (**Figure S2**). The expression of HNnov-miR-120, HNnov-miR-3 and HNnov-miR-135 have prognostic relevance regarding recurrence-free and overall survival in patients with HNSCC and may improve the current prognostic risk stratification of HNSCC.

Here, to investigate if the unannotated miRNAs discovered in head and neck tissue were tissue specific, we assessed a number of non-malignant datasets generated by TCGA, including some cohorts with low sample numbers. In general, the more samples of a tissue type analyzed, the greater likelihood of discovering additional unannotated miRNA transcripts, especially those with non-constitutive or low expression levels. Therefore, a caveat of this analysis is that some of the HNnov-miRs may have not been detected in the additional tissues analyzed because of the low sample numbers, particularly in the cohorts such as brain and cervix. However, it can indicate that they if present in these other tissues, they display different expression levels and their combined patter of in head and neck are quite tissue specific. While this study represents the first-generation analysis of these unannotated miRNAs, and focuses on head and neck tissue, future studies with additional samples will be needed to comprehensively catalog these species across human tissues.

Although we cannot weigh the HNnov-miRNAs newly discovered in this study against literature, we can assess whether the expression and function of the known miRNA observed within our custom pipeline are consistent with what is found in the literature. Our findings are consistent with a systematic review of 21 studies by Jamali et al. which indicated that

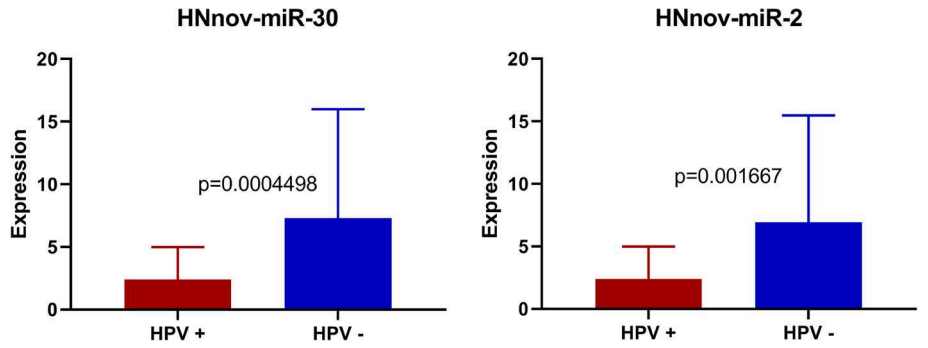

FIGURE 5 | Expression of HNnov-miR-2 and HNnov-miR-30 is significantly associated with negative HPV status in tumors (Mann Whitney *U*-test).

overexpression of miR-18a, miR-19a, miR-21, miR-134a, and miR-155, miR-181a, miR-210, were associated with poor survival, and that significantly decreased expression of let-7d, let-7g, miR-17, miR-34a, and miR-125b, miR-126a, miR-153, miR-200c, miR-203, miR-205, miR 218, miR-363, miR-375, miR-491-p5, miR-451, were associated with poor prognosis (48). In our study, we analyzed miRNA expression in the TCGA dataset (n = 523, dataset A), and found that among the abovementioned miRNAs, miR-134a, miR-153, miR-200c, miR-205, and miR-125b were significantly associated with overall survival in univariate analysis. After controlling for heterogeneity, Jamali's fixed model meta-analysis indicated that a significantly increased expression of miR-21 is associated with poor survival (Pooled HR = 1.57–95% CI: 1.22–2.02, $P < 0.05$) (48). In multivariate analysis, we found that only miR-205 remained significantly associated with overall survival. These findings add weight to the relevance and legitimacy of the novel miRNA discovered within our pipeline.

In conclusion, annotated miRNAs represent only a fraction of all the miRNAs encoded by the human genome. Here we identified 146 HNnov-miRs expressed in head and neck tissues with potential relevance to HNSCC biology, as well as diagnostic and prognostic potential. While our study was performed on a predictive platform and mainly relied on small-RNA sequencing data, the validation of 5 of these novel miRNAs by RT-qPCR supported their existence. Likewise, to understand their biological role and potential clinical utility, further functional assays will be required. An important next step would be to query the presence of these HNnov-miRNAs in liquid biopsies, such as serum samples. Here, we expand the current repertoire of head and neck miRNAs and provide an important new resource for the exploration of organ and disease specific transcripts that may guide future discoveries in head and neck cancers.

DATA AVAILABILITY STATEMENT

All data analyzed in this study are publicly available: TCGA consortium/NIH GDC (https://gdc.cancer.gov/); and GEO database accession number: GSE52663.

ETHICS STATEMENT

The studies involving human participants were reviewed and approved by University of British Columbia Research Ethics Board. The patients/participants provided their written informed consent to participate in this study.

AUTHOR CONTRIBUTIONS

LR and BM were responsible for the project design. LR, BM, EM, FG, AS, MB-F, and GS contributed to data acquisition, data analysis, interpretation of results, and manuscript preparation. CG and WL were principle investigators of this project. All authors have read, edited and approved the final manuscript, and agree to be accountable for the content of the work.

FUNDING

This work was supported by grants from the Canadian Institutes for Health Research [CIHR FDN-143345]. LR was supported by the BC Cancer Foundation and University of British Columbia Faculty of Dentistry. EM was a Vanier Canada Graduate Scholar. FG was supported by the Ligue nationale contre le cancer, the Fonds de Recherche en Santé Respiratoire (appel d'offres 2018 emis en commun avec la Fondation du Souffle), the Fondation Charles Nicolle. MB-F was supported by the São Paulo Research Foundation (2018/06138-8).

ACKNOWLEDGMENTS

The authors wish to thank Dr. Miriam P. Rosin (Department of Cancer Control Research, BC Cancer) and the British Columbia Oral Cancer Prevention Program for their assistance with the processing of tissue samples.

SUPPLEMENTARY MATERIAL

The Supplementary Material for this article can be found online at: https://www.frontiersin.org/articles/10.3389/fonc.2019.01305/full#supplementary-material

REFERENCES

1. Bray F, Ferlay J, Soerjomataram I, Siegel RL, Torre LA, Jemal A. Global cancer statistics 2018: GLOBOCAN estimates of incidence and mortality worldwide for 36 cancers in 185 countries. *CA Cancer J Clin*. (2018) 68:394–424. doi: 10.3322/caac.21492
2. Warnakulasuriya S. Living with oral cancer: epidemiology with particular reference to prevalence and life-style changes that influence survival. *Oral Oncol*. (2010) 46:407–10. doi: 10.1016/j.oraloncology.2010.02.015
3. Lozano R, Naghavi M, Foreman K, Lim S, Shibuya K, Aboyans V, et al. Global and regional mortality from 235 causes of death for 20 age groups in 1990 and 2010: a systematic analysis for the Global Burden of Disease Study 2010. *Lancet*. (2012) 380:2095–128. doi: 10.1016/S0140-6736(12)61728-0
4. Gebert LFR, MacRae IJ. Regulation of microRNA function in animals. *Nat Rev Mol Cell Biol*. (2019) 20:21–37. doi: 10.1038/s41580-018-0045-7
5. Vickers MM, Bar J, Gorn-Hondermann I, Yarom N, Daneshmand M, Hanson JE, et al. Stage-dependent differential expression of microRNAs in colorectal cancer: potential role as markers of metastatic disease. *Clin Exp Metastasis*. (2012) 29:123–32. doi: 10.1007/s10585-011-9435-3
6. Hayes J, Peruzzi PP, Lawler S. MicroRNAs in cancer: biomarkers, functions and therapy. *Trends Mol Med*. (2014) 20:460–9. doi: 10.1016/j.molmed.2014.06.005
7. Becker-Santos DD, Thu KL, English JC, Pikor LA, Martinez VD, Zhang M, et al. Developmental transcription factor NFIB is a putative target of oncofetal miRNAs and is associated with tumour aggressiveness in lung adenocarcinoma. *J Pathol*. (2016) 240:161–72. doi: 10.1002/path.4765

8. Avissar M, McClean MD, Kelsey KT, Marsit CJ. MicroRNA expression in head and neck cancer associates with alcohol consumption and survival. *Carcinogenesis*. (2009) 30:2059–63. doi: 10.1093/carcin/bgp277
9. Iorio MV, Ferracin M, Liu CG, Veronese A, Spizzo R, Sabbioni S, et al. MicroRNA gene expression deregulation in human breast cancer. *Cancer Res*. (2005) 65:7065–70. doi: 10.1158/0008-5472.CAN-05-1783
10. Lu J, Getz G, Miska EA, Alvarez-Saavedra E, Lamb J, Peck D, et al. MicroRNA expression profiles classify human cancers. *Nature*. (2005) 435:834–8. doi: 10.1038/nature03702
11. Murakami Y, Yasuda T, Saigo K, Urashima T, Toyoda H, Okanoue T, et al. Comprehensive analysis of microRNA expression patterns in hepatocellular carcinoma and non-tumorous tissues. *Oncogene*. (2006) 25:2537–45. doi: 10.1038/sj.onc.1209283
12. Roldo C, Missiaglia E, Hagan JP, Falconi M, Capelli P, Bersani S, et al. MicroRNA expression abnormalities in pancreatic endocrine and acinar tumors are associated with distinctive pathologic features and clinical behavior. *J Clin Oncol*. (2006) 24:4677–84. doi: 10.1200/JCO.2005.05.5194
13. Enfield KS, Pikor LA, Martinez VD, Lam WL. Mechanistic roles of non-coding RNAs in lung cancer biology and their clinical implications. *Genet Res Int*. (2012) 2012:737416. doi: 10.1155/2012/737416
14. Mazeh H, Deutch T, Karas A, Bogardus KA, Mizrahi I, Gur-Wahnon D, et al. Next-generation sequencing identifies a highly accurate miRNA panel that distinguishes well-differentiated thyroid cancer from benign thyroid nodules. *Cancer Epidemiol Biomarkers Prev*. (2018) 27:858–63. doi: 10.1158/1055-9965.EPI-18-0055
15. Tokar T, Pastrello C, Ramnarine VR, Zhu CQ, Craddock KJ, Pikor LA, et al. Differentially expressed microRNAs in lung adenocarcinoma invert effects of copy number aberrations of prognostic genes. *Oncotarget*. (2018) 9:9137–55. doi: 10.18632/oncotarget.24070
16. Mazumder S, Datta S, Ray JG, Chaudhuri K, Chatterjee R. Liquid biopsy: miRNA as a potential biomarker in oral cancer. *Cancer Epidemiol*. (2019) 58:137–45. doi: 10.1016/j.canep.2018.12.008
17. Vucic EA, Thu KL, Pikor LA, Enfield KS, Yee J, English JC, et al. Smoking status impacts microRNA mediated prognosis and lung adenocarcinoma biology. *BMC Cancer*. (2014) 14:778. doi: 10.1186/1471-2407-14-778
18. Rupaimoole R, Slack FJ. MicroRNA therapeutics: towards a new era for the management of cancer and other diseases. *Nat Rev Drug Discov*. (2017) 16:203–22. doi: 10.1038/nrd.2016.246
19. Tokar T, Pastrello C, Rossos AEM, Abovsky M, Hauschild AC, Tsay M, et al. mirDIP 4.1-integrative database of human microRNA target predictions. *Nucleic Acids Res*. (2018) 46:D360–70. doi: 10.1093/nar/gkx1144
20. Lubov J, Maschietto M, Ibrahim I, Mlynarek A, Hier M, Kowalski LP, et al. Meta-analysis of microRNAs expression in head and neck cancer: uncovering association with outcome and mechanisms. *Oncotarget*. (2017) 8:55511–24. doi: 10.18632/oncotarget.19224
21. Corra F, Agnoletto C, Minotti L, Baldassari F, Volinia S. The network of non-coding RNAs in cancer drug resistance. *Front Oncol*. (2018) 8:327. doi: 10.3389/fonc.2018.00327
22. Felix TF, Lopez Lapa RM, de Carvalho M, Bertoni N, Tokar T, Oliveira RA, et al. MicroRNA modulated networks of adaptive and innate immune response in pancreatic ductal adenocarcinoma. *PLoS ONE*. (2019) 14:e0217421. doi: 10.1371/journal.pone.0217421
23. Macharia LW, Wanjiru CM, Mureithi MW, Pereira CM, Ferrer VP, Moura-Neto V. MicroRNAs, hypoxia and the stem-like state as contributors to cancer aggressiveness. *Front Genet*. (2019) 10:125. doi: 10.3389/fgene.2019.00125
24. Yang X, Li Y, Zou L, Zhu Z. Role of exosomes in crosstalk between cancer-associated fibroblasts and cancer cells. *Front Oncol*. (2019) 9:356. doi: 10.3389/fonc.2019.00356
25. Yang CX, Sedhom W, Song J, Lu SL. The role of MicroRNAs in recurrence and metastasis of head and neck squamous cell carcinoma. *Cancers*. (2019) 11:E395. doi: 10.3390/cancers11030395
26. Childs G, Fazzari M, Kung G, Kawachi N, Brandwein-Gensler M, McLemore M, et al. Low-level expression of microRNAs let-7d and miR-205 are prognostic markers of head and neck squamous cell carcinoma. *Am J Pathol*. (2009) 174:736–45. doi: 10.2353/ajpath.2009.080731
27. Summerer I, Unger K, Braselmann H, Schuettrumpf L, Maihoefer C, Baumeister P, et al. Circulating microRNAs as prognostic therapy biomarkers in head and neck cancer patients. *Br J Cancer*. (2015) 113:76–82. doi: 10.1038/bjc.2015.111
28. Ludwig N, Leidinger P, Becker K, Backes C, Fehlmann T, Pallasch C, et al. Distribution of miRNA expression across human tissues. *Nucleic Acids Res*. (2016) 44:3865–77. doi: 10.1093/nar/gkw116
29. Londin E, Loher P, Telonis AG, Quann K, Clark P, Jing Y, et al. Analysis of 13 cell types reveals evidence for the expression of numerous novel primate- and tissue-specific microRNAs. *Proc Natl Acad Sci USA*. (2015) 112:E1106–15. doi: 10.1073/pnas.1420955112
30. Marshall EA, Sage AP, Ng KW, Martinez VD, Firmino NS, Bennewith KL, et al. Small non-coding RNA transcriptome of the NCI-60 cell line panel. *Sci Data*. (2017) 4:170157. doi: 10.1038/sdata.2017.157
31. Minatel BC, Martinez VD, Ng KW, Sage AP, Tokar T, Marshall EA, et al. Large-scale discovery of previously undetected microRNAs specific to human liver. *Hum Genomics*. (2018) 12:16. doi: 10.1186/s40246-018-0148-4
32. Sage AP, Minatel BC, Marshall EA, Martinez VD, Stewart GL, Enfield KSS, et al. Expanding the miRNA transcriptome of human kidney and renal cell carcinoma. *Int J Genomics*. (2018) 2018:6972397. doi: 10.1155/2018/6972397
33. Barros-Filho MC, Pewarchuk M, Minatel BC, Sage AP, Marshall EA, Martinez VD, et al. Previously undescribed thyroid-specific miRNA sequences in papillary thyroid carcinoma. *J Hum Genet*. (2019) 64:505–8. doi: 10.1038/s10038-019-0583-7
34. Martinez VD, Marshall EA, Anderson C, Ng KW, Minatel BC, Sage AP, et al. Discovery of previously undetected mircoRNAs in mesothelioma and their use as tissue-of-origin markers. *Am J Respir Cell Mol Biol*. (2019) 61:266–8. doi: 10.1165/rcmb.2018-0204LE
35. The Cancer Genome Atlas Network. Comprehensive genomic characterization of head and neck squamous cell carcinomas. *Nature*. (2015) 517:576–82. doi: 10.1038/nature14129
36. Yoon AJ, Wang S, Shen J, Robine N, Philipone E, Oster MW, et al. Prognostic value of miR-375 and miR-214-3p in early stage oral squamous cell carcinoma. *Am J Transl Res*. (2014) 6:580–92.
37. Friedlander MR, Mackowiak SD, Li N, Chen W, Rajewsky N. miRDeep2 accurately identifies known and hundreds of novel microRNA genes in seven animal clades. *Nucleic Acids Res*. (2012) 40:37–52. doi: 10.1093/nar/gkr688
38. Fehlmann T, Backes C, Kahraman M, Haas J, Ludwig N, Posch AE, et al. Web-based NGS data analysis using miRMaster: a large-scale meta-analysis of human miRNAs. *Nucleic Acids Res*. (2017) 45:8731–44. doi: 10.1093/nar/gkx595
39. Enright AJ, John B, Gaul U, Tuschi T, Sander C, Mark DS. MicroRNA targets in drosophila. *Genome Biol*. (2003) 5:R1. doi: 10.1186/gb-2003-5-1-r1
40. Rahmati S, Abovsky M, Pastrello C, Jurisica I. pathDIP: an annotated resource for known and predicted human gene-pathway associations and pathway enrichment analysis. *Nucleic Acids Res*. (2017) 45(D1):D419–26. doi: 10.1093/nar/gkw1082
41. Dobin A, Davis CA, Schlesinger F, Drenkow J, Zaleski C, Jha S, et al. STAR: ultrafast universal RNA-seq aligner. *Bioinformatics*. (2013) 29:15–21. doi: 10.1093/bioinformatics/bts635
42. Cheong WH, Tan YC, Yap SJ, Ng KP. ClicO FS: an interactive web-based service of Circos. *Bioinformatics*. (2015) 31:3685–7. doi: 10.1093/bioinformatics/btv433
43. Kolokythas A, Zhou Y, Schwartz JL, Adami GR. Similar squamous cell carcinoma epithelium microRNA expression in never smokers and ever smokers. *PLoS ONE*. (2015) 10:e0141695. doi: 10.1371/journal.pone.0141695
44. Rock LD, Rosin MP, Zhang L, Chan B, Shariati B, Laronde DM. Characterization of epithelial oral dysplasia in non-smokers: First steps towards precision medicine. *Oral Oncol*. (2018) 78:119–25. doi: 10.1016/j.oraloncology.2018.01.028
45. de la Oliva J, Larque AB, Marti C, Bodalo-Torruella M, Nonell L, Nadal A, et al. Oral premalignant lesions of smokers and non-smokers show similar carcinogenic pathways and outcomes. A clinicopathological and molecular comparative analysis. *J Oral Pathol Med*. doi: 10.1111/jop.12864. [Epub ahead of print].

46. Chang HH, Dreyfuss JM, Ramoni MF. A transcriptional network signature characterizes lung cancer subtypes. *Cancer*. (2011) 117:353–60. doi: 10.1002/cncr.25592
47. Hu J, Zhang LC, Song X, Lu JR, Jin Z. KRT6 interacting with notch1 contributes to progression of renal cell carcinoma, and aliskiren inhibits renal carcinoma cell lines proliferation *in vitro*. *Int J Clin Exp Pathol*. (2015) 8:9182–8.
48. Jamali Z, Asl Aminabadi N, Attaran R, Pournagiazar F, Ghertasi Oskouei S, Ahmadpour F. MicroRNAs as prognostic molecular signatures in human head and neck squamous cell carcinoma: a systematic review and meta-analysis. *Oral Oncol*. (2015) 51:321–31. doi: 10.1016/j.oraloncology.2015.01.008

Conflict of Interest: The authors declare that the research was conducted in the absence of any commercial or financial relationships that could be construed as a potential conflict of interest.

frontiers in Oncology

ORIGINAL RESEARCH
published: 17 January 2020
doi: 10.3389/fonc.2019.01526

HMGA2 Antisense Long Non-coding RNAs as New Players in the Regulation of HMGA2 Expression and Pancreatic Cancer Promotion

Gloria Ros[1], Silvia Pegoraro[1], Paolo De Angelis[1], Riccardo Sgarra[1], Silvia Zucchelli[2], Stefano Gustincich[3] and Guidalberto Manfioletti[1]**

[1] Department of Life Sciences, University of Trieste, Trieste, Italy, [2] Department of Health Sciences, Center for Autoimmune and Allergic Diseases, Interdisciplinary Research Center of Autoimmune Diseases, University of Piemonte Orientale, Novara, Italy, [3] Central RNA Laboratory, Istituto Italiano di Tecnologia, Genoa, Italy

OPEN ACCESS

Edited by:
Patricia P. Reis,
São Paulo State University, Brazil

Reviewed by:
Hebao Yuan,
University of Michigan, United States
Giovanni Sorrentino,
École Polytechnique Fédérale de Lausanne, Switzerland

***Correspondence:**
Silvia Pegoraro
spegoraro@units.it
Guidalberto Manfioletti
manfiole@units.it

Specialty section:
This article was submitted to Molecular and Cellular Oncology, a section of the journal Frontiers in Oncology

Received: 12 September 2019
Accepted: 18 December 2019
Published: 17 January 2020

Citation:
Ros G, Pegoraro S, De Angelis P, Sgarra R, Zucchelli S, Gustincich S and Manfioletti G (2020) HMGA2 Antisense Long Non-coding RNAs as New Players in the Regulation of HMGA2 Expression and Pancreatic Cancer Promotion. Front. Oncol. 9:1526. doi: 10.3389/fonc.2019.01526

Background: Natural antisense long non-coding RNAs (lncRNAs) are regulatory RNAs transcribed from the opposite strand of either protein coding or non-coding genes, able to modulate their own sense gene expression. Hence, their dysregulation can lead to pathologic processes. Cancer is a complex class of diseases determined by the aberrant expression of a variety of factors, among them, the oncofetal chromatin architectural proteins High Mobility Group A (HMGA) modulate several cancer hallmarks. Thus, we decided to investigate the presence of natural antisense lncRNAs in *HMGA1* and *HMGA2 loci*, and their possible involvement in gene expression regulation.

Methods: We used FANTOM5 data resources, FANTOM-CAT genome browser and Zenbu visualization tool, which employ 1,829 human CAGE and RNA-sequencing libraries, to determine expression, ontology enrichment, and dynamic regulation of natural antisense lncRNAs in *HMGA1* and *HMGA2 loci*. We then performed qRT-PCR in different cancer cell lines to validate the existence of HMGA2-AS1 transcripts. We depleted HMGA2-AS1 transcripts with siRNAs and investigated HMGA2 expression by qRT-PCR and western blot analyses. Moreover, we evaluated cell viability and migration by MTS and transwell assays, and EMT markers by qRT-PCR and immunofluorescence. Furthermore, we used bioinformatics approaches to evaluate HMGA2 and HMGA2-AS1 correlation and overall survival in tumor patients.

Results: We found the presence of a promoter-associated lncRNA (*CATG00000088127.1*) in the *HMGA1* gene and three antisense genes (*RPSAP52*, *HMGA2-AS1*, and *RP11-366L20.3*) in the *HMGA2* gene. We studied the uncharacterized HMGA2-AS1 transcripts, validating their existence in cancer cell lines and observing a positive correlation between HMGA2 and HMGA2-AS1 expression in a cancer-derived patient dataset. We showed that HMGA2-AS1 transcripts positively modulate HMGA2 expression and migration properties of PANC1 cells through HMGA2. In addition, Kaplan-Meier analysis showed that high level of HMGA2-AS1 is a negative prognostic factor in pancreatic cancer patients.

Conclusions: Our results describe novel antisense lncRNAs associated with *HMGA1* and *HMGA2* genes. In particular, we demonstrate that HMGA2-AS1 is involved in the regulation of its own sense gene expression, mediating tumorigenesis. Thus, we highlight a new layer of complexity in the regulation of HMGA2 expression, providing new potential targets for cancer therapy.

Keywords: natural antisense non-coding RNAs, HMGA, cancer, gene expression regulation, FANTOM5, HMGA2-AS1

INTRODUCTION

The advent of next-generation high throughput sequencing highlighted a new regulation layer in which RNA is a fundamental player. In fact, despite proteins were considered as final effectors in all cell regulation aspects, RNA molecules and especially non-coding RNAs have emerged as crucial and active players in cell orchestration, in particular in gene expression regulation (1–3). Non-coding RNAs are usually classified based on their length, with an artificial cutoff of 200 nucleotides (nt), in small non-coding RNAs (sncRNA) shorter than 200 nt and in long non-coding RNAs (lncRNAs) longer than 200 nt (4). LncRNAs represent a heterogeneous family and can be classified according to their position and transcription direction relative to nearby genes. Among them, natural antisense lncRNAs are characterized by being transcribed from the opposite strand of a protein-coding gene (5–8). Natural antisense lncRNAs can stimulate or reduce the gene expression of the sense transcripts at multiple levels, assuming a functional role in physiological and pathological processes (8–11).

The FANTOM5 Consortium has profiled almost 2,000 human samples from cell lines, primary cells, and tissues, using Cap Analysis of Gene Expression (CAGE) coupled to single-molecule sequencing (12), to accurately map Transcription Start Sites (TSS) and gene regulatory elements and to compile a comprehensive promoter-level mammalian expression atlas. Recently, the FANTOM5 Consortium has further expanded expression datasets, profiling thousands of samples with RNA and short RNA sequencing and paired-end CAGE (CAGEscan) protocols, to generate additional atlases of lncRNAs and miRNAs, mapping their promoters, improving annotation and providing cues of their regulatory functions (8, 13). Altogether, data from the FANTOM5 provide an invaluable tool to identify novel antisense lncRNAs with potential regulatory functions and disease association.

HMGA (High Mobility Group A) proteins are chromatin architectural factors involved in modulating the expression of a broad range of genes (14, 15). Despite HMGA proteins are not able to intrinsically trans-activate gene expression, their plasticity in binding DNA and/or transcription factors (16, 17), makes them key elements in a wide variety of biological processes (18). In physiological conditions, HMGA proteins exert their role of architectural transcription factors during embryogenesis, where they are mainly expressed. In adult tissues these proteins are almost undetectable except in cancer cells, where HMGA are over-expressed and crucial for tumor onset and progression (19, 20). In fact, HMGA drive tumor progression through the modulation of several hallmarks of cancer, such as cell proliferation, metastatic processes, drug resistance and stem cell properties (21–30). Human HMGA proteins are encoded by two distinct paralogous genes: *HMGA1*, that extends for 10 kb on chromosome 6 (6p21) and *HMGA2* that is a 160 kb long gene located on chromosome 12 (12q14-15) (20). The expression of these two genes is orchestrated both at transcriptional and post-transcriptional level (28, 31, 32). In addition, very recently, two research groups revealed that ribosomal protein SA pseudogene (RPSAP52) antisense lncRNA at the 5′ of *HMGA2* gene is able to modulate HMGA2 both at transcriptional (33) and post-transcriptional level (34, 35).

Considering the increasing importance of the antisense lncRNAs in the regulation of coding genes and their involvement in cancer progression through the modulation of crucial oncogenes and oncosuppressors and taking advantage of the genome-wide expression datasets of the FANTOM5 Consortium, we decided to evaluate the presence, expression profile and functional potentials of previously unidentified antisense lncRNAs in *HMGA1* and *HMGA2 loci*. We found novel antisense lncRNAs at both genes. In particular, we showed that a natural antisense lncRNA gene in *HMGA2 locus*, *HMGA2-AS1*, expresses a number of transcript variants involved in the regulation of sense protein-coding *HMGA2* gene. Moreover, we demonstrated that they have a role in tumorigenesis via an HMGA2-dependent mechanism. The findings reported in this paper add a further layer of complexity to the regulation of HMGA2 expression by previously uncharacterized natural antisense lncRNAs.

MATERIALS AND METHODS

Cell Culture

Human breast cancer MDA-MB 231 and MDA-MB 157, pancreatic cancer BX-PC3 and PANC1, colon cancer SW480 and HCT116, thyroid tumor ARO and TPC1, liver cancer HepG2 and Hep3B, and prostate cancer DU145 cell lines were cultured in DMEM (EuroClone: ECB7501L), whereas prostate cancer PC3 were cultured in RPMI (EuroClone: ECB9006L). Both media were supplemented with 10% tetracycline-free FBS (EuroClone: ECS0182L), L-Glutamine 2 mM (EuroClone: ECB3000D), Penicillin 100 U/ml and Streptomycin 100 μg/ml (EuroClone: ECB3001D).

Cell Transfections and Treatments

For silencing experiments in PANC1 cells, $2.1*10^4$ cells/cm^2 were treated with 12 nM of siRNA and LipofectamineTM RNAiMAX reagent (Invitrogen: 13778075) according to manufacturer instructions, for 24, 48, 72 h, depending to experiment. siCTRL was already used before (26), siHMGA2-AS1-AGI (5′-GGTGATGTATGGCCCATAA-3′) and siHMGA2-AS1-all (5′-GGGCCAACATGACACCAAA-3′) were designed using Primer Designer Tool from Thermo Fisher Scientific.

We used the following plasmids: pcDNA3.1, pEGFP-N1 (Invitrogen), pEGFP-N1-HMGA2, already available in the laboratory (36), pcDNA3.1-A2-AS1_H and pcDNA3.1-A2-AS1_G. To clone A2-AS1_H (FTMT24500018418.1), and A2-AS1_G (ENST00000536648.1) we amplified them, using primer forward 5′-CCCGCAAGCTTATAACTGGATCTT TCCATTACTTGGTAGC-3′ and primer reverse 5′-AAAGG TACCCTGAGATGCAGCTGACATGTACCA-3′, from cDNA retrotranscribed from PANC1 total RNA, then we purified the two PCR products after separation on agarose gel and we cloned them into pcDNA3.1. For A2-AS1_H and A2-AS1_G overexpression, $3.6*10^4$ cells/cm^2 PANC1 cells were transfected with 1.25 μg/ml of pcDNA3.1 as control and pcDNA3.1-A2-AS1_H or pcDNA3.1-A2-AS1_G, using LipofectamineTM 3000 (Invitrogen: L3000008) according to manufacturer instructions, for 30 h.

For rescue functional analysis, $4.0*10^4$ cells/cm^2 PANC1 cells were plated. Then cells were cotransfected, at 24 and 48 h from seeding, with 12 nM siRNA (siCTRL or siHMGA2-AS1-all) and 1.2 μg/ml of plasmid DNA (pEGFP-N1 or pEGFP-N1-HMGA2), using LipofectamineTM 3000 (Invitrogen). Experiments were done 72 h from the first transfection.

All transfections were performed in DMEM 10% tetracycline-free FBS, L-Glutamine 2 mM (EuroClone).

Immunoblotting

Cells were washed in chilled PBS and lysed using TRIzol® Reagent (Ambion® by Life Technologies: 15596026) or SDS sample buffer [62.5 mM Tris pH 6.8; 2% SDS; 10% glycerol; 50 mM DTT; Na_3Vo_4 1 mM; NaF 5 mM; PIC mammals (Sigma: P8340)]. In the case of TRIzol® Reagent usage, proteins were extracted accordingly to manufacturer instructions. The use of TRIzol® Reagent allowed to extract both RNA and proteins from the same sample. Lysates were separated by SDS-PAGE, prior to transfer to nitrocellulose membranes (GE-healthcare: GEH10600001). Western blot analyses were performed according to standard procedures using the following antibodies: anti-HMGA2 (37) and anti-β-actin (Sigma: A2066).

Immunostaining

Immunostaining was performed as described previously (30). E-Cadherin (BD: 610182), N-Cadherin (Sigma: C-2542), and Vimentin (Dako: M0725) were used as primary antibodies and anti-Mouse Alexa 488 (Invitrogen: A-11008) was used as secondary antibody. Images were visualized by a Nikon Eclipse e800 microscope and acquired by Nikon ACT-1 software.

Migration Assay

For transwell migration assay, 24-well PET inserts were used (8.0 μm pore size, Falcon: L003971 F3097) and $4*10^4$ cells were seeded. Migrated cells were fixed after 18 h in PFA 4% and stained with Crystal Violet 0.5% (Sigma: C0775). At least 4 images for insert were captured by OLYMPUS CK2 inverted optical microscope at 10× magnification through the digital camera Canon PowerShot A630. Cells were counted with ImageJ software.

MTS Cell Growth Analysis

$2.1*10^4$ cells/cm^2 were seeded in 96 well and every 24 h cell growth was revealed using CellTiter 96® AQueous One Solution Cell Proliferation Assay (Promega: G358C) according to manufacturer's instructions. For detection, at each time point, medium was replaced with a solution composed of 100 μl of PBS/glucose 4.5 g/L (Sigma: G7021) and 20 μl of CellTiter 96® AQueous One Solution in each well.

Gene Expression Analysis

Total RNA was processed as previously described (26). All RNA samples were checked for genomic contamination via qPCR. qRT-PCR was performed using IQ™ SYBRsGreen Supermix (Bio-Rad: 1708887). The CFX96 Real-Time PCR detection system (Bio-Rad) was used to perform PCR; all the primers (**Supplemental Table 1**) were designed using Primer3Plus software according to NCBI, Ensembl, and FANTOM-CAT sequence databases. For relative quantification, the GAPDH (**Supplemental Table 1**) or 18S (38) genes were used as internal standard reference. All experiments were performed at least in duplicate technical replicates. Analyses were done using DDCT method, unless otherwise specified. For classic RT-PCR we used Maxima Hot Start Green PCR master Mix 2X (Thermo Fisher Scientific: FERK1062) and BIOER xp thermal cycler (Genetouch). Amplification products were analyzed on polyacrylamide TBE gel.

Bioinformatics Analysis

HMGA1 and *HMGA2 loci* analysis was performed using Zenbu browser genomic data visualization tool from FANTOM-CAT (http://fantom.gsc.riken.jp/cat/). Zenbu was used to visualize transcripts whereas sample ontology association, dynamic expression and genetic trait association coding potential analysis were achieved in FANTOM-CAT Browser (http://fantom.gsc.riken.jp/cat/v1/#/), gene section. For correlation analysis between HMGA2 and HMGA2-AS1 we used Gene Expression Profiling Interactive Analysis (GEPIA) database (39) (http://gepia.cancer-pku.cn/) in BRCA (Breast invasive carcinoma), COAD (Colon adenocarcinoma), LIHC (Liver hepatocellular carcinoma), PAAD (Pancreatic adenocarcinoma), PRAD (Prostate adenocarcinoma), and THAC (Thyroid carcinoma) datasets. Spearman correlation coefficient was employed. For the overall survival analysis, Kaplan–Meier survival analysis of HMGA2 (90-cases) or HMGA2-AS1 (85-cases) was obtained from GEPIA (http://gepia.cancer-pku.cn/) in the PAAD dataset, using quartile (75% cutoff-high, 25% cutoff-low) as group cutoff. For Pathological Stage analysis in PAAD dataset, violin plots in

major tumor stages were obtained from GEPIA (http://gepia.cancer-pku.cn/). The method for differential gene expression analysis used was one-way ANOVA.

RESULTS

HMGA1 and *HMGA2 loci* Contain Several Natural Antisense RNAs

We used FANTOM5 data resources (40) to investigate antisense transcription in *HMGA1* and *HMGA2 loci*, across 1,829 human samples and identify novel antisense lncRNAs that may have regulatory functions. FANTOM-CAT data visualization in Zenbu (http://fantom.gsc.riken.jp/cat/) of *HMGA1* and *HMGA2 loci* revealed the presence of novel antisense transcripts with consistent Relative log expression (rle) in both *loci* (**Supplemental Figure 1** and **Figure 1**). HMGA1 antisense transcription is concentrated in the promoter region of *HMGA1* where *CATG00000088127.1* gene is located and annotated in FANTOM-CAT as "Promoter-associated lncRNAs" (p_lncRNA_divergent) (**Supplemental Figure 1**), characterized to be bidirectional transcribed. We analyzed transcriptional start site (TSS) usage from FANTOM5 datasets and observed that CATG00000088127.1 expression is mainly enriched in cells of the hemolymphoid and immuno systems (**Supplemental Figure 1**, 5′ zoom). Moreover, dynamic expression analysis highlighted the induction of this natural antisense lncRNA in macrophage upon influenza infection (**Supplemental Figure 1**, 5′ zoom).

HMGA2 locus showed a more complex pattern of antisense transcription than *HMGA1*. Indeed, we observed three independent TSS in antisense orientation relative to *HMGA2* transcription, which promoted the transcription of three genes, annotated in FANTOM-CAT as "Other RNAs" (*RPSAP52* and *RP11-366L20.2*, also named *HMGA2-AS1*), and "Enhancer lncRNA" (*RP11-366L20.3*) (**Figure 1**). The first natural antisense gene present in the *HMGA2 locus*, named *RPSAP52* (*ENSG00000241749*), includes a head-to-head divergent to 5′ HMGA2 antisense RNA (**Figure 1**) and has already been described to be involved in *HMGA2* gene expression regulation (33–35). The second natural antisense gene, originally named *RP11-366L20.2* (*uncharacterized LOC100129940: ENSG00000197301*) and now *HMGA2-AS1* according to HGNC (HUGO Gene Nomenclature Committee), is located in the first part of the *HMGA2* third intron and has not been investigated so far, as well as the third gene, *RP11-366L20.3* (*ENSG00000256083.1*), that is localized at the end of the same intron. The highest level of antisense transcription, in terms of positive expression number of libraries, is represented by RPSAP52-TSS (14% of FANTOM5 libraries), with a sum of rle CAGE signal equal to 730. On the contrary, the lowest expression is detected in RP11-366L20.3-TSS (2% of FANTOM5 libraries) with an rle sum of 33.9 (**Table 1**). RP11-366L20.3 is expressed at a very low level, in quantitative terms, compared to RPSAP52 and HMGA2-AS1. In fact, the highest CAGE signals and the mean of expression underlined that RP11-366L20.3 is poorly expressed (2.6 and 1.0, respectively), in contrast with RPSAP52 and HMGA2-AS1, which have higher and very similar values (**Table 1**). Considering that RPSAP52 has been already described and RP11-366L20.3 expression was low, we decided to focus on *HMGA2-AS1*.

HMGA2-AS1 Transcript Variants Include Natural Antisense lncRNAs

FANTOM-CAT data visualization in Zenbu of *HMGA2-AS1* revealed the presence of nine new transcript variants, not yet annotated in public databases and still uncharacterized. HMGA2-AS1 variants display different exon composition (**Figure 1**) that, for simplicity, we named from A to I as reported in **Figure 2**. From robust promoter analysis, we observed that HMGA2-AS1 transcript variants are transcribed from different TSS (**Figure 1**, HMGA2-AS1 zoom), which could be differentially used in different cell conditions. Indeed, analysis of all FANTOM5 libraries compared to dynamic expression in Saos-2 calcification and adipogenic induction libraries clearly highlighted a different TSS usage (**Figure 1**, HMGA2-AS1 zoom), suggesting a specific role for each transcript variant in space (cell type) and time (differentiation/response to external stimuli). Notably, in these time course experiments, HMGA2-AS1 is dynamically regulated similarly to HMGA2 (**Supplemental Table 2**). Moreover, GWAS analysis underline that both *HMGA2* and *HMGA2-AS1* associate with Polycystic Ovary Syndrome and Type 2 Diabetes Mellitus (**Supplemental Table 3**).

FANTOM-CAT catalog of human genes annotates *HMGA2-AS1* within the category of potentially protein-coding CAT gene class. The same gene is included within lncRNAs in NCBI and ENSEMBL. Given the complexity of transcript variants that we observed within this *locus* and the alternative expression in different cell types and during differentiation/response to external cues, we decided to further deepen this aspect and firstly analyzed the coding potential for each transcript variant individually. We took in consideration different tools based on RNA intrinsic characteristics (cPAT) or on phylogenetic conservation (RNACode, phyloCSF, and sORF ribose). Despite RNACode, phyloCSF and sORF ribose calculated no coding potential for all the transcript variants (**Supplemental Table 4**), cPAT calculated a significant coding potential for A2-AS1_C, A2-AS1_D, and A2-AS1_E (**Supplemental Table 5**), identifying A2-AS1_A, A2-AS1_B, A2-AS1_F, A2-AS1_G, A2-AS1_H, and A2-AS1_I as natural antisense lncRNAs. LncRNAs are poorly evolutionary conserved (41), thus tools based on comparative sequence analysis software, such as RNACode, phyloCSF, and sORF ribose could be less informative to predict coding potential than alignment-free programs as cPAT (42). Indeed, we analyzed the evolutionary conservation of *HMGA2-AS1* across 35 mammalian genomes using the EPO Multiple Alignment and we found that *HMGA2-AS1* DNA sequence was strongly and limitedly conserved in primates (**Supplemental Figure 2**), whereas no conservation was observed in other mammalian species suggesting an importance of *HMGA2-AS1* in this *Order* and supporting the results of cPAT. With these analyses we found a novel locus of natural antisense transcripts in *HMGA2* gene composed by six lncRNAs and three potentially coding transcripts.

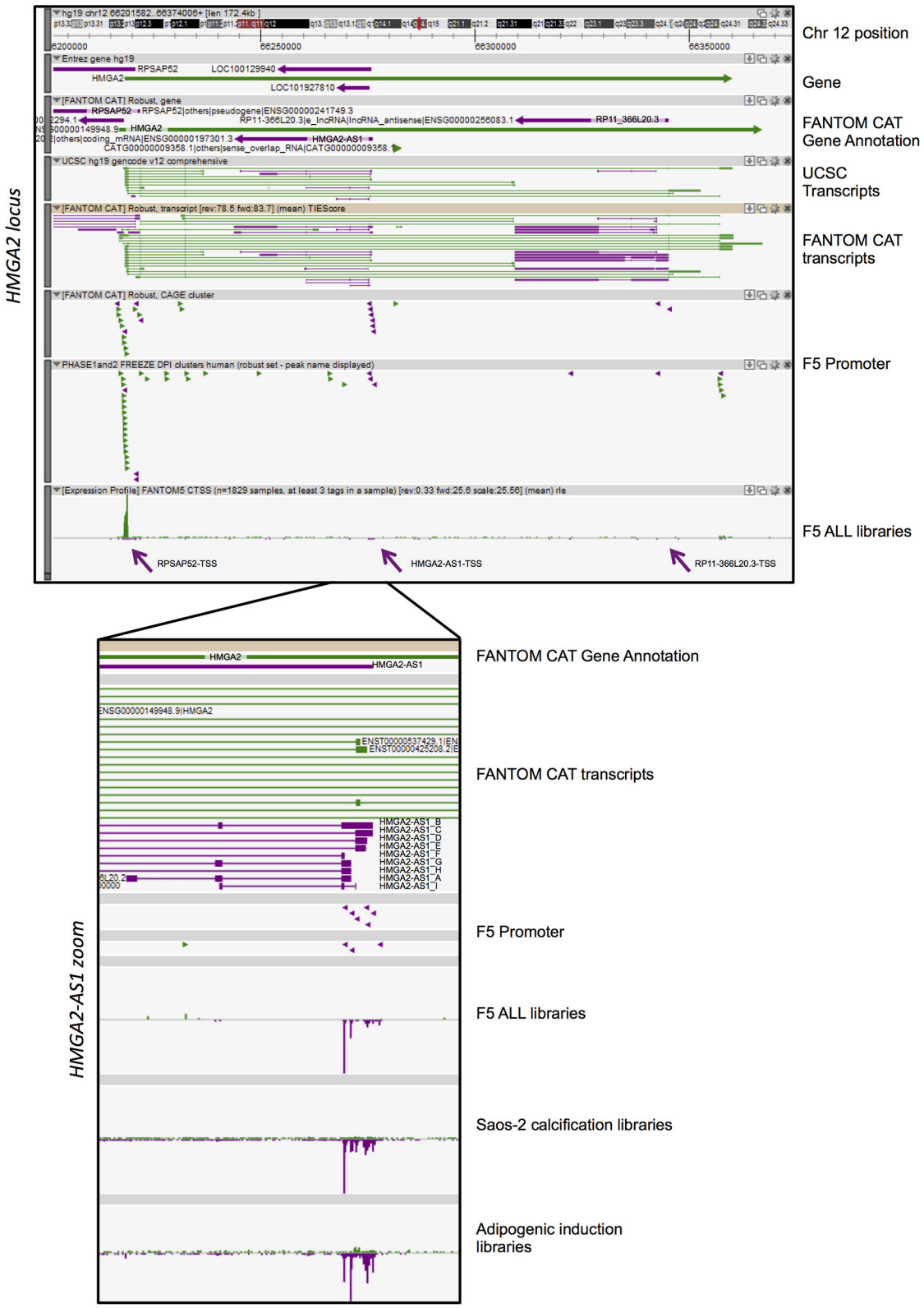

FIGURE 1 | FANTOM-CAT analyses reveal the presence of several natural antisense RNAs in *HMGA2 locus*. A Zenbu genome browser view of gene locus for human *HMGA2*. Genes and transcripts are color-coded according to their orientation in the genome (+ strand, green; – strand, purple). Upper panel reports from top to

(Continued)

FIGURE 1 | bottom: Genomic coordinates (Chr 12:66,201,582–66,374,008); NCBI Gene bodies; FANTOM-CAT Gene Annotation. Annotated UCSC transcripts and Robust FANTOM-CAT transcripts, with exon (thick lines) and intron (thin lines) boundaries. FANTOM5 promoters (robust CAT clusters and robust DPI) are indicated as arrowheads. Expression profile visualized as quantitative histogram by FANTOM5 CAGE TSS as the mean of rle (all libraries, $n = 1,829$ samples, at least three tag in a sample). Purple arrows pointed the TSS of RPSAP52, HMGA2-AS1, and RP11-366L20.3. Lower panel contains a zoom of ZENBU visualization of FANTOM-CAT analyses of HMGA2-AS1 natural antisense RNAs that localize in the first part of the HMGA2 third intron. The panel reports from top to bottom: FANTOM-CAT Gene Annotation; Robust FANTOM-CAT transcripts. We report transcript variant name, summarized in **Figure 2**. FANTOM5 promoters (robust CAT clusters and robust DPI) are indicated as arrowheads. Expression profile is reported as quantitative histogram in all FANTOM5 libraries (rle). Expression profile is shown as quantitative histogram derived from Dynamic expression in Saos-2 calcification and adipogenic induction libraries (tpm).

TABLE 1 | Expression parameters of HMGA2, RPSAP52, HMGA2-AS1, and RP11-366L20.3.

CAGE analysis	HMGA2	RPSAP52	HMGA2-AS1	RP11-366L20.3
Sum of expression (rle)	146,974.2	730.0	221.6	33.9
Positive expression number of libraries (%)	57	14	5	2
Highest signal (rle)	1,553.9	24.2	25.1	2.6
Mean of expression (rle)	140.8	2.9	2.5	1.0

HMGA2-AS1 Transcript Variants Are Expressed in Cancer Cell Lines

As a first step in characterizing the RNAs present in the *HMGA2-AS1 locus,* we analyzed their expression in human cell lines derived from breast (MDA-MB 231, MDA-MB 157), pancreatic (BX-PC3, PANC1), colon (SW480, HCT116), thyroid (ARO, TPC1), hepatic (HepG2, Hep3B), and prostatic (DU145, PC3) carcinoma. Given the complexity of the *locus* we subdivided HMGA2-AS1 transcripts in three detection-groups (Group ABGI, Group CDE, and Group FH) based on their common exons composition (**Figure 3A**), and we analyzed their expression by qRT-PCR. Results showed that all the groups of transcripts were expressed in several cell lines although at different levels (**Figure 3A**). The Group ABGI is the most expressed, whereas the Group CDE, which is composed by potential coding transcript variants, is almost undetectable in most cell lines (**Figure 3A**). Interestingly, in pancreatic tumors the highest expression of HMGA2-AS1 transcripts was found in PANC1 cell line, which is considered more aggressive than BX-PC3 (43–45). Similarly, we observed a higher expression of HMGA2-AS1 transcripts in prostatic cancer cell line PC3 with respect to DU145 cell line (**Figure 3A**). In this case PC3 cell line has also a behavior that indicates a more metastatic potential than DU145 cell line, in fact it exhibits a stellate phenotype in 3D culture instead of DU145 that is characterized by a 3D round structure (46). Considering the pro-tumorigenic role of HMGA2 in pancreatic and prostatic cancer (47–50), we checked HMGA2 mRNA and protein levels in these cell lines. Both HMGA2 mRNA and protein are more expressed in PANC1 and PC3 than BX-PC3 and DU145, respectively (**Figure 3B**) and, interestingly, HMGA2 expression parallels HMGA2-AS1 transcripts expression. Moreover, we observed a significant positive correlation between HMGA2 and HMGA2-AS1 expression in TCGA (The Cancer Genome Atlas) data derived from breast invasive carcinoma, colon adenocarcinoma, liver hepatocellular carcinoma, pancreatic adenocarcinoma, prostate adenocarcinoma, and thyroid carcinoma patient datasets (**Figure 3C**). Given these results, we reasoned about a possible role of HMGA2-AS1 transcripts in the modulation of HMGA2 expression and tumorigenesis focusing on the non-coding transcript variants (i.e., Group ABGI and Group FH).

Natural Antisense lncRNAs From *HMGA2-AS1 locus* Regulate HMGA2 Expression

Many evidences demonstrated that natural antisense lncRNAs could regulate their own sense genes, assuming a crucial role in pathological condition when their expression is impaired (51). We thus investigated whether HMGA2-AS1 natural antisense lncRNAs are involved in HMGA2 expression regulation. Firstly, we analyzed the expression of each transcript variants in PANC1 cell line demonstrating the presence of A2-AS1_G, A2-AS1_A, A2-AS1_I, and A2-AS1_H via qRT-PCR (**Figure 4A**). Since it was not possible to design suitable primers to analyze specifically A2-AS1_B, we performed classical RT-PCR able to amplify this transcript variant together with A2-AS1_G and A2-AS1_F/H. The amplified products were sequenced, confirming the expression of A2-AS1_G and A2-AS1_F/H and excluding the expression of A2-AS1_B (**Figure 4B**). Then, we silenced HMGA2-AS1 natural antisense lncRNAs in PANC1 with a small interfering RNA (siRNA) designed to target all transcript variants (siHMGA2-AS1-all) (**Figure 4C**). We observed a strong reduction of A2-AS1_H and A2-AS1_I amount and a slight decrease of the A2-AS1_A, surprisingly we detected an up-regulation of A2-AS1_G levels (**Figure 4D**), suggesting no inhibitory action on this transcript variant by siHMGA2-AS1-all. Concomitantly, we highlighted a strong reduction of HMGA2 mRNA and protein levels 72 h after siRNA transfection that was already detectable at 24 h (**Figure 4E**). Then, we used a second siRNA to confirm the results observed. Unfortunately, it was not possible to design a siRNA in a different region able to target all the four transcript variants analyzed with siHMGA2-AS1-all. Thus, we designed a siRNA, siHMGA2-AS1-AGI, able to target 3 out of the 4 transcript variants, i.e., A2-AS1_A, A2-AS1_G, and A2-AS1_I (**Supplemental Figure 3A**). We observed the silencing of A2-AS1_I and A2-AS1_A and the up-regulation of A2-AS1_G also with the second siRNA (**Supplemental Figure 3B**). Moreover, we confirmed the concomitant decrease of HMGA2 levels at 24 and 72 h both for mRNA and protein levels (**Supplemental Figure 3C**). The down-regulation of HMGA2 upon HMGA2-AS1 silencing, with both siRNAs, was also confirmed in PC3, a prostatic cancer cell line that exhibits

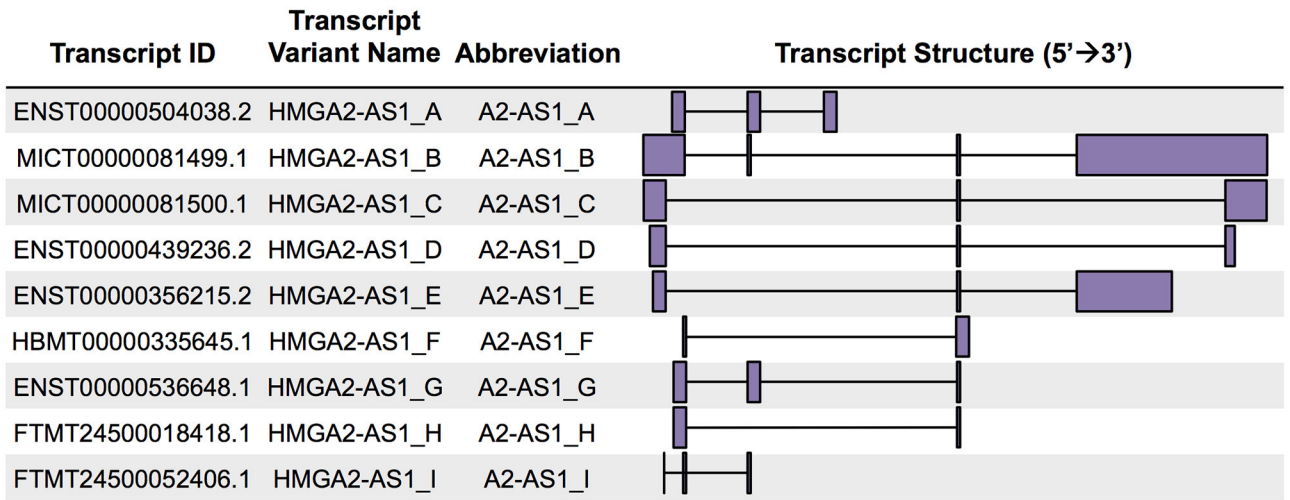

FIGURE 2 | HMGA2-AS1 natural antisense RNAs unraveled by FANTOM-CAT analysis. From left to right: transcript IDs reported in FANTOM-CAT; transcript variant names assigned in this work; abbreviations used throughout the text; and schematic representation (5′ 3′) of the HMGA2-AS1 transcripts.

high levels of HMGA2-AS1 (**Supplemental Figure 4A**). Since it was not possible to specifically target the A2-AS1_H with a second siRNA, on a different exon, without hitting A2-AS1_C, A2-AS1_D, and A2-AS1_E, we decided to assess its relevance in regulating HMGA2 expression overexpressing A2-AS1_H in PANC1 cells and we demonstrated that endogenous HMGA2 mRNA expression was up-regulated (**Supplemental Figure 4B**). As shown above (**Figure 4D** and **Supplemental Figure 3B**) upon siRNA treatment against HMGA2-AS1 we observed an unexpected up-regulation of A2-AS1_G. We are not able to explain this modulation, but we tested whether it could regulate HMGA2 expression. Therefore, we overexpressed A2-AS1_G in PANC1 cells and we did not detect any changes in HMGA2 expression levels, demonstrating that A2-AS1_G is not involved in HMGA2 regulation (**Supplemental Figure 4C**). This data clearly indicates the involvement of HMGA2-AS1 natural antisense lncRNAs, in particular A2-AS1_H, A2-AS1_I, and A2-AS1_A transcript variants, in HMGA2 gene expression regulation.

HMGA2-AS1 lncRNAs Are Involved in Cancer Promotion

The role of several lncRNAs in cancer onset and progression has been demonstrated (52), underlying that alteration in their expression could be crucial in this disease. Moreover, the involvement of HMGA2 in promoting cancer hallmarks connected with the tumorigenic processes is widely described (20, 28, 53). Therefore, we asked whether changes in the expression of HMGA2-AS1 natural antisense lncRNAs may have a role in the tumorigenic process, in particular we started analyzing cell proliferation. PANC1 cells were silenced (siHMGA2-AS1-all) or not (siCTRL) for the expression of HMGA2-AS1 natural antisense lncRNAs and cell growth was analyzed at different time points (24, 48, and 72 h). No difference in cell growth was observed in silenced with respect to control cells (**Figure 5A**). Despite PANC1 cells showed some epithelial features (54), upon HMGA2-AS1 silencing these characteristics were exacerbated. Indeed, cells were flatter exhibiting a cobblestone shape and cell culture appeared more organized (**Figure 5B**). In addition, we observed an increase of the epithelial marker E-Cadherin (**Figures 5C,D**). We analyzed also two mesenchymal markers, N-Cadherin and Vimentin, and while we did not observe changes at the RNA level (**Figure 5C**) we found a delocalization of N-Cadherin from cell membrane and a decreased perinuclear density of Vimentin (**Figure 5D**), which is connected to a decrease in cell motility (55). On the basis of these results and considering the involvement of HMGA2 in cell migration (24, 48, 56), we tested whether HMGA2-AS1 natural antisense lncRNAs were involved in this key tumor feature. Thus, we analyzed cell motility by transwell assay after siHMGA2-AS1-all treatment in PANC1 cells, highlighting a strong decrease in the ability of cells to move across the membrane pore (**Figure 5E**), suggesting an involvement of HMGA2-AS1 in metastatic process. All these results were confirmed silencing HMGA2-AS1 using the second siHMGA2-AS1-AGI (**Supplemental Figures 5A–D**). Moreover, we demonstrated the involvement of HMGA2-AS1 in cancer cell motility using PC3 cell line silenced with both siRNAs (**Supplemental Figure 6A**) and overexpressing A2-AS1_H transcript variant in BX-PC3 (**Supplemental Figures 6B,C**), a pancreatic cell line that we showed expressing low level of all HMGA2-AS1 transcript variants (see **Figure 3A**). Taking into account these results, we explored the relationship between HMGA2-AS1 and the prognosis of pancreatic adenocarcinoma patients in terms of overall-survival (OS). Kaplan-Meier analysis shows that a higher HMGA2-AS1 expression was associated with a shorter OS ($P = 0.03$) (**Figure 6A**). In addition, we observed in the same dataset an enrichment of HMGA2-AS1 expression in pathological Stage IV ($Pr \geq 0.035$) (**Figure 6B**). All these data clearly suggest a tumorigenesis function of HMGA2-AS1 in pancreatic cancer.

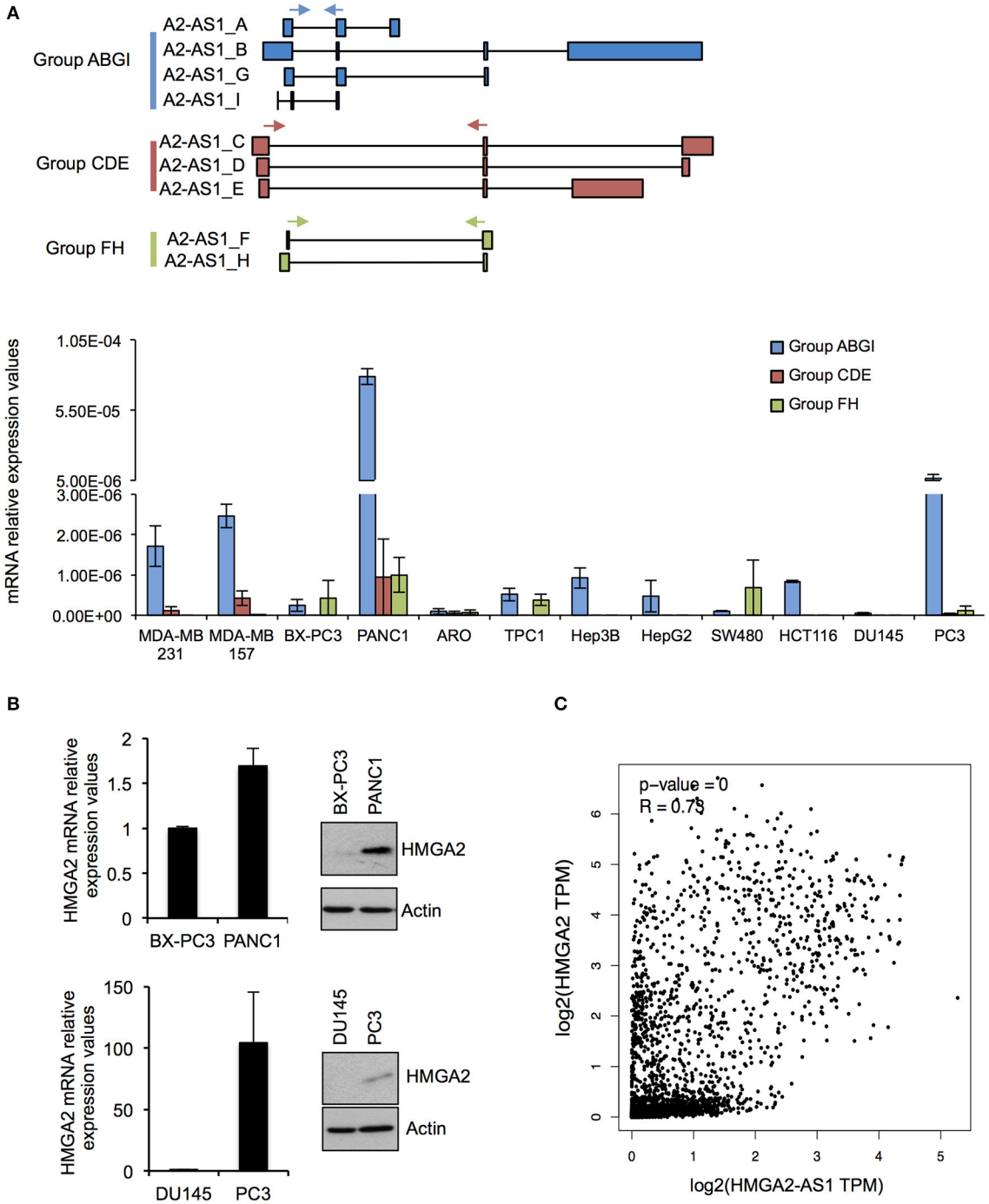

FIGURE 3 | HMGA2-AS1 transcript variants are expressed in cancer cell lines. **(A)** Upper part shows a schematic representation of primer localization (cyan, red and green arrows) used for amplifying HMGA2-AS1 transcript variants, grouped in Group ABGI (cyan), Group CDE (red), and Group FH (green). Lower part shows qRT-PCR analysis of the three transcript groups in a panel of cancer cell lines. 18S was used for normalization. Data are presented as the mean of 2∧–DCt ± range between replicates ($n = 2$). **(B)** qRT-PCR and western blot analyses of HMGA2 in BX-PC3, PANC1, DU145, and PC3 cancer cell lines. For qRT-PCR 18S was used for normalization. Data are presented as the mean ± range between replicates ($n = 2$). For protein analysis a representative western blot is reported. β-actin was used as loading control ($n = 2$). Also see uncropped figure scan in **Supplemental Images 1, 2**. **(C)** Plot of correlation of HMGA2 and HMGA2-AS1 expression in a TCGA dataset that includes BRCA (Breast invasive carcinoma), COAD (Colon adenocarcinoma), LIHC (Liver hepatocellular carcinoma), PAAD (Pancreatic adenocarcinoma), PRAD (Prostate adenocarcinoma), and THAC (Thyroid carcinoma) datasets. Data were presented in log2 scale and Spearman correlation coefficient was used.

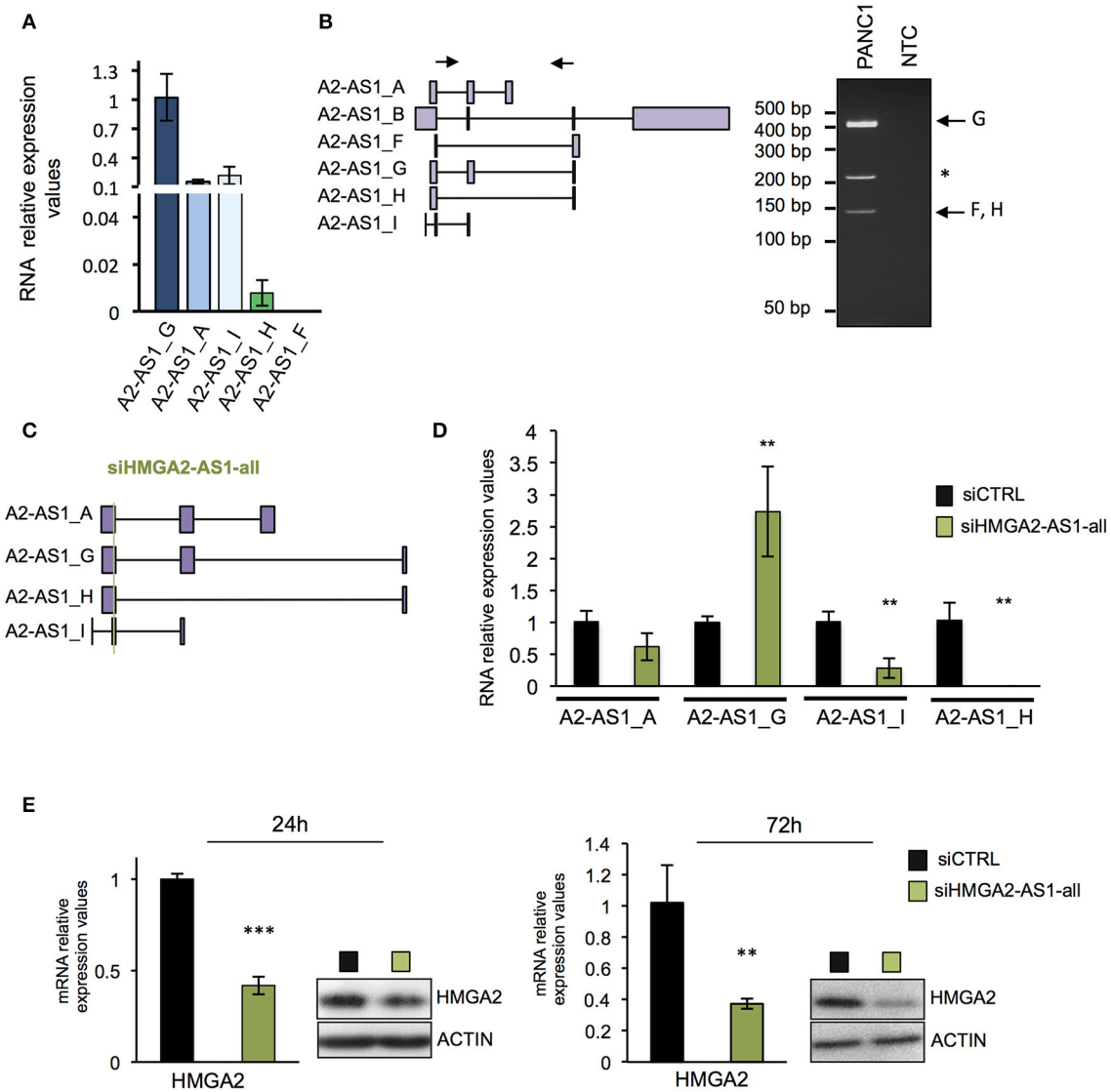

FIGURE 4 | Natural antisense lncRNAs from *HMGA2-AS1 locus* regulate HMGA2 expression. **(A)** qRT-PCR analyses of A2-AS1_G, A2-AS1_A, A2-AS1_I, A2-AS1_H, and A2-AS1_F expression in PANC1 cells. 18S was used for normalization; the data are compared to A2-AS1_G and are presented as the mean ± SD ($n = 4$). **(B)** Left part, schematic representation of primers localization used for amplifying A2-AS1_B, A2-AS1_F, A2-AS1_G, and A2-AS1_H via classical RT-PCR. Right panel shows representative RT-PCR amplification products, * indicates an unspecific product. NTC: no template control. **(C)** Schematic representation of siHMGA2-AS1-all targeting (green line) on each HMGA2-AS1 transcript variants. **(D)** Evaluation of the expression of different variants after siHMGA2-AS1-all transfection. qRT-PCR analysis of A2-AS1_A, A2-AS1_G, A2-AS1_I, and A2-AS1_H levels after 72 h of siHMGA2-AS1-all silencing in PANC1 cell line. 18S was used for normalization. The data are compared to siCTRL and are presented as the mean ± SD ($n = 3$), $^{**}p \leq 0.01$; two-tailed Student's *t*-test. **(E)** qRT-PCR and western blot analyses of HMGA2 in PANC1 cells silenced with siHMGA2-AS1-all for 24 and 72 h. For qRT-PCR GAPDH was used for normalization, the data are compared to siCTRL and are presented as the mean ± SD ($n = 3$), $^{**}p \leq 0.01$, $^{***}p \leq 0.001$; two-tailed Student's *t*-test. For protein analysis, a representative western blot is reported ($n = 3$). β-actin was used as a loading control. Also see uncropped figure scan in **Supplemental Images 3–6**.

HMGA2-AS1 lncRNAs Regulate Cell Migration Ability Through HMGA2

HMGA2 protein has a relevant and causal role in cancer onset and development, supporting metastatic process and its involvement in pancreatic cancer has been already described (48, 57). Exploring the relationship between HMGA2 and OS of pancreatic adenocarcinoma patients, we observed that higher HMGA2 expression was associated with a shorter OS ($P = 0.0013$) (**Figure 6C**), similarly to what observed for HMGA2-AS1 (**Figure 6A**), in addition, a trend in the increase of expression of HMGA2 through the different stages was found (**Figure 6D**). Our results show that natural antisense lncRNAs HMGA2-AS1 modulate motility of PANC1 cells and they regulate HMGA2 expression. We therefore asked whether the effect of HMGA2-AS1 on cell motility was mediated by HMGA2. To this aim, we silenced the expression

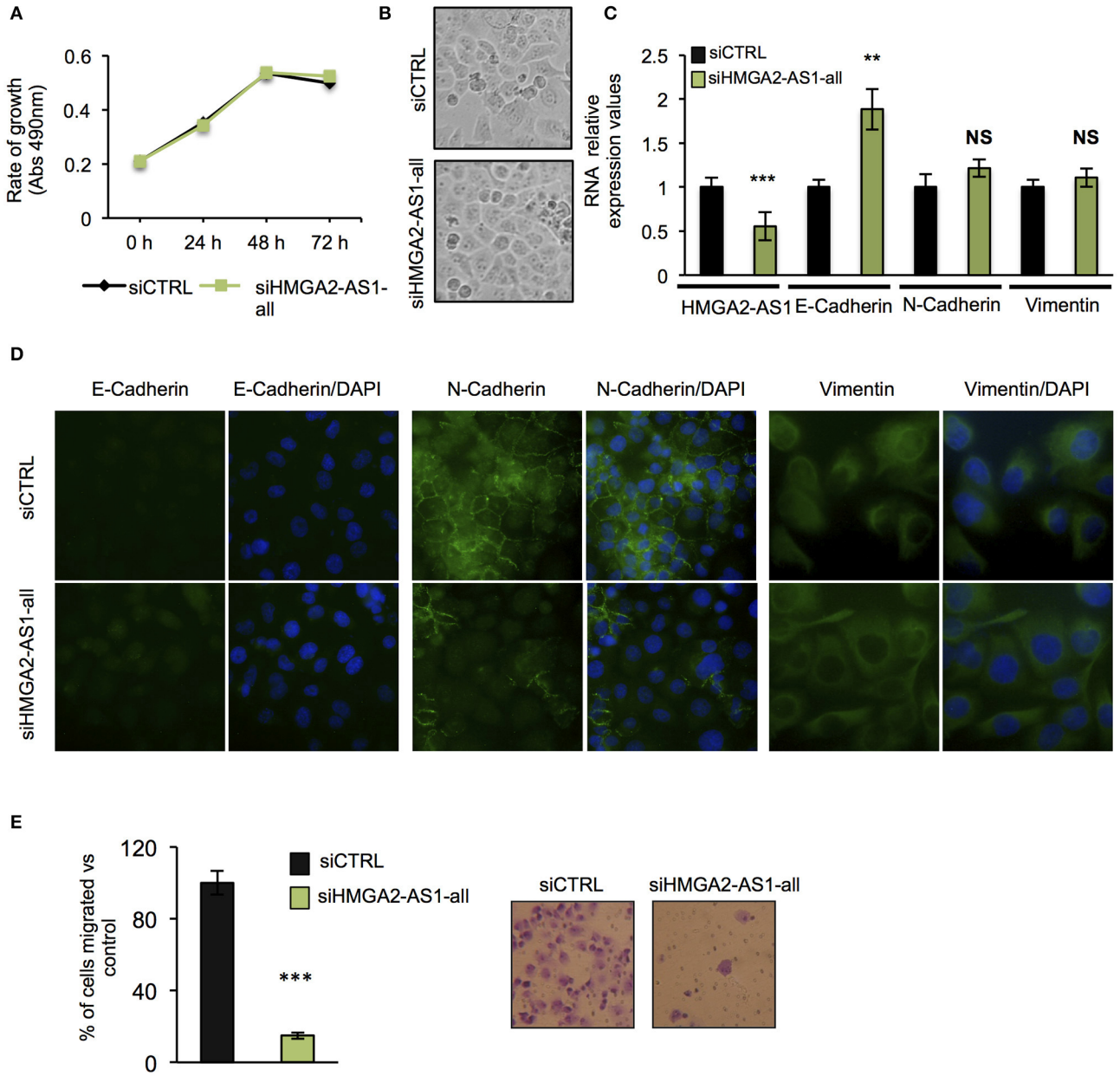

FIGURE 5 | Natural antisense lncRNAs from *HMGA2-AS1 locus* are involved in cancer promotion. **(A)** MTS proliferation assay in PANC1 cells silenced or not for HMGA2-AS1 transcript variants with siHMGA2-AS1-all. The data are presented as mean ± SD ($n = 4$). **(B)** Representative pictures of cell morphology of PANC1 cell culture in control condition and after 72 h of siHMGA2-AS1-all transfection. **(C)** qRT-PCR analysis of HMGA2-AS1, E-Cadherin, N-Cadherin, and Vimentin after 72 h of siHMGA2-AS1-all silencing in PANC1 cell line. Primers used to detect HMGA2-AS1 amplify together A2-AS1_A, A2-AS1_G, and A2-AS1_I. GAPDH was used for normalization. The data are compared to siCTRL and are presented as the mean ± SD ($n = 3$), $^{**}p \leq 0.01$, $^{***}p \leq 0.001$; two-tailed Student's *t*-test. **(D)** Representative immunofluorescence images of the epithelial marker E-Cadherin and the mesenchymal markers N-Cadherin and Vimentin localization in PANC1 control cells vs. cells silenced with siHMGA2-AS1-all. Images were taken at 40× magnification for E- and N-Cadherin and at 60× magnification for Vimentin. **(E)** Transwell assay of PANC1 cells silenced with siHMGA2-AS1-all for 72 h. On the left, quantification of the transwell assay. The data are represented as the mean of percentage of migrated cells respect to siCTRL ± SD ($n = 4$), $^{***}p \leq 0.001$; two-tailed Student's *t*-test. On the right, representative images of cells migrated across the porous membrane, stained with crystal violet.

of HMGA2-AS1 (siHMGA2-AS1-all) and we overexpressed HMGA2 (pEGFP-N1-HMGA2) to assess whether HMGA2 was able to rescue PANC1 cell migration abilities. Whereas PANC1 cells depleted for HMGA2-AS1 showed a strong decrease in cell migration compared to control, the overexpression of HMGA2 was able to completely rescue cell migration (**Figure 7**), demonstrating that HMGA2-AS1 are important players in tumorigenesis and that this function is mediated by HMGA2.

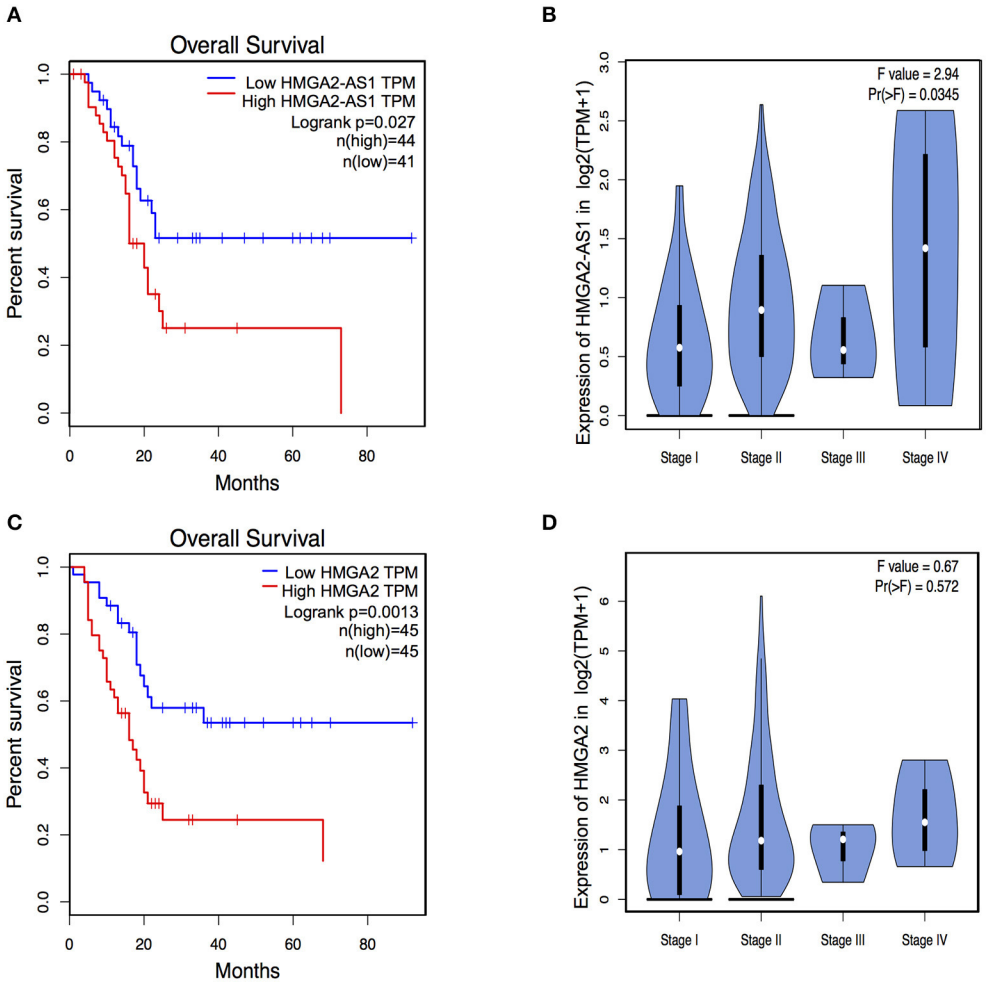

FIGURE 6 | HMGA2-AS1 and HMGA2 expression is relevant for Overall Survival (OS) in pancreatic cancer patients. **(A)** Kaplan–Meier survival curves of OS in a dataset of pancreatic adenocarcinomas patients. The patients were stratified based on the expression of HMGA2-AS1. **(B)** Violin plot of HMGA2-AS1 enrichment expression in pancreatic adenocarcinomas patients from PAAD dataset, subdivided accordingly to cancer stage. **(C)** Kaplan–Meier survival curves of OS in a dataset of pancreatic adenocarcinomas patients. The patients were stratified based on the expression of HMGA2. **(D)** Violin plot of HMGA2 enrichment expression in pancreatic adenocarcinomas patients from PAAD dataset, subdivided accordingly to cancer stage.

DISCUSSION

Deregulation of HMGA proteins in adult tissue is strictly associated with neoplastic transformation, in fact high expression levels of these proteins have been found in several types of tumor (19, 20, 58). Therefore, the fine modulation of their expression is crucial and several literature data underline that HMGA expression is controlled at different regulatory levels, from transcriptional to post-translational, and by several players (28, 59, 60). Remarkably, over the past decade, a large number of non-coding RNA molecules have been found to belong to the HMGA-expression control network (32, 60, 61). A key step derives from regulation operated by miRNA, considering that both HMGA1 and HMGA2 are targets of the tumor suppressor let-7 (62). However, the comprehension of HMGA expression regulation is still far from being completely understood.

Natural antisense lncRNAs are often expressed from cancer-associated gene *loci* together with the concordant expression of their own sense genes (63). In this context, antisense transcription is increasingly being recognized as a crucial regulator of sense gene expression in response to pathological stimuli. Therefore, with the aim to investigate the presence of sense and antisense transcripts pairing (S/AS pairs) in *HMGA loci* and the possible control of *HMGA* expression by antisense lncRNAs, we interrogated the FANTOM5 and FANTOM-CAT catalogs. FANTOM5 project enormously increased the number of ncRNA annotated, especially lncRNA, generating a comprehensive atlas of 27,919 human lncRNA genes (40). Now, a huge effort is required to understand the function of these lncRNAs. Indeed, recently, it has been demonstrated the relevance of antisense transcription in *loci* associated with hereditary neurodegenerative disease, providing evidences

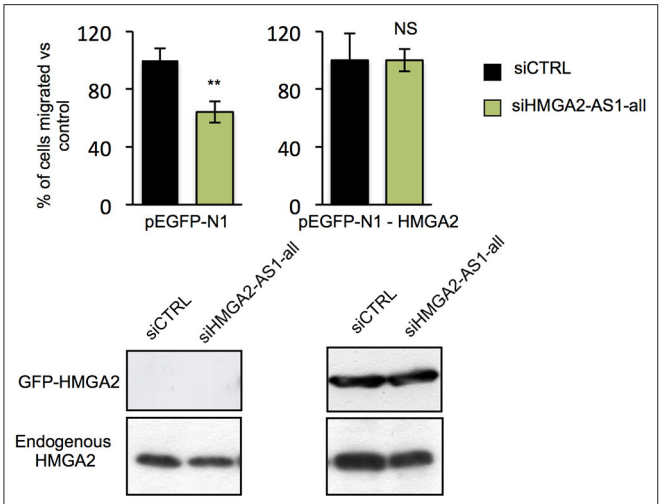

FIGURE 7 | HMGA2-AS1 lncRNAs regulate cell migration ability through HMGA2. Transwell assay in PANC1 cells transfected with empty vector (pEGFP-N1) or with a vector expressing HMGA2 (pEGFP-N1-HMGA2), treated with siCTRL or siHMGA2-AS1-all. The data are presented in pEGFP-N1 and in pEGFP-N1-HMGA2 conditions as the mean of the percentage of siHMGA2-AS1-all migrated cells relative to the siCTRL ± SD ($n = 3$) set to 100% in each condition. Lower part, a representative western blot of HMGA2 overexpression and endogenous protein is presented. β-actin was used as a loading control. $^{**}p \leq 0.01$, NS: Not Significant; two-tailed Student's *t*-test. Also see uncropped figure scan in **Supplemental Images 7–9**.

for the existence of additional regulatory mechanisms of the expression of neurodegenerative disease-causing genes (64).

Here, we show a complex picture of antisense transcription in *HMGA2* gene, increasing the number of molecules possibly involved in HMGA2 expression regulation, while *HMGA1 locus* exhibited a lower antisense transcription. Among antisense transcription genes in *HMGA2 locus,* we have found the previously characterized head-to-head natural antisense lncRNA RPSAP52 (33–35). In this study, in addition to RPSAP52, we provide, for the first time to our knowledge, evidences for the existence of previously unknown natural antisense lncRNAs within *HMGA2* gene with a function in HMGA2 expression regulation and neoplastic transformation. Indeed, our analyses on FANTOM-CAT data revealed robust antisense transcriptional activity concentrated in the third intron of *HMGA2* gene and several uncharacterized transcript variants (HMGA2-AS1_A-I) associated. Dynamic expression analysis of FANTOM5 samples showed that transcription of *HMGA2-AS1* gene is significantly up-regulated during mesenchymal stem cells differentiation to adipocyte and down-regulated throughout Saos-2 calcification similarly to what happens for *HMGA2*, suggesting a coordinated role of both genes in these processes. Notably, this observation fits very well with the well-studied role of *HMGA2* in adipogenesis and osteogenesis (65–67).

We demonstrated that some HMGA2-AS1 variants are expressed in different cancer cell lines, in particular in cells from pancreatic adenocarcinoma. Moreover, we found that HMGA2-AS1 positively correlated with HMGA2 expression in a TCGA dataset of cancer patients, and, in *in vitro* experiments, we demonstrated that HMGA2-AS1 increased HMGA2 expression. Given the relevance of fine regulation of HMGA2 expression for a normal development and a correct tissue homeostasis and considering the role of natural antisense lncRNAs in sense-gene expression regulation, the identification of these novel natural antisense lncRNAs can have significant implications in studying cancer pathogenesis. Interestingly, we found that HMGA2-AS1 promoted changes in the expression and localization of markers involved in cell-cell adhesion that support the HMGA2-mediated modulation of cell motility observed in PANC1 cells. These *in vitro* observations of the role of HMGA2-AS1 in promoting pancreatic neoplastic transformation are further reinforced by primary tumor data, showing that HMGA2-AS1 is enriched in patients with high-grade pancreatic adenocarcinoma and its high expression level correlated with poor prognosis in cancer patients.

It is still an open question how HMGA2-AS1 can regulate HMGA2 expression. Natural antisense lncRNAs can modulate their own sense gene expression at multiple levels (68). Indeed, these molecules can regulate the transcription of sense genes by controlling the epigenetic state (69–71), by forming DNA:RNA hybrids (33) or by competing for the same promoter (68, 72, 73). S/AS pairs, instead, mainly mediate post-transcriptional and translational regulation. In fact, S/AS pairs regulate RNA maturation and stability by establishing a physical obstruction to regulatory factors that induces splicing (74) or by influencing RNA stability (63, 75–77). At translational level, antisense transcript lncRNAs can compete with sense RNA for translation initiation factor (78) or induce translation by 5′UTR sense RNA binding (38, 79). Notably, using the RNAup package (80, 81), we observed a 16 nucleotides region of hybridization, localized in the 5′UTR of HMGA2 and in the common exon of natural antisense lncRNAs transcribed by *HMGA2-AS1 locus*, suggesting the existence of a possible HMGA2-AS1:HMGA2 mRNA interaction. Further studies will be needed to clarify if HMGA2-AS1 regulates HMGA2 expression through S/AS pairs.

In conclusion, the present study adds a further level of complexity to the regulation of HMGA2 expression in cancer and, considering the huge amount of data derived from the high-throughput sequencing era, it contributes to increase our knowledge of the function of lncRNAs in regulating cellular functions.

DATA AVAILABILITY STATEMENT

Publicly available datasets were analyzed in this study. This data can be found here: http://fantom.gsc.riken.jp/cat/, http://gepia.cancer-pku.cn/.

AUTHOR CONTRIBUTIONS

GR performed most of the experiments. GR and SP analyzed the data. PD performed the experiments on the function of HMGA2-AS1 in cancer cells. GR, SP, SZ, GM, RS, and SG provided the intellectual input and revised the manuscript. GR, SP, and SZ

conceptualized and designed the study. GM and SP supervised the study. GR, SP, and GM wrote the manuscript. All authors read and approved the final version of this manuscript.

FUNDING

This work was supported from Associazione Italiana per la Ricerca sul Cancro (AIRC, IG18385) and Regione Friuli Venezia Giulia (TNBCneo and RiFT) to GM.

DEDICATION

This work was dedicated to the memory of Silvia Zucchelli, who supervised the research and enthusiastically contributed to the data discussion and interpretation of the results.

ACKNOWLEDGMENTS

We thank Francesca Fasolo and Carlotta Bon for helpful discussions. We were grateful to Ilaria Persico and Valerio Mignucci for technical assistance. GR would like to thank the inspiring mentoring of who dedicated his/her own time to teach and discuss of science.

SUPPLEMENTARY MATERIAL

The Supplementary Material for this article can be found online at: https://www.frontiersin.org/articles/10.3389/fonc.2019.01526/full#supplementary-material

Supplemental Images 1–9 | Full scans of western blots.

REFERENCES

1. Mattick JS. The functional genomics of noncoding RNA. *Science.* (2005) 309:1527–8. doi: 10.1126/science.1117806
2. Cech TR, Steitz JA. The noncoding RNA revolution-trashing old rules to forge new ones. *Cell.* (2014) 157:77–94. doi: 10.1016/j.cell.2014.03.008
3. Consortium F, CLST RP, Forrest AR, Kawaji H, Rehli M, Baillie JK, et al. A promoter-level mammalian expression atlas. *Nature.* (2014) 507:462–70. doi: 10.1038/nature13182
4. Prensner JR, Chinnaiyan AM. The emergence of lncRNAs in cancer biology. *Cancer Discov.* (2011) 1:391–407. doi: 10.1158/2159-8290.CD-11-0209
5. Carninci P, Kasukawa T, Katayama S, Gough J, Frith MC, Maeda N, et al. The transcriptional landscape of the mammalian genome. *Science.* (2005) 309:1559–63. doi: 10.1126/science.1112014
6. Mercer TR, Dinger ME, Mattick JS. Long non-coding RNAs: insights into functions. *Nat Rev Genet.* (2009) 10:155–9. doi: 10.1038/nrg2521
7. Ponting CP, Oliver PL, Reik W. Evolution and functions of long noncoding RNAs. *Cell.* (2009) 136:629–41. doi: 10.1016/j.cell.2009.02.006
8. Hon CC, Ramilowski JA, Harshbarger J, Bertin N, Rackham OJ, Gough J, et al. An atlas of human long non-coding RNAs with accurate 5′ ends. *Nature.* (2017) 543:199–204. doi: 10.1038/nature21374
9. Katayama S, Tomaru Y, Kasukawa T, Waki K, Nakanishi M, Nakamura M, et al. Antisense transcription in the mammalian transcriptome. *Science.* (2005) 309:1564–6. doi: 10.1126/science.1112009
10. Faghihi MA, Wahlestedt C. Regulatory roles of natural antisense transcripts. *Nat Rev Mol Cell Biol.* (2009) 10:637–43. doi: 10.1038/nrm2738
11. Derrien T, Johnson R, Bussotti G, Tanzer A, Djebali S, Tilgner H, et al. The GENCODE v7 catalog of human long noncoding RNAs: analysis of their gene structure, evolution, and expression. *Genome Res.* (2012) 22:1775–89. doi: 10.1101/gr.132159.111
12. Kanamori-Katayama M, Itoh M, Kawaji H, Lassmann T, Katayama S, Kojima M, et al. Unamplified cap analysis of gene expression on a single-molecule sequencer. *Genome Res.* (2011) 21:1150–9. doi: 10.1101/gr.115469.110
13. de Rie D, Abugessaisa I, Alam T, Arner E, Arner P, Ashoor H, et al. An integrated expression atlas of miRNAs and their promoters in human and mouse. *Nat Biotechnol.* (2017) 35:872–8. doi: 10.1038/nbt.3947
14. Reeves R. High mobility group (HMG) proteins: Modulators of chromatin structure and DNA repair in mammalian cells. *DNA Repair (Amst).* (2015) 36:122–36. doi: 10.1016/j.dnarep.2015.09.015
15. Sumter TF, Xian L, Huso T, Koo M, Chang YT, Almasri TN, et al. The high mobility group A1 (HMGA1) transcriptome in cancer and development. *Curr Mol Med.* (2016) 16:353–93. doi: 10.2174/1566524016666160316152147
16. Munshi N, Agalioti T, Lomvardas S, Merika M, Chen G, Thanos D. Coordination of a transcriptional switch by HMGI(Y) acetylation. *Science.* (2001) 293:1133–6. doi: 10.1126/science.293.5532.1133
17. Sgarra R, Zammitti S, Lo Sardo A, Maurizio E, Arnoldo L, Pegoraro S, et al. HMGA molecular network: From transcriptional regulation to chromatin remodeling. *Biochim Biophys Acta.* (2010) 1799:37–47. doi: 10.1016/j.bbagrm.2009.08.009
18. Reeves R. Nuclear functions of the HMG proteins. *Biochim Biophys Acta.* (2010) 1799:3–14. doi: 10.1016/j.bbagrm.2009.09.001
19. Sgarra R, Rustighi A, Tessari MA, Di Bernardo J, Altamura S, Fusco A, et al. Nuclear phosphoproteins HMGA and their relationship with chromatin structure and cancer. *FEBS Lett.* (2004) 574:1–8. doi: 10.1016/j.febslet.2004.08.013
20. Fusco A, Fedele M. Roles of HMGA proteins in cancer. *Nat Rev Cancer.* (2007) 7:899–910. doi: 10.1038/nrc2271
21. Thuault S, Valcourt U, Petersen M, Manfioletti G, Heldin CH, Moustakas A. Transforming growth factor-beta employs HMGA2 to elicit epithelial-mesenchymal transition. *J Cell Biol.* (2006) 174:175–83. doi: 10.1083/jcb.200512110
22. Cleynen I, Van de Ven WJ. The HMGA proteins: a myriad of functions (Review). *Int J Oncol.* (2008) 32:289–305. doi: 10.3892/ijo.32.2.289
23. Pfannkuche K, Summer H, Li O, Hescheler J, Droge P. The high mobility group protein HMGA2: a co-regulator of chromatin structure and pluripotency in stem cells? *Stem Cell Rev.* (2009) 5:224–30. doi: 10.1007/s12015-009-9078-9
24. Morishita A, Zaidi MR, Mitoro A, Sankarasharma D, Szabolcs M, Okada Y, et al. HMGA2 is a driver of tumor metastasis. *Cancer Res.* (2013) 73:4289–99. doi: 10.1158/0008-5472.CAN-12-3848
25. Pegoraro S, Ros G, Piazza S, Sommaggio R, Ciani Y, Rosato A, et al. HMGA1 promotes metastatic processes in basal-like breast cancer regulating EMT and stemness. *Oncotarget.* (2013) 4:1293–308. doi: 10.18632/oncotarget.1136
26. Pegoraro S, Ros G, Ciani Y, Sgarra R, Piazza S, Manfioletti G. A novel HMGA1-CCNE2-YAP axis regulates breast cancer aggressiveness. *Oncotarget.* (2015) 6:19087–101. doi: 10.18632/oncotarget.4236
27. Maurizio E, Wisniewski JR, Ciani Y, Amato A, Arnoldo L, Penzo C, et al. Translating proteomic into functional data: an high mobility group A1 (HMGA1) proteomic signature has prognostic value in breast cancer. *Mol Cell Proteomics.* (2016) 15:109–23. doi: 10.1074/mcp.M115.050401
28. Sgarra R, Pegoraro S, Ros G, Penzo C, Chiefari E, Foti D, et al. High mobility group A (HMGA) proteins: molecular instigators of breast cancer onset and progression. *Biochim Biophys Acta Rev Cancer.* (2018) 1869:216–29. doi: 10.1016/j.bbcan.2018.03.001
29. Penzo C, Arnoldo L, Pegoraro S, Petrosino S, Ros G, Zanin R, et al. HMGA1 modulates gene transcription sustaining a tumor signalling pathway acting on the epigenetic status of triple-negative breast cancer cells. *Cancers (Basel).* (2019) 11:1105. doi: 10.3390/cancers11081105
30. Zanin R, Pegoraro S, Ros G, Ciani Y, Piazza S, Bossi F, et al. HMGA1 promotes breast cancer angiogenesis supporting the stability, nuclear localization and transcriptional activity of FOXM1. *J Exp Clin Cancer Res.* (2019) 38:313. doi: 10.1186/s13046-019-1307-8
31. Cleynen I, Huysmans C, Sasazuki T, Shirasawa S, Van de Ven W, Peeters K. Transcriptional control of the human high mobility group A1 gene:

basal and oncogenic Ras-regulated expression. *Cancer Res.* (2007) 67:4620–9. doi: 10.1158/0008-5472.CAN-06-4325
32. Hammond SM, Sharpless NE. HMGA2, microRNAs, and stem cell aging. *Cell.* (2008) 135:1013–6. doi: 10.1016/j.cell.2008.11.026
33. Boque-Sastre R, Soler M, Oliveira-Mateos C, Portela A, Moutinho C, Sayols S, et al. Head-to-head antisense transcription and R-loop formation promotes transcriptional activation. *Proc Natl Acad Sci USA.* (2015) 112:5785–90. doi: 10.1073/pnas.1421197112
34. D'Angelo D, Mussnich P, Sepe R, Raia M, Del Vecchio L, Cappabianca P, et al. RPSAP52 lncRNA is overexpressed in pituitary tumors and promotes cell proliferation by acting as miRNA sponge for HMGA proteins. *J Mol Med.* (2019) 97:1019–32. doi: 10.1007/s00109-019-01789-7
35. Oliveira-Mateos C, Sanchez-Castillo A, Soler M, Obiols-Guardia A, Pineyro D, Boque-Sastre R, et al. The transcribed pseudogene RPSAP52 enhances the oncofetal HMGA2-IGF2BP2-RAS axis through LIN28B-dependent and independent let-7 inhibition. *Nat Commun.* (2019) 10:3979. doi: 10.1038/s41467-019-11910-6
36. Cattaruzzi G, Altamura S, Tessari MA, Rustighi A, Giancotti V, Pucillo C, et al. The second AT-hook of the architectural transcription factor HMGA2 is determinant for nuclear localization and function. *Nucleic Acids Res.* (2007) 35:1751–60. doi: 10.1093/nar/gkl1106
37. Bozzo M, Macri S, Calzia D, Sgarra R, Manfioletti G, Ramoino P, et al. The HMGA gene family in chordates: evolutionary perspectives from amphioxus. *Dev Genes Evol.* (2017) 227:201–11. doi: 10.1007/s00427-017-0581-8
38. Zucchelli S, Cotella D, Takahashi H, Carrieri C, Cimatti L, Fasolo F, et al. SINEUPs: a new class of natural and synthetic antisense long non-coding RNAs that activate translation. *RNA Biol.* (2015) 12:771–9. doi: 10.1080/15476286.2015.1060395
39. Tang Z, Li C, Kang B, Gao G, Li C, Zhang Z. GEPIA: a web server for cancer and normal gene expression profiling and interactive analyses. *Nucleic Acids Res.* (2017) 45:W98–102. doi: 10.1093/nar/gkx247
40. Lizio M, Harshbarger J, Shimoji H, Severin J, Kasukawa T, Sahin S, et al. Gateways to the FANTOM5 promoter level mammalian expression atlas. *Genome Biol.* (2015) 16:22. doi: 10.1186/s13059-014-0560-6
41. Johnsson P, Morris KV. Expanding the functional role of long noncoding RNAs. *Cell Res.* (2014) 24:1284–5. doi: 10.1038/cr.2014.104
42. Wang L, Park HJ, Dasari S, Wang S, Kocher JP, Li W. CPAT: coding-potential assessment tool using an alignment-free logistic regression model. *Nucleic Acids Res.* (2013) 41:e74. doi: 10.1093/nar/gkt006
43. Deer EL, Gonzalez-Hernandez J, Coursen JD, Shea JE, Ngatia J, Scaife CL, et al. Phenotype and genotype of pancreatic cancer cell lines. *Pancreas.* (2010) 39:425–35. doi: 10.1097/MPA.0b013e3181c15963
44. Maupin KA, Sinha A, Eugster E, Miller J, Ross J, Paulino V, et al. Glycogene expression alterations associated with pancreatic cancer epithelial-mesenchymal transition in complementary model systems. *PLoS ONE.* (2010) 5:e13002. doi: 10.1371/journal.pone.0013002
45. Kopantzev EP, Kopantseva MR, Grankina EV, Mikaelyan A, Egorov VI, Sverdlov ED. Activation of IGF/IGF-IR signaling pathway fails to induce epithelial-mesenchymal transition in pancreatic cancer cells. *Pancreatology.* (2019) 19:390–6. doi: 10.1016/j.pan.2019.01.010
46. Harma V, Virtanen J, Makela R, Happonen A, Mpindi JP, Knuuttila M, et al. A comprehensive panel of three-dimensional models for studies of prostate cancer growth, invasion and drug responses. *PLoS ONE.* (2010) 5:e10431. doi: 10.1371/journal.pone.0010431
47. Abe N, Watanabe T, Suzuki Y, Matsumoto N, Masaki T, Mori T, et al. An increased high-mobility group A2 expression level is associated with malignant phenotype in pancreatic exocrine tissue. *Br J Cancer.* (2003) 89:2104–9. doi: 10.1038/sj.bjc.6601391
48. Watanabe S, Ueda Y, Akaboshi S, Hino Y, Sekita Y, Nakao M. HMGA2 maintains oncogenic RAS-induced epithelial-mesenchymal transition in human pancreatic cancer cells. *Am J Pathol.* (2009) 174:854–68. doi: 10.2353/ajpath.2009.080523
49. Shi Z, Li X, Wu D, Tang R, Chen R, Xue S, et al. Silencing of HMGA2 suppresses cellular proliferation, migration, invasion, and epithelial-mesenchymal transition in bladder cancer. *Tumour Biol.* (2016) 37:7515–23. doi: 10.1007/s13277-015-4625-2
50. Hawsawi O, Henderson V, Burton LJ, Dougan J, Nagappan P, Odero-Marah V. High mobility group A2 (HMGA2) promotes EMT via MAPK pathway in prostate cancer. *Biochem Biophys Res Commun.* (2018) 504:196–202. doi: 10.1016/j.bbrc.2018.08.155
51. Yang G, Lu X, Yuan L. LncRNA: a link between RNA and cancer. *Biochim Biophys Acta.* (2014) 1839:1097–109. doi: 10.1016/j.bbagrm.2014.08.012
52. Sanchez Calle A, Kawamura Y, Yamamoto Y, Takeshita F, Ochiya T. Emerging roles of long non-coding RNA in cancer. *Cancer Sci.* (2018) 109:2093–100. doi: 10.1111/cas.13642
53. Pallante P, Sepe R, Puca F, Fusco A. High mobility group a proteins as tumor markers. *Front Med.* (2015) 2:15. doi: 10.3389/fmed.2015.00015
54. Haque I, Mehta S, Majumder M, Dhar K, De A, McGregor D, et al. Cyr61/CCN1 signaling is critical for epithelial-mesenchymal transition and stemness and promotes pancreatic carcinogenesis. *Mol Cancer.* (2011) 10:8. doi: 10.1186/1476-4598-10-8
55. Jiu Y, Lehtimäki J, Tojkander S, Varjosalo M, Eriksson JE, Lappalainen P, et al. Bidirectional interplay between vimentin intermediate filaments and contractile actin stress fibers. *Cell Rep.* (2015) 11:1511–8. doi: 10.1016/j.celrep.2015.05.008
56. Tan EJ, Kahata K, Idas O, Thuault S, Heldin CH, Moustakas A. The high mobility group A2 protein epigenetically silences the Cdh1 gene during epithelial-to-mesenchymal transition. *Nucleic Acids Res.* (2015) 43:162–78. doi: 10.1093/nar/gku1293
57. Piscuoglio S, Zlobec I, Pallante P, Sepe R, Esposito F, Zimmermann A, et al. HMGA1 and HMGA2 protein expression correlates with advanced tumour grade and lymph node metastasis in pancreatic adenocarcinoma. *Histopathology.* (2012) 60:397–404. doi: 10.1111/j.1365-2559.2011.04121.x
58. Zhou X, Chada K. HMGI family proteins: architectural transcription factors in mammalian development and cancer. *Keio J Med.* (1998) 47:73–7. doi: 10.2302/kjm.47.73
59. Fedele M, Fusco A. HMGA and cancer. *Biochim Biophys Acta.* (2010) 1799:48–54. doi: 10.1016/j.bbagrm.2009.11.007
60. D'Angelo D, Esposito F, Fusco A. Epigenetic mechanisms leading to overexpression of HMGA proteins in human pituitary adenomas. *Front Med.* (2015) 2:39. doi: 10.3389/fmed.2015.00039
61. Balzeau J, Menezes MR, Cao S, Hagan JP. The LIN28/let-7 Pathway in Cancer. *Front Genet.* (2017) 8:31. doi: 10.3389/fgene.2017.00031
62. Lee YS, Dutta A. The tumor suppressor microRNA let-7 represses the HMGA2 oncogene. *Genes Dev.* (2007) 21:1025–30. doi: 10.1101/gad.1540407
63. Jadaliha M, Gholamalamdari O, Tang W, Zhang Y, Petracovici A, Hao Q, et al. A natural antisense lncRNA controls breast cancer progression by promoting tumor suppressor gene mRNA stability. *PLoS Genet.* (2018) 14:e1007802. doi: 10.1371/journal.pgen.1007802
64. Zucchelli S, Fedele S, Vatta P, Calligaris R, Heutink P, Rizzu P, et al. Antisense transcription in loci associated to hereditary neurodegenerative diseases. *Mol Neurobiol.* (2019) 56:5392–415. doi: 10.1007/s12035-018-1465-2
65. Ashar HR, Chouinard RAJr, Dokur M, Chada K. *In vivo* modulation of HMGA2 expression. *Biochim Biophys Acta.* (2010) 1799:55–61. doi: 10.1016/j.bbagrm.2009.11.013
66. Ullah M, Stich S, Notter M, Eucker J, Sittinger M, Ringe J. Transdifferentiation of mesenchymal stem cells-derived adipogenic-differentiated cells into osteogenic- or chondrogenic-differentiated cells proceeds via dedifferentiation and have a correlation with cell cycle arresting and driving genes. *Differentiation.* (2013) 85:78–90. doi: 10.1016/j.diff.2013.02.001
67. Wei J, Li H, Wang S, Li T, Fan J, Liang X, et al. let-7 enhances osteogenesis and bone formation while repressing adipogenesis of human stromal/mesenchymal stem cells by regulating HMGA2. *Stem Cells Dev.* (2014) 23:1452–63. doi: 10.1089/scd.2013.0600
68. Wight M, Werner A. The functions of natural antisense transcripts. *Essays Biochem.* (2013) 54:91–101. doi: 10.1042/bse0540091
69. Popov N, Gil J. Epigenetic regulation of the INK4b-ARF-INK4a locus: in sickness and in health. *Epigenetics.* (2010) 5:685–90. doi: 10.4161/epi.5.8.12996
70. Kotake Y, Nakagawa T, Kitagawa K, Suzuki S, Liu N, Kitagawa M, et al. Long non-coding RNA ANRIL is required for the PRC2 recruitment to and silencing of p15(INK4B) tumor suppressor gene. *Oncogene.* (2011) 30:1956–62. doi: 10.1038/onc.2010.568
71. Magistri M, Faghihi MA, St Laurent G III, Wahlestedt C. Regulation of chromatin structure by long noncoding RNAs: focus on natural antisense transcripts. *Trends Genet.* (2012) 28:389–96. doi: 10.1016/j.tig.2012.03.013

72. Shearwin KE, Callen BP, Egan JB. Transcriptional interference–a crash course. *Trends Genet.* (2005) 21:339–45. doi: 10.1016/j.tig.2005.04.009
73. Osato N, Suzuki Y, Ikeo K, Gojobori T. Transcriptional interferences in cis natural antisense transcripts of humans and mice. *Genetics.* (2007) 176:1299–306. doi: 10.1534/genetics.106.069484
74. Hastings ML, Ingle HA, Lazar MA, Munroe SH. Post-transcriptional regulation of thyroid hormone receptor expression by cis-acting sequences and a naturally occurring antisense RNA. *J Biol Chem.* (2000) 275:11507–13. doi: 10.1074/jbc.275.15.11507
75. Beltran M, Puig I, Pena C, Garcia JM, Alvarez AB, Pena R, et al. A natural antisense transcript regulates Zeb2/Sip1 gene expression during Snail1-induced epithelial-mesenchymal transition. *Genes Dev.* (2008) 22:756–69. doi: 10.1101/gad.455708
76. Faghihi MA, Modarresi F, Khalil AM, Wood DE, Sahagan BG, Morgan TE, et al. Expression of a noncoding RNA is elevated in Alzheimer's disease and drives rapid feed-forward regulation of beta-secretase. *Nat Med.* (2008) 14:723–30. doi: 10.1038/nm1784
77. Latge G, Poulet C, Bours V, Josse C, Jerusalem G. Natural antisense transcripts: molecular mechanisms and implications in breast cancers. *Int J Mol Sci.* (2018) 19:123. doi: 10.3390/ijms19010123
78. Ebralidze AK, Guibal FC, Steidl U, Zhang P, Lee S, Bartholdy B, et al. PU.1 expression is modulated by the balance of functional sense and antisense RNAs regulated by a shared cis-regulatory element. *Genes Dev.* (2008) 22:2085–92. doi: 10.1101/gad.1654808
79. Carrieri C, Cimatti L, Biagioli M, Beugnet A, Zucchelli S, Fedele S, et al. Long non-coding antisense RNA controls Uchl1 translation through an embedded SINEB2 repeat. *Nature.* (2012) 491:454–7. doi: 10.1038/nature11508
80. Hofacker IL. RNA secondary structure analysis using the Vienna RNA package. *Curr Protoc Bioinformatics.* (2004) 4: 12.2.1–12. doi: 10.1002/0471250953.bi1202s04
81. Gruber AR, Lorenz R, Bernhart SH, Neubock R, Hofacker IL. The Vienna RNA websuite. *Nucleic Acids Res.* (2008) 36:W70–4. doi: 10.1093/nar/gkn188

Conflict of Interest: The authors declare that the research was conducted in the absence of any commercial or financial relationships that could be construed as a potential conflict of interest.

frontiers in Oncology

REVIEW
published: 21 January 2020
doi: 10.3389/fonc.2019.01549

Long Non-coding RNAs Involved in Resistance to Chemotherapy in Ovarian Cancer

Cecilie Abildgaard[1,2,3], *Luisa M. Do Canto*[1], *Karina D. Steffensen*[2,3] *and Silvia R. Rogatto*[1,3]*

[1] Department of Clinical Genetics, Lillebaelt Hospital-University Hospital of Southern Denmark, Vejle, Denmark, [2] Department of Clinical Oncology, Lillebaelt Hospital-University Hospital of Southern Denmark, Vejle, Denmark, [3] Institute of Regional Health Research, University of Southern Denmark, Odense, Denmark

Ovarian cancer (OC) accounts for more than 150,000 deaths worldwide every year. Patients are often diagnosed at an advanced stage with metastatic dissemination. Although platinum- and taxane-based chemotherapies are effective treatment options, they are rarely curative and eventually, the disease will progress due to acquired resistance. Emerging evidence suggests a crucial role of long non-coding RNAs (lncRNAs) in the response to therapy in OC. Transcriptome profiling studies using high throughput approaches have identified differential expression patterns of lncRNAs associated with disease recurrence. Furthermore, several aberrantly expressed lncRNAs in resistant OC cells have been related to increased cell division, improved DNA repair, up-regulation of drug transporters or reduced susceptibility to apoptotic stimuli, supporting their involvement in acquired resistance. In this review, we will discuss the key aspects of lncRNAs associated with the development of resistance to platinum- and taxane-based chemotherapy in OC. The molecular landscape of OC will be introduced, to provide a background for understanding the role of lncRNAs in the acquisition of malignant properties. We will focus on the interplay between lncRNAs and molecular pathways affecting drug response to evaluate their impact on treatment resistance. Additionally, we will discuss the prospects of using lncRNAs as biomarkers or targets for precision medicine in OC. Although there is still plenty to learn about lncRNAs and technical challenges to be solved, the evidence of their involvement in OC and the development of acquired resistance are compelling and warrant further investigation for clinical applications.

Keywords: ovarian cancer, lncRNA, drug resistance, chemotherapy, precision medicine

OPEN ACCESS

Edited by:
Deilson Elgui De Oliveira, São Paulo State University, Brazil

Reviewed by:
Monica Montopoli, University of Padova, Italy
Raphael Carmo Valente, Rio de Janeiro State University, Brazil

***Correspondence:**
Silvia R. Rogatto
silvia.regina.rogatto@rsyd.dk

Specialty section:
This article was submitted to Molecular and Cellular Oncology, a section of the journal Frontiers in Oncology

Received: *09 August 2019*
Accepted: *20 December 2019*
Published: *21 January 2020*

Citation:
Abildgaard C, Do Canto LM, Steffensen KD and Rogatto SR (2020) Long Non-coding RNAs Involved in Resistance to Chemotherapy in Ovarian Cancer. Front. Oncol. 9:1549. doi: 10.3389/fonc.2019.01549

INTRODUCTION

Ovarian cancer (OC) is the fifth most lethal cancer in women and accounts for more than 150,000 deaths annually worldwide (1). According to molecular and pathological features, epithelial OCs are stratified into type I or type II (2). Type I OC's (including endometrioid, clear cell, mucinous, and low-grade serous carcinomas) are genetically stable with frequent mutations in *KRAS, BRAF, CTNNB1,* and *PTEN*. In contrast, type II (mainly HGSC) comprises more aggressive tumors with high-grade and propensity for invasion and metastasis leading to high mortality rates (3). These

tumors are genetically unstable, presenting a high frequency of *TP53* mutations and *BRCA1/2* alterations. Originally HGSC was thought to arise from the squamous epithelial cell layer of the ovary. However, recent findings demonstrate that the molecular profile of HGSCs has a closer resemblance to the epithelium of the distal fallopian tube, suggesting that this tissue is an alternative site of origin (4, 5). HGSC is the most common and deadliest type of OC and will be the main focus of this review.

Due to the aggressive and invasive nature of HGSC around 70% of the patients have metastatic disease (FIGO stage III-IV) at the time of diagnosis. Surgery combined with chemotherapy is the primary treatment. Platinum-based chemotherapy is the cornerstone of chemotherapeutic treatment, namely cisplatin or carboplatin, combined with a taxane, such as paclitaxel or docetaxel (6). Initially, most patients respond well to the treatment; however, the majority of them will eventually acquire resistance and experience relapse (7, 8). To improve the prognosis, targeted therapies can be applied either as adjuvant or second-line treatments. Bevacizumab, an inhibitor or of vascular endothelial growth factor (VEGF) can be administered as first-line treatment in combination with carboplatin and paclitaxel. Inhibitors of Poly (ADP-ribose) polymerase (PARP) proteins are often used as second-line treatment for recurrent disease, mainly in patients with *BRCA* mutations. A recent randomized phase 3 trial performed in patients with a germline *BRCA* mutation has shown that the addition of oral PARP inhibitor (Olaparib) as maintenance therapy after chemotherapy prolongs the median progression free survival (PFS) by at least 3 years (9).

Despite the comprehensive combination of chemotherapy and maintenance treatment with targeted therapies, most patients develop resistance to treatment. Consequently, patients with disseminated HGSC have an extremely poor prognosis with a 5-year survival rate of only ∼20% (10). The knowledge of the underlying molecular mechanisms involved in the development of resistance to chemotherapy is crucial for treatment decisions and the discovery of novel anticancer drug targets.

Advances in sequencing technologies and large-scale genomic projects such as Encyclopedia of DNA elements (ENCODE) (11) and The Cancer Genome Atlas Program (TCGA) (12) have opened avenues to improve our understanding of the mechanisms of response to treatment, development of therapeutic resistance and cancer progression (13–15). Initial studies focused on describing the small percentage of DNA transcribed into RNA encoding for proteins, whereas the non-coding RNA (ncRNA) was regarded as irrelevant and with unknown function for cellular health and disease. However, compelling evidence now reveals the involvement of these transcripts in the regulation of several cellular processes (16, 17). Furthermore, several cancer types have been associated with dysregulated expression of lncRNAs (18).

LncRNAs IN CANCER

NcRNA comprises several different classes of molecules involved in gene regulation and chromatin modification. MicroRNA (miRNA), endogenous small interfering RNA (endo-siRNA) and piwi-interacting RNA (piRNA) are different classes of small ncRNAs involved in heterochromatin formation, histone modification, DNA methylation targeting, and gene silencing. Long non-coding RNAs (lncRNAs) are a subclass of non-translated RNA-sequences defined by an arbitrary length of more than 200 base pairs. These structurally complex RNA molecules interact directly with both DNA, RNA, and proteins affecting various cellular processes including genomic imprinting, gene transcription, mRNA splicing and protein activity (19–21). We are only beginning to understand how these molecules regulate cellular function, and how dysregulation can lead to malignant transformation.

The majority of lncRNAs are physically located in the proximity of protein-coding genes. Furthermore, lncRNAs are often classified according to their position relative to those genes as sense, antisense, intronic, intergenic, and bidirectional (22). Their expression levels are usually low and often compartmentalized to the cytoplasm or nucleus (23). Many lncRNAs exhibit low inter-species homology, and their expression signatures are often tissue-specific, indicating the importance of lncRNAs in cellular differentiation and embryonic development (24–26).

The lncRNA mechanisms of action usually fall into three categories, decoys, guides, or scaffolds (**Figure 1**). The decoys function as competing endogenous RNAs (ceRNAs) and modulate gene expression by sequestering transcription factors or miRNAs (also called sponging). Consequently, the availability of the targeted molecule is limited and the downstream effect reduced. The guide lncRNAs help to localize transcription factors or chromatin modifiers to specific areas of the genome, whereby transcription can be modulated. Dynamic scaffolds support transient assembly of protein complexes that bind genomic regions to affect chromatin structure (27, 28). The functions are not mutually exclusive, and many lncRNAs have more than one function. The single-stranded circular RNA (circRNA) is a sub-group of lncRNA recently discovered (29). Although the function of circRNA is still poorly understood, evidence indicates a role in miRNA regulation by sponging and intracellular transportation. LncRNAs are also stratified into *cis*- and *trans*-acting regulators, where the *cis*-regulators, exert their effect on neighboring genes on the allele from which they are transcribed, and the *trans*-regulators control gene expression at distant genomic sites.

Unsurprisingly, aberrant expression of lncRNAs has been associated with several diseases, including cancer. Dysregulated lncRNAs can exert oncogenic or tumor suppressor functions through transcriptional regulation impacting cellular proliferation, differentiation, invasiveness, apoptosis, and metabolism (30).

Many cancer-associated lncRNAs display similar expression patterns in different cancer types. Overexpression of Hox transcript antisense RNA (HOTAIR) was first described in breast cancer, where it was associated with increased invasiveness and metastasis (31). Subsequent studies revealed an association of increased expression of *HOTAIR* with disease progression and poor prognosis in colorectal (32), non-small cell lung (33), hepatocellular (34–36), gastric (37, 38), pancreatic (39), and ovarian (40) carcinomas. Single nucleotide polymorphisms

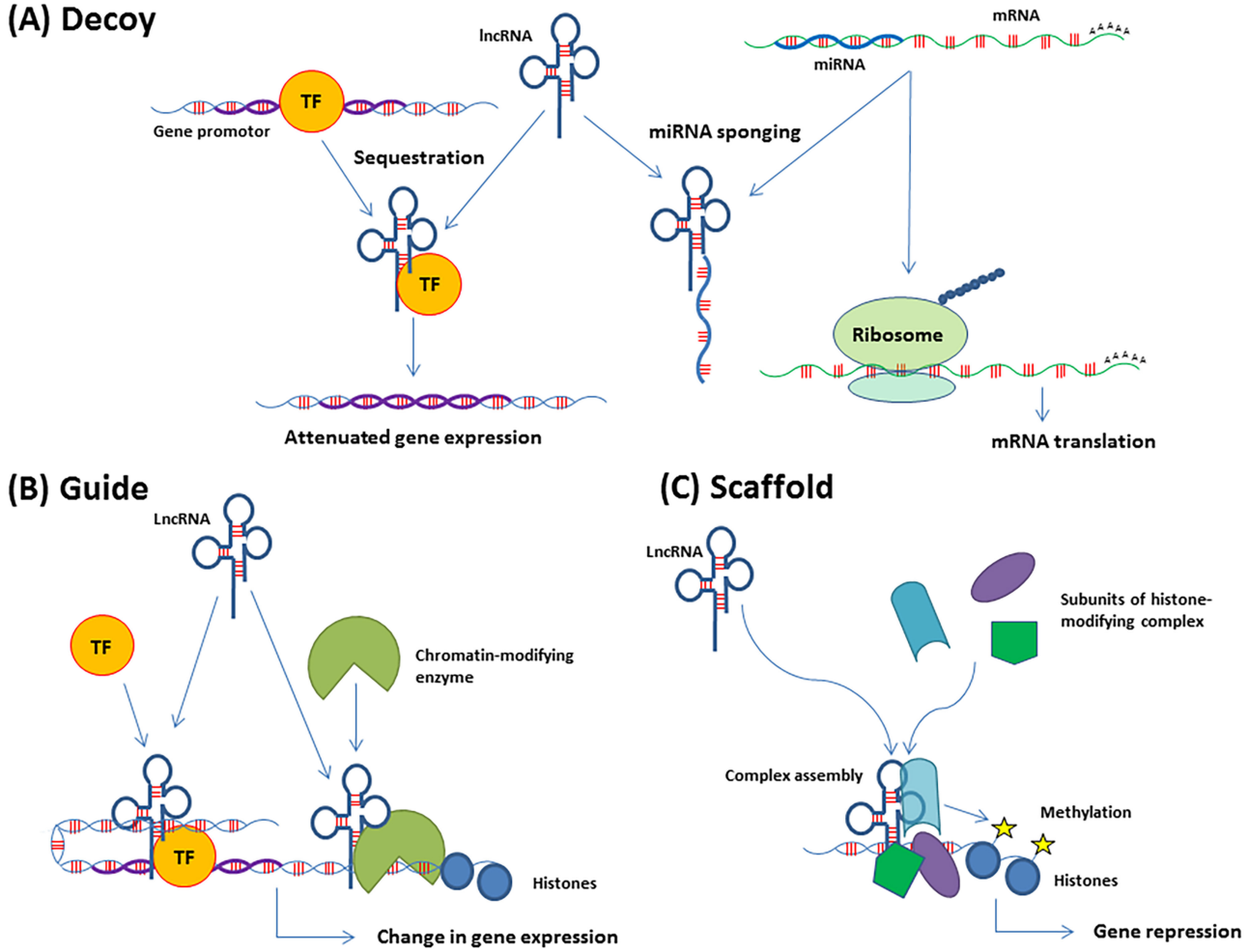

FIGURE 1 | Functions of lncRNAs in gene regulation. **(A)** Decoys can sequester transcription factors (TF) or complementary RNA transcripts, such as miRNAs (also called miRNA sponging). The consequence of TF sequestration is attenuated expression of the genes regulated by that TF. The effect of miRNA sponging is the release of the molecule e.g., mRNA which is targeted by that miRNA. The mRNA is then translated. **(B)** Guides recruit molecules, such as TFs or chromatin-modifying enzymes to their target areas of the genome, which leads to the regulation of gene expression. **(C)** Scaffolds support transient assembly of protein complexes at genomic regions, which can promote histone modifications and DNA methylation.

(SNPs) in *HOTAIR* were recently correlated with increased susceptibility to develop OC in a Chinese population (41, 42). In ovarian cancer, *HOTAIR* overexpression was associated with poor differentiation, advanced FIGO stage and lymph node metastasis (40, 43).

Metastasis associated lung adenocarcinoma transcript 1 (MALAT1) is another lncRNA widely overexpressed in various solid tumor types (44, 45), including OC (46–49). Several studies on OC cell lines showed that depletion of *MALAT1* suppresses viability, proliferation, migration, and invasion (46, 47, 50). *MALAT1* is highly conserved among mammals and is primarily known to localize to nuclear splicing speckles, where it interacts with splicing factors to regulate alternative splicing (51). In OC, *MALAT1* was demonstrated to suppress alternative splicing of pro-apoptotic factors, causing apoptotic and anoikis resistance (50).

HOTAIR and *MALAT1* are examples of widely expressed lncRNAs with oncogenic potential. Several other well-studied lncRNAs are found to be involved in the regulation of cellular processes such as proliferation, genomic stability, metabolism, and apoptosis to ensure homeostasis. These functions are executed through the lncRNAs directly or indirectly influence on the transcription of various proteins, which can lead to context-dependent oncogenic or tumor-suppressive properties. For a comprehensive overview of lncRNA's involved in cancer see (52–54).

A better understanding of the interplay between coding- and non-coding RNA and the integration of more molecular markers could potentially improve the predictive value of the molecular subtypes and provide a stronger tool for personalized therapeutic approaches.

THE MOLECULAR LANDSCAPE OF HGSC

The most prominent molecular feature of HGSC is high genomic instability (55), possibly initiated by *TP53* dysregulation and its associated effects in DNA damage repair (56). Mutations of *TP53* were reported in up to 96% of HGSC cases, mostly missense mutations (70.4%), which can result in a dominant-negative effect, gain or loss of protein function. Frameshift (12%), nonsense (8.67%), and splice site (5%) mutations, leading to loss of protein function have also been described (57). Only a few other genes were reported as commonly mutated in HGSC, including *BRCA1* (12.5%) and *BRCA2* (11.5%) (58).

Genetic predisposition is recognized in a minority of the patients with HGSC, with around 70% of familial cases presenting inherited pathogenic mutations in *BRCA1* and *BRCA2* (59). These mutations contribute to an increased risk of developing ovarian cancer (44% for *BRCA1* and 27% for *BRCA2* carriers), compared to the normal population. Mutations in other genes with low penetrance also have an important role in ovarian cancer development. The increased lifetime risk for women harboring mutations in genes involved in the DNA damage repair by homologous recombination (HR), such as *BRIP1* (5.8%) (60), *RAD51C* (5.2%), and *RAD51D* (12%) have been reported in OC (61). Alterations in genes involved in DNA mismatch repair associated with Lynch syndrome (*MSH2*, *MLH1*, *PMS2*, and *MSH6*), in rare cases prompt HGSC development (59, 62, 63).

The deficiency in DNA damage repair pathways is compatible with the high genomic instability observed in epithelial OC, with copy number alterations (CNA) affecting a significant fraction of the genome. Recurrent focal amplification of *CCNE1*, *MYC*, and *MECOM* genes are frequently identified in the TCGA cohort (58). Cases showing *CCNE1* amplification are mutually exclusive with *BRCA* mutated cases suggesting the involvement of different pathways in the tumorigenesis of HGSC (58). Deficiency of the HR pathway was described in around 50% of HGSC cases, which has been associated with *BRCA1* (20% of cases) and *BRCA2* (5%) germline or somatic mutations and, *BRCA1* promoter hypermethylation (10%). Genomic alterations in other genes involved in the HR repair pathway, such as amplification or mutation of *EMSY* (8%), focal deletion or mutation of *PTEN* (7%), hypermethylation of *RAD51C* (3%), mutation of *ATM/ATR* (2%), and mutation of Fanconi Anemia genes (58) have also been reported.

Some sporadic ovarian tumors share the phenotypic traits with tumors harboring germline mutations in *BRCA1/2* (BRCAness phenotype), which may reflect molecular similarities. The BRCAness phenotype predicts responsiveness to platinum-based chemotherapy (64) and PARP inhibitors (65). In a population-based study that evaluated the mutational profile of HR genes, a better overall survival in BRCAness patients was described (66). Another approach to identifying HR deficiency was performed based on scores of the CNA profile of tumors, named "genomic scars," which was very high in HGSC, and also correlated to PARP inhibitors or platinum-based chemotherapy sensitivity (67).

The integrative analysis of CNA, mutations, and gene expression alterations of HGSC identified RB1 and PI3K/Ras pathways deregulated in 67% and 45% of the cases, respectively (58). Amplification of *PIK3CA*, *PIK3CB,* and *PIK3K4* was correlated to the decreased overall survival of OC patients. The analysis of *PIK3CA* protein product p110α and p-Akt confirmed the involvement of the PIK3/AKT pathway in survival (68). The PIK3A/AKT/mTOR pathway was also shown to be implicated in therapy resistance. Advanced OC patients who did not respond to subsequent chemotherapy presented activation of the pathway compared to responsive patients (69). Besides, *GAB2*, a signaling intermediate of PI3K and MAPK pathways, was reported as amplified in 44% of ovarian cancer samples (70). Although HGSC rarely exhibits mutations in *KRAS* or *BRAF*, the main activators of the MAPK pathways, almost half of tumors display an expression of active downstream MAPKs (71).

In addition to the specific pathways and genes altered in HGSC, distinct molecular subtypes were identified based on the differential expression profiles (72). The expression analysis of 489 tumors performed by TCGA and compared to an external cohort revealed four HGSC subtypes: proliferative, mesenchymal, immunoreactive, and differentiated (58). The proliferative subtype was characterized by low expression of ovarian tumor markers and high expression of transcription factors and proliferation markers. The mesenchymal subtype presented a high expression of *HOX* genes and markers suggestive of increased stromal components. The immunoreactive subtype was characterized by T-cell chemokine ligands, *CXCL11* and *CXCL10*, and the receptor, *CXCR3*. The differentiated subtype was related to high expression of *MUC16*, *MUC1,* and *SLPI* (the secretory fallopian tube maker), suggesting a more mature stage of development (58). Patients with the HGSC immunoreactive subtype presented better prognosis, while patients with the mesenchymal or proliferative subtypes showed worse overall survival (73, 74).

LncRNAs SIGNATURE OF OVARIAN CANCER

Lately, the predictive value of differentially expressed lncRNAs has received increased attention due to their presence in liquid biopsies and potential as biomarkers for therapeutic response and prognosis (49, 75, 76). A meta-analysis including 1,333 OC patients established that altered lncRNAs are, in general, associated with decreased overall survival (76). In this analysis, 11 lncRNAs (*HOTAIR, TC010441, AB073614, ANRIL, MALAT1, NEAT1, CCAT2, UCA1, HOXA11-AS, SPRY4-IT1,* and *ZFAS1*) were identified with significantly increased expression in OC patients (76). Additional data have been reported to support the role of lncRNAs in OC. Eight lncRNAs were significantly correlated with overall survival, in a comprehensive analysis of lncRNA expression profiles of 544 OC patients from TCGA (75). Six of them (*RP4-799P18.3, RP11-57P19.1, RP11-307C12.11, RP11-254I22.1, RP1-223E5.4, and GACAT3*) were positively correlated with overall survival, while the last two (*PTPRD-AS1 and RP11-80H5.7*) were inversely correlated. The eight-lncRNA signature showed prognostic value and was able to

stratify patients according to clinical outcome into high- and low-risk groups. Furthermore, this signature demonstrated predictive value for the response to platinum-based chemotherapy (75). A prognostic signature was identified for recurrent disease based on datasets extracted from the Gene Expression Omnibus (GEO). The signature comprised four well-known cancer-related lncRNAs, *RUNX1-IT1, MALAT1, H19,* and *HOTAIRM1,* and two less well-described transcripts *LOC100190986* and *AL132709.8*. These lncRNAs were confirmed as differentially expressed in validation cohorts independently of tumor stage, tumor grade and histology type (49).

In silico analysis of RNA sequencing data derived from 391 patients retrieved from TCGA revealed three additional lncRNAs (*NBR2, ZNF883, and WT1-AS*) associated with recurrent OC (77). Based on the results, two interesting interactions were predicted; *WT1-AS-miR-375-RBPMS* and *WT1-AS-miR-27b-TP53*, suggesting that *WT1-AS* regulates two important tumor suppressors RBPMS and *TP53*, through miRNA sponging (77).

Several lncRNAs identified in large-scale studies have also been validated individually (46, 78–82), and across different cancer types (83). Also, functional studies have revealed that many of the dysregulated lncRNAs associated with OC are involved in one or several hallmarks of cancer such as increased proliferation, altered metabolism, evasion of apoptosis, migration or invasion (**Figure 2**) (79, 84–86).

Two lncRNAs are described specifically in ovarian cancer, ovarian adenocarcinoma amplified (OVAL) (87) and human ovarian cancer-specific transcript 2 (HOST2) (88). An intergenic region encompassing the full *OVAL* gene was found amplified in higher frequency in OC patients in comparison to other cancers. *OVAL* amplification and its increased expression suggest an oncogenic function in OC (87). So far no mechanisms or functional interactions have been described for *OVAL*. The expression of *HOST2* is dramatically increased in OC tissues and cell lines, compared to normal ovarian tissues and non-ovarian cell lines (88). Furthermore, *HOST2* was associated with increased proliferation, migration and invasion in OC. The mechanism of action of this potential driver is suggested to be through sequestration of miRNA let-7b, which is known to promote the expression of several oncogenes (89).

The involvement of dysregulated lncRNAs in the development of OC is well-documented. Considering the described oncogenic and tumor suppressor functions of lncRNA, their role in the development of resistance to therapy is expected (90–92). Differential lncRNA expression profiles were demonstrated in cisplatin-resistant and cisplatin sensitive OC, supporting their role in acquired resistance to chemotherapy (93). However, the mechanism by which lncRNAs contribute to acquired resistance remains incompletely understood. More detailed insights might lead to discoveries of new biomarkers or therapeutic targets. Signatures with the potential to predict therapeutic resistance would be valuable tools for clinicians, aiding the selection of the optimal treatment strategies for individual patients. In the following section, the involvement of lncRNAs in the development of therapeutic resistance will be highlighted, with a focus on platinum and taxane-based treatment regimens.

LncRNAs INVOLVED IN PLATINUM-RESISTANCE

The development of anti-cancer drug resistance is often complex and multifactorial, depending on the specific drug and the histological subtype of cancer. Carboplatin and cisplatin are the most commonly used drugs for the first-line treatment of advanced stages of HGSC. These platinum-based agents interact with DNA forming mono adducts or interstrand, intrastrand, and protein crosslinks mainly at guanine. The crosslinking affects DNA repair and synthesis and leads to the accumulation of single and double-strand breaks, which results in cell cycle arrest and apoptosis (94, 95). Moreover, the release of reactive oxygen species that activates inflammatory pathways may also contribute to the cytotoxic effects of these compounds (96).

Resistant clones can arise through a clonal selection of cells able to prevent, repair, or withstand DNA damage. The tumor suppressor p53 and its related nuclear transcription factors are important mediators of the cytotoxic effects of platinum therapy. DNA damage normally leads to a p53-dependent release of pro-apoptotic factors. Consequently, reduced activity of p53 or the related pathways is associated with platinum-resistance (97). Platinum-induced DNA damage can also be repaired by HR, and hence, the activity of the *BRCA1/2* genes reduces the responsiveness to platinum therapy (98). In accordance, reversions of *BRCA1/2* germline mutations have previously been reported as a mechanism of resistance to therapy (8). The mismatch repair system is another mechanism by which the cell can detect platinum induced lesions. Loss of mismatch repair-related genes such as *MLH1* and *MSH2* prevents the cells from recognizing the damage caused by platinum therapy. Consequently, apoptosis is not initiated and the cells are therefore less sensitive to the treatment (99, 100). Furthermore, platinum resistance was associated with epithelial to mesenchymal transition (EMT) (101), implying a range of molecular alterations promoting invasive properties and resistance to oncogene-induced senescence. The major pathways involved in EMT are TGF-β, HIF1-α, Wnt/β-catenin, and Notch, which have also been associated with platinum resistance (102, 103). General resistance mechanisms include reprogramming of metabolism and mitochondrial dysregulation, suppression of apoptotic mediators, up-regulated efflux pumps, reduced drug uptake, or intracellular detoxification (104). The molecular alterations leading to the platinum-resistant phenotype rarely include single nucleotide mutations in the known driver or resistance genes. Instead, it appears that the resistance arises from a highly patient-specific and adaptable pattern of altered methylation, gene amplifications, reversion of *BRCA1/2* mutations, promotor fusion, and translocation, and differential expression of ncRNAs (8, 105, 106).

Although several lncRNAs have been associated with platinum resistance in OC (**Table 1**), the resistance-associated molecular mechanisms have been elucidated in only a few of them (**Figure 3**). Next, we will present the current knowledge of the functions and roles of a set of lncRNAs associated with platinum resistance in OC.

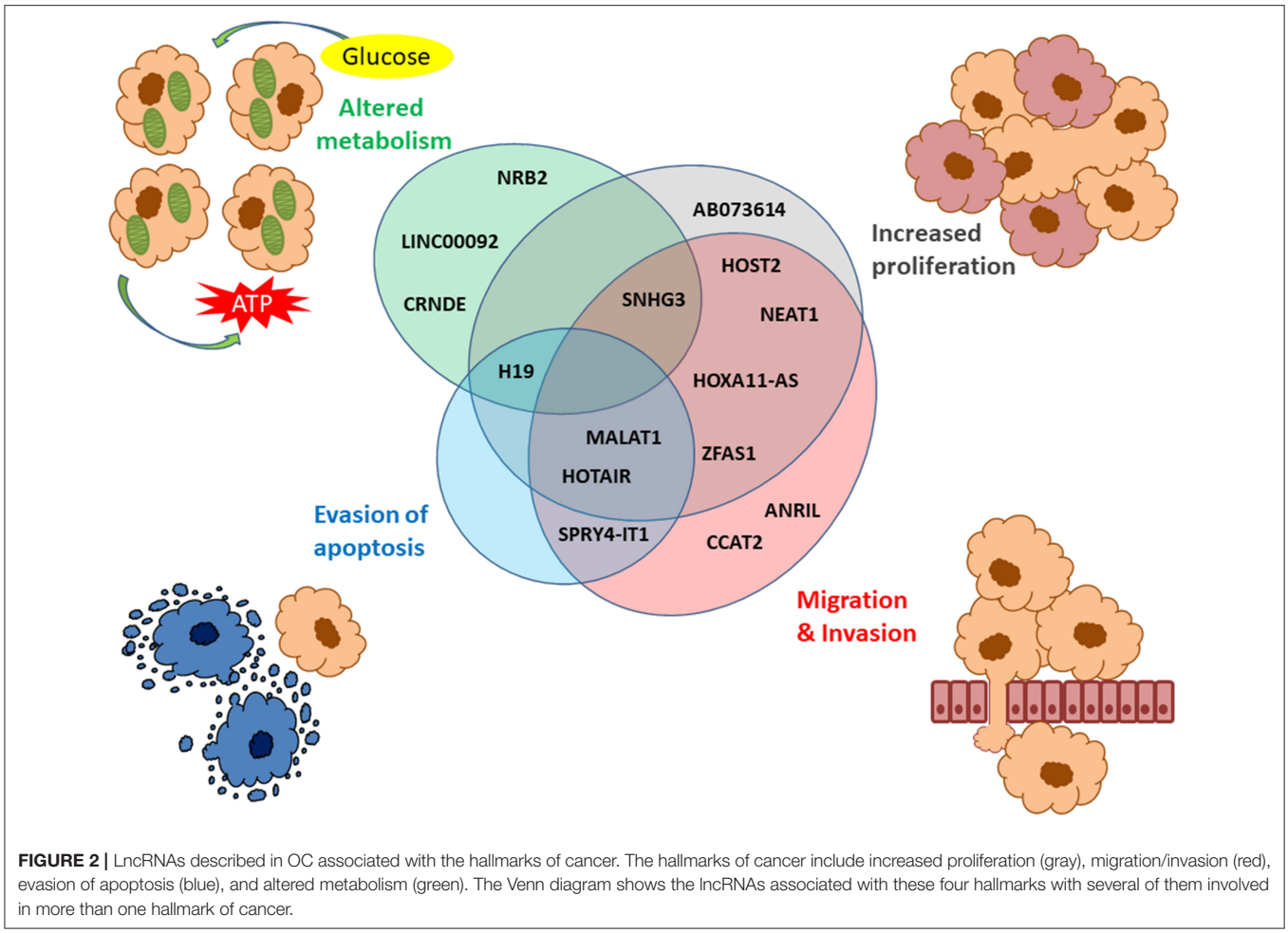

FIGURE 2 | LncRNAs described in OC associated with the hallmarks of cancer. The hallmarks of cancer include increased proliferation (gray), migration/invasion (red), evasion of apoptosis (blue), and altered metabolism (green). The Venn diagram shows the lncRNAs associated with these four hallmarks with several of them involved in more than one hallmark of cancer.

HOTAIR located within the *HOXC* gene cluster (mapped on12q13.13) was previously introduced due to its involvement in OC. *HOTAIR* recruits lysine-specific demethylase 1 (LSD1) and Polycomb Repressive Complex 2 (PRC2) and guide them to promote epigenetic silencing of *HOXD* genes (126). Additionally, *HOTAIR* regulates other HOX genes including *HOXA7*, which is consistently overexpressed in several tumor types (40, 127, 128). The knockdown of *HOTAIR* led to reduced expression of *HOXA7*, which increased susceptibility to apoptosis and restored cisplatin sensitivity in resistant OC cells (107). In general, *HOTAIR* is more abundant in advanced OC tissues and was also overexpressed in cisplatin-resistant OC cell lines, compared to sensitive controls (108). Furthermore, *HOTAIR* expression was correlated with poor survival in patients who received carboplatin compared with untreated patients (109). Knockdown of *HOTAIR* in a mouse xenograft model, enhanced the effect of treatment with cisplatin, suggesting its potential as a target to re-sensitize ovarian cancer cells to platinum treatment. This effect has been attributed to reduced activation of the Wnt/β-catenin pathway, which is known to promote excess stem cell renewal and EMT (110). Thus, overexpression of *HOTAIR* might contribute to platinum resistance by increased transcription of *HOXA7* and Wnt/β-catenin dependent induction of EMT. Overexpression of three additional lncRNAs *DNM3OS, MEG3,* and *MIAT* have been associated with EMT in ovarian cancer (129). However, the direct link between dysregulation of these transcripts and the development of platinum resistance is unexplored.

As previously mentioned, *MALAT1* plays an important oncogenic role in multiple cancers (44, 45). Recently, *MALAT1* has also been associated with resistance to therapy (130). In OC, *MALAT1* knockdown increased cell death during treatment with cisplatin, indicating its potential involvement in resistance (111). *MALAT1* was demonstrated to correlate with NOTCH1 expression, which is also up-regulated during platinum resistance in OC (112). NOTCH1 knockdown attenuates cisplatin resistance by directly down-regulating the expression of the multidrug resistance-associated protein 1 (*ABCC1*) in OC (131). *ABCC1* encodes a transporter of molecules across cellular membranes, including the efflux of a range of drugs (132). In lung adenocarcinoma and colorectal cancer, *MALAT1* promotes resistance to taxane- and platinum-based drugs, respectively. In these cases, EMT was identified as a mechanism of resistance (130, 133); however, this effect has not yet been investigated in OC.

The imprinted maternally expressed transcript *H19* gene is located in a well-conserved gene cluster also containing the

TABLE 1 | List of lncRNAs associated with platinum-resistance in ovarian cancer.

lncRNA	Category	Expression in OC tissue*	Expression in platinum-resistant cell lines**	Mechanisms of resistance***	References
HOTAIR	Antisense	↑ (cisplatin resistance or treated with carboplatin)	↑ (cisplatin/carboplatin)	↑ *HOXA7*	(107–110)
MALAT1	Intergenic	↑	↑ (cisplatin)	↑ Notch1 → ↑ abcc1	(111, 112)
H19	Intergenic	↑ (recurrent disease)	↑ (cisplatin)	↑ GSH pathway	(113)
ZFAS1	Antisense	↑ (platinum resistance)	↑ (cisplatin)	↓ miR-150-5p → ↑ SP1	(80, 114)
UCA1	Intergenic	↑ (cisplatin resistance)	↑ (cisplatin)	↑ SRPK1 ↓ miR-143 → ↑ FOSL2	(115–117)
PANDAR	Antisense	↑ (disease recurrence + wt-p53)	↑ (cisplatin)	↓ NF-YA ↑ SFRS2 - ↓ p53	(118)
PVT1	Intergenic circRNA	↑ (cisplatin resistance)	↑ (cisplatin)	↑ c-MYC	(119)
ZBED3-AS1	Antisense	↑ (platinum resistance)	↑ (cisplatin/carboplatin)	N/A	(120)
F11-AS1	Antisense	↓ (platinum resistance)	↓ (cisplatin/carboplatin)	N/A	(120)
GAS5	Intergenic	↓ (platinum resistance)	↓ (cisplatin/carboplatin)	N/A	(120)
BC200	Intergenic	↓	↓ (carboplatin)	N/A	(121)
LINC00312	Intergenic	↓ (cisplatin+paclitaxel resistance)	↓ (cisplatin)	↑ Bcl-2/Caspase-3 pathway	(122)
BX641110		N/A	↑ (cisplatin)	N/A	(123)
CRNDE	Intergenic	N/A	↑ (cisplatin)	N/A	(123)
HOXC-AS3	Antisense	N/A	↑ (cisplatin)	N/A	(123)
RP11-384P7.7	Intergenic	N/A	↑ (cisplatin)	N/A	(123)
PLAC2	Intronic	N/A	↑ (cisplatin)	N/A	(123)
RP11-6N17	Intergenic	N/A	↑ (cisplatin)	N/A	(123)
RP11-65J3.1-002	Intergenic	N/A	↓ (cisplatin)	N/A	(123)
AC141928.1	Intergenic	N/A	↓ (cisplatin)	N/A	(123)
GS1-600G8.5	Intergenic	N/A	↓ (cisplatin)	N/A	(123)
SNHG15	Intergenic	↑	↑ (cisplatin)	N/A	(124)
EBIC	Processed pseudogene	↑	↑ (cisplatin)	↑ Wnt/β-catenin pathway	(125)

The order of the lncRNAs corresponds to the appearance of the individual descriptions in the manuscript. Only the first 7 lncRNAs are described in detail in the manuscript, and are selected based on substantiating evidence in the literature.

**The expression of the lncRNAs in OC tissue is indicated by arrows, ↑ for higher and ↓ for lower expression in platinum-resistant patients (patient characteristics indicated in parenthesis), compared to expression in platinum-sensitive patients. If no patient characteristics are indicated, the expression was determined in ovarian cancer tissue from patients with unspecified sensitivity to platinum drugs and normalized to adjacent or normal ovarian tissue.*

***The expression in resistant OC cell lines is indicated by arrows; ↑ for higher and ↓ for lower expression in platinum-resistant, compared to expression in platinum-sensitive cell lines. The drug the cell lines are resistant to is indicated in parenthesis.*

****The effect of lncRNAs on associated pathways, miRNAs, genes or transcription factors involved in resistance mechanisms are indicated by arrows: ↑induction and ↓ repression. N/A, information not available.*

insulin-like growth factor 2 (IGF2). Both genes are regulated by genomic imprinting, and *H19* is only transcribed from the maternal allele, whereupon it plays an important role in embryonic development and growth control (134). Aberrant expression of *H19* has been demonstrated in several different cancers (135, 136); although its exact carcinogenic role is still under debate (137). The understanding of its function is challenged by the variety of transcriptional products deriving from the *H19* gene locus and its complex regulation. As an example, the miR-675 is transcribed from the first exon of *H19* (138) and has been associated with EMT and metastatic progression in colorectal and pancreatic cancers (139, 140). Furthermore, *H19* is directly induced by the c-Myc oncogene (141) and its expression has been associated with the hypoxic stress response, involving p53 and hypoxia-inducible factor 1-α (HIF1-α) (142). Transcriptome analysis revealed differential expression of *H19* in cisplatin-resistant OC cells compared to their sensitive progenitors. The involvement of *H19* in platinum resistance was validated in tissues from 41 cases of HGSC treated with either cisplatin or carboplatin. The patients were divided into two groups according to their recurrence-free survival (threshold of 12 months), where *H19* expression was shown to be significantly higher in patients with early recurrence (113). The role of *H19* in cisplatin resistance was related to oxidative stress and induction of the glutathione (GSH) pathway, where *H19* regulates several targets (*GSR, G6PD, GCLC, GCLM, GSTP1*, and *NQO1*) of the nuclear factor erythroid 2 (*NRF2)*, an important factor in the antioxidant defense (113). The glutathione pathway has been suggested as a detoxifying mechanism to platinum-induced oxidative toxicity and is often up-regulated during the development of resistance (143, 144). *H19* overexpression has also been correlated with cisplatin resistance in other cancers,

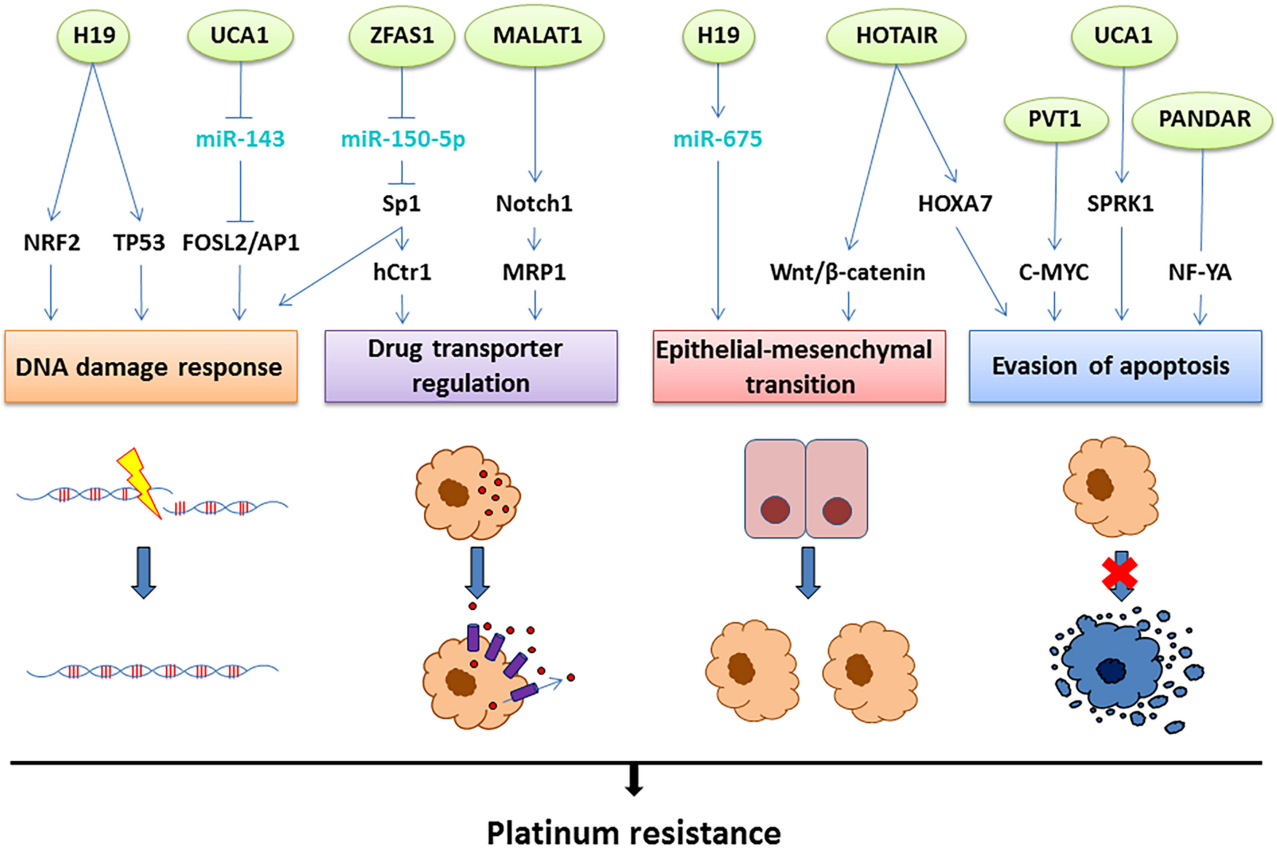

FIGURE 3 | The lncRNAs involved in platinum resistance in OC. Aberrant expression of the lncRNAs depicted on top (green circles) leads to platinum resistance through four main mechanisms: improved DNA damage response, upregulation of drug transporters leading to efflux of the drug, epithelial-mesenchymal transition or evasion of apoptosis. The molecular mechanisms suggested linking the lncRNAs to these resistance mechanisms involve interactions with miRNAs (light blue) and direct or indirect regulation of transcription factors and signaling pathways (black), as illustrated above.

including seminomas (145) and non-small cell lung cancer (146), where it was associated with evasion of apoptosis.

ZNFX1 antisense RNA 1 (ZFAS1) is transcribed from the antisense strand close to the protein-coding gene *ZNFX1*, including three C/D box small nucleolar RNAs (Snord12, Snord12b, and Snord12c) (147). The role of the lncRNA *ZFAS1* (zinc finger antisense 1) varies among human cancers. *ZFAS1* is downregulated in breast tumors compared to normal mammary tissue (147), whereas it is overexpressed in colorectal cancer (148), indicating tissue-specific functions. In OC, *ZFAS1* overexpression was identified as part of an eight-lncRNA expression signature predictive of platinum-sensitivity, based on transcriptome data from 258 patients with HGSCs (114). The authors also found increased *ZFAS1* expression in cisplatin-treated OC cell lines. Functional studies in OC cell lines revealed that the *ZFAS1* knockdown resulted in increased sensitivity to cisplatin. This effect was shown to involve sequestration of miR-150-5p, which prevents binding of the transcription factor specific protein 1 (SP1) (80). *SP1* has been appointed an important oncogene and a potential therapeutic target in several tumor types (149). Additionally, *SP1* is involved in DNA damage response (150), and regulation of a copper transporter (hCtr1), which is associated with platinum drug transport (151).

Urothelial carcinoma associated 1 (UCA1) is expressed during embryonic development and subsequently abolished in most tissues, including ovarian epithelia. In OC tissue and several other cancers, *UCA1* is re-activated and overexpressed (115, 152). In cancer tissues, *UCA1* is regulated by HIF1-α, indicating its involvement in the response to hypoxia (153). Through sponging of miR-143, *UCA1* prevents the repression of FOSL2, a subunit of the Activator protein 1 (AP-1) also involved in the hypoxic regulation. Consequently, *UCA1* overexpression might lead to the up-regulation of the hypoxic response involving AP-1. Hypoxia has been shown to promote cisplatin resistance, through HIF1-α and p53 activation (154). A significant *UCA1* overexpression in OC tissues from cisplatin-resistant patients (116) was reported. *In vitro* assays revealed that stable transfection of OC cells with *UCA1* promotes resistance toward cisplatin (115). In addition, *UCA1* was shown to affect the activity of the serine/arginine-rich protein-specific kinase 1 (SRPK1), an oncogene that suppresses apoptotic factors (115).

UCA1 is also associated with resistance to Paclitaxel in OC (155, 156), which can be reverted by *UCA1* knockdown in cell

lines (156). This effect was related to reduced sponging of miR-129 and, subsequently down-regulation of the *ABCB1* gene that encodes an efflux pump previously correlated with multidrug resistance in cancer (156, 157). These findings suggested that the mechanism of resistance involving *UCA1* is multifactorial, and could include improved response to DNA damage, reduced activation of apoptotic factors and increased efflux of the drugs.

The promoter of *CDKN1A* Antisense DNA damage Activated RNA (PANDAR) is a widely acknowledged oncogene mainly involved in regulating the response to DNA damage (158). The transcription of *PANDAR* is p53-dependent and promotes cell survival by impeding apoptosis through sequestering of the NF-YA transcription factor (159). In OC cell lines, an inverse relationship was demonstrated between *PANDAR* expression and cisplatin sensitivity. This effect involved interaction between *PANDAR* and the splicing factor arginine/serine-rich 2 (SFRS2), which led to negative feedback regulation of *TP53* (118). Patients with wild type *TP53* showed increased expression of *PANDAR* and SFRS2 at disease recurrence, compared to the time of diagnosis (118). The *PANDAR*-dependent suppression of p53 in resistant cells prevents the normal DNA damage response, whereby the cells can evade apoptosis. Since HGSCs have a very high occurrence of inactivating *TP53* mutations, the role of *PANDAR* in platinum resistance remains to be elucidated.

Plasmacytoma variant translocation 1 (PVT1) is a well-established oncogene in OC (160, 161), as well as other cancers such as gastric (162) and breast (163). *PVT1* is located in proximity to the *MYC* locus, where it encodes several alternative splice isoforms. In addition, the *PVT1* locus contains a cluster of at least six miRNAs (miR-1204,−1205,−1206,−1207-3p,−1207-5p, and−1208) (164). Transcription of *PVT1* can be regulated by p53 through a canonical binding site, indicating its involvement in the response to DNA damage. *PVT1* is often co-expressed with *MYC,* with which it interacts and stabilizes to potentiate its activity (165). *MYC* has been suggested as a potential therapeutic target in platinum-resistant OC, as its overexpression confers resistance toward cisplatin (166). The role of *PVT1* in the development of therapeutic resistance in OC is ambiguous since it was both demonstrated to promote cisplatin resistance by suppressing apoptotic factors (119), but also to be an effector in the cytotoxic response to treatment with carboplatin and docetaxel, by activating p53 and potentially promoting apoptosis (167). However, since p53 is often affected by the loss of function mutations in HGSC, the cytotoxic effect of *PVT1* in response to carboplatin and docetaxel might be blunted in these cases. Studies in other cancers support the involvement of *PVT1* in cisplatin resistance (168, 169). The opposing effects described for *PVT1* could be due to the differences in the mechanisms of action of the two treatment regimens and underlines the need for further investigation.

Other mechanisms of resistance than the ones reported here have been suggested to involve lncRNAs. As an example, the lncRNAs *MPRL* (170), *LINC00312* (122), and *SNHG3* (84) are involved in mitochondrial function and altered expression of these have been associated with platinum resistance, either through effects on energy metabolism or mitochondrial-dependent apoptosis. In general, the interactions between lncRNA and the mitochondrial genome is not yet well-understood and should be further investigated.

LncRNAs INVOLVED IN THE TAXANE RESISTANCE

Taxanes are microtubule-stabilizing agents that bind to the β-subunit of tubulin dimers to promote and stabilize polymerization. This mechanism inhibits microtubule disassembly that is a necessary event in mitosis; consequently, mitotic arrest and eventually apoptosis are promoted (171, 172). Paclitaxel is most often used in combination with the platinum-based chemotherapy as a first-line treatment, or as a single agent in platinum-resistant OC patients. Unfortunately, repeated exposure often leads to acquired resistance. Docetaxel, a second-generation taxane, can be used in some cases; however, shared resistance mechanisms result in low response rates. *In vitro* experiments have demonstrated that an inverse relationship exists between resistance to platins and taxanes, suggesting separate resistance mechanisms and emphasizing the benefits of combined treatments (173). The most common resistance mechanisms to taxanes comprise structural changes in the β-tubulin target region, altered expression of apoptotic and mitotic factors and overexpression of the multidrug resistance genes (ABC-transporters) (174, 175).

Since the taxanes are rarely used as a single agent in the treatment of OC, only a few studies have investigated the role of lncRNAs in the development of paclitaxel resistance in tissues. A combined analysis of two expression datasets comparing (1) patients with complete and incomplete response to chemotherapy and (2) two OC cell lines with paclitaxel resistance with two sensitive OC cell lines was performed. The combined analysis identified a panel of seven lncRNAs (*XR_948297, XR_947831, XR_938728, XR_938392, NR_103801, NR_073113,* and *NR_036503*) differentially expressed in both cell lines and tissues, and had predictive value for resistance to therapeutic regimens containing paclitaxel (176). However, the signature described in this study needs further validation and the functional implications for differential expression of the selected lncRNAs should be explored.

A list of lncRNAs associated with taxane resistance in OC is detailed in **Table 2**. Few of these lncRNAs have well-described functions and will be presented below. The interplay between the described lncRNAs, their molecular pathways, and resistance mechanisms are illustrated in **Figure 4**.

The Fer-1-like family member 4 (FER1L4) pseudogene is a lncRNA associated with tumor-suppressive properties in cancer (183). *FER1L4* acts as a decoy for miR-106a-5p which also interacts with the tumor suppressor *PTEN* (184). In OC, *FER1L4* is expressed at low levels compared to normal ovarian epithelial cells and, at even lower levels in paclitaxel-resistant cell lines. Transfection with *FER1L4* led to MAPK pathway suppression and restored the sensitivity to paclitaxel, indicating an important role in the development of resistance (177). Overall, PTEN-AKT-mTOR and MAPK are major cancer driver pathways deeply

TABLE 2 | List of lncRNAs associated with taxane-resistance in ovarian cancer.

lncRNA	Category	Expression in OC tissue*	Expression in paclitaxel-resistant cell lines**	Mechanisms of resistance***	Reference
UCA1	Intergenic	N/A	↑	↓ miR-129 → ↑ abcb1	(155, 156)
FER1L4	Pseudogene	↓	↓	MAPK	(177)
LINC01118	Intergenic	↑	↑	↓ miR-134 → ↑ abcc1	(178)
NEAT1	Intergenic	↑ (paclitaxel resistance)	↑	↓ miR-194 → ↑ ZEB1	(179)
Xist	Intergenic	↓ (recurrent disease)	↓	N/A	(180)
KB-1471A8.2	Antisense	↓	↓	↓ CDK4	(181)
OIP5-AS1	Antisense	N/A	↓	N/A	(182)

The order of the lncRNAs corresponds to the appearance of the individual descriptions in the manuscript. Only the first 4 lncRNAs are described in detail in the manuscript and are selected based on substantiating evidence in the literature.

**The expression of the lncRNAs in OC tissue is indicated by arrows, ↑ for higher and ↓ for lower expression in resistant patients (patient characteristics are indicated in parenthesis), compared to expression in sensitive patients. If no patient characteristics are indicated, the expression was determined in ovarian cancer tissue from patients with unspecified sensitivity to platinum drugs and normalized to adjacent or normal ovarian tissue.*

***The expression in paclitaxel-resistant OC cell lines is indicated by arrows; ↑ for higher and ↓ for lower expression and the drug they are resistant to is indicated in parenthesis.*

****The effect of lncRNAs on associated pathways, miRNAs, genes or transcription factors involved in resistance mechanisms are indicated by arrows: ↑ induction and ↓ repression. N/A, information not available.*

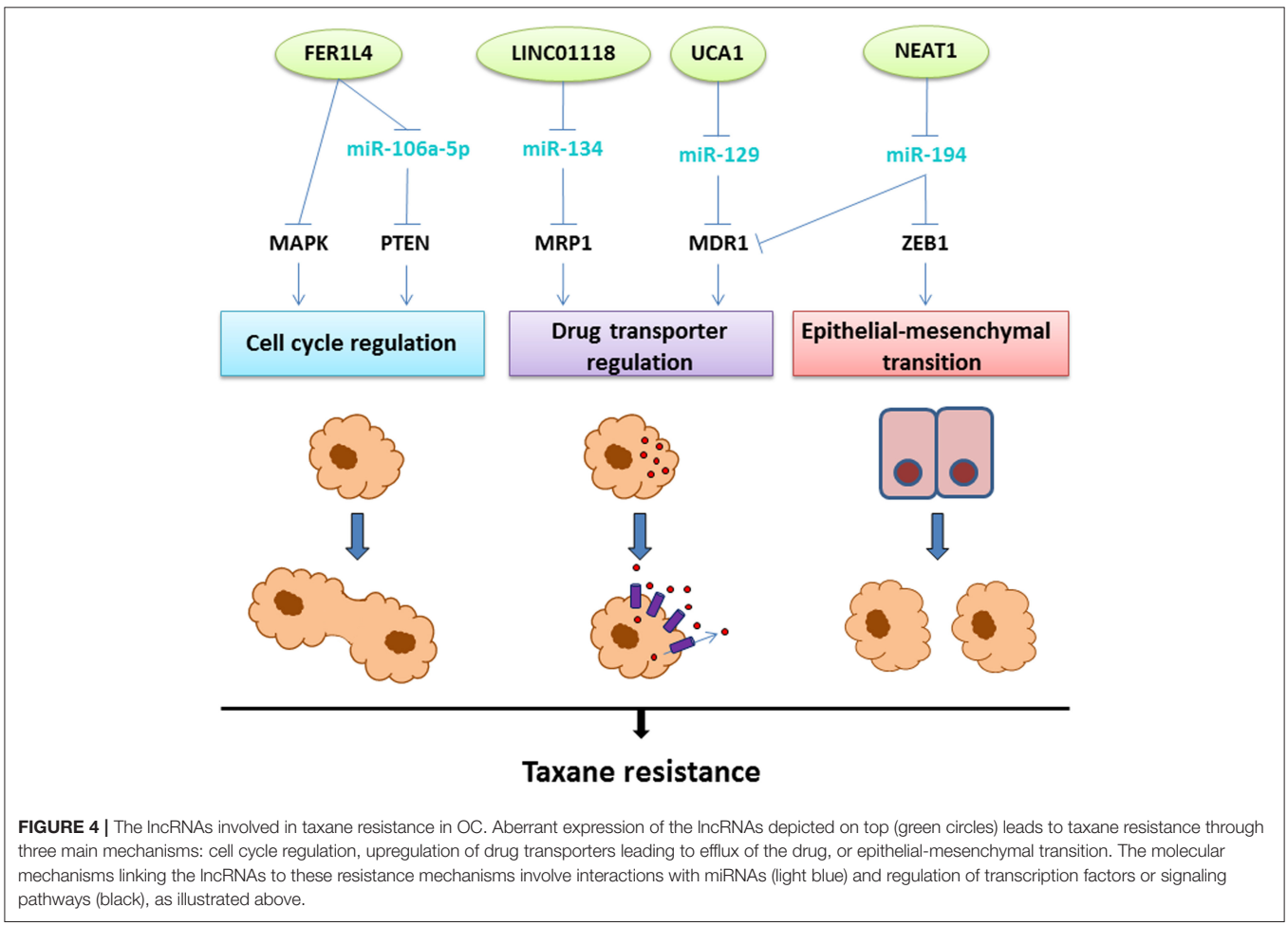

FIGURE 4 | The lncRNAs involved in taxane resistance in OC. Aberrant expression of the lncRNAs depicted on top (green circles) leads to taxane resistance through three main mechanisms: cell cycle regulation, upregulation of drug transporters leading to efflux of the drug, or epithelial-mesenchymal transition. The molecular mechanisms linking the lncRNAs to these resistance mechanisms involve interactions with miRNAs (light blue) and regulation of transcription factors or signaling pathways (black), as illustrated above.

involved in resistance to chemotherapy (including paclitaxel) in several cancers (185).

Long Intergenic Non-Coding RNA 1118 (LINC01118) was recently identified as overexpressed in paclitaxel and cisplatin-resistant cell lines and OC compared with normal and benign tissues (178). These findings were supported by *in vitro* studies showing that knockdown conferred increased sensitivity to paclitaxel, whereas overexpression led to resistance. MiR-134 was predicted as a direct target, and functional assays showed that *LINC01118* was able to regulate the *ABCC1* gene through miR-134 repression (178). As previously described, *ABCC1* upregulation is associated with multidrug resistance in cancers

(132). No additional studies have been performed correlating *LINC01118* with drug resistance or even cancer, warranting further investigations of this lncRNA.

Nuclear paraspeckle assembly transcript 1 (NEAT1) is transcribed from the *MEN1* (familial tumor syndrome multiple endocrine neoplasia type 1) locus on chromosome 11 and is a well-described oncogene (186). *NEAT1* is overexpressed in OC tissue and cell lines accordingly and is correlated with metastatic potential and poor prognosis (79, 187). In paclitaxel-resistant OC cells, *NEAT1* acts as a decoy for miR-194, promoting upregulation of *ZEB1* (zinc finger E-box-binding homeobox 1) (179). *ZEB1* is an important transcription factor and mediator of EMT and was previously associated with drug resistance (188). Besides, paclitaxel resistance was attenuated by *NEAT1* knockdown, which was associated with suppression of the efflux pump P-glycoprotein encoded by the *ABCB1* gene. This effect was also related to the interaction between *NEAT1* and miR-194, since the suppression of the efflux pump was rescued by miR-194 knockdown. The involvement of *NEAT1* in resistance to paclitaxel was validated in OC xenografts in mice, where knockdown restored paclitaxel sensitivity (179). These results substantiate the role of *NEAT1* in paclitaxel resistance and indicate the potential for therapeutic targeting.

PERSPECTIVES AND FUTURE DIRECTIONS

Collectively, the present review provides compelling evidence of the association between lncRNA expression pattern and therapeutic response in OC, indicating that the etiology of acquired resistance is more complex than originally described. We are just beginning to understand the biological role and function of some of these lncRNAs, and how they can be exploited for clinical purposes.

Two of the most obvious applications for lncRNAs in OC is the establishment of biomarker panels with predictive value for prognosis and/or drug response, or for therapeutic targeting to prevent or reverse resistance to chemotherapy. The presence of circulating lncRNAs in body fluids such as blood and urine at detectable levels, suggests that they could represent excellent biomarkers (189, 190). Several lncRNA signatures with predictive value for platinum-sensitivity in OC have recently been identified (49, 114, 120). However, further studies are needed to determine their clinical applicability.

The oncogenic behavior of some lncRNAs, combined with their tissue specificity and content of targetable residues, emphasize their potential as targets for therapeutic intervention. Furthermore, lncRNA targeting is one of the only therapeutic approaches to upregulate tumor suppressors in a locus-specific manner (191). Artificially synthesized polymers of nucleic acids, known as peptide nucleic acids (PNAs) are thermally stable, not affected by nucleases and can be modified for *in vivo* administration. Also, PNAs specific for RNA targets is much easier to design and synthesize than small-molecule oncogene inhibitors (192). For example, HOTAIR was targeted with a PNA, designed to prevent the interaction between *HOTAIR* and the EZH2 subunit of PRC2, in mice with platinum-resistant ovarian tumor xenografts. The treatment reduced *HOTAIR* expression and re-sensitized the tumors to treatment with cisplatin, which resulted in prolonged survival. The study provided proof of concept for targeting oncogenic lncRNAs as a strategy for precision medicine (193). However, more conclusive evidence of the complex molecular interactions of individual lncRNAs is paramount to determine the physiological impact of targeted treatments before clinical testing.

So far, the molecular profiling of lncRNAs and the identification of functional interactions have proved to be difficult to replicate in different studies. The main platforms for high throughput analysis of lncRNAs, such as RNA sequencing and expression arrays, offer different advantages and drawbacks, and the downstream bioinformatics is not yet standardized. Although RNA sequencing offers the advantage of including all potential lncRNA transcripts, the complexity of the following sequence assembly often hampers the correct annotation (194). In contrast, array-based methods provide a more standardized workflow and a much simpler downstream analysis but are limited to a selection of annotated transcripts. Several studies revise old data sets from publically available sources to perform *in silico* investigations. However, the experimental setup behind these data sets was rarely designed for the identification of lncRNAs. The low expression of lncRNA transcripts requires specific methodological considerations for optimal results. Furthermore, computational prediction of functional interactions should always be validated experimentally in the specific tissue of interest.

The studies investigating lncRNAs are increasing exponentially and both, experimental and bioinformatic methods are constantly improving. Several lncRNA-targeting therapeutics are already in the clinical pipeline (191), and some have reached clinical trials (195, 196). GENCODE (23), a spin-off from ENCODE is currently attempting to annotate all non-coding transcripts of the entire human genome. Complete annotation of human lncRNAs, standardization of experimental procedures and bioinformatic analysis combined with improved insights into the functional roles of lncRNAs in the development of resistance, will provide a novel paradigm for biomarker discovery and precision medicine in OC.

AUTHOR CONTRIBUTIONS

CA and SR conceived and designed the study. CA drafted the manuscript and designed the figures. LD and KS participated in drafting the molecular and clinical information, respectively. SR revised and edited the full content of the manuscript. All authors have read, revised critically and approved the final version of the manuscript.

FUNDING

The preparation of this manuscript was financially supported by the Region of Southern Denmark Research Fund.

REFERENCES

1. Reid F. The world ovarian cancer coalition atlas -global trends in incidence mortality and survival. In: Coalition WO, editor. *The Every Woman Study* (The World Ovarian Cancer Coalition) (2018). p. 1–39.
2. Kurman RJ, Shih Ie M. Pathogenesis of ovarian cancer: lessons from morphology and molecular biology and their clinical implications. *Int J Gynecol Pathol.* (2008) 27:151–60. doi: 10.1097/PGP.0b013e318161e4f5
3. Koshiyama M, Matsumura N, Konishi I. Recent concepts of ovarian carcinogenesis: type I and type II. *Biomed Res Int.* (2014) 2014:934261. doi: 10.1155/2014/934261
4. Ducie J, Dao F, Considine M, Olvera N, Shaw PA, Kurman RJ, et al. Molecular analysis of high-grade serous ovarian carcinoma with and without associated serous tubal intra-epithelial carcinoma. *Nat Commun.* (2017) 8:990. doi: 10.1038/s41467-017-01217-9
5. Labidi-Galy SI, Papp E, Hallberg D, Niknafs N, Adleff V, Noe M, et al. High grade serous ovarian carcinomas originate in the fallopian tube. *Nat Commun.* (2017) 8:1093. doi: 10.1038/s41467-017-00962-1
6. Boyd LR, Muggia FM. Carboplatin/paclitaxel induction in ovarian cancer: the finer points. *Oncology*. (2018) 32:418–20, 422–4.
7. Jayson GC, Kohn EC, Kitchener HC, Ledermann JA. Ovarian cancer. *Lancet*. (2014) 384:1376–88. doi: 10.1016/S0140-6736(13)62146-7
8. Patch AM, Christie EL, Etemadmoghadam D, Garsed DW, George J, Fereday S, et al. Whole-genome characterization of chemoresistant ovarian cancer. *Nature.* (2015) 521:489–94. doi: 10.1038/nature14410
9. Moore K, Colombo N, Scambia G, Kim BG, Oaknin A, Friedlander M, et al. Maintenance olaparib in patients with newly diagnosed advanced ovarian cancer. *N Engl J Med.* (2018) 379:2495–505. doi: 10.1056/NEJMoa1810858
10. Howlader NA, Krapcho M, Miller D, Brest A, Yu M, Ruhl J, et al. editors. *SEER Cancer Statistics Review, 1975-2016*. Bethesda, MD: National Cancer Institute (2019). Available online at: https://seer.cancer.gov/csr/1975_2016/
11. Davis CA, Hitz BC, Sloan CA, Chan ET, Davidson JM, Gabdank I, et al. The Encyclopedia of DNA elements (ENCODE): data portal update. *Nucleic Acids Res.* (2018) 46:D794–801. doi: 10.1093/nar/gkx1081
12. Institute, T. N. C. *The Cancer Genome Atlas.* Available online at: https://www.cancer.gov/about-nci/organization/ccg/research/structural-genomics/tcga
13. Longley DB, Johnston PG. Molecular mechanisms of drug resistance. *J Pathol.* (2005) 205:275–92. doi: 10.1002/path.1706
14. Chin L, Andersen JN, Futreal PA. Cancer genomics: from discovery science to personalized medicine. *Nat Med.* (2011) 17:297–303. doi: 10.1038/nm.2323
15. Tomczak K, Czerwinska P, Wiznerowicz M. The Cancer Genome Atlas (TCGA): an immeasurable source of knowledge. *Contemp Oncol.* (2015) 19:A68–77. doi: 10.5114/wo.2014.47136
16. Batista PJ, Chang HY. Long noncoding RNAs: cellular address codes in development and disease. *Cell.* (2013) 152:1298–307. doi: 10.1016/j.cell.2013.02.012
17. Tay Y, Rinn J, Pandolfi PP. The multilayered complexity of ceRNA crosstalk and competition. *Nature.* (2014) 505:344–52. doi: 10.1038/nature12986
18. Wapinski O, Chang HY. Long noncoding RNAs and human disease. *Trends Cell Biol.* (2011) 21:354–61. doi: 10.1016/j.tcb.2011.04.001
19. Engreitz JM, Haines JE, Perez EM, Munson G, Chen J, Kane M, et al. Local regulation of gene expression by lncRNA promoters, transcription and splicing. *Nature.* (2016) 539:452–55. doi: 10.1038/nature20149
20. Zampetaki A, Albrecht A, Steinhofel K. Long non-coding RNA structure and function: is there a link? *Front Physiol.* (2018) 9:1201. doi: 10.3389/fphys.2018.01201
21. Guttman M, Rinn JL. Modular regulatory principles of large non-coding RNAs. *Nature.* (2012) 482:339–46. doi: 10.1038/nature10887
22. Jarroux J, Morillon A, Pinskaya M. History, discovery, and classification of lncRNAs. *Adv Exp Med Biol.* (2017) 1008:1–46. doi: 10.1007/978-981-10-5203-3_1
23. Derrien T, Johnson R, Bussotti G, Tanzer A, Djebali S, Tilgner H, et al. The GENCODE v7 catalog of human long noncoding RNAs: analysis of their gene structure, evolution, and expression. *Genome Res.* (2012) 22:1775–89. doi: 10.1101/gr.132159.111
24. Washietl S, Kellis M, Garber M, Evolutionary dynamics and tissue specificity of human long noncoding RNAs in six mammals. *Genome Res.* (2014) 24:616–28. doi: 10.1101/gr.165035.113
25. Bouckenheimer J, Assou S, Riquier S, Hou C, Philippe N, Sansac C, et al. Long non-coding RNAs in human early embryonic development and their potential in ART. *Hum Reprod Update.* (2016) 23:19–40. doi: 10.1093/humupd/dmw035
26. Taft RJ, Pheasant M, Mattick JS. The relationship between non-protein-coding DNA and eukaryotic complexity. *Bioessays*. (2007) 29:288–99. doi: 10.1002/bies.20544
27. Balas MM, Johnson AM. Exploring the mechanisms behind long noncoding RNAs and cancer. *Noncoding RNA Res.* (2018) 3:108–17. doi: 10.1016/j.ncrna.2018.03.001
28. Fatica A, Bozzoni I. Long non-coding RNAs: new players in cell differentiation and development. *Nat Rev Genet.* (2014) 15:7–21. doi: 10.1038/nrg3606
29. Salzman J, Gawad C, Wang PL, Lacayo N, Brown PO. Circular RNAs are the predominant transcript isoform from hundreds of human genes in diverse cell types. *PLoS ONE.* (2012) 7:e30733. doi: 10.1371/journal.pone.0030733
30. Gutschner T, Diederichs S. The hallmarks of cancer: a long non-coding RNA point of view. *RNA Biol.* (2012) 9:703–19. doi: 10.4161/rna.20481
31. Gupta RA, Shah N, Wang KC, Kim J, Horlings HM, Wong DJ, et al. Long non-coding RNA HOTAIR reprograms chromatin state to promote cancer metastasis. *Nature.* (2010) 464:1071–6. doi: 10.1038/nature08975
32. Kogo R, Shimamura T, Mimori K, Kawahara K, Imoto S, Sudo T, et al. Long noncoding RNA HOTAIR regulates polycomb-dependent chromatin modification and is associated with poor prognosis in colorectal cancers. *Cancer Res.* (2011) 71:6320–6. doi: 10.1158/0008-5472.CAN-11-1021
33. Liu XH, Liu ZL, Sun M, Liu J, Wang ZX, De W. The long non-coding RNA HOTAIR indicates a poor prognosis and promotes metastasis in non-small cell lung cancer. *BMC Cancer*. (2013) 13:464. doi: 10.1186/1471-2407-13-464
34. Yang Z, Zhou L, Wu LM, Lai MC, Xie HY, Zhang F, et al. Overexpression of long non-coding RNA HOTAIR predicts tumor recurrence in hepatocellular carcinoma patients following liver transplantation. *Ann Surg Oncol.* (2011) 18:1243–50. doi: 10.1245/s10434-011-1581-y
35. Ishibashi M, Kogo R, Shibata K, Sawada G, Takahashi Y, Kurashige J, et al. Clinical significance of the expression of long non-coding RNA HOTAIR in primary hepatocellular carcinoma. *Oncol Rep.* (2013) 29:946–50. doi: 10.3892/or.2012.2219
36. Geng YJ, Xie SL, Li Q, Ma J, Wang GY. Large intervening non-coding RNA HOTAIR is associated with hepatocellular carcinoma progression. *J Int Med Res.* (2011) 39:2119–28. doi: 10.1177/147323001103900608
37. Endo H, Shiroki T, Nakagawa T, Yokoyama M, Tamai K, Yamanami H, et al. Enhanced expression of long non-coding RNA HOTAIR is associated with the development of gastric cancer. *PLoS ONE.* (2013) 8:e77070. doi: 10.1371/journal.pone.0077070
38. Hajjari M, Behmanesh M, Sadeghizadeh M, Zeinoddini M. Up-regulation of HOTAIR long non-coding RNA in human gastric adenocarcinoma tissues. *Med Oncol.* (2013) 30:670. doi: 10.1007/s12032-013-0670-0
39. Kim K, Jutooru I, Chadalapaka G, Johnson G, Frank J, Burghardt R, et al. HOTAIR is a negative prognostic factor and exhibits pro-oncogenic activity in pancreatic cancer. *Oncogene.* (2013) 32:1616–25. doi: 10.1038/onc.2012.193
40. Cui L, Xie XY, Wang H, Chen XL, Liu SL, Hu LN. [Expression of long non-coding RNA HOTAIR mRNA in ovarian cancer]. *Sichuan Da Xue Xue Bao Yi Xue Ban.* (2013) 44:57–9.
41. Qiu H, Wang X, Guo R, Liu Q, Wang Y, Yuan Z, et al. HOTAIR rs920778 polymorphism is associated with ovarian cancer susceptibility and poor prognosis in a Chinese population. *Future Oncol.* (2017) 13:347–55. doi: 10.2217/fon-2016-0290
42. Wu H, Shang X, Shi Y, Yang Z, Zhao J, Yang M, et al. Genetic variants of lncRNA HOTAIR and risk of epithelial ovarian cancer among Chinese women. *Oncotarget.* (2016) 7:41047–52. doi: 10.18632/oncotarget.8535
43. Qiu JJ, Wang Y, Ding JX, Jin HY, Yang G, Hua KQ. The long non-coding RNA HOTAIR promotes the proliferation of serous ovarian cancer cells through the regulation of cell cycle arrest and apoptosis. *Exp Cell Res*. (2015) 333:238–48. doi: 10.1016/j.yexcr.2015.03.005

44. Wang J, Xu AM, Zhang JY, He XM, Pan YS, Cheng G, et al. Prognostic significance of long non-coding RNA MALAT-1 in various human carcinomas: a meta-analysis. *Genet Mol Res.* (2016) 15:1–12. doi: 10.4238/gmr.15017433
45. Wang Y, Xue D, Li Y, Pan X, Zhang X, Kuang B, et al. The long noncoding RNA MALAT-1 is a novel biomarker in various cancers: a meta-analysis based on the GEO database and literature. *J Cancer.* (2016) 7:991–1001. doi: 10.7150/jca.14663
46. Zou A, Liu R, Wu X. Long non-coding RNA MALAT1 is up-regulated in ovarian cancer tissue and promotes SK-OV-3 cell proliferation and invasion. *Neoplasma.* (2016) 63:865–72. doi: 10.4149/neo_2016_605
47. Lin Q, Guan W, Ren W, Zhang L, Zhang J, Xu G. MALAT1 affects ovarian cancer cell behavior and patient survival. *Oncol Rep.* (2018) 39:2644–52. doi: 10.3892/or.2018.6384
48. Zhou Y, Xu X, Lv H, Wen Q, Li J, Tan L, et al. The long noncoding RNA MALAT-1 Is highly expressed in ovarian cancer and induces cell growth and migration. *PLoS ONE.* (2016) 11:e0155250. doi: 10.1371/journal.pone.0155250
49. Yang K, Hou Y, Li A, Li Z, Wang W, Xie H, et al. Identification of a six-lncRNA signature associated with recurrence of ovarian cancer. *Sci Rep.* (2017) 7:752. doi: 10.1038/s41598-017-00763-y
50. Gordon MA, Babbs B, Cochrane DR, Bitler BG, Richer JK. The long non-coding RNA MALAT1 promotes ovarian cancer progression by regulating RBFOX2-mediated alternative splicing. *Mol Carcinog.* (2019) 58:196–205. doi: 10.1002/mc.22919
51. Tripathi V, Ellis JD, Shen Z, Song DY, Pan Q, Watt AT, et al. The nuclear-retained noncoding RNA MALAT1 regulates alternative splicing by modulating SR splicing factor phosphorylation. *Mol Cell.* (2010) 39:925–38. doi: 10.1016/j.molcel.2010.08.011
52. Jiang MC, Ni JJ, Cui WY, Wang BY, Zhuo W. Emerging roles of lncRNA in cancer and therapeutic opportunities. *Am J Cancer Res.* (2019) 9:1354–66.
53. Huarte M. The emerging role of lncRNAs in cancer. *Nat Med.* (2015) 21:1253–61. doi: 10.1038/nm.3981
54. Sanchez Calle A, Kawamura Y, Yamamoto Y, Takeshita F, Ochiya T. Emerging roles of long non-coding RNA in cancer. *Cancer Sci.* (2018) 109:2093–100. doi: 10.1111/cas.13642
55. Kohn EC, Ivy SP. Whence high-grade serous ovarian cancer. *Am Soc Clin Oncol Educ Book.* (2017) 37:443–8. doi: 10.14694/EDBK_174718
56. Testa U, Petrucci E, Pasquini L, Castelli G, Pelosi E. Ovarian cancers: genetic abnormalities, tumor heterogeneity and progression, clonal evolution and cancer stem cells. *Medicines.* (2018) 5:1–74. doi: 10.3390/medicines5010016
57. Zhang Y, Cao L, Nguyen D, Lu H. TP53 mutations in epithelial ovarian cancer. *Transl Cancer Res.* (2016) 5:650–63. doi: 10.21037/tcr.2016.08.40
58. Cancer Genome Atlas Research Network. Integrated genomic analyses of ovarian carcinoma. *Nature.* (2011) 474:609–15. doi: 10.1038/nature10166
59. Bewtra C, Watson P, Conway T, Read-Hippee C, Lynch HT. Hereditary ovarian cancer: a clinicopathological study. *Int J Gynecol Pathol.* (1992) 11:180–7. doi: 10.1097/00004347-199207000-00003
60. Ramus SJ, Song H, Dicks E, Tyrer JP, Rosenthal AN, Intermaggio MP, et al. Germline mutations in the BRIP1, BARD1, PALB2, and NBN genes in women with ovarian cancer. *J Natl Cancer Inst.* (2015) 107:1–6. doi: 10.1093/jnci/djv214
61. Song H, Dicks E, Ramus SJ, Tyrer JP, Intermaggio MP, Hayward J, et al. Contribution of germline mutations in the RAD51B, RAD51C, and RAD51D genes to ovarian cancer in the population. *J Clin Oncol.* (2015) 33:2901–7. doi: 10.1200/JCO.2015.61.2408
62. Folkins AK, Longacre TA. Hereditary gynaecological malignancies: advances in screening and treatment. *Histopathology.* (2013) 62:2–30. doi: 10.1111/his.12028
63. Song H, Cicek MS, Dicks E, Harrington P, Ramus SJ, Cunningham JM, et al. The contribution of deleterious germline mutations in BRCA1, BRCA2 and the mismatch repair genes to ovarian cancer in the population. *Hum Mol Genet.* (2014) 23:4703–9. doi: 10.1093/hmg/ddu172
64. Alsop K, Fereday S, Meldrum C, A. deFazio, Emmanuel C, George J, et al. BRCA mutation frequency and patterns of treatment response in BRCA mutation-positive women with ovarian cancer: a report from the Australian Ovarian Cancer Study Group. *J Clin Oncol.* (2012) 30:2654–63. doi: 10.1200/JCO.2011.39.8545
65. Ledermann JA, Harter P, Gourley C, Friedlander M, Vergote I, Rustin G, et al. Overall survival in patients with platinum-sensitive recurrent serous ovarian cancer receiving olaparib maintenance monotherapy: an updated analysis from a randomised, placebo-controlled, double-blind, phase 2 trial. *Lancet Oncol.* (2016) 17:1579–89. doi: 10.1016/S1470-2045(16)30376-X
66. Hjortkjaer M, Malik Aagaard Jorgensen M, Waldstrom M, Ornskov D, Sogaard-Andersen E, Jakobsen A, et al. The clinical importance of BRCAness in a population-based cohort of Danish epithelial ovarian cancer. *Int J Gynecol Cancer.* (2019) 29:166–73. doi: 10.1136/ijgc-2018-000017
67. Marquard AM, Eklund AC, Joshi T, Krzystanek M, Favero F, Wang ZC, et al. Pan-cancer analysis of genomic scar signatures associated with homologous recombination deficiency suggests novel indications for existing cancer drugs. *Biomark Res.* (2015) 3:9. doi: 10.1186/s40364-015-0033-4
68. Huang J, Zhang L, Greshock J, Colligon TA, Wang Y, Ward R, et al. Frequent genetic abnormalities of the PI3K/AKT pathway in primary ovarian cancer predict patient outcome. *Genes Chromosomes Cancer.* (2011) 50:606–18. doi: 10.1002/gcc.20883
69. Levine DA, Bogomolniy F, Yee CJ, Lash A, Barakat RR, Borgen PI, et al. Frequent mutation of the PIK3CA gene in ovarian and breast cancers. *Clin Cancer Res.* (2005) 11:2875–8. doi: 10.1158/1078-0432.CCR-04-2142
70. Dunn GP, Cheung HW, Agarwalla PK, Thomas S, Zektser Y, Karst AM, et al. *In vivo* multiplexed interrogation of amplified genes identifies GAB2 as an ovarian cancer oncogene. *Proc Natl Acad Sci USA.* (2014) 111:1102–7. doi: 10.1073/pnas.1311909111
71. Hsu CY, Bristow R, Cha MS, Wang BG, Ho CL, Kurman RJ, et al. Characterization of active mitogen-activated protein kinase in ovarian serous carcinomas. *Clin Cancer Res.* (2004) 10:6432–6. doi: 10.1158/1078-0432.CCR-04-0893
72. Tothill RW, Tinker AV, George J, Brown R, Fox SB, Lade S, et al. Novel molecular subtypes of serous and endometrioid ovarian cancer linked to clinical outcome. *Clin Cancer Res.* (2008) 14:5198–208. doi: 10.1158/1078-0432.CCR-08-0196
73. Verhaak RG, Tamayo P, Yang JY, Hubbard D, Zhang H, Creighton CJ, et al. Prognostically relevant gene signatures of high-grade serous ovarian carcinoma. *J Clin Invest.* (2013) 123:517–25. doi: 10.1172/JCI65833
74. Konecny GE, Wang C, Hamidi H, Winterhoff B, Kalli KR, Dering J, et al. Prognostic and therapeutic relevance of molecular subtypes in high-grade serous ovarian cancer. *J Natl Cancer Inst.* (2014) 106:1–8. doi: 10.1093/jnci/dju249
75. Zhou M, Sun Y, Sun Y, Xu W, Zhang Z, Zhao H, et al. Comprehensive analysis of lncRNA expression profiles reveals a novel lncRNA signature to discriminate nonequivalent outcomes in patients with ovarian cancer. *Oncotarget.* (2016) 7:32433–48. doi: 10.18632/oncotarget.8653
76. Ning L, Hu YC, Wang S, Lang JH. Altered long noncoding RNAs and survival outcomes in ovarian cancer: a systematic review and meta-analysis (PRISMA Compliant). *Medicine.* (2018) 97:e11481. doi: 10.1097/MD.0000000000011481
77. Wang X, Han L, Zhou L, Wang L, Zhang LM. Prediction of candidate RNA signatures for recurrent ovarian cancer prognosis by the construction of an integrated competing endogenous RNA network. *Oncol Rep.* (2018) 40:2659–73. doi: 10.3892/or.2018.6707
78. Chang L, Guo R, Yuan Z, Shi H, Zhang D. LncRNA HOTAIR regulates CCND1 and CCND2 expression by sponging miR-206 in ovarian cancer. *Cell Physiol Biochem.* (2018) 49:1289–303. doi: 10.1159/000493408
79. Liu Y, Wang Y, Fu X, Lu Z. Long non-coding RNA NEAT1 promoted ovarian cancer cells' metastasis through regulation of miR-382-3p/ROCK1 axial. *Cancer Sci.* (2018) 109:2188–98. doi: 10.1111/cas.13647
80. Xia B, Hou Y, Chen H, Yang S, Liu T, Lin M, et al. Long non-coding RNA ZFAS1 interacts with miR-150-5p to regulate Sp1 expression and ovarian cancer cell malignancy. *Oncotarget.* (2017) 8:19534–46. doi: 10.18632/oncotarget.14663
81. Hong L, Chen W, Wu D, Wang Y. Upregulation of SNHG3 expression associated with poor prognosis and enhances malignant

progression of ovarian cancer. *Cancer Biomark.* (2018) 22:367–74. doi: 10.3233/CBM-170710
82. Szafron LM, Balcerak A, Grzybowska EA, Pienkowska-Grela B, Podgorska A, Zub R, et al. The putative oncogene, CRNDE, is a negative prognostic factor in ovarian cancer patients. *Oncotarget.* (2015) 6:43897–910. doi: 10.18632/oncotarget.6016
83. Chi Y, Wang D, Wang J, Yu W, Yang J. Long Non-coding RNA in the pathogenesis of cancers. *Cells.* (2019) 8:1–44. doi: 10.3390/cells8091015
84. Li N, Zhan X, Zhan X. The lncRNA SNHG3 regulates energy metabolism of ovarian cancer by an analysis of mitochondrial proteomes. *Gynecol Oncol.* (2018) 150:343–54. doi: 10.1016/j.ygyno.2018.06.013
85. Jin Y, Feng SJ, Qiu S, Shao N, Zheng JH. LncRNA MALAT1 promotes proliferation and metastasis in epithelial ovarian cancer via the PI3K-AKT pathway. *Eur Rev Med Pharmacol Sci.* (2017) 21:3176–84.
86. Qiu JJ, Lin YY, Ding JX, Feng WW, Jin HY, Hua KQ. Long non-coding RNA ANRIL predicts poor prognosis and promotes invasion/metastasis in serous ovarian cancer. *Int J Oncol.* (2015) 46:2497–505. doi: 10.3892/ijo.2015.2943
87. Akrami R, Jacobsen A, Hoell J, Schultz N, Sander C, Larsson E. Comprehensive analysis of long non-coding RNAs in ovarian cancer reveals global patterns and targeted DNA amplification. *PLoS ONE.* (2013) 8:e80306. doi: 10.1371/journal.pone.0080306
88. Rangel LB, Sherman-Baust CA, Wernyj RP, Schwartz DR, Cho KR, Morin PJ. Characterization of novel human ovarian cancer-specific transcripts (HOSTs) identified by serial analysis of gene expression. *Oncogene.* (2003) 22:7225–32. doi: 10.1038/sj.onc.1207008
89. Gao Y, Meng H, Liu S, Hu J, Zhang Y, Jiao T, et al. LncRNA-HOST2 regulates cell biological behaviors in epithelial ovarian cancer through a mechanism involving microRNA let-7b. *Hum Mol Genet.* (2015) 24:841–52. doi: 10.1093/hmg/ddu502
90. Huang P, Li F, Li L, You Y, Luo S, Dong Z, et al. lncRNA profile study reveals the mRNAs and lncRNAs associated with docetaxel resistance in breast cancer cells. *Sci Rep.* (2018) 8:17970. doi: 10.1038/s41598-018-36231-4
91. Hou Z, Xu C, Xie H, Xu H, Zhan P, Yu L, et al. Long noncoding RNAs expression patterns associated with chemo response to cisplatin based chemotherapy in lung squamous cell carcinoma patients. *PLoS ONE.* (2014) 9:e108133. doi: 10.1371/journal.pone.0108133
92. Hu Y, Zhu QN, Deng JL, Li ZX, Wang G, Zhu YS. Emerging role of long non-coding RNAs in cisplatin resistance. *Onco Targets Ther.* (2018) 11:3185–94. doi: 10.2147/OTT.S158104
93. Li Q, Zhang J, Zhou J, Yang B, Liu P, Cao L, et al. lncRNAs are novel biomarkers for differentiating between cisplatin-resistant and cisplatin-sensitive ovarian cancer. *Oncol Lett.* (2018) 15:8363–70. doi: 10.3892/ol.2018.8433
94. Rosenberg B, VanCamp L, Trosko JE, Mansour VH. Platinum compounds: a new class of potent antitumour agents. *Nature.* (1969) 222:385–6. doi: 10.1038/222385a0
95. Hah SS, Stivers KM, R.W. de Vere White, Henderson PT. Kinetics of carboplatin-DNA binding in genomic DNA and bladder cancer cells as determined by accelerator mass spectrometry. *Chem Res Toxicol.* (2006) 19:622–6. doi: 10.1021/tx060058c
96. Ferreira JA, Peixoto A, Neves M, Gaiteiro C, Reis CA, Assaraf YG, et al. Mechanisms of cisplatin resistance and targeting of cancer stem cells: adding glycosylation to the equation. *Drug Resist Updat.* (2016) 24:34–54. doi: 10.1016/j.drup.2015.11.003
97. Righetti SC, Della Torre G, Pilotti S, Menard S, Ottone F, Colnaghi MI, et al. A comparative study of p53 gene mutations, protein accumulation, and response to cisplatin-based chemotherapy in advanced ovarian carcinoma. *Cancer Res.* (1996) 56:689–93.
98. Turner NC, Tutt AN. Platinum chemotherapy for BRCA1-related breast cancer: do we need more evidence? *Breast Cancer Res.* (2012) 14:115. doi: 10.1186/bcr3332
99. Fink D, Nebel S, Aebi S, Zheng H, Cenni B, Nehme A, et al. The role of DNA mismatch repair in platinum drug resistance. *Cancer Res.* (1996) 56:4881–6.
100. Henkels KM, Turchi JJ. Cisplatin-induced apoptosis proceeds by caspase-3-dependent and -independent pathways in cisplatin-resistant and -sensitive human ovarian cancer cell lines. *Cancer Res.* (1999) 59:3077–83.
101. Marchini S, Fruscio R, Clivio L, Beltrame L, Porcu L, Fuso Nerini I, et al. Resistance to platinum-based chemotherapy is associated with epithelial to mesenchymal transition in epithelial ovarian cancer. *Eur J Cancer.* (2013) 49:520–30. doi: 10.1016/j.ejca.2012.06.026
102. Talbot LJ, Bhattacharya SD, Kuo PC. Epithelial-mesenchymal transition, the tumor microenvironment, and metastatic behavior of epithelial malignancies. *Int J Biochem Mol Biol.* (2012) 3:117–36.
103. Zhang W, Shi X, Peng Y, Wu M, Zhang P, Xie R, et al. HIF-1alpha Promotes Epithelial-Mesenchymal Transition and Metastasis through Direct Regulation of ZEB1 in Colorectal Cancer. *PLoS ONE.* (2015) 10:e0129603. doi: 10.1371/journal.pone.0129603
104. Norouzi-Barough L, Sarookhani MR, Sharifi M, Moghbelinejad S, Jangjoo S, Salehi R, Molecular mechanisms of drug resistance in ovarian cancer. *J Cell Physiol.* (2018) 233:4546–62. doi: 10.1002/jcp.26289
105. Bashashati A, Ha G, Tone A, Ding J, Prentice LM, Roth A, et al. Distinct evolutionary trajectories of primary high-grade serous ovarian cancers revealed through spatial mutational profiling. *J Pathol.* (2013) 231:21–34. doi: 10.1002/path.4230
106. Fang F, Cardenas H, Huang H, Jiang G, Perkins SM, Zhang C, et al. Genomic and epigenomic signatures in ovarian cancer associated with re-sensitization to platinum drugs. *Cancer Res.* (2018) 78:631–44. doi: 10.1158/0008-5472.CAN-17-1492
107. Liu S, Lei H, Luo F, Li Y, Xie L. The effect of lncRNA HOTAIR on chemoresistance of ovarian cancer through regulation of HOXA7. *Biol Chem.* (2018) 399:485–97. doi: 10.1515/hsz-2017-0274
108. Wang Y, Wang H, Song T, Zou Y, Jiang J, Fang L, et al. HOTAIR is a potential target for the treatment of cisplatinresistant ovarian cancer. *Mol Med Rep.* (2015) 12:2211–6. doi: 10.3892/mmr.2015.3562
109. Teschendorff AE, Lee SH, Jones A, Fiegl H, Kalwa M, Wagner W, et al. HOTAIR and its surrogate DNA methylation signature indicate carboplatin resistance in ovarian cancer. *Genome Med.* (2015) 7:108. doi: 10.1186/s13073-015-0233-4
110. Li J, Yang S, Su N, Wang Y, Yu J, Qiu H, et al. Overexpression of long non-coding RNA HOTAIR leads to chemoresistance by activating the Wnt/beta-catenin pathway in human ovarian cancer. *Tumour Biol.* (2016) 37:2057–65. doi: 10.1007/s13277-015-3998-6
111. Wang P, Zhang Y, Wang Q, Wu S, Zeng X, Zhou Y, et al. Down-modulation of MALAT1 inhibits proliferation, metastasis, invasion and sensitizes chemosensitivity to cisplatin in ovarian cancer cells. *Int J Clin Exp Med.* (2018). 11:13158–68.
112. Bai L, Wang A, Zhang Y, Xu X, Zhang X. Knockdown of MALAT1 enhances chemosensitivity of ovarian cancer cells to cisplatin through inhibiting the Notch1 signaling pathway. *Exp Cell Res.* (2018) 366:161–71. doi: 10.1016/j.yexcr.2018.03.014
113. Zheng ZG, Xu H, Suo SS, Xu XL, Ni MW, Gu LH, et al. The essential role of H19 contributing to cisplatin resistance by regulating glutathione metabolism in high-grade serous ovarian cancer. *Sci Rep.* (2016) 6:26093. doi: 10.1038/srep26093
114. Liu R, Zeng Y, Zhou CF, Wang Y, Li X, Liu ZQ, et al. Long noncoding RNA expression signature to predict platinum-based chemotherapeutic sensitivity of ovarian cancer patients. *Sci Rep.* (2017) 7:18. doi: 10.1038/s41598-017-00050-w
115. Wang F, Zhou J, Xie X, Hu J, Chen L, Hu Q, et al. Involvement of SRPK1 in cisplatin resistance related to long non-coding RNA UCA1 in human ovarian cancer cells. *Neoplasma.* (2015) 62:432–8. doi: 10.4149/neo_2015_051
116. Li Z, Niu H, Qin Q, Yang S, Wang Q, Yu C, et al. lncRNA UCA1 mediates resistance to cisplatin by regulating the miR-143/FOSL2-signaling pathway in ovarian cancer. *Mol Ther Nucleic Acids.* (2019) 17:92–101. doi: 10.1016/j.omtn.2019.05.007
117. Zhang L, Cao X, Zhang L, Zhang X, Sheng H, Tao K. UCA1 overexpression predicts clinical outcome of patients with ovarian cancer receiving adjuvant chemotherapy. *Cancer Chemother Pharmacol.* (2016) 77:629–34. doi: 10.1007/s00280-016-2963-4
118. Wang H, Fang L, Jiang J, Kuang Y, Wang B, Shang X, et al. The cisplatin-induced lncRNA PANDAR dictates the chemoresistance of ovarian cancer

via regulating SFRS2-mediated p53 phosphorylation. *Cell Death Dis.* (2018) 9:1103. doi: 10.1038/s41419-018-1148-y
119. Liu E, Liu Z, Zhou Y, Mi R, Wang D. Overexpression of long non-coding RNA PVT1 in ovarian cancer cells promotes cisplatin resistance by regulating apoptotic pathways. *Int J Clin Exp Med.* (2015) 8:20565–72.
120. Song J, Zhang W, Wang S, Liu K, Song F, Ran L. A panel of 7 prognosis-related long non-coding RNAs to improve platinum-based chemoresistance prediction in ovarian cancer. *Int J Oncol.* (2018) 53:866–76. doi: 10.3892/ijo.2018.4403
121. Wu DI, Wang T, Ren C, Liu L, Kong D, Jin X, et al. Downregulation of BC200 in ovarian cancer contributes to cancer cell proliferation and chemoresistance to carboplatin. *Oncol Lett.* (2016) 11:1189–94. doi: 10.3892/ol.2015.3983
122. Zhang C, Wang M, Shi C, Shi F, Pei C. Long non-coding RNA Linc00312 modulates the sensitivity of ovarian cancer to cisplatin via the Bcl-2/Caspase-3 signaling pathway. *Biosci Trends.* (2018) 12:309–16. doi: 10.5582/bst.2018.01052
123. Vera O, Rodriguez-Antolin C, de Castro J, Karreth FA, Sellers TA, I. Ibanez de Caceres. An epigenomic approach to identifying differential overlapping and cis-acting lncRNAs in cisplatin-resistant cancer cells. *Epigenetics.* (2018) 13:251–63. doi: 10.1080/15592294.2018.1436364
124. Qu C, Dai C, Guo Y, Qin R, Liu J. Long noncoding RNA SNHG15 serves as an oncogene and predicts poor prognosis in epithelial ovarian cancer. *Onco Targets Ther.* (2019) 12:101–11. doi: 10.2147/OTT.S182657
125. Xu QF, Tang YX, Wang X. LncRNA EBIC promoted proliferation, metastasis and cisplatin resistance of ovarian cancer cells and predicted poor survival in ovarian cancer patients. *Eur Rev Med Pharmacol Sci.* (2018) 22:4440–7. doi: 10.26355/eurrev_201807_15495
126. Rinn JL, Kertesz M, Wang JK, Squazzo SL, Xu X, Brugmann SA, et al. Functional demarcation of active and silent chromatin domains in human HOX loci by noncoding RNAs. *Cell.* (2007) 129:1311–23. doi: 10.1016/j.cell.2007.05.022
127. Naora H, Montz FJ, Chai CY, Roden RB, Aberrant expression of homeobox gene HOXA7 is associated with mullerian-like differentiation of epithelial ovarian tumors and the generation of a specific autologous antibody response. *Proc Natl Acad Sci USA.* (2001) 98:15209–14. doi: 10.1073/pnas.011503998
128. Zhang Y, Cheng JC, Huang HF, Leung PC. Homeobox A7 stimulates breast cancer cell proliferation by up-regulating estrogen receptor-alpha. *Biochem Biophys Res Commun.* (2013) 440:652–7. doi: 10.1016/j.bbrc.2013.09.121
129. Mitra R, Chen X, Greenawalt EJ, Maulik U, Jiang W, Zhao Z, et al. Decoding critical long non-coding RNA in ovarian cancer epithelial-to-mesenchymal transition. *Nat Commun.* (2017) 8:1604. doi: 10.1038/s41467-017-01781-0
130. Li P, Zhang X, Wang H, Wang L, Liu T, Du L, et al. MALAT1 is associated with poor response to oxaliplatin-based chemotherapy in colorectal cancer patients and promotes chemoresistance through EZH2. *Mol Cancer Ther.* (2017) 16:739–51. doi: 10.1158/1535-7163.MCT-16-0591
131. Zhou Y, Chen Q, Qin R, Zhang K, Li H. MicroRNA-449a reduces cell survival and enhances cisplatin-induced cytotoxicity via downregulation of NOTCH1 in ovarian cancer cells. *Tumour Biol.* (2014) 35:12369–78. doi: 10.1007/s13277-014-2551-3
132. Cole SP, Bhardwaj G, Gerlach JH, Mackie JE, Grant CE, Almquist KC, et al. Overexpression of a transporter gene in a multidrug-resistant human lung cancer cell line. *Science.* (1992) 258:1650–4. doi: 10.1126/science.1360704
133. Chen J, Liu X, Xu Y, Zhang K, Huang J, Pan B, et al. TFAP2C-Activated MALAT1 modulates the chemoresistance of docetaxel-resistant lung adenocarcinoma cells. *Mol Ther Nucleic Acids.* (2019) 14:567–82. doi: 10.1016/j.omtn.2019.01.005
134. Gabory A, Jammes H, Dandolo L. The H19 locus: role of an imprinted non-coding RNA in growth and development. *Bioessays.* (2010) 32:473–80. doi: 10.1002/bies.200900170
135. Esteves LI, Javaroni AC, Nishimoto IN, Magrin J, Squire JA, Kowalski LP, et al. DNA methylation in the CTCF-binding site I and the expression pattern of the H19 gene: does positive expression predict poor prognosis in early stage head and neck carcinomas? *Mol Carcinog.* (2005) 44:102–10. doi: 10.1002/mc.20126
136. Rainho CA, Pontes A, Rogatto SR. Expression and imprinting of insulin-like growth factor II (IGF2) and H19 genes in uterine leiomyomas. *Gynecol Oncol.* (1999) 74:375–80. doi: 10.1006/gyno.1999.5483
137. Yoshimura H, Matsuda Y, Yamamoto M, Kamiya S, Ishiwata T. Expression and role of long non-coding RNA H19 in carcinogenesis. *Front Biosci.* (2018) 23:614–25. doi: 10.2741/4608
138. Keniry A, Oxley D, Monnier P, Kyba M, Dandolo L, Smits G, et al. The H19 lincRNA is a developmental reservoir of miR-675 that suppresses growth and Igf1r. *Nat Cell Biol.* (2012) 14:659–65. doi: 10.1038/ncb2521
139. Costa V, Lo Dico A, Rizzo A, Rajata F, Tripodi M, Alessandro R, et al. MiR-675-5p supports hypoxia induced epithelial to mesenchymal transition in colon cancer cells. *Oncotarget.* (2017) 8:24292–302. doi: 10.18632/oncotarget.14464
140. Wang J, Zhang Y, Wei H, Zhang X, Wu Y, Gong A, et al. The mir-675-5p regulates the progression and development of pancreatic cancer via the UBQLN1-ZEB1-mir200 axis. *Oncotarget.* (2017) 8:24978–87. doi: 10.18632/oncotarget.15330
141. Barsyte-Lovejoy D, Lau SK, Boutros PC, Khosravi F, Jurisica I, Andrulis IL, et al. The c-Myc oncogene directly induces the H19 noncoding RNA by allele-specific binding to potentiate tumorigenesis. *Cancer Res.* (2006) 66:5330–7. doi: 10.1158/0008-5472.CAN-06-0037
142. Matouk IJ, Mezan S, Mizrahi A, Ohana P, Abu-Lail R, Fellig Y, et al. The oncofetal H19 RNA connection: hypoxia, p53 and cancer. *Biochim Biophys Acta.* (2010) 1803:443–51. doi: 10.1016/j.bbamcr.2010.01.010
143. Godwin AK, Meister A, O'Dwyer PJ, Huang CS, Hamilton TC, Anderson ME. High resistance to cisplatin in human ovarian cancer cell lines is associated with marked increase of glutathione synthesis. *Proc Natl Acad Sci USA.* (1992) 89:3070–4. doi: 10.1073/pnas.89.7.3070
144. Meijer C, Mulder NH, Timmer-Bosscha H, Sluiter WJ, Meersma GJ, de Vries EG. Relationship of cellular glutathione to the cytotoxicity and resistance of seven platinum compounds. *Cancer Res.* (1992) 52:6885–9.
145. Wei J, Gan Y, Peng D, Jiang X, Kitazawa R, Xiang Y, et al. Long non-coding RNA H19 promotes TDRG1 expression and cisplatin resistance by sequestering miRNA-106b-5p in seminoma. *Cancer Med.* (2018) 7:6247–57. doi: 10.1002/cam4.1871
146. Wang Q, Cheng N, Li X, Pan H, Li C, Ren S, et al. Correlation of long non-coding RNA H19 expression with cisplatin-resistance and clinical outcome in lung adenocarcinoma. *Oncotarget.* (2017) 8:2558–67. doi: 10.18632/oncotarget.13708
147. Askarian-Amiri ME, Crawford J, French JD, Smart CE, Smith MA, Clark MB, et al. SNORD-host RNA Zfas1 is a regulator of mammary development and a potential marker for breast cancer. *RNA.* (2011) 17:878–91. doi: 10.1261/rna.2528811
148. Thorenoor N, Faltejskova-Vychytilova P, Hombach S, Mlcochova J, Kretz M, Svoboda M, et al. Long non-coding RNA ZFAS1 interacts with CDK1 and is involved in p53-dependent cell cycle control and apoptosis in colorectal cancer. *Oncotarget.* (2016) 7:622–37. doi: 10.18632/oncotarget.5807
149. Vizcaino C, Mansilla S, Portugal J. Sp1 transcription factor: A long-standing target in cancer chemotherapy. *Pharmacol Ther.* (2015) 152:111–24. doi: 10.1016/j.pharmthera.2015.05.008
150. Olofsson BA, Kelly CM, Kim J, Hornsby SM, Azizkhan-Clifford J. Phosphorylation of Sp1 in response to DNA damage by ataxia telangiectasia-mutated kinase. *Mol Cancer Res.* (2007) 5:1319–30. doi: 10.1158/1541-7786.MCR-07-0374
151. Lai YH, Kuo C, Kuo MT, H.Chen HW. Modulating chemosensitivity of tumors to platinum-based antitumor drugs by transcriptional regulation of copper homeostasis. *Int J Mol Sci.* (2018) 19:E1486. doi: 10.3390/ijms19051486
152. Wang XS, Zhang Z, Wang HC, Cai JL, Xu QW, Li MQ, et al. Rapid identification of UCA1 as a very sensitive and specific unique marker for human bladder carcinoma. *Clin Cancer Res.* (2006) 12:4851–8. doi: 10.1158/1078-0432.CCR-06-0134
153. Xue M, Li X, Li Z, Chen W. Urothelial carcinoma associated 1 is a hypoxia-inducible factor-1alpha-targeted long noncoding RNA that enhances hypoxic bladder cancer cell proliferation, migration, invasion. *Tumour Biol.* (2014) 35:6901–12. doi: 10.1007/s13277-014-1925-x

154. Guo Q, Lan F, Yan X, Xiao Z, Wu Y, Zhang Q. Hypoxia exposure induced cisplatin resistance partially via activating p53 and hypoxia inducible factor-1α in non-small cell lung cancer A549 cells. *Oncol Lett.* (2018) 16:801–8. doi: 10.3892/ol.2018.8767
155. Horita K, Kurosaki H, Nakatake M, Kuwano N, Oishi T, Itamochi H, et al. lncRNA UCA1-mediated Cdc42 signaling promotes oncolytic vaccinia virus cell-to-cell spread in ovarian cancer. *Mol Ther Oncolytics.* (2019) 13:35–48. doi: 10.1016/j.omto.2019.03.003
156. Wang J, Ye C, Liu J, Hu Y. UCA1 confers paclitaxel resistance to ovarian cancer through miR-129/ABCB1 axis. *Biochem Biophys Res Commun.* (2018) 501:1034–40. doi: 10.1016/j.bbrc.2018.05.104
157. Vaidyanathan A, Sawers L, Gannon AL, Chakravarty P, Scott AL, Bray SE, et al. ABCB1 (MDR1) induction defines a common resistance mechanism in paclitaxel- and olaparib-resistant ovarian cancer cells. *Br J Cancer.* (2016) 115:431–41. doi: 10.1038/bjc.2016.203
158. Li J, Li Z, Zheng W, Li X, Wang Z, Cui Y, et al. PANDAR: a pivotal cancer-related long non-coding RNA in human cancers. *Mol Biosyst.* (2017) 13:2195–201. doi: 10.1039/C7MB00414A
159. Hung T, Wang Y, Lin MF, Koegel AK, Kotake Y, Grant GD, et al. Extensive and coordinated transcription of noncoding RNAs within cell-cycle promoters. *Nat Genet.* (2011) 43:621–9. doi: 10.1038/ng.848
160. Chen Y, Du H, Bao L, Liu W. LncRNA PVT1 promotes ovarian cancer progression by silencing miR-214. *Cancer Biol Med.* (2018) 15:238–50. doi: 10.20892/j.issn.2095-3941.2017.0174
161. Yang Q, Yu Y, Sun Z, Pan Y. Long non-coding RNA PVT1 promotes cell proliferation and invasion through regulating miR-133a in ovarian cancer. *Biomed Pharmacother.* (2018) 106:61–7. doi: 10.1016/j.biopha.2018.06.112
162. Ding J, Li D, Gong M, Wang J, Huang X, Wu T, et al. Expression and clinical significance of the long non-coding RNA PVT1 in human gastric cancer. *Onco Targets Ther.* (2014) 7:1625–30. doi: 10.2147/OTT.S68854
163. Guan Y, Kuo WL, Stilwell JL, Takano H, Lapuk AV, Fridlyand J, et al. Amplification of PVT1 contributes to the pathophysiology of ovarian and breast cancer. *Clin Cancer Res.* (2007) 13:5745–55. doi: 10.1158/1078-0432.CCR-06-2882
164. Huppi K, Volfovsky N, Runfola T, Jones TL, Mackiewicz M, Martin SE, et al. The identification of microRNAs in a genomically unstable region of human chromosome 8q24. *Mol Cancer Res.* (2008) 6:212–21. doi: 10.1158/1541-7786.MCR-07-0105
165. Tseng YY, Moriarity BS, Gong W, Akiyama R, Tiwari A, Kawakami H, et al. PVT1 dependence in cancer with MYC copy-number increase. *Nature.* (2014) 512:82–6. doi: 10.1038/nature13311
166. Reyes-Gonzalez JM, Armaiz-Pena GN, Mangala LS, Valiyeva F, Ivan C, Pradeep S, et al. Targeting c-MYC in platinum-resistant ovarian cancer. *Mol Cancer Ther.* (2015) 14:2260–9. doi: 10.1158/1535-7163.MCT-14-0801
167. Liu E, Liu Z, Zhou Y. Carboplatin-docetaxel-induced activity against ovarian cancer is dependent on up-regulated lncRNA PVT1. *Int J Clin Exp Pathol.* (2015) 8:3803–10.
168. Chen L, Han X, Hu Z, Chen L. The PVT1/miR-216b/Beclin-1 regulates cisplatin sensitivity of NSCLC cells via modulating autophagy and apoptosis. *Cancer Chemother Pharmacol.* (2019) 83:921–31. doi: 10.1007/s00280-019-03808-3
169. Iden M, Fye S, Li K, Chowdhury T, Ramchandran R, Rader JS. The lncRNA PVT1 contributes to the cervical cancer phenotype and associates with poor patient prognosis. *PLoS ONE.* (2016) 11:e0156274. doi: 10.1371/journal.pone.0156274
170. Tian T, Lv X, Pan G, Lu Y, Chen W, He W, et al. Long noncoding RNA MPRL promotes mitochondrial fission and cisplatin chemosensitivity via disruption of pre-miRNA processing. *Clin Cancer Res.* (2019) 25:3673–88. doi: 10.1158/1078-0432.CCR-18-2739
171. Rao S, Orr GA, Chaudhary AG, Kingston DG, Horwitz SB. Characterization of the taxol binding site on the microtubule. 2-(m-Azidobenzoyl)taxol photolabels a peptide (amino acids 217-231) of beta-tubulin. *J Biol Chem.* (1995) 270:20235–8. doi: 10.1074/jbc.270.35.20235
172. Jordan MA, Wendell K, Gardiner S, Derry WB, Copp H, Wilson L. Mitotic block induced in HeLa cells by low concentrations of paclitaxel (Taxol) results in abnormal mitotic exit and apoptotic cell death. *Cancer Res.* (1996) 56:816–25.
173. Stordal B, Pavlakis N, Davey R. A systematic review of platinum and taxane resistance from bench to clinic: an inverse relationship. *Cancer Treat Rev.* (2007) 33:688–703. doi: 10.1016/j.ctrv.2007.07.013
174. Yusuf RZ, Duan Z, Lamendola DE, Penson RT, Seiden MV. Paclitaxel resistance: molecular mechanisms and pharmacologic manipulation. *Curr Cancer Drug Targets.* (2003) 3:1–19. doi: 10.2174/1568009033333754
175. Parekh H, Wiesen K, Simpkins H, Acquisition of taxol resistance via P-glycoprotein- and non-P-glycoprotein-mediated mechanisms in human ovarian carcinoma cells. *Biochem Pharmacol.* (1997) 53:461–70. doi: 10.1016/S0006-2952(97)83383-7
176. Wang L, Hu Y, Xiang X, Qu K, Teng Y, Identification of long non-coding RNA signature for paclitaxel-resistant patients with advanced ovarian cancer. *Oncotarget.* (2017) 8:64191–202. doi: 10.18632/oncotarget.19828
177. Liu S, Zou B, Tian T, Luo X, Mao B, Zhang X, et al. Overexpression of the lncRNA FER1L4 inhibits paclitaxel tolerance of ovarian cancer cells via the regulation of the MAPK signaling pathway. *J Cell Biochem.* (2018). doi: 10.1002/jcb.28032. [Epub ahead of print].
178. Shi C, Wang M. LINC01118 modulates paclitaxel resistance of epithelial ovarian cancer by regulating miR-134/ABCC1. *Med Sci Monit.* (2018) 24:8831–9. doi: 10.12659/MSM.910932
179. An J, Lv W, Zhang Y. LncRNA NEAT1 contributes to paclitaxel resistance of ovarian cancer cells by regulating ZEB1 expression via miR-194. *Onco Targets Ther.* (2017) 10:5377–90. doi: 10.2147/OTT.S147586
180. Huang KC, Rao PH, Lau CC, Heard E, Ng SK, Brown C, et al. Relationship of XIST expression and responses of ovarian cancer to chemotherapy. *Mol Cancer Ther.* (2002) 1:769–76.
181. Zhang M, Liu S, Fu C, Wang X, Zhang M, Liu G, et al. LncRNA KB-1471A8.2 Overexpression suppresses cell proliferation and migration and antagonizes the paclitaxel resistance of ovarian cancer cells. *Cancer Biother Radiopharm.* (2019) 34:316–24. doi: 10.1089/cbr.2018.2698
182. Xu J, Wu J, Fu C, Teng F, Liu S, Dai C, et al. Multidrug resistant lncRNA profile in chemotherapeutic sensitive and resistant ovarian cancer cells. *J Cell Physiol.* (2018) 233:5034–43. doi: 10.1002/jcp.26369
183. Liu Z, Shao Y, Tan L, Shi H, Chen S, Guo J. Clinical significance of the low expression of FER1L4 in gastric cancer patients. *Tumour Biol.* (2014) 35:9613–7. doi: 10.1007/s13277-014-2259-4
184. Xia T, Chen S, Jiang Z, Shao Y, Jiang X, Li P, et al. Long noncoding RNA FER1L4 suppresses cancer cell growth by acting as a competing endogenous RNA and regulating PTEN expression. *Sci Rep.* (2015) 5:13445. doi: 10.1038/srep13445
185. Liu Z, Zhu G, Getzenberg RH, Veltri RW. The upregulation of PI3K/Akt and MAP kinase pathways is associated with resistance of microtubule-targeting drugs in prostate cancer. *J Cell Biochem.* (2015) 116:1341–9. doi: 10.1002/jcb.25091
186. Yu X, Li Z, Zheng H, Chan MT, Wu WK. NEAT1: A novel cancer-related long non-coding RNA. *Cell Prolif.* (2017) 50:1–13. doi: 10.1111/cpr.12329
187. Chen ZJ, Zhang Z, Xie BB, Zhang HY. Clinical significance of up-regulated lncRNA NEAT1 in prognosis of ovarian cancer. *Eur Rev Med Pharmacol Sci.* (2016) 20:3373–7.
188. Zhang P, Sun Y, Ma L. ZEB1: at the crossroads of epithelial-mesenchymal transition, metastasis and therapy resistance. *Cell Cycle.* (2015) 14:481–7. doi: 10.1080/15384101.2015.1006048
189. Tinzl M, Marberger M, Horvath S, Chypre C. DD3PCA3 RNA analysis in urine–a new perspective for detecting prostate cancer. *Eur Urol.* (2004) 46:182–6; discussion: 187. doi: 10.1016/j.eururo.2004.06.004
190. Isin M, Ozgur E, Cetin G, Erten N, Aktan M, Gezer U, et al. Investigation of circulating lncRNAs in B-cell neoplasms. *Clin Chim Acta.* (2014) 431:255–9. doi: 10.1016/j.cca.2014.02.010
191. Slaby O, Laga R, Sedlacek O. Therapeutic targeting of non-coding RNAs in cancer. *Biochem J.* (2017) 474:4219–51. doi: 10.1042/BCJ20170079
192. Ray A, Norden B. Peptide nucleic acid (PNA): its medical and biotechnical applications and promise for the future. *FASEB J.* (2000) 14:1041–60. doi: 10.1096/fasebj.14.9.1041
193. Ozes AR, Wang Y, Zong X, Fang F, Pilrose J, Nephew KP. Therapeutic targeting using tumor specific peptides inhibits long non-coding RNA HOTAIR activity in ovarian and breast cancer. *Sci Rep.* (2017) 7:894. doi: 10.1038/s41598-017-00966-3

194. Uszczynska-Ratajczak B, Lagarde J, Frankish A, Guigo R, Johnson R. Towards a complete map of the human long non-coding RNA transcriptome. *Nat Rev Genet*. (2018) 19:535–48. doi: 10.1038/s41576-018-0017-y
195. Vidaurre S, Fitzpatrick C, Burzio VA, Briones M, Villota C, Villegas J, et al. Down-regulation of the antisense mitochondrial non-coding RNAs (ncRNAs) is a unique vulnerability of cancer cells and a potential target for cancer therapy. *J Biol Chem*. (2014) 289:27182–98. doi: 10.1074/jbc.M114.558841
196. *Andes Biotechnologies -Clinical Trials and Pipelines*. Available online at: http://andesbio.com/clinical-trials-pipeline/ (cited June 05, 2019).

Conflict of Interest: The authors declare that the research was conducted in the absence of any commercial or financial relationships that could be construed as a potential conflict of interest.

frontiers in Oncology

REVIEW
published: 20 February 2020
doi: 10.3389/fonc.2020.00150

The Role of microRNAs, Long Non-coding RNAs, and Circular RNAs in Cervical Cancer

Maria Lina Tornesello[1], Raffaella Faraonio[2], Luigi Buonaguro[3], Clorinda Annunziata[1], Noemy Starita[1], Andrea Cerasuolo[1], Francesca Pezzuto[1], Anna Lucia Tornesello[1] and Franco Maria Buonaguro[1]*

[1] Molecular Biology and Viral Oncology Unit, Istituto Nazionale Tumori IRCCS "Fondazione G. Pascale", Naples, Italy, [2] Department of Molecular Medicine and Medical Biotechnology, University of Naples Federico II, Naples, Italy, [3] Cancer Immunoregulation Unit, Istituto Nazionale Tumori IRCCS "Fondazione G. Pascale", Naples, Italy

Prolonged infection of uterine cervix epithelium with human papillomavirus (HPV) and constitutive expression of viral oncogenes have been recognized as the main cause of the complex molecular changes leading to transformation of cervical epithelial cells. Deregulated expression of microRNAs (miRNA), long non-coding RNAs (lncRNA), and circular RNAs (circRNA) is involved in the initiation and promotion processes of cervical cancer development. Expression profiling of small RNAs in cervical neoplasia revealed up-regulated "oncogenic" miRNAs, such as miR-10a, miR-21, miR-19, and miR-146a, and down regulated "tumor suppressive" miRNAs, including miR-29a, miR-372, miR-214, and miR-218, associated with cell growth, malignant transformation, cell migration, and invasion. Also several lncRNAs, comprising among others HOTAIR, MALAT1, GAS5, and MEG3, have shown to be associated with various pathogenic processes such as tumor progression, invasion as well as therapeutic resistance and emerged as new diagnostic and prognostic biomarkers in cervical cancer. Moreover, human genes encoded circular RNAs, such as has_circ-0018289, have shown to sponge specific miRNAs and to concur to the deregulation of target genes. Viral encoded circE7 has also demonstrated to overexpress E7 oncoprotein thus contributing to cell transformation. In this review, we summarize current literature on the complex interplay between miRNAs, lncRNAs, and circRNAs and their role in cervical neoplasia.

Keywords: cervical cancer, long non-coding RNA, circular RNA, microRNA, human papillomavirus (HPV)

OPEN ACCESS

Edited by:
Patricia P. Reis,
São Paulo State University, Brazil

Reviewed by:
Apollonia Tullo,
National Research Council, Italy
Hua Zhang,
Guangdong Medical University, China

****Correspondence:***
Maria Lina Tornesello
m.tornesello@istitutotumori.na.it

Specialty section:
This article was submitted to Molecular and Cellular Oncology, a section of the journal Frontiers in Oncology

Received: *07 October 2019*
Accepted: *28 January 2020*
Published: *20 February 2020*

Citation:
Tornesello ML, Faraonio R, Buonaguro L, Annunziata C, Starita N, Cerasuolo A, Pezzuto F, Tornesello AL and Buonaguro FM (2020) The Role of microRNAs, Long Non-coding RNAs, and Circular RNAs in Cervical Cancer. Front. Oncol. 10:150. doi: 10.3389/fonc.2020.00150

INTRODUCTION

Cervical cancer is the fourth most frequently diagnosed tumor and the fourth leading cause of cancer death in women in the world with ∼570,000 cases and 311,000 deaths in 2018 (1). The persistent infection with carcinogenic human papillomaviruses (HPV) has shown to be the necessary cause of ∼95% of invasive cervical cancer, including cervical squamous cell carcinoma (SCC) and adenocarcinoma (AC) histotypes (2). Cervical SCC is generally preceded by persistent squamous intraepithelial lesions (SIL) caused by HPV infection, therefore the detection of viral nucleic acids has shown to be valuable for the effective prevention of cervical cancer development in oncologic screening programs (3).

The E6 and E7 oncoproteins encoded by high risk HPVs are considered the main players of the multistep transformation process affecting the infected cervical cells. Indeed, they are able to inhibit p53 and pRb oncosuppressors, respectively, and to interact with a plethora of cell signaling factors regulating cell cycle, genome stability and epigenetic modifications (4, 5). Moreover, the HPV E5 protein has also a relevant role in tumor cell invasion and metastasis for its ability to increase the expression of the epidermal growth factor receptor (EGFR) and c-MET, the latter being also critical for viral gene expression (6, 7).

Nevertheless, the gradually accumulation of genetic and epigenetic alterations in HPV infected cells is also crucial for the ultimate progression to cervical cancer. The mutational profile of cervical carcinoma showed the presence of non-synonymous somatic nucleotide changes in PIK3CA, PTEN, TP53, STK11, and KRAS genes (8–11). Recent advances in cancer genome sequencing allowed to identify further unknown mutations in MAPK1, HLA, EP300, FBXW7, NFE2L2, ERBB3, CASP8, TGFBR2, and SHKBP1 genes as well as sequence amplifications in CD274 (PD-L1), PDCD1LG2 (PD-L2), and BCAR4 (lncRNA BCAR4) genes (12, 13). In addition, activating mutations creating *de novo* transcription factor binding sites in regulatory regions, such as the TERT promoter sequence, have been identified in a significant fraction of cervical SCC (14).

Epigenetic modifications, including deregulation of microRNA (miRNA), long non-protein coding RNA (lncRNA) and circular RNA (circRNA) levels, have shown to play important roles in cell transformation during distinct stages of cervical intraepithelial neoplasia and cervical carcinoma development [**Figure 1**; (15–17)].

MiRNAs are small (19–25 nucleotides long), single-stranded non-coding RNAs that regulate gene expression mainly by binding to sequence motifs located within the 3′ untranslated region (UTR) of mRNA transcripts (18, 19). Other regulatory functions include their reciprocal interaction on primary miRNA transcription processes, binding to double-stranded DNA to form triple helixes as well as interaction with RNA G-quadruplex structures that interfere at specific gene regulatory sites (20). The differential expression of the ∼2,500 miRNAs encoded by the human genome has an important role in the embryo development and in the physiological functioning of tissues and organs (21, 22). Several miRNAs have oncogenic or tumor suppressor activities and play a fundamental role in cancer development, progression and dissemination (23). A recent meta-analysis of miRNA profiles in cervical neoplasia cases and normal cervical epithelium samples identified 42 up regulated and 21 down regulated miRNAs among different stages of cervical neoplasia (24). The pathway enrichment analysis of genes targeted by these miRNAs revealed the alteration of p53, ErbB, MAPK, mTOR, Notch, TGFβ, and Wnt pathways all contributing to hallmarks of cancer (24).

lncRNAs are regulatory transcripts longer than 200 nucleotides mostly transcribed by RNA pol II and characterized by a 5′ 7-methylguanosine cap and a 3′ poly (A) tail similarly to messenger RNAs (25). Despite being not translated into full-length proteins, lncRNAs are implicated in a variety of biological activities such as regulation of gene transcription mediated by their interaction with chromatin-modifying complexes at specific regulatory regions, decoy for transcription factors and miRNAs as well as scaffolding for functional ribonucleoprotein complexes organization (26, 27). Deregulation of lncRNAs expression is associated with cardiovascular and neurodegenerative diseases as well as with cancer development (27, 28). Around 14 lncRNAs have shown to be altered in cervical carcinoma affecting important metabolic pathways such as STAT3, wnt/β-catenin, PI3K/AKT, and Notch signaling (29). Moreover, some lncRNAs, including MALAT1, CCEPR, and TMPOP2, are reciprocally regulated by HPV16 E6 and E7 expression hence enhancing the oncogenic effect of viral oncoproteins in the progression of cervical neoplasia (30, 31).

The single-stranded closed RNA molecules (circRNA) are a new class of non-coding RNAs, originating from back-splicing of pre-mRNAs, that have several biological functions in normal cells including the ability to act as sponges to efficiently subtract microRNAs and proteins (32). CircRNAs have shown to be aberrantly expressed in a tissue-specific manner in cancer cells and to contribute to cancer development by perturbing cell proliferation, migration, and angiogenesis processes (33). Several studies indicated that circRNAs play a significant role in cervical cancer development by different molecular mechanisms, which among them miRNA sponging is the most important (34). A recent study investigating circRNA expression in cervical cancer tissues by microarray analysis showed that 45 circRNAs were upregulated and that the most expressed has_circ_0018289 was involved in the direct binding of miR-497 (35).

The aim of this review is to summarize the recent studies on the role of miRNAs, lncRNAs, and circRNAs as well as their reciprocal regulation in different stages of cervical neoplasia. Moreover, it provides an overview of the potential impact of non-coding RNAs in the diagnosis and therapy of cervical cancer.

THE ROLE OF miRNAs IN CERVICAL NEOPLASIA

Many studies have evaluated the expression levels of miRNAs in cervical neoplasia biopsies as well as in exfoliated cervical cells, in cervical mucus and in the serum of women diagnosed with cervical cancer (**Table 1**). The first study describing the differential expression of six miRNAs (let-7b, let-7c, miR-21, miR-23b, miR-196b, and miR-143) in human cervical carcinoma cell lines in comparison with normal cervical samples was published by Lui et al. (107). Numerous investigations since then have been conducted in order to characterize the mechanisms causing miRNAs deregulation as well as their expression pattern in cervical cancer tissues vs. normal cervical epithelia. Indeed, genetic alterations of miRNA loci such as gene deletions, amplifications, or mutations as well as epigenetic silencing such as DNA methylation or deregulation of miRNA processors and transcription factors have been all associated with aberrant expression of miRNAs in cervical cancer (108). For example, Wilting et al. identified 89 deregulated miRNAs in cervical SCC with miR-9 over expression significantly

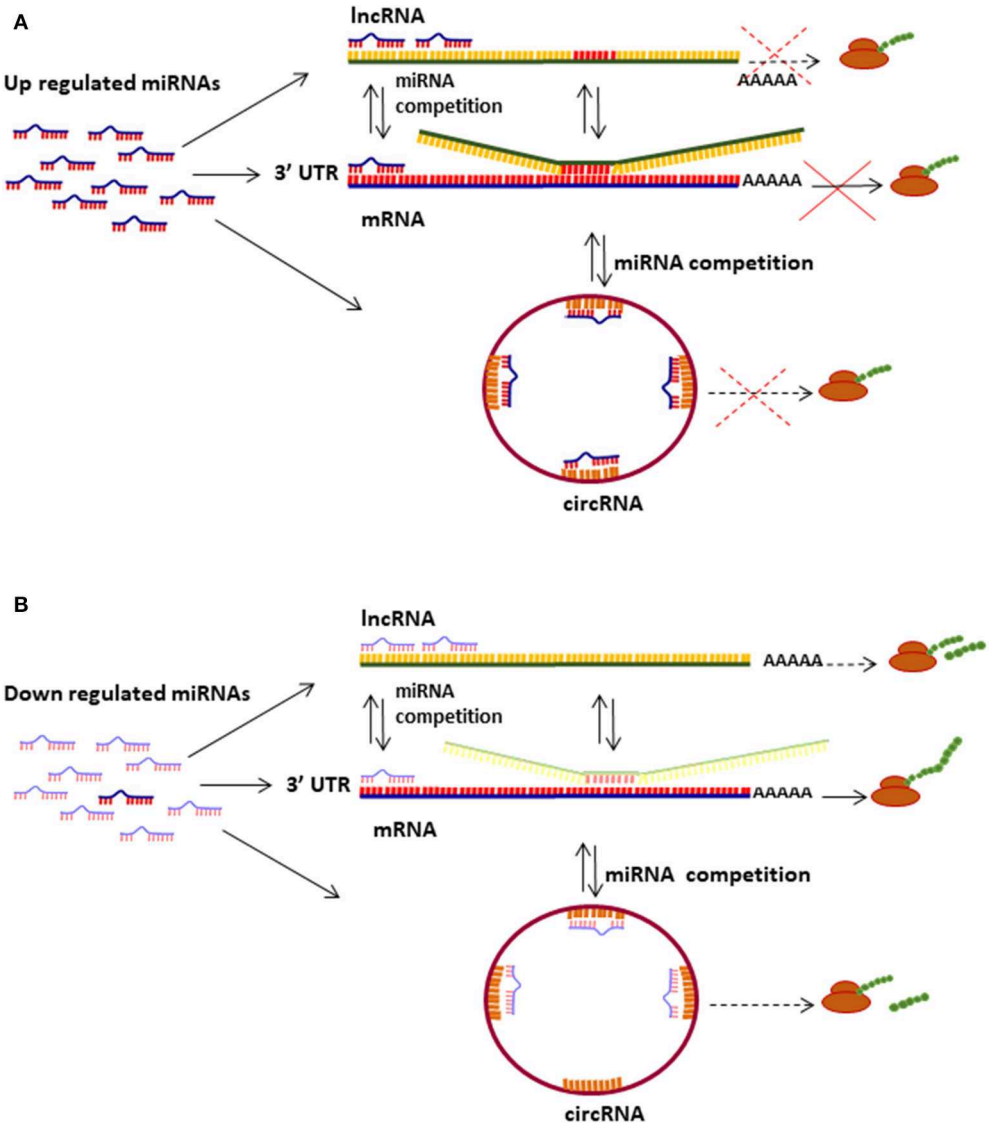

FIGURE 1 | Mechanisms of miRNas/lncRNAs/circRNAs regulating mRNA translation. **(A)** Up regulated miRNAs bind to mRNA 3′UTR and inhibit translation depending on the sponging effect of lncRNAs and circRNAs. **(B)** miRNAs down regulation induces protein translation from diverse types of transcripts (mRNA, lncRNA, and circRNA); several lncRNAs and circRNAs can be translated into small proteins and peptides.

associated with chromosome 1q gain and with increased cell viability, anchorage-independent growth and cell migration (36). Moreover, Muralidhar et al. identified 16 deregulated miRNAs, including miR-21, miR-29a, miR-31, and miR-203, in advanced cervical SCC which were associated with the up regulation of miRNA processor Drosha transcript and gain of chromosome 5p (109).

Numerous studies over the past decade have analyzed the miRNAs expression to identify significant variations during the transition from low to high grade cervical neoplasia and to invasive cervical cancer in order to define novel biomarkers for cervical cancer diagnosis, prognosis and cancer stage (24, 37). Pereira et al. described eight down regulated miRNAs (miR-26a, miR-29a, miR-99a, miR-143, miR-145, miR-199a, miR-203, miR-513) and five upregulated miRNAs (miR-148a, miR-302b, miR-10a, miR-196a, and miR-132) in low SIL, high SIL and cervical SCC in comparison with normal samples (110). Only five miRNAs (miR-106a, miR-197, miR-16, miR-27a, and miR-142-5p) were found specifically deregulated in pre-neoplastic lesions but not in cervical carcinoma (110). Subsequently, many research groups reported the identification of specific miRNA signatures during the transition from SIL to cervical cancer with variable results mainly due to the small sample size, the type of specimens (i.e., formalin fixed paraffin embedded vs. fresh biopsies), the number of miRNAs included in each panel (ranging from one to 7788 miRNAs) as well as the diverse methods used to quantify (37, 96, 111, 112).

TABLE 1 | miRNAs identified in cervical tissues, cell exfoliates, and mucus as well as in the serum of high grade SIL and cervical cancer patients.

Deregulated miRNAs*	HSIL**	Cervical Cancer	References
Up regulated miRNAs in tissue biopsies		*miR-20a-5p*; ***miR-31-5p***; *miR-96-5p*; *miR-142-5p*; *miR-189-5p; miR-200b*; *miR-224-5p*; *miR-944*; miR-*1246*; *let-5p*;	(24, 36–62)
	let-7; *miR-10a-5p*; *miR-16-5p*; miR21-5p; *miR-25-5p*; *miR-26a; miR-29a; miR-29b; miR-29c; miR-30a; miR-34b; miR-34c-5p*; *miR-92a-3p*; *miR-101; miR-125a-5p; miR-135b; miR- 143; miR-145*; *miR-196a-5p*; *miR-223; miR-338; miR-301b; miR-345; miR-424; miR-466; miR-512-5p; miR-518a*	***miR-9-5p***; ***miR-10a-5p***; **miR-15b**; ***miR-16-5p***; **miR-17**; miRNA-19a/b; **miR-20b**; **miR-21-5p**; ***miR-25-5p***; **miR-27a**; miR-29a; miR-30a; ***miR-92a-3p***; **miR-92b**; **miR-93**; **miR-106a**; miR-125b; miR-127; miR-130a; miR-133a; miR-133b; miR-135b; miR-141b; miR-145b; **miR-146a**; miR-150; **miR-155**; miR-181b; miR-182; **miR-185**; *miR-196a-5p*; miR-199a; **miR-199a**; miR-199b; miR-199-s; miR-203b; miR-205; miR-215; miR-221; miR-222; miR-223; miR-301b; miR-320a; miR-361-5p; miR-373; miR-378; miR-425-5p; miR-449; miR-451a; miR-466; miR-486-5p miR-494; miR-500; miR-505; miR-519d; miR-543; miR-590-5p; miR-711; miR-720; miR-886-5p; miR-888; miR-892b; miR-944; miR-1290; miR-2392; miR-3147; miR-3162; miR-4484; miR-6852;	
Down regulated miRNAs in tissue biopsies		*miR-1*; *miR-99b-5p*; *miR-126-3p*; *miR-140-5p*; *miR-196b-5p*;	(24, 36, 37, 39, 40, 55, 58, 63–93)
	Let-7a; miR-22; *miR-29a*; *miR-34a; miR-99a-5p; miR-100-5p*; miR-129b-5p; miR-193a-3p; *miR-199a-3p*; *miR-203*; miR-205; miR-216-5p; *miR-218-5p*; miR-212; miR-221; miR-27a; miR-27b; miR-342; *miR-376c-3p****; miR-433; miR-484; miR-636; miR-770-5p	Let-7a; Let-7b; Let-7c; Let-7g; miR-7; miR-10b; miR-17-5p; miR-22; miR-24; *miR-26a*; miR-27b; ***miR-29a***; miR-29b; miR-30a; miR-30e; ***miR-34a***; ***miR-99a-5p***; ***miR-100-5p***; miR-101; miR-103b; miR-107; miR-124-3p; miR-125a-5p; **miR-125b**; miR-129b-5p; miR-132; miR-133a; miR-138; miR-139-3p; miR-141; miR-142-3p; miR-143; miR-144; **miR-145**; miR-149; miR-152; miR-154; miR-181; miR-182; miR-183; miR-186; miR-187; miR-193a; **miR-193b; miR-195**; miR-199a-3p; miR-199b; miR-200b; miR-200c; miR-202; ***miR-203***; miR-204; miR-205; miR-211; miR-212; miR-214; miR-216-5p; ***miR-218***; miR-223; miR-296; miR-320; miR-326; miR-328; miR-329; miR-331-3p; miR-335; miR-337; miR-338-3p; miR-342; miR-362; miR-374c-5p; **miR-375**; miR-376c; miR-379; miR-383; miR-376a; **miR-424**; miR-429; miR-451; miR-484; miR-486-3p; miR-489-3p; miR-491-5p; miR-494; **miR-497**; miR-503; miR-506; miR-544; miR-630; miR-634; miR-638; miR-720; miR-758; miR-892b; miR-1297; miR-1246; miR-2861; miR-3185; miR- 3156-3p; miR- 3666; miR-3960; miR-4262; miR-4467; miR-4488; miR-4525	
Up regulated miRNAs in cervical exfoliated cells	miRNA-16-2; miRNA-20a		(94)
Down regulated miRNAs in exfoliated cervical cells	miR-424; miR-375; *miR-34a*; miR-218; miRNA-195; miRNA-29a	miR-758	(93–95)
Up regulated miRNAs in the serum		*miR-20a-5p*	(39, 59, 61, 96–103)
	miR-9-5p; *miR-10a-5p*; miR-20a-5p; *miR-92a-3p*; miR-196a-5p;	**miR-9-5p**; **miR-21-5p**; miR-29a-3p; *miR-92a-3p*; miR-101-3p; miR-122-5p; miR-132-3p; miR-141-3p; miR-150; **miR-155**; miR-191-5p; *miR-196a-5p*; miR-200c-3p; miR-203a-3p; miR-205-5p; miR-212-3p; miR-214–3p; miR-370; miR-425-5p; miR-486-5p; miR-494; miR-1246	
Down regulated miRNAs in the serum	Let-7a-5p; miR-101; miR-142-3p	Let-7a-5p; miR-17-5p; miR-24; miR-101; miR-103a-3p; miR-106a-5p; miR-106a-5p; miR-139-3p; miR-142-3p miR-144-3p; miR-191-5p**; miR-195-5p**; miR-212-3p; ***miR-218-5p***; miR-370; miR-425-5p; miR-451a; miR-758	(93, 99, 102, 104–106)
Up regulated miRNAs in cervical mucus	Let-7a-5p; *miR-10a-5p*; miR-21-5p; miR-141-3p; miR-144-3p; miR-155-5p; miR-205-5p; miR-451a	Let-7a-5p; ***miR-10a-5p***; **miR-17-5p**; **miR-21-5p**; **miR-106a-5p**; miR-141-3p; miR-144-3p; **miR-155-5p**; miR-205-5p; miR-451a; miR-758;	(96)
Down regulated miRNAs in cervical mucus	Not reported	Not reported	

**miRNAs up-regulated or down regulated in more than one study as determined by Pardini et al. (37) have been highlighted in bold; miRNAs with statistically significant expression changes in cervical neoplasia samples vs. normal epithelia as reported by He et al. (24) have been written in italics; miRNAs which have been found specifically expressed in in cervical cancer and not in HSIL are underlined and listed as a separated group.*

***HSIL group comprises CIN2-3 lesions.*

****The miR-376c-3p has been found significantly down regulated in CIN3 compared to CIN2 (24).*

He et al. performed a systematic study to identify miRNAs with statistically significant expression changes among 827 CIN and 3,095 cervical carcinomas as well as 2,099 non-tumor tissues from 85 selected studies (24). All studies analyzing miRNA profile in human cancerous and non-cancerous cervical tissues were included in such analysis. This approach allowed to identify 42 up regulated and 21 down-regulated miRNAs in different stages of cervical neoplasia. In particular, seven miRNAs (miR-29a, miR-34a, miR-99a-5p, miR-100-5p, miR-199a-3p, miR-203, and miR-218-5p) were found down-regulated and five miRNAs (miR10a-5p, 16-5p, 25-5p, 92a-3p, and 196a-5p) up regulated in CIN1 as well as in CIN 2–3 and cervical SCC compared to cervical non-tumor tissues. In CIN2-3 there were eight additional down regulated miRNAs and 27 new upregulated miRNAs with the miR-376c-3p specifically down regulated in CIN3 compared to CIN2. The functional target of miR-376c-3p is the BMI1 polycomb ring finger proto-oncogene which is highly expressed in several cancer types, including cervical cancer (113). Thus, the miR-376c-3p and the BMI1 factor may represent novel biomarkers for diagnosis as well as for target therapy in cervical cancer patients. Moreover, five new down regulated (miR-1, miR-99b-5p, miR-126-3p, miR-140-5p, miR-196b-5p) and ten additional up-regulated miRNAs (miR-20a-5p, miR-31-5p, miR-96-5p, miR-142-5p, miR-189-5p, miR224-5p, miR-200b, miR-944, miR-1246, and Let-5p) were identified in cervical carcinoma compared to CIN3 miRNA profile (24). Among these, miR-96-5p and miR-126-3p, which are predicted to target PTEN and MARK1 tumor-associated genes, have shown to be associated with metastatic potential of cervical cancer and to have a great potential as prognostic biomarkers or therapeutic targets (114, 115).

The expression levels of miRNAs consistently altered in all stages of cervical neoplasia may be directly deregulated by early viral proteins produced soon after infection. Gocze et al. performed the miRNA profiling of cervical neoplasia biopsies and identified the over expression of miR-21, miR-34a, miR-196a, miR-27a, and miR-221 as specific signature of HPV positivity irrespective of the clinical tumor grading (38). Indeed, the E6 protein encoded by oncogenic HPVs has shown to down regulate both the tumor suppressors miR-34a, through the viral E6-mediated degradation of the oncosuppressor p53 (116, 117), and the miR-218, in a p53-independent manner thus causing over expression of its target laminin 5 β3 (LAMB3) gene in cervical SCC cells (63, 118). Furthermore, the HPV E6 was demonstrated to up regulate miR-20a thereby enhancing cell proliferation, through the AKT/p38 pathway activation, and tumor growth by down regulation of the target gene PDCD6 (119). The E6 protein has also shown to increase miR-20b levels which in turn inhibits metastasis suppressor TIMP-2 expression and promotes epithelial-mesenchymal transition, migration and invasion of cervical cancer cells (120). Both E6 and E7 oncoproteins have shown to strongly suppress miR-424 levels in HPV16 and HPV31-positive cells causing increased expression of its target gene CHK1 encoding a damage repair factor (25).

Integration of HPV DNA into host genome, with disruption of E2 viral gene and host chromosomal loci, is a critical event in cancer development and progression. Interestingly, the viral status has shown to affect the levels of several miRNAs. Mandal et al. reported that cervical cancer biopsies either carrying integrated or episomal HPV16 genomes have a common expression signature of miR-200a associated with HPV16 genotype. Conversely, down regulation of miR-181c and expression of its target gene CKS1B was observed only in cases harboring HPV16 episomes but not in cancer tissues with the integrated virus (121). Therefore, miR-200a and miR-181c could represent useful biomarkers of cervical neoplasia progression if will be validated in clinical studies.

The HPV genome encodes the HPV-16-miR-H1-1 and HPV-16-miR-H2-1 which, besides being essential for viral infection and maintenance, are able to target critical cell genes, including those regulating cell cycle progression, migration, and immunological response (122). On the other hand, the miR-375 has shown to suppress HPV E6 and E7 expression and to induce increased levels of p53 and p21, higher activity of caspase-3 and caspase-9, suppression of E6AP, IGF-1R, cyclin D1, and survivin protein expression (123). Development of therapeutic strategies able to increase miR-375 levels and re-expression of tumor suppressors may be effective to improve the clinical outcomes in cervical cancer patients.

Recently, Pardini et al. performed a comprehensive evaluation of those miRNAs found deregulated in more than one study in order to identify consistent signatures occurring during the progression from normal cervical epithelium to SIL stages and cervical SCC. Among the 24 studies included in the analysis 17 and 13 miRNAs were found up or down regulated, respectively, in relation to cervical carcinoma progression (37). Among the over expressed miRNAs, one (miR-21) was found associated with cervical carcinogenesis in five studies, and nine (miR-9, miR-16, miR-25, miR-10a, miR-20b, miR-31 miR-92a, miR-106a, and miR-155) in three studies. Among under expressed miRNAs, miR-218 was described in six studies, miR-375 and miR-203 in four studies and six miRNAs (miR-99a, miR-29a, miR-195, miR-125b, miR-34a, and miR-100) in three studies. These findings suggest that specific panels including commonly deregulated miRNAs may serve as effective diagnostic biomarkers for early diagnosis and disease progression as well as for therapy in cervical cancer patients.

Identification of novel cancer biomarkers in cervical exfoliated cells as well as biological fluids may have an important role in early cancer detection and/or recurrence monitoring following therapy. Interestingly, Tian et al. showed that the expression level of miR-424, miR-375, miR-34a, and miR-218 in cervical exfoliated cells was statistically significant lower in high grade lesions than in low-grade lesions with a sensitivity superior to the cytology, suggesting that their detection may provide a new triage choice for the follow up of HPV-positive women (95). Moreover, the levels of miR-34a, miR-125, and miR-375 were also found deregulated in cervical exfoliated cells in association with cancer progression (37). Accordingly, Ye et al. observed that the relative low expression of miRNA-195 and miRNA-29a and the high expression of miRNA16-2 and miRNA20a in the cervical exfoliated cells was predictive of high grade SIL in the women group diagnosed with low grade SIL. Among these, miR-29a expression achieved the highest sensitivity (92.6%) and specificity (80.7%) in the identification of high grade SIL (94). These results indicate that miRNA expression profiles may

represent promising biomarkers for the early diagnosis of high grade cervical lesions and cervical cancer.

Profiling of miRNAs in cervical mucus has also shown to be a good strategy for the identification of cervical neoplastic lesions (96). Indeed, four miRNAs (miR-126-3p, miR-20b-5p, miR-451a, and miR-144-3p) detected in cervical mucus have been shown effective for diagnosis of cervical adenocarcinoma and high-grade intraepithelial lesions. However, more investigations are needed in order to establish the clinical value of miRNA detection in cervical mucus.

Few studies evaluated the parallel expression of miRNAs in cervical cancer biopsies and in serum samples and the potential of circulating miRNAs as cancer biomarkers. Chen et al. examined the levels of 1,450 miRNAs in cervical carcinoma tissues as well as in sera and identified 62 up regulated and 27 down regulated in comparison with normal controls (39). Among these, the miR-1246, miR-20a, miR-2392, miR-3147, miR-3162-5p, miR-4484, and miR-4667-5p were all over expressed in patients sera consistently with their high levels in cervical cancer tissues (39). More recently, Shukla et al. identified 14 miRNAs differentially expressed in cervical cancer tissue and serum specimens by performing sequencing analysis and real time PCR (124). Among them, miR-17-5p, miR-32-5p, and miR-454-3p were over expressed while miR-409-3p was down regulated both in serum samples and tumor biopsies of cervical cancer patients. Moreover, an inverse correlation was observed between the miR-409-3p and miR-454-3p levels and the expression of their target genes MTF2 and ST18, respectively, in cervical cancer biopsies. The MTF2 is a polycomb-like (PCL) protein which, in association with the polycomb repressive complex 2 (PRC2), mediates transcriptional repression and regulates several biological processes including cell differentiation (125). The ST18 genes has shown to inhibit colony formation of cancer cells in soft agar and to regulate pro-apoptotic and pro-inflammatory gene expression in fibroblast and in pancreatic B-cells (126, 127). Further studies need to be performed to fully characterize the role of such genes in cervical carcinogenesis.

Few studies investigated the expression of specific circulating miRNAs in distinct stages of cervical carcinoma. Yu et al. detected lower levels of miR-218 in cervical cancer patients sera compared to healthy women matched by age. Importantly such reduction was significantly associated with lymph node metastasis suggesting its potential use as circulating prognostic marker for cervical cancer invasion and metastasis (104). Several other circulating miRNAs have been proposed to be predictive of lymph node metastasis in patients with early stages cervical cancer (39, 97, 128). Among these, promising candidate biomarkers for their limited variations between tumor tissue and serum are represented by miR-1246, miR-20a, miR-2392, miR-3147, miR-3162-5p and miR-4484 (39).

DEREGULATED lncRNAs IN CERVICAL CANCER

lncRNAs have the ability to bind proteins, mRNAs or miRNAs, are involved in multiple biological functions and have an important role in cancer development. Several lncRNAs, including HOTAIR, H19, MALT1, CCAT2, SPRY4-IT1, GAS5, CCHE1, MEG3, LET, EBIC, and PVT1, are recognized to play crucial functions in cervical cancer progression, invasion and metastasis as well as in radio-resistance [**Table 2**; (29, 165)].

The 2.2 kb HOX transcript antisense intergenic RNA, namely HOTAIR, is a lncRNA encoded by the antisense strand of the HOXC gene located in the chromosome 12 q13.13 (166). Similarly to other lncRNAs, HOTAIR has shown to recruits chromatin-modifying proteins and to affect cancer epigenome modulation (81, 167). Indeed, the HOTAIR 5′ domain binds the zeste homolog 2 (EZH2) and concurs to the silencing of the target gene nemo-like kinase (NLK) (168). In cervical cancer HOTAIR levels have shown to be strictly controlled by the HPV E7 protein (129). Furthermore, HOTAIR has shown to act as sponge for several miRNAs and to cause deregulation of the respective target genes. Indeed, HOTAIR has shown to alter the miR-143-3p/BCL2 axis favoring cervical cancer cell growth (130) and miR-23b/MAPK1 axis contributing to cell proliferation and metastasis (139). Moreover, the over expression of HOTAIR has demonstrated to regulate diverse metabolic functions such as the activation of mTOR pathway in cervical carcinoma cell lines Hela, CaSki, and C33A (131), as well as the activation of Notch-Wnt signaling in SiHa cells (132). HOTAIR expression causes the up regulation of the vascular endothelial growth factor (VEGF), matrix metalloproteinase-9 (MMP-9) and EMT-related genes thus promoting tumor aggressiveness in cervical carcinoma (133). HOTAIR levels have observed to be consistently high in cervical cancer tissues and associated with lymph node metastasis and reduced overall survival (133). Moreover, the HOTAIR levels are higher also in the serum of cervical cancer patients and significantly associated with increased tumor size, lymph vascular space invasion, lymph node metastasis, and reduced survival (132). These data indicated that HOTAIR might represent a novel diagnostic circulating biomarker as well as a promising therapeutic target in cervical cancer. The single nucleotide polymorphism rs920778 T located in the HOTAIR enhancer has shown to be associated with elevated expression of HOTAIR and with cancer susceptibility (169). In addition, the frequency of the rs920778 C HOTAIR allele is reported to be significantly higher in HPV-positive cervical cancer cases while its expression level is observed to be low due to the ability of miR-22 to bind rs920778 C sequence and to suppress the HOTAIR expression (170).

The lncRNA H19, encoded by the H19 gene located in the chromosome loci 11p15.5, is expressed only from the maternally-inherited chromosome (171). It was the first lncRNA identified as a riboregulator and shown to be expressed in fetal tissues and adult muscles as well in many kinds of cancer (172, 173). The lncRNA H19 is modulated by the HPV16 E6 oncoprotein and demonstrated to act as a molecular sponge for miR-138-5p in epithelial cells (160, 174). Kim et al. reported that the lncRNA H19 which is abnormally expressed in cervical cancer may be associated with the cervical cancer progression (140).

The metastasis-associated lung adenocarcinoma transcript 1 (MALAT1), first identified in non-small cell lung cancer, is an 8,000 nucleotides lncRNA located in the chromosome

TABLE 2 | lncRNAs that are reported to have oncogenic or tumor suppressor functions in cervical cancer.

lncRNAs	Function	Sponged miRNAs	Deregulated pathways in cervical cancer	References
HOTAIR	Oncogenic	miR-22, miR-23b, miR-143-3p	BCL2, PRC2, LSD1, VEGF, mmP-9, mTOR, Notch, Wnt, STAT3, wnt/β-catenin, PI3K/AKT, HPV E7 oncoprotein	(129–139)
H19	Oncogenic	miR-138-5p	IGF2, HPV E6 oncoprotein	(140)
MALAT1	Oncogenic	miR-124, miR-145, miR-206	RBG2, E-cadherin, β-catenin, vimentin, ZO-1, caspase-3, caspase-8, Bax, Bcl-2, and BclxL	(141)
CCAT2	Oncogenic	miR-17-5p, miR-20a	MYC, wnt in colon cancer	(142)
SPRY4-IT1	Oncogenic	miR-101-3p	ZEB1, EMT, E-cadherin, vimentin	(143)
GAS5	Oncosuppressive	miR-106b	IER3	(144)
CCHE1	Oncogenic		PCNA, ERK/MAPK	(145, 146)
MEG3	Oncosuppressive	miR-21-5p		(147)
LET	Oncosuppressive		LIN28	
EBIC	Oncogenic		EZH2, Wnt/β-catenin, E-cadherin	(148, 149)
PVT1	Oncogenic	miR-200, miR-424, miR-195	EZH2, Myc, Nop2, p15, p16, H3K27me3, NF-kB	(150–157)
LINC00675	Oncogenic		Wnt/β-catenin, Bax and GSK-3β Bcl-2	(158)
C5orf66-AS1	Oncogenic	miR-637	RING1	(159)
FAM83H-AS1	Oncogenic		HPV E6, E6-p300	(160)
CCAT1	Oncogenic	miR-181a-5p	MMP14	(161)
NOC2L-4.1	Oncogenic	miR-630	YAP1	(162)
PAX8 AS1	Oncosuppressive		PAX8, NOTCH1 (pancreatic carcinoma)	(163)
RSU1P2	Oncogenic	let-7a	IGF1R, N-myc	(164)

11q13.1. MALAT1 has shown to promote epigenetic changes and to modulate gene expression, nuclear organization as well as regulation of alternative splicing by acting as decoy for splicing factors (175). It is found largely expressed in many cancer types in relation to the accumulation of aberrant splicing products (176). The MALAT1 is over expressed in cervical cancer cell lines and cancer tissues infected with high risk HPVs (177), acts as a sponge for several miRNAs, including miR-124, miR-145, and miR-206, and favors cervical cancer progression (178). Accordingly, down regulation of MALAT1 in cervical cancer cell lines and in cervical cancer tissues reduces invasion and metastasis through the inhibition of epidermal mesenchymal transition and modulation of the MALAT1-miR-124-RBG2 axis (141). The sponging of miR-145 by MALAT1 has suggested to be involved in the mechanisms of radio-resistance in cervical cancer radiotherapy (178). Moreover, MALAT1 expression has recognized to be an independent prognostic factor in addition to tumor size, FIGO stage, and lymph node metastasis (179). The knockdown of MALAT1 in CaSki cell line caused decrease of cell cycle regulators, such as cyclin D1, cyclin E, and CDK6, leading the cells to accumulate in G1 phase (180).

LncRNA colon cancer-associated transcript 2 (CCAT2) is a 1,752 nucleotide sequence located in the chromosome 8q24 and expressed in microsatellite-stable colorectal cancers (181). Next, CCAT2 has shown to be over expressed and defined as biomarker of poor prognosis in gastric, bladder, non-small cell lung, small cell lung, breast, and ovary cancers as well as in esophageal squamous cell carcinoma and glioma (182). CCAT2 has found to be up regulated in HeLa, CaSki, and SiHa cervical cancer cells as well as in cervical cancer tissues (183). The inhibition of CCAT2 expression by siRNA in cervical cancer cells has shown to suppress cell proliferation. In cervical cancer patients the high expression of CCAT2 is correlated to advanced FIGO stage, lymph node metastasis, deep cervical invasion and reduced survival (183). However, the molecular mechanism mediating the activity of CCAT2 in cervical cancer remain uncharacterized.

SPRY4 intronic transcript 1 (SPRY4-IT1) derives from the intron two of the SPRY4 gene and has shown to act as an oncogenic factor or a tumor suppressor in different cancer types (19, 184). Indeed, it is reported to be over expressed in melanoma, non-small cell lung, esophageal cancer and under expressed in gastric cancer (19, 185, 186). The expression levels of SPRY4-IT1 have been found higher in cervical cancer than in normal tissues and associated with advanced clinical stages and shorter overall survival of cervical cancer patients (187). More recently, the silencing of SPRY4-IT1 in cervical cancer cell lines has shown to inhibit migration and invasion through the SPYR4-IT1/miR-101-3p/ZEB1 axis. This effect is associated with suppression of EMT changes, increased E-cadherin levels and decreased the N-cadherin and vimentin expression (143).

Growth arrest-specific transcript 5 (GAS5) is 651 nucleotide lncRNA encoded by a sequence located in the chromosome 1q25 (188). GAS5 has tumor suppressor activity in several cancer types (189). Accordingly, its decreased expression has a strong association with tumor development and worse clinical outcome in cervical cancer patients (190). Moreover, inhibition of GAS5 in cervical cancer cells has shown to increase the proliferation, migration and invasion confirming its oncosuppressor activity in the cervical cancer progression (190). Gao et al. reported that GAS5 acts as miR-106b sponge causing up regulation of IER3 expression and enhanced radio-sensitivity of cervical cancer cells (144).

Cervical carcinoma high-expressed 1 (CCHE1) lncRNA is 2,500 nucleotide sequence transcribed from a region located in the chromosome 10. It is over expressed in cervical cancer in association with advanced tumor stages, increasing tumor size, invasion and poor prognosis (191). The CCHE1 has demonstrated to bind and stabilize the mRNA of proliferating cell nuclear antigen (PCNA) thus promoting its over expression and increased cervical cancer cell proliferation (145). Peng and Fan, demonstrated that CCHE1 inhibition causes inactivation of the ERK/MAPK pathway, growth arrest and apoptosis (146).

Maternally expressed gene (MEG3) is a 1,600 nucleotide lncRNA derived from the DLK1-MEG3 locus located on the chromosomal region 14q32.3, first identified as the ortholog of gene trap locus 2 (Gtl2) in mice (192). MEG3 is expressed in many normal tissues and its loss has been reported in many cancer types. The over expression of MEG3 can inhibit proliferation and increase apoptosis in cancer cells either in a p53 dependent or independent manner (193). Expression of MEG3 is low both in cervical cancer tissues and in cervical cancer cell lines. Increased levels of MEG3 in cervical cancer cell lines have shown to inhibit cell proliferation, induce cell cycle arrest and cause apoptosis (194). MEG3 has shown to act as a cancer suppressor through its ability to down regulate the miR-21-5p levels in cervical cancer cell lines (147). Indeed, knockdown of MEG3 in HeLa and CaSki cells induced significant up regulation of miR-21-5p expression (147). Thus, could act as a tumor suppressor able to inhibit tumor growth in cervical cancer.

LncRNA-Low Expression in Tumor (LET), is a 2,600 nucleotide long RNA transcribed from a region located in the chromosome locus 15q24.1. It is down-regulated in hepatocellular, gallbladder, esophageal and cervical carcinoma (182, 195). In cervical cancer patients has been reported a significant correlation between LET expression levels and clinico-pathological parameters suggesting that it might be considered a prognostic biomarker if confirmed by more clinical studies (196).

EZH2-binding lncRNA (EBIC) is a 1,500 nucleotide RNA encoded by a sequence located in the chromosome locus 12q22. The over expression of EBIC has shown to deregulate the Wnt/β-catenin signaling pathway and to promote cell proliferation, invasion and migration as well as to increase cisplatin resistance in ovarian cancer (148). EBIC has been described as an oncogenic lncRNA also in cervical cancer, indeed it was demonstrated to promote tumor cell invasion by binding to EZH2 and inhibiting E-cadherin expression (149).

Plasmacytoma variant translocation 1 (PVT1) is a highly conserved lncRNA, which is located downstream of MYC gene and is frequently co-amplified with MYC in several cancer types (150–152, 193). Iden et al. utilized siRNA and LNA-mediated knockdown to analyze the effect of reduced levels of PVT1 in cervical cancer cells obtaining inhibition of cell proliferation, migration, invasion and cisplatin resistance (153). Furthermore, PVT1 has shown to decrease miR-195 and miR-200b expression in cervical cancer either by enhancing histone H3K27me3 in the miR-195 and miR-200b promoters or by direct binding of miR-195 and miR-200b (154, 155). MiR-195 is associated with epithelial-mesenchymal transition and chemo resistance, whereas miR-200b is associated with cell proliferation, invasion and migration of cervical cancer cells. Yang et al. reported that serum levels of PVT1 positively correlate with PVT1 expression in cancer tissues indicating that it could serve as a biomarker for diagnosis of cervical cancer (156).

Along with the above-mentioned lncRNAs, many other novel sequences, such as LINC00675, C5orf66-AS1, FAM83H-AS1, CCAT1, NOC2L-4.1, PAX8 AS1, and RSU1P2, have identified as playing multiple roles in cervical tumorigenesis (**Table 2**). Their ability to sponge specific miRNAs and to deregulate metabolic pathways have been mainly investigated in cell culture models. Therefore, clinical studies are needed to determine the possible use of these novel lncRNAs as biomarkers for diagnosis and prognosis of cervical cancer.

CIRCULAR RNAs IN CERVICAL CANCER

CircRNAs are highly expressed in many cancer types, such as breast, lung and colorectal cancer (197–200). Several circRNAs are abnormally expressed in cervical cancer tissues as well as derived cell lines and contribute to tumorigenesis mostly by sequestering miRNAs [**Table 3**; (34)]. Among these, hsa_circ_0141539 (circRNA-000284), encoded by the Clorf116 gene, was found significantly over expressed in cervical cancer tissues compared to adjacent non-tumor tissues and directly associated with tumor size, FIGO stage as well as myometrium invasion (202). The hsa_circ_0141539 is able to sponge miR-518d-5p/519-5p causing increased expression of the target gene CBX8 and promotion of malignant transformation of cervical cells (202). This circRNA was also demonstrated to sponge miR-506 causing an increased expression of Snail-2 which is a direct target of miR-506 (201). Silencing of hsa_circ_0141539 has been proposed as a novel treatment strategy for cervical cancer patients.

The circRNA Hsa_circ_0023404, derived from the RNF121 gene located on the chromosome 11, was significantly over expressed in cervical cancer and associated with poor prognosis (203). Hsa_circ_0023404 has shown to sequester miR-136 thus promoting over expression of target gene TFCP2, consequent activation of YAP signaling pathway and consequent cervical cancer development and progression (203). More recently, Guo et al. reported a novel biological effect of hsa_circ_0023404 relying on the subtraction of miR-5047 with consequent induction of VEGFA expression and increased cervical cancer metastasis and chemoresistance. Moreover, hsa_circ_0023404 and VEGFA were found concordantly up regulated in cervical tumors, while miR-5047 was under expressed (213).

Gao et al. performed a microarray analysis of 35 cervical cancer cases and identified 45 significantly up regulated circRNAs with hsa_circ_0018289 as the most deregulated (35). Hsa_circ_0018289 was observed to directly bind miR-497 causing increased cell proliferation, migration and invasion of cervical cancer cells (35). Thus, hsa_circ_0018289, similarly to other circRNA, has demonstrated to have an oncogenic role in cervical cancer development. Cai et al. reported that also hsa_circ_0000263 has an oncogenic role being significantly up regulated in cervical cancer cells, able to bind miR-150-5p

TABLE 3 | CircRNA that were reported to be deregulated in cervical neoplasia.

CircRNAs	Targets	Effect in cervical cancer and/or cell lines	References
Hsa_circ_000284	miR-506, Snail-2	Promote proliferation and invasion	(201)
Hsa_circ_0141539	miR-518d-5p, miR-519-5p, CBX8	Promote proliferation, migration and invasion	(202)
Hsa_circ_0023404	miR-136, TFCP2, YAP	Promote proliferation and invasion	(203)
Hsa_circ_0018289	miR-497	Promote cell proliferation, migration and invasion	(35)
Hsa_circ_0000263	miR-150-5p, MDM4, p53	Promote cell proliferation, migration	(204)
Hsa_circ_0001445	miR-620	Suppress proliferation and invasion	(205)
Hsa_circRNA_101996	miR-8075, TPX2		
Hsa_circ_0031288	HuR, PABPN1	Decrease cell proliferation	(206)
Hsa_circ_0004015	miR-1183, and PDPK1	Promote cell migration, angiogenesis and radio-resistance	(207)
CircATP8A2	miR-433, EGFR	Promote cervical cancer progression	(208)
Circ_0067934	miR-545	Promote cervical cancer progression	(209)
CircEIF4G2	miR-218, HOXA1	Promote cell proliferation and migration	(210)
CircCLK3	miR-320a, FoxM1	Promote cervical cancer progression	(211)
CircE7	pRb	HPV encoded circular E7 RNA promoting cell transformation	(212)

and to promote cell proliferation and migration through the hsa_circ_0000263/miR-150-5p/MDM4/p53 regulatory network affecting p53 activity (204). Conversely, the hsa_circ_0001445 (circSMARCA5) is able to sponge the miR-620 and to act as an oncosuppressor being its expression decreased in cervical cancer cells and its over expression causing inhibition of cell proliferation, invasion and migration (205).

Very recently, Song et al. by performing *in silico* analyses detected higher expression of hsa_circRNA_101996 in cervical cancer and observed a correlation with tumor stage, tumor size, lymph node metastasis, and poor outcomes (214). The oncogenic activity of hsa_circRNA_101996 has shown to be mediated by sequestration of miR-8075 and deregulation of TPX2 gene expression which represents a new mechanism of cervical cancer development (214). Others up regulated circRNAs in cervical cancer cells are circATP8A2 promoting cervical cancer progression through the circATP8A2/miR-433/EGFR axis, and circ_0067934 which binds miR-545 and is associated with advanced cancer stage, lymph node metastasis, and poor prognosis (208, 209). Moreover, Mao et al. identified the circEIF4G2 as over expressed in cervical cancer cells and able to interact with miR-218 causing enhancement of cervical cancer progression through the circEIF4G2-miR-218/HOXA1 axis (210). Recently, the circCLK3, which is a novel circRNA found over expressed in cervical carcinoma, has demonstrated to sponge miR-320a and to abolish its ability to suppress FoxM1 transcription factor expression as well as to promote cell proliferation, epidermal mesenchymal transition, migration, and invasion of cervical cancer cells (211). A recent study evaluating the expression profile of circRNAs by high-throughput RNA sequencing in three HPV16 positive cervical cancer cases identified 99 deregulated circRNAs (58 over expressed and 41 under expressed circRNAs) of which 44 have not been previously described and their role in cancer has not yet established (215). All these findings clearly show that many circRNAs play key roles in cervical cancer development and that they can be used as novel diagnostic and prognostic biomarkers as well as for targeted therapies. However, more studies are needed to establish their significance as biomarkers of early disease and clinical outcome indicators.

High risk HPVs have recently demonstrated to encode a circRNA encompassing the E7 oncogene (circE7) (212). Such viral circRNA has shown to be modified by the N6-methyladenosine (m6A), to localize in the cytoplasm, to associate with polysomes, and to produce E7 oncoprotein. CircE7 is expressed in HPV16 positive CaSki cells and its targeted disruption causes reduction of E7 oncoprotein levels and cell growth inhibition (212). These results provide evidence of a new molecular mechanism of viral related tumorigenesis in HPV-related human malignancies and the possibility to search for new types of viral nucleic acids in order to discriminate progressing vs. regressing cervical lesions.

CONCLUSION

The discovery of aberrantly expressed miRNAs, lncRNAs, and circRNAs in cervical cancer have defined new molecular mechanisms of cervical cancer tumorigenesis and provided considerable opportunities for translating the non-coding RNAs research into clinical settings. Data from emerging studies clearly highlight the significance of specific miRNA signatures in the diagnosis and prognosis of cervical cancer. Particularly, miRNAs with oncogenic potential differently expressed in different stages of cervical cancer and those associated with high risk HPV infection might represent promising biomarkers for oncologic screening and cancer recurrence monitoring. Indeed, the analysis of specific miRNA panels have demonstrated a greater diagnostic value, higher sensitivity and specificity, in patients with cervical lesions and cancer. More importantly, circulating miRNAs appear valuable for the early detection of cervical cancer and for monitoring the clinical outcome of advanced cancer considering that the majority of cancer associated deaths are caused by metastases to distant organs. In addition, miRNA testing may reduce the need for invasive

cervical biopsies and are useful in predicting the prognosis of cervical cancer. However, larger studies are required to validate miRNA assays as diagnostic marker in comparison with cytology and HPV screening methods. Several molecules able to target oncogenic miRNAs have been developed such as the synthetic antisense oligonucleotides encoding miRNA complementary sequences. Hypomethylation agents such as decitabine or 5-azacitidine have also shown effective to induce epigenetic silencing of miRNAs and they are the approved treatments for downregulating the expression of several non-coding RNAs and mRNAs in myelodysplastic syndromes. Therefore, such therapeutic approaches, although in the early stage of clinical translation, might become effective drugs providing insight into the treatment of all types of cancers.

lncRNAs are important as potential biomarkers for cervical prognosis, invasion, metastasis, chemo-radio-resistance. Several lncRNAs can be detected in the serum and other biological fluids. Indeed, circulating HOTAIR, MALAT1, and MEG3 transcripts were found significantly higher in cancer patients compared to healthy subjects suggesting their potential as diagnostic biomarkers. Moreover, the increased HOTAIR levels in the serum of cervical cancer patients is also indicative of the metastatic tumor phase, adenocarcinoma, lymphatic node metastasis and tumor recurrence. The molecular mechanisms of lncRNAs in cervical cancer need further characterization. Particularly the interplay with miRNAs and circRNAs needs to be fully discovered. Inhibition of the oncogenic activity of lncRNAs is also in the early phase of research since no RNA-interference drugs have been approved for clinical use.

CircRNAs have been recently discovered and their role in cervical cancer pathogenesis recognized. Massive parallel sequencing and bioinformatics techniques allowed uncovering many circRNAs differentially expressed in cervical cancer tissues compared to normal cells suggesting that they have relevant roles in this cancer type. Their activity is mainly mediated by the sponging of specific miRNAs. The study of circRNAs potentially represents a new promising strategy for diagnosis and treatment of cervical cancer. However, the characterization of biological functions of circRNAs in cancer cells is in a nascent stage and most activities have not been fully elucidated.

More studies mainly based on high-throughput sequencing technologies, which simultaneously evaluate the network of miRNAs, lncRNAs, and circRNAs are needed to further reveal the complexity of the interplay between diverse classes of non-coding RNAs and deregulation of new actionable metabolic pathways for treatment of cervical cancer.

AUTHOR CONTRIBUTIONS

MT, RF, LB, CA, NS, AC, FP, AT, and FB contributed to the writing and editing of the manuscript.

FUNDING

This work and the publication cost was supported by the research grants Ricerca Corrente (No. 2611892) and Ministero della Salute (RF-2018-12366163).

REFERENCES

1. Bray F, Ferlay J, Soerjomataram I, Siegel RL, Torre LA, Jemal A. Global cancer statistics 2018: GLOBOCAN estimates of incidence and mortality worldwide for 36 cancers in 185 countries. *CA Cancer J Clin.* (2018) 68:394–424. doi: 10.3322/caac.21492
2. Schiffman M, Wentzensen N, Wacholder S, Kinney W, Gage JC, Castle PE. Human papillomavirus testing in the prevention of cervical cancer. *J Natl Cancer Inst.* (2011) 103:368–83. doi: 10.1093/jnci/djq562
3. Ronco G, Dillner J, Elfstrom KM, Tunesi S, Snijders PJ, Arbyn M, et al. Efficacy of HPV-based screening for prevention of invasive cervical cancer: follow-up of four European randomised controlled trials. *Lancet.* (2014) 383:524–32. doi: 10.1016/S0140-6736(13)62218-7
4. Tornesello ML, Annunziata C, Tornesello AL, Buonaguro L, Buonaguro FM. Human oncoviruses and p53 tumor suppressor pathway deregulation at the origin of human cancers. *Cancers.* (2018) 10:E213. doi: 10.3390/cancers10070213
5. Yeo-Teh NSL, Ito Y, Jha S. High-risk human papillomaviral oncogenes E6 and E7 target key cellular pathways to achieve oncogenesis. *Int J Mol Sci.* (2018) 19:E1706. doi: 10.3390/ijms19061706
6. Venuti A, Paolini F, Nasir L, Corteggio A, Roperto S, Campo MS, et al. Papillomavirus E5: the smallest oncoprotein with many functions. *Mol Cancer.* (2011) 10:140. doi: 10.1186/1476-4598-10-140
7. Scott ML, Coleman DT, Kelly KC, Carroll JL, Woodby B, Songock WK, et al. Human papillomavirus type 16 E5-mediated upregulation of Met in human keratinocytes. *Virology.* (2018) 519:1–11. doi: 10.1016/j.virol.2018.03.021
8. Wright AA, Howitt BE, Myers AP, Dahlberg SE, Palescandolo E, Van HP, et al. Oncogenic mutations in cervical cancer: genomic differences between adenocarcinomas and squamous cell carcinomas of the cervix. *Cancer.* (2013) 119:3776–83. doi: 10.1002/cncr.28288
9. Tornesello ML, Annunziata C, Buonaguro L, Losito S, Greggi S, Buonaguro FM. TP53 and PIK3CA gene mutations in adenocarcinoma, squamous cell carcinoma and high-grade intraepithelial neoplasia of the cervix. *J Transl Med.* (2014) 12:255. doi: 10.1186/s12967-014-0255-5
10. Tornesello ML, Buonaguro L, Buonaguro FM. Mutations of the TP53 gene in adenocarcinoma and squamous cell carcinoma of the cervix: a systematic review. *Gynecol Oncol.* (2013) 128:442–8. doi: 10.1016/j.ygyno.2012.11.017
11. Wingo SN, Gallardo TD, Akbay EA, Liang MC, Contreras CM, Boren T, et al. Somatic LKB1 mutations promote cervical cancer progression. *PLoS ONE.* (2009) 4:e5137. doi: 10.1371/journal.pone.0005137
12. Ojesina AI, Lichtenstein L, Freeman SS, Pedamallu CS, Imaz-Rosshandler I, Pugh TJ, et al. Landscape of genomic alterations in cervical carcinomas. *Nature.* (2014) 506:371–5. doi: 10.1038/nature12881
13. Cancer Genome Atlas Research Network, Albert Einstein College of Medicine, Analytical Biological Services, Barretos Cancer Hospital, Baylor College of Medicine, Beckman Research Institute of City of Hope, et al. Integrated genomic and molecular characterization of cervical cancer. *Nature.* (2017) 543:378–84. doi: 10.1038/nature21386
14. Annunziata C, Pezzuto F, Greggi S, Ionna F, Losito S, Botti G, et al. Distinct profiles of TERT promoter mutations and telomerase expression in head and neck cancer and cervical carcinoma. *Int J Cancer.* (2018) 143:1153–61. doi: 10.1002/ijc.31412
15. Peng L, Yuan X, Jiang B, Tang Z, Li GC. lncRNAs: key players and novel insights into cervical cancer. *Tumour Biol.* (2016) 37:2779–88. doi: 10.1007/s13277-015-4663-9
16. Reshmi G, Pillai MR. Beyond HPV: oncomirs as new players in cervical cancer. *FEBS Lett.* (2008) 582:4113–6. doi: 10.1016/j.febslet.2008.11.011
17. Yi Y, Liu Y, Wu W, Wu K, Zhang W. Reconstruction and analysis of circRNAmiRNAmRNA network in the pathology of cervical cancer. *Oncol Rep.* (2019) 41:2209–25. doi: 10.3892/or.2019.7028

18. Lai EC. Micro RNAs are complementary to 3' UTR sequence motifs that mediate negative post-transcriptional regulation. *Nat Genet.* (2002) 30:363–4. doi: 10.1038/ng865
19. Xie M, Nie FQ, Sun M, Xia R, Liu YW, Zhou P, et al. Decreased long noncoding RNA SPRY4-IT1 contributing to gastric cancer cell metastasis partly via affecting epithelial-mesenchymal transition. *J Transl Med.* (2015) 13:250. doi: 10.1186/s12967-015-0595-9
20. Liu H, Lei C, He Q, Pan Z, Xiao D, Tao Y. Nuclear functions of mammalian MicroRNAs in gene regulation, immunity and cancer. *Mol Cancer.* (2018) 17:64. doi: 10.1186/s12943-018-0765-5
21. Friedlander MR, Lizano E, Houben AJ, Bezdan D, Banez-Coronel M, Kudla G, et al. Evidence for the biogenesis of more than 1,000 novel human microRNAs. *Genome Biol.* (2014) 15:R57–15. doi: 10.1186/gb-2014-15-4-r57
22. Jens M, Rajewsky N. Competition between target sites of regulators shapes post-transcriptional gene regulation. *Nat Rev Genet.* (2015) 16:113–26. doi: 10.1038/nrg3853
23. Romano G, Veneziano D, Acunzo M, Croce CM. Small non-coding RNA and cancer. *Carcinogenesis.* (2017) 38:485–91. doi: 10.1093/carcin/bgx026
24. He Y, Lin J, Ding Y, Liu G, Luo Y, Huang M, et al. A systematic study on dysregulated microRNAs in cervical cancer development. *Int J Cancer.* (2016) 138:1312–27. doi: 10.1002/ijc.29618
25. Hong S, Cheng S, Songock W, Bodily J, Laimins LA. Suppression of MicroRNA 424 levels by human papillomaviruses is necessary for differentiation-dependent genome amplification. *J Virol.* (2017) 91:e01712-17. doi: 10.1128/JVI.01712-17
26. Ulitsky I, Bartel DP. lincRNAs: genomics, evolution, and mechanisms. *Cell.* (2013) 154:26–46. doi: 10.1016/j.cell.2013.06.020
27. Sun Q, Hao Q, Prasanth KV. Nuclear long noncoding RNAs: key regulators of gene expression. *Trends Genet.* (2018) 34:142–57. doi: 10.1016/j.tig.2017.11.005
28. Marchese FP, Raimondi I, Huarte M. The multidimensional mechanisms of long noncoding RNA function. *Genome Biol.* (2017) 18:206. doi: 10.1186/s13059-017-1348-2
29. Dong J, Su M, Chang W, Zhang K, Wu S, Xu T. Long non-coding RNAs on the stage of cervical cancer (review). *Oncol Rep.* (2017) 38:1923–31. doi: 10.3892/or.2017.5905
30. Sharma S, Munger K. Expression of the cervical carcinoma expressed PCNA regulatory (CCEPR) long noncoding RNA is driven by the human papillomavirus E6 protein and modulates cell proliferation independent of PCNA. *Virology.* (2018) 518:8–13. doi: 10.1016/j.virol.2018.01.031
31. He H, Liu X, Liu Y, Zhang M, Lai Y, Hao Y, et al. Human papillomavirus E6/E7 and long noncoding RNA TMPOP2 mutually upregulated gene expression in cervical cancer cells. *J Virol.* (2019) 93:e01808-18. doi: 10.1128/JVI.01808-18
32. Haddad G, Lorenzen JM. Biogenesis and function of circular RNAs in health and in disease. *Front Pharmacol.* (2019) 10:428. doi: 10.3389/fphar.2019.00428
33. Bach DH, Lee SK, Sood AK. Circular RNAs in cancer. *Mol Ther Nucleic Acids.* (2019) 16:118–29. doi: 10.1016/j.omtn.2019.02.005
34. Chaichian S, Shafabakhsh R, Mirhashemi SM, Moazzami B, Asemi Z. Circular RNAs: a novel biomarker for cervical cancer. *J Cell Physiol.* (2019) 235:718–24. doi: 10.1002/jcp.29009
35. Gao YL, Zhang MY, Xu B, Han LJ, Lan SF, Chen J, et al. Circular RNA expression profiles reveal that hsa_circ_0018289 is up-regulated in cervical cancer and promotes the tumorigenesis. *Oncotarget.* (2017) 8:86625–33. doi: 10.18632/oncotarget.21257
36. Wilting SM, Snijders PJ, Verlaat W, Jaspers A, van de Wiel MA, van Wieringen WN, et al. Altered microRNA expression associated with chromosomal changes contributes to cervical carcinogenesis. *Oncogene.* (2013) 32:106–16. doi: 10.1038/onc.2012.20
37. Pardini B, De MD, Francavilla A, Di GC, Ronco G, Naccarati A. MicroRNAs as markers of progression in cervical cancer: a systematic review. *BMC Cancer.* (2018) 18:696. doi: 10.1186/s12885-018-4590-4
38. Gocze K, Gombos K, Juhasz K, Kovacs K, Kajtar B, Benczik M, et al. Unique microRNA expression profiles in cervical cancer. *Anticancer Res.* (2013) 33:2561–7.
39. Chen J, Yao D, Li Y, Chen H, He C, Ding N, et al. Serum microRNA expression levels can predict lymph node metastasis in patients with early-stage cervical squamous cell carcinoma. *Int J Mol Med.* (2013) 32:557–67. doi: 10.3892/ijmm.2013.1424
40. Zhang J, Zheng F, Yu G, Yin Y, Lu Q. miR-196a targets netrin 4 and regulates cell proliferation and migration of cervical cancer cells. *Biochem Biophys Res Commun.* (2013) 440:582–8. doi: 10.1016/j.bbrc.2013.09.142
41. Hou T, Ou J, Zhao X, Huang X, Huang Y, Zhang Y. MicroRNA-196a promotes cervical cancer proliferation through the regulation of FOXO1 and p27Kip1. *Br J Cancer.* (2014) 110:1260–8. doi: 10.1038/bjc.2013.829
42. Xu XM, Wang XB, Chen MM, Liu T, Li YX, Jia WH, et al. MicroRNA-19a and−19b regulate cervical carcinoma cell proliferation and invasion by targeting CUL5. *Cancer Lett.* (2012) 322:148–58. doi: 10.1016/j.canlet.2012.02.038
43. Liu C, Lin J, Li L, Zhang Y, Chen W, Cao Z, et al. HPV16 early gene E5 specifically reduces miRNA-196a in cervical cancer cells. *Sci Rep.* (2015) 5:7653. doi: 10.1038/srep07653
44. Wang N, Zhou Y, Zheng L, Li H. MiR-31 is an independent prognostic factor and functions as an oncomir in cervical cancer via targeting ARID1A. *Gynecol Oncol.* (2014) 134:129–37. doi: 10.1016/j.ygyno.2014.04.047
45. Yao T, Lin Z. MiR-21 is involved in cervical squamous cell tumorigenesis and regulates CCL20. *Biochim Biophys Acta.* (2012) 1822:248–60. doi: 10.1016/j.bbadis.2011.09.018
46. Zhang S, Liu F, Mao X, Huang J, Yang J, Yin X, et al. Elevation of miR-27b by HPV16 E7 inhibits PPARgamma expression and promotes proliferation and invasion in cervical carcinoma cells. *Int J Oncol.* (2015) 47:1759–66. doi: 10.3892/ijo.2015.3162
47. Zhou C, Shen L, Mao L, Wang B, Li Y, Yu H. miR-92a is upregulated in cervical cancer and promotes cell proliferation and invasion by targeting FBXW7. *Biochem Biophys Res Commun.* (2015) 458:63–9. doi: 10.1016/j.bbrc.2015.01.066
48. Lao G, Liu P, Wu Q, Zhang W, Liu Y, Yang L, et al. Mir-155 promotes cervical cancer cell proliferation through suppression of its target gene LKB1. *Tumour Biol.* (2014) 35:11933–8. doi: 10.1007/s13277-014-2479-7
49. Yang L, Wang YL, Liu S, Zhang PP, Chen Z, Liu M, et al. miR-181b promotes cell proliferation and reduces apoptosis by repressing the expression of adenylyl cyclase 9 (AC9) in cervical cancer cells. *FEBS Lett.* (2014) 588:124–30. doi: 10.1016/j.febslet.2013.11.019
50. Zheng W, Liu Z, Zhang W, Hu X. miR-31 functions as an oncogene in cervical cancer. *Arch Gynecol Obstet.* (2015) 292:1083–9. doi: 10.1007/s00404-015-3713-2
51. Kang HW, Wang F, Wei Q, Zhao YF, Liu M, Li X, et al. miR-20a promotes migration and invasion by regulating TNKS2 in human cervical cancer cells. *FEBS Lett.* (2012) 586:897–904. doi: 10.1016/j.febslet.2012.02.020
52. Xie H, Zhao Y, Caramuta S, Larsson C, Lui WO. miR-205 expression promotes cell proliferation and migration of human cervical cancer cells. *PLoS ONE.* (2012) 7:e46990. doi: 10.1371/journal.pone.0046990
53. Zhao S, Yao D, Chen J, Ding N, Ren F. MiR-20a promotes cervical cancer proliferation and metastasis *in vitro* and *in vivo*. *PLoS ONE.* (2015) 10:e0120905. doi: 10.1371/journal.pone.0120905
54. Wu X, Xi X, Yan Q, Zhang Z, Cai B, Lu W, et al. MicroRNA-361–5p facilitates cervical cancer progression through mediation of epithelial-to-mesenchymal transition. *Med Oncol.* (2013) 30:751. doi: 10.1007/s12032-013-0751-0
55. Wang LQ, Zhang Y, Yan H, Liu KJ, Zhang S. MicroRNA-373 functions as an oncogene and targets YOD1 gene in cervical cancer. *Biochem Biophys Res Commun.* (2015) 459:515–20. doi: 10.1016/j.bbrc.2015.02.138
56. Sun Y, Zhang B, Cheng J, Wu Y, Xing F, Wang Y, et al. MicroRNA-222 promotes the proliferation and migration of cervical cancer cells. *Clin Invest Med.* (2014) 37:E131. doi: 10.25011/cim.v37i3.21380
57. Xie H, Lee L, Scicluna P, Kavak E, Larsson C, Sandberg R, et al. Novel functions and targets of miR-944 in human cervical cancer cells. *Int J Cancer.* (2015) 136:E230-E241. doi: 10.1002/ijc.29160
58. Lee JW, Choi CH, Choi JJ, Park YA, Kim SJ, Hwang SY, et al. Altered MicroRNA expression in cervical carcinomas. *Clin Cancer Res.* (2008) 14:2535–42. doi: 10.1158/1078-0432.CCR-07-1231
59. Nagamitsu Y, Nishi H, Sasaki T, Takaesu Y, Terauchi F, Isaka K. Profiling analysis of circulating microRNA expression in cervical cancer. *Mol Clin Oncol.* (2016) 5:189–94. doi: 10.3892/mco.2016.875
60. Sharma S, Hussain S, Soni K, Singhal P, Tripathi R, Ramachandran VG, et al. Novel MicroRNA signatures in HPV-mediated cervical

carcinogenesis in Indian women. *Tumour Biol.* (2016) 37:4585–95. doi: 10.1007/s13277-015-4248-7
61. Jia W, Wu Y, Zhang Q, Gao GE, Zhang C, Xiang Y. Expression profile of circulating microRNAs as a promising fingerprint for cervical cancer diagnosis and monitoring. *Mol Clin Oncol.* (2015) 3:851–8. doi: 10.3892/mco.2015.560
62. Cheung TH, Man KN, Yu MY, Yim SF, Siu NS, Lo KW, et al. Dysregulated microRNAs in the pathogenesis and progression of cervical neoplasm. *Cell Cycle.* (2012) 11:2876–84. doi: 10.4161/cc.21278
63. Yamamoto N, Kinoshita T, Nohata N, Itesako T, Yoshino H, Enokida H, et al. Tumor suppressive microRNA-218 inhibits cancer cell migration and invasion by targeting focal adhesion pathways in cervical squamous cell carcinoma. *Int J Oncol.* (2013) 42:1523–32. doi: 10.3892/ijo.2013.1851
64. Liu L, Yu X, Guo X, Tian Z, Su M, Long Y, et al. miR-143 is downregulated in cervical cancer and promotes apoptosis and inhibits tumor formation by targeting Bcl-2. *Mol Med Rep*. (2012) 5:753–60. doi: 10.3892/mmr.2011.696
65. Liu S, Song L, Yao H, Zhang L, Xu D, Gao F, Li Q. MiR-375 is epigenetically downregulated by HPV-16 E6 mediated DNMT1 upregulation and modulates EMT of cervical cancer cells by suppressing lncRNA MALAT1. *PLoS ONE*. (2016) 11:e0163460. doi: 10.1371/journal.pone.0163460
66. Wen Z, Lei Z, Jin-An M, Xue-Zhen L, Xing-Nan Z, Xiu-Wen D. The inhibitory role of miR-214 in cervical cancer cells through directly targeting mitochondrial transcription factor A (TFAM). *Eur J Gynaecol Oncol.* (2014) 35:676–82. doi: 10.12892/ejgo24572014
67. Qiang R, Wang F, Shi LY, Liu M, Chen S, Wan HY, et al. Plexin-B1 is a target of miR-214 in cervical cancer and promotes the growth and invasion of HeLa cells. *Int J Biochem Cell Biol.* (2011) 43:632–41. doi: 10.1016/j.biocel.2011.01.002
68. Peng RQ, Wan HY, Li HF, Liu M, Li X, Tang H. MicroRNA-214 suppresses growth and invasiveness of cervical cancer cells by targeting UDP-N-acetyl-alpha-D-galactosamine:polypeptide N-acetylgalactosaminyltransferase 7. *J Biol Chem.* (2012) 287:14301–9. doi: 10.1074/jbc.M111.337642
69. Yang Z, Chen S, Luan X, Li Y, Liu M, Li X, et al. MicroRNA-214 is aberrantly expressed in cervical cancers and inhibits the growth of HeLa cells. *IUBMB Life.* (2009) 61:1075–82. doi: 10.1002/iub.252
70. Zhu X, Er K, Mao C, Yan Q, Xu H, Zhang Y, et al. miR-203 suppresses tumor growth and angiogenesis by targeting VEGFA in cervical cancer. *Cell Physiol Biochem.* (2013) 32:64–73. doi: 10.1159/000350125
71. Mao L, Zhang Y, Mo W, Yu Y, Lu H. BANF1 is downregulated by IRF1-regulated microRNA-203 in cervical cancer. *PLoS ONE.* (2015) 10:e0117035. doi: 10.1371/journal.pone.0117035
72. Sun J, Ji J, Huo G, Song Q, Zhang X. miR-182 induces cervical cancer cell apoptosis through inhibiting the expression of DNMT3a. *Int J Clin Exp Pathol*. (2015) 8:4755–63. doi: 10.1007/978-1-4939-1692-4
73. Song X, Shi B, Huang K, Zhang W. miR-133a inhibits cervical cancer growth by targeting EGFR. *Oncol Rep.* (2015) 34:1573–80. doi: 10.3892/or.2015.4101
74. Zhao Q, Zhai YX, Liu HQ, Shi YA, Li XB. MicroRNA-491–5p suppresses cervical cancer cell growth by targeting hTERT. *Oncol Rep.* (2015) 34:979–86. doi: 10.3892/or.2015.4013
75. Deng B, Zhang Y, Zhang S, Wen F, Miao Y, Guo K. MicroRNA-142–3p inhibits cell proliferation and invasion of cervical cancer cells by targeting FZD7. *Tumour Biol.* (2015) 36:8065–73. doi: 10.1007/s13277-015-3483-2
76. Zhou WY, Chen JC, Jiao TT, Hui N, Qi X. MicroRNA-181 targets Yin Yang 1 expression and inhibits cervical cancer progression. *Mol Med Rep.* (2015) 11:4541–6. doi: 10.3892/mmr.2015.3324
77. Zhou C, Li G, Zhou J, Han N, Liu Z, Yin J. miR-107 activates ATR/Chk1 pathway and suppress cervical cancer invasion by targeting MCL1. *PLoS ONE*. (2014) 9:e111860. doi: 10.1371/journal.pone.0111860
78. Wan HY, Li QQ, Zhang Y, Tian W, Li YN, Liu M, et al. MiR-124 represses vasculogenic mimicry and cell motility by targeting amotL1 in cervical cancer cells. *Cancer Lett.* (2014) 355:148–58. doi: 10.1016/j.canlet.2014.09.005
79. Liang X, Liu Y, Zeng L, Yu C, Hu Z, Zhou Q, et al. miR-101 inhibits the G1-to-S phase transition of cervical cancer cells by targeting Fos. *Int J Gynecol Cancer*. (2014) 24:1165–72. doi: 10.1097/IGC.0000000000000187
80. Dong J, Sui L, Wang Q, Chen M, Sun H. MicroRNA-26a inhibits cell proliferation and invasion of cervical cancer cells by targeting protein tyrosine phosphatase type IVA 1. *Mol Med Rep.* (2014) 10:1426–32. doi: 10.3892/mmr.2014.2335
81. Luo M, Li Z, Wang W, Zeng Y, Liu Z, Qiu J. Long non-coding RNA H19 increases bladder cancer metastasis by associating with EZH2 and inhibiting E-cadherin expression. *Cancer Lett.* (2013) 333:213–21. doi: 10.1016/j.canlet.2013.01.033
82. Xin JX, Yue Z, Zhang S, Jiang ZH, Wang PY, Li YJ, et al. miR-99 inhibits cervical carcinoma cell proliferation by targeting TRIB2. *Oncol Lett*. (2013) 6:1025–30. doi: 10.3892/ol.2013.1473
83. Wang L, Chang L, Li Z, Gao Q, Cai D, Tian Y, et al. miR-99a and−99b inhibit cervical cancer cell proliferation and invasion by targeting mTOR signaling pathway. *Med Oncol.* (2014) 31:934. doi: 10.1007/s12032-014-0934-3
84. Wen SY, Lin Y, Yu YQ, Cao SJ, Zhang R, Yang XM, et al. miR-506 acts as a tumor suppressor by directly targeting the hedgehog pathway transcription factor Gli3 in human cervical cancer. *Oncogene.* (2015) 34:717–25. doi: 10.1038/onc.2014.9
85. Cui F, Li X, Zhu X, Huang L, Huang Y, Mao C, et al. MiR-125b inhibits tumor growth and promotes apoptosis of cervical cancer cells by targeting phosphoinositide 3-kinase catalytic subunit delta. Cell Physiol Biochem (2012) 30:1310–8. doi: 10.1159/000343320
86. Wei Q, Li YX, Liu M, Li X, Tang H. MiR-17–5p targets TP53INP1 and regulates cell proliferation and apoptosis of cervical cancer cells. *IUBMB Life.* (2012) 64:697–704. doi: 10.1002/iub.1051
87. Xu J, Li Y, Wang F, Wang X, Cheng B, Ye F, et al. Suppressed miR-424 expression via upregulation of target gene Chk1 contributes to the progression of cervical cancer. *Oncogene.* (2013) 32:976–87. doi: 10.1038/onc.2012.121
88. Kogo R, How C, Chaudary N, Bruce J, Shi W, Hill RP, et al. The microRNA-218∼Survivin axis regulates migration, invasion, and lymph node metastasis in cervical cancer. *Oncotarget.* (2015) 6:1090–100. doi: 10.18632/oncotarget.2836
89. Wang F, Li Y, Zhou J, Xu J, Peng C, Ye F, et al. miR-375 is down-regulated in squamous cervical cancer and inhibits cell migration and invasion via targeting transcription factor SP1. *Am J Pathol.* (2011) 179:2580–8. doi: 10.1016/j.ajpath.2011.07.037
90. Pang RT, Leung CO, Ye TM, Liu W, Chiu PC, Lam KK, et al. MicroRNA-34a suppresses invasion through downregulation of Notch1 and Jagged1 in cervical carcinoma and choriocarcinoma cells. *Carcinogenesis.* (2010) 31:1037–44. doi: 10.1093/carcin/bgq066
91. Li XR, Chu HJ, Lv T, Wang L, Kong SF, Dai SZ. miR-342-3p suppresses proliferation, migration and invasion by targeting FOXM1 in human cervical cancer. *FEBS Lett*. (2014) 588:3298–307. doi: 10.1016/j.febslet.2014.07.020
92. Li MY, Hu XX. Meta-analysis of microRNA expression profiling studies in human cervical cancer. *Med Oncol.* (2015) 32:510. doi: 10.1007/s12032-015-0510-5
93. Meng X, Zhao Y, Wang J, Gao Z, Geng Q, Liu X. Regulatory roles of miRNA-758 and matrix extracellular phosphoglycoprotein in cervical cancer. *Exp Ther Med.* (2017) 14:2789–94. doi: 10.3892/etm.2017.4887
94. Ye J, Cheng XD, Cheng B, Cheng YF, Chen XJ, Lu WG. MiRNA detection in cervical exfoliated cells for missed high-grade lesions in women with LSIL/CIN1 diagnosis after colposcopy-guided biopsy. *BMC Cancer.* (2019) 19:112. doi: 10.1186/s12885-019-5311-3
95. Tian Q, Li Y, Wang F, Li Y, Xu J, Shen Y, et al. MicroRNA detection in cervical exfoliated cells as a triage for human papillomavirus-positive women. *J Natl Cancer Inst.* (2014) 106:dju241. doi: 10.1093/jnci/dju241
96. Kawai S, Fujii T, Kukimoto I, Yamada H, Yamamoto N, Kuroda M, et al. Identification of miRNAs in cervical mucus as a novel diagnostic marker for cervical neoplasia. *Sci Rep*. (2018) 8:7070. doi: 10.1038/s41598-018-25310-1
97. Zhao S, Yao D, Chen J, Ding N. Circulating miRNA-20a and miRNA-203 for screening lymph node metastasis in early stage cervical cancer. *Genet Test Mol Biomarkers.* (2013) 17:631–6. doi: 10.1089/gtmb.2013.0085
98. Liu P, Xin F, Ma CF. Clinical significance of serum miR-196a in cervical intraepithelial neoplasia and cervical cancer. *Genet Mol Res.* (2015) 14:17995–8002. doi: 10.4238/2015.December.22.25
99. Zhang Y, Zhang D, Wang F, Xu D, Guo Y, Cui W. Serum miRNAs panel (miR-16–2*, miR-195, miR-2861, miR-497) as novel non-invasive biomarkers for detection of cervical cancer. *Sci Rep.* (2015) 5:17942. doi: 10.1038/srep17942

100. Xin F, Liu P, Ma CF. A circulating serum miRNA panel as early detection biomarkers of cervical intraepithelial neoplasia. *Eur Rev Med Pharmacol Sci.* (2016) 20:4846–51.
101. Li C, Zheng X, Li W, Bai F, Lyu J, Meng QH. Serum miR-486–5p as a diagnostic marker in cervical cancer: with investigation of potential mechanisms. *BMC Cancer.* (2018) 18:61. doi: 10.1186/s12885-017-3753-z
102. Wang WT, Zhao YN, Yan JX, Weng MY, Wang Y, Chen YQ, et al. Differentially expressed microRNAs in the serum of cervical squamous cell carcinoma patients before and after surgery. *J Hematol Oncol.* (2014) 7:6. doi: 10.1186/1756-8722-7-6
103. You W, Wang Y, Zheng J. Plasma miR-127 and miR-218 Might Serve as Potential Biomarkers for Cervical Cancer. *Reprod Sci.* (2015) 22:1037–41. doi: 10.1177/1933719115570902
104. Yu J, Wang Y, Dong R, Huang X, Ding S, Qiu H. Circulating microRNA-218 was reduced in cervical cancer and correlated with tumor invasion. *J Cancer Res Clin Oncol.* (2012) 138:671–4. doi: 10.1007/s00432-012-1147-9
105. Jiang W, Pan JJ, Deng YH, Liang MR, Yao LH. Down-regulated serum microRNA-101 is associated with aggressive progression and poor prognosis of cervical cancer. *J Gynecol Oncol.* (2017) 28:e75. doi: 10.3802/jgo.2017.28.e75
106. Tang BB, Liu SY, Zhan YU, Wei LQ, Mao XL, Wang J, et al. microRNA-218 expression and its association with the clinicopathological characteristics of patients with cervical cancer. *Exp Ther Med.* (2015) 10:269–74. doi: 10.3892/etm.2015.2455
107. Lui WO, Pourmand N, Patterson BK, Fire A. Patterns of known and novel small RNAs in human cervical cancer. *Cancer Res.* (2007) 67:6031–43. doi: 10.1158/0008-5472.CAN-06-0561
108. Lin S, Gregory RI. MicroRNA biogenesis pathways in cancer. *Nat Rev Cancer.* (2015) 15:321–33. doi: 10.1038/nrc3932
109. Muralidhar B, Goldstein LD, Ng G, Winder DM, Palmer RD, Gooding EL, et al. Global microRNA profiles in cervical squamous cell carcinoma depend on Drosha expression levels. *J Pathol.* (2007) 212:368–77. doi: 10.1002/path.2179
110. Pereira PM, Marques JP, Soares AR, Carreto L, Santos MA. MicroRNA expression variability in human cervical tissues. *PLoS ONE.* (2010) 5:e11780. doi: 10.1371/journal.pone.0011780
111. Nahand JS, Taghizadeh-Boroujeni S, Karimzadeh M, Borran S, Pourhanifeh MH, Moghoofei M, et al. microRNAs: new prognostic, diagnostic, and therapeutic biomarkers in cervical cancer. *J Cell Physiol.* (2019) 234:17064–99. doi: 10.1002/jcp.28457
112. Berti FCB, Salviano-Silva A, Beckert HC, de Oliveira KB, Cipolla GA, Malheiros D. From squamous intraepithelial lesions to cervical cancer: circulating microRNAs as potential biomarkers in cervical carcinogenesis. *Biochim Biophys Acta Rev Cancer.* (2019) 1872:188306. doi: 10.1016/j.bbcan.2019.08.001
113. Deng Y, Xiong Y, Liu Y. miR-376c inhibits cervical cancer cell proliferation and invasion by targeting BMI1. *Int J Exp Pathol.* (2016) 97:257–65. doi: 10.1111/iep.12177
114. Shao S, Wang C, Wang S, Zhang H, Zhang Y. LncRNA STXBP5-AS1 suppressed cervical cancer progression via targeting miR-96–5p/PTEN axis. *Biomed Pharmacother.* (2019) 117:109082. doi: 10.1016/j.biopha.2019.109082
115. Natalia MA, Alejandro GT, Virginia TJ, Alvarez-Salas LM. MARK1 is a novel target for miR-125a-5p: implications for cell migration in cervical tumor cells. *Microrna.* (2018) 7:54–61. doi: 10.2174/2211536606666171024160244
116. Navarro F, Lieberman J. miR-34 and p53: new insights into a complex functional relationship. *PLoS ONE.* (2015) 10:e0132767. doi: 10.1371/journal.pone.0132767
117. Wang X, Meyers C, Guo M, Zheng ZM. Upregulation of p18Ink4c expression by oncogenic HPV E6 via p53-miR-34a pathway. *Int J Cancer.* (2011) 129:1362–72. doi: 10.1002/ijc.25800
118. Martinez I, Gardiner AS, Board KF, Monzon FA, Edwards RP, Khan SA. Human papillomavirus type 16 reduces the expression of microRNA-218 in cervical carcinoma cells. *Oncogene.* (2008) 27:2575–82. doi: 10.1038/sj.onc.1210919
119. Liu X. Up-regulation of miR-20a by HPV16 E6 exerts growth-promoting effects by targeting PDCD6 in cervical carcinoma cells. *Biomed Pharmacother.* (2018) 102:996–1002. doi: 10.1016/j.biopha.2018.03.154
120. Cheng Y, Geng L, Zhao L, Zuo P, Wang J. Human papillomavirus E6-regulated microRNA-20b promotes invasion in cervical cancer by targeting tissue inhibitor of metalloproteinase 2. *Mol Med Rep.* (2017) 16:5464–70. doi: 10.3892/mmr.2017.7231
121. Mandal P, Saha SS, Sen S, Bhattacharya A, Bhattacharya NP, Bucha S, et al. Cervical cancer subtypes harbouring integrated and/or episomal HPV16 portray distinct molecular phenotypes based on transcriptome profiling of mRNAs and miRNAs. *Cell Death Discov.* (2019) 5:81. doi: 10.1038/s41420-019-0154-x
122. Qian K, Pietila T, Ronty M, Michon F, Frilander MJ, Ritari J, et al. Identification and validation of human papillomavirus encoded microRNAs. *PLoS ONE.* (2013) 8:e70202. doi: 10.1371/journal.pone.0070202
123. Wu S, Chen H. Anti-Condyloma acuminata mechanism of microRNAs-375 modulates HPV in cervical cancer cells via the UBE3A and IGF-1R pathway. *Oncol Lett.* (2018) 16:3241–7. doi: 10.3892/ol.2018.8983
124. Shukla V, Varghese VK, Kabekkodu SP, Mallya S, Chakrabarty S, Jayaram P, et al. Enumeration of deregulated miRNAs in liquid and tissue biopsies of cervical cancer. *Gynecol Oncol.* (2019) 155:135–43. doi: 10.1016/j.ygyno.2019.08.012
125. Li H, Liefke R, Jiang J, Kurland JV, Tian W, Deng P, et al. Polycomb-like proteins link the PRC2 complex to CpG islands. *Nature.* (2017) 549:287–91. doi: 10.1038/nature23881
126. Jandrig B, Seitz S, Hinzmann B, Arnold W, Micheel B, Koelble K, et al. ST18 is a breast cancer tumor suppressor gene at human chromosome 8q11.2. *Oncogene.* (2004) 23:9295–302. doi: 10.1038/sj.onc.1208131
127. Yang J, Siqueira MF, Behl Y, Alikhani M, Graves DT. The transcription factor ST18 regulates proapoptotic and proinflammatory gene expression in fibroblasts. *FASEB J.* (2008) 22:3956–67. doi: 10.1096/fj.08-111013
128. Ma Q, Wan G, Wang S, Yang W, Zhang J, Yao X. Serum microRNA-205 as a novel biomarker for cervical cancer patients. *Cancer Cell Int.* (2014) 14:81. doi: 10.1186/s12935-014-0081-0
129. Sharma S, Mandal P, Sadhukhan T, Roy CR, Ranjan MN, Chakravarty B, et al. Bridging links between long noncoding RNA HOTAIR and HPV oncoprotein E7 in cervical cancer pathogenesis. *Sci Rep.* (2015) 5:11724. doi: 10.1038/srep11724
130. Liu M, Jia J, Wang X, Liu Y, Wang C, Fan R. Long non-coding RNA HOTAIR promotes cervical cancer progression through regulating BCL2 via targeting miR-143–3p. *Cancer Biol Ther.* (2018) 19:391–9. doi: 10.1080/15384047.2018.1423921
131. Zhang D, Zhou XH, Zhang J, Zhou YX, Ying J, Wu GQ, et al. Propofol promotes cell apoptosis via inhibiting HOTAIR mediated mTOR pathway in cervical cancer. *Biochem Biophys Res Commun.* (2015) 468:561–7. doi: 10.1016/j.bbrc.2015.10.129
132. Lee M, Kim HJ, Kim SW, Park SA, Chun KH, Cho NH, et al. The long non-coding RNA HOTAIR increases tumour growth and invasion in cervical cancer by targeting the Notch pathway. *Oncotarget.* (2016) 7:44558–71. doi: 10.18632/oncotarget.10065
133. Kim HJ, Lee DW, Yim GW, Nam EJ, Kim S, Kim SW, et al. Long non-coding RNA HOTAIR is associated with human cervical cancer progression. *Int J Oncol.* (2015) 46:521–30. doi: 10.3892/ijo.2014.2758
134. Huang L, Liao LM, Liu AW, Wu JB, Cheng XL, Lin JX, et al. Overexpression of long noncoding RNA HOTAIR predicts a poor prognosis in patients with cervical cancer. *Arch Gynecol Obstet.* (2014) 290:717–23. doi: 10.1007/s00404-014-3236-2
135. Li D, Feng J, Wu T, Wang Y, Sun Y, Ren J, et al. Long intergenic noncoding RNA HOTAIR is overexpressed and regulates PTEN methylation in laryngeal squamous cell carcinoma. *Am J Pathol.* (2013) 182:64–70. doi: 10.1016/j.ajpath.2012.08.042
136. Li L, Liu B, Wapinski OL, Tsai MC, Qu K, Zhang J, et al. Targeted disruption of Hotair leads to homeotic transformation and gene derepression. *Cell Rep.* (2013) 5:3–12. doi: 10.1016/j.celrep.2013.09.003
137. Ding C, Cheng S, Yang Z, Lv Z, Xiao H, Du C, et al. Long non-coding RNA HOTAIR promotes cell migration and invasion via down-regulation of RNA binding motif protein 38 in hepatocellular carcinoma cells. *Int J Mol Sci.* (2014) 15:4060–76. doi: 10.3390/ijms15034060

138. Zhang H, Cai K, Wang J, Wang X, Cheng K, Shi F, et al. MiR-7, inhibited indirectly by lincRNA HOTAIR, directly inhibits SETDB1 and reverses the EMT of breast cancer stem cells by downregulating the STAT3 pathway. *Stem Cells.* (2014) 32:2858–68. doi: 10.1002/stem.1795
139. Li Q, Feng Y, Chao X, Shi S, Liang M, Qiao Y, et al. HOTAIR contributes to cell proliferation and metastasis of cervical cancer via targetting miR-23b/MAPK1 axis. Biosci Rep. (2018) 38:BSR20171563. doi: 10.1042/BSR20171563
140. Kim SJ, Park SE, Lee C, Lee SY, Jo JH, Kim JM, et al. Alterations in promoter usage and expression levels of insulin-like growth factor-II and H19 genes in cervical carcinoma exhibiting biallelic expression of IGF-II. *Biochim Biophys Acta.* (2002) 1586:307–15. doi: 10.1016/S0925-4439(01)00109-0
141. Sun R, Qin C, Jiang B, Fang S, Pan X, Peng L, et al. Down-regulation of MALAT1 inhibits cervical cancer cell invasion and metastasis by inhibition of epithelial-mesenchymal transition. *Mol Biosyst.* (2016) 12:952–62. doi: 10.1039/C5MB00685F
142. Ling H, Spizzo R, Atlasi Y, Nicoloso M, Shimizu M, Redis RS, et al. CCAT2, a novel noncoding RNA mapping to 8q24, underlies metastatic progression and chromosomal instability in colon cancer. *Genome Res.* (2013) 23:1446–61. doi: 10.1101/gr.152942.112
143. Fan MJ, Zou YH, He PJ, Zhang S, Sun XM, Li CZ. Long non-coding RNA SPRY4-IT1 promotes epithelial-mesenchymal transition of cervical cancer by regulating the miR-101-3p/ZEB1 axis. *Biosci Rep.* (2019) 39:BSR20181339. doi: 10.1042/BSR20181339
144. Gao J, Liu L, Li G, Cai M, Tan C, Han X, et al. LncRNA GAS5 confers the radio sensitivity of cervical cancer cells via regulating miR-106b/IER3 axis. *Int J Biol Macromol.* (2019) 126:994–1001. doi: 10.1016/j.ijbiomac.2018.12.176
145. Yang M, Zhai X, Xia B, Wang Y, Lou G. Long noncoding RNA CCHE1 promotes cervical cancer cell proliferation via upregulating PCNA. *Tumour Biol.* (2015) 36:7615–22. doi: 10.1007/s13277-015-3465-4
146. Peng W, Fan H. Long noncoding RNA CCHE1 indicates a poor prognosis of hepatocellular carcinoma and promotes carcinogenesis via activation of the ERK/MAPK pathway. *Biomed Pharmacother.* (2016) 83:450–455. doi: 10.1016/j.biopha.2016.06.056
147. Zhang J, Yao T, Wang Y, Yu J, Liu Y, Lin Z. Long noncoding RNA MEG3 is downregulated in cervical cancer and affects cell proliferation and apoptosis by regulating miR-21. *Cancer Biol Ther.* (2016) 17:104–13. doi: 10.1080/15384047.2015.1108496
148. Xu QF, Tang YX, Wang X. LncRNA EBIC promoted proliferation, metastasis and cisplatin resistance of ovarian cancer cells and predicted poor survival in ovarian cancer patients. *Eur Rev Med Pharmacol Sci.* (2018) 22:4440–7. doi: 10.26355/eurrev_201807_15495
149. Sun NX, Ye C, Zhao Q, Zhang Q, Xu C, Wang SB, et al. Long noncoding RNA-EBIC promotes tumor cell invasion by binding to EZH2 and repressing E-cadherin in cervical cancer. *PLoS ONE.* (2014) 9:e100340. doi: 10.1371/journal.pone.0100340
150. Guan Y, Kuo WL, Stilwell JL, Takano H, Lapuk AV, Fridlyand J, et al. Amplification of PVT1 contributes to the pathophysiology of ovarian and breast cancer. *Clin Cancer Res.* (2007) 13:5745–55. doi: 10.1158/1078-0432.CCR-06-2882
151. Barsotti AM, Beckerman R, Laptenko O, Huppi K, Caplen NJ, Prives C. p53-dependent induction of PVT1 and miR-1204. *J Biol Chem.* (2012) 287:2509–19. doi: 10.1074/jbc.M111.322875
152. Li MY, Tang XH, Fu Y, Wang TJ, Zhu JM. Regulatory mechanisms and clinical applications of the long non-coding RNA PVT1 in cancer treatment. *Front Oncol.* (2019) 9:787. doi: 10.3389/fonc.2019.00787
153. Iden M, Fye S, Li K, Chowdhury T, Ramchandran R, Rader JS. The lncRNA PVT1 contributes to the cervical cancer phenotype and associates with poor patient prognosis. *PLoS ONE.* (2016) 11:e0156274. doi: 10.1371/journal.pone.0156274
154. Zhang S, Zhang G, Liu J. Long noncoding RNA PVT1 promotes cervical cancer progression through epigenetically silencing miR-200b. *APMIS.* (2016) 124:649–58. doi: 10.1111/apm.12555
155. Shen CJ, Cheng YM, Wang CL. LncRNA PVT1 epigenetically silences miR-195 and modulates EMT and chemoresistance in cervical cancer cells. *J Drug Target.* (2017) 25:637–44. doi: 10.1080/1061186X.2017.1307379
156. Yang JP, Yang XJ, Xiao L, Wang Y. Long noncoding RNA PVT1 as a novel serum biomarker for detection of cervical cancer. *Eur Rev Med Pharmacol Sci.* (2016) 20:3980–6.
157. Wang C, Zou H, Yang H, Wang L, Chu H, Jiao J, et al. Long noncoding RNA plasmacytoma variant translocation 1 gene promotes the development of cervical cancer via the NFkappaB pathway. *Mol Med Rep.* (2019) 20:2433–40. doi: 10.3892/mmr.2019.10479
158. Ma S, Deng X, Yang Y, Zhang Q, Zhou T, Liu Z. The lncRNA LINC00675 regulates cell proliferation, and invasion by affecting Wnt/beta-catenin signaling in cervical cancer. *Biomed Pharmacother.* (2018) 108:1686–93. doi: 10.1016/j.biopha.2018.10.011
159. Rui X, Xu Y, Jiang X, Ye W, Huang Y, Jiang J. Long non-coding RNA C5orf66-AS1 promotes cell proliferation in cervical cancer by targeting miR-637/RING1 axis. *Cell Death Dis.* (2018) 9:1175–228. doi: 10.1038/s41419-018-1228-z
160. Barr JA, Hayes KE, Brownmiller T, Harold AD, Jagannathan R, Lockman PR, et al. Long non-coding RNA FAM83H-AS1 is regulated by human papillomavirus 16 E6 independently of p53 in cervical cancer cells. *Sci Rep.* (2019) 9:3662. doi: 10.1038/s41598-019-40094-8
161. Shen H, Wang L, Xiong J, Ren C, Gao C, Ding W, et al. Long non-coding RNA CCAT1 promotes cervical cancer cell proliferation and invasion by regulating the miR-181a-5p/MMP14 axis. *Cell Cycle.* (2019) 18:1110–21. doi: 10.1080/15384101.2019.1609829
162. Wang Q, Ding J, Nan G, Lyu Y, Ni G. LncRNA NOC2L-4.1 functions as a tumor oncogene in cervical cancer progression by regulating the miR-630/YAP1 pathway. *J Cell Biochem.* (2019) 120:16913–20. doi: 10.1002/jcb.28949
163. Qi C, Xiaofeng C, Dongen L, Liang Y, Liping X, Yue H, et al. Long non-coding RNA MACC1-AS1 promoted pancreatic carcinoma progression through activation of PAX8/NOTCH1 signaling pathway. *J Exp Clin Cancer Res.* (2019) 38:344. doi: 10.1186/s13046-019-1332-7
164. Liu Q, Guo X, Que S, Yang X, Fan H, Liu M, et al. LncRNA RSU1P2 contributes to tumorigenesis by acting as a ceRNA against let-7a in cervical cancer cells. *Oncotarget.* (2017) 8:43768–81. doi: 10.18632/oncotarget.10844
165. Aalijahan H, Ghorbian S. Long non-coding RNAs and cervical cancer. *Exp Mol Pathol.* (2019) 106:7–16. doi: 10.1016/j.yexmp.2018.11.010
166. Chen FJ, Sun M, Li SQ, Wu QQ, Ji L, Liu ZL, et al. Upregulation of the long non-coding RNA HOTAIR promotes esophageal squamous cell carcinoma metastasis and poor prognosis. *Mol Carcinog.* (2013) 52:908–15. doi: 10.1002/mc.21944
167. Ren Y, Wang YF, Zhang J, Wang QX, Han L, Mei M, et al. Targeted design and identification of AC1NOD4Q to block activity of HOTAIR by abrogating the scaffold interaction with EZH2. *Clin Epigenetics.* (2019) 11:29. doi: 10.1186/s13148-019-0624-2
168. Zhang JX, Han L, Bao ZS, Wang YY, Chen LY, Yan W, et al. HOTAIR, a cell cycle-associated long noncoding RNA and a strong predictor of survival, is preferentially expressed in classical and mesenchymal glioma. *Neuro Oncol.* (2013) 15:1595–603. doi: 10.1093/neuonc/not131
169. Guo L, Lu X, Zheng L, Liu X, Hu M. Association of long non-coding RNA HOTAIR polymorphisms with cervical cancer risk in a chinese population. *PLoS ONE.* (2016) 11:e0160039. doi: 10.1371/journal.pone.0160039
170. Sharma Saha S, Roy CR, Mondal NR, Chakravarty B, Chatterjee T, Roy S, et al. Identification of genetic variation in the lncRNA HOTAIR associated with HPV16-related cervical cancer pathogenesis. *Cell Oncol.* (2016) 39:559–72. doi: 10.1007/s13402-016-0298-0
171. Lecerf C, Le B, X, Adriaenssens E. The long non-coding RNA H19: an active player with multiple facets to sustain the hallmarks of cancer. *Cell Mol Life Sci.* (2019) 76:4673–87. doi: 10.1007/s00018-019-03240-z
172. Kallen AN, Zhou XB, Xu J, Qiao C, Ma J, Yan L, et al. The imprinted H19 lncRNA antagonizes let-7 microRNAs. *Mol Cell.* (2013) 52:101–12. doi: 10.1016/j.molcel.2013.08.027
173. Matouk IJ, DeGroot N, Mezan S, Ayesh S, bu-lail R, Hochberg A, et al. The H19 non-coding RNA is essential for human tumor growth. *PLoS ONE.* (2007) 2:e845. doi: 10.1371/journal.pone.0000845
174. Ou L, Wang D, Zhang H, Yu Q, Hua F. Decreased expression of miR-138–5p by lncRNA H19 in cervical cancer promotes tumor proliferation.

Oncol Res. (2018) 26:401–10. doi: 10.3727/096504017X15017209042610
175. Sun Y, Ma L. New insights into long non-coding RNA MALAT1 in cancer and metastasis. *Cancers.* (2019) 11:E216. doi: 10.3390/cancers11020216
176. Wilusz JE, Freier SM, Spector DL. 3' end processing of a long nuclear-retained noncoding RNA yields a tRNA-like cytoplasmic RNA. *Cell.* (2008) 135:919–32. doi: 10.1016/j.cell.2008.10.012
177. Jiang Y, Li Y, Fang S, Jiang B, Qin C, Xie P, et al. The role of MALAT1 correlates with HPV in cervical cancer. *Oncol Lett.* (2014) 7:2135–41. doi: 10.3892/ol.2014.1996
178. Lu H, He Y, Lin L, Qi Z, Ma L, Li L, et al. Long non-coding RNA MALAT1 modulates radiosensitivity of HR-HPV+ cervical cancer via sponging miR-145. *Tumour Biol.* (2016) 37:1683–91. doi: 10.1007/s13277-015-3946-5
179. Yang L, Bai HS, Deng Y, Fan L. High MALAT1 expression predicts a poor prognosis of cervical cancer and promotes cancer cell growth and invasion. *Eur Rev Med Pharmacol Sci.* (2015) 19:3187–93.
180. Guo F, Li Y, Liu Y, Wang J, Li Y, Li G. Inhibition of metastasis-associated lung adenocarcinoma transcript 1 in CaSki human cervical cancer cells suppresses cell proliferation and invasion. *Acta Biochim Biophys Sin.* (2010) 42:224–9. doi: 10.1093/abbs/gmq008
181. Kasagi Y, Oki E, Ando K, Ito S, Iguchi T, Sugiyama M, et al. The expression of CCAT2, a novel long noncoding RNA transcript, and rs6983267 single-nucleotide polymorphism genotypes in colorectal cancers. *Oncology.* (2017) 92:48–54. doi: 10.1159/000452143
182. Zhou B, Jing XY, Wu JQ, Xi HF, Lu GJ. Down-regulation of long non-coding RNA LET is associated with poor prognosis in gastric cancer. *Int J Clin Exp Pathol.* (2014) 7:8893–8.
183. Wu L, Jin L, Zhang W, Zhang L. Roles of long non-coding RNA CCAT2 in cervical cancer cell growth and apoptosis. *Med Sci Monit.* (2016) 22:875–9. doi: 10.12659/MSM.897754
184. Khaitan D, Dinger ME, Mazar J, Crawford J, Smith MA, Mattick JS, et al. The melanoma-upregulated long noncoding RNA SPRY4-IT1 modulates apoptosis and invasion. *Cancer Res.* (2011) 71:3852–62. doi: 10.1158/0008-5472.CAN-10-4460
185. Jin J, Chu Z, Ma P, Meng Y, Yang Y. Long non-coding RNA SPRY4-IT1 promotes proliferation and invasion by acting as a ceRNA of miR-101-3p in colorectal cancer cells. *Tumour Biol.* (2017) 39:1010428317716250. doi: 10.1177/1010428317716250
186. Liu D, Li Y, Luo G, Xiao X, Tao D, Wu X, et al. LncRNA SPRY4-IT1 sponges miR-101-3p to promote proliferation and metastasis of bladder cancer cells through up-regulating EZH2. *Cancer Lett.* (2017) 388:281–91. doi: 10.1016/j.canlet.2016.12.005
187. Cao Y, Liu Y, Lu X, Wang Y, Qiao H, Liu M. Upregulation of long noncoding RNA SPRY4-IT1 correlates with tumor progression and poor prognosis in cervical cancer. *FEBS Open Bio.* (2016) 6:954–60. doi: 10.1002/2211-5463.12102
188. Schneider C, King RM, Philipson L. Genes specifically expressed at growth arrest of mammalian cells. *Cell.* (1988) 54:787–93. doi: 10.1016/S0092-8674(88)91065-3
189. Pickard MR, Williams GT. The hormone response element mimic sequence of GAS5 lncRNA is sufficient to induce apoptosis in breast cancer cells. *Oncotarget.* (2016) 7:10104–16. doi: 10.18632/oncotarget.7173
190. Cao S, Liu W, Li F, Zhao W, Qin C. Decreased expression of lncRNA GAS5 predicts a poor prognosis in cervical cancer. *Int J Clin Exp Pathol.* (2014) 7:6776–83.
191. Chen Y, Wang CX, Sun XX, Wang C, Liu TF, Wang DJ. Long non-coding RNA CCHE1 overexpression predicts a poor prognosis for cervical cancer. *Eur Rev Med Pharmacol Sci.* (2017) 21:479–83.
192. Zink F, Magnusdottir DN, Magnusson OT, Walker NJ, Morris TJ, Sigurdsson A, et al. Insights into imprinting from parent-of-origin phased methylomes and transcriptomes. *Nat Genet.* (2018) 50:1542–52. doi: 10.1038/s41588-018-0232-7
193. Paci P, Colombo T, Farina L. Computational analysis identifies a sponge interaction network between long non-coding RNAs and messenger RNAs in human breast cancer. *BMC Syst Biol.* (2014) 8:83. doi: 10.1186/1752-0509-8-83
194. Gomez N, Unzeta M, Tipton KF, Anderson MC, O'Carroll AM. Determination of monoamine oxidase concentrations in rat liver by inhibitor binding. *Biochem Pharmacol.* (1986) 35:4467–72. doi: 10.1016/0006-2952(86)90765-3
195. Zhou CX, Wang X, Yang N, Xue SK, Li WC, Xie PP. LncRNA LET function as a tumor suppressor in breast cancer development. *Eur Rev Med Pharmacol Sci.* (2018) 22:6002–7. doi: 10.26355/eurrev_201809_15935
196. Jiang S, Wang HL, Yang J. Low expression of long non-coding RNA LET inhibits carcinogenesis of cervical cancer. *Int J Clin Exp Pathol.* (2015) 8:806–11.
197. Zhang HD, Jiang LH, Sun DW, Hou JC, Ji ZL. CircRNA: a novel type of biomarker for cancer. *Breast Cancer.* (2018) 25:1–7. doi: 10.1007/s12282-017-0793-9
198. Zhu X, Wang X, Wei S, Chen Y, Chen Y, Fan X, et al. hsa_circ_0013958: a circular RNA and potential novel biomarker for lung adenocarcinoma. *FEBS J.* (2017) 284:2170–82. doi: 10.1111/febs.14132
199. Salzman J, Gawad C, Wang PL, Lacayo N, Brown PO. Circular RNAs are the predominant transcript isoform from hundreds of human genes in diverse cell types. *PLoS ONE.* (2012) 7:e30733. doi: 10.1371/journal.pone.0030733
200. Han YN, Xia SQ, Zhang YY, Zheng JH, Li W. Circular RNAs: A novel type of biomarker and genetic tools in cancer. *Oncotarget.* (2017) 8:64551–63. doi: 10.18632/oncotarget.18350
201. Ma HB, Yao YN, Yu JJ, Chen XX, Li HF. Extensive profiling of circular RNAs and the potential regulatory role of circRNA-000284 in cell proliferation and invasion of cervical cancer via sponging miR-506. *Am J Transl Res.* (2018) 10:592–604.
202. Liu J, Wang D, Long Z, Liu J, Li W. CircRNA8924 promotes cervical cancer cell proliferation, migration and invasion by competitively binding to MiR-518d-5p/519–5p family and modulating the expression of CBX8. *Cell Physiol Biochem.* (2018) 48:173–84. doi: 10.1159/000491716
203. Zhang J, Zhao X, Zhang J, Zheng X, Li F. Circular RNA hsa_circ_0023404 exerts an oncogenic role in cervical cancer through regulating miR-136/TFCP2/YAP pathway. *Biochem Biophys Res Commun.* (2018) 501:428–33. doi: 10.1016/j.bbrc.2018.05.006
204. Cai H, Zhang P, Xu M, Yan L, Liu N, Wu X. Circular RNA hsa_circ_0000263 participates in cervical cancer development by regulating target gene of miR-150-5p. *J Cell Physiol.* (2019) 234:11391–400. doi: 10.1002/jcp.27796
205. Tian JDC, Liang L. Involvement of circular RNA SMARCA5/microRNA-620 axis in the regulation of cervical cancer cell proliferation, invasion and migration. *Eur Rev Med Pharmacol Sci.* (2018) 22:8589–98. doi: 10.26355/eurrev_201812_16622
206. Abdelmohsen K, Panda AC, Munk R, Grammatikakis I, Dudekula DB, De S, et al. Identification of HuR target circular RNAs uncovers suppression of PABPN1 translation by CircPABPN1. *RNA Biol.* (2017) 14:361–9. doi: 10.1080/15476286.2017.1279788
207. Zhou Y, Zheng X, Xu B, Chen L, Wang Q, Deng H, et al. Circular RNA hsa_circ_0004015 regulates the proliferation, invasion, and TKI drug resistance of non-small cell lung cancer by miR-1183/PDPK1 signaling pathway. *Biochem Biophys Res Commun.* (2019) 508:527–35. doi: 10.1016/j.bbrc.2018.11.157
208. Ding L, Zhang H. Circ-ATP8A2 promotes cell proliferation and invasion as a ceRNA to target EGFR by sponging miR-433 in cervical cancer. *Gene.* (2019) 705:103–8. doi: 10.1016/j.gene.2019.04.068
209. Hu C, Wang Y, Li A, Zhang J, Xue F, Zhu L. Overexpressed circ_0067934 acts as an oncogene to facilitate cervical cancer progression via the miR-545/EIF3C axis. *J Cell Physiol.* (2019) 234:9225–32. doi: 10.1002/jcp.27601
210. Mao Y, Zhang L, Li Y. circEIF4G2 modulates the malignant features of cervical cancer via the miR218/HOXA1 pathway. *Mol Med Rep.* (2019) 19:3714–22. doi: 10.3892/mmr.2019.10032
211. Hong H, Zhu H, Zhao S, Wang K, Zhang N, Tian Y, et al. The novel circCLK3/miR-320a/FoxM1 axis promotes cervical cancer progression. *Cell Death Dis.* (2019) 10:950. doi: 10.1038/s41419-019-2183-z
212. Zhao J, Lee EE, Kim J, Yang R, Chamseddin B, Ni C, et al. Transforming activity of an oncoprotein-encoding circular RNA from human papillomavirus. *Nat Commun.* (2019) 10:2300. doi: 10.1038/s41467-019-10246-5
213. Guo J, Chen M, Ai G, Mao W, Li H, Zhou J. Hsa_circ_0023404 enhances cervical cancer metastasis and chemoresistance through VEGFA and

autophagy signaling by sponging miR-5047. *Biomed Pharmacother.* (2019) 115:108957. doi: 10.1016/j.biopha.2019.108957

214. Song T, Xu A, Zhang Z, Gao F, Zhao L, Chen X, et al. CircRNA hsa_circRNA_101996 increases cervical cancer proliferation and invasion through activating TPX2 expression by restraining miR-8075. *J Cell Physiol.* (2019) 234:14296–305. doi: 10.1002/jcp.28128
215. Wang H, Zhao Y, Chen M, Cui J. Identification of novel long non-coding and circular RNAs in human papillomavirus-mediated cervical cancer. *Front Microbiol.* (2017) 8:1720. doi: 10.3389/fmicb.2017.01720

Conflict of Interest: The authors declare that the research was conducted in the absence of any commercial or financial relationships that could be construed as a potential conflict of interest.

frontiers in Oncology

ORIGINAL RESEARCH
published: 20 May 2020
doi: 10.3389/fonc.2020.00633

Long Non-coding RNA AK025387 Promotes Cell Migration and Invasion of Gastric Cancer

Yi-Yuan Sun[1,2], *Hui Zhang*[1,2], *Ran-Ran Ma*[1,2], *Guo-Hao Zhang*[1,2], *Ya-Ru Tian*[1,2], *Lei Liu*[1,2], *Lin Liu*[1,2] *and Peng Gao*[1,2]*

[1] Department of Pathology, Qilu Hospital, Shandong University, Jinan, China, [2] Key Laboratory for Experimental Teratology of the Ministry of Education, Department of Pathology, School of Basic Medical Sciences, Cheeloo College of Medicine, Shandong University, Jinan, China

Gastric cancer is one of the most common cancers in the world, and long non-coding RNAs (lncRNAs) play a crucial role in proliferation, metastasis, and invasion of gastric cancer. However, there are very few researches focusing on the effects of lncRNAs on metastatic gastric cancer. In this research, we identify one kind of lncRNA, called AK025387, which is highly expressed in metastatic gastric cancer samples compared with non-metastatic gastric cancer samples. The expression of AK025387 is significantly positively correlated with lymph node metastasis. The *in situ* hybridization demonstrates that AK025387 is located in both nucleus and cytoplasm, but mostly in cytoplasm. AK025387 promotes gastric cancer cells migratory and invasive ability, but it inhibits apoptosis *in vitro*. Furthermore, AK025387 regulates Raf-1, mitogen-activated protein kinase/extracellular signal-regulated kinase (MEK), and extracellular signal-regulated kinase (ERK) and is involved in mitogen-activated protein kinase (MAPK) signaling pathway to perform its biological functions. We conclude that AK025387 is highly expressed in metastatic gastric cancer, and its biological functions suggest the potential of AK025387 to be a biomarker of metastatic gastric cancer.

Keywords: long non-coding RNA, gastric cancer, AK025387, migration and invasion, MAPK signaling pathway

OPEN ACCESS

Edited by:
Patricia P. Reis,
São Paulo State University, Brazil

Reviewed by:
Smrithi Rajendiran,
University of California, Santa Cruz, United States
Estela de Oliveira Lima,
São Paulo State University, Brazil

***Correspondence:**
Peng Gao
gaopeng@sdu.edu.cn

Specialty section:
This article was submitted to Molecular and Cellular Oncology, a section of the journal Frontiers in Oncology

Received: *05 August 2019*
Accepted: *06 April 2020*
Published: *20 May 2020*

Citation:
Sun Y-Y, Zhang H, Ma R-R, Zhang G-H, Tian Y-R, Liu L, Liu L and Gao P (2020) Long Non-coding RNA AK025387 Promotes Cell Migration and Invasion of Gastric Cancer. Front. Oncol. 10:633. doi: 10.3389/fonc.2020.00633

INTRODUCTION

Gastric cancer is the fifth most commonly diagnosed cancers and the third most common cause of cancer death worldwide (1). Despite the global downward trends in gastric cancer mortality rates, further efforts are still needed (2). The two main features of gastric cancer, tumor invasion and metastasis, cause poor prognosis (3). Therefore, proposition of new treatments via the exploration of the molecular mechanisms of gastric cancer tumorigenesis and development, especially invasion and metastasis, are stringent.

Long non-coding RNAs (lncRNAs) are defined as transcriptional products that are composed of more than 200 nucleotides in length with little or no protein-coding potential (4). LncRNAs were initially thought to be spurious transcriptional noise with little biological function. However, widespread functionality of lncRNAs has been discovered and investigated in recent studies, and some new methods to research lncRNAs were used (5, 6). LncRNAs regulate gene expression at various levels, such as transcriptional regulation, post-transcriptional, protein localization, and RNA interference (7–10). Aberrant lncRNA expression is also involved in tumor proliferation, invasion, and metastasis process (11). For example, the lncRNA Hox transcript antisense intergenic RNA (HOTAIR) promotes migration and invasion of gastric cancer cells by performing as a

competing endogenous RNA to regulate HER2 expression (12). In this research, we first identify an lncRNA called AK025387, which is overexpressed in metastatic gastric cancer sample. Then, we investigate migration, invasion, proliferation, and apoptosis ability of gastric cancer cells by downregulating or upregulating AK025387 level. We further explore underlying signaling pathways of AK025387 in gastric cancer cells.

MATERIALS AND METHODS

Human Gastric Cancer Samples

Fresh-frozen tissues of 37 metastatic and 33 non-metastatic gastric cancers between 2013 and 2014 were obtained from the Qilu Hospital of Shandong University. All samples were collected for RNA expression analysis. Methods were performed according to the approved guidelines. All the participants have provided informed consents. The research was approved by the Ethical Committee of Shandong University, China.

Real-Time Quantitative PCR

Total RNA was extracted using TRIzol (Invitrogen, Carlsbad, CA, USA), according to the manufacturer's recommended protocol, and was reverse transcribed into complementary DNA (cDNA) using a Rever Tra Ace qPCR RT Kit (Toyobo, Osaka, Japan). SYBR Green Real-Time PCR Master Mix (Roche Diagnostic GmbH, Mannheim, Germany) and Applied Biosystems 7900HT were used to perform the real-time quantitative PCR. The relative expression of RNAs was standardized by glyceraldehyde 3-phosphate dehydrogenase (GAPDH).

Cell Culture and Transfection

The human gastric cancer cell lines MKN45 and SGC7901 were obtained from the Shanghai Cancer Institute. Gastric cancer cells were grown in Roswell Park Memorial Institute (RPMI) 1640 supplemented with 10% fetal bovine serum (FBS, Gibco BRL, Grand Island, NY, USA). X-tremeGENE transfection reagent (Roche Applied Science, Indianapolis, IN, USA) was used to transfect small interfering RNA (siRNA) (siRNA target sequence: GCTATCATTTCCCAGGTTT) or the negative control (RiboBio, Guangzhou, China) into gastric cancer cells according to the manufacturer's instructions. The pcDNA3.1 and pcDNA3.1-AK025387 plasmids (BioSune, Shanghai, China) transfected gastric cancer cells using TurboFect transfection reagent (Thermo Scientific, Shanghai, China) according to the manufacturer's instructions.

RNA *in situ* Hybridization

The digoxin-labeled *in situ* hybridization (ISH) probe used for detecting AK025387 was designed and synthesized by BioSune Co., Ltd. (Shanghai, China). Cells were seeded on polylysine-processed coverslips. The fresh-frozen tissue was cut at a thickness of 4 μm per section in a cryostat microtome and then was fixed on coverslips with formaldehyde. Coverslips were processed using the Enhanced Sensitive ISH Detection Kit I (POD) (cat: MK1030; Boster, Wuhan, China) according to the manufacturer's protocol. The Biotin-Mouse Anti-Digoxin was used after hybridization. The cell coverslips were visualized with fluorescein isothiocyanate (FITC)-streptavidin–biotin complex (SABC) (Boster, Wuhan, China) for probe and 4′,6-diamidino-2-phenylindole (DAPI) for nucleus. The positive results were stained in green and visualized under a fluorescent microscope (Olympus, Japan). The tissue-frozen sections were processed with SABC and biotin peroxidase and then visualized with 3,3′-diaminobenzidine (DAB) stain for probe and hematoxylin for nucleus. The positive results were stained in yellow.

RNA Stability Assay

The cells were grown in 12-well plates (Corning, NY, USA) until adherence. All cells were treated with Actinomycin D (Solarbio, Beijing, China) for 0 h, 30 min, 1 h, and 4 h and collected for real-time quantitative PCR (RT-qPCR). C-myc level was used as control.

Cell Migration and Invasion Assays *in vitro*

Migration assays were performed in Transwell chambers inserts with 8.0-μm pore size membrane (24-well plate, Coster, Corning Inc., Corning, NY, USA), and in invasion assays, membranes of Transwell chambers were coated with the Matrigel matrix (BD Science, Sparks, MD, USA). Gastric cancer cells (loss-of-function experiment, 8×10^4 in migration assays and 1.2×10^5 in invasion assays; gain-of-function experiment, 6×10^4 in migration assays and 1×10^5 in invasion assays) in 200 μl RPMI 1640 media were transferred into the upper chamber 24 h after transfection, and 600 μl RPMI 1640 media with 10% FBS was transferred into the lower chamber. Then, the 24-well plate was transferred into a CO_2 incubator at 37°C for 24 h. The non-migrating or non-invading cells stayed on the upper surface of the membrane, while the migrated or invaded cells reached the lower surface. The cotton swabs were used to remove non-migrating or non-invading cells; migrated or invaded cells were fixed, stained, and counted under the microscope (Olympus, Japan).

MTS Assay

Cell proliferation was measured at 24, 48, and 72 h after transfection in 96-well plates (Corning, NY, USA). First, 20 μl of 3-(4,5-dimethylthiazol-2-yl)-5-(3-carboxymethoxyphenyl)-2-(4-sulfophenyl)-2H-tetrazolium (MTS) solution (5 mg/ml) was added to the culture medium in each well, and absorbance was read at 490 nm using a microplate reader (Bio-Rad, Foster City, CA, USA).

EdU Assay

The transfected gastric cancer cells were seeded into 96-well plates for use. Proliferation of cells was also assessed by a Cell-Light™ EdU DNA Cell Proliferation (RiboBio, Guangzhou, China) assay according to the manufacturer's instructions. Gastric cancer cells were treated with DAPI (mark nucleus) after the 5-ethynyl-2′-deoxyuridine (EdU) incubation and counted under a fluorescent microscope (Olympus, Japan).

Apoptosis Assay

Gastric cancer cells were obtained 48 and 72 h after transfection and were stained using Annexin V-FITC/PI Apoptosis Detection Kit (BestBio, Shanghai, China) according to the manufacturer's instructions and immediately analyzed by flow cytometry.

Western Blot

Western blot was performed according to standard methods. Proteins were collected 48 h after transfection. Primary antibodies used included h-Ras (1:1,000, Sangon Biotech), Raf-1 (1:1,000, Cell Signaling), mitogen-activated protein kinase/extracellular signal-regulated kinase (MEK) (1:1,000, Cell Signaling), extracellular signal-regulated kinase (ERK) (1:2,000, Cell Signaling), p90RSK (1:1,000, Cell Signaling), AKT (1:10,000, Abcam), AKT3 (1:2,000, Proteintech), PIK3-CD (1:2,000, Proteintech), and β-actin (1:1,000, OriGene). The antibody binding was detected using a FluorChem Q system (Cell Biosciences, San Jose, CA, USA).

Statistical Analysis

All statistical analyses were performed using GraphPad Prism 5 (GraphPad Software, Inc., San Diego, CA, USA). The significance of the differences was determined by the Student's *t*-test between two groups. Non-parametric test was used in calculating RNA expression in samples. The chi-square test was used to analyze the relationship between clinicopathological factors and AK025387 expression. The receiver operating

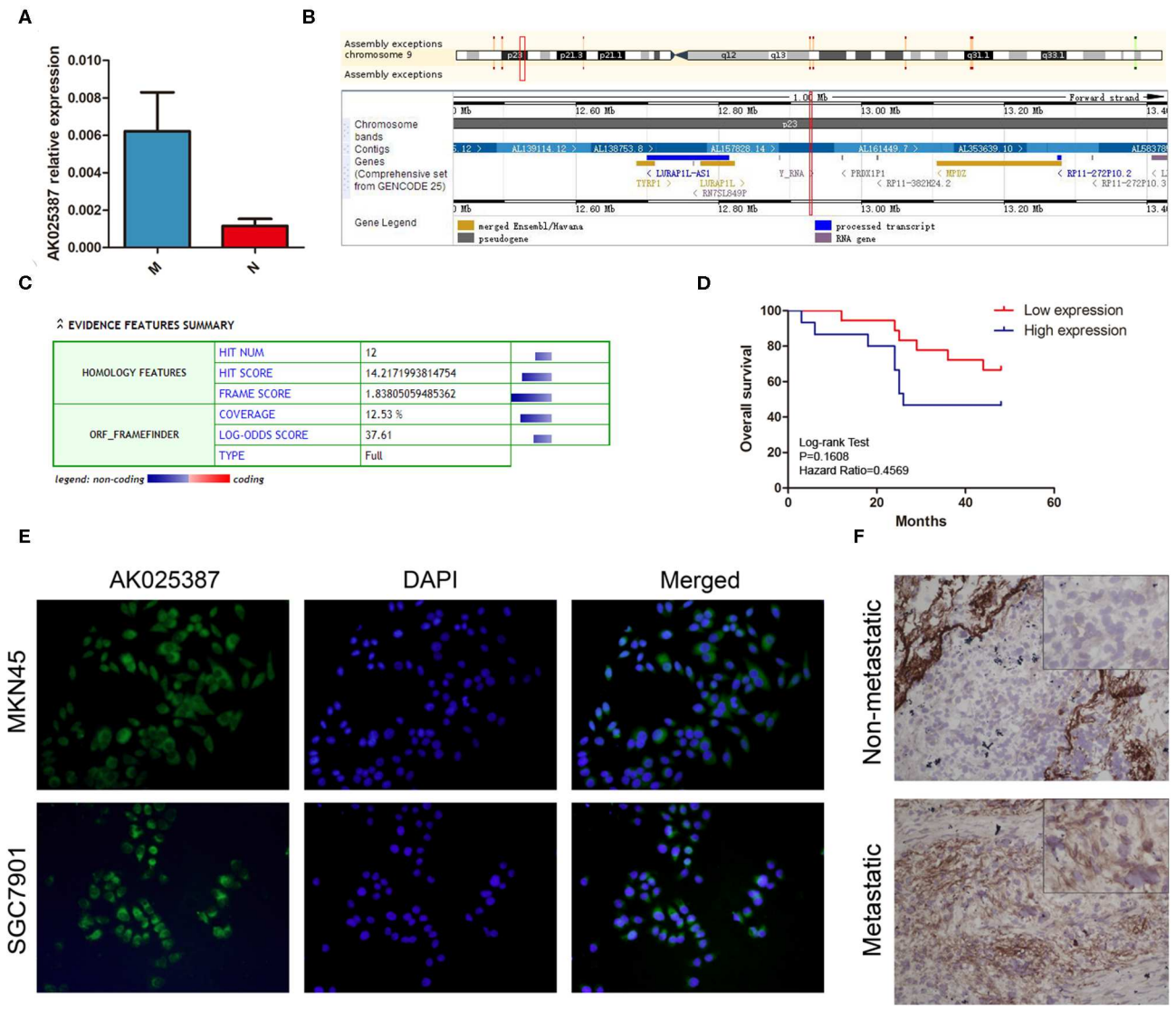

FIGURE 1 | Expression of AK025387 in gastric cancer tissues and intracellular location of AK025387. **(A)** The relative expression of AK025387 was higher in the metastatic (M) group than that in the non-metastatic (N) group ($P = 0.010$). **(B)** Gene information of AK025387. AK025387 is transcribed on chromosome 9 p23, with a length of 1,892 nucleotides, containing two exons and one intron. **(C)** Coding Potential Calculator (CPC) results of AK025387 (coding potential score: 0.024, weak coding potential). **(D)** Correlation of AK025387 expression with survival of patients with gastric cancer. No significant correlation was observed between overall survival and AK025387 expression ($P = 0.161$). **(E)** Fluorescence *in situ* hybridization results of AK025387 in gastric cancer cell lines. AK025387 was located in both nucleus and cytoplasm, but mainly in cytoplasm in both MKN45 and SGC7901 cell lines. **(F)** The *in situ* hybridization results of AK025387 in metastatic and non-metastatic gastric cancer tissues (200×). AK025387 was located mainly in the cytoplasm.

characteristics (ROC) curve was used to measure the diagnostic value of AK025387 expression in gastric cancer. The survival analysis was assessed by the Kaplan–Meier method, and the differences between groups were examined by the log-rank test. In this study, all *in vitro* experiments were repeated for at least three times. $P < 0.05$ was considered to be statistically significant.

RESULTS

LncRNA AK025387 Is Upregulated in Metastatic Gastric Cancer Sample

In our previous study, we had assessed the expression profiles of 33,045 lncRNAs through microarray analysis on five gastric cancer samples with lymphatic metastasis and five gastric cancer samples without lymphatic metastasis (array data were available in the GEO database, GSE72307; Probe name, ASHG19A3A038370). The result revealed that lncRNA, AK025387, was upregulated in metastatic gastric cancer sample with a 2.9-fold change ($P = 0.04$). To verify the microarray result, qRT-PCR was used to test AK025387 relative expression in both metastatic and non-metastatic gastric cancer samples (37 in metastatic group, 33 in non-metastatic group). The relative expression of AK025387 was higher in metastatic group than that in non-metastatic group ($P = 0.010$, **Figure 1A**), which was consistent with the microarray result. Furthermore, we analyzed the correlation between AK025387 expression and clinicopathological features in metastatic and non-metastatic gastric cancer (**Table 1**). A ROC curve was used to evaluate the AK025387 expression in predicting metastasis and non-metastasis (sensitivity = 69.0%, specificity = 73.3%, $P = 0.008$). AK025387 expression was found to be positively correlated with lymph node metastasis ($P = 0.025$). No significant correlation was observed between AK025387 expression and age, gender, tumor size, depth of invasion, and differentiation ($P = 0.763$, $P = 0.700$, $P = 1.000$, $P = 0.369$, $P = 1.000$, respectively). This result indicates a strong relationship with gastric cancer metastasis but not other clinicopathological factors. Furthermore, we evaluated the association of AK025387 expression with the prognosis of gastric cancer patients. However, the survival analysis indicates no significant correlation between overall survival and AK025387 expression ($P = 0.161$, **Figure 1D**).

Next, we used UCSC Genome Browser (http://genome.ucsc.edu/) to search genetic information of AK025387 (**Figure 1B**). AK025387 is transcribed on chromosome 9 p23, with a length of 1,892 nucleotides. Coding Potential Calculator (https://opendata.pku.edu.cn/dataset.xhtml?persistentId=doi:10.18170/DVN/8BO9C9) (13) was used to estimate protein-coding potential. The result illustrated that AK025387 had a low coding potential (**Figure 1C**). In order to investigate the subcellular localization of AK025387, we designed *in situ* hybridization in gastric cancer cells and tissues. The result showed that AK025387 was located in both nucleus and cytoplasm, mostly in cytoplasm (**Figures 1E,F**). This finding may demonstrate the potential function of AK025387 in gastric cancer cell.

TABLE 1 | Association between AK025387 expression and clinicopathological factors in primary gastric cancer.

Variable	*N*	AK025387 expression		*P*-value
		Low	High	
AGE				
≤60	23	9	14	
>60	20	9	11	
Missing	3	1	2	0.763
GENDER				
Male	38	15	23	
Female	8	4	4	0.700
TUMOR SIZE				
≤4	17	7	10	
>4	24	10	14	
Missing	5	2	3	1.000
DEPTH OF INVASION				
T1	1	0	1	
T2	6	4	2	
T3	16	7	9	
T4	22	7	15	0.369
Missing	1	1	0	
LYMPH NODE METASTASIS				
Negative	15	10	5	
Positive	31	9	22	0.025
DIFFERENTIATION				
Well	0	0	0	
Moderate	8	3	5	
Poor	35	13	22	
Missing	3	3	0	1.000

AK025387 Promotes Migration and Invasion of Gastric Cancer Cell *in vitro*

To evaluate the biological functions of AK025387 *in vitro*, we chose two gastric cancer cell lines, MKN45 and SGC7901, for further experiments (**Supplementary Figure 4**). RNA stability assay was used to test the stability of AK025387 in gastric cancer cells. Compared with c-myc, AK025387 expression was stable in 0 h, 30 min, 1 h, and 4 h in MKN45 (**Figures 2A,B**). The same results were also seen in other gastric cancer cell lines (data not shown). Then, a small interfering RNA (siRNA) was designed to knock down AK025387 in MKN45 and SGC7901 ($P = 0.038$ in MKN45; $P < 0.001$ in SGC7901, **Figures 2C,D**). Transwell experiments were performed to investigate migratory ability of MKN45 and SGC7901 cells. The migratory ability was inhibited with the silence of AK05387 in both MKN45 and SGC7901 cell lines, which means that AK025387 may promote migration of gastric cancer cells ($P < 0.001$ in MKN45; $P = 0.005$ in SGC7901, **Figures 2E,F**; **Supplementary Figures 1A,B**). In addition, we tested invasive ability of MKN45 and SGC7901 cells using Matrigel-coated Transwell experiments to determine whether AK025387 could promote invasive behavior or not. The invasive ability was inhibited in MKN45 and SGC7901

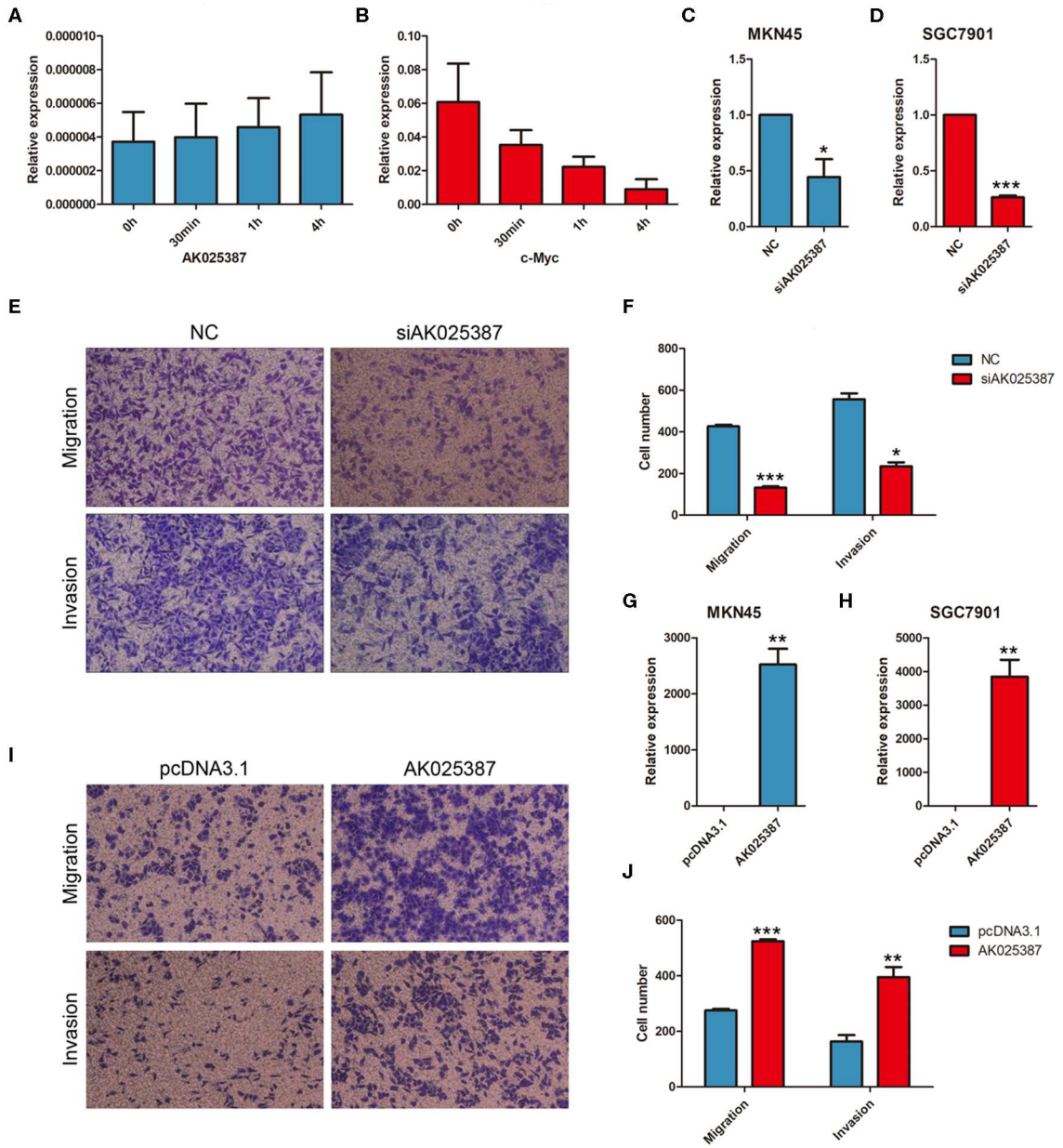

FIGURE 2 | AK025387 promoted migratory and invasive ability of gastric cancer cells. Actinomycin D could inhibit the synthesis of RNA. AK025387 maintained its expression level in MKN45 after treated **(A)** with Actinomycin D **(B)** compared with c-myc. **(C,D)** The small interfering RNA (siRNA) could sufficiently downregulate the expression level of AK025387 in both MKN45 and SGC7901 cell lines ($P = 0.038$ in MKN45; $P < 0.001$ in SGC7901). **(E,F)** Transwell experiments showed an inhibition of migration ($P < 0.001$) and invasion ($P = 0.010$) with knockdown of AK025387 in MKN45 cell line. **(G,H)** Upregulation of AK025387 in MKN45 and SGC7901 cell lines ($P = 0.006$ in MKN45; $P < 0.009$ in SGC7901). **(I,J)** The overexpression of AK025387 promoted migration ($P < 0.001$) and invasion ($P = 0.007$) in MKN45 cell line. *$P < 0.05$, **$P < 0.01$, and ***$P < 0.001$.

cell lines with downregulated AK025387 ($P = 0.010$ in MKN45; $P = 0.004$ in SGC7901. **Figures 2E,F** for MKN45; **Supplementary Figures 1A,B** for SGC7901).

Then, AK025387 was overexpressed in MKN45 and SGC7901 cell lines ($P = 0.006$ in MKN45; $P = 0.009$ in SGC7901, **Figures 2G,H**). The migratory and invasive abilities were enhanced with the upregulation of AK05387 in MKN45 cell line ($P < 0.001$ in migration; $P = 0.007$ in invasion, **Figures 2I,J**). An increased tendency but not significant difference of migration and invasion was observed in SGC7901 cell line with AK025387 upregulated ($P = 0.336$ in migration; $P = 0.081$ in invasion, **Supplementary Figures 1C,D**). Altogether, these results confirm that AK025387 could promote gastric cancer cell migratory and invasive ability.

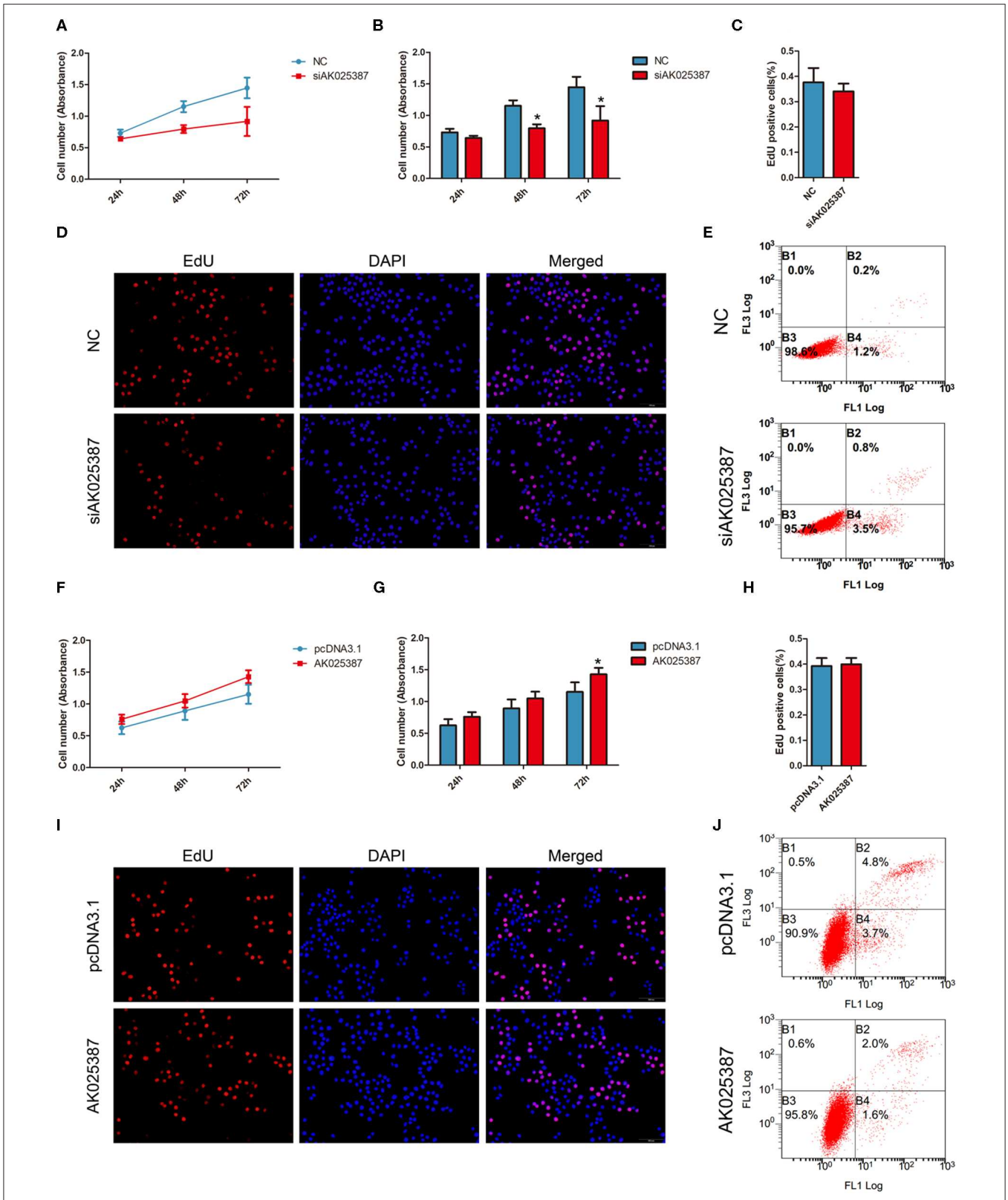

FIGURE 3 | AK025387 promoted gastric cancer growth via inhibiting apoptosis *in vitro*. **(A,B)** 3-(4,5-Dimethylthiazol-2-yl)-5-(3-carboxymethoxyphenyl)-2-(4-sulfophenyl)-2H-tetrazolium (MTS) assay showed an inhibition of growth ability with AK025387 knockdown in MKN45 cell line. The absorbance of siAK025387 group had no

(Continued)

FIGURE 3 | difference with the control group in 24 h ($P = 0.082$) but was lower in 48 h ($P = 0.020$) and 72 h ($P = 0.017$) in MKN45 cell line. **(C,D)** The 5-ethynyl-2′-deoxyuridine (EdU) assay showed no difference between the control and siAK025387 groups in MKN45 ($P = 0.352$). **(E)** Flow cytometry indicated a higher apoptosis rate with AK025387 knockdown in MKN45 cell line. FL1: Annexin V-FITC. FL3: PI. **(F,G)** The overexpression of AK025387 promoted growth ability in the MKN45 cell line. The absorbance of AK025387-upregulated group was higher in 72 h ($P = 0.020$) but not in 24 h ($P = 0.090$) and 48 h ($P = 0.051$) in MKN45. **(H,I)** The EdU assay showed no difference between the control and pcDNA3.1-AK025387 groups in MKN45 ($P = 0.408$). **(J)** Upregulation of AK025387 inhibited apoptosis in the MKN45 cell line. FL1: FITC. FL3: PI. *$P < 0.05$.

AK025387 Promotes Growth of Gastric Cancer by Inhibiting Apoptosis *in vitro*

To investigate the effect of AK025387 on growth, MTS assay was performed in both MKN45 and SGC7901 cell lines. An inhibition of cell growth ability was shown in AK025387-downregulated expression group (**Figures 3A,B**; **Supplementary Figures 2A,B**). To verify this result, cell proliferation ability was further detected via EdU assay. However, we found that there was no difference between control and AK025387-downregulated group in two gastric cancer cell lines ($P = 0.352$ in MKN45; $P = 0.402$ in SGC7901, **Figures 3C,D**; **Supplementary Figures 2C,D**). As cancer cell growth involved proliferation and apoptosis, we detected the effect of AK025387 on the apoptosis rate of gastric cancer cell lines. The result indicates that both MKN45 and SGC7901 cell lines transfected with AK025387 siRNA show a tendency of higher apoptosis ability compared with control group (**Figure 3E**; **Supplementary Figures 2E, 5A,C**).

Next, we overexpressed AK025387 in MKN45 and SGC7901 cell lines. A promotion of cell growth ability was observed in both cell lines with AK025387 upregulated by MTS assay (**Figures 3F,G**; **Supplementary Figures 2F,G**). No significant differences were found between control and AK025387-upregulated group by EdU assay ($P = 0.408$ in MKN45; $P = 0.247$ in SGC7901, **Figures 3H,I**; **Supplementary Figures 2H,I**). In addition, a lower apoptosis tendency was observed in AK025387-upregulated group in both cell lines (**Figure 3J**; **Supplementary Figures 2J, 5B,D**). All the above results suggests that AK025387 promotes growth of gastric cancer by inhibiting apoptosis without promoting proliferation directly.

AK025387 Performs Its Biological Function via MAPK Pathway

To explore how AK025387 regulated migration and invasion of gastric cancer cell, we first focused on the expression change of neighboring gene of AK025387, but no significant association was observed as AK025387 downregulated (data not shown). Then, several classical signaling pathways were tested via qRT-PCR and Western blot analysis. MAPK pathway mediated invasion and proliferation in many types of human cancers (14), and lncRNAs might be involved in this signaling pathway. Several genes in MAPK pathway were tested in MKN45 and SGC7901 gastric cancer cell lines with different levels of AK025387. The messenger RNA (mRNA) expression levels of Raf-1, MEK2, and ERK showed a parallel change with AK025387 downregulation (**Figure 4A**, $P = 0.022$, $P < 0.001$, $P = 0.015$, respectively) and AK025387 upregulation (**Figure 4B**, $P = 0.042$, $P = 0.023$, $P = 0.043$, respectively). Additionally, Western blot was performed to confirm this result at protein level (**Figures 4C-F**). In addition, we tested several representative genes in the PI3K-AKT pathway, but no significant difference was observed between the AK025387 and PI3K-AKT pathway ((**Supplementary Figures 3A-C**). All the above results imply that AK025387 may play a role in MAPK signaling pathway to perform its biological function.

DISCUSSION

As gastric cancer is one of the most common carcinomas worldwide, it is essential to research on the mechanism of gastric cancer occurrence and development. LncRNA is one of the indispensable molecules involved in this process. Zhang et al. identified the lncRNA HOXC-AS3 that regulated gastric cancer cell proliferation and migration via interacting with YBX1 (15). LncRNA ZFPM2 antisense RNA 1 (ZFPM2-AS1) was reported to promote proliferation and suppress apoptosis of gastric cancer cells via a novel ZFPM2-AS1/MIF/p53 signaling axis (16). Besides, lncRNA metastasis-associated lung adenocarcinoma transcript 1 (MALAT1) was overexpressed in gastric cancer cells and promote cell proliferation in gastric cancer by recruiting SF2/ASF (17). Another famous lncRNA HOTAIR was also associated with gastric cancer (12). HOTAIR might act as competing endogenous RNA and interact with microRNA (miRNA), such as miR-331-3p and miR-152, to regulate human epidermal growth factor receptor 2 (HER2) and human leukocyte antigen-G (HLA-G) expression in gastric cancer cells (12, 18–20).

Since most lncRNAs were found between cancer and non-cancerous tissue in gastric cancer, there was a lack of attention on the aberrant lncRNAs between metastatic and non-metastatic cancer. We thus focused on this area, which might be more significant in metastasis and invasion of tumor. In this study, we validated that AK025387 expression was significantly increased in metastatic gastric cancer sample compared with the non-metastatic gastric cancer samples. The clinicopathological analysis elaborated a strong relationship between AK025387 expression and gastric cancer metastasis, ruling out other factors. However, no correlation was observed between overall survival of gastric cancer patients and AK025387 expression. We also testified that AK025387 was located in both nucleus and cytoplasm, but mainly in cytoplasm. Then, the expression of AK025387 was downregulated in gastric cancer cell lines using siRNA transfection, and a reduction in migration and invasion was found. Interestingly, the migratory and invasive ability was significantly promoted with AK025387 upregulated in MKN45 but not in SGC7901 cell lines. We consider that SGC7901 cell line represents gastric cancer cells with limited migration and invasion due to AK025387 upregulation. Thus, the enhancement of migration and invasion by upregulating AK025387 in SGC7901 is limited.

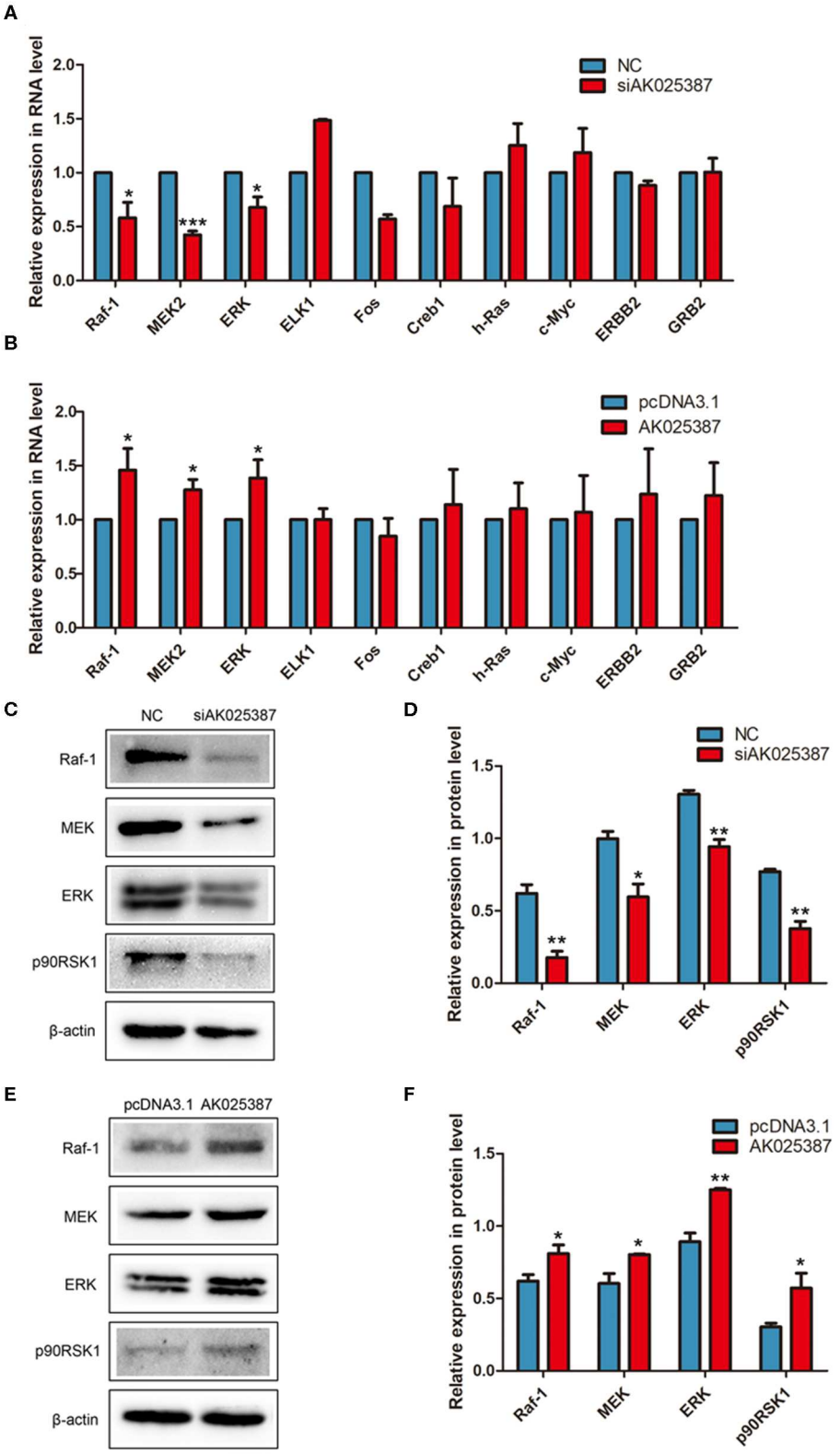

FIGURE 4 | AK025387 was involved in mitogen-activated protein kinase (MAPK) signaling pathway. **(A,B)** The expression levels of some RNAs in MAPK pathway in the MKN45 cell line. **(A)** Raf-1 ($P = 0.022$), MEK2 ($P < 0.001$), and ERK ($P = 0.015$) were significantly downregulated with knockdown of AK025387. **(B)**

(Continued)

FIGURE 4 | Raf-1 ($P = 0.042$), MEK2 ($P = 0.023$), and ERK ($P = 0.043$) were significantly upregulated with overexpression of AK025387. **(C–F)** The Western blot results of some proteins in MAPK pathway in the MKN45 cell line. **(C,D)** Raf-1, MEK, ERK, and p90RSK1 were significantly downregulated with knockdown of AK025387 ($P = 0.004$, $P = 0.018$, $P = 0.003$, $P = 0.002$, $P = 0.001$, respectively). **(E,F)** Raf-1, MEK, ERK, and p90RSK1 were significantly upregulated with overexpression of AK025387 ($P = 0.031$, $P = 0.023$, $P = 0.002$, $P = 0.032$, $P = 0.001$, respectively). $^{*}P < 0.05$, $^{**}P < 0.01$, and $^{***}P < 0.001$.

The function of AK025387 in proliferation and apoptosis was also investigated. Different results performed by MTS and EdU assays indicated that AK025387 promoted growth of gastric cancer in another way. An apoptosis assay was explored, and it was demonstrated that AK025387 promoted growth of gastric cancer by inhibiting apoptosis but not promoting proliferation directly. Additionally, some apoptosis-relative markers were tested [such as BCL2 and BCL2-antagonist of cell death (BAD), data not shown], and no significance was found. More researches on the mechanism of apoptosis are still required.

MAPK cascades regulate several cellular processes such as cell proliferation, differentiation, metabolism, motility, survival, apoptosis, etc. and contribute to many physiological and pathological processes (21). The ERK pathway is one of the most well-known MAPK pathways in mammals. The ERK is activated upon phosphorylation by MEK, which is itself activated when phosphorylated by Raf (22). The ERK/MAPK pathway is also one of the most frequently affected pathways in cancer (23, 24). In recent years, more researches have proposed that lncRNAs regulate signaling pathways in cancer, including ERK/MAPK pathway (25). It is reported that lncRNA MALAT-1 inactivates ERK/MAPK pathway to mediate tumor suppression in glioma cells (26) and may promote the proliferation and metastasis of gallbladder cancer cells by activating the ERK/MAPK pathway (27). LncRNA CCHE1 (cervical carcinoma expressed PCNA regulatory lncRNA) promoted carcinogenesis and indicated a poor prognosis of hepatocellular carcinoma via activation of ERK/MAPK pathway (28). In this study, we discovered a reduction in the expression level of Raf-1, MEK2, and ERK with AK025387 knockdown. However, some upstream and downstream molecules in MAPK pathway, such as growth factor receptor-bound protein 2 (GRB2), c-myc, and Erb-B2 receptor tyrosine kinase 2, showed no expression level change with AK025387 interfered. These results indicate that AK025387 might activate the Raf-MEK-ERK pathway to promote migration and invasion and inhibit apoptosis of gastric cancer cells, but a specific signaling pathway to regulate its biological function is still unknown. Further research on molecular mechanism of AK025387 in gastric cancer, such as direct or indirect interaction with MAPK pathway, is still needed.

CONCLUSIONS

In summary, we find that AK025387 is significantly upregulated in metastatic gastric cancer samples. The expression of AK025387 is confirmed to be significantly positively correlated only with lymph node metastasis and is not associated with overall survival of gastric cancer patients. AK025387 is located in both nucleus and cytoplasm, but mainly in cytoplasm. AK025387 promotes gastric cancer cells' migratory and invasive ability but inhibited apoptosis *in vitro*. Moreover, AK025387 increases the expression level of Raf-1, MEK2, and ERK. Therefore, AK025387 may activate the Raf-MEK-ERK pathway to perform its biological function. Taken together, AK025387 is a potential molecule and needs to be further investigated to determine if it can be used as a biomarker of metastatic gastric cancer.

DATA AVAILABILITY STATEMENT

The datasets generated for this study can be found in the GEO database (GSE72307).

ETHICS STATEMENT

The studies involving human participants were reviewed and approved by Ethical Committee of Shandong University, China. The patients/participants provided their written informed consent to participate in this study.

AUTHOR CONTRIBUTIONS

Y-YS, HZ, R-RM, and PG designed the study. Y-YS, G-HZ, Y-RT, and LeL performed the experiments. LiL collected the gastric cancer samples. Y-YS analyzed the data and wrote the manuscript. All authors read the manuscript and approved the final draft that was submitted.

FUNDING

This study was supported by the National Natural Science Foundation of China (Grant Nos. 81672842 and 81872362). The sponsors had no roles in study design, data collection and analysis, writing, and submitting the article.

SUPPLEMENTARY MATERIAL

The Supplementary Material for this article can be found online at: https://www.frontiersin.org/articles/10.3389/fonc.2020.00633/full#supplementary-material

REFERENCES

1. Bray F, Ferlay J, Soerjomataram I, Siegel RL, Torre LA, Jemal A. Global cancer statistics 2018, GLOBOCAN estimates of incidence and mortality worldwide for 36 cancers in 185 countries. *CA Cancer J Clin.* (2018) 68:394–424. doi: 10.3322/caac.21492
2. Ferro A, Peleteiro B, Malvezzi M, Bosetti C, Bertuccio P, Levi F, et al. Worldwide trends in gastric cancer mortality (1980–2011), with predictions to 2015, and incidence by subtype. *Eur J Cancer.* (2014) 50:1330–44. doi: 10.1016/j.ejca.2014.01.029
3. Steeg PS. Metastasis suppressors alter the signal transduction of cancer cells. *Nat Rev Cancer.* (2003) 3:55–63. doi: 10.1038/nrc967
4. Jin C, Shi W, Wang F, Shen X, Qi J, Cong H, et al. Long non-coding RNA HULC as a novel serum biomarker for diagnosis and prognosis prediction of gastric cancer. *Oncotarget.* (2016) 7:51763–72. doi: 10.18632/oncotarget.10107
5. Fanelli GN, Gasparini P, Coati I, Cui R, Pakula H, Chowdhury B, et al. LONG-NONCODING RNAs in gastroesophageal cancers. *Noncoding RNA Res.* (2018) 3:195–212. doi: 10.1016/j.ncrna.2018.10.001
6. Koch L. Functional genomics, screening for lncRNA function. *Nat Rev Genet.* (2017) 18:70. doi: 10.1038/nrg.2016.168
7. Pedro Batista J, Howard Chang Y. Long noncoding RNAs, cellular address codes in development and disease. *Cell.* (2013) 152:1298–307. doi: 10.1016/j.cell.2013.02.012
8. Choudhari R, Sedano MJ, Harrison AL, Subramani R, Lin KY, Ramos EI, et al. Long noncoding RNAs in cancer: from discovery to therapeutic targets. *Adv Clin Chem.* (2020) 95:105–47. doi: 10.1016/bs.acc.2019.08.003
9. Schmitz SU, Grote P, Herrmann BG. Mechanisms of long noncoding RNA function in development and disease. *Cell Mol Life Sci.* (2016) 73:2491–509. doi: 10.1007/s00018-016-2174-5
10. Sun W, Yang Y, Xu C, Xie Y, Guo J. Roles of long noncoding RNAs in gastric cancer and their clinical applications. *J Cancer Res Clin Oncol.* (2016) 142:2231–7. doi: 10.1007/s00432-016-2183-7
11. Wang Z, Wang J, Wang J, Song Y, Gao P, Shi J, et al. Long noncoding RNAs in gastric cancer: functions and clinical applications. *Onco Targets Ther.* (2016) 9:681–97. doi: 10.2147/ott.s95412
12. Liu XH, Sun M, Nie FQ, Ge YB, Zhang EB, Yin DD, et al. Lnc RNA HOTAIR functions as a competing endogenous RNA to regulate HER2 expression by sponging miR-331-3p in gastric cancer. *Mol Cancer.* (2014) 13:92 doi: 10.1186/1476-4598-13-92
13. Kong L, Zhang Y, Ye ZQ, Liu XQ, Zhao SQ, Wei L, et al. CPC: assess the protein-coding potential of transcripts using sequence features and support vector machine. *Nucleic Acids Res.* (2007) 35(Suppl. 2):W345–9. doi: 10.1093/nar/gkm391
14. Masliah-Planchon J, Garinet S, Pasmant E. RAS-MAPK pathway epigenetic activation in cancer: miRNAs in action. *Oncotarget.* (2016) 7:38892–907. doi: 10.18632/oncotarget.6476
15. Zhang E, He X, Zhang C, Su J, Lu X, Si X, et al. A novel long noncoding RNA HOXC-AS3 mediates tumorigenesis of gastric cancer by binding to YBX1. *Genome Biol.* (2018) 19:154. doi: 10.1186/s13059-018-1523-0
16. Kong F, Deng X, Kong X, Du Y, Li L, Zhu H, et al. ZFPM2-AS1, a novel lncRNA, attenuates the p53 pathway and promotes gastric carcinogenesis by stabilizing MIF. *Oncogene.* (2018) 37:5982–96. doi: 10.1038/s41388-018-0387-9
17. Wang J, Su L, Chen X, Li P, Cai Q, Yu B, et al. MALAT1 promotes cell proliferation in gastric cancer by recruiting SF2/ASF. *Biomed Pharmacother.* (2014) 68:557–64. doi: 10.1016/j.biopha.2014.04.007
18. Kim HP, Han SW, Song SH, Jeong EG, Lee MY, Hwang D, et al. Testican-1-mediated epithelial–mesenchymal transition signaling confers acquired resistance to lapatinib in HER2-positive gastric cancer. *Oncogene.* (2013) 33:3334–41. doi: 10.1038/onc.2013.285
19. Matsui Y, Inomata M, Tojigamori M, Sonoda K, Shiraishi N, Kitano S. Suppression of tumor growth in human gastric cancer with HER2 overexpression by an anti-HER2 antibody in a murine model. *Int J Oncol.* (2005) 27:681–5. doi: 10.3892/ijo.27.3.681
20. Song B, Guan Z, Liu F, Sun D, Wang K, Qu H. Long non-coding RNA HOTAIR promotes HLA-G expression via inhibiting miR-152 in gastric cancer cells. *Biochem Biophys Res Commun.* (2015) 464:807–13. doi: 10.1016/j.bbrc.2015.07.040
21. Low HB, Zhang Y. Regulatory roles of MAPK phosphatases in cancer. *Immune Netw.* (2016) 16:85. doi: 10.4110/in.2016.16.2.85
22. Dhillon AS, Hagan S, Rath O, Kolch W. MAP kinase signalling pathways in cancer. *Oncogene.* (2007) 26:3279–90. doi: 10.1038/sj.onc.1210421
23. Fey D, Matallanas D, Rauch J, Rukhlenko OS, Kholodenko BN. The complexities and versatility of the RAS-to-ERK signalling system in normal and cancer cells. *Semi Cell Dev Biol.* (2016) 58:96–107. doi: 10.1016/j.semcdb.2016.06.011
24. Samatar AA, Poulikakos PI. Targeting RAS–ERK signalling in cancer: promises and challenges. *Nat Rev Drug Discov.* (2014) 13:928–42. doi: 10.1038/nrd4281
25. Zong W, Ju S, Jing R, Cui M. Long non-coding RNA-mediated regulation of signaling pathways in gastric cancer. *Clin Chem Lab Med.* (2018) 56:1828–37. doi: 10.1515/cclm-2017-1139
26. Han Y, Wu Z, Wu T, Huang Y, Cheng Z, Li X, et al. Tumor-suppressive function of long noncoding RNA MALAT1 in glioma cells by downregulation of MMP2 and inactivation of ERK/MAPK signaling. *Cell Death Dis.* (2016) 7:e2123. doi: 10.1038/cddis.2015.407
27. Wu X-S, Wang X-A, Wu W-G, Hu Y-P, Li M-L, Ding Q, et al. MALAT1 promotes the proliferation and metastasis of gallbladder cancer cells by activating the ERK/MAPK pathway. *Cancer Biol Ther.* (2014) 15:806–14. doi: 10.4161/cbt.28584
28. Peng W, Fan H. Long noncoding RNA CCHE1 indicates a poor prognosis of hepatocellular carcinoma and promotes carcinogenesis via activation of the ERK/MAPK pathway. *Biomed Pharmacother.* (2016) 83:450–55. doi: 10.1016/j.biopha.2016.06.056

Conflict of Interest: The authors declare that the research was conducted in the absence of any commercial or financial relationships that could be construed as a potential conflict of interest.

frontiers in Oncology

ORIGINAL RESEARCH
published: 04 September 2020
doi: 10.3389/fonc.2020.01544

Comparison of microRNA Expression Profile in Chronic Myeloid Leukemia Patients Newly Diagnosed and Treated by Allogeneic Hematopoietic Stem Cell Transplantation

*Juliana Ravelli Baldassarre Martins[1], Leonardo Nazario de Moraes[2], Sarah Santiloni Cury[3], Juliane Dadalto[1], Juliana Capannacci[1], Robson Francisco Carvalho[3], Célia Regina Nogueira[1], Newton Key Hokama[1] and Paula de Oliveira Montandon Hokama[1]**

[1] Department of Internal Medicine, São Paulo State University (UNESP-FMB), Botucatu, Brazil, [2] Department of Bioprocesses and Biotechnology, São Paulo State University (UNESP-FCA), Botucatu, Brazil, [3] Department of Structural and Functional Biology, São Paulo State University (UNESP-IBB), Botucatu, Brazil

OPEN ACCESS

Edited by:
Deilson Elgui De Oliveira,
São Paulo State University, Brazil

Reviewed by:
Mohammad Sarwar Jamal,
King Abdulaziz University, Saudi Arabia
Clement M. Lee,
Icahn School of Medicine at Mount Sinai, United States

***Correspondence:**
Paula de Oliveira Montandon Hokama
paula.hokama@unesp.br

Specialty section:
This article was submitted to Molecular and Cellular Oncology, a section of the journal Frontiers in Oncology

Received: 13 July 2019
Accepted: 20 July 2020
Published: 04 September 2020

Citation:
Martins JRB, Moraes LN, Cury SS, Dadalto J, Capannacci J, Carvalho RF, Nogueira CR, Hokama NK and Hokama POM (2020) Comparison of microRNA Expression Profile in Chronic Myeloid Leukemia Patients Newly Diagnosed and Treated by Allogeneic Hematopoietic Stem Cell Transplantation. Front. Oncol. 10:1544. doi: 10.3389/fonc.2020.01544

Chronic myeloid leukemia (CML) results from a translocation between chromosomes 9 and 22, which generates the Philadelphia chromosome. This forms BCR/ABL1, an active tyrosine kinase protein that promotes cell growth and replication. Despite great progress in CML treatment in the form of tyrosine kinase inhibitors, allogeneic-hematopoietic stem cell transplantation (allo-HSCT) is currently used as an important treatment alternative for patients resistant to these inhibitors. Studies have shown that unregulated expression of microRNAs, which act as oncogenes or tumor suppressors, is associated with human cancers. This contributes to tumor formation and development by stimulating proliferation, angiogenesis, and invasion. Research has demonstrated the potential of microRNAs as biomarkers for cancer diagnosis, prognosis, and therapeutic targets. In the present study, we compared the circulating microRNA expression profiles of 14 newly diagnosed patients with chronic phase-CML and 14 Philadelphia chromosome-negative patients after allo-HSCT. For each patient, we tested 758 microRNAs by reverse transcription quantitative polymerase chain reaction (RT-qPCR) analysis. The global expression profile of microRNAs revealed 16 upregulated and 30 downregulated microRNAs. Target genes were analyzed, and key pathways were extracted and compared. Bioinformatics tools were used to analyze data. Among the downregulated miRNA target genes, some genes related to cell proliferation pathways were identified. These results reveal the comprehensive microRNA profile of CML patients and the main pathways related to the target genes of these miRNAs in cytogenetic remission after allo-HSCT. These results provide new resources for exploring stem cell transplantation-based CML treatment strategies.

Keywords: miRNAs, chronic myeloid leukemia, allogeneic hematopoietic stem cell transplantation, biomarkers, Philadelphia chromosome

INTRODUCTION

Chronic myeloid leukemia (CML) is a myeloproliferative disease accounting for ∼20% of diagnosed adult cases (1, 2). CML was the first human malignant disease to be linked to a chromosomal abnormality. A translocation between chromosomes 9q34 and 22q11 generates the Philadelphia chromosome. This encodes the BCR/ABL1 oncoprotein, an active tyrosine kinase protein that is the main driver of CML pathogenesis (2, 3). There have been great developments and improvements in anticancer targeted therapy associated with CML (4). Imatinib was the first member of a class of small molecules that prevent tyrosine kinase activity to be developed, and acts by binding to the BCR-ABL1 protein. Tyrosine kinase inhibitors (TKIs) act upon the interaction between the BCR-ABL1 oncoprotein and ATP, blocking cellular proliferation of the malignant clone. However, ∼2% of patients become resistant to TKIs. Allogeneic-hematopoietic stem cell transplantation (allo-HSCT) is the only curative treatment for CML and provides an important alternative for TKI-resistant or advanced phase CML patients (2). However, the mortality and morbidity of this method, as well as a lack of suitable donors, limits the application of allo-HSCT (5).

The natural course of CML begins in the chronic phase and progresses to the blast phase, passing through the accelerated phase. The transformation mechanisms involved with this process are varied and not yet fully understood. The interruption of differentiation, genomic instability, shortening of telomeres, and loss of tumor suppressor functions are among the steps of this transformation that have already been described (6, 7).

Recent advancements in gene expression profiling technology have demonstrated that microRNAs (miRNAs) are promising prognostic predictors of different types of cancers. miRNAs, which modulate post-transcriptional gene expression, are 18–25-nucleotide non-coding RNAs (8–10). They regulate gene expression and modify cancer processes such as differentiation, proliferation, and apoptosis. Previous studies have suggested that miRNAs play important roles in regulating angiogenesis and metastasis (11, 12). Additionally, miRNAs are very stable molecules in the blood, suggesting that they can be applied as molecular markers (13).

Bioinformatics is an important research approach that can be applied for understanding gene regulation pathways. Cancer bioinformatics is an emerging field that integrates knowledge from cancer and information technology. Integrating cancer research and bioinformatics is important for advancing the diagnosis, prognosis, and treatment of cancer (14). Additionally, bioinformatics analyses have contributed to the identification of candidate genes and miRNA-mRNA target pairs (15).

This study was conducted to determine the profiles of miRNAs and their target genes in CML patients treated with allo-HSCT. These profiles were then compared to those of a newly diagnosed and untreated patient group.

PATIENTS AND METHODS

The study was previously approved by the Research Ethics Committee of the Dr. Amaral Carvalho Hospital, Jahu, SP, Brazil (CEPHAC-−2.917.389). The patients provided informed consent to participate in the study, in accordance with the Declaration of Helsinki.

Patients and Samples

A total of 28 patients diagnosed with chronic phase-CML and treated at the Dr. Amaral Carvalho Hospital were included in the study. The patients were separated into two groups: (1) 14 patients newly diagnosed with Philadelphia chromosome-positive (Ph+) CML who had not been treated with TKIs; and (2) 14 patients who achieved complete cytogenetic remission (Philadelphia chromosome-negative) post-allo-HSCT. Patient characteristics are described in **Table 1**. The present study used a leukocyte pool of 14 healthy blood donors as a control group. To determine the miRNA profiles of each patient group, the control group was compared to the patient groups to determine which miRNAs were upregulated or downregulated. All transplanted patients received BuCy-2 as a conditioning regimen and cyclosporine and methotrexate as graft-vs.-host disease prophylaxis (16, 17).

Total RNA Isolation and RT-qPCR

Total RNA isolation was performed using a QIAamp® RNA Blood Mini Kit (QIAGEN, Hilden, Germany) with 5 mL peripheral blood. RNA integrity and quantity were evaluated by NanoDrop (Thermo Scientific, Waltham, MA, USA) and RNA 2100 Bioanalyzer (Agilent Technologies, Santa Clara, CA, USA) according to the manufacturer's instructions.

The total RNA was reverse-transcribed using a Taqman MicroRNA Reverse Transcription Kit, and a TaqMan™ MGB probe was used for real-time qPCR according to the manufacturer's instructions. RT-qPCR and TaqMan® Low Density Array Human MicroRNA Arrays A v2.0 and B v3.0 (ABIV®, Life Technologies, Carlsbad, CA, USA) were performed on a ViiA7 platform (ABIV®) following the manufacturer's instructions. miRNAs were quantified using the comparative Ct-method (18). Each Human Pool Set contains 377 unique human miRNAs, three internal controls, and one negative control. A total of 758 miRNAs were analyzed.

Bioinformatic Analysis

The study followed the experimental procedure detailed in **Figure 1**. Expression Suite Software Version 1.1 Program was used to identify differentially expressed miRNAs. To identify possible differentially expressed miRNA targets, we conducted RT-qPCR using miRWalk 2.0, which includes target prediction data generated by different algorithms (including own algorithm) (19). The following algorithms were selected: miRWalk, miRDB, Micro T4, miRanda, RNAhybrid, and Targetscan. Only targets predicted by at least three of the selected algorithms were accepted. We then verified whether the predicted targets have been identified as being differentially expressed in CML using microarray data available from Gene Expression Omnibus (https://www.ncbi.nlm.nih.gov/geo), accession number GSE 43225. Microarray data were analyzed using the GEO2R script (https://www.ncbi.nlm.nih.gov/geo/geo2r/).

TABLE 1 | Patient clinical data.

Patient	Gender	Age	BCR-ABL (%)	Breakpoint
Untreated group				
1	M	61	92	b2a2
2	M	52	100	b2a2
3	M	35	100	b2a2
4	F	54	100	b2a2
5	M	46	73	b3a2
6	M	72	100	b2a2
7	F	80	100	b3a2
8	M	67	100	b3a2
9	M	59	40	b2a2
10	M	60	82	b2+b3
11	F	52	100	b3a2
12	M	37	100	b3a2
13	F	53	100	b3a2
14	M	72	100	b3a2

Patients	Gender	Age	HSCT indication	Source	DAT	BCR-ABL (%)	Breakpoint	Mutation	Follow up
Hematopoietic stem cell transplantation group									
1	M	37	Disease progression	BM	224	1.60	b2a2	Absence	Relapsed
2	F	44	Failed therapy	BM	231	1,20	b3a2	Absence	Relapsed
3	F	03	Disease progression	BM	208	0.20	b3a2	_	Relapsed
4	F	63	FC	BM	1569	0.20	b3a2	Absence	Relapsed
5	M	37	Failed therapy	BM	110	0.50	b2a2	_	Relapsed
6	M	43	FC	BM	2450	0.30	b3a2	_	MMR
7	M	48	Disease progression	PBSC	80	0.75	b3a2	Absence	MMR
8	M	35	Failed therapy	BM	2352	0.03	b3a2	Absence	Relapsed
9	M	42	Failed therapy	PBSC	3561	0.01	b2a2	_	Relapsed
10	F	42	Disease progression	PBSC	3708	0.01	b3a2	_	MMR
11	F	56	FC	BM	3932	0.03	b2a2	Absence	MMR
12	M	32	FC	PBSC	3242	0.08	b2a2	_	Relapsed
13	M	21	FC	BM	1949	0.30	b3a2	Absence	Relapsed
14	M	58	Disease progression	BM	41	0.02	b2a2	_	MMR

DAT, days after transplantation; BM, bone marrow; PBSC, peripheral blood stem cell; (-), BCR-ABL mutation test was not performed; MMR, Major molecular response (BCR-ABL1 transcript level ≤ 0.1%).

FIGURE 1 | Flowchart showing the experimental procedure.

TABLE 2 | Dysregulated miRNAs in chronic myeloid leukemia.

miR	miRBase ID	FC	*P*-value
hsa-miR-1260a	MIMAT0005911	0.013	0.000
hsa-miR-27a-3p	MIMAT0000084	0.082	0.000
hsa-miR-140-3p	MIMAT0004597	0.083	0.000
mmu-miR-374b-5p	MIMAT0003727	0.105	0.000
hsa-miR-143-3p	MIMAT0000435	0.150	0.000
hsa-miR-181c-5p	MIMAT0000258	0.159	0.000
hsa-miR-26b-5p	MIMAT0000083	0.160	0.000
hsa-miR-212-3p	MIMAT0000269	0.164	0.000
hsa-miR-29c-3p	MIMAT0000681	0.172	0.000
hsa-miR-26a-1-3p	MIMAT0004499	0.180	0.000
hsa-miR-181a-5p	MIMAT0000256	0.189	0.000
hsa-miR-19a-3p	MIMAT0000073	0.224	0.008
hsa-miR-363-3p	MIMAT0000707	0.243	0.001
hsa-miR-30d-5p	MIMAT0000245	0.252	0.000
hsa-miR-10a-5p	MIMAT0000253	0.259	0.014
hsa-miR-29a-3p	MIMAT0000086	0.291	0.000
hsa-miR-16-5p	MIMAT0000069	0.291	0.002
hsa-miR-486-5p	MIMAT0002177	0.292	0.029
hsa-miR-345-5p	MIMAT0000772	0.310	0.000
hsa-miR-26a-5p	MIMAT0000082	0.318	0.000
hsa-miR-18a-3p	MIMAT0002891	0.329	0.000
hsa-miR-27b-3p	MIMAT0000419	0.331	0.003
hsa-miR-374a-5p	MIMAT0000727	0.343	0.009
hsa-miR-362-5p	MIMAT0000705	0.350	0.000
hsa-let-7g-5p	MIMAT0000414	0.402	0.000
hsa-miR-324-3p	MIMAT0000762	0.417	0.000
hsa-miR-550a-5p	MIMAT0004800	0.417	0.003
hsa-miR-125a-3p	MIMAT0004602	0.444	0.046
hsa-miR-106b-5p	MIMAT0000680	0.477	0.001
hsa-miR-191-5p	MIMAT0000440	0.496	0.000
hsa-miR-15b-3p	MIMAT0004586	2.005	0.039
hsa-miR-328-3p	MIMAT0000752	2.179	0.013
hsa-miR-222-3p	MIMAT0000279	2.233	0.000
hsa-miR-139-5p	MIMAT0000250	2.338	0.039
hsa-miR-92a-3p	MIMAT0000092	2.492	0.002
hsa-miR-628-3p	MIMAT0003297	2.589	0.010
hsa-miR-150-5p	MIMAT0000451	2.748	0.034
hsa-miR-574-3p	MIMAT0003239	2.764	0.001
hsa-miR-484	MIMAT0002174	2.820	0.000
hsa-miR-127-3p	MIMAT0000446	3.969	0.007
hsa-miR-146a-5p	MIMAT0000449	3.973	0.000
hsa-miR-193a-5p	MIMAT0004614	4.513	0.000
hsa-miR-342-3p	MIMAT0000753	5.070	0.000
hsa-miR-7-1-3p	MIMAT0004553	5.650	0.000
mmu-miR-134-5p	MIMAT0000146	6.473	0.002
hsa-miR-409-3p	MIMAT0001639	10.905	0.004

FC, fold-change; miR, microRNA.

We considered genes to be differentially expressed when they showed a fold-change of at least 1.5. Gene Ontology (GO) (http://www.geneontology.org/) was used to search for enriched terms among differentially expressed genes, accepting only terms with $P \leq 0.05$ and using Bonferroni's correction. Differentially expressed genes related to upregulated and downregulated miRNAs were analyzed according to EnrichR (https://amp.pharm.mssm.edu/Enrichr/) for enrichment analysis. Reactome was used for analysis. To assess the protein-protein interaction (PPI) network based on a list of genes, the online tool STRING Version 11.0 (https://string-db.org/) was utilized. Experiments, databases, co-expression data, neighborhood, and co-occurrence were considered active interaction sources. The minimum required interaction score was 0.700. Finally, we used Cytoscape Version 3.8.0 (http://www.cytoscape.org) software to visualize the enrichment results. Network nodes represent genes, while edges represent protein-protein associations.

Statistical Analysis

Comparative C_T analysis was used to quantify miRNA gene expression. The differences were estimated by Student's *t*-test. Values of $P < 0.05$ were considered statistically significant.

RESULTS

Differentially Expressed miRNAs

The miRNA expression data set is available in the NCBI GEO database (accession number GSE 148567). A total of 758 miRNAs were analyzed by RT-qPCR in peripheral blood samples from 14 newly diagnosed patients and untreated chronic phase CML patients, and 14 patients in cytogenetic remission after allo-HSCT. According to the cut-off criteria (fold-change $\leq$ 0.5 and fold-change $\geq$ 2.0), 46 differentially expressed miRNAs were identified. Sixteen (34.8%) miRNAs were upregulated, and thirty (65.2%) were downregulated (**Table 2**). Among them, miR-1260a was the most downregulated miRNA, whereas miR-409-3p was the most upregulated miRNA. The main functions of all differentially expressed miRNAs are listed in **Table 3**.

MiRNA Target Genes

Upregulated and downregulated miRNAs were analyzed in miRWalk to identify the miRNA target genes. Using microarray analysis, 1,069 genes were identified.

Gene Expression

We evaluated whether the identified target genes were previously differentially expressed in CML using available microarray data in the Gene Expression Omnibus. The microarray data were analyzed using GEO2R script. The identified genes were compared to our results. Of the 822 genes related to downregulated miRNA, 789 (96%) were also identified among the Gene Expression Omnibus microarray data genes. Among the genes associated with upregulated miRNAs, 247 genes were found in the patients included in the experiment, and 234 (95%) were found in the data searched.

Pathway Enrichment Analysis and PPI Network Construction

GO analysis (including Molecular Function, Biological Process and Cellular Component) was performed on 1,069 target genes. A total of 461 results were obtained from GO analysis. The top 30 terms are shown in **Figure 2**.

TABLE 3 | Functions of dysregulated miRNAs in chronic myeloid leukemia.

miR Name	Dysregulation in cancer	References
hsa-miR-1260a	Down-regulated in follicular B-cell lymphoma	(20)
hsa-miR-27a-3p	Involved in tumor growth: cell proliferation and cell invasion	(21)
hsa-miR-140-3p	Chemoresistance in osteosarcoma and colon cancer	(22)
mmu-miR-374b-5p	Inhibits cell migration, proliferation and invasion in cervical cancer	(23)
hsa-miR-143-3p	Low expression level contributes to tumor development, differentiation, proliferation, invasion and metastasis	(24)
hsa-miR-181c-5p	Inhibits chemoresistance in chronic myelocytic leukemia	(25)
hsa-miR-26b-5p	Down-regulated in breast cancer	(26)
hsa-miR-212-3p	Inhibits cell proliferation and promotes apoptosis	(27)
hsa-miR-29c-3p	Deregulated in hematological malignances	(28)
hsa-miR-26a-1-3p	Tumor suppressor	(29)
hsa-miR-181a-5p	Downregulation in resistance to imatinib	(30, 31)
hsa-miR-19a-3p	Potential biomarker for CML	(32)
hsa-miR-363-3p	Tumor suppressor in gastric cancer	(33)
hsa-miR-30d-5p	Downregulation in resistance to imatinib	(30, 31)
hsa-miR-10a-5p	Biomarker of drug response in CML	(34)
hsa-miR-29a-3p	Deregulated in hematological malignances	(28)
hsa-miR-16-5p	Regulation of cell cycle and apoptosis in myeloid leukemogenesis	(35)
hsa-miR-486-5p	Expression increased in erythroid differentiation in CML	(36)
hsa-miR-345-5p	Tumor suppressor in pancreatic cancer	(37)
hsa-miR-26a-5p	Tumor suppressor	(29)
hsa-miR-18a-3p	Potential biomarker for CML	(32)
hsa-miR-27b-3p	Oncogene; expression increased in lymphoma	(38)
hsa-miR-374a-5p	Promotes proliferation and migration of transformed mesenchymal stem cells	(39)
hsa-miR-362-5p	Induces apoptosis resistance and cell proliferation in gastric cancer	(40)
hsa-let-7g-5p	Downregulated in Burkitt's lymphoma	(41)
hsa-miR-324-3p	Overexpression promotes cell growth and decreases apoptosis	(42)
hsa-miR-550a-5p	Tumor suppressor	(43)
hsa-miR-125a-3p	Induces apoptosis in pancreatic cancer	(44)
hsa-miR-106b-5p	Inhibits metastasis and invasion colorectal cancer cells	(45)
hsa-miR-191-5p	Disregulated in human gliobastoma tissues	(46)
hsa-miR-15b-3p	High expression in poor prognosis for hepatocellular carcinoma	(47)
hsa-miR-328-3p	CML progression	(48)
hsa-miR-222-3p	Cancer development as oncomiR or as oncosuppressor	(49)
hsa-miR-139-5p	Antimetastic and anti-oncogenic activity	(50)
hsa-miR-92a-3p	Higher levels in acute myeloid leukemia and acute lymphoblastic leukemia	(51)
hsa-miR-628-3p	Inhibits proliferation of acute myeloid leukemia cells	(52, 53)
hsa-miR-150-5p	CML progression; CML biomarker	(54)
hsa-miR-574-3p	Tumor suppressor in ovarian cancer	(55)
hsa-miR-484	Highly expressed in breast cancer patients	(56)
hsa-miR-127-3p	Tumor suppressors in gastric cancer	(57)
hsa-miR-146a-5p	Development and maintenance of neoplastic processes	(58)
hsa-miR-193a-5p	Low expression in lung cancer	(59)
hsa-miR-342-3p	Suppresses acute myeloid leukemia cell proliferation	(60)
hsa-miR-7-1-3p	Up-regulated in metastatic prostate cancer	(61)
mmu-miR-134-5p	Cancer cell proliferation	(62)
hsa-miR-409-3p	Tumor suppressor in endometrial carcinoma cells	(63)

Fc, fold change; miR, microRNA.

EnrichR is a free web-based gene signature search tool. It was used to evaluate the 247 target genes of upregulated miRNAs, among which 573 terms were identified. Among the 822 target genes of downregulated miRNAs, 1,017 terms were found. EnrichR provides a visualization summary of the pathways based on a collective gene function list. The free pathway database tool Reactome is available for online use, and provides biological interpretation and visualization models for network analysis. STRING analysis was performed on the target genes of upregulated miRNAs (**Figure 3**) and downregulated miRNAs (**Figure 4**). The results were visualized using Cytoscape.

DISCUSSION

Differentially Expressed miRNAs

MiRNAs can act as oncogenes or tumor suppressor genes in CML, contributing to the pathogenesis, disease progression, and therapeutic responses (1, 52). Following the advent of TKIs as specific target drugs, hematopoietic stem cell transplantation began to play an important role in treating CML patients that are in the disease phase or are resistant to TKIs. This study investigated the miRNA profile of a group of 14 CML patients treated with allo-HSCT, who were in complete cytogenetic remission at the time of sample collection. Among the evaluated group, five patients underwent transplantation due to disease progression (patients 1, 3, 7, 10, and 14) and four others underwent transplantation due to a failed therapeutic response (patients 2, 5, 8, and 9). These comprised a total of 64.3% of the evaluated patients.

miR-10a

MiR-10a has been extensively studied due to its potential as a CML marker. Flamant et al. suggested the relevance of miR-10a as a drug response biomarker. By means of microarray analysis, a significant increase in miR-10a was observed in patient samples 2 weeks

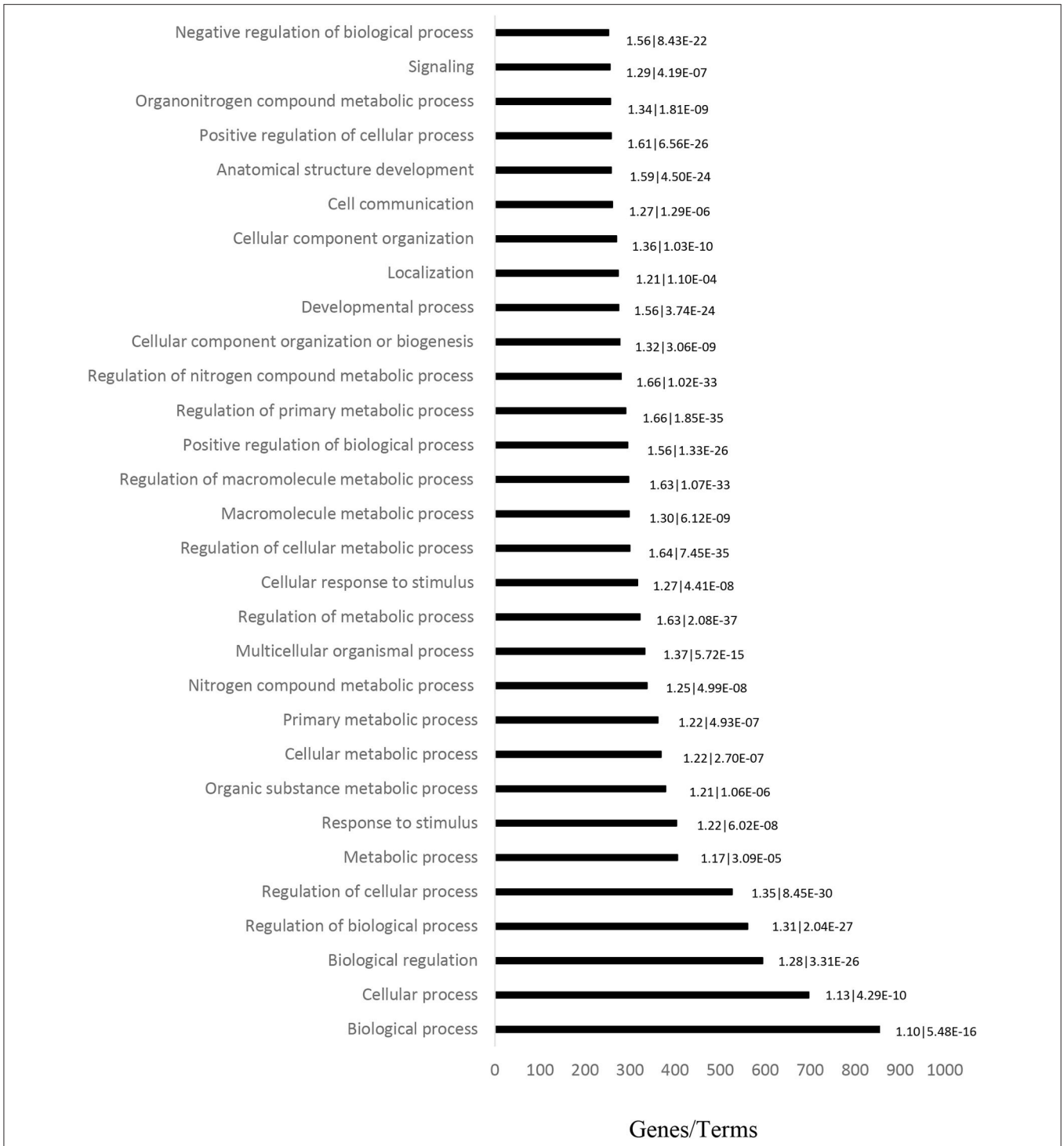

FIGURE 2 | Ontology analysis of differentially expressed genes in CML patient blood samples, performed to determine the main altered pathways. Horizontal bars represent the number of genes found in each term. The fold-enrichment and *P*-values are displayed on the sides of the horizontal bars, and are separated by a vertical line.

post-imatinib treatment (34). miR-10a downregulation was also detected in the transplanted patient group in the present study.

miR-17/92 Cluster

The miR-17/92 cluster is another potential biomarker for CML progression, and may be detected from the chronic phase to

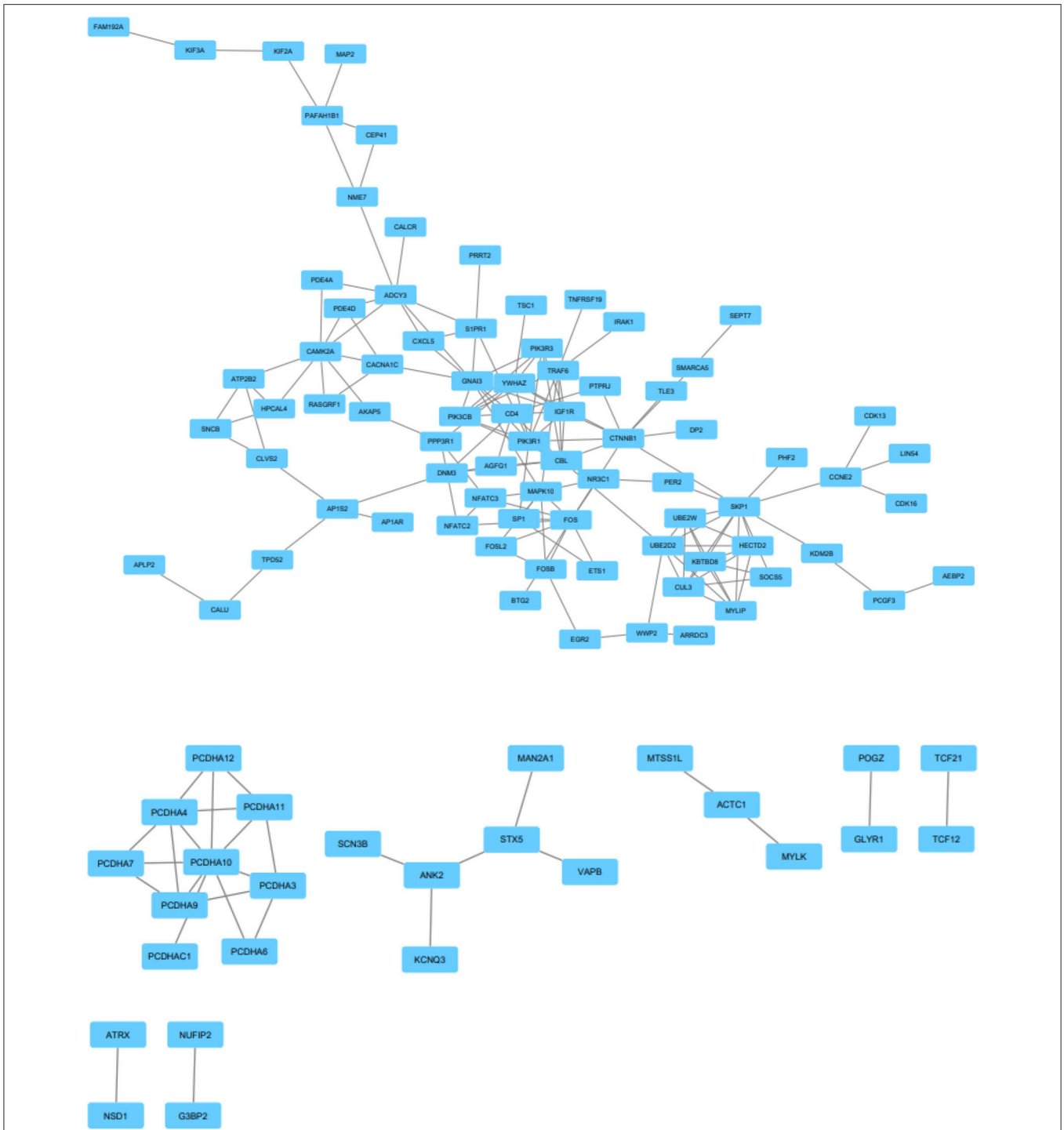

FIGURE 3 | Protein-protein interaction network analysis of the target genes of upregulated miRNAs. Gene interactions were constructed using the STRING online database and Cytoscape. Network nodes represent genes, and the edges represent protein-protein associations.

the blastic phase. This cluster is comprised of miR-17, miR18a, miR-19a, miR19b-1, miR20a, and miR92a-1 (32). In our study, a downregulation in the expression of miR-18a and miR-19a was observed, both of which are present in this cluster.

miR-328 and miR150

miR-328 and miR-150 are also related to disease progression (32, 48, 54, 64). Eiring et al. (48) have previously demonstrated the loss of miR-328 in blastic crisis $CD34^{+}$ cells, which did

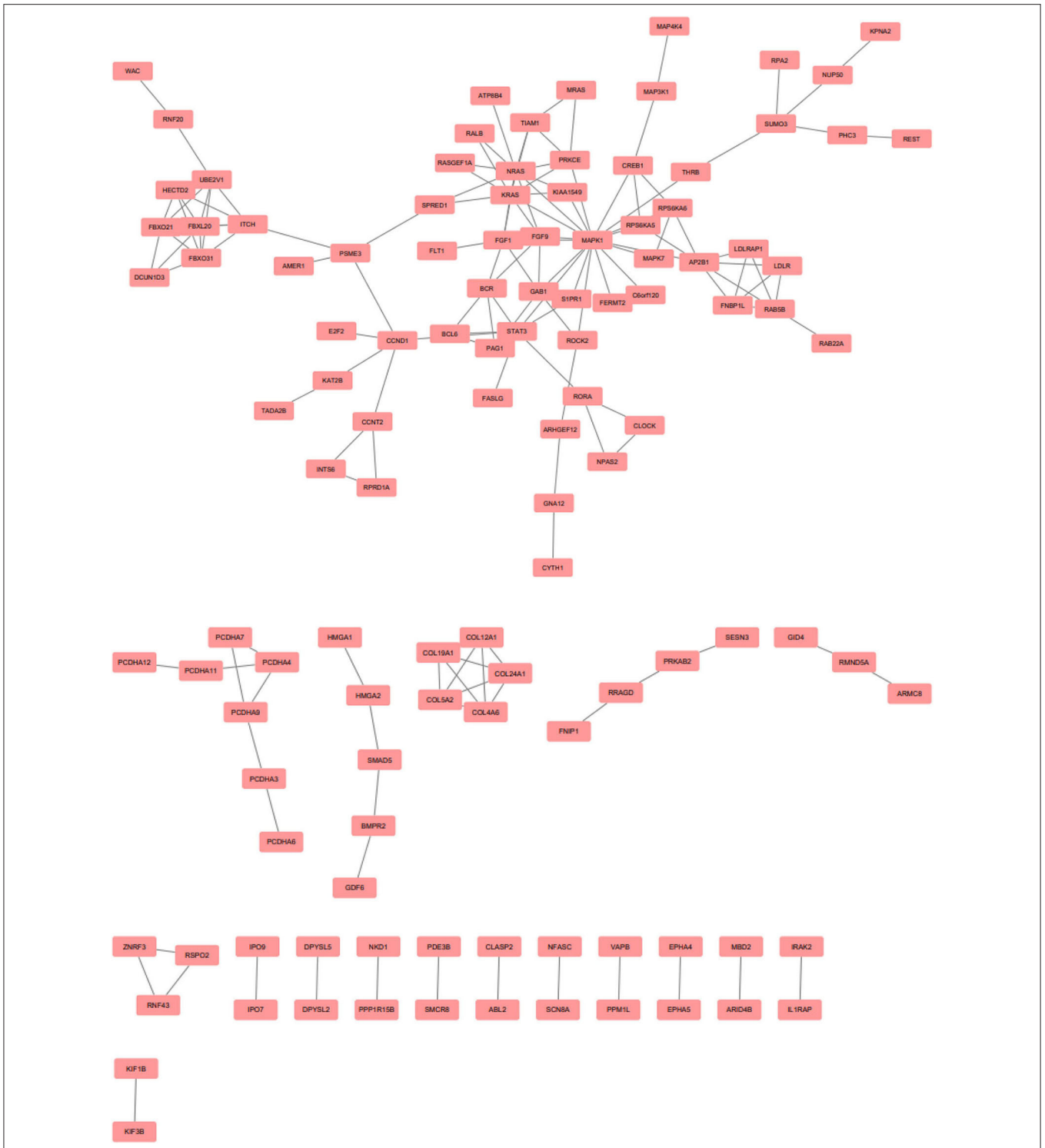

FIGURE 4 | Protein-protein interaction network analysis of the target genes of downregulated microRNAs. Gene interactions were constructed using the STRING online database and Cytoscape. Network nodes represent genes, and the edges represent protein-protein associations.

not otherwise occur in chronic phase $CD34^{+}$ myeloid cells. Poláková et al. (52) detected a negative correlation between the levels of *BCR-ABL* transcript and miR-150, further substantiating previous findings by Agirre et al. (64) and Fallah et al. (54) suggested that the downregulation of miR-150 is a potential diagnostic marker of CML. RT-PCR was performed for 50

samples from patients newly diagnosed with CML, revealing a downregulation in miR-150. In our study, both miRNAs were found to be upregulated, suggesting that miR-328 and miR-150 are useful as molecular biomarkers of the treatment response.

miR-486

The results of previous studies have also suggested miR-486 as an effective treatment response marker. Wang et al. compared miRNA expression in normal human $CD34^+$ cells with that in CML $CD34^+$ cells, using human leukemia cell lines and $CD34^+$ cells isolated from chronic phase CML patients who had not been treated with imatinib. The results showed that miR-486 was overexpressed in CML cells, especially in megakaryocytes and erythroid progenitor cells (36). In our study, miR-486 was downregulated, further suggesting the potential of this miRNA to act as a biomarker of the treatment response.

miR-181c and miR-30

According to studies carried out in the K562 cell line, miR-181c, and miR-30 downregulation is related to imatinib resistance (30, 31). Yu et al. demonstrated that the downregulation of miR-30 in this CML cell line was related to the autophagy process and imatinib resistance mechanisms (30, 31). These results were reflected in the current study, with our findings demonstrating that miR-181c and miR-30 were downregulated.

Let-7g and miR-16

Let-7a and miR-16 also have important functions in myeloid leukemogenesis, such as regulating the cell cycle and apoptosis. Let-7a regulates oncogenes such as RAS and HMGA, while Mir-16 targets MCL1, BCL2, WNT3A, and CCNDI (35). Let-7a is also a member of the let-7 family, and it has been found that it may suppress CML via *CRKL* (20). Zuo et al. (35) examined the plasma levels of miR-16 and let-7a in a group of 50 patients with myelodysplastic syndrome (MDS). After comparing these results with those from a group of 76 healthy donors, it was found that both miRNAs were significantly lower in MDS patients than in healthy controls. In the present study, we found that let-7g and miR-16 were downregulated.

Pathway Enrichment Analysis and PPI Network Construction

In the analysis conducted using STRING and EnrichR, it was possible to determine which pathways were enriched by observing the target genes of unregulated miRNAs. Through our analysis, we found that MAPK, NRAS, KRAS, and ROCK had important functions related to CML regulation pathways.

The mitogen-activated protein kinase (MAPK) pathway is an important signaling cascade in several types of cancer, including CML (65). This pathway controls fundamental cellular processes such as cell proliferation, migration, growth, differentiation, and death (66). The MAPK pathway therefore plays a fundamental role in cell growth and survival, and irregularities in this pathway can lead to cells developing cancerous properties. This may include exacerbated cell proliferation, metastasis, and evasion of apoptosis (67).

RAS proteins are involved in signal transduction, and are mutated in different types of human cancer. The RAS family comprises three genes associated with carcinogenesis: HRAS, KRAS, and NRAS (68). These three genes encode a protein located on the inner cell membrane, which has GTPase activity. This protein participates in extracellular signal transduction into the cell, and the signal is transmitted by a cascade of kinases. As a result, MAPK is activated, which then activates transcription factors. Mutations in the RAS genes in human cancer inhibit GTP hydrolysis, and mutated RAS proteins remain in their GTP-linked active form. This, leads to disordered cell proliferation (69). KRAS and NRAS mutations are frequently found in myeloid disorders, including CML (70).

ROCK proteins perform different functions in cells. They are involved in organization of the actin cytoskeleton, human tumor pathogenesis, and in the signaling pathways that lead to cell proliferation. The RAS and ROCK pathways are interconnected, with RAS activating PI3K, which then activates the ROCK pathway. This interaction network can lead to continuous cell proliferation and survival (68).

The MAPK, RAS, and ROCK genes had increased expression in the patient group of our study. As these genes are involved in cell proliferation during leukemogenesis, it can be concluded that these genes play an important role in post-transplant evolution. Nine of the 14 patients (64.3%) had leukemia relapse, and the other five (35.7%) did not achieve a deep molecular response (BCR-ABL transcript level $\leq 0.01\%$).

This study explored miRNAs in CML patients and their target genes, and analyzed the pathways involved. Our study was based on original and clinical samples. However, as there were scarce samples available and these were insufficient to validate the 46 altered miRNAS, the study was limited by this factor. The bioinformatics analyses predicted interactions that require further biological validation before their therapeutic application.

Despite the small sample size, these findings showed that aggressive therapy such as transplantation did not alter the disease course in these group of CML patients. Furthermore, the demonstrated pattern of gene expression is suggestive of disease progression.

DATA AVAILABILITY STATEMENT

All datasets generated for this study are included in the article/**Supplementary Material**.

ETHICS STATEMENT

This study was reviewed and approved by Research Ethics Committee of Dr. Amaral Carvalho Hospital–Jahu-SP- Brazil

(CEPHAC—2.917.389). The patients/participants provided their written informed consent to participate in this study.

AUTHOR CONTRIBUTIONS

PH, NH, and CN designed and coordinated the study and prepared the manuscript. JM, LM, and SC performed bioinformatics analysis and prepared the manuscript. JD and JC collected and analyzed the data. RC offered laboratory support and helped with discussions about the study. All authors critically reviewed and approved the final version of the manuscript.

FUNDING

This study received financial support by São Paulo Research Foundation (FAPESP 2011/50629-7).

SUPPLEMENTARY MATERIAL

The Supplementary Material for this article can be found online at: https://www.frontiersin.org/articles/10.3389/fonc.2020.01544/full#supplementary-material

REFERENCES

1. Wang K, Xu Z, Wang N, Tian Y, Sun X, Ma Y. Analysis of microRNA and gene networks in human chronic myelogenous leukemia. *Mol Med Rep.* (2016) 13:453–60. doi: 10.3892/mmr.2015.4502
2. Jabbour E, Kantarjian H. Chronic myeloid leukemia: 2018 update on diagnosis, therapy and monitoring. *Am J Hematol.* (2018) 93:442–59. doi: 10.1002/ajh.25011
3. Spagnuolo M, Regazzo G, De Dominici M, Sacconi A, Pelosi A, Korita E, et al. Transcriptional activation of the miR-17-92 cluster is involved in the growth-promoting effects of MYB in human Ph-positive leukemia cells. *Haematologica.* (2019) 104:82–92. doi: 10.3324/haematol.2018.191213
4. Baccarani M, Pane F. A critical history of chronic myeloid leukemia. *Mediterr J Hematol Infect Dis.* (2014) 6:1 doi: 10.4084/MJHID.2014.010
5. Goldman JM. Chronic myeloid leukemia: a historical perspective. *Semin Hematology.* (2010) 47:302–11. doi: 10.1053/j.seminhematol.2010.07.001
6. Garcia-Manero G, Faderl S, O'Brien S, Cortes J, Talpaz M, Kantarjian HM. Chronic myelogenous leucemia: a review and update of therapeutic strategies. *Cancer.* (2003) 98:437–57. doi: 10.1002/cncr.11520
7. Chakraborty C, Sharma AR, Patra BC, Bhattacharya M, Sharma G, Lee SS. MicroRNAs mediated regulation of MAPK signaling pathways in chronic myeloid leukemia. *Oncotarget.* (2016) 7:42683–97. doi: 10.18632/oncotarget.7977
8. Liang L, Wei DM, Li JJ, Luo DZ, Chen G, Dang YW, et al. Prognostic microRNAs and their potential molecular mechanism in pancreatic cancer: a study based on The cancer genome atlas and bioinformatics investigation. *Mol Med Rep.* (2018) 17:939–51. doi: 10.3892/mmr.2017.7945
9. Keklikoglou I, Koerner C, Schmidt C, Zhang JD, Heckmann D, Shavinskaya A, et al. MicroRNA-520/373 family functions as a tumor suppressor in estrogen receptor negative breast cancer by targeting NF-κB and TGF-β signaling pathways. *Oncogene.* (2012) 31:4150–63. doi: 10.1038/onc.2011.571
10. Cao Z, Moore BT, Wang Y, Peng XH, Lappe JM, Recker RR, et al. MiR-422a as a potential cellular microRNA biomarker for postmenopausal osteoporosis. *PLoS ONE.* (2014) 9:e97098 doi: 10.1371/jornal.pone.0097098
11. Guessous F, Velez MA, Marcinkiewicz L, Zhang Y, Kim J, Heister S, et al. Oncogenic effects of miR-10b in glioblastoma stem cells. *J Neurooncol.* (2013) 112:153–63. doi: 10.1007/s11060-013-1047-0
12. Garofalo M, Croce CM. Role of microRNAs in mantaining cancer stem cells. *Adv Drug Deliv Rev.* (2015) 81:53–61. doi: 10.1016/j.addr.2014.11.014
13. Li A, Yu J, Kim H, Wolfgang CL, Canto MI, Hruban RH, et al. MicroRNA array analysis finds elevated serum miR-1290 accurately distinguishes patients with low-stage pancreatic cancer from healthy and disease controls. *Clin Cancer Res.* (2013) 19:3600–10. doi: 10.1158/1078-0432.CCR-12-3092
14. Banwait JK, Bastola DR. Contribution of bioinformatics prediction in microRNA-based cancer therapeutics. *Adv Drug Deliv Rev.* (2015) 81:94–103. doi: 10.1016/j.addr.2014.10.030
15. Gao C, Zhou C, Zhuang J, Liu L, Wei J, Liu C, et al. Identification of key candidate genes and miRNA-mRNA target pairs in chronic lymphocytic leukemia by integrated bioinformatics analysis. *Mol Med Rep.* (2019) 19:362–74. doi: 10.3892/mmr.2018.9636
16. Tutscha PJ, Copelan EA, Klein JP. Bone marrow transplantation for leukemia following a new busulfan and cyclosphosphamide regimen. *Blood.* (1987) 70:1382–8.
17. Storb R, Deeg HJ, Whitehead J, Appelbaum F, Beatty P, Bensinger W, et al. Methotrexate and cyclosporine alone for prophylaxis of acute graft versus host disease after marrow transplantation for leukemia. *N Engl J Med.* (1986) 314:729–35. doi: 10.1056/NEJM198603203141201
18. Schmittgen T, Livak K. Analyzing real-time PCR data by the comparative CT method. *Nat Protoc.* (2008) 3:1101–8. doi: 10.1038/nprot.2008.73
19. Dweep H, Gretz N. MiRWalk2.0: a comprehensive atlas of microRNA-target interactions. *Nat Methods.* (2015) 12:697. doi: 10.1038/nmeth.3485
20. Rokah OH, Geva P, Divon MS, Shpilberg O, Aronov SL. Network analysis of microRNAs, genes and their regulation in diffuse and follicular B-cell lymphomas. *Oncotarget.* (2018) 9:7928–41. doi: 10.18632/oncotarget.23974
21. Li X, Xu M, Ding L, Tang J. miR-27a: A novel biomarker and potential therapeutic target in tumors. *J Cancer.* (2019) 10:2836–48. doi: 10.7150/jca.31361
22. Song B, Wang Y, Xi Y, Kudo K, Bruheim S, Botchkina G I, et al. Mechanism of chemoresistance mediated by miR-140 in human osteosarcoma and colon cancer cells. *Oncogene.* (2009) 28:4065–74. doi: 10.1038/onc.2009.274
23. Xia N, Tan WF, Peng QZ, Lai HN. MiR-374b reduces cell proliferation and cell invasion of cervical cancer through regulating FOXM1. *Eur Rev Med Pharmacol Sci .* (2019) 23:513–21. doi: 10.26355/eurrev_201901_16863
24. Takai T, Tsujino T, Yoshikawa Y, Inamoto T, Sugito N, Kuranaga Y. Synthetic miR-143 exhibited an anti-cancer effect via the downregulation of K-RAS networks of renal cell cancer cells *in vitro* and i*n vivo*. *Mol Ther.* (2019) 27:1017–27. doi: 10.1016/j.ymthe.2019.03.004
25. Zhao L, Li Y, Song X, Zhou H, Li N, Miao Y, et al. Upregulation of miR-181c inhibits chemoresistance by targeting ST8SIA4 in chronic myelocytic leukemia. *Oncotarget*. (2016) 7:60074–86. doi: 10.18632/oncotarget.11054
26. Verghese ET, Drury R, Green CA, Holliday DL, Lu X, Nash C. MiR-26b is down-regulated in carcinoma-associated fibroblasts from ER-positive breast cancers leading to enhanced cell migration and invasion. *J Pathol.* (2013) 231:388–99. doi: 10.1002/path.4248
27. Wu X, Chen H, Zhang G, Wu J, Zhu W, Gu Y, et al. MiR-212-3p inhibits cell proliferation and promotes apoptosis by targeting nuclear factor IA in bladder cancer. *J Biosci.* (2019) 44:80. doi: 10.1007/s12038-019-9903-5
28. Fiserova B, Kubiczkova L, Sedlarikova L, Hajek R, Sevcikova S. The miR-29 family in hematological malignancies. *Biomed Pap Med Fac Univ Palacky Olomouc Czech Repub.* (2015) 159:184–91. doi: 10.5507/bp.2014.037
29. Wen L, Cheng F, Zhou Y, Yin C. MiR-26a enhances the sensitivity of gastric cancer cells to cisplatin by targeting NRAS and E2F2. *Saudi J Gastroenterol.* (2015) 21:313–9.doi: 10.4103/1319-3767.166206

30. Zimmerman EI, Dollins CM, Crawford M, Grant S, Sinkam SPN, Richards KL, et al. Lyn kinase-dependent regulation of miR181 and myeloid cell leukemia-1 expression: Implications for drug resistance in myelogenous leukemia. *Mol Pharmacol.* (2010) 78:811–7. doi: 10.1124/mol.110.066258
31. Yu Y, Yang L, Zhao M, Zhu S, Kang R, Vernon P, et al. Targeting microRNA-30a-mediated autophagy enhances imatinib activity against human chronic myeloid leukemia cells. *Leukemia.* (2012) 26:1752–60. doi: 10.1038/leu.2012.65
32. Venturini L, Battmer K, Castoldi M, Schultheis B, Hochhaus A, Muckenthaler MU, et al. Expression of the miR-17-92 polycistron in chronic myeloid leukemia (CML) CD34+ cells. *Blood.* (2007) 109:4399–405. doi: 10.1182/blood-2006-09-045104
33. Song B, Yan J, Liu C, Zhou H, Zheng Y. Tumor suppressor role of miR-363-3p in gastric cancer. *Med Sci Monit.* (2015) 21:4074–80. doi: 10.12659/MSM.896556
34. Flamant S, Ritchie W, Guilhot J, Holst J, Bonnet ML, Chomel JC, et al. Micro-RNA response to imatinib mesylate in patients with chronic myeloid leukemia. *Haematologica.* (2010) 95:1325–33. doi: 10.3324/haematol.2009.020636
35. Zuo Z, Calin GA, de Paula HM, Medeiros LJ, Fernandez MH, Shimizu M, et al. Circulating microRNAs let-7a and miR-16 predict progression-free survival and overall survival in patients with myelodysplastic syndrome. *Blood.* (2011) 118:413–5. doi: 10.1182/blood-2011-01-330704
36. Wang LS, Li L, Li L, Chu S, Shiang KD, Li M, et al. MicroRNA-486 regulates normal erythropoiesis and enhances growth and modulates drug response in CML progenitors. *Blood.* (2015) 125:1302–13. doi: 10.1182/blood-2014-06-581926
37. Mou T, Xie F, Zhong P, Hua H, Lai L, Yang Q, et al. MiR-345-5p functions as a tumor suppressor in pancreatic cancer by directly targeting CCL8. *Biomed Pharmacother.* (2019) 111:891–900. doi: 10.1016/j.biopha.2018.12.121
38. Hannafon BN, Cai A, Calloway CL, Xu YF, Zhang R, Fung KM, et al. miR-23b and miR-27b are oncogenic microRNAs in breast cancer: evidence from a CRISPR/Cas9 deletion study. *BMC Cancer.* (2019) 19:642. doi: 10.1186/s12885-019-5839-2
39. Ji R, Zhang X, Gu H, Ma J, Wen X, Zhou J, et al. miR-374a-5p: A new target for diagnosis and drug resistance therapy in gastric cancer. *Mol Ther Nucleic Acids.* (2019) 18:320–31. doi: 10.1016/j.omtn.2019.07.025
40. Xia J T, Chen L Z, Jian W H, Wang K B, Yang Y Z, He W L. MicroRNA-362 induces cell proliferation and apoptosis resistance in gastric cancer by activation of NF-κB signaling. *J Transl Med.* (2014) 12:33. doi: 10.1186/1479-5876-12-33
41. Chadrashekar K, Jayaram S. Role of *let-7* family microRNA in breast cancer. *Non-Cod RNA Res.* (2016) 1:77–82. doi: 10.1016/j.ncrna.2016.10.003
42. Sun GL, Li Z, Wang WZ, Chen Z, Zhang L, Li Q. miR-324-3p promotes gastric cancer development by activating Smad4-mediated Wnt/beta-catenin signaling pathway. *J Gastroenterol.* (2018) 53:725–39. doi: 10.1007/s00535-017-1408-0
43. Choe MH, Yoon Y, Kim J, Hwang SG, Han YH, Kim JS. miR-550a-3-5p acts as a tumor suppressor and reverses BRAF inhibitor resistance through the direct targeting of YAP. *Cell Death Dis.* (2018) 9:640. doi: 10.1038/s41419-018-0698-3
44. Pan L, Zhou L, Yin W, Bai J, Liu R. miR-125a induces apoptosis, metabolism disorder and migration impairment in pancreatic cancer cells by targeting Mfn2-related mitochondrial fission. *Int J Oncol.* (2018) 53:124–136. doi: 10.3892/ijo.2018.4380
45. Ni S, Weng W, Xu M, Wang Q, Ian C, Sun H. miR-106b-5p inhibits the invasion and metastasis of colorectal cancer by targeting CTSA. *Onco Targets Ther.* (2018) 11:3835–45. doi: 10.2147/OTT.S172887
46. Xue J, Yang M, Hua L-H, Wang Z-P. MiRNA-191 functions as an oncogene in primary glioblastoma by directly targeting NDST1. *Eur Rev Med Pharmacol Sci.* (2019) 23:6242–9. doi: 10.26355/eurrev_201907_18443
47. Ji WB, Liu X, Luo Y, Zhang WZ. High expression of miR-15b predicts poor prognosis for hepatocellular carcinoma after curative hepatectomy. *Oncol Rep.* (2016) 36:1901–8. doi: 10.3892/or.2016.4982
48. Eiring AM, Harb JG, Neviani P, Garton C, Oaks JJ, Spizzo R, et al. MiR-328 functions as an RNA decoy to modulate hnRNP E2 regulation of mRNA translation in leukemic blasts. *Cell.* (2010) 140:652–65. doi: 10.1016/j.cell.2010.01.007
49. Garofalo M, Quintavalle C, Romano G, Croce CM, Condorelli G. miR221/222 in cancer: their role in tumor progression and response to therapy. *Curr Mol Med.* (2012) 12:27–33. doi: 10.2174/156652412798376170
50. Zhang H, Jiang L, Sun D, Li J, Tang J. MiR-139-5p: promising biomarker for cancer. *Tumor Biol.* (2015) 36:1355–65. doi: 10.1007/s13277-015-3199-3
51. Li M, Guan X, Sun Y, Mi J, Shu X, Liu F, et al. miR-92a family and their target genes in tumorigenesis and metastasis. *Exp Cell Res.* (2014) 323:1–6. doi: 10.1016/j.yexcr.2013.12.025
52. Poláková KM, Lopotová T, Klamová H, Burda P, Trněný M, Stopka T, et al. Expression patterns of micro-RNAs associated with CML phases and their disease related targets. *Mol Cancer.* (2011) 10:41. doi: 10.1186/1476-4598-10-41
53. Chen L, Jiang X, Chen H, Han Q, Liu C, Sun M. microRNA-628 inhibits the proliferation of acute myeloid leukemia cells by directly targeting IGF-1R. *Onco Targets Ther.* (2019) 12:907–19. doi: 10.2147/OTT.S192137
54. Fallah P, Amirizadeh N, Poopak B, Toogeh G, Arefian E, Kohram F, et al. Expression pattern of key microRNAs in patients with newly diagnosed chronic myeloid leukemia in chronic phase. *Int J Lab Hematol.* (2015) 37:560–8. doi: 10.1111/ijlh.12351
55. Zheng J, Zhou Y, Li XJ, Hu JM. MiR-574-3p exerts as a tumor suppressor in ovarian cancer through inhibiting MMP3 expression. *Eur Rev Med Pharmacol Sci.* (2019) 23:6839–48. doi: 10.26355/eurrev_201908_18723
56. Zearo S, Kim E, Zhu Y, Zhao JT, Sidhu SB, Robinson BG, et al. MicroRNA-484 is more highly expressed in serum of early breast cancer patients compared to healthy volunteers. *BMC Cancer.* (2014) 14:200. doi: 10.1186/1471-2407-14-200
57. Guo LH, Li H, Wang F, Yu J, He JS. The tumor suppressor roles of miR-433 and miR-127 in gastric cancer. *Int J Mol Sci.* (2013) 14:14171–84. doi: 10.3390/ijms140714171
58. Labbaye C, Testa U. The emerging role of MIR-146A in the control of hematopoiesis, immune function and cancer. *J Hematol Oncol.* (2012) 5:13. doi: 10.1186/1756-8722-5-13
59. Chen J, Gao S, Wang C, Wang Z, Zhang H, Huang K, et al. Pathologically decreased expression of miR-193a contributes to metastasis by targeting WT1-E-cadherin axis in non-small cell lung cancers. *J Exp Clin Cancer Res.* (2016) 35:173. doi: 10.1186/s13046-016-0450-8
60. Wang H, He H, Yang C. miR-342 suppresses the proliferation and invasion of acute myeloid leukemia by targeting Naa10p. *Artif Cell Nanomed Biotechnol.* (2019) 47:3671–6. doi: 10.1080/21691401.2019.1596930
61. Ravichandran K, Sekar D, Subramanian G, Devanathan S. Role of microRNA-7-1-3p in prostate cancer progression. *HIV Adv Res Dev.* (2014) 1:1–4. doi: 10.14437/HARDOA-1-103
62. Pan JY, Zhang F, Sun CC, Li SJ, Li G, Gong FY, et al. miR-134: A human cancer suppressor? *Mol Ther Nucl Acids.* (2017) 6:140–9. doi: 10.1016/j.omtn.2016.11.003
63. Zhang C, Wang B, Wu L. MicroRNA-409 may function as a tumor suppressor in endometrial carcinoma cells by targeting Smad2. *Mol Med Rep.* (2019) 19:622–8. doi: 10.3892/mmr.2018.9642
64. Agirre X, Velasco AJ, Enériz ESJ, Garate L, Bandrés E, Cordeu L, et al. Down-regulation of hsa-miR-10a in chronic myeloid leukemia CD34+ cells increases USF2-mediated cell growth. *Mol Cancer Res.* (2008) 6:1830–40. doi: 10.1158/1541-7786.MCR-08-0167
65. Koul HK, Pal M, Koul S. Role of p38 MAP kinase signal transduction in solid tumors. *Genes Cancer.* (2013) 4:342–59. doi: 10.1177/1947601913507951
66. Meister M, Tomasovic A, Banning A, Tikkanen R. Mitogen-activated protein (MAP) kinase scaffolding proteins: a recount. *Int J Mol Sci.* (2013) 14:4854–84. doi: 10.3390/ijms14034854
67. Dhillon AS, Hagan S, Rath O, Kolch W. MAP kinase signalling pathways in cancer. *Oncogene.* (2007) 26:3279–90. doi: 10.1038/sj.onc.1210421
68. Rocca S, Carrà G, Poggio P, Morotti A, Brancaccio M. Targeting few to help hundreds: JAK, MAPK and ROCK pathways as druggable targets in atypical chronic myeloid leukemia. *Mol Cancer.* (2018) 17:40. doi: 10.1186/s12943-018-0774-4

69. Zhang F, Cheong JK. The renewed battle against RAS-mutant cancers. *Cell Mol Life Sci.* (2016) 73:1845–58. doi: 10.1007/s00018-016-2155-8
70. Wang AS, Hasserjian RP, Fox PS, Rogers HJ, Geyer JT, Chabot-Richards D, et al. Atypical chronic myeloid leukemia is clinically distinct from unclassifiable myelodysplaastic/myeloproliferative neoplasms. *Blood.* (2015) 123:2645–52. doi: 10.1182/blood-2014-02-553800

Conflict of Interest: The authors declare that the research was conducted in the absence of any commercial or financial relationships that could be construed as a potential conflict of interest.

The handling editor declared a shared affiliation, though no other research collaboration, with the authors.

Advantages of publishing in Frontiers

OPEN ACCESS
Articles are free to read for greatest visibility and readership

FAST PUBLICATION
Around 90 days from submission to decision

HIGH QUALITY PEER-REVIEW
Rigorous, collaborative, and constructive peer-review

TRANSPARENT PEER-REVIEW
Editors and reviewers acknowledged by name on published articles

Frontiers
Avenue du Tribunal-Fédéral 34
1005 Lausanne | Switzerland

Visit us: www.frontiersin.org
Contact us: frontiersin.org/about/contact

REPRODUCIBILITY OF RESEARCH
Support open data and methods to enhance research reproducibility

DIGITAL PUBLISHING
Articles designed for optimal readership across devices

FOLLOW US
@frontiersin

IMPACT METRICS
Advanced article metrics track visibility across digital media

EXTENSIVE PROMOTION
Marketing and promotion of impactful research

LOOP RESEARCH NETWORK
Our network increases your article's readership